Replacement of Neanderthals by Modern Humans Series

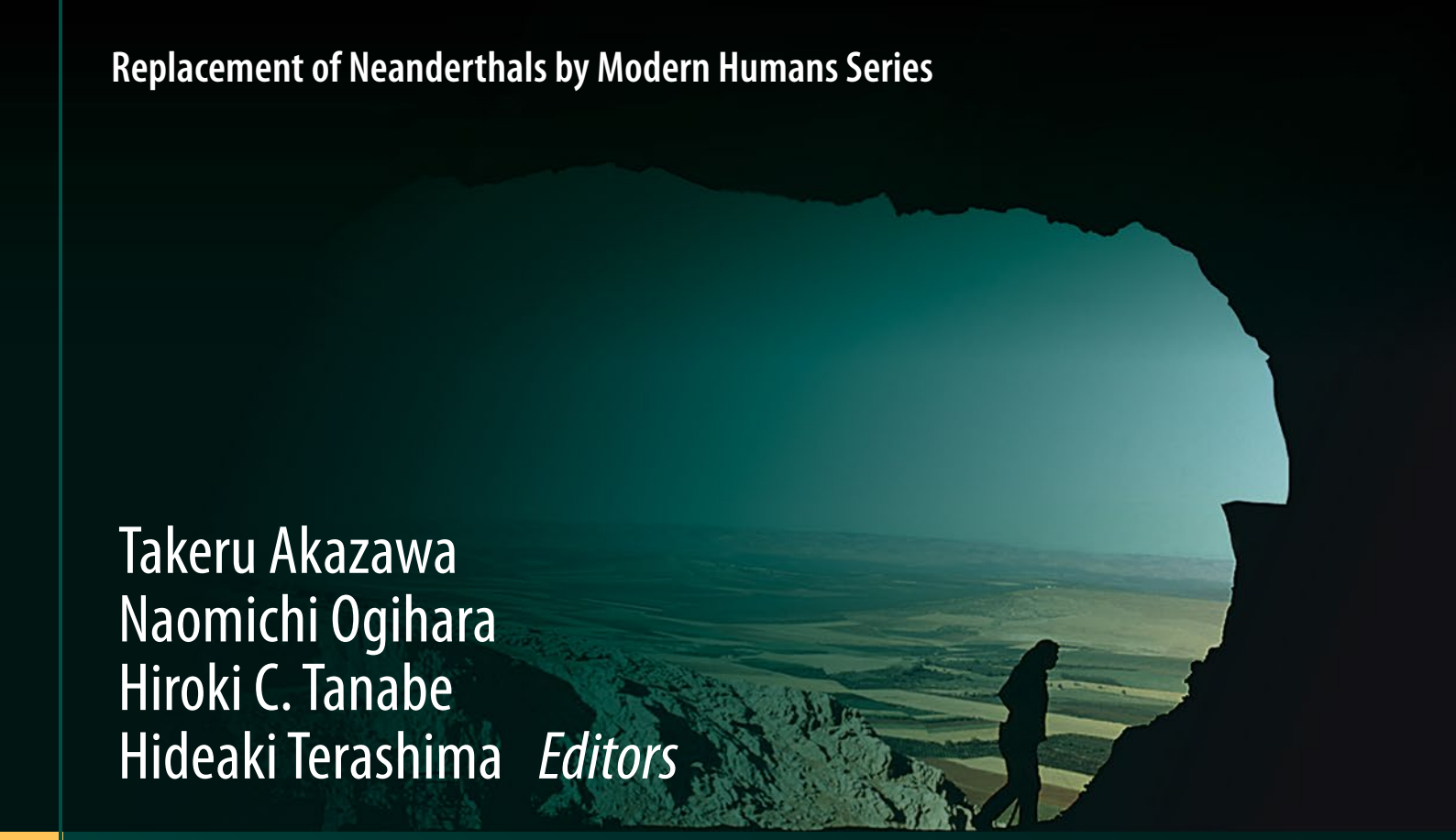

Takeru Akazawa
Naomichi Ogihara
Hiroki C. Tanabe
Hideaki Terashima *Editors*

Dynamics of Learning in Neanderthals and Modern Humans

Volume 2

Cognitive and Physical Perspectives

Springer

Replacement of Neanderthals by Modern Humans Series

Edited by

Takeru Akazawa
Research Institute, Kochi University of Technology
Kochi 782-8502, Japan
akazawa.takeru@kochi-tech.ac.jp

Ofer Bar-Yosef
Department of Anthropology, Harvard University
Cambridge, Massachusetts 02138, USA
obaryos@fas.harvard.edu

The planned series of volumes will report the results of a major research project entitled "Replacement of Neanderthals by Modern Humans: Testing Evolutionary Models of Learning", offering new perspectives on the process of replacement and on interactions between Neanderthals and modern humans and hence on the origins of prehistoric modern cultures. The projected volumes will present the diverse achievements of research activities, originally designed to implement the project's strategy, in the fields of archaeology, paleoanthropology, cultural anthropology, population biology, earth sciences, developmental psychology, biomechanics, and neuroscience. Comprehensive research models will be used to integrate the discipline-specific research outcomes from those various perspectives. The series, aimed mainly at providing a set of multidisciplinary perspectives united under the overarching concept of learning strategies, will include monographs and edited collections of papers focusing on specific problems related to the goals of the project, employing a variety of approaches to the analysis of the newly acquired data sets.

For further volumes:
http://www.springer.com/series/11816

Takeru Akazawa • Naomichi Ogihara
Hiroki C. Tanabe • Hideaki Terashima
Editors

Dynamics of Learning in Neanderthals and Modern Humans Volume 2

Cognitive and Physical Perspectives

Proceedings of the international conference on "*Replacement of Neanderthals by Modern Humans: Testing Evolutionary Models of Learning*", organized by Takeru Akazawa, Shunichi Amari, Kenichi Aoki, Ofer Bar-Yosef, Ralph L. Holloway, Shiro Ishii, Tasuku Kimura, Yoshihiro Nishiaki, Naomichi Ogihara, Hiroki C. Tanabe, Hideaki Terashima, and Minoru Yoneda, which took place in Tokyo, November 18–24, 2012, Volume 2.

Edited by

Takeru Akazawa
Kochi University of Technology, Kochi, Japan

Naomichi Ogihara
Keio University, Yokohama, Japan

Hiroki C. Tanabe
Nagoya University, Nagoya, Japan

Hideaki Terashima
Kobe Gakuin University, Kobe, Japan

Springer

Editors
Takeru Akazawa
Research Institute
Kochi University of Technology
Kochi, Japan

Hiroki C. Tanabe
Graduate School of Environmental Studies
Nagoya University
Nagoya, Japan

Naomichi Ogihara
Department of Mechanical Engineering
Faculty of Science and Technology
Keio University, Yokohama, Japan

Hideaki Terashima
Department of Human Psychology
Faculty of Humanities and Sciences
Kobe Gakuin University
Kobe, Japan

ISBN 978-4-431-54552-1 ISBN 978-4-431-54553-8 (eBook)
DOI 10.1007/978-4-431-54553-8
Springer Tokyo Heidelberg New York Dordrecht London

Library of Congress Control Number: 2013957874

Preface

Knowledge about the pathways of human evolution has expanded dramatically as a result of advances in genetic, paleontological, and archaeological studies in the twentieth century. One excellent example is the resolution of the issue of the origin of modern humans, long a source of great controversy; namely, the idea that modern *Homo sapiens* are direct related genealogically to Eurasian archaic humans was rejected, and the "Out of Africa" theory, which is now the accepted evolutionary model, was vindicated. However, this new theory only gave rise to a flurry of new questions, one of which centers on the drama of the replacement of the archaic Neanderthals by modern *Homo sapiens*.

Modern humans appeared in Africa about 200,000 years ago; as they subsequently spread across Eurasia, they encountered the indigenous Neanderthals. The two populations coexisted until 30,000 years ago or perhaps even later, but the Neanderthals eventually went extinct. What governed the fates of the two groups? A number of current hypotheses have been proposed to explore the possible mechanics of the replacement of Neanderthals by modern humans, and there has been extensive debate as to whether or not the presence of the modern humans accelerated the extinction of the Neanderthals. This question is being hotly debated among archaeologists, anthropologists, and geneticists around the world.

We are actively engaged in a 5-year (2010–2014) major research project entitled "Replacement of Neanderthals by Modern Humans: Testing Evolutionary Models of Learning" (RNMH). In launching RNMH we have adopted a large scale innovative assault on this research question. The RNMH project implements a pioneering framework structured around the contrast between the success of modern human societies in solving strategic survival problems, and the failure of Neanderthal societies to do so. In that context, we attribute the contrasting fates of the two societies to a difference in learning abilities between the two populations. This is the basis of our working hypothesis ("learning hypothesis").

The specific goal of this project is to verify the learning hypothesis within an interdisciplinary research framework incorporating new perspectives and methods in the fields of archaeology, paleoanthropology, cultural anthropology, population biology, earth sciences, developmental psychology, biomechanics, and neuroscience. The two present volumes are the proceedings of the first international RNMH conference held in Tokyo in November 2012. Some results have already been published separately in various scholarly journals, but these two volumes constitute the first full attempt to disseminate the findings of our RNMH project to the international research communities. A major purpose in doing so at this halfway point of our project is to solicit scholarly evaluation of these findings.

The 43 submitted manuscripts have been classified into seven sections based on content, and then divided into two groups to be published as two volumes in the Replacement of Neanderthals by Modern Humans series. The first volume is devoted to discussion of cultural perspectives, the second to cognitive and physical perspectives. We hope that these two volumes may contribute significant new insights on the process of replacement and on interactions between Neanderthals and modern humans, and hence on the origins of prehistoric modern cultures.

The editors of this volume are greatly indebted to all our colleagues who supported the publication with their reviews and comments: Juko Ando (Keio University), Emiliano Bruner

(Centro National de Investigación Sobre la Evolución Humana), Nicole Creanza (Stanford University), Laurel Fogarty (Stanford University), Kaoru Imamura (Nagoya Gakuin University), Hiroaki Kawamichi (National Institute for Physiological Sciences), Ryosuke Kimura (University of the Ryukyus), Tasuku Kimura (University of Tokyo), Yasushi Kobayashi (National Defense Medical College), Takanori Kochiyama (Kyoto University), Osamu Kondo (University of Tokyo), Tadashi Koyama (Kobe Gakuin University), Naoko Matsumoto (Okayama University), Alex Mesoudi (Durham University), Takashi Michikawa (University of Tokyo), Naoki Miura (Tohoku Institute of Technology), Masaaki Mochimaru (National Institute of Advanced Industrial Science and Technology), Masaki Moriguchi (Chuo University), Yoshihiro Nishiaki (University of Tokyo), Ryutaro Ohtsuka (Japan Wildlife Research Center), Hiroki Oota (Kitazato University), Herman Pontzer (Hunter College), Makoto Shimada (Fujita Health University), Dietrich Stout (Emory University), Nobuyuki Takahashi (Hokkaido University), Kyoko Yamaguchi (University of the Ryukyus), Eiko Yamagami (Kobe Gakuin University), Taro Yamauchi (Hokkaido University), Kazufumi Yoshihara (Kyushu University). These colleagues read the manuscripts and made critical but constructive comments on the early drafts; this valuable input greatly improved the quality of the volumes. Many thanks to all of them.

We are pleased to acknowledge the Japanese Ministry of Education, Culture, Science, and Technology for their interest in our project and for their financial support, which has made possible our RNMH Project, the conference, and the preparation of this volume.

We would like to thank Ken Kimlicka and Taeko Sato of Springer Japan for heir most valuable guidance and support, and for their tireless encouragement during the preparation of this volume.

May 2013

Takeru Akazawa
Naomichi Ogihara
Hiroki C. Tanabe
Hideaki Terashima

Contents

Part IV Neuroscience

Contributors

Takeru Akazawa Research Institute, Kochi University of Technology, Kami-shi, Kochi, Japan

Hideki Amano Department of Mechanical Engineering, Faculty of Science and Technology, Keio University, Yokohama, Kanagawa, Japan

Juko Ando Department of Humanities and Social Sciences, Faculty of Letters, Keio University, Tokyo, Japan

Emiliano Bruner Centro Nacional de Investigación sobre la Evolución Humana, Burgos, Spain

Izumi Hagino Laboratory of Human Ecology, Graduate School of Health Sciences, Hokkaido University, Sapporo, Hokkaido, Japan

Yoshinori Haizuka Department of Anatomy, Kyorin University School of Medicine, Tokyo, Japan

Ayaka Hatano Graduate School of Letters, Hokkaido University, Sapporo, Hokkaido, Japan

Naoki Hirai Department of Integrative Physiology, Kyorin University School of Medicine, Tokyo, Japan

Hiroyuki Hishida Research Center for Advanced Science and Technology, University of Tokyo, Tokyo, Japan

Yukinobu Hoshino Engineering Course of Graduate School, Kochi University of Technology, Kami-shi, Kochi, Japan

Misato Inaba Graduate School of Letters, Hokkaido University, Sapporo, Hokkaido, Japan

Hajime Ishida Department of Human Biology and Anatomy, Graduate School of Medicine, University of the Ryukyus, Nishihara, Okinawa, Japan

Hiroaki Kawamichi Division of Cerebral Integration, Department of Cerebral Research, National Institute for Physiological Sciences, Okazaki, Aichi, Japan

Ryosuke Kimura Graduate School of Medicine, University of the Ryukyus, Okinawa, Japan

Ryo Kitada Division of Cerebral Integration, Department of Cerebral Research, National Institute for Physiological Sciences, Okazaki, Aichi, Japan

Yasushi Kobayashi Department of Anatomy and Neurobiology, National Defense Medical College, Tokorozawa, Saitama, Japan

Takanori Kochiyama The Hakubi project, Primate Research Institute, Kyoto University, Inuyama, Aichi, Japan

Brain Activity Imaging Center, Advanced Telecommunications Research Institute International, Kyoto, Japan

Osamu Kondo Department of Biological Sciences, Graduate School of Science, University of Tokyo, Tokyo, Japan

Tadashi Koyama Department of Human Psychology, Faculty of Humanities and Sciences, Kobe Gakuin University, Kobe, Hyogo, Japan

Daisuke Kubo Department of Biological Sciences, Graduate School of Science, University of Tokyo, Tokyo, Japan

Toshiyasu Matsui Department of Anatomy and Neurobiology, National Defense Medical College, Tokorozawa, Saitama, Japan

George Matsumura Department of Anatomy, Kyorin University School of Medicine, Tokyo, Japan

Masahiro Matsunaga Division of Cerebral Integration, Department of Cerebral Research, National Institute for Physiological Sciences, Okazaki, Aichi, Japan

Alex Mesoudi Department of Anthropology and Centre for the Coevolution of Biology and Culture, Durham University, Durham, UK

Takashi Michikawa Research Center for Advanced Science and Technology, University of Tokyo, Tokyo, Japan

Keita Mitani Kochi University of Technology, Kami-shi, Kochi, Japan

Steven Mithen University of Reading, Whiteknights, Reading, UK

Naoki Miura Department of Information and Communication Engineering, Faculty of Engineering, Tohoku Institute of Technology, Sendai, Miyagi, Japan

Kei Mizuno Molecular Probe Dynamics Laboratory, RIKEN Center for Molecular Imaging Science, Kobe, Hyogo, Japan

Pathophysiological and Health Science Team, RIKEN Center for Life Science Technologies, Kobe, Hyogo, Japan

Masaki Moriguchi Department of Information and System Engineering, Chuo University, Tokyo, Japan

Yusuke Morita Department of Mechanical Engineering, Faculty of Science and Technology, Keio University, Yokohama, Kanagawa, Japan

Sadayuki Murayama Department of Radiology, Graduate School of Medicine, University of the Ryukyus, Nishihara, Okinawa, Japan

Kenji Nagai Department of Historic Heritage, Tohoku University of Art and Design, Yamagata, Japan

Hiroyasu Nagano Department of Mechanical Engineering, Faculty of Science and Technology, Keio University, Yokohama, Kanagawa, Japan

Masato Nakatsukasa Laboratory of Physical Anthropology, Graduate School of Science, Kyoto University, Sakyo, Kyoto, Japan

Naomichi Ogihara Department of Mechanical Engineering, Faculty of Science and Technology, Keio University, Yokohama, Kanagawa, Japan

Yutaka Ohtake Department of Precision Engineering, University of Tokyo, Tokyo, Japan

Keiichi Omura Studies in Language and Culture, Graduate School of Language and Culture, Osaka University, Toyonaka, Osaka, Japan

Ryoichi Onoda Graduate School of Letters, Hokkaido University, Sapporo, Hokkaido, Japan

Satoshi Oota RIKEN BioResource Center, Tsukuba, Ibaraki, Japan

Norihiro Sadato Division of Cerebral Integration, Department of Cerebral Research, National Institute for Physiological Sciences, Okazaki, Aichi, Japan

Akihiro Sasaki Division of Cerebral Integration, Department of Cerebral Research, National Institute for Physiological Sciences, Okazaki, Aichi, Japan

Dora Simunovic Graduate School of Letters, Hokkaido University, Sapporo, Hokkaido, Japan

Hiromasa Suzuki Research Center for Advanced Science and Technology, University of Tokyo, Tokyo, Japan

Haruka Takahashi Division of Cerebral Integration, Department of Cerebral Research, National Institute for Physiological Sciences, Okazaki, Aichi, Japan

Nobuyuki Takahashi Center for Experimental Research in Social Sciences, Graduate School of Letters, Hokkaido University, Sapporo, Hokkaido, Japan

Hiroki C. Tanabe Department of Social and Human Environment, Graduate School of Environmental Studies, Nagoya University, Nagoya, Aichi, Japan

Division of Cerebral Integration, Department of Cerebral Research, National Institute for Physiological Sciences, Okazaki, Aichi, Japan

Hideaki Terashima Department of Human Psychology, Faculty of Humanities and Sciences, Kobe Gakuin University, Kobe, Hyogo, Japan

Eiko Yamagami Department of Human Psychology, Faculty of Humanities and Sciences, Kobe Gakuin University, Kobe, Hyogo, Japan

Taro Yamauchi Laboratory of Human Ecology, Faculty of Health Sciences, Hokkaido University, Sapporo, Hokkaido, Japan

Mika Yamazaki Child Development Research Center, Graduate School of Medical Sciences, National University Corporation University of Fukui, Fukui, Japan

Akira Yogi Department of Radiology, Graduate School of Medicine, University of the Ryukyus, Nishihara, Okinawa, Japan

Yumiko Yoshida Division of Cerebral Integration, Department of Cerebral Research, National Institute for Physiological Sciences, Okazaki, Aichi, Japan

Kazufumi Yoshihara Department of Psychosomatic Medicine, Graduate School of Medical Sciences, Kyushu University, Fukuoka, Japan

Introduction

1

Naomichi Ogihara, Hiroki C. Tanabe, Hideaki Terashima, and Takeru Akazawa

The "Replacement of Neanderthals by Modern Humans" (RNMH) project aims to validate the working hypothesis, or "learning hypothesis," that seeks to explain the replacement of Neanderthals (*Homo neanderthalensis*) by early modern humans (*H. sapiens*). The RNMH project focuses on evidence—such as innate differences in learning capacity between the two populations—within an interdisciplinary research framework that incorporates new perspectives and methods from the humanities and biological sciences, including neuroscience and engineering. This volume, the second of a two-volume book, is the result of papers presented at the first international conference of the RNMH project, held in Tokyo in November 2012. The first volume covers cultural perspectives addressing the process of the replacement of Neanderthals and learning strategies based on changing patterns in archaeological evidence and theoretical interpretation using mathematical models. The second volume deals with cognitive and physical perspectives on the replacement process, exploring the innate differences in learning and cognitive abilities that may have existed between Neanderthals and early modern humans. The editors of the second volume have selected a total of 26 contributed papers, divided into four parts according to research topic.

The first part is devoted to cognitive and psychological perspectives on the learning hypothesis. Here, the authors work to clarify which cognitive and psychological functions helped shape the fate of the two species. Mithen (Chap. 2) reviews the similarities and differences in cognition of Neanderthals and early modern humans and discusses the possible differences in cognitive ability between them, offering examples such as the use of pigment. The next two chapters deal with learning style and ability in modern humans. Ando (Chap. 3) introduces three learning types, individual, imitative and instructed, and discusses the differences in their characteristics based on original experiments. Omura (Chap. 4) considers the evolutionary basis for theories on learning ability in modern humans, modifying the cumulative cultural evolution hypothesis proposed by Tomasello, and proposes that the most important ability for cumulative cultural learning is the ability to objectify and manipulate the relationships between culture and the environment. The subsequent two chapters report field research conducted with children. It is important to understand the basic learning characteristics required for modern humans to survive as innovative hunter-gatherers. In particular, it is critical to focus on the learning behaviors seen in children and children's play groups, since childhood is the most active period for learning, and because play groups served as the primary learning place for children until the introduction of modern school education. Koyama (Chap. 5) and Yamagami (Chap. 6) joined Baka society in Cameroon and performed experiments with Baka children. They found evidence of cognitive flexibility as demonstrated by object-making and drawings, which might be important in the construction of a flexible learning attitude in modern humans. The last two chapters of the first part of this volume offer experimental psychological evidence.

N. Ogihara (✉)
Department of Mechanical Engineering, Faculty of Science and Technology, Keio University, 3-14-1 Hiyoshi, Kohoku-ku, Yokohama, Kanagawa 223-8522, Japan
e-mail: ogihara@mech.keio.ac.jp

H.C. Tanabe
Department of Social and Human Environment, Graduate School of Environmental Studies, Nagoya University, Furo-cho, Chikusa-ku, Nagoya, Aichi 464-8601, Japan

Division of Cerebral Integration, Department of Cerebral Research, National Institute for Physiological Sciences, 38 Nishigo-naka, Myodaiji, Okazaki, Aichi 444-8585, Japan
e-mail: htanabe@lit.nagoya-u.ac.jp

H. Terashima
Department of Human Psychology, Faculty of Humanities and Sciences, Kobe Gakuin University, 518 Arise, Ikawadani-cho, Nishi-ku, Kobe, Hyogo 651-2180, Japan
e-mail: terasima@human.kobegakuin.ac.jp

T. Akazawa
Research Institute, Kochi University of Technology, 185 Miyanokuchi, Tosayamada, Kami-shi, Kochi 782-8502, Japan
e-mail: akazawa.takeru@kochi-tech.ac.jp; akazawa0823@qd6.so-net.ne.jp

T. Akazawa et al. (eds.), *Dynamics of Learning in Neanderthals and Modern Humans Volume 2: Cognitive and Physical Perspectives*, Replacement of Neanderthals by Modern Humans Series, DOI 10.1007/978-4-431-54553-8_1, © Springer Japan 2014

Evolutional mathematical models assume that there are two types of learning process: individual learning (i.e., learning by oneself, by trial-and-error) and social learning (i.e., learning from others, by imitation). However, from a cognitive psychology viewpoint, this dichotomy might be misleading or inadequate, because there are more cognitive factors operating in the learning situation. Takahashi et al. (Chap. 7) claim that individual learning has two different components: trial-and-error and creativity. They clarify the relationship between the abilities of imitation, trial-and-error, and creativity from an experimental psychology point of view. Mesoudi (Chap. 8) investigates social and individual learning behavior in an archaeological context, examining how contemporary humans behaved when faced with a relatively complex and novel technology design task and elucidating their adaptive performance under constraint.

The second part of this volume deals with biology and genetics as related to the replacement of Neanderthals by modern humans. Hoshino et al. (Chap. 9) present a preliminary analysis of the three-dimensional kinematics of knapping motion in stone tool-making. Such replication studies are important for identifying the motor skills required for recurrent Levallois techniques, as well as possible differences in learning ability between Neanderthals and early modern humans. Hagino and Yamauchi (Chap. 10) and Yamauchi and Hagino (Chap. 11) report the results of field studies on Baka hunter-gatherers. In Chap. 10 the authors quantify the daily physical activities and time-space of hunter-gatherers' children, and in Chap. 11 they compare the growth patterns of hunter-gatherer children with those of populations in other parts of the world. These studies provide a solid biological basis for understanding and characterizing learning behavior in hunter-gatherer societies, allowing extrapolation to potential differences in learning ability between Neanderthals and early modern humans. In the last paper in the second part of this volume, Kimura (Chap. 12) discusses statistical analyses of population genomics. Reconstructing modern human population dispersal is crucial for understanding the replacement of Neanderthals by early modern humans, and Kimura's computer simulation study represents a step towards better interpretation of results obtained by genetic analyses for the reconstruction of the complex demographic history of modern human populations.

The third part of this volume contains studies on the computerized reconstruction of fossil crania and brain morphology, which is expected to facilitate empirical validation of the learning hypothesis by providing anatomical proof of differences in learning ability between Neanderthals and early modern humans. Bruner (Chap. 13) reviews recent advances in functional craniology in Neanderthals and demonstrates that Neanderthals generally display a plesiomorphic organization of the braincase. Bruner hypothesizes that a morphogenetic limit (caused by geometric and structural constraints between the endocranial soft and hard tissues) and a thermal limit (rooted in the plesiomorphic vascular system) led to differences in cranial morphology between Neanderthals and early modern humans. Kobayashi et al. (Chaps. 14 and 15) present their attempts to establish a connection between cranial and brain morphology in extant macaques. In Chap. 14, they report that endocasts of macaque skulls show marked impressions of the cerebral sulci and gyri through the entire surface, indicating that the extent of major subdivisions of the macaque cerebral cortex can be determined from endocasts. In Chap. 15, the authors present their results on the morphological correspondence between the location of sutures and the location of major sulci. These studies provide important data for the estimation of brain morphology based on fossil crania.

The next four papers in the third part of the volume focus on geometric morphometrics for the digital reconstruction of fossil crania. Geometric morphometrics is a quantitative approach used to analyze shape variations based on landmark coordinates. However, the human cranial vault has few definable landmarks, and semi-landmarks must be introduced for quantification of the overall shape of the cranial vault. Using the modern Japanese population as an example, Ogihara et al. (Chap. 16) evaluate how two types of semi-landmark configurations affect the analysis of morphological variability in neurocranial shape, concluding that the results do not seem to be significantly affected by the choice of landmark configuration, provided that a sufficient number of semi-landmarks are evenly distributed across the neurocranial surface. Morita et al. (Chap. 17) also focus on the modern Japanese population, analyzing the detailed morphological variability of cranial shape using geometric morphometrics. The results presented by Morita et al. serve as a reference database of human cranial morphology for computerized reconstruction of fossil crania, such as the assembly of fossil cranial fragments and the interpolation of missing parts in fossil crania. Using this cranial database, Amano et al. (Chap. 18) propose a method for mathematically interpolating missing parts of crania, and discuss the usefulness and limitations of the proposed interpolation method for the reconstruction of fossil crania. In the above three studies, semi-landmarks were placed by sliding a "template" landmark configuration along the cranium in order to minimize spatial bending energy. However, Moriguchi et al. (Chap. 19) proposes a new approach to the transfer of semi-landmarks based on the minimization of bending energy on the surface.

The final three chapters in the third part of this volume deal with the reconstruction of fossil crania and brain morphology. Suzuki et al. (Chap. 20) propose an automatic CT segmentation method using structural analysis for the disassembly of fragments of an assembled fossil cranium in order to permit reassembly of the fragments. The proposed method would be a valuable tool for the digital reassembly of fossil materials. Kondo et al. (Chap. 21) present a semi-virtual method for the reconstruction of the endocast of Qafzeh 9, a representative early modern human fossil, using CT images,

and discuss possible asymmetries found in the cranial morphology. Lastly, Kochiyama et al. (Chap. 22) propose a framework for a computerized method of digitally reconstructing Neanderthal brain morphology. Specifically, mapping from a human cranium to a fossil cranium was defined by means of a spatial deformation function using computational anatomy methodology, and this function was then applied to the estimation of the shape of the brain inside the fossil cranium. Although this method has methodological limitations that have yet to be resolved, the proposed framework is promising for application to the mathematical reconstruction of fossil brain morphology.

The fourth and final part of this volume is devoted to neuroscience. The authors adopt cognitive neuroscientific and computational neuroanatomical approaches to search for weaknesses in the learning hypothesis. By assuming that morphological changes in fossil skulls reflect functional differences between the brains of modern humans and those of Neanderthals, the authors seek out possible gaps in learning abilities based on differences in brain morphology and region-specific activities. Tanabe et al. (Chap. 23) introduce a scheme for comparing the Neanderthal brain to the modern human brain using computational neuroanatomy and functional neuroimaging techniques, and illustrate their attempt to elucidate the difference between the two species. As an example of this approach, Kubo et al. (Chap. 24) show the correlation between the cerebellar and posterior cranial fossa volumes using structural magnetic resonance imaging data, and attempt to develop a method for estimating the cerebellar volume of fossil hominins.

Tanabe et al. (Chap. 23) also clarify which brain functions relate to learning ability under focus. The authors assume that the formation of innovative activities is strongly correlated with two components of cognitive ability: the intrinsic drive (internal motivation and perspective) to produce creative activity, and the social cognitive ability to make predictions about the actions and intentions of others on the basis of their mental states. Early modern humans might have been superior to Neanderthals in these abilities and this difference may have determined the fates of both species. Based on this hypothesis, Tanabe et al. attempt to identify functional brain maps related to social cognition and motivation, and clarify the neural mechanisms of eye contact and joint attention, which are both markers of social cognitive ability during early development in humans. Kawamichi et al. (Chap. 25) examine the neural correlates of sense of acceptance, which is thought to be one of the key factors for maintaining an innovative society. Miura et al. (Chap. 26) identify the neural substrates of imitative learning of stone tool-making actions, and Mizuno (Chap. 27) examines the neural substrates associated with motivation to learn. These studies contribute to the creation of maps of specific brain functions. Using this input, it is possible to examine the differences in learning abilities between Neanderthals and early modern humans by integrating morphological analyses of fossilized brains with functional mapping of the modern human brain.

We hope this edited volume will promote further integration of different disciplines and enrich ongoing discussions to promote better understanding of the dynamics of learning in the replacement of Neanderthals by early modern humans.

Part I

Cognition and Psychology

2 The Cognition of *Homo neanderthalensis* and *H. sapiens*: Does the Use of Pigment Necessarily Imply Symbolic Thought?

Steven Mithen

Abstract

Zilhão and his colleagues have argued that the discovery of pigment use in Middle Palaeolithic contexts in Cuevas de los Aviones and Antón, Spain, provides "secure evidence that, approximately 50 ka cal B.P., 10 millennia before modern humans are first recorded in Europe, the behaviour of Neanderthals was symbolically organised and continues to be so until the very end of their evolutionary trajectory". This derived from some outstanding archaeological research but is it a valid interpretation? To address this question I will initially review the evidence for similarities and differences in the cognition of *H. neanderthalensis* and *H. sapiens*, and then consider the impact on existing theories of the recently discovered and/or published evidence for Neanderthal pigment use. My conclusion is that while such evidence supports proposals for a socially complex, emotionally driven Neanderthal lifestyle, it does not provide *prima facie* evidence for symbolic thought and behaviour. Neither does the evidence for pigment use by *H. sapiens* when found without any additional evidence for symbolic thought, such as that from Pinnacle Point at c. 164 kya in the Middle Stone Age of South Africa.

Keywords

Cognition • Colour • Pigments • Ritual • Symbols

2.1 Introduction

The nature of *H. neanderthalensis* cognition is of enduring interest for two reasons. First, the close evolutionary relationship between *H. neanderthalensis* and *H. sapiens* means that the cognitive similarities and differences (if any) between these species enables us to better understand the modern human mind—our own mind. In this regard, the study of *H. neanderthalensis* cognition plays the same role as that of chimpanzees and other non-human primates: it contributes towards a comparative framework for exploring which characteristics of the modern human mind are unique to our species and which are shared with other primates. Second, *H. neanderthalensis* cognition is of inherent interest itself, irrespective of what it may tell us about ourselves: archaeologists have an obligation to explain the observed character of the *H. neanderthalensis* archaeological record and cannot do so without reference to the *H. neanderthalensis* mind, just as they also need to understand the minds of all other hominin species.

Our views of *H. neanderthalensis* and *H. sapiens* cognition continue to evolve with the discovery of new fossil and archaeological evidence and by developments in associated disciplines such as the cognitive sciences and evolutionary genetics. Elsewhere I have considered how the latter requires us to place greater emphasis on neural plasticity; indeed we must view the brain as much as a cultural artefact as a biological entity (Mithen and Parsons 2008). Here I will address the recently published evidence for the use pigments by

S. Mithen (✉)
University of Reading, Whiteknights, Shinfield Rd, Reading, West Berkshire RG6 6UR, UK
e-mail: s.j.mithen@rdg.ac.uk

T. Akazawa et al. (eds.), *Dynamics of Learning in Neanderthals and Modern Humans Volume 2: Cognitive and Physical Perspectives*, Replacement of Neanderthals by Modern Humans Series, DOI 10.1007/978-4-431-54553-8_2, © Springer Japan 2014

H. neanderthalensis, interpreting this within the context of recent research within the cognitive anthropology of religion.

2.1.1 Different, but Neither Better nor Worse

There has been a series of well-documented swings of academic opinion regarding *H. neanderthalensis* cognition that can only be fully understood by being placed into their historical context, whether of the late nineteenth century or relatively recent twentieth century (Trinkaus and Shipman 1994; Mellars 1996). Ultimately, of course, our own theories and models of the *H. neanderthalensis* mind are just as much a product of our time, unconsciously influenced by the culture and politics of our day as were those of Marcellin Boule and Carlton Coon.

One difference, however, is that we are now explicit that reference to potential differences in cognitive characteristics between *H. neanderthalensis and H. sapiens* is entirely unrelated to making value judgements between these species. At least that should be the case: persisting use of phrases such as "cognitive inferiority" (Zilhão et al. 2010) is unfortunate.

The starting point for any consideration of the similarities and differences between *H. neanderthalensis* and *H. sapiens* cognition is the close evolutionary relationship between these species, sharing a common ancestor c. 500,000 years ago. This, together with shared anatomical features, would appear to diminish the extent of any cognitive difference between the two species. Their brain sizes are equivalent and the evolved vocal tract of *H. neanderthalensis* appears no different, in essence, to that of *H. sapiens*. Why would these costly adaptations exist if they were not delivering the same type of cognition and language? We should also note that many of the stone tools used by *H. neanderthalensis* were extraordinarily complex to manufacture, no less so than many of those of the Late Stone Age and Upper Palaeolithic. Moreover, *H. neanderthalensis* endured for an extensive period of time throughout a wide variety of challenging environmental conditions. Could members of this species have possibly done so without the type planning and decision making regarding both the natural and social worlds as found among *H. sapiens*?

2.2 Archaeological Evidence for Cognitive Differences Between *H. neanderthalensis* and *H. sapiens*

Despite these considerable anatomical and behavioural similarities between *H. neanderthalensis* and *H. sapiens* further lines of evidence makes it not unreasonable to posit a significant difference in the nature of their cognition. Specifically, the archaeological record has three characteristics that lead us in this direction: the relative homogeneity of the *H. neanderthalensis* archaeological record in space and time when compared to that of *H. sapiens*; the absence/rarity of evidence for visual symbolism by *H. neanderthalensis*; and the swift replacement of *H. neanderthalensis* by *H. sapiens*.

2.2.1 Cultural Homogeneity

Despite more than 350,000 years of existence, the extent of cultural and behavioural innovation by the *H. neanderthalensis* appears to have been limited (for reviews see Stringer and Gamble 1993; Mellars 1999; Mithen 2005; Stringer 2011). Throughout their existence the *H. neanderthalensis* remained as stone-age hunter-gatherers with a narrow cultural repertoire when compared to that of *H. sapiens*. Similarly the extent of geographical variation is strikingly limited. There are few, if any, technological innovations in *H. neanderthalensis* stone tool technology throughout this period, with a considerable amount of the existing technological variability being attributable to the impact of raw material availability and environmental conditions effecting mobility patterns (Rolland and Dibble 1990; Dibble and Rolland 1992). Similarly, variability in Neanderthal subsistence behaviour appears to be adaptive responses to environmental conditions of the type we would expect for any large brained, bipedal, tool-using primate—as illustrated by the changing hunting patterns throughout the Combe Grenal sequence (Chase 1986). The records of other activities, such as burial and hearth constructions are so slight that identifying chronological or spatial patterns is hugely problematic. One might point to a possible increase in such types of activity after 60,000 years ago, such as in pigment use (Soressi and d'Errico 2007) and burial (Wynn and Coolidge 2012), but this may be a consequence of preservation and discovery.

In all of these regards, the contrast with *H. sapiens* is striking: having been in existence for approximately half of the temporal span of *H. neanderthalensis*, *H. sapiens* has undertaken continual cultural innovation, whether of new hunting and gathering technology during the Pleistocene or the invention of agriculture, towns, civilisations, science and so forth during the Holocene. While the latter developments are restricted to the last 11,600 years—during the relatively warm, wet and stable Holocene period—the Neanderthals also lived through similar environmental conditions (isotope stage 5e, c. 130–115,000 years ago) without making any fundamental changes in their behaviour.

Contrasts in demography are most likely to have played a key role in this dramatic contrast between *H. neanderthalensis* and *H. sapiens*—although there is no evidence to

suggest that *H. sapiens* were forced into farming lifestyles by population pressure, whether in the Levant, Mesoamerica or other areas of independent invention (Barker 2006; Mithen 2003). Nevertheless, the transmission of new ideas requires a demographic threshold to be passed if they are to be sustained. The apparent absence or at least interrupted nature of cultural innovation by *H. sapiens* prior to c. 50,000 years is likely to derive from low population densities (Powell et al. 2009). Similarly, step changes in localised population densities arising from the development of sedentary farming communities after 10,000 years ago and then from towns/cities after 5,000 years ago are likely to be integral to step changes in the rate of cultural innovation. If the *H. neanderthalensis* never passed the first of these demographic thresholds because of their life history parameters (Zubrow 1989; Trinkaus 1995), the lack of cultural change in the *H. neanderthalensis* archaeological record might be argued as being entirely unrelated to their cognitive capacities. This appears to be the position favoured by Zilhão et al. (2010).

The problem with this argument is that if the *H. neanderthalensis* had the same cognitive capacity as *H. sapiens* we ought to see the traces of un-sustained innovations, as we appear to see in the archaeological record of the earliest *H. sapiens* when at low population densities (Powell et al. 2009; e.g., the Howiesons Poort industry). This is especially the case because *H. neanderthalensis* appears to have been under considerable adaptive stress such that their communities teetered on survival (Trinkaus 1995): if ever there were human communities which needed to enhance their hunting technology, such as by inventing spear throwers or bows and arrows, or their protection from the cold, such as by sewn clothing and substantial dwellings, it was those of the *H. neanderthalensis*. The absence of any such evidence suggests a cognitive constraint on innovation irrespective of whether population densities were such that new ideas and technologies could then be sustained.

The contrast in the *H. neanderthalensis* and *H. sapiens* response to post/interglacial conditions is especially striking and, I would argue, cognitively informative. When communities of *H. sapiens* first encountered postglacial conditions at c. 11,600 years ago following their dispersal from Africa c. 50,000 years, they responded by inventing multiple forms of sedentism and agriculture in several different locations around the world without seeming to have been under pressure from food shortages (Mithen 2003; Barker 2006). This was a creative response to post/inter-glacial conditions. When *H. neanderthalensis* encountered inter-glacial conditions at 115,000 years ago, we have no trace of a similar response. Why didn't the *H. neanderthalensis* invent agriculture or at least engage in the creative manipulation of the natural world?

2.2.2 The Absence or Rarity of Visual Symbols

There is no unambiguous evidence for the creation of visual symbols by *H. neanderthalensis*—although numerous highly contentious artefacts have been put forward for such evidence. This absence is the case whether we use the term symbol in its precise sense of an image with a meaning entirely arbitrary to its appearance, or in its more general sense to include icons and indexes, the former having a visual similarity to their meaning (my photographs stands for me) and the latter having a functional association (smoke means fire). The first sense is the more important and synonymous with metaphor, widely regarded as not only being fundamental to the religious thought and art of modern humans but also to science.

We must, of course, be enormously cautious. Among modern-*day H. sapiens* anything and everything might be a symbol, including the most apparently mundane artefacts, entirely unmodified natural objects, such shells, and features of the landscape, such as hills and rivers. It might have been the same for the *H. neanderthalensis*. Moreover, in light of their hunting and gathering activity it would be most unlikely that *H. neanderthalensis* did not use icons and indexes of the natural world, notably the tracks and trails of the animals they were hunting. Interestingly, images of these are frequently found in hunter-gatherer rock art (McDonald and Veth 2012), including that of the Upper Palaeolithic (Mithen 1988), and play a role in plausible theories for the evolution of scientific thought (for which metaphor is essential) (Carruthers 2002). But we have no unambiguous evidence that the *H. neanderthalensis* were creating such images even if they were using those unintentionally present in the natural world.

Might the absence of visual symbols be a consequence of preservation (as argued by Bednarik 1994)? Maybe *H. neanderthalensis* symbols were entirely made in transient materials, such as ice sculptures, or organic materials that have since decayed. Restricting their symbolic behaviour to such materials seems intuitively unlikely. Moreover, as noted above, the *H. neanderthalensis* archaeological record is extensive in scope; it contains numerous sites with excellent bone preservation and a significant portion of this record has been analysed in meticulous detail. If the *H. neanderthalensis* were creating symbols surely some direct and unambiguous evidence would have been recovered, such as carved figurines, body ornaments or rock paintings?

Such evidence might exist in the form of the much disputed Châtelperronian "personal ornaments" recovered from Grotte du Renne at Arcy-sur-Cure—a series of pierced teeth and ivory pendants for which symbolic interpretation is not unreasonable. There has been a substantial debate as to whether or

not these artefacts had been made by *H. neanderthalensis*, and if so whether they were manufactured before *H. sapiens* had arrived in Europe, and hence represent an entirely innovative behaviour, or afterwards such that they may be a form imitation (d'Errico et al. 1998; Mellars 1999, 2004; Conard and Bolus 2003; Bar-Yosef and Bordes 2010).

This debate has primarily informed us about the enormous challenge of interpreting cave deposits excavated prior to modern methods of record keeping and analysis rather than throwing any conclusive light on these intriguing artefacts. Recently derived AMS dates suggest that the Grotte du Renne deposits are so heavily disturbed that the species affiliation of the pierced teeth and pendants is impossible to ascertain unless they can be directly dated themselves (HighamT et al. 2010; Mellars 2010)—although even this may be unable to resolve the issue. As such, the most reasonable interpretation is that the Châtelperronian ornaments were made by *H. sapiens* in light of the entire absence of similar material manufactured by *H. neanderthalensis* from elsewhere (with exception of the even more disputed evidence from Quinçay). Nevertheless, François Caron and his colleagues challenge the reliability of the dates and continue to argue that the site stratigraphy is sufficiently intact to attribute the ornaments to the *H. neanderthalensis* (Caron et al. 2011). Personally, I find their arguments unpersuasive.

Further examples of possible *H. neanderthalensis* personal ornaments have been described by Zilhão et al. (2010) in the form of three pierced marine shells from Cueva de los Aviones, Spain. By making a comparative study with modern day shell collections the authors argue that rather than having been drilled these shells had natural perforations. Nevertheless, they suggest that the *H. neanderthalensis* had selected them from the range of shells with natural perforations, choosing those with holes of an appropriate dimension for threading to create a pendant. I remain cautious that any selection had occurred in light of the small number of samples and further work required on the rates of hole weathering. It remains unclear whether the natural perforations occurred prior to or post-deposition, and even if the former what further expansions of the hole occurred following discard within the heavily disturbed cave deposit. Moreover, the excavation provides no evidence that the perforated shells had been used as pendants or indeed in any manner at all—perhaps they had been collected as collected a curios, as we know that *N.neanderthalensis* was occasionally prone to do. Although certainly intriguing, there is insufficient evidence at presence to be confident that the *H. neanderthalensis* at Cueva de los Aviones wore shell pendants.

2.2.3 Scratched Bones, Burials and Pigments

I have been careful to refer to "unambiguous" evidence for *H. neanderthalensis* symbolism because three much disputed categories of archaeological materials are regularly forwarded as evidence for symbolic behaviour. There are a number of stone and bone artefacts dating to the Lower and Middle Palaeolithic that have surface scratches claimed to have been made intentionally (e.g., Mania and Mania 1988; Bednarik 1995; Marshack 1997). These are unlikely to be visual symbols for two reasons. First, there are no recurrent images to suggest a symbolic code; indeed an extensive degree of over-interpretation is often required to infer any geometric pattern at all (Mithen 1996a). Second, if such marks derive from hominin activity, it is more reasonable to conclude that they are the unintentional by-products of tasks such as chopping plant material or cutting meat. This is also the most plausible interpretation of the cut marks on the talon of a golden eagle from Combe Grenal (c. 90 kya) and on two talons of white-tailed eagle from Les Fieux (c. 50–40 kya) as described by Morin and Laroulandie (2012). Their interpretation of these as derivative of symbolic behaviour, suggesting "complex cognitive abilities similar to those of coeval EMH" (early modern humans) (Morin and Laroulandie 2012) is unwarranted unless utilitarian explanations can be confidently dismissed.

Neanderthal burials have also been cited as evidence for symbolic behaviour (Chase and Dibble 1987). To do so requires that two challenges are overcome. First that deliberate burial does indeed exist, this having been disputed by Gargett (1989, 1999). The weight of evidence suggests that some *H. neanderthalensis* bodies were most likely positioned within shallow depressions or in crevices in a manner that can be reasonably described as burial. The second challenge is to precisely identify what is symbolic about making such burials. Evidence for graveside ritual is absent, and—as I will further argue below—burial itself does not necessarily imply symbolic thought. With the type of close social bonds attributable to *H. neanderthalensis* and evidence for care of the sick and old such as from Shanidar Cave (Trinkaus 1983), we should expect that the dead would be mourned and corpses treated with respect. Indeed, it is surprising that the evidence for *H. neanderthalensis* burial is not considerably more extensive. But there is nothing unambiguously symbolic in that which exists.

The potential use of pigments by *H. neanderthalensis* is a third body of evidence that has been used to argue for symbolic thought and behaviour. Because this is relatively more recent and less discussed type of evidence than the scratched artefacts and burials, I will address pigment use below.

Finally, we should note that symbolic communication plays a key role in the adaptation of *H. sapiens* to challenging environments. This is exemplified in the abundance of art objects and implied ritual behaviour at the last glacial maximum in Europe (Jochim 1983). As such, and in light of the environmental stress that the *H. neanderthalensis* appear to have experienced, it is again surprising that they did not use symbolic communication more prolifically than would appear to have been the case even if all of the ambiguous

evidence for symbolism was found acceptable. The only reasonable conclusion is that *H. neanderthalensis* lacked the capacity for symbolic thought.

2.2.4 Rapid Replacement

A third reason to argue for significant cognitive differences between *H. sapiens* and *H. neanderthalensis* is simply the fact that *H. sapiens* is extant while *H. neanderthalensis* are extinct—not only the Neanderthals but all other members of the *Homo* genus that ever existed. The dispersal of *H. sapiens* from Africa at c. 50,000 years ago and their rapid colonisation of the Old and New Worlds is such a remarkable event that some overriding explanation is required: what could be so fundamentally different about this particular member of *Homo* that led to such a radically different pattern of behaviour to that of all its relatives and ancestors?

With regard to the replacement of *H. neanderthalensis* in Europe there may have been around 5,000 years of overlap. As several authors have remarked, *H. neanderthalensis* had evolved in Europe with physiological adaptations to northern hemisphere environments (Stringer and Gamble 1993). To have been so quickly replaced by an African-adapted *H. sapiens* population suggests the latter must have had some competitive advantage that over-rode that which the physiology of the *H. neanderthalensis* would have provided. Few, if any, suggestions have been forthcoming other than an enhanced cognitive capability, perhaps situated in language.

In light of the extensive mobility patterns of hunter-gatherers, both the *H. neanderthalensis* and *H. sapiens* must have been aware of each other's presence in Europe. Indeed, recent genetic evidence suggests some degree of interbreeding (Stringer 2011). When the possibility remained that the Châtelperronian pierced teeth and pendants may have been manufactured by *H. neanderthalensis*, imitation of those being made and worn by *H. sapiens* was a feasible interpretation. Even if that had remained viable, the lack of imitation or adoption of *H. sapiens* material culture by *H. neanderthalensis* during this period of overlap is striking. The strong technological traditions of the Neanderthals suggest that various forms of social learning were employed, including imitation and emulation (as with earlier hominins, e.g., Mithen 1994). Intuitively we might have expected such social learning to have led to a substantial adoption of the technology and material culture of *H. sapiens* by the *H. neanderthalensis* during the period of overlap, just as we have seen throughout human prehistory and history when indigenous people have been colonised, and ultimately replaced, by immigrant people. Even if the Châtelperronian artefacts were the result of such imitation, the extent of this is surprisingly low suggesting there was a cognitive constraint in the application of social learning processes to novel circumstances. More generally, there appears to have been limited response, if any, by the *H. neanderthalensis* to the arrival of *H. sapiens* in Europe. This is strikingly different to the response of the indigenous Mesolithic hunter-gatherers when Neolithic farmers spread into Europe (Mithen 2003).

2.3 Models for *H. neanderthalensis* Mind and Language

2.3.1 Domain-Specific and Cognitive Fluid Mentalities

It was an attempt to resolve the apparent contradictions between the fossil record with its evidence for large brains and evolved vocal tracts and the archaeological record with its ambiguous evidence for symbolism, cultural homogeneity and rapid replacement that I introduced notions of mental modularity into the 1990s discussions about *H. neanderthalensis* and *H. sapiens* cognition. This also sought to bring discussions of cognitive evolution by archaeologists into line with those currently underway in related disciplines such as evolutionary psychology and neuroscience, with those disciplines themselves suffering from the absence of an archaeological perspective. In my 1996 book *The Prehistory of the Mind*, I argued that Neanderthals had a domain-specific mentality while *H. sapiens* possessed the capability for cognitive fluidity, the latter largely deriving from the use of spoken compositional language and providing the capacity for metaphorical thought, and hence science as well as art and religion (Mithen 1996b).

By domain-specific mentality I meant that the Neanderthals had bodies of knowledge and types of thought processes equivalent to those of modern humans in the domains of social, technical and natural history intelligence, but lacked the capability to integrate these to come up novel ideas. This was heavily influenced by arguments within evolutionary psychology that stressed mental modularity (e.g., Fodor 1983; Hirschfeld and Gelman 1994) and/or multiple intelligences (e.g., Gardner 1993), although these did not appear to appreciate the extent of cross-modal thinking by modern humans.

Cognitive capabilities within each domain explain the complexity of *H. neanderthalensis* technology, the sophistication of their hunting and gathering behaviour and the inferred intricacy of their social lives (Mithen 1996b). As Dunbar (1993, 1996) has argued, social life with its attendant cognitive challenges may be the primary explanation for the relatively large brains of both *H. neanderthalensis* and *H. sapiens*.

Cognitively fluidity lay at the essence of those behaviours at which *H. sapiens* excelled—and still do—but which appear rare or entirely absent among the *H. neanderthalensis* (Mithen 1996b). Symbolic thought, for instance, involves creating arbitrary associations between entities that reside in different

cognitive domains, although the use of icons and indexes could be domain specific and within the *H. neanderthalensis* capability. Complex hunting technology—manufacturing tools dedicated to hunting particular types of animals in particular circumstances—requires combining knowledge about animals and technology into a single thought. Similarly, developing the types of relationships with animals and plants that led to domestication and agriculture had required a "social" interaction with the natural world, caring for seedlings or juvenile animals as one does for children (Mithen 1996b, 2007). Without such cognitive fluidity, the *H. neanderthalensis* could never develop such relationships and initiate a process of domestication.

H. neanderthalensis did, of course, achieve some degree of cognitive integration between its domains—tools had to be used for hunting and food sharing was used to mediate social relations. *The Prehistory of the Mind* suggested that the *H. neanderthalensis* degree of integration was achieved by generalised intelligence, this being insufficiently powerful, however to create cognitive fluidity. This reminds us that superficially similar mental processes can be achieved by quire different cognitive/neural mechanisms. For instance my own second language speaking ability, acquired as an adult, is most likely undertaken by quite different neural networks in my brain than is the second language speaking of someone who grew up to be bi-lingual. Similarly, those who suffer from autism may learn to interact socially by using cognitive processes other than those of empathy (theory of mind) on which the majority of us rely.

The Prehistory of the Mind provided no suggestion for how either domain-specific thought or cognitive fluidity were actually constituted within the brain, other than proposing that compositional language might play a role. There was no suggestion that a particular cognitive domain would map onto a particular part of the brain.

Wynn and Coolidge (2004) argued that the Neanderthals had a limited degree of working memory that constrained their ability at maintaining multiple ideas in their mind at the same time—which is in effect another description of an absence of cognitive fluidity. In their later work they acknowledged that their limited working memory model for the *H. neanderthalensis* provided the mechanism for the domain-specific thought that I had proposed, and that an extension of working memory enables cognitive fluidity (Wynn and Coolidge 2012).

While I am sympathetic to their extended working memory hypothesis as a means to achieve cognitive fluidity, I suspect that multiple processes are in play with regard to the modern human mind. One of these is the use of material culture itself to provide a scaffold for articulating and discussing complex, cross-domain ideas such as notions about supernatural beings. As I have suggested elsewhere (Mithen 1998), while cognitive fluidity enables ideas about such beings to be entertained, they remain intuitively difficult to sustain and to communicate to others. One means of resolving this problem is by the use of visual images—figurines and paintings—as a support to cognitive fluidity. The fact that *H. neanderthalensis* did not do so, suggests to me that this species lacked the ability to come up with such ideas.

2.3.2 Hmmmmm and Compositional Language

Wynn and Coolidge (2012) remained unspecific about Neanderthal language. My own view in *The Prehistory of the Mind* was that *H. neanderthalensis* lacked compositional language—this involving a large lexicon and set of grammatical rules from which an infinite set of novel utterances could be made. How could it be otherwise when spoken language is the motor for cultural innovation by easing cognitive fluidity? That left unresolved, however, how Neanderthals communicated especially in light of their effectively modern vocal tracts and large brains. Those anatomical features suggest that the rather minimalist "proto-language" capabilities as proposed by Bickerton (1990, 1995) must be a serious under-estimation of the *H. neanderthalensis* vocal capabilities. To address this my 2005 book, *The Singing Neanderthals*, proposed that a sophisticated communication system had been present, one with a greater reliance in variations in tone, rhythm and pitch and a less reliance on words and grammar than does compositional language as used by *Homo sapiens* today (and presumably in the past; Mithen 2005).

The Singing Neanderthals proposed that *H. neanderthalensis* language holistic, multi-modal, mimetic and musical (the Hmmmm model). This model also sought to bring archaeological studies into greater alignment with those in the cognitive sciences by drawing on recent studies in neuroscience, psychology and linguistics (e.g., Wray 1998; Wallin et al. 2000; Cross 2001). It also served to place greater emphasis on the socially complex and emotionally driven character of Neanderthal life than had been present in previous studies. Communal dancing and singing were placed at the centre of *H. neanderthalensis* social life, these acting to build trust between individuals who would engage in dangerous pursuits (e.g., big mammal hunting) and to negotiate social relationships, partly via the expression and manipulation of emotional states.

2.4 The Use of Pigments

The domain-specific model for the *H. neanderthalensis* mind can be easily falsified such as by the discovery of an unambiguous figurine in a secure context such that it could have only been manufactured by an *H. neanderthalensis*.

Does the increasing evidence for the use of pigments by *H. neanderthalensis,* all of which has been published since the domain-specific model was proposed, provide an equivalent degree of falsification?

This evidence is of considerable interest, although requires further analysis before its full implications can be confidently understood. Soressi and d'Errico (2007) describe more than 70 horizons dating to the Lower and Middle Palaeolithic in Europe from which blocks of pigment or objects that had served to grind colorants have been recovered. They describe 250 nodules of soft stone from Middle Palaeolithic levels at Pech I and 20 from Pech IV showing signs of pigment use. The pigment was predominantly black, deriving from manganese oxide. Although the species affiliation is more difficult to assess, several concave fragments of stalagmite from Middle Palaeolithic contexts of Cioarei-Borosteni Cave, Romania, appear to contain residues from ochre (Carciumaru et al. 2002). Most recently, Zilhão et al. (2010) have described blocks of pigment, pigment-stained marine shells and a horse metatarsal coming from Middle Palaeolithic contexts at Cueva de los Aviones and Cueva Antón, Spain, which they confidently attribute to *H. neanderthalensis*.

Does this evidence indicate symbolic thought? I suspect not, although it certainly adds to the view that *H. neanderthalensis* engaged in complex, emotionally driven social behaviour. Precisely the same applies to the use of pigment by *H. sapiens* when there is no additional evidence for symbolism, such as at Pinnacle Point, South Africa at c. 164 thousand years ago. As such, entirely equal standards of interpretation are being applied to the *H. neanderthalensis* and *H. sapiens* archaeological records: rather than attributing symbolic behaviour to the former we should become more restrictive about its attribution to the latter.

The most striking example of over-interpretation of *H. neanderthalensis* pigment use comes from the 2010 paper by Zilhão and his colleagues entitled "Symbolic use of marine shells and marine pigments by Iberian Neanderthals." Here they describe evidence for pigments having been applied to a bone and shells at Cueva de los Aviones and Cueva Antón , or possibly the use of these artefacts as a tool and palette for mixing pigments. The scientific analysis remains contentious in some aspects, such as the inability to detect the chemical nature of the observed orange pigment on the tip of the horse metatarsal and hence validate that observation as deliberately applied pigment rather than the consequence of a post-depositional process. But let us assume that the identification of pigment use at both sites has been adequately established.

There is no evidence for how the pigments were then further used but the authors appear to favour body painting which appears quite reasonable. Zilhão and his colleagues argue that the pigment use from Cuevas de los Aviones and Antón provide "secure evidence that, approximately 50 ka cal B.P., 10 millennia before modern humans are first recorded in Europe, the behaviour of Neanderthals was symbolically organised and continues to be so until the very end of their evolutionary trajectory" (Zilhão et al. 2010). There is not one but three non-sequiteurs in this statement. The first is that one can generalise from the evidence from two cave sites in Iberia to *H. neanderthalensis* as a whole; the second is that pigment use necessarily implies symbolic thought; the third is that if symbolic thought is granted then symbolism had been used to "organise" behaviour—whatever that might mean.

It is the second of these three unwarranted inferences that is most serious and one which regrettably pervades so much literature about the *H. neanderthalensis*. Why should the use of pigment imply symbolism? Modern humans, today and in the past, use pigment in all manner of ways which is non-symbolic. For instance, we use colour to attract attention, and to express and arouse emotions in others. In this regard we are no different to a great many other species in the animal world.

Here we can do no better than refer to the seminal 1976 essay by Nicholas Humphrey entitled "the colour currency of nature" (Humphrey 1984). As he explains, the ability to see colour can only have evolved because it contributes towards biological survival. Humphrey uses the term "organic colours," to refer to those carried by the tissues of plants and animals and explains that these have only evolved to be seen because of the messages they send—"come here" as in a flower attracting a pollinating insect or "keep away" as in the colour of a poisonous toadstool to deter a potential consumer. As Humphrey describes, the message may sometimes be more complex as when the colour is used in a social context such as courtship or an aggressive encounter—a peacock displaying his fan or a monkey flashing his genitals. In summary:

> whatever the level of the message, signal colours commonly have three functions: they catch attention, they transmit information, and they directly affect the emotions of the viewer – an orange arouses appetite in a monkey, a yellow wasp fear in a fly-catcher, the red lips of a young woman passion in a man (Humphrey 1984).

2.4.1 Non-Symbolic Colour Use and Ritual

Even though wasps, peacocks, monkeys and fly-catchers make extensive use of colour we do not describe their behaviour as being organised in a symbolic manner. Why should it be necessarily any different for *Homo*—whether *sapiens, neanderthalensis* or otherwise? With regard to modern-day humans, our use of cosmetics need not be symbolic: red lipstick draws attention to the lips as does mascara to the eyes. These pigments are used to exaggerate what are thought to

be visually attractive parts of the anatomy and can be characterised as a sexual display. But they need not have any symbolic meaning at all in the sense of standing for something entirely different. This is not to deny that symbolic meanings can be attached to cosmetics or other forms of pigment use—but there is no necessity for these to be present.

Colour in a great deal of "art" plays exactly the same non-symbolic but emotionally-stimulating role. At the extreme we have the paintings of Mark Rothko. These are held in high regard as "works of art" but they lack any symbolic meaning: Rothko painted them to express the big emotions—tragedy, ecstasy, and doom—and appears to have been highly successful in doing so. This art is non-symbolic but emotionally potent. In this regard I would not be surprised if *H. neanderthalensis* did indeed paint on their bodies or even the walls of caves in which they may have been undertaken social activities as a means to manipulate the emotional responses of those involved. The Neanderthals may even have worn shell beads or other natural objects to draw attention to themselves. I envisage this as certainly being within the cognitive capacity of their generalised intelligence but having no implications for symbolic thought.

We have no evidence for cave painting by *H. neanderthalensis*. It is most unfortunate that the public headlines of what appears to be an outstanding piece of archaeological science, the uranium-series dating of calcite deposits underlying or overlying painting in 11 Spanish caves (Pike et al. 2012) became fixated on the possibility that the earliest of these paintings could have been made by *H. neanderthalensis*. By producing a minimum date of 40.8 Ka for a red disk on the wall of El Castillo this is indeed by a possibility—but one which is highly remote. The immense stylistic continuity of the art throughout the Upper Palaeolithic and the match of this date with the arrival of *H. sapiens* in the region at 4.15Ka suggest that the El Castillo disk and all cave art was the product of *H. sapiens*.

We should acknowledge that much of Upper Palaeolithic art and its associated rituals may have lacked explicit symbolic intent, having been produced to manipulate the emotions of the artists themselves and whoever watched them work and looked at the outcomes. Such rituals would fall within what the cognitive social anthropologist Harvey Whitehouse has described as the "imagistic mode of religiosity," in contrast to the "doctrinal" mode (Whitehouse 2004). The latter refers to rituals within societies with centralised institutions, religious leaders and—by definition—fixed doctrines of religious belief. Such rituals are frequently and meticulously performed according to set rules, having explicit symbolic meanings relating to the religious ideology of the group.

The imagistic mode of religiosity is typical of hunter-gatherer and small scale farming communities. While ritual activities of the imagistic mode can have symbolic meaning these are not essential to their performance. According to Whitehouse:

> rituals that are only rarely performed are also typically felt to be personally consequential, extraordinary, and emotionally arousing occasions. These features result in long-lasting episodic memories. But the memories are problematic. They specify at least some of the details of what happened in a particular ritual performance, but they do not specify the meanings of those happenings. Rituals are capable of being accorded a wide range of symbolic motivations, but people do not reflect extensively on matters of symbolism in the absence of very special inducements. Theologians and art critics (for example) engage in that kind of activity but only because they have undergone, routinized education into that particular mode of intellectual activity, backed up by complex systems of rewards and incentives. Where no such educational framework exists to support exegetical reflection, why should it happen at all? (Whitehouse 2004).

Whitehouse goes on to describe why the search for meaning might often occur, but the case is made that this is not essential for the ritual activities to be potent for both the individual and group: they function to mediate social relations, express and induce emotions and to instigate long-lasting episodic memories. This is the type of non-symbolic ritual behaviour that the socially complex "singing and dancing" Neanderthals could have undertaken, using artificially applied pigment to enhance their emotional impact. Likely occasions would be at various rites of passage—birth of a child, "marriage/formation of a pair-bond," death and burial—or significant events such as the kill of an especially large beast or the long waited thaw. Such colourful rituals may have involved icons and indexes but have been symbol-free. As such the discovery of pigment use or even shell pendants by either *H. neanderthalensis* or *H. sapiens* need not imply symbolic thought. This is especially the case for the former because of so many other elements of the *H. neanderthalensis* archaeological record that suggests the absence of symbolic thought and the presence of a domain-specific mentality.

2.5 Conclusion

Discussion and debate will continue around the nature of *H. neanderthalensis* cognition and its similarities and differences to that of *H. sapiens*. This will continue to be driven by new archaeological discoveries, novel analyses of existing materials and developments in the cognitive sciences as a whole. At the present time, the character of the archaeological record suggests there were profound difference between *H. neanderthalensis* and *H. sapiens* cognition. The domain-specific/cognitive fluid model remains as a feasible interpretation of this difference, while recent discoveries of pigment use have reinforced the views that the *H. neanderthalensis* engaged in emotionally-rich but non-symbolic social activities similar to those found in many *H. sapiens* communities.

References

Barker G (2006) The agricultural revolution in prehistory: why did foragers become farmers? Oxford University Press, Oxford

Bar-Yosef O, Bordes JG (2010) Who were the makers of the Châtelperronian culture? J Hum Evol 59:586–593. doi:10.1016/j.jhevol.2010.06.009

Bednarik RG (1994) A taphonomy of palaeoart. Antiquity 68:68–74

Bednarik RG (1995) Concept-mediated marking in the Lower Palaeolithic. Curr Anthropol 36:605–634

Bickerton D (1990) Language and species. University of Chicago Press, Chicago

Bickerton D (1995) Language and human behavior. University of Washington Press, Seattle, WA.

Carciumaru M, Moncel M-H, Anghelinu M, Carciumaru R (2002) The Cioarei-Borosteni Cave (Carpathian Mountains, Romania): Middle Palaeolithic finds and technological analysis of the lithic assemblages. Antiquity 76:681–690

Caron F, d'Errico F, del Moral P, Santos F, Zilhão J (2011) The reality of Neandertal symbolic behavior at the Grotte du Renne, Arcy sur-Cure, France. PLoS One 6:e21545

Carruthers P (2002) The roots of scientific reasoning: infancy, modularity and the art of tracking. In: Carruthers P, Stitich S, Siegal M (eds) The cognitive basis of science. Cambridge University Press, Cambridge, pp 73–97

Chase P (1986) The hunters of Combe Grenal: approaches to Middle Palaeolithic subsistence. British Archaeological Reports International Series, Oxford

Chase P, Dibble H (1987) Middle Palaeolithic symbolism: a review of current evidence and interpretations. J Anthropol Archaeol 6:263–293

Conard NJ, Bolus M (2003) Radiocarbon dating the appearance of modern humans and timing of cultural innovations in Europe: new results and new challenges. J Hum Evol 44:331–371

Cross I (2001) Music, mind and evolution. Psychol Music 29:95–102

d'Errico F, Zilhao J, Julien M, Baffier D, Pelegrin J (1998) Neanderthal acculturation in Western Europe? A critical review of the evidence and its interpretation. Curr Anthropol 39 (S1). doi: 10.1086/204689

Dibble HL, Rolland N (1992) On assemblage variability in the Middle Palaeolithic of western Europe: history, perspectives and a new interpretation. In: Dibble HL, Mellars P (eds) The Middle Palaeolithic: adaptation, behaviour and variability. The University Museum, University of Pennsylvania, Philadelphia, pp 1–28

Dunbar RIM (1993) Coevolution of neocortical size, group size and language in humans. Behav Brain Sci 16:681–735

Dunbar RIM (1996) Gossip, grooming and the evolution of language. Faber & Faber, London

Fodor J (1983) The modularity of mind. MIT, Cambridge

Gardner H (1993) Multiple Intelligences: the theory in practice. Basic Books, New York

Gargett RH (1989) Grave shortcomings: the evidence for Neanderthal burial. Curr Anthropol 30:157–190

Gargett RH (1999) Middle Palaeolithic burial is not a dead issue: the view from Qafzeh, Saint-Césaire, Kebara, Amud, and Dederiyeh. J Hum Evol 37:27–90

HighamT JR, Julien M, David F, Basell L, Wood R, Davies W, Bronk Ramsey C (2010) Chronology of the Grotte du Renne (France) and implications for the context of ornaments and human remains within the Chatelperronian. Proc Natl Acad Sci U S A 107:20234–20239

Hirschfeld LA, Gelman SA (eds) (1994) Mapping the mind: domain specificity in cognition and culture. Cambridge University Press, Cambridge

Humphrey N (1984) Consciousness regained: chapters in the development of mind. Oxford University Press, Oxford

Jochim M (1983) Palaeolithic art in ecological perspective. In: Bailey GN (ed) Hunter-gatherer economy in prehistory: a European perspective. Cambridge University Press, Cambridge, pp 212–219

Mania D, Mania U (1988) Deliberate engravings on bone artefacts of Homo Erectus. Rock Art Res 5:919–927, qtd in Scarre 2005

Marean C, Bar-Matthews M, Bernatchez J, Fisher E, Goldberg P, Herries AIR, Jacobs Z, Jeradino A, Karkanas P, Minichillio T, Nilssen P, Thompson E, Watts I, Williams HM (2007) Early human use of marine resources and pigment in South Africa during the Middle Pleistocene. Nature 449:905–909

Marshack A (1997) The Berekhat Ram figurine: a late Acheulian carving from the Middle East. Antiquity 71:327–337

McDonald J, Veth P (2012) A companion to rock art. Wiley, London

Mellars P (1996) The Neanderthal legacy. Princeton University Press, Princeton, New Jersey

Mellars P (1999) The Neanderthal problem continued. Curr Anthropol 40:341–350

Mellars P (2004) Neanderthals and the modern human colonization of Europe. Nature 432:461–465

Mellars P (2010) Neanderthal symbolism and ornament manufacture: the bursting of a bubble? Proc Natl Acad Sci U S A 107:20147–20148

Mithen SJ (1988) Looking and learning: Upper Palaeolithic art and information gathering. World Archaeol 19:119–137

Mithen SJ (1994) Technology and society during the Middle Pleistocene: hominid group size, social learning and industrial variability. Cam Archaeol J 3:3–36

Mithen SJ (1996a) Early Palaeolithic 'concept mediated' marks, mental modularity and the origins of art. Curr Anthropol 37:666–670

Mithen SJ (1996b) The prehistory of the mind: a search for the origins of art, science and religion. Thames & Hudson, London & New York

Mithen SJ (1998) The supernatural beings of prehistory: the external symbolic storage of religious ideas. In: Scarre C, Renfrew C (eds) Cognition and culture: the archaeology of symbolic storage. McDonald Institute, Cambridge, pp 97–106

Mithen SJ (2003) After the ice: a global human history, 20,000–5000 BC. Weidenfeld & Nicolson, London

Mithen SJ (2005) The singing Neanderthals: the origins of music, language, mind and body. Weidenfeld & Nicolson, London

Mithen SJ (2007) Did farming arise from a misapplication of social intelligence? Phil Trans R Soc B 362:705–718

Mithen SJ, Parsons L (2008) The brain as a cultural artefact. Cam Archaeol J 18:401–441

Morin E, Laroulandie V (2012) Presumed symbolic use of diurnal raptors by Neanderthals. PLoS One 7:e32856

Pike AWG, Hoffmann DL, García-Diez M, Pettitt PB, Alcolea J, De Balbín R, González-Sainz C, de las Heras C, Lasheras JA, Montes R, Zilhão J (2012) U-seies dating of Paleolithic art in 11 caves in Spain. Science 336:1409–1413

Powell A, Shennan S, Thomas M (2009) Late Pleistocene demography and the appearance of modern human behavior. Science 324:1298–1301. doi:10.1126/science.1170165

Rolland N, Dibble HL (1990) A new synthesis of Middle Palaeolithic variability. Am Antiquity 55:480–499

Soressi M, D'Errico F (2007) Pigments, gravures, parures: Les comportements symboliques controversés des Néandertaliens. In: Vandermeersch B, Maureille B (eds) Les Néandertaliens. Biologie et Cultures. Document Préhistoriques 23. Éditions du CTHS, Paris, pp 297–309

Stringer C (2011) The origin of our species. Allen Lane, London

Stringer C, Gamble C (1993) In search of the Neanderthals. Thames & Hudson, London

Trinkaus E (1983) The Shanidar Neandertals. Academic, New York

Trinkaus E, Shipman P (1994) The Neandertals. Vintage Books, New York

Trinkaus E (1995). Neanderthal mortality patterns. J. Arch Sci 22: 121–142

Wallin NL, Merker B, Brown S (eds) (2000) The origins of music. Massachusetts Institute of Technology, Cambridge

Whitehouse H (2004) Modes of religiosity: a cognitive theory of religious transmission. Altamira, Walnut Creek

Wray A (1998) Protolanguage as a holistic system for social interaction. Lang Commun 18:47–67

Wynn T, Coolidge FL (2004) The expert Neandertal mind. J Hum Evol 46:467–487

Wynn T, Coolidge FL (2012) How to think like a Neandertal. Oxford University Press, Oxford

Zilhão J, Angelucci DE, Badal-Garcia E, d'Errico F, Daniel F, Dayet L, Douka K, Higham TFG, Martinez-Sánchez J, Montes-Bernárdez R, Murcia-Mascarós S, Pérez-Sirvent R-G, Vanhaere M, Villaverde V, Wood R, Zapata J (2010) Symbolic use of marine shells and mineral pigments by Iberian Neandertals. Proc Natl Acad Sci U S A 107: 1023–1028

Zubrow E (1989) The demographic modeling of Neanderthal extinction. In: Mellars P, Stringer CB (eds) The human revolution: behavioural and biological perspectives on the origins of modern humans. Edinburgh University Press, Edinburgh, pp 212–231

Comparisons Between Individual, Imitative and Instructed Learning

3

Juko Ando

Abstract

Although the Neanderthals were social learners (i.e., learning by imitation) whereas modern humans are individual learner-focused, modern humans can be characterized as unique social learners who can learn from a teacher/model. However, we do not know the most effective method of learning: individual, imitative or instructed. Nor do we know the psychological characteristics of each respective style. In this study, we compared the efficiency and psychological characteristics of individual, imitative and instructed learning by asking 20 Japanese university students to disentangle a series of puzzles and then statistically analyzing each style for its effectiveness. We found that individual learning was the most efficient strategy when the number of successful trials completed in 10 min was used as a measure of learning efficiency. The motivation to teach was affected by the imitator's attentiveness towards a teacher while imitating, and their feelings of direct and indirect relationship to a teacher when being instructed. Feeling of the task's difficulty and having an ambitious/competitive attitude were predispositions for attentiveness towards a model. Although teaching is not always the most efficient strategy to transfer skills and knowledge, we discovered that those who had high ability and interest in others' behavior and who were not competitive would be in charge of teaching.

Keywords

Imitative learning • Individual differences of attitudes • Individual learning • Instructed learning • Learning efficiency • Modern humans • Neanderthals

3.1 Background and Purpose

One of the most important research questions on the differences of learning abilities between the Neanderthals and modern humans is how to clarify the differences between social learning and individual learning psychologically. It is evident that the Neanderthals transmitted their stone axe-making skills by means of social learning, probably via learning by imitation. The modern humans could perform creative individual learning as well as imitation. This creative individual learning found in the modern human is obviously different from the individual learning universally conducted by non-social animals.

An additional learning characteristic in the modern human is that they can perform instructed learning as a special style of learning specific to *modern humans* (Strauss 2005; Strauss and Ziv 2011; Csibra and Gergely 2009; Ando 2009, 2012). Although the Neanderthals might have had the ability to learn by teaching, it must have been quite primitive. On the other hand, the modern humans apparently use learning by teaching as a unique and universal method for transmitting skills and knowledge to others.

Imitative learning is a kind of social learning in the sense that learning occurs in a social situation in which models to be imitated exist. However, imitative learning is also a kind of

J. Ando (✉)
Department of Humanities and Social Sciences, Faculty of Letters, Keio University, 2-15-45 Mita, Minato-ku, Tokyo 108-8345, Japan
e-mail: juko@msa.biglobe.ne.jp

T. Akazawa et al. (eds.), *Dynamics of Learning in Neanderthals and Modern Humans Volume 2: Cognitive and Physical Perspectives*, Replacement of Neanderthals by Modern Humans Series, DOI 10.1007/978-4-431-54553-8_3, © Springer Japan 2014

individual learning in contrast with instructed learning. This is because imitative learning occurs individually without another's social support during the learning process, but rather depends the learner's subjective understanding of how to reproduce the model's skills and regulate his or her own learning processes. On the other hand, instructed learning occurs in socially interactive situation in which there exists a person who controls their behavior in a costly and altruistic manner in order to facilitate the learning of other people (the learners).

Instructed learning is an evolutionarily unique way of learning. According to the operational definition of animal teaching (Caro and Hauser 1992). instructed learning can be defined as follows:

a. An individual, "A," modifies its behaviour only in the presence of a naïve observer, "B."
b. "A" incurs some cost, or derives no immediate benefit.
c. As a result of "A"'s behaviour, "B" acquires knowledge or skills more rapidly or efficiently than it would otherwise, or that it would not have learned at all.

That is, teachers change their behavior, without any immediate benefits for teachers, to let novices acquire novel survival skills and knowledge.

Additionally, in the modern human, both teachers and learners usually use the "Theory of Mind (ToM)" to infer mental states such as the intentions and knowledge of others. This kind of instructed learning must not have occurred in the Neanderthals, even if they could have had a kind of "natural pedagogy" (Csibra and Gergely 2009).

Instructed learning could take an important role in evolution in two ways: accurate transfer and reification of invisible knowledge. In imitative learning, a learner has to infer relevant knowledge while observing a model's behavior, and sometimes acquires irrelevant knowledge or inefficient skills. However, in instructive learning, a teacher explicitly verbally explains or visually illustrates the knowledge and procedures to be transmitted to naïve learners, which (usually) leads to accurate transmission of knowledge. Furthermore, verbal explanation and visual illustration facilitate reification of invisible knowledge (i.e., making invisible knowledge visible and understandable) to be transferred intentionally and objectively. This "reification" has the function of the "ratchet" effect (Tomasello 1999) which urges innovation of knowledge.

If instructed learning is so adaptive, it raises of the question of why the Neanderthals or other species did not acquire this type of learning. Thornton and Raihani (2008) report that there are only three species (meerkats, tandem running ants, and pied babblers) verified up to now that meet the operational definitions of teaching by Caro and Hauser (1992).

All these ways of teaching are limited to a single specific domain; eating (foraging or feeding). Even chimpanzees, the genetically closest species to modern humans, cannot conduct teaching (Matsuzawa 2011). Unlike the chimpanzee and maybe even the Neanderthal, the teaching of the modern human can be applied to a wide range of knowledge domains by means of cultural innovation and heritage. One of the possible answers for the absence of a "general instructive learning strategy" in other species is that imitative learning is sufficient or effective enough for them to survive in their niches. So then, one might ask what the advantage of imitative learning over instructed learning is. Another important question to investigate is the advantage of individual learning versus imitative and instructed learning.

In our current preliminary study, therefore, we compared three different styles of learning—individual, imitative and instructed—to clarify the nature of learning in the modern human. We compared how efficient each style was, and how motivations to imitate or to be imitated and to teach or to be taught were regulated. The efficiency and psychological attitudes of different learning styles vary depending on characteristics and difficulties of tasks. Individual learning might be most effective and preferred if a task is easy enough, whereas imitative learning might be better if a task is complex and visible. It is important to choose an appropriate task to be compared for the current research question. In this study, disentangled puzzles with a medium level of difficulty were chosen as an experimental task, because they were not so easy to solve for most participants while appropriately complex enough to perform with visual demonstration and verbal explanations.

3.2 Methods

3.2.1 Participants

Twenty university students (12 females, 8 males); mean age = 20.8 years (SD = 0.77) participated in the current experiment.

3.2.2 Materials

Three sets of disentangled puzzles were asked to be solved: Puzzle 1 (Key), 2 (Horse), and 3 (Disk) (Fig. 3.1).

3.2.3 Procedure

There were three phases: individual, imitative, and instructed learning.

i. Individual learning: participants solved the first puzzle (a target puzzle) alone without any assistance from others.
ii. Imitative learning: participants solved the second puzzle. When solving the second puzzle, the learner was permitted to observe and imitate a model (who had learned the target puzzle in Phase (i)) solving the target puzzle.
iii. Instructed learning: participants solved the third puzzle. When solving the third puzzle, a teacher (who had learned the target puzzle in Phase (i)) was permitted to

Fig. 3.1 Disentangled puzzles as experimental tasks

teach and a learner was permitted to ask the teacher to teach how to solve a puzzle.

The participants made teams of three people and each participant in the teams solved a different puzzle in each phase (Fig. 3.2). The trial was deemed successful when participants could disentangle two pieces of the puzzle and put them together again. The number of successful trials completed in 10 min was a measure of learning efficiency (a behavioral measure).

After each phase, participants were asked to answer psychological questions about their attitudes and feelings while they completed each task phase. The question items (psychological measures) and their factored analytic results are given in the left column of Table 3.1.

3.3 Results

3.3.1 Behavioral Measure

The frequency of success in each phase for the three puzzle tasks is shown in Fig. 3.3. Although no significant differences were found for these frequencies of each material, individual learning tended to be the most efficient of the three learning styles.

3.3.2 Psychological Measurements

Table 3.1 shows factor loading patterns of psychological items in three experimental phases. In Phase (i), three factors were extracted. They were learners' feelings of the task's easiness (*easiness*), learners' sense of *involvement* and challenge when completing the task (*challenge*). In Phase (ii), two factors were extracted. They were feelings of *attention* to one's partner and *competition* as a model and learner (imitator). In Phase (iii), only one factor—*teaching* motivation—was extracted as an instructor, and two factors were extracted as a learner; the learners' feelings of *direct* and *indirect relations* with an instructor.

Table 3.2 shows the correlation matrix among the factored scores shown above and the bolded, asterisked figures indicate significant relationships between factors. Participants who felt confident tended to pay more attention to imitators ($r=0.55$). Participants who felt more competitive while imitating tended to feel more competitive while being imitated ($r=0.76$) and less competitive when being directly taught. ($r=-0.72$). Those who were competitive as a model reported less relating feeling feelings when they were taught directly ($r=-0.70$).

Path analysis where motivation to teach is put as the final dependent variable was conducted to depict the causal relationship among these psychological attitudes and feelings. Figure 3.4 indicates only statistically significant ($p<0.05$) paths and correlation. Direct predictors of the dependent variable were an attentive attitude while teaching as an instructor, and direct and indirect attitudes while being taught as a student. Feeling that a task was challenging and feeling competitive as an imitator were both negatively related to attention toward an imitator as a model which lead to (lesser) motivation to teach. Feeling confident while solving a task in the individual learning phase lead to an attentive attitude towards an imitator while being observed, which in turn lead to motivation to teach.

3.4 Discussion

According to the behavioral results, imitative and instructed learning conditions were more time consuming than individual learning to solve these tasks. Individual learning tended to be the most efficient among three learning styles. Instructed learning is not an efficient way for this kind of task as far as efficiency is evaluated by time for the first trial, although it would be possible that imitative and instructed learning have some beneficial effects on learning over a long-term period or for other types of tasks.

In the first phase of learning, it took time for the learners to observe the models' behavior and to understand the instructors' explanation and demonstration. If the instructors' demonstration and explanation are poor, difficult, or inappropriate for learners, imitative and instructed learning might not be selected as a good strategy. Also, competitive people were not motivated to be taught. The task chosen in the current study (solving disentangled puzzles) might be more appropriate for individual learning than imitative and instructed learning because its final goal is easy to understand and some participants could enjoy trying out different

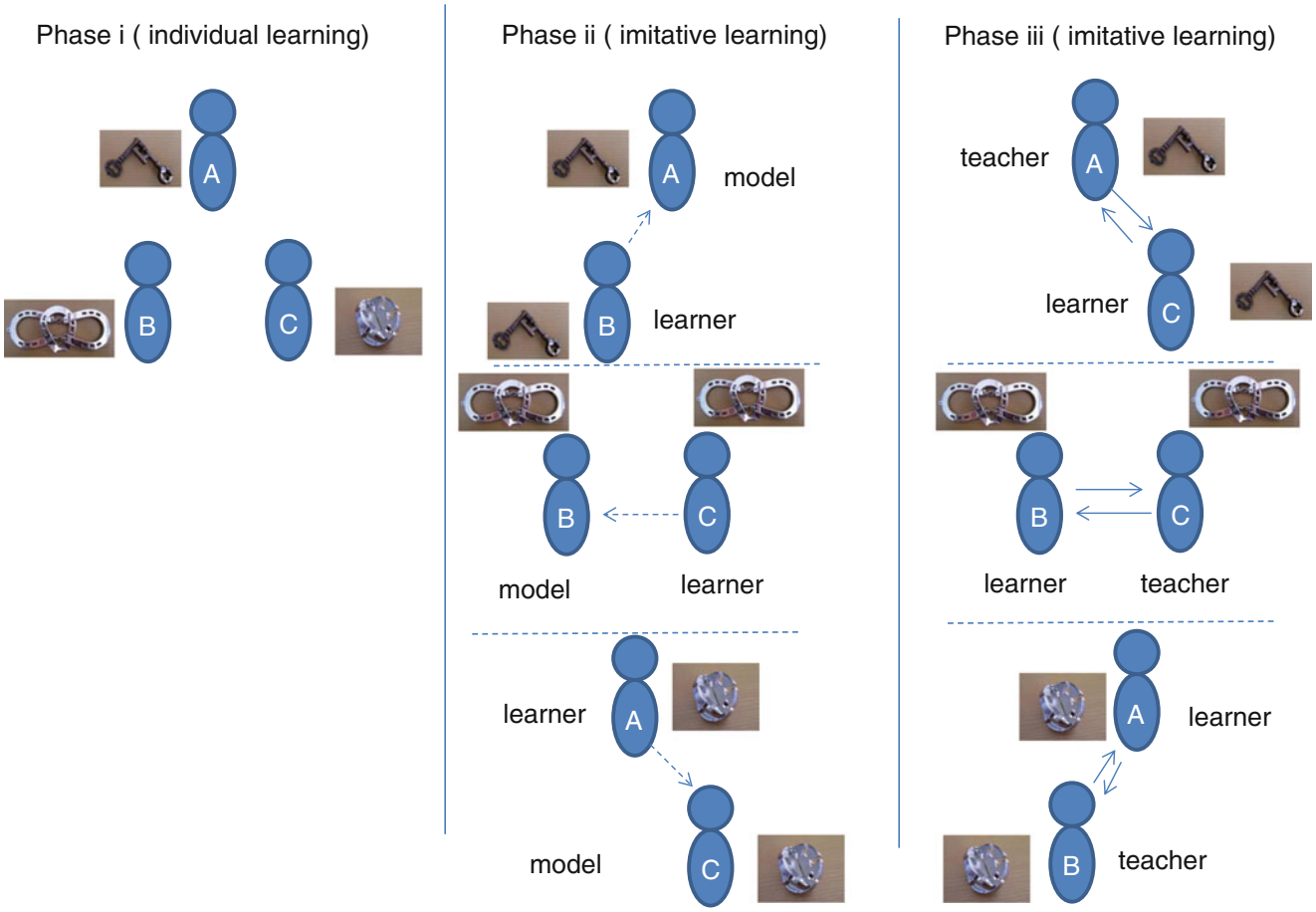

Fig. 3.2 Procedures of the experiment (10 min). Phase (i): each participant solves the first disentangle puzzle as a target task for him/herself individually. Phase (ii): each participant (a learner) solves the second puzzle while his/her partner as a model is individually solving the target puzzle. A learner is permitted to observe a model's behavior, but a model is not permitted to teach (not only verbally but also even with eye contact) a learner how to solve the target puzzle (10 min for each participant). Phase (iii): each participant solves the third puzzle while his/her partner as a teacher (different from the person paired in Phase ii) is individually solving the target puzzle. A teacher can teach the way of solving a target task and a learner can ask any assistance from a teacher

solutions for a single task by themselves to find the most effective way to solve rather than imitating and being taught by another person's behavior. Therefore, in future studies, measurement methodology (e.g., measuring not only the time it takes to solve the task but also the retention or application of solving strategies) and task choice (e.g., using more difficult tasks) should be considered carefully when testing the efficiency of these learning styles.

The participants showed individual differences in the process of becoming interested in teaching. According to the psychological analysis of attitude and feeling during each type of learning, attention towards a model, and feelings of direct and indirect relationship to a teacher are relevant predispositions to motivate a person to teach others. One's feeling of the task's difficulty (high or low), and having a challenging/competitive attitude are indirect predispositions. To return to the question of teaching in the Neanderthals and modern humans, it could be imagined that not all individuals taught others how to make hand axes. Presumably, those who had high ability and interest in others' behavior and who were not competitive would be in charge of teaching. It does not mean that a person who is motivated to teach is a "good" teacher. Even the modern humans who probably possess a potential ability to teach universally show a wide variety of individual difference in teaching ability. The current study indicates possible psychological conditions in which teaching behavior emerges; having high ability to perform a task, high interest in others and being uncompetitive (probably altruistic). In order to verify this kind of hypothesis, it will be informative to conduct observational studies of modern hunter-gatherers in traditional African villages.

Table 3.1 Items of psychological measurement (attitudes and feelings during learning) and their factor loadings by factor analysis (The bolded figures are loadings over 0.30)

Individual learning	Easiness	Involvement	Challenge
Felt easy	**0.925**	0.034	–0.042
Felt difficult	**–0.814**	–0.149	**0.316**
Wanted to challenge more difficult tasks	**0.692**	–0.057	**0.339**
Felt joy	0.241	**0.764**	0.121
Wanted to quit	**–0.357**	**–0.738**	0.172
Got involved	–0.217	**0.680**	0.180
Thought about other things	**0.332**	**–0.651**	**–0.438**
Wanted to solve puzzles more smoothly	0.019	0.172	**0.851**
Imitative learning	Attention	Compete	
As a model			
Felt involved	**–0.881**	0.190	
Looked carefully at imitator	**0.856**	0.185	
Felt uneasy about imitator's behavior	**0.848**	0.165	
Tried to imitate imitator's method	**0.532**	**0.492**	
Tried to compete with imitator	–0.159	**0.849**	
Worried about imitator watching	**0.444**	**0.548**	
As an imitator			
Tried to imitate model's method	**0.950**	0.162	
Looked carefully at model	**0.930**	0.052	
Felt uneasy about model's behavior	**0.879**	0.109	
Involved myself	**–0.814**	**0.346**	
Tried to compete with model	–0.205	**0.805**	
Worried about model watching	**0.370**	**0.715**	
Instructed learning	Teaching		
As an instructor			
Had strong motivation to teach	**0.888**		
Could understand how partner felt being taught	**0.828**		
Wanted to let a partner do his/herself	**–0.655**		
Felt it was interesting to teach	**0.567**		
Teaching was annoying	**–0.492**		
As a student	Direct relation	Indirect relation	
Thought instructor was good at teaching	**0.822**	0.156	
Wanted to get a hint from instructor	**0.772**	0.021	
Could understand instructor's motivation to teach	–0.297	**0.880**	
Being taught was annoying	**–0.367**	**–0.665**	
Wanted to be taught step by step	**0.329**	**0.497**	

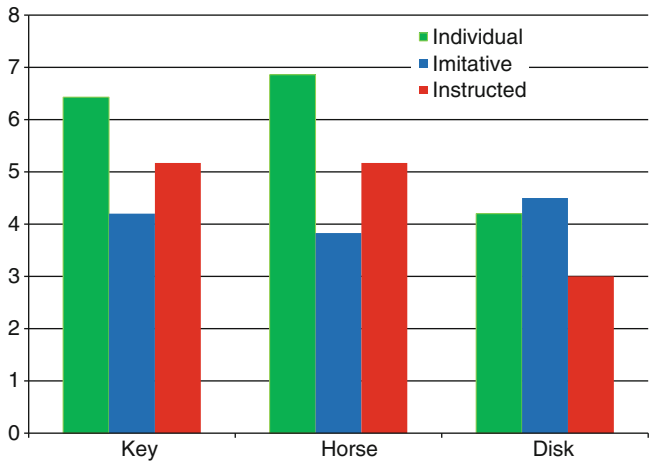

Fig. 3.3 The number of successes in the first 10-min trial

Table 3.2 Correlations among the psychological factors of attitudes and feelings during learning

		Individual			Imitative				Instructed		
					As a model		As an imitator		As an instructor	As a learner	
		Easiness	Involvement	Challenge	Attention	Compete	Attention	Compete	Teaching	Direct relation	Indirect relation
Easiness		1									
Involvement		0.013	1								
Challenge		−0.029	0.049	1							
Attention	As a model	**0.547***	0.153	−0.284	1						
Compete		0.312	0.104	0.436	0	1					
Attention	As an imitator	−0.113	−0.153	0.192	0.202	−0.089	1				
Compete		0.153	−0.002	0.429	0.143	**0.755****	0	1			
Teaching	As an instructor	0.328	−0.064	−0.013	0.319	−0.008	0.340	0.146	1		
Direct relation	As a learner	−0.303	−0.055	−0.221	−0.344	**−0.704****	0.360	**−0.718****	0.233	1	
Indirect relation		−0.165	−0.123	0.093	−0.144	0.072	0.427	0.087	0.333	0.000	1

*$p<0.05$; **$p<0.01$

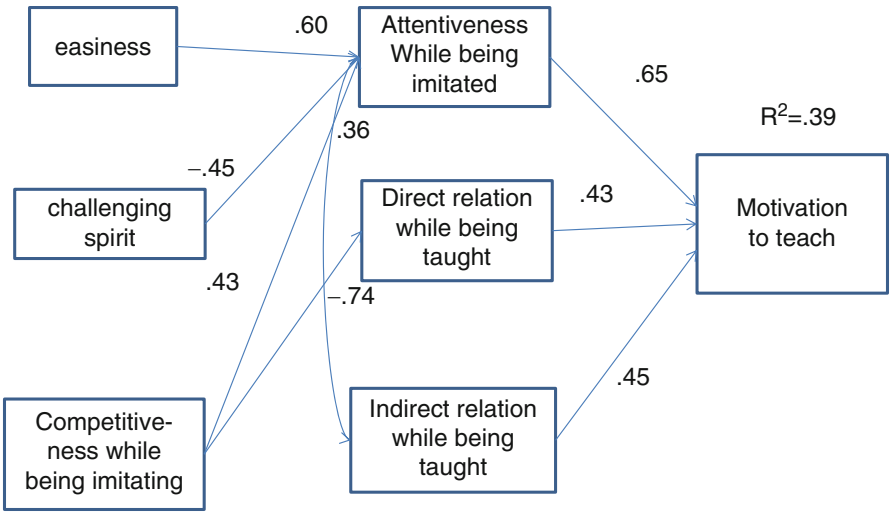

Fig. 3.4 Path analysis of psychological factors of attitudes and feelings of learning

References

Ando J (2009) Evolutionary and genetic bases of education: an adaptive perspective. Annu Rep Educ Psychol Jpn 48:235–246

Ando J (2012) On "Homo educans" hypothesis. In: Watanabe S (ed) CARLS series of advanced study of logic and sensibility. Keio University Press, Tokyo, pp 147–156

Caro TM, Hauser MD (1992) Is there teaching in nonhuman animals? Q Rev Biol 67:151–174

Csibra G, Gergely G (2009) Natural pedagogy. Trends Cogn Sci 13(4):148–253

Matsuzawa T (2011). Souzousuru chikara-Chimpanzee ga oshiete kuretakoto (Imagination ability: what chimpanzees teach us) (in Japanese) Iwanami Shoten

Strauss S (2005) Teaching as a natural cognitive ability: `implications for classroom practice and teacher education. In: Pillemer D, White S (eds) Developmental psychology and social change. Cambridge University Press, New York, pp 368–388

Strauss S, Ziv M (2011) What nonhuman animal teaching teaches us about teaching. In: Watanabe S (ed) CARLS series of advanced studies of logic and sensibility, vol 5. Keio University Press, Tokyo, pp 363–371

Thornton, Raihani NJ (2008) The evolution of teaching. Animal Behaviour, 75:1823–1836

Tomasello M (1999) The cultural origins of human cognition. Harvard University Press, Cambridge

4 The Ability to Objectify Conventional Styles of Problem-Solving: A Hypothesis on the Difference in Learning Ability Between Modern Humans and Neanderthals

Keiichi Omura

Abstract

In this paper, based on the Bateson's model regarding the evolution of learning, I will attempt to examine and modify the hypothesis of 'cumulative cultural evolution' proposed by Tomasello in order to consider the evolutionary basis of the learning ability of modern humans and thus construct a hypothesis about the difference in learning ability between Neanderthals and modern humans. First, I will briefly review Tomasello's hypothesis about differences in learning ability between modern humans and other primate species. Then, based on Bateson's model regarding the evolution of learning, I will examine the hypothesis of 'cumulative cultural evolution' proposed by Tomasello in order to modify it to include the evolutionary process of learning ability from Neanderthals to modern humans. Finally, I will propose the hypothesis that the most important ability required for the full achievement of 'cumulative cultural learning' is the modern humans' ability to objectify and manipulate the relationships between their culture and the environment, which might distinguish them from Neanderthals.

Keywords

Bateson • Cultural learning • Cumulative cultural evolution • Objectification • Tomasello

4.1 Introduction

When studying the learning process of modern humans, it is necessary to consider social learning as the basis of their varied kinds of learning because they have culture. All modern human individuals are born into society and begin their lifelong learning processes with socially learning each culture. However, this doesn't mean that they never learn individually. As noted in anthropological studies on creativity in human societies (e.g., Boas 1928; Lavie et al. 1993), new customs and styles are frequently innovated by individuals learning independently of others, with the result that their existing culture is changed. Such individual learning is nevertheless based on the cultural knowledge and techniques learned through social learning. In modern human societies, any kind of innovation could not be possible without the pool of knowledge and techniques—the so-called cultural traditions—which have been accumulated through historical processes. In this sense, the social learning of culture can be said to be the basis for any kind of learning done by modern humans.

Above all, as pointed out by Tomasello (1999), 'cultural learning,' (including 'imitative learning,' 'instructed learning' and 'collaborative learning') which is one of the forms of social learning but is unique to modern humans, plays the most important role in the learning process of modern humans. This is because cultural learning is essential to modern humans' species-unique modes of cultural transmission, that is, 'cumulative cultural evolution.' This unique mode enables them to develop the cognitive skills necessary to invent and maintain complex tool-use industries and technologies,

K. Omura (✉)
Studies in Language and Culture, Graduate School of Language and Culture, Osaka University, 1-8 Machikaneyama-cho, Toyonaka, Osaka 560-0043, Japan
e-mail: BXQ06636@nifty.com

T. Akazawa et al. (eds.), *Dynamics of Learning in Neanderthals and Modern Humans Volume 2: Cognitive and Physical Perspectives*, Replacement of Neanderthals by Modern Humans Series, DOI 10.1007/978-4-431-54553-8_4, © Springer Japan 2014

complex forms of symbolic communication and representation, and complex social organizations and institutions. All of these developments only occurred in the last 250,000 years, which is a very short time evolutionarily speaking.

Tomasello's hypothetical model of 'cumulative cultural evolution' can be considered to provide a convincing explanation for the way modern humans developed their species-unique cognitive skills in only 250,000 years. However, Tomasello's hypothesis tells us nothing about the difference in learning ability between modern humans and Neanderthals, because his hypothesis only considers the evolutionary process of learning ability between modern humans and other animal species. If it were certain that the difference between modern humans and other animal species is the ability to learn culturally, what is the difference in the learning ability of modern humans and Neanderthals?

In this paper, based on the Bateson's model regarding the evolution of learning (Bateson 1972), I will examine and modify the hypothesis of 'cumulative cultural evolution' proposed by Tomasello (1999) in order to consider the evolutionary basis of the learning ability of modern humans and thus construct a hypothesis about the difference in learning ability between Neanderthals and modern humans. First, I will briefly review Tomasello's hypothesis about differences in learning ability between modern humans and other primate species. Then, based on Bateson's model regarding the evolution of learning (Bateson 1972), I will examine the hypothesis of 'cumulative cultural evolution' proposed by Tomasello (1999) in order to modify it to include the evolutionary process of learning ability from Neanderthals to modern humans. Then, I will propose the hypothesis that the most important ability required for full achievement of 'cumulative cultural learning' is the modern humans' ability to objectify and manipulate the relationships between their artificial culture and natural environment, which might distinguish them from Neanderthals.

4.2 Tomasello's Hypothesis of 'Cumulative Cultural Learning'

According to Tomasello (1999), only modern humans acquired their species-unique modes of cultural transmission, that is, 'cumulative cultural evolution.' This process "requires not only creative invention but also, and just as importantly, faithful social transmission that can work as a ratchet to prevent slippage backward—so that the newly invented artifact or practice preserves its new and improved form at least somewhat faithfully until a further modification or improvement comes along" (Tomasello 1999, p. 5). It is this mechanism of 'cumulative cultural evolution,' which works on time scales many orders of magnitude faster than those of biological evolution, that enables modern humans, in only 250,000 years, to develop the cognitive skills and products that other animal species never achieved. As mentioned before, 250,000 years is not enough time for normal processes of biological evolution involving genetic variation and natural selection to have created them.

This 'cumulative cultural evolution' consists of the following two stages (see Fig. 4.1).

(1) Child Cultural Learning: The Ratchet of Cumulative Cultural Evolution

This is the process in which children or novices learn existing cognitive skills through cultural learning. It is through this process that the pool of cognitive skills and products that

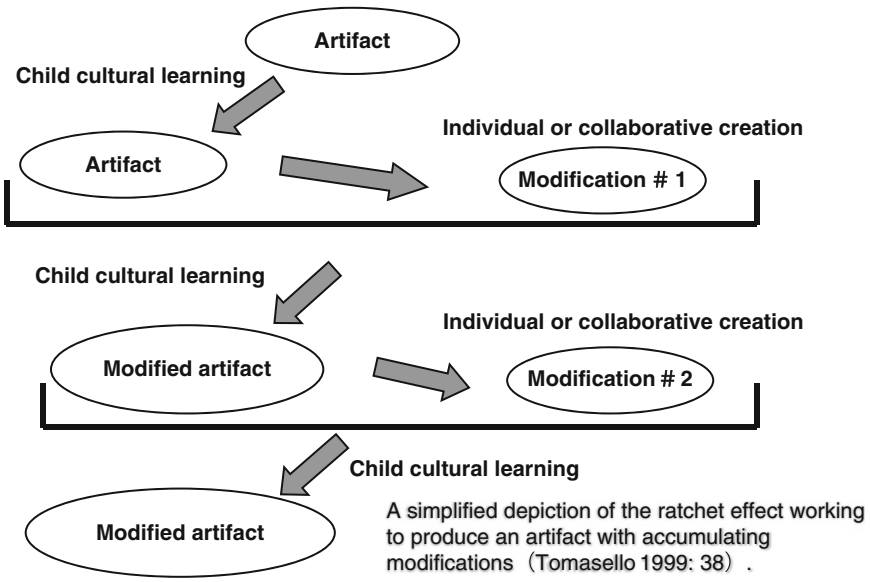

Fig. 4.1 The ratchet effect of cultural learning (Tomasello 1999, p. 38)

have been created or invented in the past are faithfully transmitted over generations and preserved as the resources for innovations in the future. This process functions as Tomasello's 'ratchet.'

(2) Individual or Collaborative Creation: The Driving Force of Cumulative Cultural Evolution

In this process, individuals or groups of individuals modify existing cognitive skills and products or invent new ones based on the accumulated pool of cognitive resources, such as tools, technical processes, the devices for symbolic communication, social institutions, and so on. This process advances the gears of cumulative cultural evolution and thus can be considered its driving force.

Tomasello points out that the ability of cultural learning functioning as the ratchet of cumulative cultural evolution, which enables modern humans to accumulate modifications through historical time, is restricted to modern humans. However, the ability to create new inventions is commonly shared among modern humans and other animal species. For example, "many nonhuman primate individuals regularly produce intelligent behavioral innovations and novelties, but then their groupmates do not engage in the kinds of social learning that would enable, over time, the cultural ratchet to do its work" (Tomasello 1999, p. 5). Thus, it is difficult for other animal species to preserve and accumulate over generations the modifications their predecessors have achieved. As the result, they always have to create and invent new skills by themselves without any help from an accumulated pool of skills and knowledge.

According to Tomasello, this mode of learning essential to cumulative cultural evolution, that is, cultural learning, is based on "the ability of individual organisms to understand conspecifics as beings like themselves who have intentional and mental lives like their own," (Tomasello 1999, p. 5) and is composed of three types of learning: 'imitative learning,' 'instructed learning,' and 'collaborative learning' (see Fig. 4.2). 'Imitative learning' is the learning in which "youngsters actually reproduce the behavior or behavioral strategy of the demonstrator, for the same goal as the demonstrator" (Tomasello 1999, p. 26). 'Instructive learning' is the learning process, which "comes from the 'top down,' as knowledgeable or skilled individuals seek to impart knowledge or skills to others" (Tomasello 1999, p. 33). 'Collaborative learning' is the form of learning in which novices learn through the experience of collaboration with knowledgeable and skilled individuals. These types of cultural learning would be impossible without the ability of learners to understand the intentions behind the behaviors of others. Thus, Tomasello concludes that the difference in learning ability between modern humans and other animal species can be seen in their ability to learn culturally, which is based on the ability of learners to understand conspecifics as beings that have intentional and mental lives like their own.

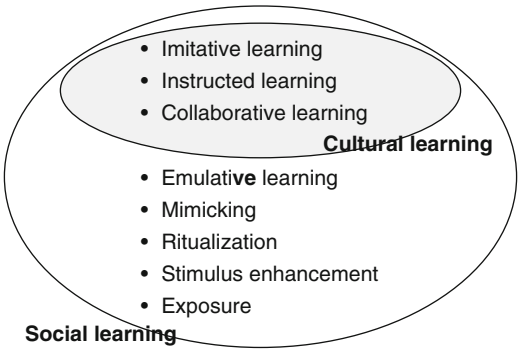

Fig. 4.2 Social learning and cultural learning

Tomasello's hypothetical model of 'cumulative cultural evolution' can be considered as providing a convincing explanation for the way modern humans developed their species-unique cognitive skills in only 250,000 years, which is too short for biological evolutionary mechanisms to have created them. It seems reasonable to consider 250,000 years as enough time for modern humans to develop their cognitive skills required for their complex products—such as technologies, communication devices, and social institutions—through their species-unique mechanism of cumulative cultural evolution, which requires only one biological basis of cultural learning: the ability to understand the intentions of others behind their behaviors.

However, as mentioned previously, Tomasello's hypothesis tells us nothing about the difference in learning ability between modern humans and Neanderthals. His hypothesis only concerns the differences in the evolutionary processes between modern humans and other species. If it were certain that the difference between modern humans and other animal species can be seen in the ability of cultural learning, it begs the question of where we can see the differences in learning ability between modern humans and Neanderthals.

4.3 Hints from Batson's Evolutionary Model of Learning

Bateson's evolutionary model of learning (Bateson 1972) is instructive in considering this question, because his model provides a clue to modifying Tomasello's model to include the evolutionary process from Neanderthals to modern humans.

Bateson classified and arranged the types of learning processes into the following hierarchical series according to the level of logical types:

(1) Zero Learning

This level of learning "is characterized by *specificity of response*, which—right or wrong—is not subject to correction" (Bateson 1972, p. 293). This learning process is "the case in which an entity shows minimal change in its response to a repeated item of sensory input" (Bateson 1972, p. 283).

(2) Learning I

This level of learning "is *change in specificity of response* by correction of errors of choice within a set of alternatives" (Bateson 1972, p. 293). This learning process includes "the cases in which an entity gives at Time 2 a different response from what it gave at Time 1, and again we encounter a variety of cases variously related to experience, physiology, genetics, and mechanical process" (Bateson 1972, p. 287).

In this level of learning, learners learn specific ways of problem-solving one at a time and through trial and error to suit specific situations, but do not learn generalized styles of problem-solving proper to contexts abstracted from these situations. The result of this style of learning is that the learners always have to examine which way of problem-solving is commensurate to each situation and cannot flexibly alter it according to changing contexts. In this sense, the learners at this level are still bound by specific situations and cannot abstract generalized contexts from situations through objectification.

(3) Learning II

This level of learning is the meta-learning of Learning I, that is, "*change in the process of Learning I*, e.g., a corrective change in the set of alternatives from which choice is made, or it is a change in how the sequence of experience is punctuated" (Bateson 1972, p. 293). This level of learning entails "changes in the manner in which the stream of action and experience is segmented or punctuated into contexts" (Bateson 1972, p. 293).

At this level of learning, learners learn the styles of problem-solving proper to contexts abstracted from situations so that they can flexibly and properly adjust their styles of problem-solving according to given contexts without the need for laborious case-by-case examination. In this sense, "Learning II is an economy of the thought processes (or neural pathways) which are used for problem-solving or Learning I" (Bateson 1972, p. 303). However, at this level of learning, the ability to abstract generalized contexts from specific situations is fixed as a template for how to understand the situations. Therefore, the specific styles of problem-solving are bound to the specific contexts, with the result that the learners are conservative in their habits and resist any innovation.

Thus, all kinds of habits are learned on this level, including conventional technical processes, socially proper manners, conventional ways of understanding the world etc., which can be called 'character' (Bateson 1972, p. 303), style, or culture. In the case of modern humans, this level of learning is acquired in infancy and is likely to persist through life as the reflectively unexamined premise of learning, which often functions as cultural bias. In this sense, the learners of this level are still bound by conventional styles of problem-solving, which is in turn bound to specific contexts.

(4) Learning III

This level of learning is the meta-learning of Learning II and is "*change in the process of Learning II*, e.g., a corrective change in the system of sets of alternatives from which choice is made" (Bateson 1972, p. 293). Learners at this level acquire the ability to objectify the unexamined premises learned in Learning II and the relationships between themselves and the circumstances so that they can creatively and flexibly change the unexamined and fixed premises or make creative modifications to them according to the circumstances.

In this sense, "Learning III will throw these unexamined premises open to question and change," (Bateson 1972, p. 303) and brings to the learners "freedom from the bondage of habit" (Bateson 1972, p. 30). The learners learn to objectify the relationships between contexts and styles of problem-solving as well as the how to abstract generalized contexts from situations. Thus, they can freely change their styles of problem-solving as well as their ways of understanding the world according to changing circumstances.

This level of learning is acquired as the result of resolving what Bateson (1972, p. 303) called 'double binds,' that is, paradoxes among the unexamined premises learned in Learning II or between the premises and the circumstances. Thus, this level of learning is "likely to be difficult and rare even in human beings," (Bateson 1972, p. 30) and requires the patience not to give up hope of resolving paradoxes. This tenacity and ability to hold two equally viable ideas in mind are illustrated beautifully in the example of "the Zen candidate" who has been assigned a *koan* (paradox) and must labor at his task "like a mosquito biting on an iron bar" (1972, p. 303).

In this arrangement of learning processes by Bateson, the higher the level of learning, the more freedom, economy and flexibility the learners acquire. The learners, who are bound to specific ways of problem-solving for specific situations at the level of Learning I, will acquire the ability to abstract the contexts from situations and economically select the proper styles of problem-solving suited to a specific context at the level of Learning II. At Learning Level III the learners who are bound by conventional styles of problem-solving and understanding only from specific contexts will acquire the ability to objectify the sets of their conventional styles of

problem-solving and the contexts, and are then able to flexibly change them according to circumstances. It is important, however, to note that the higher levels of learning are always based on the lower levels. Learning III could not be possible without acquiring Learning II, which is also impossible without Learning I. In this sense, Bateson's arrangement of learning processes can be considered as the evolutionary model of learning processes.

4.4 An Attempt to Modify Tomasello's Model

When comparing Bateson's evolutionary model of learning with Tomasello's model of cumulative cultural evolution, it should be noted that cultural learning as the ratchet of cultural evolution in Tomasello's model corresponds to Learning II in Bateson's model, because what is learned in Learning II is culture. It is through Learning II that children learn existing cognitive skills as conventional styles of problem-solving and thus the pool of knowledge and skills are transmitted over generations as the resources for innovations in the future. How, then, does one move onto Learning III? If Learning II corresponds to cultural learning, Learning III could be nothing else but the acquirement of the ability to partake in 'individual or collaborative creations.' These individual or collaborative creations function as the driving force of cumulative cultural evolution, because it is through Learning III that the learners acquire the ability to objectify the conventionally fixed styles of problem-solving and thereby flexibly change or make modifications to them.

It is important, however, to point out that what is learned in Learning III is different from the ability of innovations or inventions, which is commonly shared among other animal species and modern humans. Learning III is possible only after acquiring Learning II—that is, cultural learning—the ability of which other animal species do not acquire. Rather, the ability of innovations and inventions, which is also shared among other animal species, corresponds to Learning I, in which the specific ways of problem-solving proper to given situations are learned one by one without help of accumulated skills and knowledge. Therefore, it is reasonable to consider the following correspondence between Tomasello's model and Batson's model (see Fig. 4.3).

1. Learning I: individual learning and social learning, which are commonly shared among all animal species.
2. Learning II: the cultural learning unique to modern humans, which functions as the ratchet of cumulative cultural evolution.
3. Learning III: the learning necessary for innovation and invention, which is also unique to modern humans and functions as the driving force of the gear of cumulative cultural evolution.

If it is accepted that cumulative cultural evolution is composed of two stages respectively based on two types of learning: (1) cultural learning acquired by Learning II, and (2) creative innovations and inventions, the ability of which is acquired by Learning III, and if there are supposed to be differences in learning ability between modern humans and Neanderthals, there is logically no other choice but to infer that Neanderthals lack the ability of Learning III even if they share the ability of cultural learning enabled by Learning II with modern humans. This is because Learning III without Learning II is logically impossible even if Learning II without Learning III is possible. Thus, it is reasonable to set up the hypothesis that the difference in learning ability between modern humans and Neanderthals can be seen in the ability of Learning III, which Neanderthals lack but modern humans acquire.

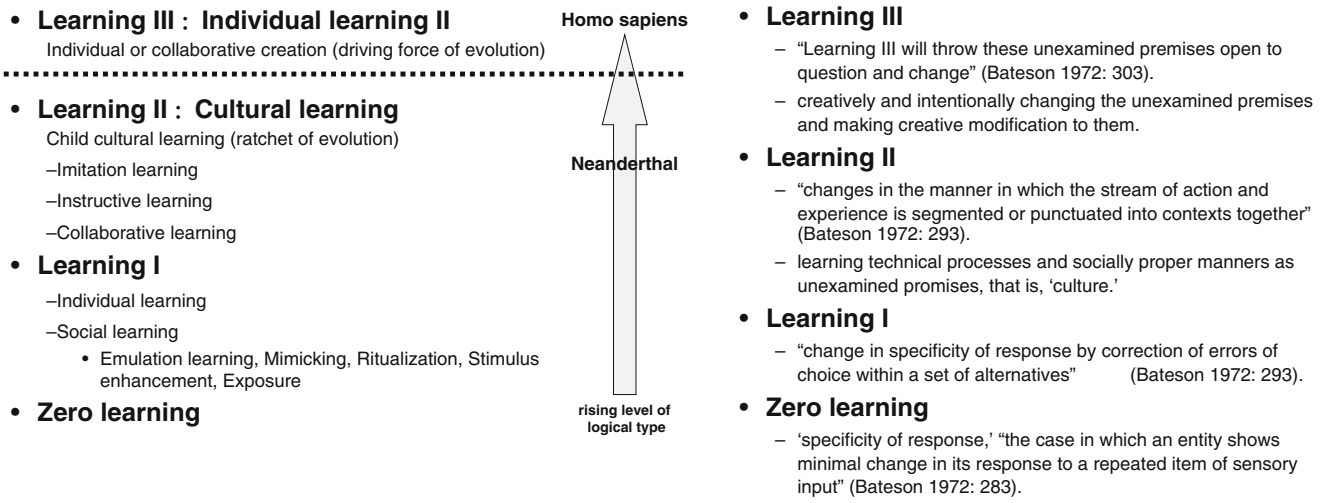

Fig. 4.3 A hypothesis about the evolutionary process from Neanderthals to Modern Humans

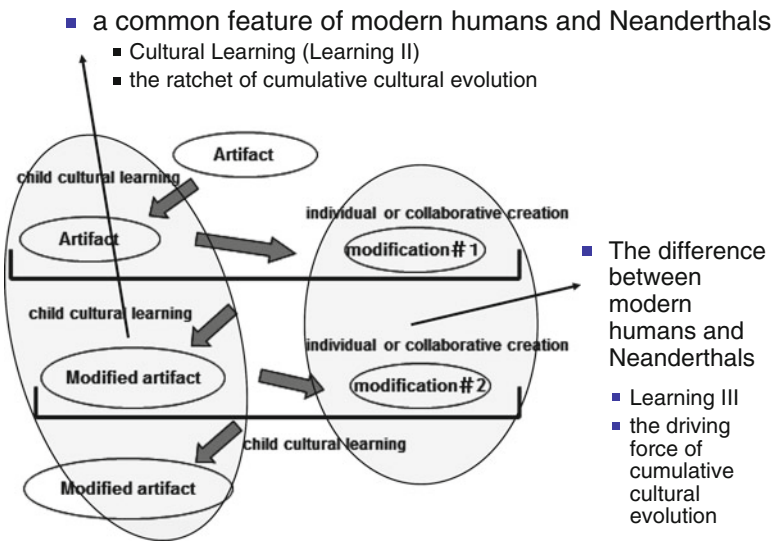

Fig. 4.4 A hypothesis about the evolution of learning

This hypothesis seems to be further supported by the archaeological fact that stone-crafting techniques believed to originate with the Neanderthals (such as the Levallois technique) were preserved for several hundred thousand years without any innovations (cf. Mithen 1996). This fact can be reasonably explained by the hypothesis that the Neanderthals acquired the ability of Learning II but lacked the ability of Learning III such that they were able to preserve their conventional techniques as a culture but unable to make modifications to them.

Thus, based on Bateson's model regarding the evolution of learning, Tomasello's model can be modified to include the evolutionary process from Neanderthals to modern humans as in the following figure: (see Fig. 4.4). This is the hypothesis that Neanderthals might have acquired the ability for Learning II, which functions as the ratchet of cumulative cultural evolution, but did not acquire the ability for Learning III, which is required for individual or collaborative creations (the driving force of cumulative cultural evolution). Ultimately, the result of this non-learning was that Neanderthals might not have been able to make creative modifications to their original artifacts and practices. In contrast to the case of Neanderthals, modern humans acquired the ability for both Learning II and Learning III, and fully realized cumulative cultural evolution. In short, it can be concluded that it is the ability for Learning III that distinguishes modern humans from Neanderthals.

4.5 A Tentative Conclusion to and Future Perspective on the RNMH Project

In this paper, I have examined and modified Tomasello's hypothetical model of 'cumulative cultural evolution' to include the evolutionary process from Neanderthals to modern humans on the basis of Bateson's evolutionary model of learning processes. I concluded that if there is any one difference in learning ability between Neanderthals and modern humans, it is the ability of Learning III in Bateson's model, which is the foundation of 'individual or collaborative creation'; that is, the driving force of cumulative cultural evolution. Thus, Neanderthals most likely acquired the ability of Learning II, which enabled them to preserve their styles of problem-solving. On the other hand, it might be supposed that they lacked the ability of Learning III, that is, the ability to make creative modifications to preserved styles of problem-solving, with the result that they might not be able to fully operate cumulative cultural evolution and thus were conservative in their techniques of stone-crafting. In this sense, Neanderthals might have acquired but perhaps were strictly bound by their cultures.

If this hypothesis is accepted, it might be safely inferred from Tomasello's model that Neanderthals acquired the ability to understand conspecifics as beings that have intentional and mental lives like their own, because Tomasello pointed out that the ability of cultural learning is based on the ability to understand the intentions behind the behaviors of others. In this sense, Neanderthals might be considered to share the ability of 'theory of mind' with modern humans.

So, what kind of ability is required for Learning III, on which creative innovations and inventions are based? It could be inferred from Bateson's model that Learning III is based on the ability to objectify the existing styles of problem-solving, which are learned as unexamined premises through cultural learning enabled by Learning II. This is because Bateson pointed out that what is learned by Learning III is how to open these unexamined premises to question and change them. It is essential to objectify what are already learned as unexamined premises in order to do so. In this sense, it is the ability to objectify what is already learned via cultural learning on the

basis of a 'theory of mind' that is required for Learning III. Modern humans acquired this ability so that they could fully operate cumulative cultural evolution and thus develop their species-unique cognitive skills and products.

Moreover, it follows from this hypothesis that modern humans might be considered to have developed the ability to objectify not only the existing styles of problem-solving but also the relationships between self and the environment as that ability is indispensable for objectifying and changing what has already been learned. In order to flexibly and effectively change the existing styles of problem-solving according to changing circumstances, it is essential not only to objectify one's styles of problem-solving but also to objectify the relationship between self and the environment on each occasion and then place one's styles of problem-solving in the relationship to evaluate and change said styles.

In this sense, the most important ability required for cumulative cultural evolution may be the ability to objectify the relationships between self and the environment to attentively observe the circumstances and thereupon properly evaluate and flexibly change one's existing styles of problem-solving according to the circumstances. This must be done while conducting daily life on the basis of what is learned through cultural learning. Thus, it can be concluded that the most important species-unique ability of modern humans is the ability to objectify the relationships between their own culture as unexamined styles of problem-solving and their surrounding environments.

These are, of course, only the hypotheses deductively lead to by examining Tomasello's and Bateson's models, and therefore should be examined and proved on the basis of positive evidence. Moreover, tentative conclusions of this paper should raise more questions about the learning ability of modern humans. For example, what kind of ability enabled modern humans to acquire the ability to objectify the relationships between their cultures and environments? Is it biologically acquired or is socially fostered? If it is socially fostered, then how is it fostered in social interactions? There are a number of questions about the learning ability of modern humans that remain unsolved. Based on my ethnographic research on the learning processes of Inuit (an indigenous people living in Canadian Arctic), I shall address these questions on the basis of ethnographic evidence in the future.

References

Bateson G (1972) Steps to an ecology of mind. The University of Chicago Press, Chicago

Boas F (1928) Primitive art. Harvard University Press, Cambridge

Lavie S, Narayan K, Rosaldo R (eds) (1993) Creativity/anthropology. Cornell University Press, Ithaca

Mithen S (1996) The prehistory of the mind: a search for the origins of art, religion and science. Thames and Hudson Ltd., London

Tomasello M (1999) The cultural origins of human cognition. Harvard University Press, Cambridge

Cognitive Flexibility and Making Objects in Baka Pygmy Children

5

Tadashi Koyama

Abstract

Cognitive flexibility, especially representational flexibility is a crucial element of human creativity. This paper provides some insight on the cognitive flexibility of the Baka Pygmy children of southeastern Cameroon based on observations of their play and object-making activities. It seems that children until about 2 years of age engage in sensorimotor interactions with the materials around them, and those around 3 years of age begin to make objects. However, while we often observed sensorimotor activities, object-making was observed almost exclusively in solitary play. The development of Baka Pygmy children's cognitive flexibility appears in their daily creation of objects, substitution of objects, and when using broken parts of entities. Those activities in their play enhance the development of symbolic functions.

Keywords

Baka Pygmy children • Cognitive flexibility • Object-making • Representational flexibility • Symbolic function

5.1 Introduction

Drawing from Piaget's theory, Anthony D. Pellegrini (2009) pointed out that children's cognitive development could be rooted in their sensorimotor interactions with objects. Through repeated interactions with objects, children construct mental representations of those objects (Pellegrini 2009). These representations come to be expressed in their own object-making. Some aspects of children's cognitive development such as causal cognition and their ongoing interests to the real life are reflected in their object-making. Furthermore, participation in these activities may develop their creativity. Children's behavior with objects has been studied from the viewpoints of exploration, play, construction, and tool use (Bock 2005). I observed that children were often absorbed in object-making such as making a basket of leaves for primarily play. I think these activities may have a relation with their creativity and cognitive flexibility in their later lives.

In recent research in developmental psychology, cognitive flexibility is defined as a child's ability to switch his or her strategy to suit new task he or she must accomplish. For example, the Dimensional Change Card Sorting (DCCS) (Zelazo 2006), a cognitive-flexibility test, assesses the capacity of examinees to flexibly shift between two sorting rules based on color and shape. Kloo et al. (2010) suggested that we have to distinguish between two different kinds of flexibility: response flexibility and representational flexibility. Object-making also requires children's cognitive flexibility, especially when using representation. In this study, I hope to demonstrate the creativity of the children who are raised and nurtured in hunter-gathering societies. I observed the Baka Pygmy children creating objects in their daily life and speculated on their cognitive flexibility demonstrated by this object-making.

T. Koyama (✉)
Department of Human Psychology, Faculty of Humanities and Sciences, Kobe Gakuin University, 518 Arise, Ikawadani-cho, Nishi-ku, Kobe, Hyogo 651-2180, Japan
e-mail: t-koyama@human.kobegakuin.ac.jp

T. Akazawa et al. (eds.), *Dynamics of Learning in Neanderthals and Modern Humans Volume 2: Cognitive and Physical Perspectives*, Replacement of Neanderthals by Modern Humans Series, DOI 10.1007/978-4-431-54553-8_5, © Springer Japan 2014

5.2 Method

I conducted my research on Baka children's object-making and object-play in Baka villages in southeastern Cameroon from the 13th through the 18th of August, 2012. I observed the children in their camp site for about 2 h in the morning and 2 h in the afternoon every day in that period, recording the children's object-making activities for their play with a Sony Handy Cam.

5.3 Results

Baka Pygmy children were very often observed making objects for play (Fig. 5.1). However, Baka Pygmy children under 2 years of age engaged in sensorimotor interactions with the materials around them. From about 3 years of age object-making was observed often in children's solitary play. Object-making and constructing objects were also infrequently observed in collaborative symbolic play such as pretending and substituting one object for another as shown in Fig. 5.1. This type of play was particularly observed in the girls. For example, I once observed this type of play in four girls ranging from the age of 3–5. They first selected the location for play in their camp site. Then they used object-substitution to simulate scenes of food-gathering, real cooking, having meals, and going to bed. This one period of play lasted for 37 min.

Some children incorporated "new" materials such as cans from their camp sites for making play-objects (Figs. 5.2 and 5.3). The products in Figs. 5.2 and 5.3 were made by a 5-year-old boy. He used cans, strings, and food scraps. Those products then were used and further elaborated upon by the other children at the same site. Figure 5.3 shows that the boy used a concave space on the ground as a representation of a river and made a little bridge over it with a piece of wood. It seemed to represent a real-life scene with a loaded car passing across the bridge.

Figure 5.4 shows a 4-year-old boy making an object by himself. The boy in Fig. 5.4 was concentrating on attaching some pieces of wood to a wheel. Object-making as shown in Fig. 5.4 was not observed often, but boys were more likely to engage in it. In fact, children often incorporated broken odds and ends from the camp into object-making activities. One thing I noticed was that children played with peers at first and later began to play solitarily. Figure 5.5 shows that a boy was making a steering wheel out of the broken parts of a motorcycle. Those kinds of play reflected children's awareness of the real world around them.

5.4 Discussion

Children up to 3 years of age engaged in sensorimotor interactions with materials around them. At around 3 years of age, children would begin to make objects. But these observations reported here were not observed frequently and object-making was often observed in solitary play.

Sex differences were also noted. In their collaborative symbolic play, girls were observed constructing objects that were similar to those that adult women used to cook and prepare meals. Those kinds of activities were interpreted as the playful uses of objects as simulations of real-world subsistence activities. They used leaves, woods, food scraps, and cloths for substitutions of utensils which adults used daily. The object substitution enacted during that type of play might reflect a child's cognitive flexibility.

On the other hand, boys preferred making objects used to play pretend, such as cars, trucks and motorcycle. When making these objects, boys tended to bring together new materials such as cans with leaves, stones, wood, and string

Fig. 5.1 Girls making objects in collaborative symbolic play

Fig. 5.2 Making an object with a can

Fig. 5.3 Making a river and its bridge with wood

Fig. 5.4 Making an object from wood and a wheel

based on their representation. It seems that Baka Pygmy children construct objects flexibly, for example using a can for a toy car, or a piece of wood for food. It reflects their cognitive flexibility and their representational faculties by forcing them to use the various cognitive abilities mentioned above.

Kamei (2009) reported on the materials that the Baka Pygmy children used for their play and he particularly emphasized the richness and creativity shown in their use of those materials. Kloo et al. (2010) demonstrated that flexibility is a key competency in daily life. We can see the Baka Pygmy children's cognitive flexibility in their daily object-making,

Fig. 5.5 Using broken parts of a motorcycle

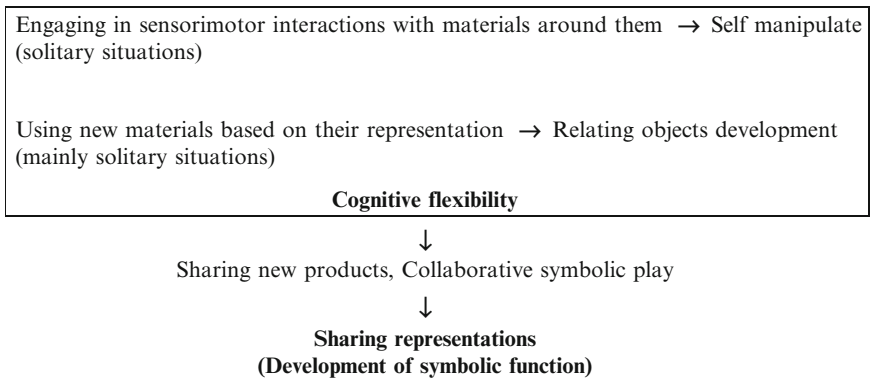

Fig. 5.6 Cognitive flexibility in object-making, Sharing representations, and development of symbolic function

object substitutions for play and their creative use of broken parts to build new toys. In child development object substitution could be achieved by their symbolic function (McCune 2008). It is thought that those activities in Baka Pygmy children's play further enhanced their symbolic functioning in which one thing (signified) was represented by another thing (signifier). In Fig. 5.6 I summarize these cognitive developments from the view point of symbolic function. Tomasello and Call (1977) pointed out the importance of self-manipulating in representing means for achieving goal behavior. Self-manipulating with old and new materials in solitary situations enriches children's cognitive flexibility. Then new products are shared in their collaborative play. It leads to the development of Baka Pygmy children's symbolic function.

In this research I noticed that the use of new materials, for example, the can in Figs. 5.1 and 5.2, might affect their object-making and object-relations development. Koyama (2012) pointed out that younger when Baka Pygmy children showed their intuitional and representational abilities in responding to visual reception signals which was required to gain meaning from visual symbols. This intuition and the ability to create representations might be related to the development of their object-making. This research also impressed on me that Baka Pygmy children's development of cognitive flexibility is based on their awareness of the real world around them.

Acknowledgments This research was supported by the "Grant-in-aid-for Scientific Research on Innovative Areas 2010–2014, 1201." The project leader was Takeru Akazawa, PhD. The title is: Replacement of Neanderthals by Modern Humans: Testing Evolutionary Models of Learning. Potions of this research were presented to RNMH 2012, The Frist International Conference in Tokyo.

References

Bock J (2005) Farming, foraging, and children's in the Okavango Delta, Botswana. In: Pellegrini AD, Smith PK (eds) The nature of play: Great Apes and Humans. Guilford, New York, pp 254–284

Kamei N (2009) Anthropology of Play. Showado, Tokyo (In Japanese)

Kloo D, Perner J, Aichhorn M, Schmidhuber M (2010) Perspective taking and cognitive flexibility in the dimensional change card sorting (DCCS) task. Cogn Dev 25:208–217

Koyama T (2012) Comprehension of pictures in Baka children who grow up in the hunter gatherer culture. In: Terashima H (ed) Replacement of Neanderthals by Modern Humans: A-02 Team Annual Report, No.2:55-59. Kobe Gakuin Uni. (In Japanese)

McCune L (2008) How children learn to learn language. Oxford University Press, New York

Pellegrini AD (2009) The role of play in human development. Oxford University Press, New York

Tomasello M, Call J (1977) Primate cognition. Oxford University Press, New York

Zelazo PD (2006) The Dimensional Change Card Sort (DCCS): a method of assessing executive function in children. Nat Protoc 1:297–301

The Demonstration of Resilience in the Drawings of Baka Pygmy Children

6

Eiko Yamagami

Abstract

This paper reveals the resilience of hunter-gatherer Baka Pygmy children, as demonstrated by their drawings. Twenty-five boys and six girls were asked to draw their favorite things on paper with pencils, colored pens and pastel crayons. The results should be considered from different angles such as their drawing process, style, and the content of their works. Their spontaneity, curiousness, adjustability to the unfamiliar stimuli and joy in the new experience were shown during the drawing process. Their final products also revealed resilient factors such as "Productive activity" "Insight and warmth," "Confident Optimism," "Skilled expressiveness," "Adaptability to change." Through their resilience, i.e., a flexible learning attitude to a transitional and critical situation, I speculate that humans have also been thriving similarly in the face of adversity throughout history.

Keywords

Baka Pygmy children • Drawings • Innovators and followers • Productive activity • Resilience • Skilled expressiveness

6.1 Introduction

"Resilience" is a key word in understanding how humans cope with extreme stress such as the traumas of child abuse, war, or natural disaster. Although some childhood trauma victims suffer from Posttraumatic Stress Disorder (PTSD) and develop a personality disorder after growing up, some survive without developing any problems. The group that encounters the least difficulties after a trauma may find strength in their flexibility and ability to learn from their difficult situation. The most important aspect of this flexible attitude is "resilience," the ability to "bounce back" from a difficult situation. This psychological concept "resilience" could be said to characterize humanity as a whole, because of our ability to succeed in a harsh environment that has included extreme temperatures, food shortages and varied threats over our long history. Having examined the drawings of hunter-gatherer Pygmy children in Cameroon—who are not greatly influenced by a systematic school education or technology, but rather by tradition—I would like to posit that their drawings are a clear example of humanity's intrinsic resilience.

6.2 Literature Review on "Resilience"

The word "resilience" originally comes from physics, and is usually paired with the word "stress." Spring-back, or resilience, occurs when stress is applied to something. It has come to be used as a term of psychological strength for recovery after traumatic events, such as child abuse or disaster. Connor and Davidson (2003) give the definition of "resilience" as "the personal qualities that enable one to thrive in the face of adversity." They developed the Resilience Scale (CD-RISC) which is comprised of 25 items important to having a sense of overall resilience that were

E. Yamagami (✉)
Department of Human Psychology, Faculty of Humanities and Sciences, Kobe Gakuin University, 518 Arise, Ikawadani-cho, Nishi-ku, Kobe, Hyogo 651-2180, Japan
e-mail: yamagami@human.kobegakuin.ac.jp

T. Akazawa et al. (eds.), *Dynamics of Learning in Neanderthals and Modern Humans Volume 2: Cognitive and Physical Perspectives*, Replacement of Neanderthals by Modern Humans Series, DOI 10.1007/978-4-431-54553-8_6, © Springer Japan 2014

drawn from a variety of sources. For example, the qualities "Views change or stresses as a challenge/opportunity," "Commitment" and "Recognition of limits to control" were drawn from Kobasa (1979). "Close secure attachment to others," "Strong self esteem," "Sense of humor" "Adaptability to change" and so on were drawn from Rutter (1985). "Patience" and "Tolerance of negative affect" were drawn from Lyons (1991). Klohnen (1996) also suggested possible factors of "resilience" such as "Productive activity," "Insight and warmth," "Confident optimism" and "Skilled expressiveness."

Although the concept of "resilience" has been accepted in some fields, some researchers are critical. Luthar et al. (2000) produced an article which critically appraised the construct of resilience. They insisted that "this construct falls into four broad categories: (1) ambiguities in definitions and terminology, (2) variations in interdomain functioning and risk experiences among ostensibly resilient children, (3) instability in the phenomenon of resilience, and (4) theoretical concerns, including questions about the utility of resilience as a scientific construct." Nevertheless, the authors concluded that "the continuation of scientific work in this "resilience" area is of substantial value" and that "there is clearly a need for resilience researchers to enhance the scientific rigor of their work."

Therefore, I am examining the drawings of the Pygmy children in as scientific a manner as possible, (such as referring to the CD-RISC and other resilience factors) to ultimately suggest the overall resilience of human beings.

6.3 Baka Pygmy Children

The Baka people inhabit the central or west area of Africa, and I had an opportunity to see and communicate with the Baka people in Cameroon. In the summer of 2011, I stayed at Lomie, a small village located 6 hours drive from the capitol of Yaunde. There were several small Baka settlements around the village, and I visited them to collect data through observation and psychological techniques. The Baka Pygmies are hunter-gatherers, which is the longest and most enduring typical lifestyle of human beings with few industrialized products. I would posit that they maintain the resourcefulness innate to human begins, perhaps more than people in industrialized societies who undergo organized education. In fact, the children there had few opportunities to go and learn in school due to poverty and tradition. This means that they responded to my stimuli without any systematic educational influence tempering their answers, rather replying traditionally. However, it should be noted that as some of them had received a little education in school, their learning situation might be considered to be in a transitional stage.

6.4 Method

6.4.1 Participants

Thirty-one Baka Pygmy children (25 boys and 6 girls, ranging from 5 to 15 years old).

6.4.2 Procedure

I asked the children to draw their favorite things on paper with tools such as pencils, colored pens and pastel crayons, which they could choose from. They mostly drew in small groups of their friends. After observing what they were drawing, I examined the data in terms of the style and content of their pictures. As drawing is an image expression with tools, it should reflect their intellectual and emotional capacities, interests, attitude and behaviors involving resilience.

6.5 Results

6.5.1 Drawing Process and Attitude

They chose from the tools that were set up in front of them. Then, according to my instruction, they started to draw spontaneously without hesitation or help from others. After making images they pointed to and named their favorite things on the paper. Finally, they told me that they had enjoyed drawing very much.

6.5.2 Drawing Style and Content

I am describing each drawing of the children in terms of the drawing content and styles (forms). The characteristics of their drawings are summarized below.

6.5.2.1 Drawing Style

Their drawing styles were examined based on iconic development. As Eng (1954) noted, most children's sensorimotor functions begin with collaboration between the eyes and hands in terms the drawing development, and they are eventually able to represent something in their drawings. Even though they are in their representational drawing stage, the styles (forms) of early childhood are still simple such as scribbles of lines and circles. As children enter the formative drawing stage (around 4 years old), they become able to draw X-ray paintings, head-feet person drawings and other incomplete gestalt drawings.

The realistic drawing stage usually starts for children at around 6 years of age, when art education in school might

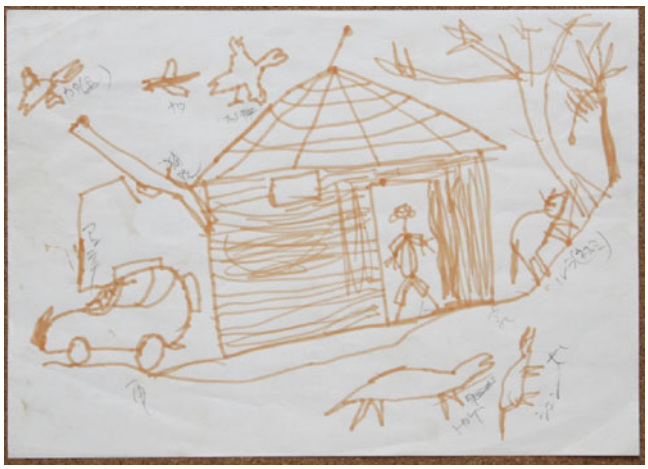

Fig. 6.1 Nine-year-old boy: "a car with an antenna, house, person, lizard, dog, mouse, trees, rifle and birds" drawn with an orange pen. Constructed painting. Kinetic painting

Fig. 6.2 Ten-year-old boy: "car, boy, ball" drawn with a black pen. X-ray painting. Kinetic painting

have an effect on their style. In fact, art education appeared to make the children draw realistically and from a single-viewpoint perspective.

One constructed painting (Fig. 6.1), 12 imaginary X-ray paintings (Figs. 6.2, 6.3, 6.4, 6.5, 6.7, 6.8, 6.9, 6.11, 6.12, 6.19, 6.21, 6.25), 17 incomplete gestalt paintings including two head-feet representations (Figs. 6.5, 6.7, 6.9, 6.10, 6.11, 6.12, 6.13, 6.14, 6.16, 6.17, 6.19, 6.20, 6.22, 6.25, 6.26, 6.27, 6.28), 16 multiple viewpoint paintings (Figs. 6.4, 6.5, 6.7, 6.9, 6.11, 6.14, 6.15, 6.17, 6.18, 6.21, 6.22, 6.26, 6.27, 6.28, 6.29, 6.30), five kinetic paintings (Figs. 6.1, 6.2, 6.8, 6.9, 6.19), and two skillful and artistic paintings (Figs. 6.29, 6.30).

6.5.2.2 Drawing Content (Rate of Drawing)

Vehicles and airplanes 80.6 %, human beings 74.1 %, food (edible animals and fruit) 64.5 %, plants 61.2 %, houses including a traditional *mongle* 38.7 %, tools (pump, rifle, traditional knife, drum, pan, umbrella, spectacles, wooden boat and table) 38.7 %, animals 32.2 %, fish 32.2 %, a soccer ball

Fig. 6.3 Ten-year-old boy: "person, corn, caterpillar, T.V." drawn with a blue pen. X-ray painting

Fig. 6.4 Eight-year-old boy: "car, house, snake, person, cook, fish, T.V., cook, fish, ball, leaf, sun, helicopter, papaya" drawn with a red pen. X-ray painting. Multiple viewpoints

29.0 %, electrical appliances (T.V., DVD, mobile phone, antenna etc.) 19.3 %, the sun, moon and stars 19.3 %, letters and numbers 16.1 %, cloth 6.4 %, the national flag 6.4 %.

6.6 Discussion

6.6.1 The Drawings of Children in Traditional Societies

Although there are not many articles about forager children's drawings, Iwata (1985) showed that the children in a small, tradition Laotian village did not draw landscapes but rather

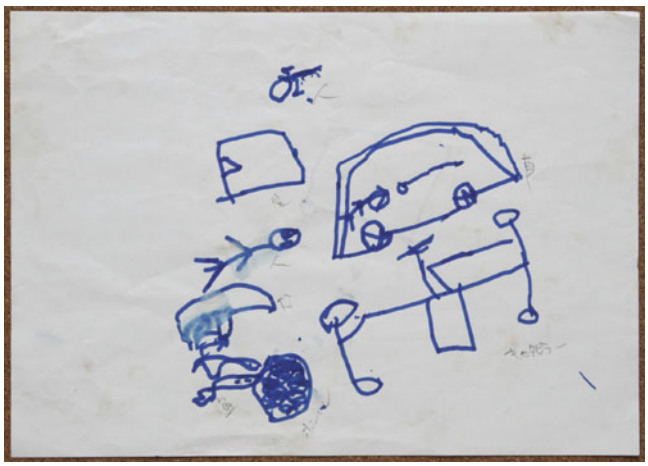

Fig. 6.5 Eleven-year-old boy: "the car and caterpillar" are bigger than the "house." "People, dog, fish, ball" drawn with a blue pen. X-ray painting. Incomplete gestalt painting. "Stick people." Multiple viewpoints

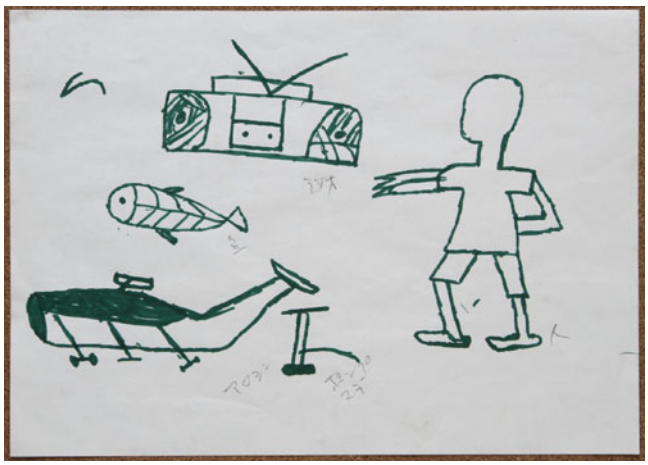

Fig. 6.6 Eleven-year-old boy: "a person without eyes, a nose or a mouth," "helicopter, radio, fish and pump" drawn with a green pen

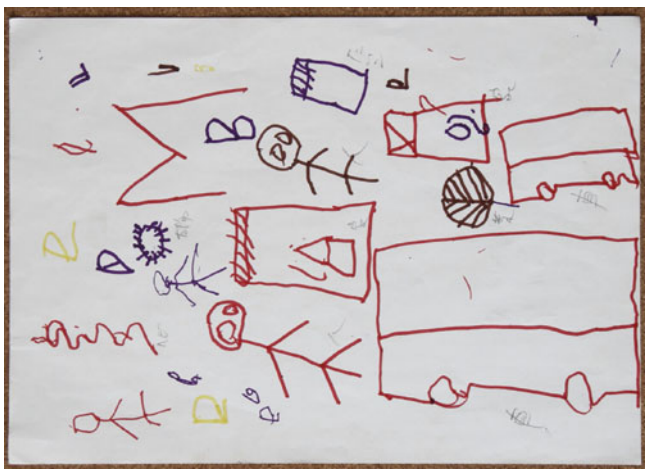

Fig. 6.7 Seven-year-old girl: "cars, houses, people, drum, leaf, sun, snake and the letter B" drawn with "red, blue and brown pens." "Stick people." Incomplete gestalt painting. Multiple viewpoints. X-ray painting

Fig. 6.8 Ten-year-old boy: "car, house, person, ball, pump, hand, fish, cook, tomato and flower" drawn with a blue pen. Kinetic painting. X-ray painting

familiar things like tools and instruments from everyday life. None of their drawings were from a bird's-eye view, but rather a worm's-eye view. One Pygmy boy out of 31 members drew a short distance landscape, and the others drew tools, animals and industrialized products like T.V.s and motorbikes from a worm's-eye view as they did in Laos. It might be speculated that children in traditional societies depict the objects surrounding them from a worm's-eye view due to the lack of knowledge of how to draw from a bird's-eye view.

In a recent study involving children's drawings and resilience, Huss and Alhaiga-Taz (2013) tried to understand stress and resilience in Bedouin children's drawings in Israel. Bedouin children there have been living in either townships under government control or illegal villages. Although both groups have settled under great stress due to their poverty, political conflicts and exposure to unfamiliar cultures, they still showed their resilience in their drawings. In particular, the children in townships showed resilience by integrating cultural traditions and westernized cultural traditions, while the children in the illegal villages are making an effort to maintain cultural traditions. The drawings showed that "the children utilize their communities to enhance resilience" through reflecting their reality and their mind. I have found this same resilience in my research which I will show in the next paragraph.

6.6.2 The Resilience of Pygmy Children

The Pygmy children's drawings of their favorite things seem to reveal the resilience through their drawing process and drawing itself. For example, one of the CD-RISC resilience factors listed by Connor and Davidson (2003) is to "View change or stress as a challenge/opportunity" and might be revealed by their drawing style and attitude. That is, more than half of them drew from multiple viewpoints, not decid-

Fig. 6.9 Nine-year-old boy: "cars, person jump roping, houses, T.V., tree, tomato, mobile phone, ball" drawn with yellow and red pens. Incomplete gestalt painting. Multiple viewpoints. Kinetic painting. X-ray painting

Fig. 6.10 Six-year-old girl: "house, people, the numbers 5, 7, and 8" drawn with red and yellow pens. Incomplete gestalt painting

Fig. 6.11 Eleven-year-old boy: "person, radio, and a ball in a house," "car, porcupine, cook, glasses, snake and tomato" drawn with purple and red pens. Incomplete gestalt painting. Multiple viewpoints. X-ray painting

ing on a fixed position and changing it freely. Other traits of resilience listed on the CD-RISC such as "Commitment," "Adaptability to change" and "Can deal with whatever situation comes up" were shown by their acceptance of the unfamiliar situation in which they were asked to draw by a stranger (the author). "Not easily discouraged by failure" was shown by the overall completion of their drawings even though their drawings were at an early stage of iconic development. In fact, 15 children drew imaginary X-ray paintings, and 10 of them incomplete gestalt paintings including two head-feet representations.

Klohnen (1996) also suggested some resilience factors. One of them, "Productive activity," might be shown by their active attitude for an unfamiliar situation and kinetic and energetic drawing style. The drawing content also indicates "Productive activity." Namely, "shooting a rifle" and "kicking a soccer ball" are important activities in their life. Moreover, some children drew a "hand" which might be a symbol of power, labor, will, protection and so on, and a lot of them drew "food" which might be a symbol of desire or greediness to live. All these figures might reveal "Productive activity."

In addition, some content might show other component factors of resilience. For example, the high rate of "human beings" that were drawn might mean friendship with others,

Fig. 6.12 Ten-year-old boy:"car with a person, person, ball, leaf" drawn with a yellow pen. X-ray painting. Incomplete gestalt painting

Fig. 6.15 Fourteen-year-old boy: "fish, tree, corn, umbrella" drawn with a brown pen. Meticulous painting. Multiple viewpoints

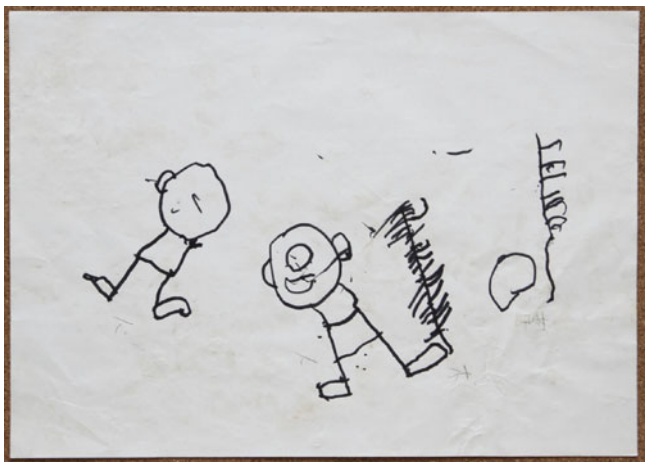

Fig. 6.13 Five-year-old boy: "people, trees, leaf" drawn with a black pen. Incomplete gestalt painting

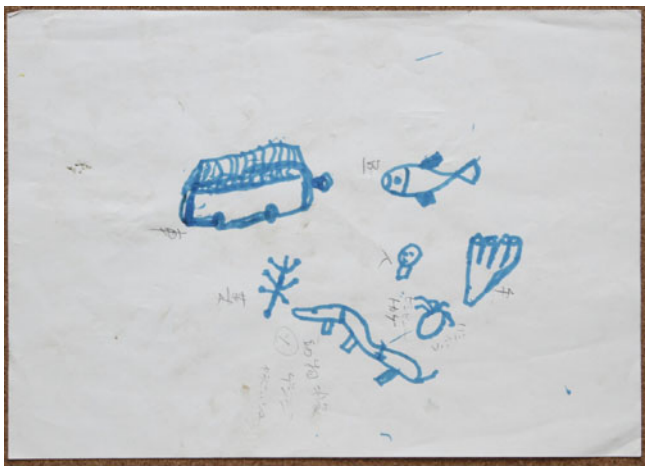

Fig. 6.16 Eleven-year-old boy: "car, animal, lizard, person, fish, leaf, hand" drawn with a blue pen. Incomplete gestalt painting

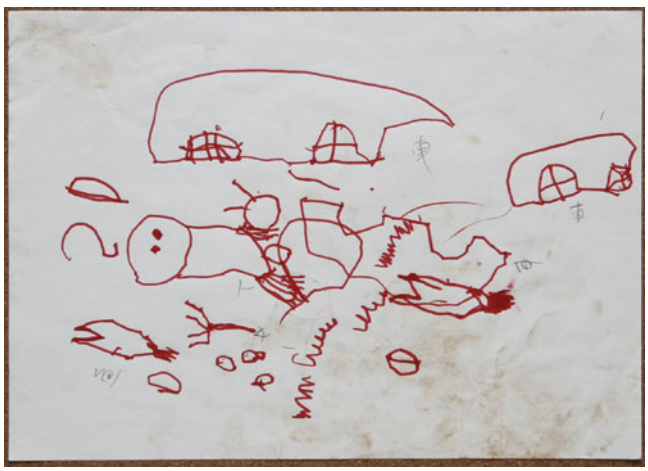

Fig. 6.14 Ten-year-old boy: "cars, person, fish, tree, leaf" drawn with a red pen. Incomplete gestalt painting. Multiple viewpoints

perhaps indicating the resilience factor, "Insight and warmth." "Vehicles, airplanes, and electrical appliances," which belong to a different culture, are far removed from the daily life of Pygmy children, but they are fond of such unfamiliar things and expect to obtain them in future. The children are likely able to imagine how the new and strange things are desirable. Likewise, they expressed in their drawings that they are in favor of both their own culture and things from foreign cultures. This openness in their transitional stage from tradition to innovation might lead the resilience factor, "Confident optimism."

6.6.3 Innovators and Followers

The last resilience factor listed by Klohnen, "Skilled expressiveness" was especially shown by two ingenious boys

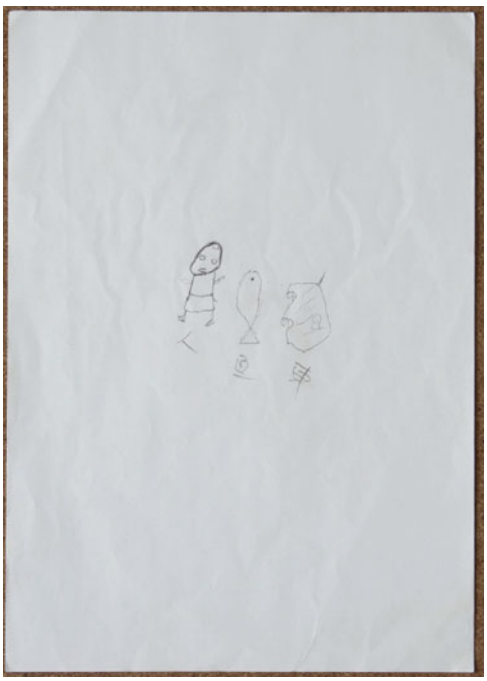

Fig. 6.17 Nine-year-old girl: "person, fish, car" drawn with a pencil. Incomplete gestalt painting. Weak. Multiple viewpoints

Fig. 6.19 Seven-year-old boy: "man with rifle, persons, cook, car, cacao, hand" Incomplete gestalt painting. Kinetic painting. X-ray painting

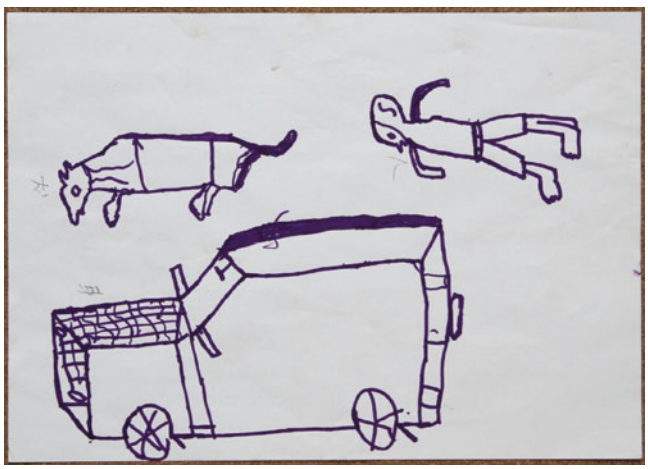

Fig. 6.18 Eleven-year-old boy: "car, person, dog" drawn with a purple pen. Strong. Multiple viewpoints

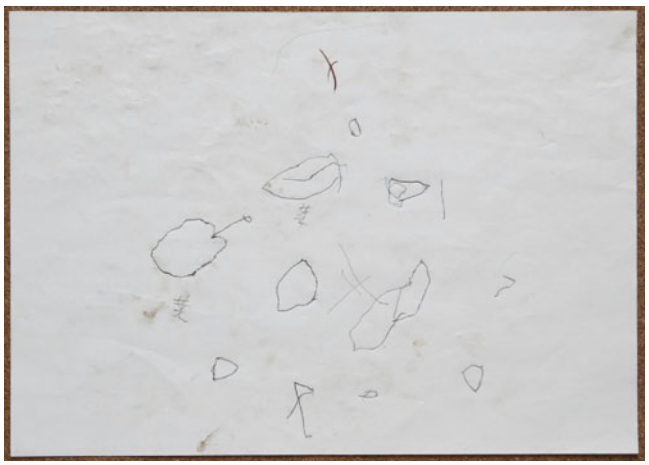

Fig. 6.20 Seven-year-old boy: "leaves, circle, line" drawn with a pencil. Incomplete gestalt painting. Weak

(Figs. 6.29 and 6.30) who exhibited skillful and artistic expression through their drawings. Although they had not had any opportunity to learn drawing skills, they drew accurate shapes and colored them originally. They drew some familiar things such as a banana, a traditional knife and the moon realistically; on the other hand, unfamiliar things like helicopters and audio-decks were colored fantastically. The key point is that they were able to depict their favorite things without any models but rather by using their memories of their everyday life or magazines.

This ability reflects that their perceptional, intellectual and emotional capacities are extremely high. The two boys became innovators as they challenged new ways to paint beautifully. On the other hand, limited opportunities to learn drawing skills tended to make most of the children stay at the early stage of iconic development, typified by the X-ray painting style, in which they drew what they knew instead of what they saw (intellectual realism). Therefore, most of the children looked like followers. The two innovative boys and the other boys who followed them usually played together.

Fig. 6.21 Five-year-old boy: "car, person, palm, pineapple, fish, leaf" with an orange pen. Multiple viewpoints. X-ray painting

Fig. 6.24 Fourteen-year-old boy: "house, airplane, peanut, star, moon" drawn with a red pen

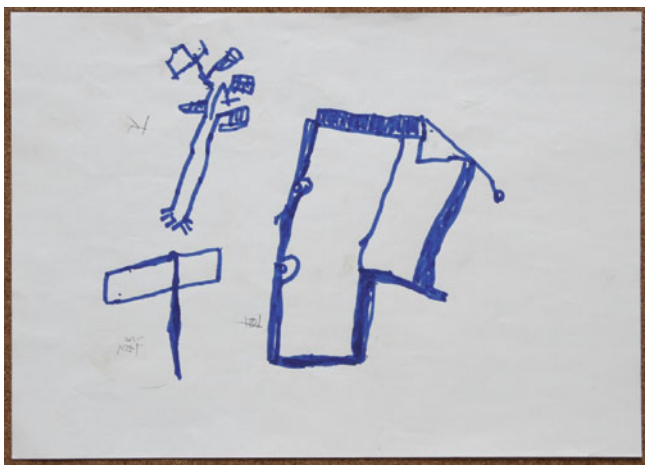

Fig. 6.22 Thirteen-year-old boy: "car with antenna, tree, flag" drawn with a blue pen. Incomplete gestalt painting. Multiple viewpoints

Fig. 6.25 Six-year-old girl: "people, car with a person, fish, leaf, cloth, cacao" drawn with a red pen. Incomplete gestalt painting. X-ray painting

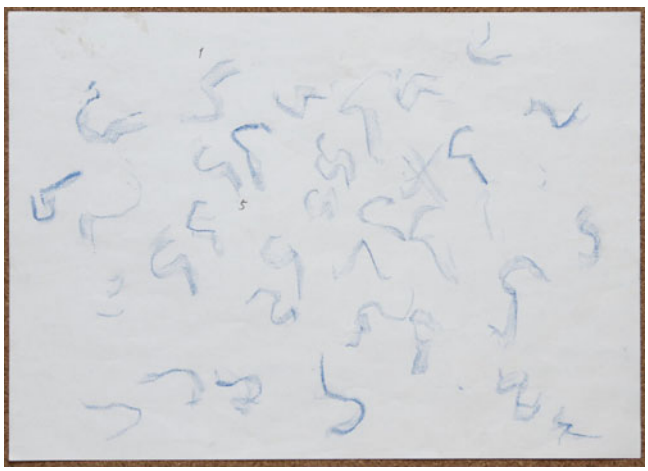

Fig. 6.23 Five-year-old boy: "1, 5 (numbers)" drawn with a blue pastel

If drawings were introduced into their everyday life, the followers would learn how to paint from the gifted boys, perhaps raising the group level of iconic development. As I mentioned before, their learning situation should be considered to be at a transitional stage in terms of the school education system. The two innovative boys had little formal education; nevertheless, they showed a high level of perception, memory and artistic emergence. That is why I called

Fig. 6.26 Twelve-year-old boy: "people, cars, tree, house, soccer ball, tomato, moon, turtle, butterfly. Person with a traditional knife" drawn with blue, black and orange pens. Incomplete gestalt painting. Multiple viewpoints

Fig. 6.28 Eleven-year-old girl: "car, people, me, house, flower, leaf" drawn with purple, orange, green pens. Incomplete gestalt painting. Multiple viewpoints

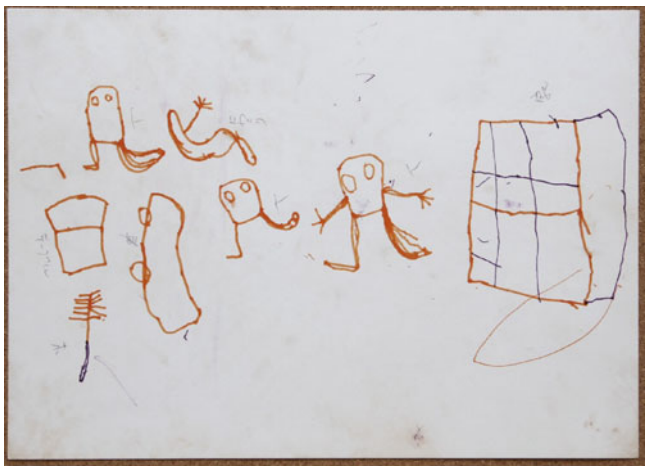

Fig. 6.27 Eleven-year-old girl: "house, people, car, cook, table, tree" drawn with orange and purple pens. Incomplete gestalt painting. Multiple viewpoints

Fig. 6.29 Twelve-year-old boy: "helicopter, motorbike, radio, DVD, ball, boat, mobile phone and moon" with pastel crayons. Artistic painting. Multiple viewpoints

them innovators and speculated that there is not a serious relation between innovation and school education.

Moreover, Drucker (2000) noted that, "innovation essentially starts as a tiny, provisional and fussy thing" and "the occasion of innovation is usually found around the field." In fact, the two boys in my research disclosed their new method through small drawings at their sites. Although their new discoveries did not affect other Baka members at that time, in the future they might expand their innovation with the "continu[ed] learning and self-enlightenment which are essential for social innovation" (Drucker 2000).

6.7 Conclusion

In conclusion, the Baka Pygmy children can be considered to be resilient. Through the psychologically involved task of drawing, "resilience, i.e., an acceptable and flexible attitude to a transitional and critical situation" was observed. If art instruction was introduced, the skillful, expressive, innovative boys especially should raise the iconic development in the group. Likewise, human beings might be speculated to have been thriving in the face of adversity in much the same manner as the Pygmy children developed their own learning skills.

Fig. 6.30 Fifteen-year-old boy: "car with a person, man, pot, cap, flag, table, notebook, banana, papaya, star, moon" drawn with pastel crayons. Artistic painting. Multiple viewpoints

Fig. 6.31 Fifteen-year-old boy: "houses, traditional tent *mongle,* car, motor bike, boat" drawn with pastel crayons

References

Connor KM, Davidson JRT (2003) Development of a new resilience scale: the Connor-Davidson Resilience Scale (CD-RISC). Depress Anxiety 18:76–82

Drucker P (2000) The essential Drucker on society. Tuttle-Mori Agency Inc., Tokyo

Eng H (1954) The psychology of children's drawings. Routledge and Kegan Paul Ltd., London

Huss E, Alhaiga-Taz S (2013) Bedouin children's experience of growing up in illegal villages, versus townships in Israel: Implications of social context for understanding stress, and resilience in children's drawings. Int J Art Therapy 18(1):10–19

Iwata K (1985) Kodomo-bunnka eno shiten. In Iwata K (ed) Kodomo-Bunka no gennzou. The publisher association of Japan Broadcast, Tokyo. (In Japanese)

Klohnen EC (1996) Conceptual analysis and measurement of the construct of ego-resiliency. J Pers Soc Psychol 70(5):1067–1079

Kobasa SC (1979) Stressful life events, personality, and health: an inquiry into hardiness. J Pers Soc Psychol 37:1–11

Luthar SS, Cicchetti D, Becker B (2000) The construct of resilience: a critical evaluation and guidelines for future work. Child Dev 71(3):543–562

Lyons J (1991) Strategies for assessing the potential for positive adjustment following trauma. J Traumatic Stress 4:93–111

Rutter M (1985) Resilience in the face of adversity: protective factors and resistance to psychiatric disorders. Br J Psychiatry 147:598–611

Social Learning, Trial-and-Error, and Creativity

7

Nobuyuki Takahashi, Ayaka Hatano, Misato Inaba, Ryoichi Onoda, and Dora Simunovic

Abstract

Homo sapiens is a species whose behaviors are determined heavily by learning. Typically, research on learning has assumed implicitly a dichotomy between individual learning and social learning, and examined under what conditions each type of learning ability can be adaptive. These previous studies have two problems, however. First, there is little empirical data on the relationship between individual learning and social learning among humans. Second, they assume that social learning is usually represented by the single ability of imitation, while individual learning is represented by either trial-and-error or creativity, although these two abilities are quite different from each other. The current study investigated the relationships between these three major human learning abilities for the first time. The results of the two experiments showed that there is a positive relationship between creativity and imitation, and no relationship between trial-and-error and imitation. The relationship between creativity and trial-and-error remains ambiguous. These results suggest that there is no trade-off between individual learning and social learning. Thus, it partly supports a new theoretical argument that a social learner-explorer, who combines accurate social learning with exploratory individual learning, is most adaptive under certain fluctuating environments.

Keywords

Creativity • Imitation • Intelligence • Learning • Trial-and-error

7.1 Introduction

Learning is a means to collect information, which enables individuals to acquire appropriate behaviors. Although many species have the ability to learn, learning is one of the key characteristics uniquely developed in humans. *Homo sapiens* is the species whose behavioral plasticity is most likely the highest. People have to acquire a considerable number of behaviors after they are born into the world. Another characteristic which is equally important to note is that only *Homo sapiens* has cumulative culture (e.g., Dean et al. 2012; Tennie et al. 2009).[1] A piece of new knowledge which is discovered by a single individual is transmitted to others if it is useful. This process prevents new knowledge from being lost, which produces cumulative culture. These two characteristics clearly show that learning behaviors among humans are extraordinary. In order to explain this fact, various research has been conducted.

Previous research on learning has typically assumed a dichotomy between individual learning and social learning

N. Takahashi (✉)
Center for Experimental Research in Social Sciences, Graduate School of Letters, Hokkaido University, N10, W7, Kita-ku, Sapporo, Hokkaido 060-0810, Japan
e-mail: ntakahas@let.hokudai.ac.jp

A. Hatano • M. Inaba • R. Onoda D. Simunovic
Graduate School of Letters, Hokkaido University, N10, W7, Kita-ku, Sapporo, Hokkaido 060-0810, Japan
e-mail: ahatano@lynx.let.hokudai.ac.jp; minaba@lynx.let.hokudai.ac.jp; onoda@lynx.let.hokudai.ac.jp; saveusmilkboy@gmail.com

[1] There are, however, a counter argument that other primates are capable of cumulative culture (e.g., Horner et al. 2006; Yamamoto et al. 2013).

T. Akazawa et al. (eds.), *Dynamics of Learning in Neanderthals and Modern Humans Volume 2: Cognitive and Physical Perspectives*, Replacement of Neanderthals by Modern Humans Series, DOI 10.1007/978-4-431-54553-8_7,

(e.g., Aoki et al. 2005; Cavalli-Sforza and Feldman 1981; Boyd and Richerson 1985; Rogers 1988). The key difference between these two is whether the source of information originates in oneself or others. We call learning from ones' own behavior individual learning, and learning from others' behavior social learning. Usually individual learning is considered a more basic ability since species who have very limited cognitive abilities, such as *Paramecium caudatum*, have it, whereas social learning is a more advanced ability since it requires sophisticated cognitive and mental abilities.

One of the key insights in previous research is that cost and benefit of individual and social learning abilities are different. For an individual to learn by himself, he has to invest his resources. However, other individuals can imitate the fruit of his labor at no extra cost to themselves. This presents us with a free-rider problem. For each individual, it is better to engage in social learning. However, if everyone engages in social learning, no new knowledge would be acquired. Therefore, many previous studies assumed that individual learning and social learning are alternative ways to acquire information, and examined under what conditions social learning can be adaptive (e.g., Borenstein et al. 2008; Kameda and Nakanishi 2002; Wakano et al. 2004).

One of the most ambitious arguments is the one adopted as a working hypothesis by the Replacement of Neanderthals by Modern Humans (RNMH) project which was launched in 2010 by the grant from the Ministry of Education, Culture, Sports, Science and Technology of Japan. In this project, theoretical studies on learning are applied to explain why *Homo neanderthalensis* went extinct and left *Homo sapiens* the only hominin still existing on earth. The working hypothesis, which is called the learning hypothesis, states that there is a genetic difference in the learning strategies employed by Neanderthals and *Homo sapiens*. Archeological evidence suggests that Neanderthals had produced virtually unchanged stone tools during the Middle Paleolithic period (about 300,000 years ago until 30,000 years ago). These Mousterian tools, as they are called, are characterized by Levallois points. Since making Levallois points is extremely difficult and probably requires years of training, it is speculated that the continuation of Mousterian industry was possible thanks to the Neanderthals' social learning ability. At the same time, since Neanderthals had not developed a new industry for at least about 270,000 years (Diamond 1991), it also suggests that they had a low level of individual learning ability. The story of *Homo sapiens* is quite different. *Homo sapiens* is characterized by cumulative yet rapidly changing culture. During the Upper Paleolithic (about 50,000–10,000 years ago), there have been number of industries (e.g., Chatelperronian, Aurignacian) for stone tools exhibiting varying techniques and characteristics. For that to have come about, both social learning ability and individual learning ability (innovation) should be high among *Homo sapiens*.

Whether or not this conceptualization is a good one is questionable, however. First, we believe that the dichotomy of social versus individual learning does not reflect the true nature of learning. Although social learning is usually represented by the single ability of imitation in the previous literature, two abilities represent individual learning—trial-and-error and creativity. Although trial-and-error and creativity have been used interchangeably in the previous literature, we believe that these two should be distinguished. Thus, we need to think about the relationships among the three learning abilities. However, there have been few studies that empirically examined the relationships among different learning abilities.

Since these three learning concepts have been defined in various ways in each discipline, here we describe a working definition for each ability. First, we consider imitation to be the acquisition of new behavior through the observation of others engaging in it. Examples include learning craftsmanship, farmwork, and how to play musical instruments. It has been found that there are other species, such as chimpanzees, marmosets, capuchin monkeys, dolphins, rats, and pigeons, which have the ability of imitation (e.g., Bouchard et al. 2007; Bugnyar and Huber 1997; Custance et al. 1995; Custance et al. 1999; Heyes et al. 1992; Krützen et al. 2005; Voelkl and Huber 2000, 2007). Compared to the other two learning abilities suggested here, there is a relatively clear consensus on what imitation means.

Second, we consider trial-and-error to be a method of problem solving, repair, tuning, or obtaining new knowledge. In trial-and-error, individuals learn by making a first attempt, analyzing the failure, making a change, and trying a new behavior. It is a solution-oriented, problem-specific, non-optimal method that needs little prior knowledge. It is a method which requires little insight and theory. It is usually not the most desirable option but a last resort for a problem when all other means turn out to be futile. It is tedious and time-consuming. By trial-and-error animals engage in operant conditioning. Examples include evolution by natural selection in biology, finding new drugs, and deciphering cryptographs by a computer. We know that many species (pigeons, mice, and even *Paramecium caudatum*) have the trial-and-error ability. In this sense, there is a relatively clear consensus on what trial-and-error means.

The last learning ability we investigate here is creativity, which is also the most controversial one. There is a long history of research in psychology and other related disciplines since Galton in the nineteenth century. Initially researchers who focused on intelligence assumed that creativity is a subcategory of intelligence, but in the middle of the twentieth century some researchers began to consider creativity a separate concept from intelligence (Guilford 1950). Since then, many theories, experiments, and perspectives have proposed. The concepts that have been considered synonymous with creativity include fluid intelligence (Dunker 1945), divergent

thinking (Guilford 1967), conceptual blending (Koestler 1964), counterfactual thinking (Markman et al. 2009), and so on. Thus, there is no consensus on what creativity means. Typical examples include innovation, new behavior based on insight, various types of art, giving a new meaning to a familiar object, and application of an already acquired knowledge to unknown situations. Thus, there is a huge variety.[2] From an evolutionary perspective, creativity has its significance because it enables humans to acquire a completely new and complex behavioral pattern very fast. Also, a new behavioral pattern adopted by creativity can be generalizable to other situations since humans understand why it is adaptive. Based on these observations, we decided our working definition of creativity as the ability to re-imagine an observed state of affairs as something other than what it strictly is, or transfer it into another context.

Based on the working definitions shown above, the current study investigated the relationships between these three major human learning abilities for the first time. There have been empirical studies that focused on a particular learning ability. A few empirical studies have examined the relationship between two learning abilities—individual learning and social learning—in species other than *Homo sapiens* (e.g., Bouchard et al. 2007; Giraldeau and Caraco 2000; Reader and Laland 2002). In humans, a few studies have empirically examined the relationship between individual learning and social learning (e.g., Kameda and Nakanishi 2002, 2003; McElreath et al. 2005, 2008; Morgan et al. 2012; Toelch et al. 2010; Mesoudi and O'Brien 2008; Mesoudi 2008, 2011). However, none of them distinguished creativity from trial-and-error ability. If we use the working definitions discussed above, what these studies measured as individual learning may correspond to either trial-and-error or creativity, while what they measured as social learning may correspond to imitation. The second problem in the previous literature is that often it is not clear whether they examined strategies or abilities. According to the learning hypothesis in RNMH, what we should focus on is learning ability. However, in the previous empirical studies it is often not clear whether individuals who engaged in social learning could engage in individual learning if they wished or they were not capable of individual learning (and vice versa). Therefore, the current study is the first attempt to examine the relationships among three types of learning abilities in humans.

Although the current study was intended as an exploratory examination of the three learning abilities, we could expect different patterns of relationships based on each theoretical perspective. First, regarding the relationship between trial-and-error and creativity both of which have been considered individual learning, from the majority of mathematical modeling studies we would expect that these two abilities are positively correlated. From their perspective, as long as people learn from their own experience, the difference between a trial-and-error method and creativity does not matter. However, our common sense tells us that these two abilities are quite different. It is often said that trial-and-error is the last resort for those who are not creative. Also, although computer is the best tool to solve a problem by trial-and-error, we would never consider the computer to be creative. Based on these intuitions, we would expect that between trial-and-error and creativity there is no relationship or a negative one.

Second, regarding the relationship between imitation and the two individual learning abilities (trial-and-error and imitation), if there is a trade-off between social learning and individual learning as most of the theoretical studies suggest, we would expect that both individual learning abilities are negatively correlated with imitation. However, we could also expect the opposite. Aoki (2010) suggested that a combination of social learning and individual learning is most adaptive under certain fluctuating environments. In addition, Reader and Laland (2002) argued that social learning is positively related to individual learning, although their unit of analysis is a species. Furthermore, Mesoudi (2011) found a positive correlation between individual learning and social learning, but it is not clear whether this relationship exists in learning abilities rather than learning strategies. Based on these opposite argument, we might expect that both individual learning abilities are positively correlated with imitation.

While there could be other possibilities as well, we conducted two laboratory experiments to test what the actual connection between different learning abilities is with these most plausible relationships in mind.

7.2 Method

We have conducted two experiments. Both experiments were conducted in the Group Experiment Lab at Center for Experimental Research in Social Sciences (CERSS), Hokkaido University. Participants were asked to perform tasks designed to measure trial-and-error, creativity, imitation, and certain other abilities.

7.2.1 Experiment 1

7.2.1.1 Method of Experiment 1

Fifty-eight undergraduate students participated in Experiment 1.[3] The total length of an experimental session was about 90 min.

[2] Since the amount of psychological literature on creativity is huge, we do not discuss them further. See, for example, Hocevar (1981) for a review.

[3] In the analysis, we excluded five participants who had known at least one of the tasks described below.

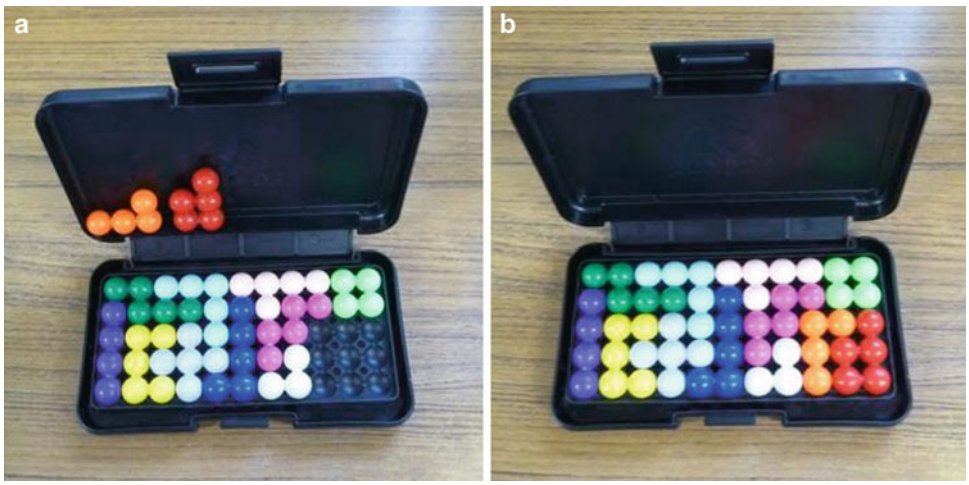

Fig. 7.1 Lonpos task. Initial setting (**a**) and solved setting (**b**). Participants were asked to fill in empty spaces on a board with different-shaped pieces. This task was intended to measure trial-and-error ability

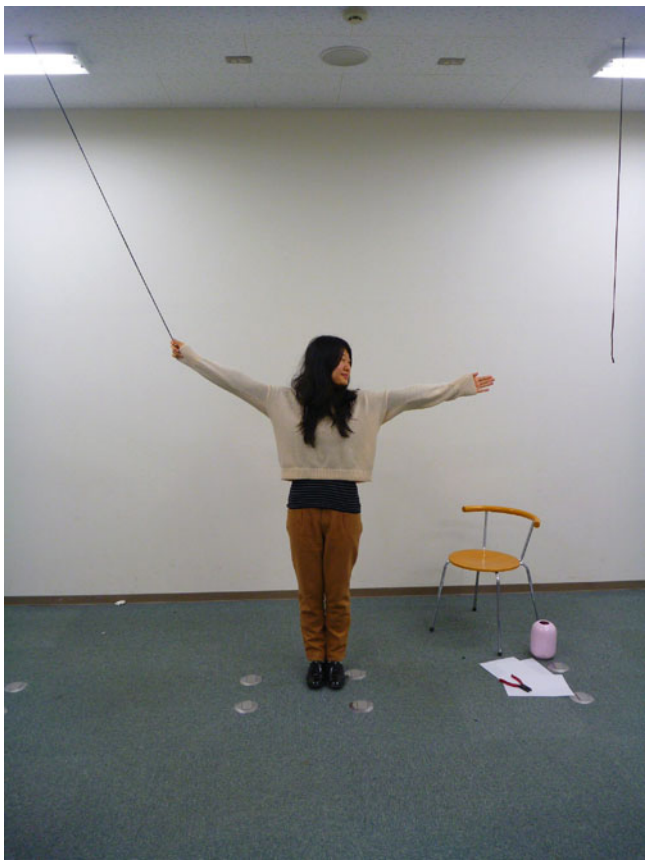

Fig. 7.2 Photo for the two-string problem. Participants were given the above photo in which they saw a chair, a vase, pliers, and several sheets of paper on the floor. They were presented with the following problem: "You want to tie together two strings that are hanging down from the ceiling too far apart for you to grab them both at the same time. What would you do?" This task was intended to measure creativity

The first experiment consisted of three types of tasks. The first one measured trial-and-error. We used the Lonpos game in which participants were asked to fill in empty spaces on a board with different-shaped pieces within a ten-minute time limit (see Fig. 7.1a, b). We measured how long it took to solve the problem.

The second task measured creativity. For this purpose, we used the two-string problem (Maier 1933) and the candle holder problem (Dunker 1945), both of which are known to measure functional fixedness (a mental block against using an object in a new way that is required to solve a problem, Dunker 1945) in cognitive psychology. In the two-string problem, participants were given a photo of a person who was trying to tie together two strings that hung down from the ceiling (see Fig. 7.2). There was a chair, a vase, pliers, and several sheets of paper on the floor. Participants were presented with the following problem: "You want to tie together two strings that are hanging down from the ceiling too far apart for you to grab them both at the same time. What would you do?" Then they wrote down up to three answers. Later, five undergraduate students rated whether the answers qualified as feasible. We used the average of five feasibility evaluations as our variable.

In the candle holder problem, participants were given a matchbox, a candle, and tacks, and asked to attach the candle to a corkboard, which represented a wall (see Fig. 7.3a, b) within a ten-minute time limit. We measured whether or not, and how long it took participants to attach the candle to the wall.

The third task measured imitation. For that we used a wire puzzle. First, participants were handed a wire puzzle and tried to solve it within 3 min. After examining various wire puzzles, we chose the one that most of the people could not solve it within 3 min.[4] Then, they watched a

[4]Only three participants could solve it without watching the video (see Table 7.1).

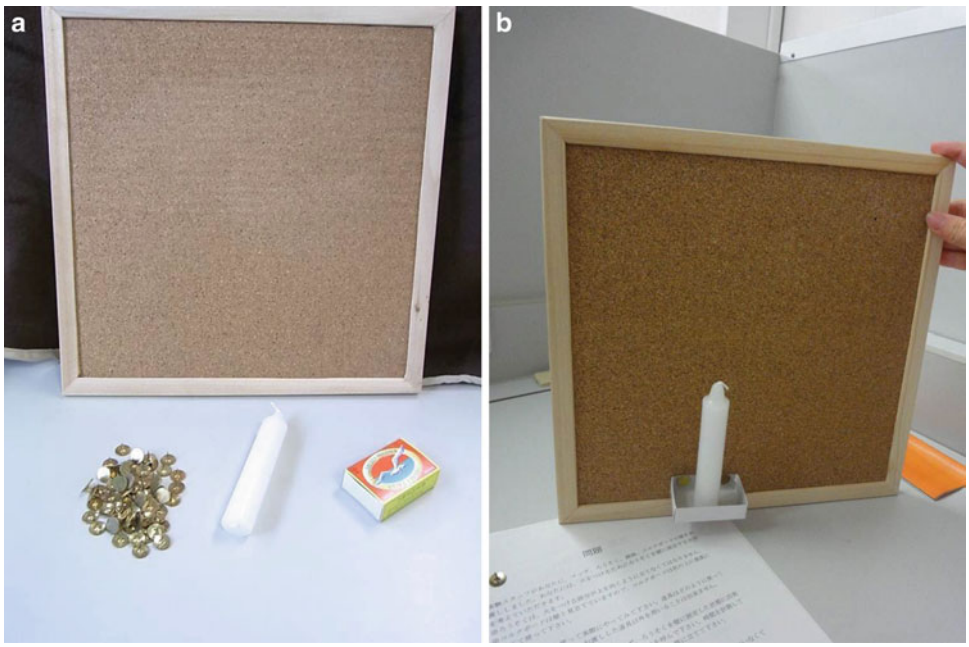

Fig. 7.3 Photo for the candle holder problem. Initial setting (**a**) and model answer (**b**). Participants were given a matchbox, a candle, and tacks, and asked to attach the candle to a corkboard, which represented a wall. This task was intended to measure creativity

Table 7.1 Descriptive statistics of variables in Experiment 1

	N	Mean	Standard deviation
Trial-and-error			
Lonpos (time-remaining)	40	420.01	102.91
Lonpos-alt (time-remaining)	53	360.25	147.17
Creativity			
String (feasibility)	52	4.76	0.74
Candle (solved)	53	0.49	0.50
Candle (time-remaining)	26	182.01	130.16
Candle-alt (time-remaining)	53	89.43	128.88
Imitation			
Wire (solved)	50	0.72	0.45
Wire (time-remaining)	36	119.64	48.05
Wire-alt (time-remaining)	50	86.14	67.78

N of wire (solved) is 50 because three participants solved the wire task before watching the demonstration video

Fig. 7.4 Wire puzzle. Participants were asked to solve the puzzle after watching a video of a demonstrator solving it. This task was intended to measure imitation

video of a demonstrator solving it. We measured whether or not, and how long it took participants to solve the puzzle within a three-minute time limit for the second time (see Fig. 7.4).

In addition to the three learning abilities, we measured working memory capacity. Although there is no theoretical reason to predict that trial-and-error and imitation abilities in general are influenced by memory capacity, the specific tasks that we used for this experiment might be influenced. If this is the case, we could use the score of the memory task as a control variable to measure the true trial-and-error and imitation abilities. For this purpose, we used the find-the-pair task, which is a single player PC game in which the objective is to match all the cards with identical pictures on them in the least number of moves. We measured how long it took participants to finish it within a five-minute time limit as well as how many times participants turned the cards.[5]

[5]We agree with the reviewer that controlling for memory capacity is not the best option. Nevertheless, we measured memory capacity because it is a feasible option. Fortunately, it turned out that memory had no relationship with either trial-and-error or imitation abilities in Experiment 1.

Table 7.2 Correlation coefficients among three learning abilities in Experiment 1

	Lonpos (time-remaining)	String (feasibility)	Candle (solved)	Candle (time-remaining)
String (feasibility)	–0.049	–	–	–
	–0.116			
Candle (solved)	0.177	0.345*	–	–
	0.052	0.329*		
Candle (time-remaining)	–0.437+	–0.100	–	–
	–0.333	–0.046		
Wire (solved)	0.143	0.276+	0.218	0.033
	0.136	0.307*	0.218	0.052
Wire (time-remaining)	0.247	0.118	–0.010	–0.093
	0.232	0.127	–0.056	0.069

In each cell, Pearson correlation coefficients are shown above, and Spearman correlation coefficients are shown below
The value of the time-remaining variable of those who could not solve the task was treated as missing
Measures for creativity are shown in red, measures for imitation are shown in blue, and measures for trial-and-error are shown in yellow
+$p<0.10$, *$p<0.05$

Table 7.3 Correlation coefficients among three learning abilities in Experiment 1

	Lonpos-alt (time-remaining)	String (feasibility)	Candle (solved)	Candle-alt (time-remaining)
String (feasibility)	–0.021	–	–	–
	–0.002			
Candle (solved)	0.162	0.345*	–	–
	0.110	0.329*		
Candle-alt (time-remaining)	0.041	0.195	–	–
	0.012	0.291*		
Wire (solved)	0.366**	0.276+	0.218	0.166
	0.363**	0.307*	0.218	0.218
Wire-alt (time-remaining)	0.347*	0.276+	0.170	0.106
	0.334*	0.292*	0.142	0.168

In each cell, Pearson correlation coefficients are shown above, and Spearman correlation coefficients are shown below
The value of the time-remaining variable of those who could not solve the task was set to 0
Measures for creativity are shown in red, measures for imitation are shown in blue, and measures for trial-and-error are shown in yellow
+$p<0.10$, *$p<0.05$, **$p<0.01$

7.2.1.2 Results of Experiment 1

We were primarily interested in correlations among variables. We used two types of variables: (1) whether participants could solve the problem (coded as 1) or not (coded as 0),[6] and (2) how long it took to solve the problem. For ease of understanding and for convenience, we reversed the score of the second type of variables so that they represent time-remaining. Therefore, the smaller the number, the lower the ability.

Descriptive statistics are shown in Table 7.1. Both the standard variables and the alternative variables that measured timing are shown. In Lonpos (time-remaining), Candle (time-remaining), and Wire (time-remaining), the value for those who could not solve the task was treated as missing, while in Lonpos-alt, Candle-alt, and Wire-alt, the value was set to zero. Often it did not matter whether we used the standard variables or the alternative variables, but below we report the difference when existed.

The main results are shown in Tables 7.2 and 7.3. Since distributions of most of the variables were not normal, in addition to Pearson's correlation coefficients, we report Spearman's rank-order correlation.[7] In most cases, these two correlation coefficients gave us qualitatively identical results. First, there is a significant positive correlation between the two-string problem and the candle holder problem. Those who could solve the two-string problem were more likely to solve the candle holder problem. This result suggests that there is a certain level of validity in the two tasks to measure creativity.

[6]When we needed to have evaluations as objective as possible, we asked undergraduate students who had not themselves participated in the experiment or the preparation of the experiment to evaluate whether or not each participant solved a problem. In this case, we took the average of the evaluations. For this type of variables, the larger number also means that a participant's answer was evaluated as correct.

[7]For one dichotomous and one continuous variables, point-biserial correlation coefficient is identical with Pearson's correlation coefficient. For the correlations between two dichotomous variables, Person, Spearman, and Phi are all identical.

Next, we turn to the relationship between creativity and imitation. We found a weak but positive correlation between the two abilities. Those who could solve the two-string problem were more likely to solve the wire puzzle after watching a video of a demonstrator solving it. However, the correlation coefficient between the candle holder problem and the wire puzzle did not reach significance.

Next, we turn to the relationship between trial-and-error and imitation. We found no significant correlation between the remaining time of Lonpos task and whether participants could solve the wire puzzle or the remaining time of it when we used the standard variables (Table 7.2). However, when we used the alternative variables, we found positive relationship between the performance of Lonpos task and that of the wire puzzle (Table 7.3). The implication of this finding is discussed later.

Finally, we turn to the relationship between trial-and-error and creativity. The correlation coefficients between the performance of Lonpos task and any of the creativity tasks did not reach significance. We could see, however, a weak negative relationship between the Lonpos task and the candle holder problem when we used the standard variables. This non-significance may be due to a small number of observations. However, in either case, since this is not strong evidence, we need to be cautious when we interpret the results.

7.2.1.3 Discussion of Experiment 1

Results of Experiment 1 suggested that, first, there is a positive relationship between creativity and imitation. Participants who could solve the two-string problem were more likely to solve the wire puzzle after they watched the experimenter's demonstration. Second, there seems to be no relationship between trial-and-error and imitation among those who could solve the tasks. However, the results suggested that those who could solve the wire puzzle are more likely to solve the Lonpos task. One interpretation is that both tasks seem to involve space perception ability. If this is the case, in the next experiment we should include a measure of imitation or trial-and-error that is not influenced by space perception ability. Third, there was no positive relationship between trial-and-error and creativity. Rather, the relationship, if there is any, would be negative, even though both abilities are considered individual learning in previous studies. These results were confirmed both when we used Pearson correlation coefficients and when we partialled out performance in the memory task.[8] Therefore, we could suggest that there was no trade-off between individual learning ability and social learning ability since no ability was negatively related to imitation. Also, only creativity was positively related to imitation, which partly supports a new theoretical argument that a combination of social learning and individual learning is most adaptive under certain fluctuating environments (e.g., Aoki 2010).

7.2.2 Experiment 2

7.2.2.1 Method of Experiment 2

Although the results of Experiment 1 are informative, since it was the first attempt, it was merely a prototype and as such had many issues. First, we needed to refine our measurements. The problem we had is how to treat the remaining time for those who could not solve the task. We tried two methods to minimize the problem. First, we used the standard variables in which we treated them as missing. Obviously, however, such a method decreased the number of observations significantly. Second, we used the alternative variables in which we treated them as zero. By using them, we did not lose observations, but obviously the values were biased. Therefore, we needed to increase the number of observations without involving an artificial method. Second, we needed to use more objective evaluations of the participants' performance. Third, we needed to include more tasks to measure each learning ability, especially creativity. In order to resolve these issues as much as possible, and to replicate Experiment 1 conceptually, we conducted Experiment 2.

In Experiment 2, participants were 60 undergraduate students. The total length of an experimental session was about 150 min. As in Experiment 1, in each session, several participants were recruited and performed various tasks to measure trial-and-error, creativity, and imitation. Since memory had little influence on any of the learning abilities in Experiment 1, we dropped it from Experiment 2. However, since we suspected that the performance of the Lonpos puzzle and the wire puzzle may have been influenced by space perception ability in Experiment 1, in Experiment 2 we included a space perception task in order to control the influence of that factor statistically when necessary.

In order to measure trial-and-error, as our new original task, we developed the coin task. On the participants' computer screens, three buttons, a circle, triangle and a star, were displayed (Fig. 7.5). If the participants clicked the buttons in a certain way, they would be rewarded with coins on the computer. Their objective was to figure out what pattern of clicking the buttons would get the coins. This is conceptually equivalent to the Skinner box used in psychology of learning, except that participants were not compensated in reality. The time limit was 7 min, and participants wrote down what they believed to be the correct answer. We measured whether their answers were correct and how many coins they had collected. Participants took part in two problems, each of which

[8] Since how long it took participants to finish the memory task as well as how many times participants turned the cards did not show any correlation with either of trial-and-error or imitation, we omit presenting the results regarding memory capacity.

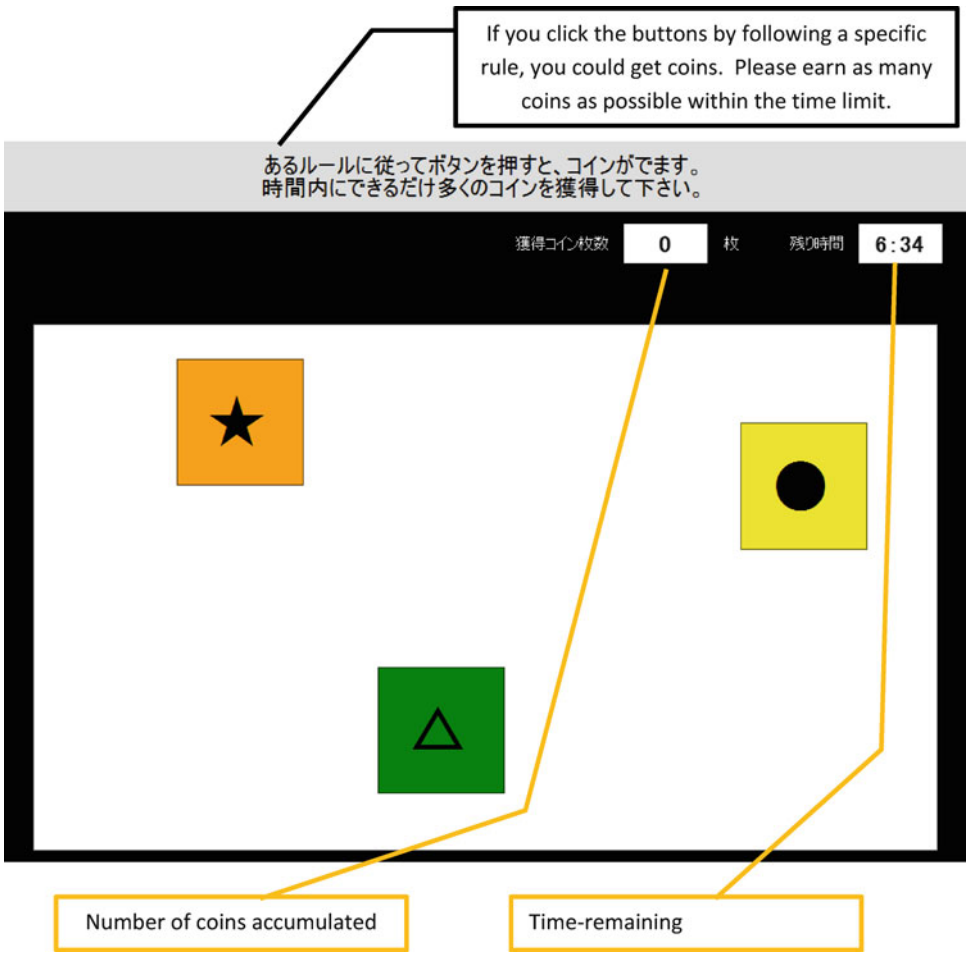

Fig. 7.5 Coin task. On the participants' computer screens, three buttons: a circle, triangle and a star, were displayed. If the participants clicked the buttons in a certain way, they would be rewarded with coins on the computer. Their objective was to figure out what pattern of clicking the buttons would get the coins. The time limit was 7 min, and participants wrote down what they believed to be the correct answer. This task was intended to measure trial-and-error

had a unique pattern as a correct answer. This new task does not involve space perception ability. Therefore, spurious correlation due to space perception ability should not be observed.

We used numerous tasks to measure creativity in Experiment 2. First, we used Cattell CFIT Scale 3 Form A, which is one of the established tests developed to measure fluid intelligence. Cattell (1971) classified intelligence into two categories: crystallized intelligence and fluid intelligence. Crystallized intelligence includes the ability to use skills, knowledge, and experience. It reflects one's lifetime or intellectual achievement, such as vocabulary, depth and breadth of general knowledge, and ability to reason using words and numbers. Thus, it is a product of educational and cultural experience. On the contrary, fluid intelligence includes ability to think logically and solve problems in novel situations, independent of acquired knowledge. Thus, fluid intelligence is a closer concept to what we consider creativity. CFIT is one of the most popular non-verbal multiple choice IQ tests that measure fluid intelligence.

In addition to Cattell CFIT, to measure creativity we had two tasks that participants had to perform and two paper-and-pencil tasks. One of the performing tasks is the candle holder problem used in Experiment 1, and the other is the ring task (McCaffrey 2012). The ring task originally developed in McCaffrey (2012) was a paper-and-pencil task, but we modified it into a live performance task. Participants were handed two rings, a match box, and a candle, and asked to securely fasten the rings so that they would not fall apart when lifted up (see Fig. 7.6a, b). The time limit was 10 min. The answer was to remove the wick from the candle and use it to tie the rings together.[9] Using the candle for an unusual purpose is the key to solving this problem. We measured

[9]In addition to the original answer in McCaffrey (2012), we also accepted binding the rings with the matchbox paper as an answer.

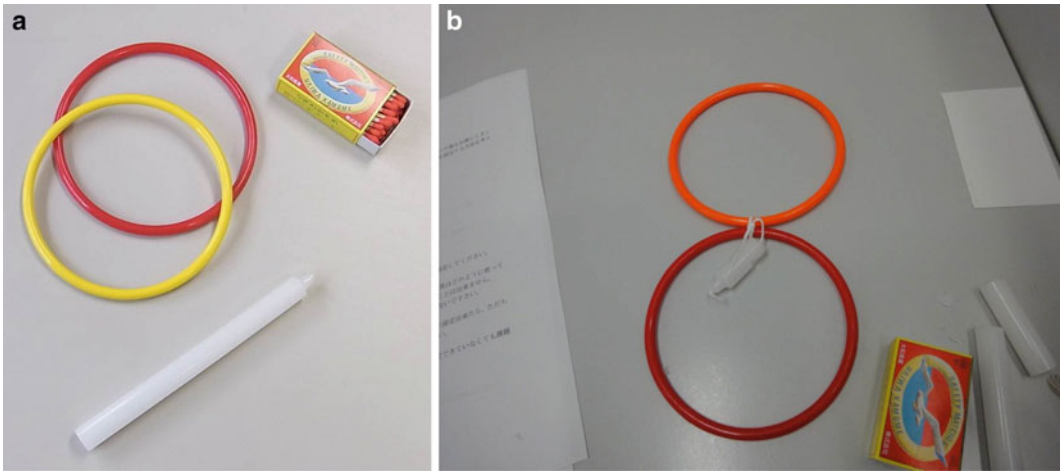

Fig. 7.6 Ring problem. Initial setting (**a**) and model answer (**b**). Participants were handed two rings, a match box, and a candle, and asked to securely fasten the rings so that they would not fall apart when they lift them up. This task was intended to measure creativity

whether or not the participants securely fastened the rings together, and how long it took them to do so within a ten-minute time limit.

The two paper-and-pencil tasks were also adopted from McCaffrey (2012). One was the truck task. Participants read a scenario describing a truck stuck under an overpass. The height of the overpass was just barely as high as the truck. The truck top had become wedged so tightly beneath it that the driver could not go forward or backward. Participants had to write down a solution for the driver so that he could get his truck unstuck all by himself without damaging either the top of the truck or the overpass. The time limit was 4 min. There are two model answers; either to deflate all the tires, or to add new weight so the truck would go down. We used the average of evaluations by six undergraduate students as the performance indicator. We also measured how long it took to finish the task.[10] The other paper-and-pencil measure of creative thinking was the light task. Participants read a scenario describing three light bulbs in a room. Outside the room were three switches, all in the off position. In the scenario, the participants themselves were placed outside of the room where they could not see the light bulbs. Participants had to write down a solution to determine which switch turns on which light bulb. They could only open the door once and once they opened the door they could not change the position of any of the switches. The solution is to turn on two of the switches for several minutes and then turn one of them off before entering the room. The light bulb which is warm (but off) matches the first switch that had been turned on and off. The light bulb which is currently on matches the second switch that had been turned on (and left on). The light bulb which is off and cold matches the switch that had not been touched. We used the average of evaluations by ten undergraduate students as the performance indicator. We also measured how long it took to finish the task.

In order to measure imitation ability, we used the wire puzzle that was used in Experiment 1. Of course, using multiple measures of the imitation ability would be ideal, however, due to practical constraints such as participants' fatigue and the length of an experimental session, we placed our priority to the measures of creativity.

Finally, we included two tasks meant to measure space perception. One was the dice task. Participants needed to reach the goal by rolling a dice so that the spots on the top of it correspond to the red spots on the ground. Participants were instructed to draw the correct path on the answer sheet (see Fig. 7.7a, b). The second one was the cube task. Participants were presented with a three-dimensional figure composed of many cubes. They could also see several holes which go through it. They had to count how many smaller cubes there were (see Fig. 7.8). Please note that they only saw the image: they did not see the actual cubic. The correct answer was 47 cubes. The time limit was 4 min for each task.

7.2.2.2 Result of Experiment 2

Descriptive statistics are shown in Table 7.4. As in Experiment 1, both the standard variables and the alternative variables that measured timing are shown.

Since creativity was the one we judged most critical, we increased the number of tasks to measure creativity in Experiment 2. Thus, we first examined if there were any positive correlations among the measurements of creativity. As in Experiment 1, both Pearson and Spearman correlation

[10]This variable and similar others are not the best indicator of how long it took to solve the problem, since sometimes participants wrote down more than one answer, and the correct answer was not necessarily the last one, and sometimes there was no correct answer.

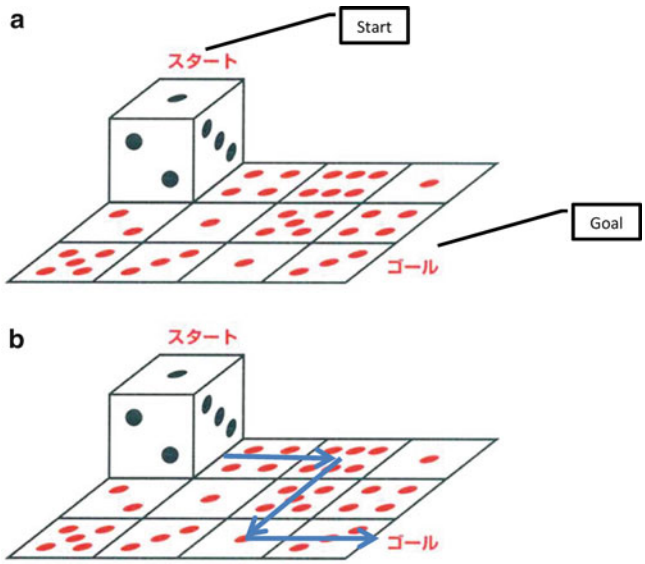

Fig. 7.7 Dice problem. Answer sheet (**a**) and correct answer (**b**). Participants needed to reach the goal by rolling a dice so that the spots on the top of it corresponds to the red spots on the ground. Participants wrote down the correct path on the sheet. This task was intended to measure space perception

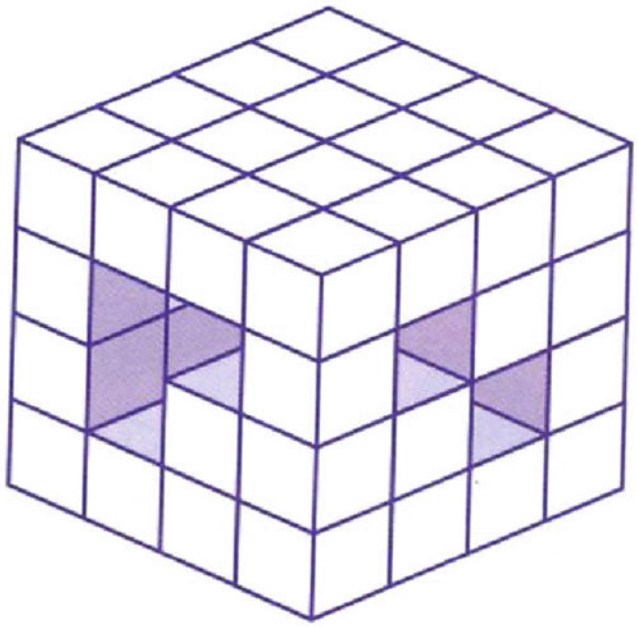

Fig. 7.8 Cube problem. Participants were presented with a three-dimensional figure composed of many cubes. They could also see several holes which go through it. They had to count how many smaller cubes there were. This task was intended to measure space perception

coefficients are shown in Tables 7.5 and 7.6. We found a positive correlation between whether participants solved the ring task and whether they solved the candle task, indicating that there is a positive relationship between two performing creativity tasks. In Table 7.6, we could also see that there is a

Table 7.4 Descriptive statistics of variables in Experiment 2

	N	Mean	Standard deviation
Trial-and-error			
Coin 1 (solved)	59	0.46	0.50
Coin 1 (# of coins collected)	60	26.30	29.54
Coin 2 (solved)	60	0.43	0.50
Coin 2 (# of coins collected)	60	18.15	16.82
Creativity			
Cattell	60	32.93	3.72
Ring (solved)	60	0.42	0.50
Ring (time-remaining)	25	287.08	149.86
Ring-alt (time-remaining)	60	119.62	171.77
Candle (solved)	60	0.40	0.49
Candle (time-remaining)	24	320.42	166.36
Candle-alt (time-remaining)	60	128.17	189.33
Truck (solved)	57	0.55	0.24
Truck (time-remaining)	57	42.35	50.00
Truck-alt (time-remaining)	60	40.23	49.59
Light (solved)	39	0.56	0.41
Light (time-remaining)	39	23.67	40.99
Light-alt (time-remaining)	60	15.38	34.81
Imitation			
Wire (solved)	58	0.60	0.49
Wire (time-remaining)	35	132.26	47.66
Wire-alt (time-remaining)	58	79.81	74.93

N of wire (solved) is 58 because 2 participants solved the wire task before watching the demonstration video

positive correlation between the other variables of the ring task and the candle task. However, we believe that this is an artifact of the positive correlation between the two dichotomous variables. Virtually no other correlations reached significance, suggesting that the other paper-and-pencil tasks as well as Cattell CFIT might measure something different from the performing creativity tasks. As we explained earlier, creativity may mean various things, and each task might measure a different ability. Among them, however, we believe that performing tasks are most relevant to our study because participants actually engaged in behaviors.

Next, we turn to the main results. First, we examined the relationship between creativity and imitation. The results are shown in Tables 7.7 and 7.8. We observe a positive relationship between the candle task and the wire task. Qualitatively these results replicate Experiment 1. In Table 7.7, we could also observe that there is a strong positive correlation between the performance of the light task and the remaining time of the wire puzzle. Since the number of observations is only 26, we may not be able to rely on this result.

Next, we turn to the relationship between trial-and-error and imitation (Tables 7.9 and 7.10). We found no significant correlation between them. Thus, it is more likely that the positive correlation found in Experiment 1 was due to space perception ability.

Table 7.5 Correlation coefficients among the measures of creativity in Experiment 2

	Cattell	Ring (solved)	Ring (time-remaining)	Candle (solved)	Candle (time-remaining)	Truck (solved)	Truck (time-remaining)	Light (solved)
Ring (solved)	0.061	–	–	–	–	–	–	–
	0.088							
Ring (time-remaining)	−0.148	–	–	–	–	–	–	–
	−0.156							
Candle (solved)	0.107	0.345**	0.063	–	–	–	–	–
	0.072	0.345**	0.000					
Candle (time-remaining)	0.129	0.120	−0.088	–	–	–	–	–
	0.180	0.118	−0.150					
Truck (solved)	−0.064	−0.163	−0.136	0.003	−0.151	–	–	–
	−0.073	−0.170	−0.120	0.043	−0.124			
Truck (time-remaining)	0.054	−0.035	0.126	0.188	−0.006	0.191	–	–
	0.068	−0.048	0.163	0.183	−0.075	0.190		
Light (solved)	0.226	0.084	−0.195	0.133	−0.051	0.005	−0.004	–
	0.228	0.021	−0.170	0.116	−0.018	−0.017	0.050	
Light (time-remaining)	0.162	−0.137	−0.126	−0.040	0.221	−0.028	0.156	0.247
	0.283+	−0.102	−0.096	−0.052	0.213	0.012	0.108	0.290+

In each cell, Pearson correlation coefficients are shown above, and Spearman correlation coefficients are shown below
The value of the time-remaining variable of those who could not solve the task was treated as missing
$+p<0.10$, $**p<0.01$

Table 7.6 Correlation coefficients among the measures of creativity in Experiment 2

	Cattell	Ring (solved)	Ring-alt (time-remaining)	Candle (solved)	Candle-alt (time-remaining)	Truck (solved)	Truck-alt (time-remaining)	Light (solved)
Ring (solved)	0.061	–	–	–	–	–	–	–
	0.088							
Ring-alt (time-remaining)	−0.014	–	–	–	–	–	–	–
	0.071							
Candle (solved)	0.107	0.345**	0.309*	–	–	–	–	–
	0.072	0.345**	0.343**					
Candle-alt (time-remaining)	0.134	0.329*	0.279*	–	–	–	–	–
	0.100	0.352**	0.341**					
Truck (solved)	−0.064	−0.163	−0.184	0.003	−0.054	–	–	–
	−0.073	−0.170	−0.194	0.043	0.020			
Truck-alt (time-remaining)	0.069	−0.084	−0.009	0.186	0.146	0.191	–	–
	0.077	−0.105	−0.041	0.180	0.150	0.190		
Light (solved)	0.226	0.084	0.027	0.133	0.099	0.005	0.004	–
	0.228	0.021	−0.011	0.112	0.111	−0.017	0.052	
Light-alt (time-remaining)	0.131	−0.132	−0.106	−0.067	0.003	0.015	0.161	0.247
	0.203	−0.107	−0.080	−0.083	−0.060	0.052	0.130	0.290+

In each cell, Pearson correlation coefficients are shown above, and Spearman correlation coefficients are shown below
The value of the time-remaining variable of those who could not solve the task was set to 0
$+p<0.10$, $*p<0.05$, $**p<0.01$

Finally, we turn to the relationship between trial-and-error and creativity (Tables 7.11 and 7.12). The pattern is ambiguous, but there seems to be a positive relationship between trial-and-error and creativity. Although the correlation coefficients are only marginally significant, the higher the performance in the coin task #1, the higher the score of Cattell CFIT. The performance of the coin task #1 seems to be positively related to the performance of the candle task, while the performance of the coin task #2 seems to be positively related to the performance of the ring task.[11]

[11] A weak negative relationship was found between the speed of solving the candle task and the coin task 1 in Table 7.11. Currently we do not have an explanation for this result, however.

Table 7.7 Correlation coefficients between creativity and imitation

	Imitation	
Creativity	Wire (solved)	Wire-alt (time-remaining)
Cattell	0.087	0.216
	0.041	0.297+
Ring (solved)	–0.006	0.299+
	–0.006	0.215
Ring-alt (time-remaining)	0.140	–0.239
	0.057	–0.295
Candle (solved)	0.225+	0.021
	0.225+	0.187
Candle-alt (time-remaining)	0.498*	0.156
	0.493*	0.233
Truck (solved)	–0.194	0.141
	–0.173	0.162
Truck-alt (time-remaining)	–0.043	0.013
	–0.052	–0.028
Light (solved)	–0.199	0.452*
	–0.201	0.707**
Light-alt (time-remaining)	0.143	0.238
	0.113	0.214

In each cell, Pearson correlation coefficients are shown above, and Spearman correlation coefficients are shown below
The value of the time-remaining variable of those who could not solve the task was treated as missing
+$p<0.10$, *$p<0.05$, **$p<0.001$

Table 7.8 Correlation coefficients between creativity and imitation

	Imitation	
Creativity	Wire (solved)	Wire-alt (time-remaining)
Cattell	0.087	0.155
	0.041	0.159
Ring (solved)	–0.006	0.109
	–0.006	0.109
Ring-alt (time-remaining)	0.047	0.130
	0.029	0.115
Candle (solved)	0.225+	0.204
	0.225+	0.242+
Candle-alt (time-remaining)	0.342**	0.330*
	0.294*	0.325*
Truck (solved)	–0.194	–0.117
	–0.173	–0.079
Truck-alt (time-remaining)	–0.078	–0.066
	–0.091	–0.066
Light (solved)	–0.199	–0.018
	–0.201	0.155
Light-alt (time-remaining)	0.166	0.230+
	0.157	0.190

In each cell, Pearson correlation coefficients are shown above, and Spearman correlation coefficients are shown below
The value of the time-remaining variable of those who could not solve the task was set to 0
+$p<0.10$, *$p<0.05$, **$p<0.01$

This result is different from Experiment 1 where there was none or a weak negative relationship between them.

Table 7.9 Correlation coefficients between trial-and-error and imitation

	Imitation	
Trial-and-error	Wire (solved)	Wire-alt (time-remaining)
Coin 1 (solved)	0.064	0.209
	0.064	0.171
Coin 1 (# of coins collected)	0.160	0.161
	0.085	0.215
Coin 2 (solved)	0.065	0.177
	0.065	0.102
Coin 2 (# of coins collected)	–0.154	0.099
	–0.120	–0.080

In each cell, Pearson correlation coefficients are shown above, and Spearman correlation coefficients are shown below
The value of the time-remaining variable of those who could not solve the task was treated as missing

Table 7.10 Correlation coefficients between trial-and-error and imitation

	Imitation	
Trial-and-error	Wire (solved)	Wire-alt (time-remaining)
Coin 1 (solved)	0.064	0.135
	0.064	0.129
Coin 1 (# of coins collected)	0.160	0.209
	0.085	0.166
Coin 2 (solved)	0.065	0.125
	0.065	0.101
Coin 2 (# of coins collected)	–0.154	–0.102
	–0.120	–0.094

In each cell, Pearson correlation coefficients are shown above, and Spearman correlation coefficients are shown below
The value of the time-remaining variable of those who could not solve the task was set to 0

7.2.2.3 Discussion of Experiment 2

Results of experiment 2 suggested that, first, there is a positive relationship between creativity and imitation, although the correlation coefficients were not large. In this sense, Experiment 2 replicated the results of Experiment 1. Second, there was no relationship between trial-and-error and imitation, as in Experiment 1. Third, trial-and-error was positively related with creativity, although the correlation coefficients were not large. In general, these results were confirmed both when we used Pearson correlation coefficients and when we partialled out space perception ability.[12] In conclusion, the results of Experiment 2 replicated most of the ones from the first experiment, except for the relationship between creativity and trial-and-error. The candle holder problem was used in both experiments, yet there was

[12] Since the scores of the dice task and the cube task did not show any correlation with imitation, we omit presenting the results regarding space perception.

Table 7.11 Correlation coefficients between creativity and trial-and-error

	Trial-and-error			
Creativity	Coin 1 (solved)	Coin 1 (# of coins collected)	Coin 2 (solved)	Coin 2 (# of coins collected)
Cattell	0.200	0.232+	0.198	−0.082
	0.198	0.218+	0.215+	−0.093
Ring (solved)	0.140	0.176	0.216+	0.153
	0.140	0.155	0.216+	0.173
Ring-alt (time-remaining)	0.244	0.114	0.302	0.454*
	0.242	0.010	0.330	0.518**
Candle (solved)	0.209	0.254+	0.179	−0.007
	0.209	0.270*	0.179	−0.030
Candle-alt (time-remaining)	−0.334	−0.305	0.205	0.198
	−0.342	−0.396+	0.223	0.196
Truck (solved)	−0.221	−0.175	−0.206	−0.147
	−0.226+	−0.144	−0.178	−0.121
Truck-alt (time-remaining)	0.060	0.016	0.068	−0.003
	0.094	0.134	0.010	−0.032
Light (solved)	0.043	0.149	0.075	−0.127
	0.015	0.133	0.078	−0.192
Light-alt (time-remaining)	0.115	0.119	−0.090	−0.133
	0.196	0.162	−0.053	−0.190

In each cell, Pearson correlation coefficients are shown above, and Spearman correlation coefficients are shown below
The value of the time-remaining variable of those who could not solve the task was treated as missing
+$p < 0.10$, *$p < 0.05$, **$p < 0.01$

Table 7.12 Correlation coefficients between creativity and trial-and-error

	Trial-and-error			
Creativity	Coin 1 (solved)	Coin 1 (# of coins collected)	Coin 2 (solved)	Coin 2 (# of coins collected)
Cattell	0.200	0.232+	0.198	−0.082
	0.198	0.218+	0.215+	−0.093
Ring (solved)	0.140	0.176	0.216+	0.153
	0.140	0.155	0.216+	0.173
Ring-alt (time-remaining)	0.203	0.189	0.288*	0.291*
	0.197	0.174	0.286*	0.284*
Candle (solved)	0.209	0.254+	0.179	−0.007
	0.209	0.270*	0.179	−0.030
Candle-alt (time-remaining)	0.058	0.101	0.221+	0.062
	0.137	0.192	0.212	0.010
Truck (solved)	−0.221	−0.175	−0.206	−0.147
	−0.226+	−0.144	−0.178	−0.121
Truck-alt (time-remaining)	0.069	0.021	0.074	−0.002
	0.104	0.137	0.016	−0.040
Light (solved)	0.043	0.149	0.075	−0.127
	0.015	0.133	0.078	−0.192
Light-alt (time-remaining)	0.149	0.158	−0.089	−0.095
	0.231+	0.198	−0.056	−0.162

In each cell, Pearson correlation coefficients are shown above, and Spearman correlation coefficients are shown below
The value of the time-remaining variable of those who could not solve the task was set to 0
+$p < 0.10$, *$p < 0.05$

none or a negative relationship with the Lonpos task in Experiment 1 and there was a positive relationship with the coin game in Experiment 2.

7.3 General Discussion

Combining the results of two experiments, we are relatively confident that there is a positive relationship between creativity and imitation, and there is no relationship between trial-and-error and imitation. The relationship between creativity and trial-and-error still remains ambiguous. These results suggest that there is no trade-off between individual learning ability and social learning ability since no variable was negatively related to imitation. The level of individual learning ability of an individual does not depend on the level of social learning ability. Thus, we could conclude that creative people can be better imitators.[13] This finding partly supports a new theoretical argument that a social learner-explorer, who combines accurate social learning with exploratory individual learning, is most adaptive when the environment is assumed to vary spatially and the migration rate is relatively high (Aoki 2010). *Homo sapiens* may have been more adaptive than Neanderthals because they had a higher level of creativity as well as a high level of imitation ability.

However, it is premature to conclude this since caution is necessary when interpreting the results of two experiments. There are several important problems that need to be resolved in the current study. First, because of various practical constraints, participants were not a representative sample of the whole population of *Homo sapiens* but were undergraduate students at Hokkaido University only. Undergraduate students at a particular university are obviously very homogeneous in various aspects. Therefore, it is very possible that correlations we found could underestimate the true correlations which exist in a population. We are relatively confident that correlations we found would exist in the general population as well. At the same time, testing a larger and more diverse sample might reveal correlations that we did not uncover in the two experiments reported in this paper. Therefore, in the next step, we plan to collect data from a larger, more heterogeneous sample.

Second, the above results were obtained from only a few specific tasks. Reliability of multiple measures of each ability is still low. Also, the fact that we could only use the wire puzzle as the measure of imitation ability is a critical problem. Therefore, a new study which uses refined measures of each learning ability, especially the imitation ability, should be conducted.

Third, since the current study is an exploratory one, we examined if there are any significant correlations among a large number of variables. It means that the possibility of Type 1 errors is high. We tried to minimize this problem by conducting two experiments and examining if there are any common patterns in the data. However, such a method is far from the true solution. There is therefore a long way to go. We need to continue collecting data from various samples by using various measures of each learning ability.

[13] Here what we focus on is not learning strategy but learning ability. An individual who has a high level of individual learning ability and social learning ability may experience a tradeoff when he decides how to allocate his resources to each learning activity.

References

Aoki K (2010) Evolution of the social-learner-explorer strategy in an environmentally heterogeneous two-island model. Evolution 64:2575–2586

Aoki K, Wakano JY, Feldman MW (2005) The emergence of social learning in a temporally changing environment: a theoretical model. Curr Anthropol 46:334–340

Borenstein E, Feldman MW, Aoki K (2008) Evolution of learning in fluctuating environments: when selection favors both social and exploratory individual learning. Evolution 62:586–602

Bouchard J, Goodyer W, Lefebvre L (2007) Social learning and innovation are positively correlated in pigeons (Columba livia). Anim Cogn 10:259–266

Boyd R, Richerson PJ (1985) Culture and the evolutionary process. Unitersity of Chicago Press, Chicago

Bugnyar T, Huber L (1997) Push or pull: an experimental study on imitation in marmosets. Anim Behav 54:817–831

Cattell RB (1971) Abilities: their structure, growth, and action. Houghton Mifflin, New York

Cavalli-Sforza LL, Feldman MW (1981) Cultural transmission and evolution. Princeton University Press, Princeton

Custance DM, Whiten A, Bard KA (1995) Can young chimpanzees (*Pan troglodytes*) imitate arbitrary actions? Hayes & Hayes (1952) revisited. Behaviour 132:837–859

Custance DM, Whiten A, Fredman T (1999) Social learning of an artificial fruit task in capuchin monkeys (Cebus apella). J Comp Psychol 113:13–23

Dean LG, Kendal RL, Schapiro SJ, Thierry B, Laland KN (2012) Identification of the social and cognitive processes underlying human cumulative culture. Science 335:1114–1118

Diamond J (1991) The rise and fall of the third chimpanzee. Harper Collins, New York

Dunker K (1945) On problem-solving. Psychological Monographs 58 (5, Whole No. 270): 1–113

Giraldeau LA, Caraco T (2000) Social foraging theory. Princeton University Press, Princeton

Guilford JP (1950) Creativity. Am Psychol 5:444–454

Guilford JP (1967) The Nature of Human intelligence. McGraw-Hill, London

Heyes CM, Dawson GR, Nokes T (1992) Imitation in rats: initial responding and transfer evidence. Q J Exp Psychol 45:229–240

Hocevar D (1981) Measurement of creativity: review and critique. J Pers Assess 45(5):450–464

Horner V, Whiten A, Flynn E, de Waal FB (2006) Faithful replication of foraging techniques along cultural transmission chains by chimpanzees and children. Proc Natl Acad Sci 103:13878–13883

Kameda T, Nakanishi D (2002) Cost-benefit analysis of social/cultural learning in a nonstationary uncertain environment: an evolutionary

simulation and an experiment with human subjects. Evol Hum Behav 23:373–393
Kameda T, Nakanishi D (2003) Does social/cultural learning increase human adaptability? Rogers's question revisited. Evol Hum Behav 24:242–260
Koestler A (1964) The act of Creation. Pan Books, London
Krützen M, Mann J, Heithaus MR, Connor RC, Bejder L, Sherwin WB (2005) Cultural transmission of tool use in bottlenose dolphins. Proc Natl Acad Sci U S A 102:8939–8943
Maier NRF (1933) An aspect of human reasoning. Br J Psychol 24:144–155
Markman KD, Klein WMP, Suhr JA (eds) (2009) Handbook of mental simulation. Psychology, Hove
McCaffrey T (2012) Innovation relies on the obscure: a key to overcoming the classic problem of functional fixedness. Psychol Sci 23:215–218
McElreath R, Lubell M, Richerson PJ, Waring TM, Baum W, Edsten E, Efferson C, Paciotti B (2005) Applying evolutionary models to the laboratory study of social learning. Evol Hum Behav 26:483–508
McElreath R, Bell AV, Efferson C, Lubell M, Richerson PJ, Waring T (2008) Beyond existence and aiming outside the laboratory: estimating frequency-dependent and pay-off-biased social learning strategies. Philos T Roy Soc B 363:3515–3528
Mesoudi A (2008) An experimental simulation of the "copy-successful-individuals" cultural learning strategy: adaptive landscapes, producer-scrounger dynamics and informational access costs. Evol Hum Behav 29:350–363
Mesoudi A (2011) An experimental comparison of human social learning strategies: payoff-biased social learning is adaptive but underused. Evol Hum Behav 32:334–342
Mesoudi A, O'Brien MJ (2008) The cultural transmission of Great Basin projectile-point technology I: an experimental simulation. Am Antiq 73:3–28
Morgan TJH, Rendell LE, Ehn M, Hoppitt W, Laland KN (2012) The evolutionary basis of human social learning. Proc R Soc B 279:653–662
Reader SM, Laland KN (2002) Social intelligence, innovation and enhanced brain size in primates. Proc Natl Acad Sci U S A 99: 4436–4441
Rogers AR (1988) Does biology constrain culture? Am Anthropol 90(4):819–831
Tennie C, Call J, Tomasello M (2009) Ratcheting up the ratchet: on the evolution of cumulative culture. Phil Trans R Soc B 364:2405–2415
Toelch U, Bruce MJ, Meeus MT, Reader SM (2010) Humans copy rapidly increasing choices in a multiarmed bandit problem. Evol Hum Behav 31:326–333
Voelkl B, Huber L (2000) True imitation in marmosets. Anim Behav 60:195–202
Voelkl B, Huber L (2007) Imitation as faithful copying of a novel technique in marmoset monkeys. PLoS One 2:e611
Wakano JY, Aoki K, Feldman MW (2004) Evolution of social learning: a mathematical analysis. Theor Popul Biol 66:249–258
Yamamoto S, Humle T, Tanaka M (2013) Basis for Cumulative Cultural Evolution in Chimpanzees: social learning of a more efficient tool-use technique. PLoS One 8:e55768. doi:10.1371/journal.pone.0055768

8 Experimental Studies of Modern Human Social and Individual Learning in an Archaeological Context: People Behave Adaptively, But Within Limits

Alex Mesoudi

Abstract

It has been proposed that one reason for the success of *Homo sapiens* is our advanced learning abilities. Theoretical models suggest that complex cultural adaptations can arise from an optimal mix of (1) individual learning that is of sufficient accuracy plus (2) social learning that is of sufficiently high fidelity and is payoff-biased. Here I review the findings of a series of experimental studies of human learning, designed to simulate the kind of technology-based tasks that our ancestors would have faced. Results of these studies support the predictions of the models, and show that contemporary humans' learning strategies are broadly adaptive. Performance typically improves through effective individual learning and payoff-biased social learning. The latter crucially allows participants to escape low-fitness locally optimal artifact designs and jump to higher-fitness designs, assuming a realistic multimodal adaptive landscape underlying artifact fitness. On the other hand, people also exhibited predictable flaws in their learning, such as the copying of neutral traits exhibited by successful models along with their functional traits (i.e., cultural hitchhiking), and an unwillingness to share information with others under certain circumstances.

Keywords

Cultural evolution • Cumulative culture • Individual learning • Social learning

8.1 Introduction

In a relatively brief period of evolutionary time, our species has successfully colonised and inhabited virtually every terrestrial environment on the planet, from the driest deserts to frozen tundra, from high-altitude mountain ranges to remote island chains, such that we now account for about eight times the biomass of all other wild terrestrial vertebrates combined (Hill et al. 2009). Other hominin species such as the Neanderthals have gone extinct, possibly due in part to the success of *Homo sapiens*, while our closest living relative species, chimpanzees, are limited to a few small, scattered populations across Africa. What accounts for the extraordinary evolutionary success of our species?

One possibility, proposed by the Replacement of Neanderthals by Modern Humans (RNMH) Project (Akazawa 2012), is that anatomically modern *Homo sapiens* possessed superior learning abilities compared to their fellow hominins and other primates. This hypothesis has its roots in theoretical modelling work in the field of cultural evolution going back several decades, which has linked evolutionary rates of change and phenotypic adaptation to learning strategies (Aoki et al. 2005, 2011; Boyd and Richerson 1985; Cavalli-Sforza and Feldman 1981; Rogers 1988). A primary focus of these models has been the interplay between individual (or asocial) learning, in which novel solutions to problems are invented by a single individual, and social learning (or cultural transmission), in which solutions are copied from one or more other individuals in the population. The latter can take on different modes,

A. Mesoudi (✉)
Department of Anthropology and Centre for the Coevolution of Biology and Culture, Durham University, Dawson Building, South Road, Durham DH1 3LE, UK
e-mail: a.a.mesoudi@durham.ac.uk

T. Akazawa et al. (eds.), *Dynamics of Learning in Neanderthals and Modern Humans Volume 2: Cognitive and Physical Perspectives*, Replacement of Neanderthals by Modern Humans Series, DOI 10.1007/978-4-431-54553-8_8, © Springer Japan 2014

such as vertical transmission from one's biological parents (Cavalli-Sforza and Feldman 1981), conformist transmission of the most popular solution in one's group (Henrich and Boyd 1998), or payoff/prestige biased transmission in which the most successful/prestigious individual in one's group is preferentially copied (Boyd and Richerson 1985; Henrich and Gil-White 2001).

Although the results of these models are varied, a general finding seems to be that some mix of individual and social learning is adaptive in fluctuating environments that change too rapidly for innate, genetic responses to evolve, yet not so rapid that previous generations' solutions to problems are out-of-date (Aoki et al. 2005; Boyd and Richerson 1988). Moreover, if individual learning is sufficiently accurate, and social learning is of sufficiently high fidelity and is payoff-biased such that adaptive solutions are preferentially copied, then this mix of social and individual learning can result in cumulative cultural evolution (Aoki et al. 2012; Ehn and Laland 2012; Enquist et al. 2008; Mesoudi 2011b; Powell et al. 2009). Just as cumulative genetic evolution can result in complex genetic adaptations such as eyes or wings, cumulative cultural evolution can similarly generate complex cultural adaptations that most likely underlie our species' success, from bow-and-arrows, kayaks and celestial navigation to agriculture, airplanes and quantum physics (Richerson and Boyd 2005).

Did anatomically modern humans uniquely possess an optimal mix of sufficiently accurate individual learning plus sufficiently high fidelity, payoff-biased social learning? Was one of these ingredients missing in other hominin, or other primate, species? It is, of course, extremely difficult to infer the learning abilities of extinct hominin species from the incomplete and often ambiguous artifactual record. We can, however, test these predictions in contemporary humans. If groups of people solve problems in the way predicted by the aforementioned theoretical models, then we can be more confident in the validity of those models, and more confident in asserting that our species' learning capacities are evolutionarily adaptive. Just as importantly, if people do *not* behave as predicted (e.g., if they eschew payoff-biased social learning in favour of, say, conformist or random copying), then this requires modification of the assumptions of the models and/or modification of the original hypothesis that modern humans possess adaptive learning capacities.

With this aim in mind, in this paper I will review the results of a series of experimental studies conducted by myself and collaborators that have probed the learning abilities of contemporary humans when faced with a novel and complex task—what we have dubbed the *Virtual Arrowhead Task*—that is designed to resemble technology found in the material record. Hopefully, the findings of these experiments can inform both theoretical models of the evolution of human learning capacities, and interpretation of the often ambiguous archaeological record. This is not to say that experimental simulations are a perfect tool: far from it. While they offer many advantages, such as the ability to control extraneous conditions, manipulate variables, replicate findings and generate complete behavioural datasets, they are limited by their lack of external validity, such as their short time spans, lower incentives, restricted social interaction and the assumption that the behaviour of contemporary humans can be extrapolated to that of past people. I therefore conclude with an extended discussion of the limitations and real-life applications of experimental methods in this context.

8.2 The Virtual Arrowhead Task

The Virtual Arrowhead Task was originally designed by myself and archaeologist Michael O'Brien to capture the key aspects of North American projectile points (Mesoudi and O'Brien 2008a, b), although we have since used it to explore the learning of complex technology in general (Atkisson et al. 2012; Mesoudi 2008, 2011a). One limitation of many of the theoretical models of cultural evolution discussed above, as well as some experimental tests of such models (e.g., McElreath et al. 2005), is that the 'task' or 'problem' that must be solved is unrealistically simple: often it is assumed that individuals can exhibit just one of two possible discrete traits, with one of those traits giving a higher payoff than the other trait as specified by the state of the environment. Even the simplest of human technology, however, comprises multiple component traits, some of which might be continuous (e.g., the length or width of a handaxe: Lycett and von Cramon-Taubadel 2008), others discrete but with more than two states (e.g., arc-shaped vs. curved vs. triangular base shapes of projectile points: O'Brien et al. 2001); some might be functional (e.g., the thickness or length of arrowheads: Cheshier and Kelly 2006) and some might be functionless (e.g., decorative patterns on canoes: Rogers and Ehrlich 2008). The overall 'cultural fitness' of an artifact will be a combination of these component trait values, each of which interacts with one another, as well as with the skill of the manufacturer/user, and stochastic factors such as weather conditions.

We therefore sought to design a task that was simultaneously complex enough to give us insights about how people solve real-life technology-based problems, and simple enough to be able to inform the theoretical models described above and yield tractable findings. In our task (see Mesoudi and O'Brien 2008a for a full description), participants in small groups of 5–6 each design an arrowhead via a computer program (Fig. 8.1). This virtual arrowhead is composed of three continuous traits (Height, Width and Thickness), which can each take any value from 1–100 arbitrary units, and two discrete traits (Shape and Colour), which can each take one of

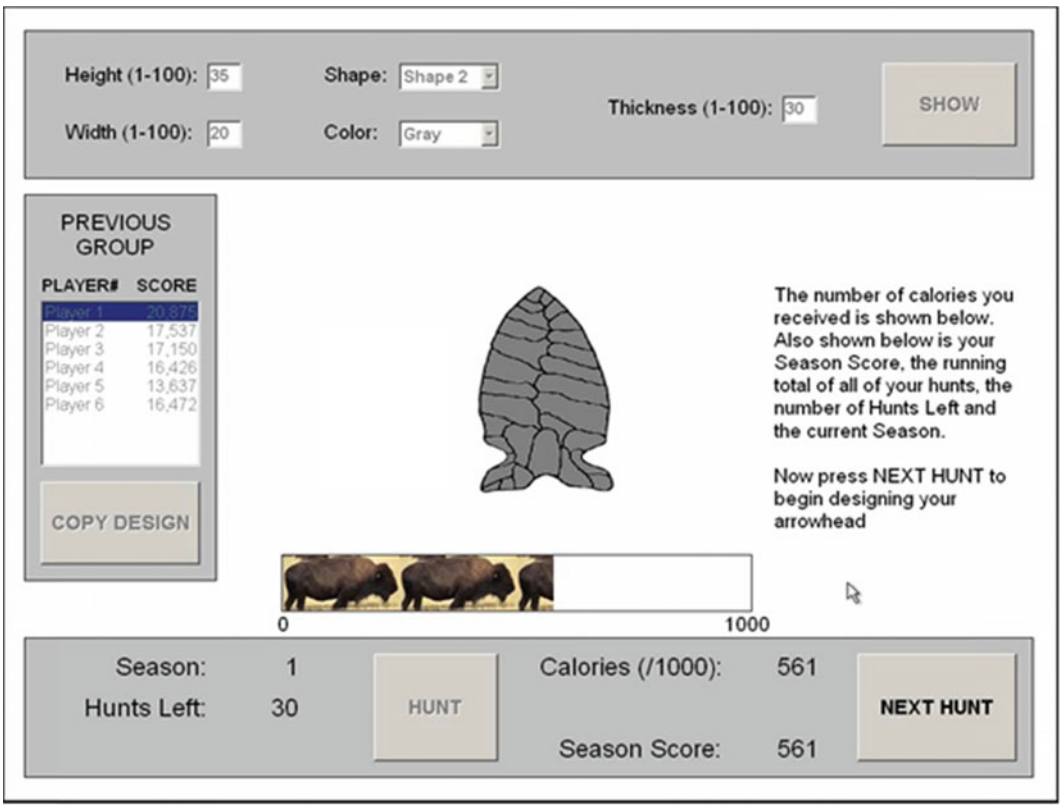

Fig. 8.1 A screenshot of the Virtual Arrowhead Task. Participants can choose to directly change the traits in the box at the top (individual learning) or copy the design of another participant in the box on the left (social learning). Feedback is given in calories depending on how close the design is to one or more hidden optimal designs

four categorical values. Over a series of trials (or 'hunts'), participants can improve their arrowhead by either individual trial-and-error learning, by directly altering the values of one or more of the traits, or social learning, by copying the design of another group member. The form of this social learning (e.g., payoff bias, conformity) can be manipulated.

On each hunt the participant tests their arrowhead in a virtual hunting environment, receiving a score in calories out of 1,000. The closer their design is to one or more hidden optimal designs pre-specified by us using fitness functions, the higher the score ('fitness' is used here to refer to cultural fitness of an artifact, which may, or may not, correspond to the biological fitness of the individual using that artifact). The overall fitness of the arrowhead is given by the sum of the separate fitness functions for the constituent traits (Fig. 8.2). The discrete trait Shape has a step fitness function, with the four shapes randomly assigned either 100 %, 90 %, 66 % or 33 % of the maximum possible fitness from that trait. Colour is neutral and does not contribute to fitness in any way. The continuous traits (Height, Width and Thickness) each have bimodal fitness functions. For each, one randomly chosen value gives 100 % of the fitness contribution (the global optimum), and another random value gives 66 % of that maximum (the local optimum).

When added together, these bimodal functions generate a multimodal adaptive landscape (Wright 1932), where each coordinate represents a different arrowhead design and the height of the landscape represents the fitness of that design. With three bimodal traits there are $2^3 = 8$ peaks in our adaptive landscape, with each peak varying in its maximum payoff. For example, an arrowhead with Height, Width and Thickness all at their globally optimal values gives the full 1,000 calories; an arrowhead with Height and Width at their global optima and Thickness at its local optimum gives a slightly lower maximum payoff; an arrowhead with Height, Width and Thickness all at their local optima gives the lowest maximum payoff. Given that most real-life problems can typically be solved in multiple ways, with some solutions better than others, this is likely to be representative of real-life technological fitness (Boyd and Richerson 1992). Note, however, that participants were told nothing about these fitness functions (just as, presumably, real-life hunter-gathers have no a priori knowledge of the effectiveness of most of the technology they use). Finally, there is always a small random error in the score, simulating stochastic conditions such as weather or prey availability.

After each hunt, participants are informed of their score out of 1,000 calories. Participants go through three seasons

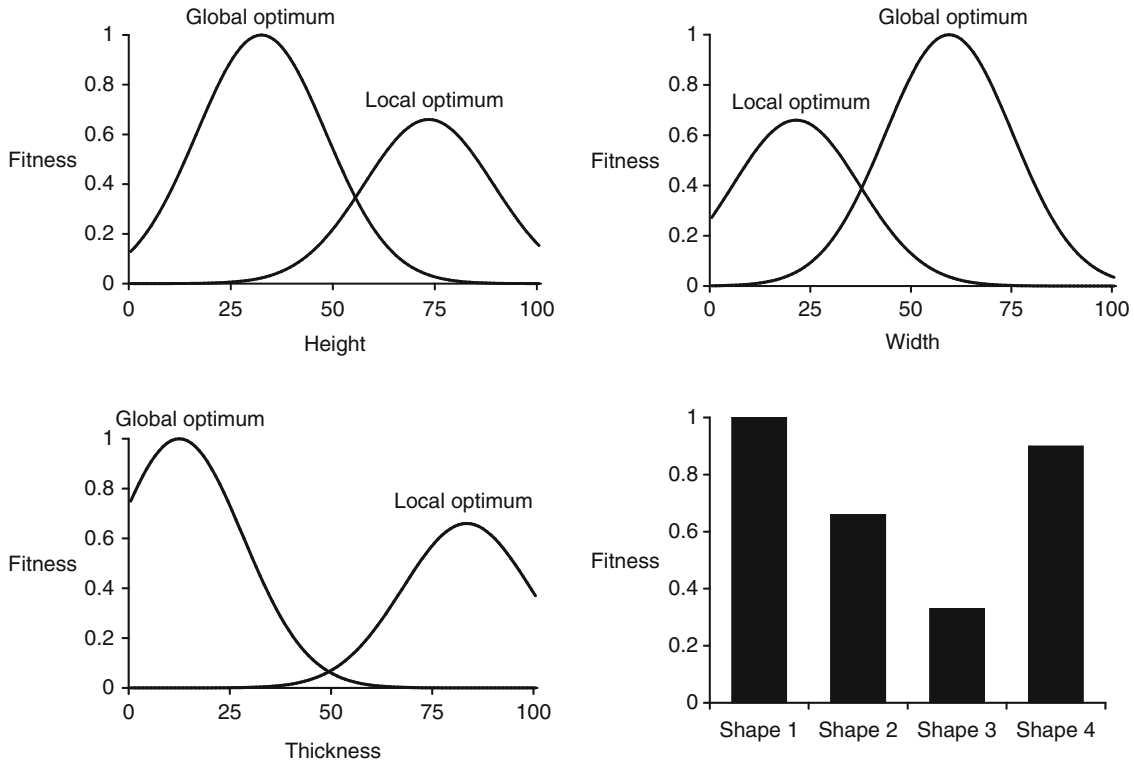

Fig. 8.2 Fitness functions for the constituent traits. The overall fitness of an arrowhead was given by the sum of these fitness functions. The continuous traits (Height, Width and Thickness) had bimodal functions, generating a multimodal adaptive landscape. A fifth trait, Colour, was neutral and did not affect arrowhead fitness. From Mesoudi and O'Brien (2008a)

of hunting, with each season comprising 30 hunts. Optimal values change between seasons, but not during seasons, and participants are informed about both of these facts. During each season the participant can see their cumulative score (the sum of the scores on every hunt up to that point), and in group conditions their relative rank compared to other group members' cumulative scores. Motivational reward has varied across the studies described below: in some studies participants were rewarded monetarily based on their absolute score, in others based on their relative rank, and in others no monetary reward is given at all (interestingly, no obvious differences have been observed across these different motivational regimes).

This task is intended to capture the key aspects of most complex technology, including that used by both modern humans and Neanderthals around the time of their coexistence: a technology composed of multiple constituent traits (some continuous and some discrete, some functional and some neutral), that is cognitively opaque (there is no obvious, intuitive relation between an artifact and its effectiveness: Gergely and Csibra 2006) and which has multiple locally optimal alternative designs (i.e., a multimodal adaptive landscape). In a series of studies we have explored how contemporary humans engage with this task, with the following key findings.

8.3 Key Findings

8.3.1 People Are Effective Individual Learners, But Can Get Stuck on Local Optima

While much theoretical modelling work has looked at a diverse range of social learning strategies (Laland 2004), individual learning is often under-theorised in models, where it is often assumed that individuals come up with the correct solution to a problem with some fixed probability. We were interested in opening this 'black box' and exploring the strategies that people use when engaging in individual learning.

When playing alone, participants on average show effective individual learning. Figure 8.3 shows that mean score increases over successive hunts, plateauing to a level significantly higher than that of the starting (random) design. Analyses of these data revealed that participants appear to engage in a simple but effective reinforcement learning, or 'win-stay-lose-shift', strategy (Mesoudi and O'Brien 2008a, b): pick a trait at random (e.g., Width), modify the trait (e.g., increase Width), if the payoff increases then keep modifying the trait in that way (e.g., increase Width further); if the payoff decreases then do the opposite (e.g., decrease Width). This is repeated until the

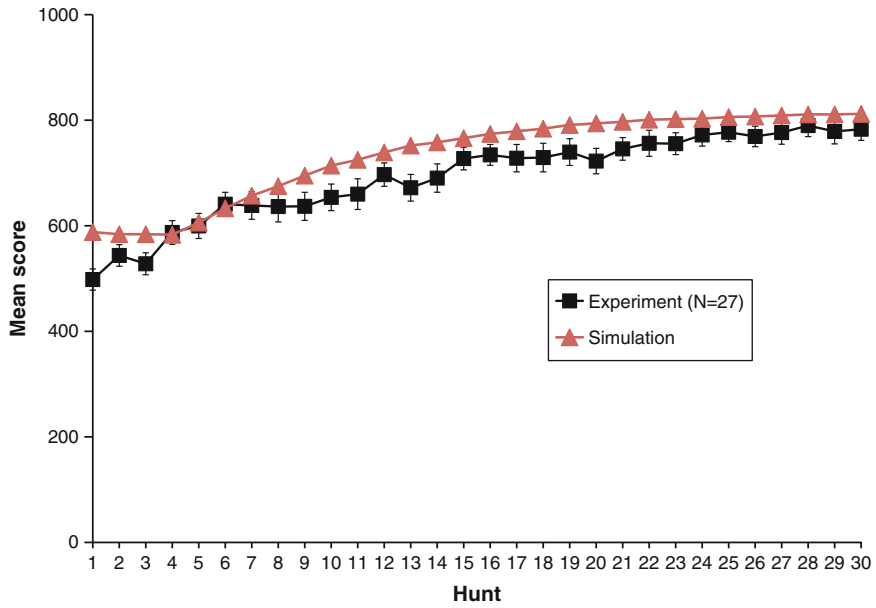

Fig. 8.3 The mean score of a sample of individual learners (N = 27) showing a gradual increase and plateauing over successive hunts (*black line with squares*), along with the simulated performance of the reinforcement learning strategy with $d = 1$ and $c = 5$ (*red line with triangles*)

payoff no longer changes, at which point the whole process is repeated for the next trait. In terms of the multimodal adaptive landscape, this simple hill-climbing algorithm results in the participant converging on the nearest peak in the landscape.

Formally, we can define two parameters in this strategy: d, which we defined as the number of traits that a participant changed on a single hunt ($0 \leq d \leq 5$), and c, the amount by which a continuous trait is modified during one hunt ($0 \leq c \leq 99$). If more than one continuous trait was changed in a hunt then c represents the mean of these traits, and we focus on the continuous traits because these are responsible for most of the improvement and variation in payoffs. Empirically, our participants typically had a d of 1 (mean = 1.43, median = 1, mode = 1) and a c of 5 (mean = 9.50, median = 5, mode = 5), meaning that on each hunt they changed one trait by 5 units. To test our hypothesised individual learning strategy, an agent-based model was constructed that followed the rules specified above with $d = 1$ and $c = 5$ (Mesoudi and O'Brien 2008b). As shown in Fig. 8.3, the simulated values match well with the actual data from participants, reaching virtually identical end points and showing a similar gradual increase then plateau.

Interestingly, the participants do best relative to the simulation during early hunts (see hunts 4, 5 and 6 in Fig. 8.3). Further analyses showed that this is because c was not, in fact, constant across all hunts, as suggested by the slightly higher mean of 9.50. During earlier hunts, when participants generally had low scores, they responded by increasing c, i.e., making larger modifications to their arrowheads. Consequently, score was negatively and significantly correlated with c ($r_s = -0.368$, $p < 0.01$). In a multimodal adaptive landscape this is an adaptive individual learning strategy: if your score is low, you are most likely to be in a low-fitness valley, and large modifications may well transport you to a higher-fitness part of the landscape. If your score is high, then modifications should be small, otherwise you may move off your peak and into a valley.

Note also from Fig. 8.3 that the maximum mean score at hunt 30 of around 750–800 calories, which appears to have levelled off at a kind of equilibrium, falls quite short of the maximum possible 1,000 calories. This, again, is because of the multimodal adaptive landscape. The individual learning strategy followed by our participants, and simulated in the model, leads participants uphill from a random starting point to the top of the nearest peak. This might be the globally optimal peak, but equally might be one of the seven other locally optimal but globally suboptimal peaks. So even though participants saw that their score was less than the maximum of 1,000, the majority chose to stick with their pretty-good-but-not-perfect design, what Simon (1956) called 'satisficing'. This represents a disadvantage of pure individual learning in a multimodal adaptive landscape: independent individual learners can get stuck on locally optimal, but globally suboptimal peaks.

Note also that this individual learning strategy was employed for a range of randomly generated optimal arrowhead designs, with these random optima changing between seasons and across studies. Participants did not exhibit any intuitive notion of what an effective arrowhead design looked

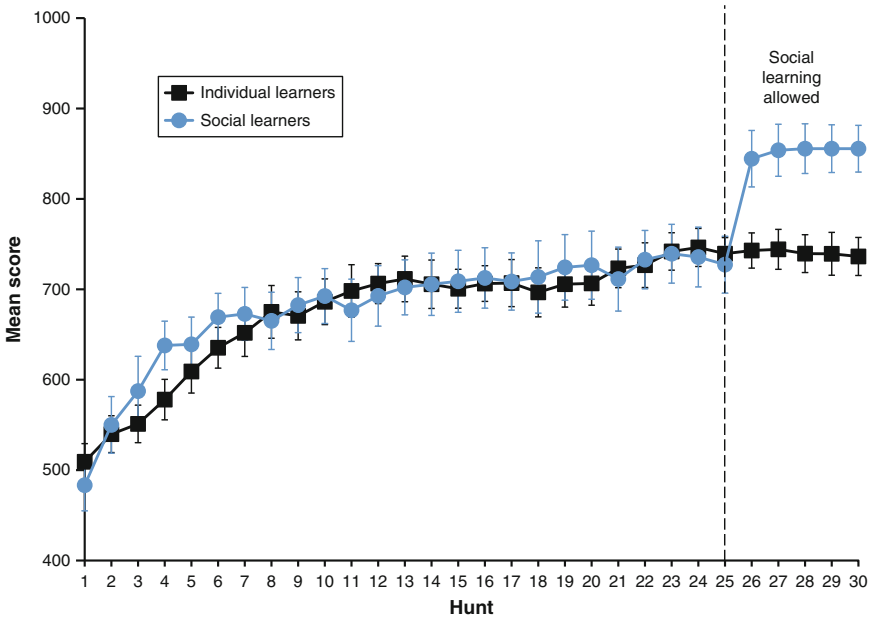

Fig. 8.4 The mean score of individual learners (*black line with squares*) compared to payoff-biased social learners (*blue line with circles*). The latter could copy one another only during the last five hunts, during which their score significantly increased relative to the individual learners, who could not copy on any hunt

like, or if they did, it was (1) different for each participant given that they each started at different points in the landscape (see Mesoudi and O'Brien 2008b), and (2) quickly overridden when the a priori intuitively good arrowhead design was found to perform poorly in the experiment. In this case, then, general-purpose learning rules override any pre-existing intuitive content biases or cultural attractors (Sperber 1996) regarding projectile point characteristics (at least in our non-expert participants; we explicitly excluded archaeology students and amateur replica-arrowhead-makers from the studies to avoid too specialised knowledge).

8.3.2 People Use Payoff-Biased Social Learning to Jump to Higher-Fitness Designs

We can now ask how social learning, and in particular payoff-biased social learning, changes participants' performance on the task. Payoff-biased social learning was implemented by allowing participants to view the arrowhead design of another member of their group, given information about those group members' cumulative scores up to that point. When this is allowed, either after a long period of individual learning (Mesoudi and O'Brien 2008a) or concurrently with individual learning (Mesoudi 2008), participants readily engage in payoff-biased social learning, copying the design of the most successful person in their group rather than copying a random group member or continuing with individual learning. The result of payoff-biased social learning is a significant jump in the mean score relative to individual learners (Fig. 8.4).

Payoff-biased social learning is adaptive here because it allows participants to abandon their locally optimal designs and jump, almost instantaneously, to the globally optimal peak, or at least the highest peak found by anyone in the group. Payoff-biased social learning has this effect almost by definition, because participants who have found higher peaks will have higher scores, and they are preferentially copied. To confirm that the multimodal shape of the adaptive landscape was responsible for the advantage of social learning, it was shown that (1) there were significantly more participants with designs at or near a locally optimal peak immediately before social learning is allowed than after, and conversely, significantly more participants at globally optimal peaks after social learning than before (Mesoudi and O'Brien 2008a), and (2) when the adaptive landscape was made unimodal (by removing the local optima from the fitness functions for Height, Width and Thickness shown in Fig. 8.2, to create a single globally optimal design/peak), the advantage of social learning disappeared, and individual learners achieved mean scores identical to multimodal social learners (Mesoudi 2008).

Moreover, just as a participant's individual learning strategy changed in response to the participant's score, so too did their social learning. The lower a participant's score, the more use they made of social information (Mesoudi 2008). This was indicated by a significant and negative correlation ($r = -0.29$, $p < 0.001$) between participants' scores and a measure of social influence, defined as the amount by which a participant changed their existing arrowhead to make it more similar to the arrowhead of the participant who they had chosen to view.

This performance-dependent payoff-biased social learning, or "copy-successful-individuals-when-behaviour-is-unproductive" (Laland 2004), is again adaptive. Boyd and Richerson (1995) showed that this flexible and selective

learning strategy of engaging in social learning only when individual learning is particularly costly or difficult is one way of solving 'Rogers' paradox' (Rogers 1988). Rogers suggested that social learners can be seen as 'information scroungers' free-riding on the costly efforts of individual learners (or 'information producers'), with a net result that a mixed population of social and individual learners will never have a higher mean fitness than a population solely comprised of individual learners. Boyd and Richerson (1995) showed that making learners selective, engaging in social learning only when individual learning is costly or difficult, removes this problem, allowing social learning to evolve and mean fitness to increase. That our participants behave in this way, only engaging in social learning when their scores are low (which we can infer is because they are finding individual learning difficult), is encouraging. It is also encouraging that other studies using different tasks have found similar effects, such as Morgan et al.'s (2012) finding that the lower a participant's confidence in their performance, the more they rely on social learning.

8.3.3 Payoff-Biased Social Learning Is Preferred to Other Forms of Social Learning

The Virtual Arrowhead studies discussed so far compared individual learning with payoff-biased social learning, with alternative social learning strategies difficult or impractical for participants to use. In one study (Mesoudi 2011a), participants were given the option to engage in three additional strategies: random copying (copying the arrowhead of a randomly-chosen fellow group member), conformity (in which continuous traits were divided into 10-unit intervals, i.e., 1–10, 11–20, 21–30…, and the conforming participant is assigned the mid-value of the most popular interval in their group) and averaging (in which participants were assigned the arithmetic mean of everyone in the groups' values for each trait, similar to Boyd and Richerson's (1985) blending inheritance), along with payoff bias (copying the arrowhead of the highest-scoring group member) and individual learning (directly changing the traits with no social influence) as before.

Payoff-biased social learning was the clear favourite compared to the other social learning strategies. Across all hunts played by all participants, 78 % involved individual learning, 19 % payoff-biased social learning, and only around 1 % each of conformity, random copying and averaging (Mesoudi 2011a). Again, this choice of social learning strategy is adaptive in the multimodal adaptive landscape implemented here. As shown using agent-based models simulating each of these strategies (Mesoudi and O'Brien 2008b), only payoff-biased social learning outperforms individual learning, due to the aforementioned reason that individual learners stuck on locally optimal peaks can jump to higher-fitness peaks found by more successful group members. Random copying also allows participants to jump peaks, but to a random, not necessarily high, peak. Conformity allows participants to jump to the most popular peak, but again there is no reason that this most-popular peak is the highest (unless payoff-bias has already acted). Averaging is particularly bad, as the mean trait value of several peaks is likely to be mid-way between all of them, i.e., in a valley.

8.3.4 Payoff Biased Social Learning Leads to "Cultural Hitchhiking"

In Sects. 3.2 and 3.3 we saw how payoff-biased social learning is adaptive, allowing participants to jump to high-fitness peaks in the multimodal adaptive landscape. Yet this social learning strategy also comes with disadvantages. As noted above, the Colour trait was neutral and had no effect on the score shown to participants. Despite this, Colour was copied by our participants just as faithfully as the other functional traits during payoff-biased social learning (Mesoudi and O'Brien 2008a).

This was measured by calculating pair-wise inter-trait correlations across all participants in a group, i.e., the correlation between all participants' Height and Width, the correlation between all participants' Height and Thickness, and so on. Following periods of individual learning, these inter-trait correlations were found to be quite low, around $r = 0.1–0.3$. This is to be expected, as different individual learners would diverge to different peaks in the adaptive landscape, thus reducing between-participant similarity. Once payoff-biased social learning was permitted, however, the inter-trait correlations increased significantly to around $r = 0.3–0.9$. This is because all participants in the group copied the single most-successful group member (apart from that most-successful participant him or herself, of course, who could not copy themselves), thus all participants ended up with extremely similar arrowheads. Colour showed the same pattern of inter-trait correlations as the other traits, indicating that Colour was copied along with the other functional traits in a complete package.

This is an example of a neutral trait hitchhiking on functional traits, and represents the downside of payoff-biased social learning: while copying a successful individual will on average lead to the acquisition of adaptive behaviour, occasional neutral or even maladaptive traits might also be copied. This hitchhiking was explored formally by Boyd and Richerson (1985) as 'indirect' bias, which encompasses payoff-biased social learning, in which successful people are preferentially copied, and prestige bias, in which people with high social status are preferentially copied (which may, or

may not, correspond to objective measures of success in tasks such as hunting). If this 'cultural hitchhiking' is an intrinsic side-effect of payoff- or prestige-biased social learning then we might expect neutral traits to be common in the archaeological record, and not necessarily seek functional explanations for all observed traits (see also Bentley et al. 2004; Dunnell 1978; Neiman 1995).

A more recent study illustrates further the power of prestige bias. Henrich and Gil-White (2001) suggested that people often identify from whom to copy based on quite minimal and subtle cues of prestige, such as looking times. Highly prestigious individuals should be looked at more by others than less prestigious individuals because they are good sources of information, and so looking times might constitute a cheap and quick cue regarding who to copy. Atkisson et al. (2012) tested this prediction in the Virtual Arrowhead Task, presenting participants with objective success information—the scores of other group members—as before, but also fictional looking time information concerning how long each group member had chosen to view every other group members' arrowheads. Even though the looking times were fictional and therefore useless, this marker of prestige was used at least as much as the objective success information when participants were choosing from whom to copy. So again, while this prestige-biased social learning may be broadly adaptive, it can easily misfire.

Further studies might look more systematically at the conditions under which we would expect neutral or maladaptive to hitchhike via generally prestigious models. We might predict hitchhiking to be particularly prevalent when it is difficult to directly assess the efficacy of different traits. In the arrowhead task, the constant random error in feedback likely obscured the fact that Colour had no systematic effect on payoffs; future studies might vary the size of this feedback error to determine whether hitchhiking disappears below some error threshold. Whether maladaptive traits hitchhike, meanwhile, is likely dependent on their cost relative to the fitness benefits of the adaptive traits exhibited by prestigious demonstrators. One might predict that highly maladaptive traits would not spread beyond an initial accidental copying event after which their negative effects are detected (although cases such as kuru [Durham 1991] or celebrity-driven copycat suicides [Mesoudi 2009] might suggest otherwise).

8.3.5 Informational Access Costs Block Social Learning

In the Virtual Arrowhead experiments discussed so far, participants could freely view other participants' arrowhead designs. This is unlikely to hold true for all real-life situations, however. Henrich and Gil-White (2001) suggested that even though many hunter-gatherer societies are relatively egalitarian, highly skilled individuals will often receive material benefits (e.g., food) or non-material benefits (e.g., status) from letting others watch them engage in their skilled activity. Stout (2002) found that knowledge of stone tool production in adze makers of Indonesian Irian Jaya was carefully protected through the use of highly selective apprenticeships. Similarly, in industrialised societies, it is commonplace for highly skilled or knowledgeable people, from car mechanics to lawyers, to set prices for access to their skills or knowledge. Moreover, the level of skill and knowledge often covaries with their price: more knowledgeable lawyers set higher fees than less knowledgeable lawyers, for example. These prices can be seen as 'informational access costs', which potential social learners must pay in order to access social information.

In one study, I therefore added informational access costs to the Virtual Arrowhead Task (Mesoudi 2008). Each participant could set their own access cost, in terms of calories, that other group members had to pay in order to view their arrowhead design. These costs were added and subtracted to the participants' actual cumulative scores. For example, if Participant 1 set an access cost of 450 calories and Participant 2 chose to copy Participant 1, then 450 calories would be deducted from the cumulative score of Participant 2 and 450 calories would be added to the cumulative score of Participant 1.

As expected, participants with higher scores set higher informational access costs than participants with lower scores. Participants were clearly aware, then, that their fellow participants will engage in payoff-biased social learning and preferentially copy the highest-scoring participant, such that their information would be in the highest demand and therefore be most valuable. But unexpectedly, rather than seeking to profit from the access costs of potential copiers, the highest-scoring participants in the group typically set excessively high access costs (mean = 2,500 calories, although ranging up to 23,000 calories) which no other group member was willing to pay. Consequently, the frequency of social learning dropped, and the frequency of payoff-biased social learning dropped to almost zero. At the group level, the overall increase in mean score illustrated in Fig. 8.4 disappeared, and groups of social learners with informational access costs performed no better than groups of individual learners.

In a sense, this use of informational access costs to block social learning is a product of the competitive nature of the task as it was set up in that study. Participants were informed not only of their absolute score but also their relative rank in their group (although participants in this particular study were unpaid, they seemed to be motivated primarily by rank rather than absolute performance). It was therefore in the interest of high-scoring participants to maintain their advantage by protecting their high quality information. If the incentives were to be changed such that participants are only

shown or rewarded for their absolute performance and not provided with information about relative performance, then access costs might be lower and copying more frequent (although there would still be no positive incentive to sharing one's information, just no negative consequence). Alternatively, if groups rather than individuals are rewarded for their overall relative group score, then we might expect more information sharing to occur between group members (but not with members of other groups, if permitted). Adding environmental change might also encourage information sharing even in the most individually competitive situation, as participants might seek to profit from their high-quality information before it becomes out-of-date.

Nevertheless, this study is valuable in demonstrating that people (at least Western people) are not indiscriminately egalitarian with their information. Indeed, the apprenticeships observed by Stout (2002), as well as other institutions such as guilds, might be seen as following the same principles, with high-quality skills and knowledge protected from outsiders.

8.4 Limitations and Applications

There are, of course, many limitations of laboratory experiments. Generally, experiments lack 'external validity', the degree to which the experimental situation resembles the real-life situation of interest. This is true of all experiments, but particularly so when seeking to simulate past technological change in traditional societies, as we are here. The computer-based task described above is obviously a highly abstracted and simplified version of real-life artifact design practiced by past hunter-gatherers. The task lacks any kind of motor activity and physical object affordances. The incentive (a few pounds or dollars) is very different to the incentive to feed oneself and one's family. The participants—typically Western college students—are different in many ways to the long-dead hunter-gatherers responsible for manufacturing artifacts found in the archaeological record. The time-frame is very different: an hour or so in the experiment versus years or decades acquiring the skills needed to manufacture complex artifacts such as arrowheads or handaxes. So too is the social structure: a closed and small group of unrelated strangers in the experiments versus a much larger kin-based society with overlapping generations, migration from other groups, and so on.

All of these limitations should be recognised. Yet experiments make up for their obvious lack of external validity by having high 'internal validity', the degree to which they afford experimental control (Mesoudi 2007). In experiments we can isolate and manipulate specific variables in order to test their causal effect; we can randomly assign participants into different conditions in order to test hypotheses; we can re-run situations in multiple groups to determine whether observed effects are robust or historically contingent; and we can obtain complete and unbiased data regarding our participants' behaviour. None of these are possible with historical or ethnographic methods for both practical and ethical reasons. Archaeologists cannot 're-run' history or manipulate key variables to see how history would have changed in response to that variable, and seldom have uninterrupted or unbiased historical data sets. Ethnographers cannot randomly assign contemporary hunter-gatherers into different control and experimental societies to see how a key variable affects behaviour. Essentially, historical and observational methods are limited in being correlational, whereas experiments can test causal hypotheses.

Experiments can therefore be seen as a useful bridge between theoretical models and historical/ethnographic methods. The key point is that these methods should be used in combination. Theoretical models and experiments that are not informed by real-life historical and observational data will simply reflect the uninformed and probably incorrect intuitions of the modeller/experimenter. Conversely, historical and observational data alone cannot be used to test causal hypotheses due to their non-interventionist and correlational nature.

This interplay is hopefully illustrated in our previous application of the Virtual Arrowhead Task to a specific archaeological case study. Bettinger and Eerkens (1999) documented how projectile points from the Great Basin region of the south-western United States from around 300–600 AD exhibited systematic differences between two sites. In one site, in central Nevada, the inter-trait correlations were very high, indicative of a small number of uniform types. In eastern California, in contrast, inter-trait correlations were significantly lower, such that there were no systematic links between the dimensions of different arrowheads. Having ruled out any differences in prey or material type between the two sites, Bettinger and Eerkens (1999) suggested that the difference lay in learning strategies: prehistoric Nevada featured strong payoff- or prestige-biased social learning, such that hunters copied a small number of designs exhibited by a few high-status individuals, whereas prehistoric California featured much more individual learning, which increased variation as different hunters experimented in different ways.

As noted above, our experimental simulation supported this hypothesised scenario (Mesoudi and O'Brien 2008a): when our participants were allowed to engage in payoff-biased social learning then inter-trait correlations increased (like in Nevada), and when our participants had to rely on individual learning then inter-trait correlations were low (like in California). This supports Bettinger and Eerkens (1999) hypothesis, and shows that it is consistent with actual human behaviour.

Yet we also showed that this hypothesis only works under certain assumptions that were not specified by Bettinger and Eerkens (1999). For example, the hypothesis only works under the assumption of a multimodal adaptive landscape. If there is a single optimal point design, then individual learners will converge on this design, and inter-trait correlations will remain high. Indeed, independent work testing the functional characteristics of projectile points suggests that multiple locally optimal designs are a reasonable assumption. Cheshier and Kelly (2006) found that long, thin points were easier to aim and hit prey with but less likely to result in a kill due to the small wounds they create, whereas thick, wide points were harder to fire but more likely to result in a kill because they created a larger wound. Here we have at least two optima: one maximising firing power, the other maximising the likelihood of a kill.

Moreover, our experimental programme suggests possible reasons why prehistoric Nevada might have featured more social learning than prehistoric California. Perhaps individual learning was more costly in Nevada due to its harsher environment making social learning more adaptive, or perhaps informational access costs were higher in California therefore blocking social learning. These hypotheses, suggested by our experiments, can hopefully guide further archaeological research. In sum, the interplay of theoretical models, archaeological data and lab experiments provides a richer understanding of the past than any one of these methods alone.

8.5 Conclusions

The aim of this series of studies (Atkisson et al. 2012; Mesoudi 2008, 2011a; Mesoudi and O'Brien 2008a, b) was to test the predictions of theoretical models concerning the adaptiveness of contemporary humans' learning strategies, using a complex task designed to be representative of real-life human technology. Participants in small groups designed virtual arrowheads via individual and social learning, while we manipulated key variables such as the form of the underlying fitness functions, the possible social learning strategies permitted, the cost of individual learning, and whether social information was free or costly to access.

Our findings demonstrated that people approached this task in a broadly adaptive manner. They used a simple but effective reinforcement-based individual learning strategy that improved their payoff by leading them to a locally-optimal arrowhead design. They engaged in payoff-biased social learning in preference to alternative and less effective social learning strategies such as conformity, random copying and averaging, with this payoff-biased social learning uniquely allowing participants to jump from low-fitness locally optimal designs to high-fitness globally optimal designs that had been found by more successful group members. At a larger scale, payoff-biased social learning is especially likely to lead to cumulative cultural evolution (Aoki et al. 2012; Enquist et al. 2008; Mesoudi 2011b; Powell et al. 2009) by selectively preserving and building on effective cultural traits. It is therefore encouraging that our participants readily and preferentially engaged in this particular social learning strategy.

Moreover, both individual and social learning flexibly responded to the participants' performance in real-time. When participants were performing poorly, they made larger changes to their arrowhead when learning individually, and they were more likely to engage in payoff-biased social learning. This latter 'selective learning'—copying others only when individual learning is costly or difficult—has been shown to be adaptive relative to a mix of pure individual learners and pure social learners, allowing our participants to avoid the detrimental effect of information scrounging (Boyd and Richerson 1995).

Yet there were also flaws in our participants' learning strategies. Payoff-biased social learning was indiscriminate such that participants readily copied functionless traits from successful individuals alongside their functional traits. Indirect cues to prestige, such as looking times, were used as guides to who to copy as much as objective measures of success, even when it was inappropriate to do so, which may exacerbate the spread of neutral or even maladaptive traits. Finally, when participants were allowed to set access costs that others had to pay in order to see their arrowhead, they used these to block all social learning. At a population level, this may be detrimental to the overall preservation and accumulation of knowledge, and highlights how the cooperative motivation to share information on the part of the demonstrator is just as important as the social learners' choice of who to copy.

A comparison of contemporary humans' learning abilities with those of prehistoric hominins (either anatomically modern humans or Neanderthals) is beyond the scope of this paper, and will be left to those expert in interpreting the archaeological record. It is instructive, however, to compare the results of these studies with similar learning studies of chimpanzees. Some studies suggest that, in contrast to our human participants, chimpanzees are less likely to switch to superior solutions to tasks. Marshall-Pescini and Whiten (2008), for example, found that chimpanzees will readily copy and use a quite-good method for extracting honey from a puzzle box (sticking a wand into the box and licking honey off the end) but, when shown an even better method (using the wand to open the top of the box to expose all of the honey), fail to switch to this superior solution (see also Hrubesch et al. 2009). This stands in contrast to our participants, who readily abandoned their own arrowheads and switched to superior designs. This lack of payoff-biased social learning in chimps might explain why their cultural

traditions remain non-cumulative (Tennie et al. 2009), if they fail to selectively copy and switch to superior traits.

On the other hand, more recent studies suggest that chimpanzees *will* switch to superior methods if they are dissatisfied with their current payoff (Dean et al. 2012; Yamamoto et al. 2013), suggesting that they do exhibit some form of payoff-biased social learning. Dean et al. (2012) attributed a lack of cumulative culture in chimpanzees instead to a lack of teaching, imitation and/or prosociality. The latter finding in particular might be of particular importance. Chimpanzees have been shown to be inordinately self-interested, failing to share food with others even when there is no cost to sharing (Jensen et al. 2007; Silk et al. 2005). As we showed in our studies using informational access costs, a lack of cooperation can severely block social learning. Human cumulative culture may therefore be intimately tied to our cooperative motivations (Dean et al. 2012; Hill et al. 2009; Mesoudi and Jensen 2012).

Assuming that chimpanzees are closer behaviourally to the common ancestor of chimpanzees and humans that lived around 6 million years ago (which is, admittedly, a contestable assumption), we can speculate that somewhere in the hominin lineage the capacities for high fidelity and flexible payoff-biased social learning, tied to cooperative motivations to allow individuals to copy one other, evolved and facilitated the emergence of cumulative cultural adaptations. As illustrated in Sect. 4, it is possible to detect the signatures of different learning strategies in the archaeological record, as we did in the Great Basin by inferring payoff-biased social learning from high inter-trait correlations and individual learning from low inter-trait correlations. Perhaps the same might be possible with earlier material culture to determine, say, whether Neanderthals exhibited payoff-biased social learning. The appearance of culturally hitchhiking neutral or maladaptive traits might also serve as an indication of payoff-biased social learning. In sum, hopefully the further interplay of lab experiments and theoretical models, along with comparative studies of non-human primates and the archaeological study of prehistoric hominin material culture, will lead us to a better understanding of our species' success story.

References

Akazawa T (ed) (2012) Replacement of Neanderthals by modern humans (RNMH) project series, vol 1. RNMH Project Group, Kochi University of Technology, Tokyo

Aoki K, Wakano JY, Feldman MW (2005) The emergence of social learning in a temporally changing environment: a theoretical model. Curr Anthropol 46:334–340

Aoki K, Lehmann L, Feldman MW (2011) Rates of cultural change and patterns of cultural accumulation in stochastic models of social transmission. Theor Popul Biol 79:192–202

Aoki K, Wakano JY, Lehmann L (2012) Evolutionarily stable learning schedules and cumulative culture in discrete generation models. Theor Popul Biol 81:300–309

Atkisson C, Mesoudi A, O'Brien MJ (2012) Adult learners in a novel environment use prestige-biased social learning. Evol Psychol 10:519–537

Bentley RA, Hahn MW, Shennan SJ (2004) Random drift and culture change. Proc R Soc B 271:1443–1450

Bettinger RL, Eerkens J (1999) Point typologies, cultural transmission, and the spread of bow-and-arrow technology in the prehistoric Great Basin. Am Antiq 64:231–242

Boyd R, Richerson PJ (1985) Culture and the evolutionary process. University of Chicago Press, Chicago

Boyd R, Richerson PJ (1988) An evolutionary model of social learning: the effects of spatial and temporal variation. In: Zentall T, Galef BG (eds) Social learning. Erlbaum, Hillsdale, pp 29–48

Boyd R, Richerson PJ (1992) How microevolutionary processes give rise to history. In: Nitecki M, Nitecki DV (eds) History and evolution. State University of New York Press, Albany, pp 178–209

Boyd R, Richerson PJ (1995) Why does culture increase human adaptability? Ethol Sociobiol 16:125–143

Cavalli-Sforza LL, Feldman MW (1981) Cultural transmission and evolution. Princeton University Press, Princeton

Cheshier J, Kelly RL (2006) Projectile point shape and durability: the effect of thickness: length. Am Antiq 71:353–363

Dean LG, Kendal RL, Schapiro SJ, Thierry B, Laland KN (2012) Identification of the social and cognitive processes underlying human cumulative culture. Science 335:1114–1118

Dunnell RC (1978) Style and function: a fundamental dichotomy. Am Antiq 35:305–319

Durham WH (1991) Coevolution: genes, culture, and human diversity. Stanford University Press, Stanford

Ehn M, Laland KN (2012) Adaptive strategies for cumulative cultural learning. J Theor Biol 301:103–111

Enquist M, Ghirlanda S, Jarrick A, Wachtmeister CA (2008) Why does human culture increase exponentially? Theor Popul Biol 74:46–55

Gergely G, Csibra G (2006) Sylvia's recipe: the role of imitation and pedagogy in the transmission of cultural knowledge. In: Enfield NJ, Levenson SC (eds) Roots of human sociality: culture, cognition, and human interaction. Berg, Oxford

Henrich J, Boyd R (1998) The evolution of conformist transmission and the emergence of between-group differences. Evol Hum Behav 19:215–241

Henrich J, Gil-White FJ (2001) The evolution of prestige. Evol Hum Behav 22:165–196

Hill K, Barton M, Hurtado AM (2009) The emergence of human uniqueness. Evol Anthropol 18:187–200

Hrubesch C, Preuschoft S, van Schaik C (2009) Skill mastery inhibits adoption of observed alternative solutions among chimpanzees (Pan troglodytes). Anim Cogn 12:209–216

Jensen K, Call J, Tomasello M (2007) Chimpanzees are rational maximizers in an ultimatum game. Science 318:107–109

Laland KN (2004) Social learning strategies. Learn Behav 32:4–14

Lycett SJ, von Cramon-Taubadel N (2008) Acheulean variability and hominin dispersals: a model-bound approach. J Archaeol Sci 35:553–562

Marshall-Pescini S, Whiten A (2008) Chimpanzees (Pan troglodytes) and the question of cumulative culture: an experimental approach. Anim Cogn 11:449–456

McElreath R, Lubell M, Richerson PJ, Waring TM, Baum W, Edsten E, Efferson C, Paciotti B (2005) Applying evolutionary models to the laboratory study of social learning. Evol Hum Behav 26:483–508

Mesoudi A (2007) Using the methods of social psychology to study cultural evolution. J Soc Evol Cult Psychol 1:35–58

Mesoudi A (2008) An experimental simulation of the 'copy-successful-individuals' cultural learning strategy: Adaptive landscapes, producer-scrounger dynamics and informational access costs. Evol Hum Behav 29:350–363

Mesoudi A (2009) The cultural dynamics of copycat suicide. PLoS One 4:e7252

Mesoudi A (2011a) An experimental comparison of human social learning strategies: payoff-biased social learning is adaptive but underused. Evol Hum Behav 32:334–342

Mesoudi A (2011b) Variable cultural acquisition costs constrain cumulative cultural evolution. PLoS One 6:e18239

Mesoudi A, Jensen K (2012) Culture and the evolution of human sociality. In: Vonk J, Shackelford T (eds) The oxford handbook of comparative evolutionary psychology. Oxford University Press, Oxford, pp 419–433

Mesoudi A, O'Brien MJ (2008a) The cultural transmission of Great Basin projectile point technology I: an experimental simulation. Am Antiq 73:3–28

Mesoudi A, O'Brien MJ (2008b) The cultural transmission of Great Basin projectile point technology II: an agent-based computer simulation. Am Antiq 73:627–644

Morgan TJH, Rendell LE, Ehn M, Hoppitt W, Laland KN (2012) The evolutionary basis of human social learning. Proc R Soc B 279:653–662

Neiman FD (1995) Stylistic variation in evolutionary perspective - inferences from decorative diversity and interassemblage distance in Illinois woodland ceramic assemblages. Am Antiq 60:7–36

O'Brien MJ, Darwent J, Lyman RL (2001) Cladistics is useful for reconstructing archaeological phylogenies: Palaeoindian points from the southeastern United States. J Archaeol Sci 28:1115–1136

Powell A, Shennan S, Thomas MG (2009) Late Pleistocene demography and the appearance of modern human behavior. Science 324:1298–1301

Richerson PJ, Boyd R (2005) Not by genes alone. University of Chicago Press, Chicago

Rogers AR (1988) Does biology constrain culture? Am Anthropol 90:819–831

Rogers DS, Ehrlich PR (2008) Natural selection and cultural rates of change. Proc Natl Acad Sci U S A 105:3416

Silk JB, Brosnan SF, Vonk J, Henrich J, Povinelli DJ, Richardson AS, Lambeth SP, Mascaro J, Schapiro SJ (2005) Chimpanzees are indifferent to the welfare of unrelated group members. Nature 437:1357–1359

Simon HA (1956) Rational choice and the structure of the environment. Psychol Rev 63:129–138

Sperber D (1996) Explaining culture: a naturalistic approach. Oxford University Press, Oxford

Stout D (2002) Skill and cognition in stone tool production. Curr Anthropol 43:693–722

Tennie C, Call J, Tomasello M (2009) Ratcheting up the ratchet: on the evolution of cumulative culture. Philos Trans R Soc B 364: 2405–2415

Wright S (1932) The roles of mutation, inbreeding, crossbreeding and selection in evolution. Proceedings of the sixth international congress of genetics 1:356–366

Yamamoto S, Humle T, Tanaka M (2013) Basis for cumulative cultural evolution in chimpanzees: social learning of a more efficient tool-use technique. PLoS One 8:e55768

Part II

Body Science and Genetics

Motion Analysis for Stone-Knapping of the Skilled Levallois Technique

9

Yukinobu Hoshino, Keita Mitani, Naoki Miura, Hiroki C. Tanabe, and Kenji Nagai

Abstract

Motion analysis is an important factor verifying skill learning. The subject has special skills for manufacturing stone-tools based on the Recurrent Levallois technique. The motion data was collected for the kinematic analysis. In January 2011, we acquired the 3D motion data by using the motion capture system. Taken data are the knapping motion data about stone flakes. The motion capture system is able to capture 3D motion data of the subject's motion and hammer stone movement with high resolution. That data includes any knap styles, which are the peeling stone operation, adjusting operation stone surface. Based on interview comments, we analyzed the detailed motion data and the fabrication characteristics of Levallois flake production. The knapping technique with Recurrent Levallois is also a kind of valuable archaeological materials. This paper reports the results of the knapping motion analysis of making stone tools and discuss of the Recurrent Levallois technique.

Keywords

3D motion • Recurrent Levallois technique • Skill learning

Y. Hoshino (✉)
Engineering Course of Graduate School,
Kochi University of Technology, Tosayamada-cho,
Kami-shi, Kochi 782-8502, Japan
e-mail: hoshino.yukinobu@kochi-tech.ac.jp

K. Mitani
Kochi University of Technology, Tosayamada-cho,
Kami-shi, Kochi 782-8502, Japan
e-mail: keita.mitani.kut@gmail.com

N. Miura
Department of Information and Communication Engineering,
Faculty of Engineering, Tohoku Institute of Technology,
35-1 Yagiyama, Kasumi-cho, Taihaku-ku, Sendai, Miyagi
982-8577, Japan
e-mail: miura.naoki@tohtech.ac.jp

H.C. Tanabe
Graduate School of Environmental Studies, Nagoya University,
furo-cho, chikusa-ku, Nagoya, Aichi 464-8601, Japan
e-mail: htanabe@lit.nagoya-u.ac.jp

K. Nagai
Department of Historic Heritage, Tohoku University of Art
and Design, 3-4-5 Kami-sakurada, Yamagata 990-9530, Japan
e-mail: nagai.kenji@aga.tuad.ac.jp

9.1 Introduction

Motion analysis is an important factor verifying skill learning (Michiyoshi et al. 1992). In this research, 3D motion data of a special subject were measured (Okuda et al. 2006). The subject has special skills for manufacturing stone-tools based on the Recurrent Levallois technique. The motion data was collected for the kinematic analysis. Most famous research is analysys the Oldowan industrial stone tools. In this research, any type analysis examples are shown(de la Torre et al. 2003). They used digital-image-analysis techniques to investigate the intensity of reduction in single-platform core stone of the Developed Oldowan. For analysis based on the experimental archaeology, it is important to consider the body control of the knapping process of Levallois point (LP) and Levallois flake (LF). In this paper, the analysis of making a stone tool using Recurrent Levallois technique is reported. In January 2011, we acquired the 3D motion data. We took the knapping motion data about stone flakes by using the motion capture system. In this experiment, the subject is an expert knapper of Recurrent Levallois

T. Akazawa et al. (eds.), *Dynamics of Learning in Neanderthals and Modern Humans Volume 2: Cognitive and Physical Perspectives*, Replacement of Neanderthals by Modern Humans Series, DOI 10.1007/978-4-431-54553-8_9, © Springer Japan 2014

technique. The knapper formed the core stone's edges from one side as Recurrent Levallois technique. Before taking a target flake, the knapper declared the process of flaking off pieces. After that, the subject made a stone flake by strongly knapping. When using the motion capture system, three tracers are placed around the target subject. The motion capture system is able to capture 3D motion data of the subject's motion and hammer stone movement with high resolution. That data includes any knap styles, which are the peeling stone operation, adjusting operation stone surface. We previously reported the analyzed results of motion analysis using image video and the illocutionary acts by interviews with the knapper (Miura et al. 2011a, b). Previously, we reported the analysis and results of the interview data from the subject about the operation process together with the detailed motion data and the fabrication characteristics of Levallois flake production. We also reported the analysis and results using interview data from the subject. In this report, we described the operation process and thinking points of the force value and a hit point (Dibble 1997).

Based on interview and comments, we analyzed the detailed motion data and the fabrication characteristics of Levallois flake production. In the RNMH project, the learning ability of Neanderthal is the main topic. As main hypothesis, this learning ability would be mandatory for the survival of mankind. Archaeological material would be the only evidence that reveals the learning behavior of prehistoric times (Nishiaki and Nagai 2012). We analyzed archaeological materials in order to determine the difference between modern human beings and the New Learning of archaic humans. We took and analyzed archaeological materials in order to determine the difference between modern human beings and the New Learning of archaic humans. The knapping technique with Recurrent Levallois is also a kind of valuable archaeological materials. Modern humans begin with a cognitive behavior. More specifically, they obtained this skill during a relatively short time period of 250,000 to 6 million years. Those are from the evolution and a group production by mixing group learning and individual learning. This paper reports the results of the knapping motion analysis of making stone tools and discuss of the Recurrent Levallois technique.

9.2 Two Process of Recurrent Levallois Technique for the Motion Analysis

In this paper, we report the analysis results of an expert knapper's motion using the Recurrent Levallois technique (Nonaka et al. 2010). It is important to analyze the process in order to understand human's learning ability. However, the analysis is very difficult because those are no precedent. First, we analyzed a difference of kinematic information of arm motion between each procedure to product a stone-tool using the Recurrent Levallois technique. The 3D motion data is measured from a skilled subject by this experiment. For the analyses, we consider 2 level procedures about Recurrent Levallois technique (see Fig. 9.1). We catalog two process

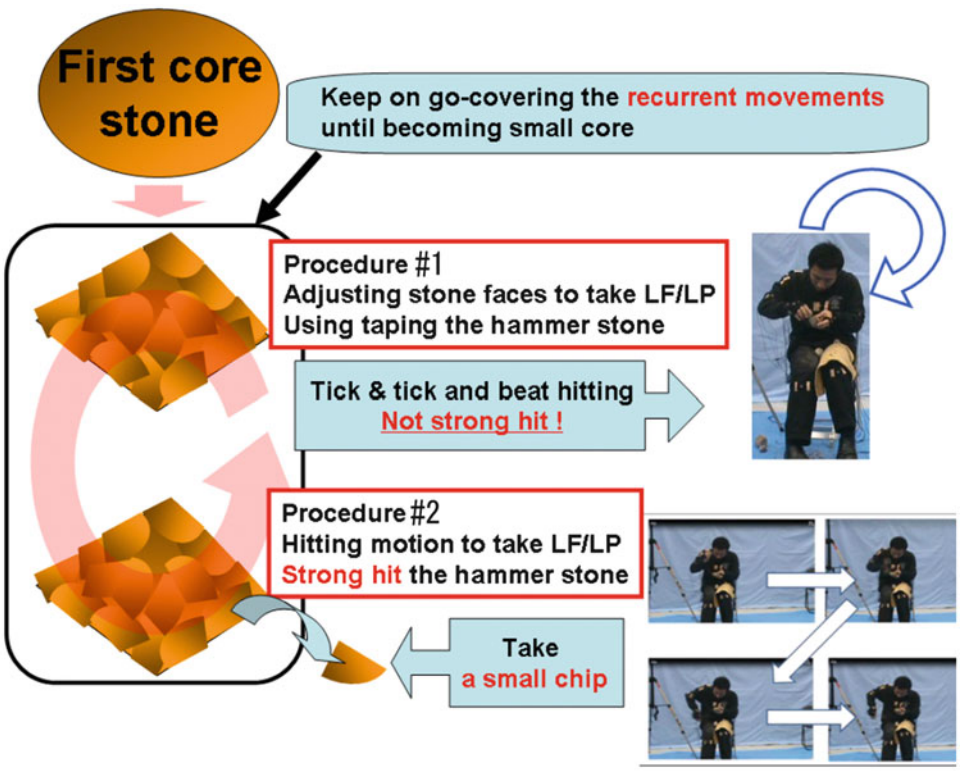

Fig. 9.1 Two process diagram of the Recurrent Levallois technique

data classes for our analysis. The first process is a beat knap to make a form called a stone testudinal style. The second process is a strong knap to flake off a piece of stone. So, a procedure #1 is in the process of forming the testudinal style by finely knapping. The core stone is deformed visually by a beat knapping, so with the former it is possible to check this hitting motion visually and acquire the deforming technique by the observational learning (group learning). The knapper should proceeds with consideration of the flakes in the acquired process about a procedure #2, it is predicted to advance (prediction) the transition state to the process of a procedure#2. This paper, we discuss about #2 that is process of taking LF and LP. So, a procedure #1 is outside from a main discussion. Using experiential knowledge to make stone tools is important, is considered.

9.3 The Outline of the Stone-Tool Production Experiment for a Motion Analysis

The experiment to make the stone-tools and analysis the production motion was tried (see Fig. 9.2). This experiment consisted from three phases, the rehearsal experiment and two main experiments. The rehearsal experiment was conducted one time. Next day, we conducted a full-scale experiment. One hour later, a final experiment is conducted. LP involves the former of an object with a tip such as a spear, dart, or arrow, or perhaps something used as a knife. If the knapper has an image of that behavior, the knapper declares “LP”in the experiment. LF motion is the behavior to take the flakes objects. If the knapper has an image of that behavior, the knapper declares “LF”in the experiment. In the rehearsal session, the knapper tried five times to form a LP/LF. In this case,the total number of strong knaps was 28 times during 11 min. In the first experiment, the knapper tried 14 times to form a LP/LF. In this case, the total number of strong knaps was 52 times during 27 min. In the final experiment, the knapper tried 16 times to form a LP/LF. In this case, the total number of strong knaps was 66 times during 55 min. The knapper was carefully shaping the core stone. After that, the knapper hit the stone strongly. Is this same process used by Neanderthals? or only modern humans? In this experiment, we use 4 sets video and the motion capturing system Visualize3000. All motions were analyzed from video data and 3D x-y-z motion data.

9.4 The Motion Capturing System Visualize3000

For motion analysis, we used the Visualize3000 of motion capture system. Visualize3000 is product by PhoeniX Technologies, BC, Canada. The motion capturing is the process of sampling the posture and location information of a subject over time. The subject is usually a person, an animal or a machine. The technical goal of motion capture is to get the motion data,which are the certain points on the subject. So that either some parameters of the motion (e.g., speed, angle, distance, etc.) can be calculated or the data can be used to control or drive (Taniguchi et al. 2012). In case parameters of the motion are calculated, the application may be motion analysis, sports analysis, biomechanics, biodynamic and so on. This motion capture system has three tracker, many LED markers and TMC. TMC system is radio waves transmission system LED signal to motion trackers. The tracker system is able to track LED’s light signal and send signal data to computer. This tracker uses an infrared ray and measures the distance between trackers and LED. See Fig. 9.3, we show data sheet of the tracker spec at Visualize3000 system. This tracker is possible to measure ±45 ° vertical direction and horizontal direction. About 4 m triangle area is a real capture area using three tracker. In our experiment, a subject knapper stays in this area.

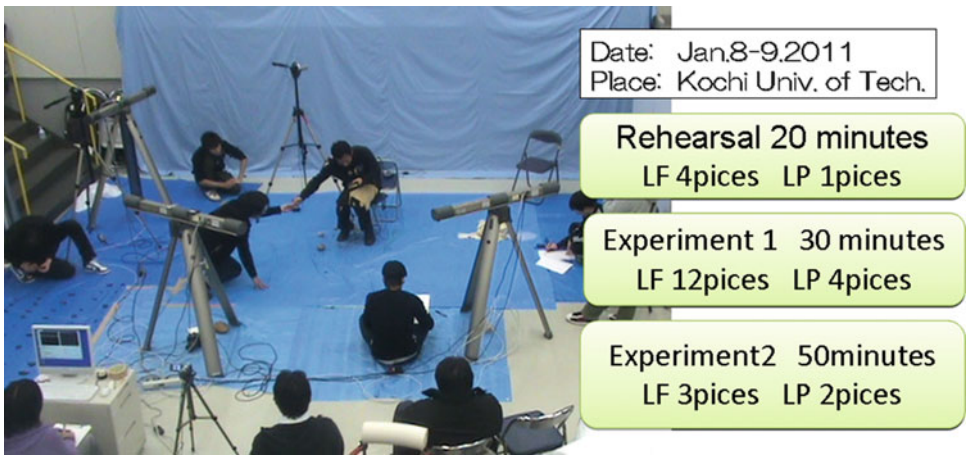

Fig. 9.2 Picture of experiment

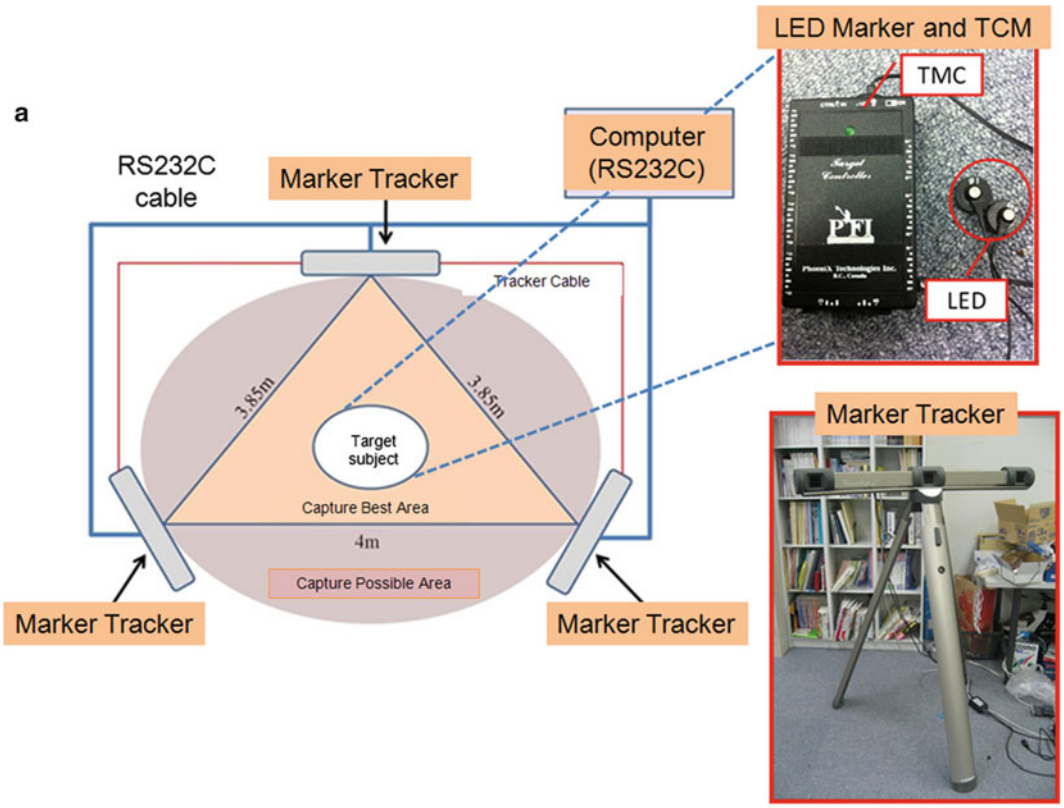

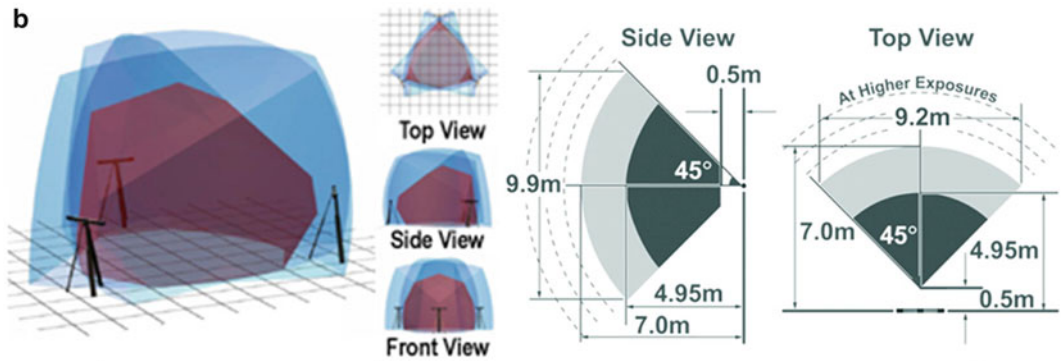

3D space resolution	under than 0.015[mm] about 1D
Duplication error	under than 0.050[mm] about 3D
3D sensing accuracy	0.6~2.2[mm], Horizontal angle ±40° , Vertical angle ±35°
Sampling rate	3300 times/sec

Fig. 9.3 (**a**) System framework of Visualize 3000, (**b**) Data sheet of Visualize 3000

This system have VZSoft Application, show the visualize computer graphics (CG) using bone and dots (see Fig. 9.4). This software is able to show the basic CG information and recode 3D motion xyz position. In our experiment, we took 13 marker's 3D movement data (xyz -position) during 800 thousand steps.

9.5 Analysis About Getting to LF/LP Motion

In this research, we have processed a detailed analysis of behavior. Our focusing is the motion at the time of getting flakes. Figure 9.5 is the marker position and setup stones in this

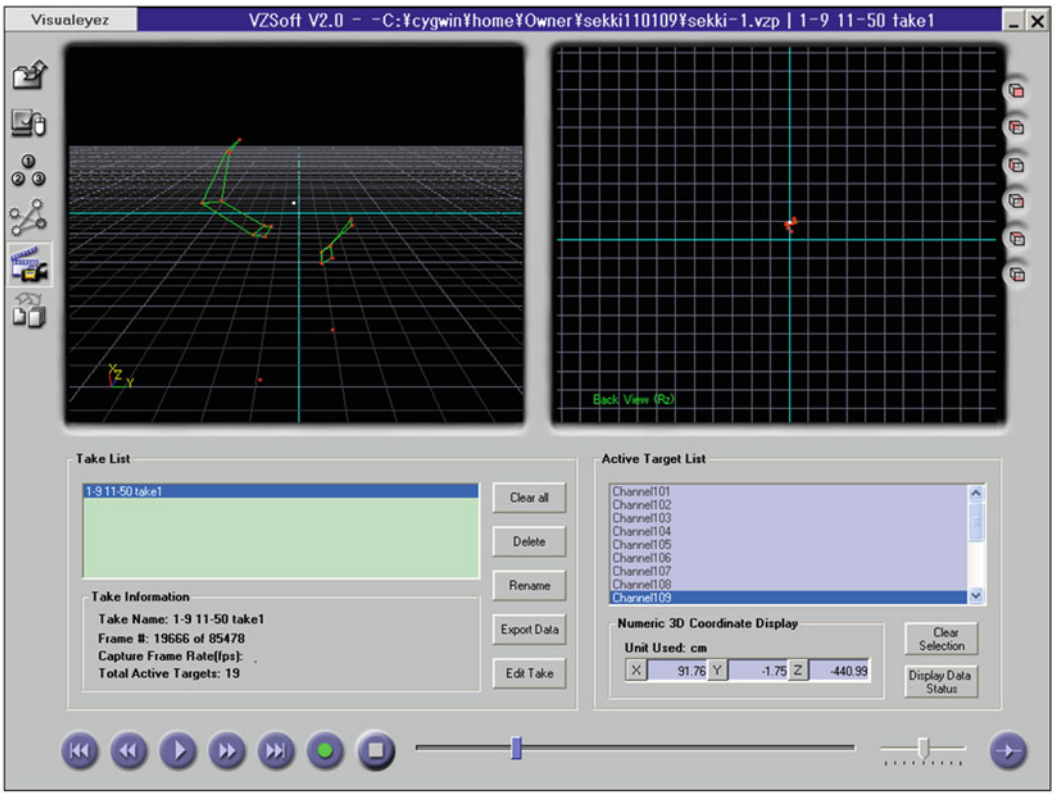

Fig. 9.4 "VZ Soft": Viewing the marker motion

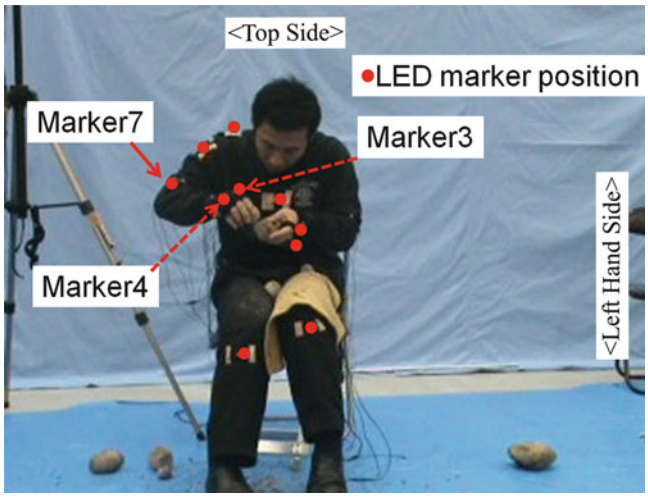

Fig. 9.5 Setup the motion LED markers and a hammer

experiment. Knapper gives us declaration for getting flakes. Some hammer stones always were selected by knapper decision (see Fig. 9.6). Then knapper decide LF/LP motion from small and medium size core stone, mostly selected lightweight stone, 115 g. This is likely to be a result of determining the controllable easy than the powerful impact. Before the motion, knapper declared the process of getting LF. We would be able to see the behavior of twisting wrist, and to see the behavior of pulling elbow behind is a graph of speed on the hammer stone at getting LF/LP. This curve explains the big impact and hitting stone. After this impact, stone speed has changed slowly.The knapper decides thenecessary acceleration for getting LF/LP. See Fig. 9.7, the curve is a marker 3's speed.Marker 3 is almost a hammer stone movement. This curve's direction is increasing rapidly between about 0.37–0.43 s. This area is a curve before the stone hammer collides with the core stone. The impact point is a little bit before from a top about 0.43–0.45 s. The curve direction is drop down rapidly between about 0.45–0.60 s. This area is a curve after the stone hammer collides with the core stone. A small upper curve on left side is upstroke the hammer to side of a head. The valley curve point is stopping period of the hammer. In this period, knapper decides and starts action to hit the core stone. Those top speeds are 3.34 ± 0.51 m/s (=Median ± Standard Deviation). The coefficient of variation is 0.15(C.V. = 15 %). So values of top speed are spread out 15 % within an average. We consider that the hammer's top speed is impeded on all cases for taking LF/LP. Basically, the hammer stone is not heavy and controllable is not hard. Thus, we checked all videos about the griping hammer stones, are hold tight or not. See Fig. 9.8, the knapper is change the gripping hammer stone as Opening stage and Final stage. So usually, knapper motion does not work about a detail speed control and keep the constant top speed. So, we decided to check the controllable ability of knapper.

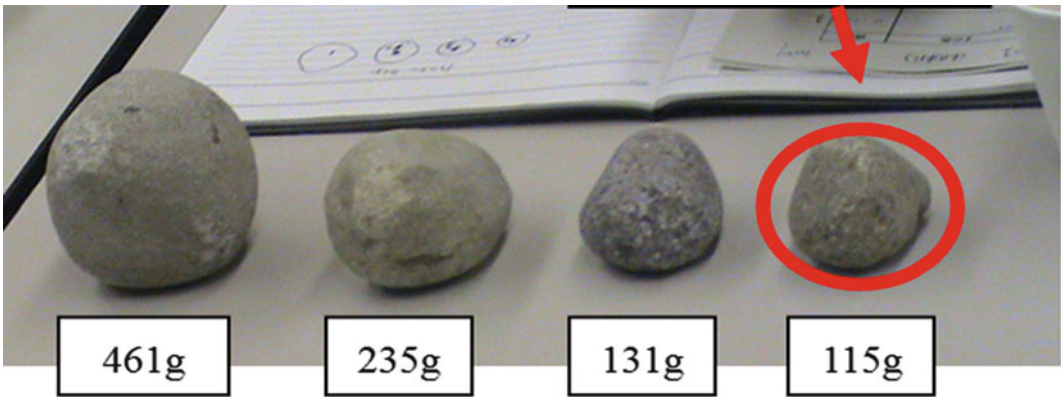

Fig. 9.6 Characteristic of using hammer stones

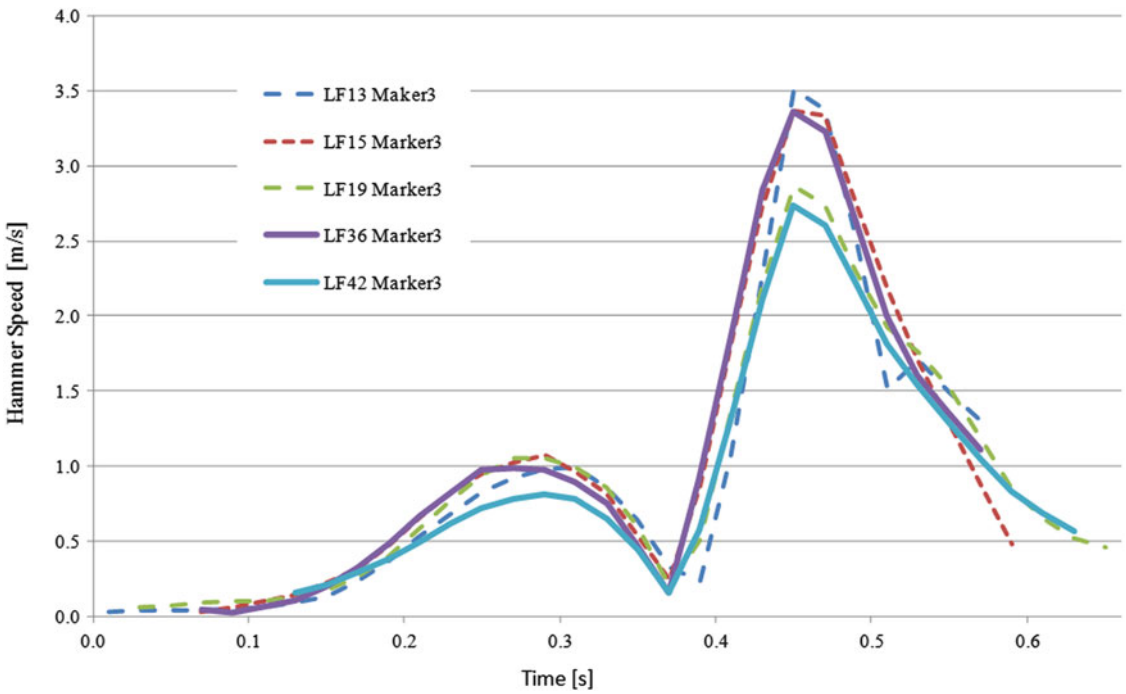

Fig. 9.7 Speed curve a marker 3 at getting LF/LP

We have discussed to be categorized LF/LP motion as Table 9.1. Let's read it carefully that LF/LP is not getting stones. In this experiment, LF/LP is the decision making results of knapper. The knapper declared taking the LF/LP with a current core stone. Knapper is not necessarily to acquire the real LF/LP. We are not care for getting real LF/LP. Let we check LF13, LF19, LF36 and LP42. Firstly, we classified three stages by core size and hammer's weight. Three stages are Opening, Stable and Final. On the opening stage, knapper took the surface parts of the core and took LF sometimes. On the stable stage, knapper changes the hammer stone and declared LF at six times. The motion is very smooth. The core size is medium and a hitting was looks so easy by watching a video. The twisting motion changed to quick motion in this stage. Changing hammer stone is very important point. See Fig. 9.8, this picture shows a period start to swing down the hammer stone. When knapper took LF13, he grips a holding tight the hammer stone. When knapper took LP43, he grips a holding not-tight the hammer stone. Table 9.1 describes double heavy hammer stone within LF13 and LP42. Knapper keeps a balance between holding a hammer stone and the centrifugal force of circular motion as swing down. The centripetal force is $F = mv^2/r$ with a hammer stone, vis constant speed by Fig. 9.7, ris constant radius of the path (aim length) and m is mass. The force is, of course, this acceleration multiplied by the mass of the hammer stone. If swing down is speed up 15 % then this force up just 32 %. If hammer weight is double mass then this force

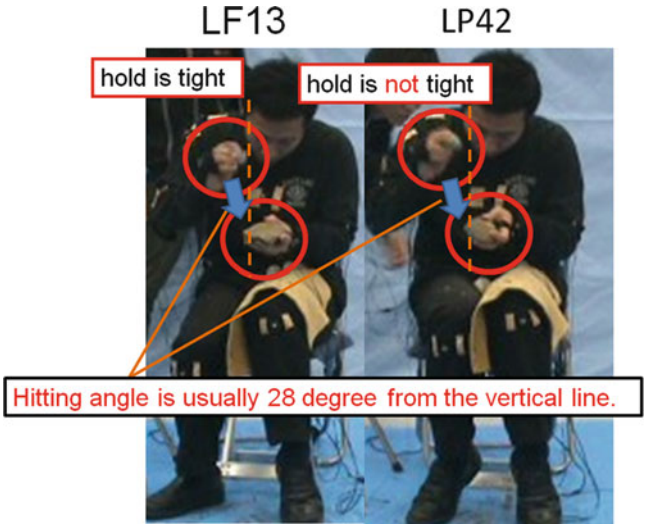

Fig. 9.8 Motion pictures of gripping a hammer

up 100 %, is like double force. So hammer weight works directly force. Knapper need to hold tight using heavy hammer stone during Opening stage. Hitting angle is usually 28 ° from the vertical line.

9.6 Detail Analysis About LF13 Motion

Figure 9.9a–c shows motion pictures and follow speed vector of the hammer stone. This speed vector has colors that show the maker speed. Red-Orange color arrows are shown between 2.90 and 2.00 m/s of the maker speed. Yellow-Green color arrows are shows between 1.90 and 1.00 m/s of the maker speed. Light blue-Deep blue color arrows are shows between 0.90 and 0.00 m/s of the maker speed. In this picture, knapper hold tight hammer stone and swing down to the core. In this case, the hammer stone is dropped down with straight to the core. Top speed is very high but knapper did not twist and pulling elbow a little. We consider that knapper availed a heavy weight of hammer stone. After the picture analysis, we checked 3D curve and the vector of finishing period about marker3 and marker4. During 2 circle's area, the hammer stone is going up stroking. After that, knapper swing down with straight to take LF13 from the core stone. In this motion, knapper did not twisting action, because those arrows of finishing period are mostly straight parallel.

9.7 Detail Analysis About LF19 Motion

Figure 9.10a–c shows motion pictures and follow speed vector of the hammer stone. In this picture, knapper hold tight hammer stone and swing down to the core. In this case, the hammer stone is dropped down with a little twist to the core. Top speed is very low. Knapper did little twist and pulling elbow a little. We consider that knapper availed a heavy weight of hammer stone, like almost same case of LF13. After the picture analysis, we checked 3D curve about the vector tail marker3 and marker4. Blue arrows area is upstroke area of the hammer. After that, knapper swing down with a curving to take LF19 from the core stone. In this motion, knapper did not twisting action, because those arrow tails are mostly curving parallel. So, this case is almost same case of LF13 by an arrow graph analysis. If knapper tried curving swing down the hammer, the centripetal force of hammer is big. Thus, knapper keep hold tight a hammer stone. Generally, the wrist snapping and twisting motion are not controllable, if a handhold is tight (Okuda et al. 2006). Especially, the centripetal force will be big then knapper must hold a hammer stone strongly.

Table 9.1 LF/PL motion class of Experiment 2

	LF/LP	Hammer weight (g)	Core size	Pulling elbow	Twist action	Top speed of hammer (m/s)
Opening stage	LF13	235	Big	Little	Non	3.51
	LF15	235	Big	Quick	Little	3.37
	LF19	235	Big	Little	Non	2.87
Stable stage	LF30	115	Mid	Quick	Little	3.04
	LF32	115	Mid	Quick	Little	3.18
	LF35	115	Mid	Little	Quick	2.55
	LF36	115	Mid	Little	Quick	3.36
	LF38	115	Mid	Little	Quick	3.69
	LF39	115	Mid	Quick	Quick	3.14
Final stage	LP42	115	Small	Quick	Quick	2.74
	LF43	115	Small	Little	Little	4.53
	LF44	115	Small	Little	Little	3.37
	LP47	115	Small	Non	Non	3.85
	LF51	115	Small	Non	Non	3.88

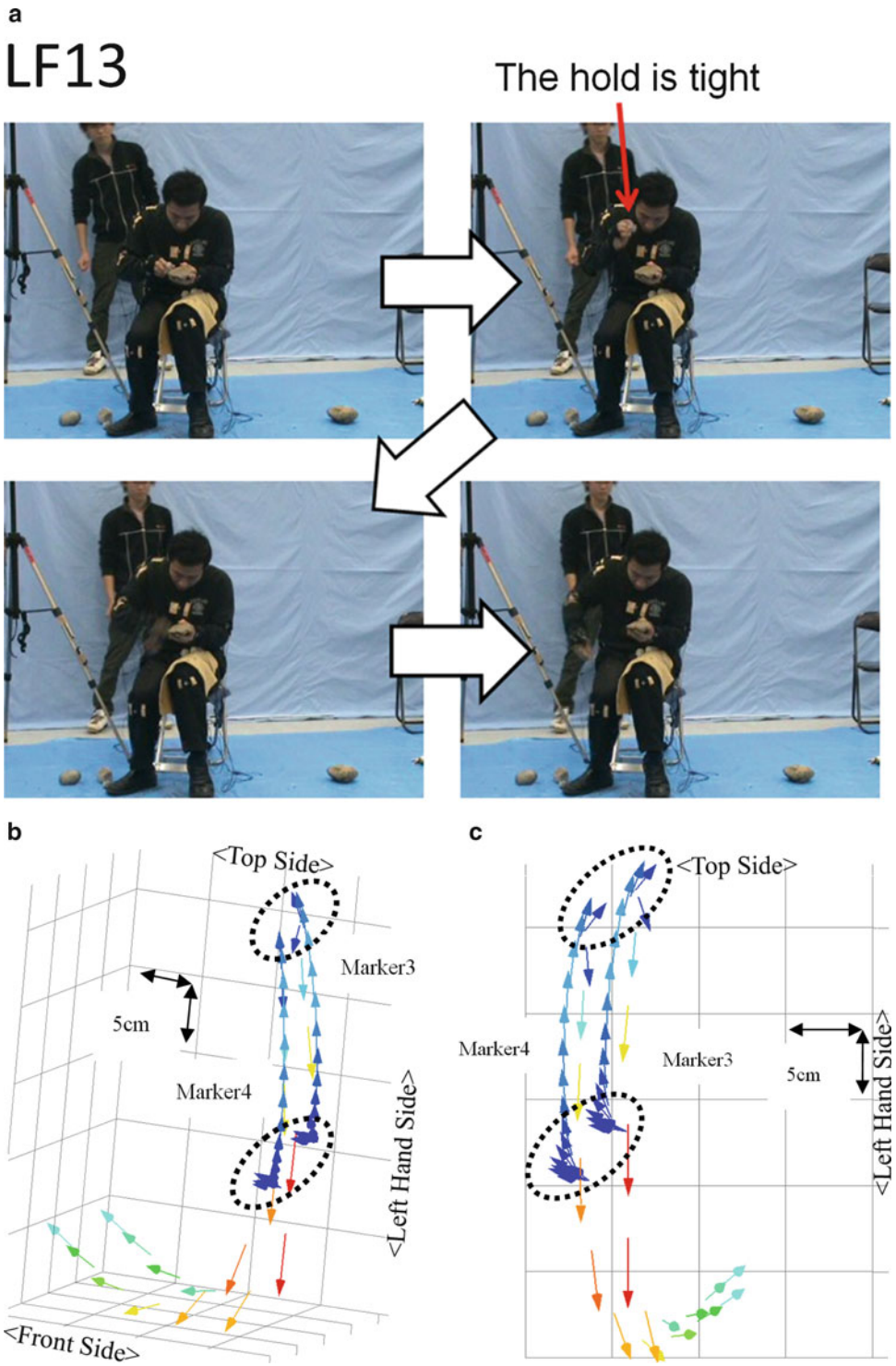

Fig. 9.9 (**a**) Camera pictures of hitting about LF13, (**b**) Motion curve of hitting about LF13, (**c**) Motion curve of hitting about LF13 (*Front side view*)

9.8 Detail Analysis About LP42 Motion

Figure 9.11a–c shows motion pictures and follow speed vector of the hammer stone. In this picture, knapper did not hold tight hammer stone and swing down to the core. In this case, the hammer stone is dropped down with a circle curve to the core. Top speed is very low. Knapper did twist quickly and pulling elbow too. We consider that knappercontrolled the hammer stone to hitting target point of a core. After the picture analysis, we checked 3D curve about the vector tail marker3 and marker4. Blue arrows

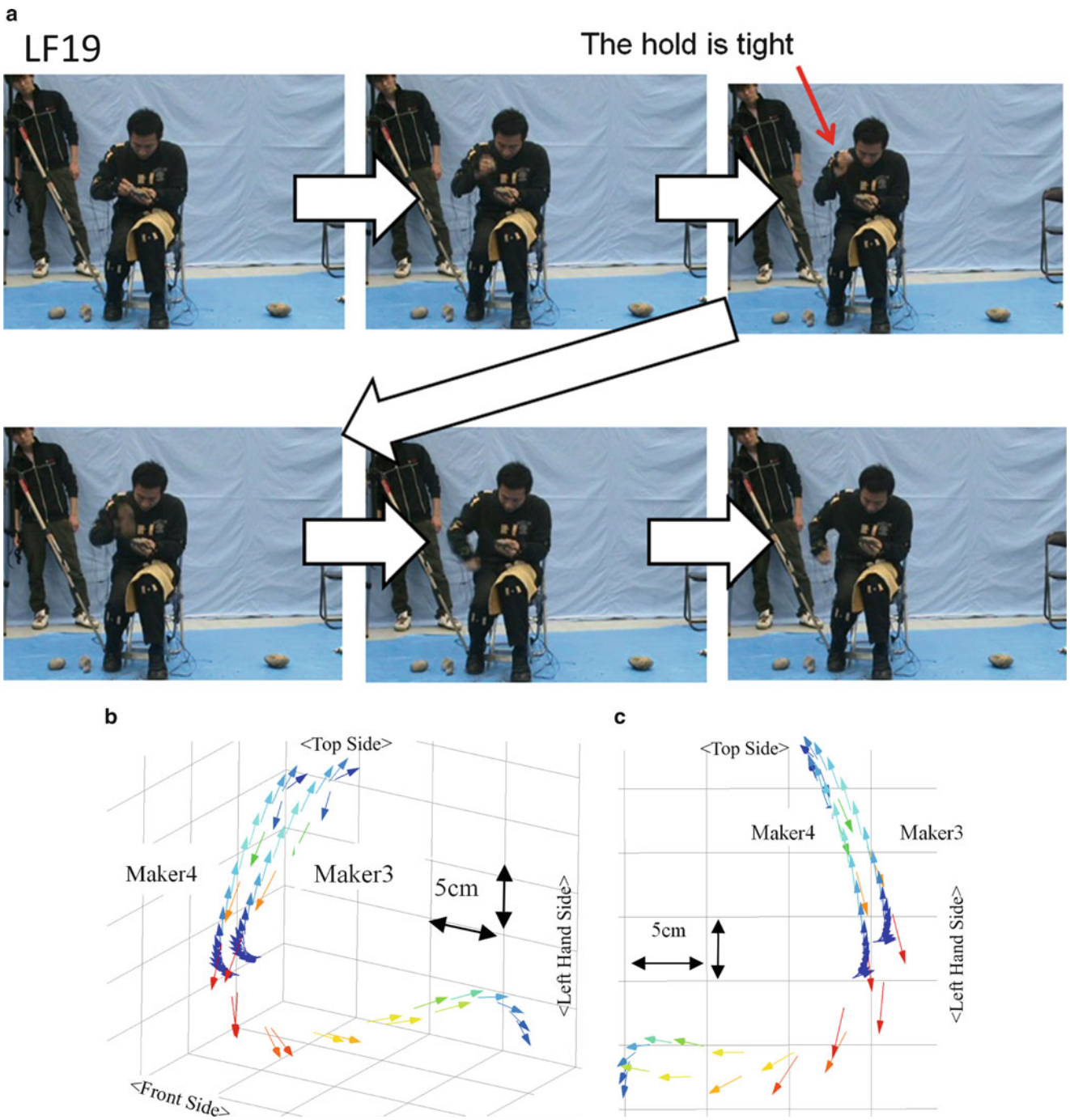

Fig. 9.10 (**a**) Camera pictures of hitting about LF19, (**b**) Motion curve of hitting about LF19, (**c**) Motion curve of hitting about LF19 (*Front side view*)

area is upstroke area of the hammer. After this motion, knapper swing down with straight to take LF42 from the core stone. In this motion, knapper dose not twisting action, because those arrow tails are mostly curving parallel. Knapper motion is like a whipping and his arm is like a swish (see Fig. 9.11a–c).

9.9 Detail Analysis About the Hammer Swing Motion About LF13, LF19 and LP42

In Table 9.1, we show an analysis table about Exp.2. This table describes some characteristic of the knapper at Opening stage, Stable stage and Final stage. We described the

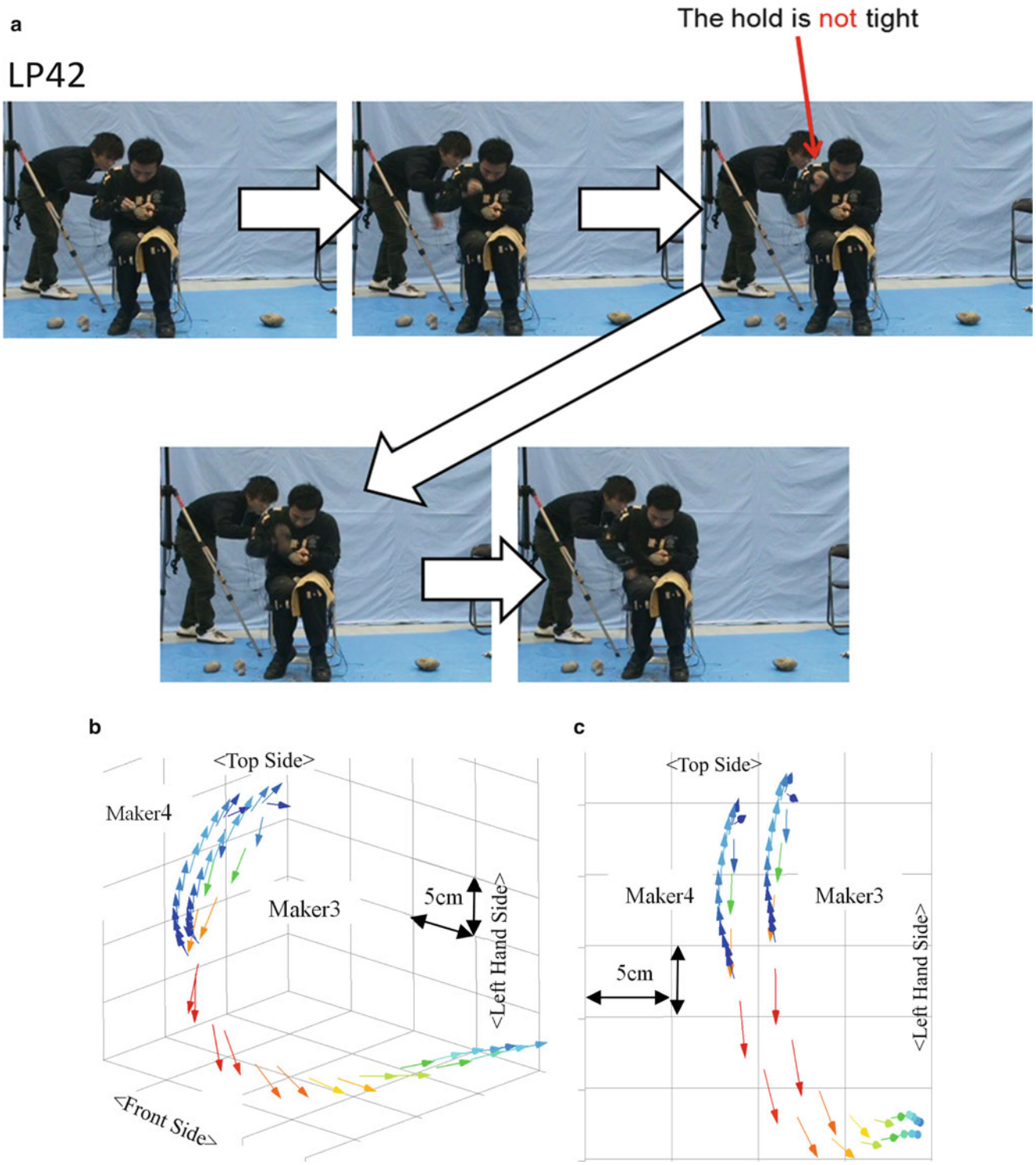

Fig. 9.11 (**a**) Camera pictures of hitting about LF42**,** (**b**) Motion curve of hitting about LP42, (**c**) Motion curve of hitting about LP42 (*Front side view*)

relationship between hammer speed and tails. Figures 9.9a–c, 9.11a–c shown the 3D speed applied to the hammer stone vector and some example video's scene. Additionally, Marker 3 and marker 4 are representing the movement of the hammer stone from the front view. The acceleration reaches to target stone by the momentum conservation law. It shows that the knapper accelerated the hammer stone at the same time pulling the elbow and twist of the wrist. From the impact point, the speed vectors of the hammer stone are changing curve directions and velocity value. Let's discuss this area. We can

consider the vector direction of this graph is due to a twisting wrist. In order to obtain a constant speed of this very short time, twisting of the knapper motion conducts a full advantage of the human skeleton. This twist makes a small shift of hit points. A greater speed is easy control for the small skeleton. If the skeleton is strong, the twist motion increases a shift of hit points. In order to suppress the deviation, knapper must slow down. If the hammer stone heavier then, knapper can make the impulse of the same degree. Skeletal differences make a difference of hammer selection and hitting speed to target stone. In other words, 3D graph and using light hammer-stone explain that modern small person's motion. This motion date represents the smart control of an arm than Neanderthals. This twist process is possible to become the special motion for the mass production of small flakes because a knapper hits continually with the low muscle power.

9.10 Elbow Motion Analysis

Figure 9.12a, b shows the pulling elbow motion about LF13, LF19 and LP42. Those data are from a marker 7. This marker 7 set up the outside elbow. Blue arrows are pulling up elbow when is the same time of upstroke the hammer stone. After the swing down, knapper was pulling an elbow, is like to through. LF13 and LF14 arrow tail is curve to outside. In this case, knapper is hitting and pulling elbow to straight and small twist. Motion of LP42 is curve the near body. In this case, knapper tightened anunderarm and he swung out through the near body. This arrow curve shows the special twist. This twisting motion becomes possible by light hammer stone and the long term personal learning. This twisting technique is able to get LP42 from a small core using light hammer stone, we are considering.

9.11 Discussion

We are considering that *Homo sapiens* have survived by twisting motion and the smart control of an arm. This is a necessary element of both individual learning and social learning. To determine the LP and LF motion is a kind of particularly important individual learning. The individual learning is the most important and need long time learning. This learning method is highly suitable for modern people life. Assistance of the swing operation and arm acceleration becomes pulling an elbow. Neanderthals were 80–90 kg body weight, height 160 cm. Their muscles were well developed. They also had strong bones. We speculate that they were inferior the ability of learning and did not control the twist of the arm. Therefore, we believe that they were making crushed stone instinctively by the Recurrent Levallois technique. In addition, the life expectancy of the Neanderthals is about 20 years old, they were short-lived. The technical tradition to the next generation has been hard. In the future, we will proceed with the investigation and analysis of the literature (Nishiaki 2011). We will be looking for a material that represents the difference of the learning ability between Neanderthal and modern human. Because twisting technique of LP42 work on the special condition. Those conditions are a small core, a light hammer stone, slow speed swing down and quick snap twisting (Nishiaki and Nagai 2012). Knapper need long term training to experiment this complex condition. For developing knapper's skill, knapper need the long term learning. This case is a kind of the personal learning. However those data and the result of this analysis is from modern knapper. We cannot compare real Neanderthal with modern human production skill.

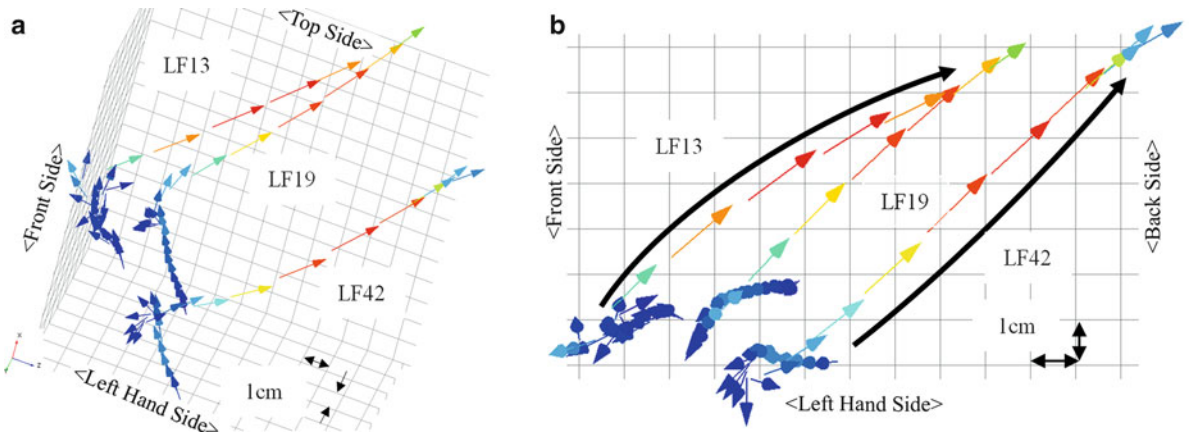

Fig. 9.12 (**a**) Elbow's arrow tail LF13, LF19 and LP42, (**b**) Elbow's arrow tail LF13, LF19 and LP42 (*Top view*)

References

de la Torre I, Mora R, Dominguez RM et al (2003) The Oldowan industry of Peninj and its bearing on the reconstruction of the technological skills of Pleistocene hominids. J Hum Evol 44:203–224

Dibble HL (1997) Platform variability and flake morphology: a comparison of experimental and archaeological data and implications for interpreting prehistoric lithic technological strategies. Lithic Technol 22:150–170

Michiyoshi A, Tang H, Yokoi T (1992) Estimation of inertia properties of the body segments in Japanese athletes. Society of Biomechanisms Japan (SOBIM)

Miura N, Hoshino Y, Nagai K (2011a) Extracting kinematic features of skilled behavior on Levallois flake production. In: Nishiaki Y (ed) Replacement of Neanderthals by Modern Humans: testing evolutionary models of learning, vol 3. Proceedings of the 3rd conference on RNMH, National Center of Sciences Building, Tokyo, Japan, 2010, p 55

Miura N, Nagai K, Hoshino Y (2011b) 3D body motion analysis of stone tool making by a skilled subject. In: Terashima H (ed) Replacement of Neanderthals by Modern Humans: testing evolutionary models of learning, vol 2. Proceedings of the 2nd conference on RNMH. Kobe Gakuin University, Hyogo, Japan, 2011, p 62–64

Nishiaki Y (2010) Research Team A01 archaeological research of the learning behaviors of the Neanderthals and early Modern Humans. In: Proceedings of the 1st conference on the RNMH project. National Center of Sciences Building, Tokyo, Japan, 2010, p 19–20

Nishiaki Y, Nagai K (2011) Knapping skill and Levallois flake production: insights from experimental replication. In: Proceedings of the 2nd conference on the RNMH project Kobe Gakuin University, Hyogo, Japan, 2011, p 6–8

Nonaka T, Bril B, Rein R (2010) How do stone knappers predict and control the outcome of flaking? Implications for understanding early stone tool technology. J Hum Evol 59:155–167

Okuda A, Okamoto S, Nanba R (2006) Three dimensional analysis of baseball batting using motion capture technique, Proceedings of Formu on Information Technology 2006 (FIT2006),Fukuoka University, Fukuoka, Japan, p I.006

Taniguchi S, Kino H, Ozawa R et al (2012) Inverse dynamics of human passive motion based on iterative learning control. IEEE Trans Syst Cybern A Syst Hum 42(2):307

Daily Physical Activity and Time-Space Using of Pygmy Hunter-Gatherers' Children in Southeast Cameroon

10

Izumi Hagino and Taro Yamauchi

Abstract

Previous studies described the active daily lives and various daily behaviors for children of pygmy hunter-gatherers, however, there were only a few studies which reported daily physical activities and time-space using quantitatively for hunter-gatherers' children. This study aimed to clarify following three topics for children of pygmy hunter-gatherers: (1) daily physical activities, (2) time-space use and (3) relationship between physical activities and time-space using. A field survey was conducted on 44 Baka children (28 boys and 16 girls) in a same village located southeast Cameroon. GPS log tracks were obtained from all 44 children, and acceleration monitoring were performed for 21 children each for consecutive 3 days. Baka children showed a generally high level of physical activity. They walked more than 20,000 steps per day (boys: 25,331 ± 9,348, girls: 22,400 ± 4,258), and the mean of their estimated PALs (boys: 2.08 ± 0.21, girls: 2.10 ± 0.15) were classified "vigorous." Total travel distances and active radii were become significantly greater as their age increased, and a dispersion was appeared in older boys. The sex-/age- difference for daily time-space using were observed from GPS log data, moreover, it was considered that boys changed their daily lives greater than girls as they grew up. In addition, it was suggested that activities outside of their own village were related to increasing children's physical activities.

Keywords

Children • Physical activity • Pygmy hunter-gatherers • Time-space using

10.1 Introduction

Pygmy hunter-gatherers, who are called as "Forest people," are thought to be original inhabitants of central African rainforest (Turnbull 1965). They are living in semi-settled villages and remaining the traditional hunting-gathering society still nowadays.

Our previous study showed that pygmy adults had moderate physical activities both in semi-settled village and forest camp (Yamauchi et al. 2009). From detail field observation, it was known that some playing of pygmy children was born from imitating for adults' livelihood, and the frequency for variety of playing was different by their sex-/age- group (Kamei 2005). It is expected that hunter-gatherers' children had greater physical activities, and their daily time use would be changed with their physical and psychological development. However, there was no study which reported children's daily physical activities and daily time allocation for quantitatively about pygmy hunter-gatherers children who live in the traditional society.

I. Hagino
Laboratory of Human Ecology, Graduate School of Health Sciences, Hokkaido University, JPPS Research Fellow, N12-W5, Kita-ku, Sapporo, Hokkaido 060-0812, Japan
e-mail: hagino.is.me@gmail.com

T. Yamauchi (✉)
Laboratory of Human Ecology, Faculty of Health Sciences, Hokkaido University, N12-W5, Kita-ku, Sapporo, Hokkaido 060-0812, Japan
e-mail: taroy@med.hokudai.ac.jp

T. Akazawa et al. (eds.), *Dynamics of Learning in Neanderthals and Modern Humans Volume 2: Cognitive and Physical Perspectives*, Replacement of Neanderthals by Modern Humans Series, DOI 10.1007/978-4-431-54553-8_10, © Springer Japan 2014

The objectives of present study were to clarify three topics as below: (1) daily physical activities, (2) time-space using and (3) relationship between physical activities and time-space using for children of pygmy hunter-gatherers.

10.2 Subjects and Methods

10.2.1 Participants

A field survey was conducted on 44 Baka children (28 boys and 16 girls) who were living in one village (86 total inhabitants) located East Region of Cameroon. The Baka are one of the groups of pygmy hunter-gatherers that are living in central African rainforest (Joiris 1998). Our study village is 5 km away from the nearest town, and the inhabitants were only Baka people. The population maintain a traditional lifestyle, hunting, gathering, trapping and planting some subsistence crops like cassava and plantain banana. We defined "children" as people who were under 20 years old and unmarried. They usually went to school in neighboring village; however that school broke up for the summer during our research periods. All children were participated our study, and they were divided into two age groups (older and younger) by pre-/post- the onset of adolescent growth spurt. The ages for onset of adolescent growth spurt were calculated by using mathematical method (Hagino et al. 2013). The number of older children was 17 (9 boys and 8 girls), and younger one was 27 (19 boys and 8 girls). All children were healthy, and were not contracted any disease. The field survey was conducted during short dry season in 2011. The study was approved by the ethics committee of the Graduate School of Health Sciences, Hokkaido University (No.11-13). Participation in the study was voluntary using explanations of the study for participants and care persons using local languages. Consent was obtained from the children and their parents or the chiefs of villages.

Fig. 10.1 Children are wearing GPS unites

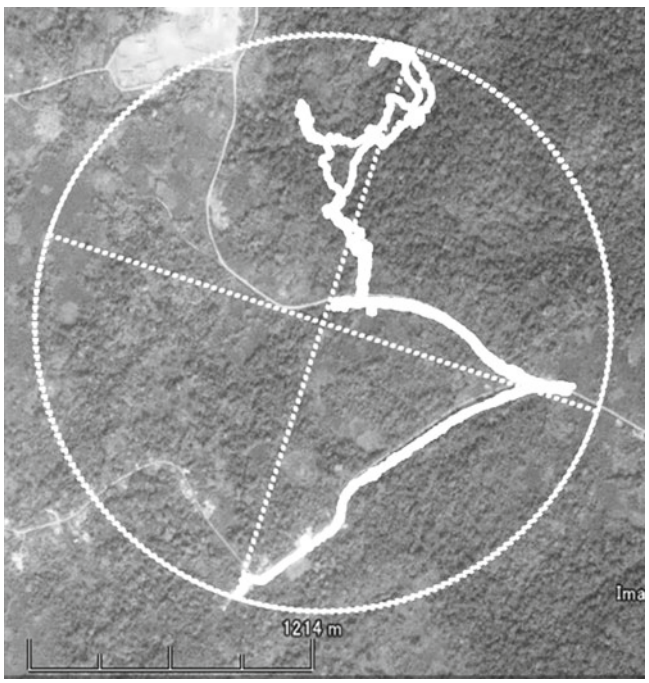

Fig. 10.2 Daily travel route (*solid lines*) and active radius (*dotted straight line*)

10.2.2 Methods and Data Analyses

10.2.2.1 Age Estimation

All ages of the participants were estimated by three following methods; (1) birth-ordering of 44 children, (2) interviewing their birth date for local informants, and (3) matching their birth date with national/local events. As a result, we could obtain their estimated age for 1-year range.

10.2.2.2 Daily Time Allocation

Each participant wore the small GPS (Global Positioning Satellite, WPL-2000, Wintec) units for consecutive 3 days including the sleeping time (Fig. 10.1). GPS log points which including latitude and longitude at each time point were obtained for total 131 days. Unfortunately, data of 1 day was lacked by flat battery. Figure 10.2 shows the sample of daily track obtained from GPS log data. Solid line means the daily travel route, and dotted line means daily active radius.

The daily travel durations (hours/day) were calculated for six activity areas. Using the GPS log data and direct observations, activity areas of children surrounding their village were divided into following areas (their own village, forest, river, water, village of other ethnics, and miscellaneous) shown in Fig. 10.3. "Forest" surrounded their village, and "River" was located about 900 m away from the village (Fig. 10.3). "Own village" was defined as a circle which includes all houses and that radius was about 50 m, and

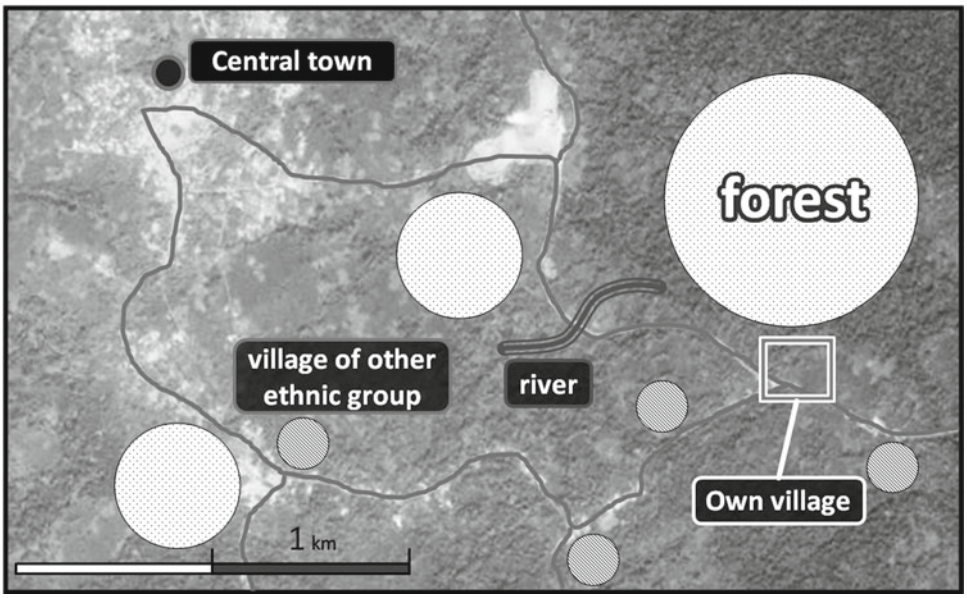

Fig. 10.3 Map for wide area around of the village. River and central of town are located for each 900 m and 5 km from the village. Forest are surrounded the village, and agriculturists' villages are dotted around the village

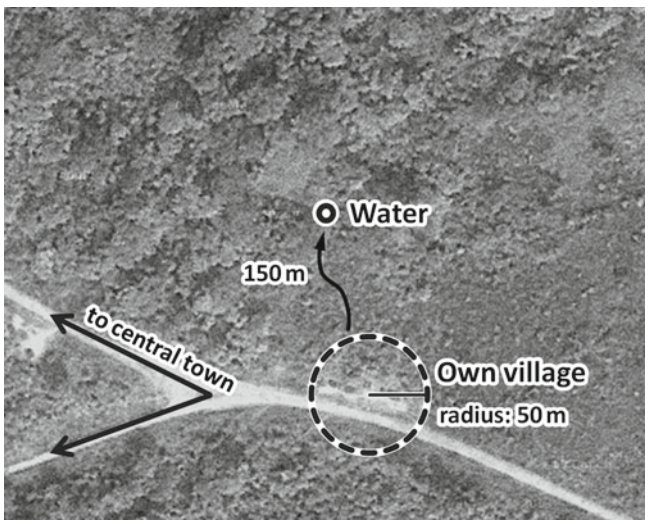

Fig. 10.4 Map for the surroundings of the village. Own village were defined as area circled by *dotted line*, and the radius was (*solid line*) about 50 m. Water was located about 150 m from the center of village

"Water" was about 150 m away from the center of the village (Fig. 10.4). "Miscellaneous" included the nearest town, and road faced to the village. Travel durations (hours/day) were determined as a period between the time of leaving from their village and that of returning their village. Furthermore, the trend of daily time-space using for children were evaluated from comparing travel durations of 4 sex-/age- groups. Sex-/age- difference of time-space using was assessed by two-way ANOVA.

10.2.2.3 Daily Physical Activity

For the physical activity monitoring, 21 children (13 boys and 8 girls) were chosen to wear the pedometer with a built-in uniaxial accelerometer (Lifecorder EX, Suzuken, Japan). 13 children were excluded because of their small physique not to be able to wear accelerometer units. Each participant wore the accelerometer with GPS units at the same periods. Finally, 63 person-days acceleration data and step counts were obtained.

The physical activities were assessed by four indices. From the GPS log data, daily travel distance (TD, km/day) and active radius (AR, m/day) were calculated for each person-day. TDs were calculated from GPS log data as the sum of distances participants moved for a day, and ARs were calculated as the radius of the circle which included all the GPS log points for each day (shown as Fig. 10.2). Daily step count (step) was obtained from pedometer, and physical activity level (PAL) was calculated for both total 63 person-days. PAL is determined as the ratio of total energy expenditure (TEE) to basal metabolic rate (BMR), and widely used for assessing the physical activity. PAL was directly calculated by converting activities levels (0, 0.5, 1–9) which were recorded in accelerometer to METs using regression equation previously developed by Kumahara et al. (2004). PALs were calculated as the values which multiply average of converted METs and 1.1 as the ratio of resting metabolic rate (RMR) and BMR (Institute of Medicine 2005) together. Sexual differences were evaluated by non-paired t-test. Steps and PALs were compared with international references (Tudor-Locke et al. 2004; FAO 2004).

10.2.2.4 Correlation Between Daytime use and Physical Activities

The Pearson's correlation coefficients were calculated between 4 indices of physical activities (TD, AR, steps, PAL) and travel durations for six activity areas (Own village, Forest, River, Water, Other village, Others). This analysis was performed by using data of 63 person-days (TD and AR) and 131 person-days (step and PAL).

10.2.2.5 Statistical Analysis

All statistical analyses were performed by using JMP 10.0.0 software package (SAS institute. inc). All data were shown by mean ± S.D. The significance levels were defined as $P<0.05$.

10.3 Results and Discussion

10.3.1 Daily Physical Activity

Table 10.1 presents the means and standard deviations for four indices about physical activities of children. Baka children generally had high physical activities, and there was no significant difference between the sexes. The means of daily steps were greater than 20,000, and 95.2 % of observations had greater steps than developed country's children and international reference (Tudor-Locke et al. 2004; Owen et al. 2009). The means of PAL were also high in both sexes, where 66.7 % boys' person-days and 80.0 % girls' person-days were classified as "vigorous" based on the criteria established by FAO (FAO 2004).

Figures 10.5 and 10.6 shows the increment of total travel distance (TD) and active radius (AR) of children. As their age increased, TDs were become significantly longer ($N=131$, $r=0.59$, $P<0.001$) and AR were become significantly greater ($N=131$, $r=0.54$, $P<0.001$). The variations of ARs among individuals were observed in older boys. There was strong positive correlation between steps and PALs ($N=63$, $r=0.82$, $P<0.001$). There were also strong positive correlation between steps and TDs ($N=63$, $r=0.83$, $P<0.001$) and ARs ($N=63$, $r=0.83$, $P<0.001$).

Table 10.1 Physical activities of participants

	Boys		Girls		
	N[a]	Mean ± SD	N[a]	Mean ± SD	*P*
Steps (steps/day)	39	25,331 ± 9,348	24	22,400 ± 4,258	ns
PAL[b]	39	2.08 ± 0.21	24	2.10 ± 0.15	ns
TD[c] (km/day)	83	10.0 ± 5.1	48	8.6 ± 4.0	ns
AR[d] (m/day)	83	480.1 ± 347.9	48	496.9 ± 440.6	ns

Non-paired t-test, *ns* no significant difference ($P \geq 0.05$)
[a]Person-days
[b]Physical activity level
[c]Travel distance per day
[d]Activity radius per day

Two characteristics might explain the high physical activities for our participants which were the "children" of "traditional hunter-gatherers' society." In general, previous studies reported that the physical activities become vigorous during childhood or adolescence, and then decrease as the age increase during adulthood (Tudor-Locke et al. 2011; Ndiaye and Bénéfice 2007). It is also reviewed that the inhabitants of traditional or rural societies generally had high physical activities in

Fig. 10.5 Daily travel distances (TDs) for children. As ages of children increased, TDs were become significantly longer ($N=131$, $r=0.59$, $P<0.001$)

Fig. 10.6 Activity radii (ARs) for children. As ages of children increased, ARs were become significantly greater ($N=131$, $r=0.54$, $P<0.001$), and variations of ARs were observed in older boys

Table 10.2 Daily travel durations for each place (hours/day) by sex-age distribution

	Younger[a]		Older[a]				
Place	Boys (19)	Girls (8)	Boys (9)	Girls (8)	Sex	Age	Sex × Age
Own village	21.6	21.2	16.9	20.1	*	***	**
Forest	1.07	2.02	3.03	1.92		**	**
River	0.61	0.72	0.83	0.58			
Water	0.15	0.03	0.27	0.44		**	
Other village	0.05	0.00	1.85	0.41	**	***	**
Miscellaneous	0.40	0.09	0.79	0.56		*	

Two-way ANOVA, $*P<0.05$, $**P<0.01$, $***P<0.001$
[a]Classified by pre-/post- the onset of adolescent growth spurt (Hagino et al. 2013)

some sub-Saharan countries (Yamauchi et al. 2000; Sobngwi et al. 2002). Although it is known that the physical activities of Baka hunter-gatherers greatly reduced in semi-settled village during rainy season (Yamauchi et al. 2009), it is expected that the physical activities of them would increase during dry season because of their food procurements. Same as Munroe et al. (1984) described in developing countries, Baka children are regularly involved in domestic tasks in their family, and they somewhat contributed to household works. In addition, children usually use most of their daily time for "playing," and it is known that many of their plays are by using their own bodies (Kamei 2010). For these reasons, even if the participation for housework were excluded, it would be thought that Baka children have vigorous daily physical activities.

Similarly to our previous study for Baka adults reported the same trend (Yamauchi et al. 2009), there was strong correlation between steps and PALs which meant the physical activities of children were related to walking in this traditional hunter-gatherers society. Daily steps are known as the indices which reflect physical activities (Welk et al. 2000). As children walked a lot around their village, their daily steps increased, and that lead their considerable physical activities. It is considered that physical and psychological developments cause the variations of daily activities based on "playing" or "imitation of adult's livelihood" in older children. Those variations among older children should have led the variations of daily physical activities or selecting active areas, which might generate various TDs and ARs. As Baka adult and youth men often participated in public relations to other ethnics, the social function was also considered as a factor which generated variations of TDs and ARs.

10.3.2 Daily Time-Space Using

Table 10.2 presents the time-space using of participants for divided four sex-/age- groups. The figures show the mean daily travel durations to six activity areas for each group. In general, there were two findings for time-space using of children. At first, the older groups generally went out from their own village more than younger groups. Secondary, children spent their time mainly in two areas which were own village and forest. From the two-way ANOVA, the sex-/age-differences were observed for five activity areas except the area "River." As their age increased, the great changing of time-space using was observed in boys more than in girls. In older girls, they spent more time on going "Water" as they fetch the water for household works than younger girls, and they visited more time to agriculturists' village. However, the travel durations for main two areas (own village and forest) were almost same between younger and olders, so that it was revealed that girls' time-space using was not changed as they grow. On the contrary, in boys, the drastic changes of time-space using were observed for following three points. First important variation was the increment of travel durations for "Forest." Second characteristic was the increment of the travel duration for "Other village." At last, the time staying in own village was greatly decreased.

It was suggested that these variations about time-space using between boys and girls was generated by the major livelihood of adults. There was a strong positive correlation between heights and TDs ($N=44$, $r=0.71$, $P<0.0001$). Pontzer and Wrangham (2006) showed that developments of body lengths make daily travel distance increase, and it is possible for adults to travel longer than juveniles with same energy cost in their study for Chimpanzees. Thus, it would be possible for both boys and girls to go farther, and to change their trend for space using similarly as their age increased. However, because of the sexual difference in daily lives for Baka people, time-space using of Baka children were varied. The most important livelihood of adult Baka women is gathering daily provisions in the forest. It was considered the reason why young girls went to forest for longer than boys was that they took along with their mothers' food procuring in forest. In addition, travel durations for "Forest" were not changed between younger and older girls, and that time were near to the time Baka women spent for gathering in forest camp (137 min, Yamauchi et al. 2009). It was also implied that the frequency for girls to go to food gathering might not change with their age increased. On the contrary, it was considered that young boys did not take along with adult men because their main livelihood is hunting which need much physical strength as previous studies showed that hunting was

Table 10.3 Correlation between travel durations and physical activities

	Steps	PAL	TD	AR
Place	N = 63[a]		N = 131[a]	
Own village	−0.63****	−0.42***	−0.73****	−0.67****
Forest	0.43***	0.25*	0.53****	0.40****
River	0.06[ns]	0.01[ns]	0.18*	0.20*
Water	−0.19[ns]	0.03[ns]	0.03[ns]	−0.02[ns]
Other village	0.56****	0.36**	0.49****	0.49****
Miscellaneous	0.13[ns]	0.14[ns]	0.25**	0.38****

Pearson's correlation coefficient
*$P<0.05$, **$P<0.01$, ***$P<0.001$, ****$P<0.0001$
[a]Person-days

conducted in wider range than gathering (Yasuoka 2006; Sato et al. 2012). Due to this reason, young boys stayed longer time in their own village. However, as boys grew up, they obtained physical strength that they become possible to go forest and make playing related to hunting, so that older boys tended to stay longer time in forest. Yamauchi et al. (2009) described that adult men spent a larger time out of their camps than adult women. These results showed the trend for the changes of time-space using as children grew up to adults. It was considered that boys had changed their daily activity vigorously as they grew whereas girls generally had been moderately active since they were young.

10.3.3 Correlation Between Physical Activity and Time-Space Using

Table 10.3 presents the correlation between physical activities and time-space using. There was moderate relationship between daily time-space using and physical activity. Travel durations for "Forest" and "other village" had significant positive correlations between all physical activity indices, whereas travel duration for "Own village" had negative correlations. Travel durations for "River" and "Miscellaneous" had significant positive correlation between only TD and AR. Travel duration for "Water" didn't have any significant correlation between physical activity indices.

From direct observations, it was found that the six divided areas have different characteristics for children's activities. In "Own village," children often spent time with their family, and their common activities were sleeping, resting and housework. Because of limited village radius (about 50 m), if they played long time in their village, it is considered difficult to increase their physical activities greatly. By contrast, children always walk around in "Forest," thereby we could observe various activities such as fruit gathering, fish bailing, playing with tree vine and small animal hunting. "River" located little a bit far from village, children mainly spend their time for playing in river or personal activities as laundering and bathing. Though "Water" was near from the village, children visited there only few times per day, hence travel for "Water" did not contribute the increment of children's physical activities. It was considered that going out from village generally have positive correlation with physical activity. Additionally, it was also implied that housework and personal time do not significantly increase the physical activity. Harold and Karen (1998) described that there were some (e.g., physiologic, environmental, psychological and social) factors which influence physical activity development of children. According to physical development and skills acquisition about viability in the forest, children tend to go out from village and spread their wings. It was suggested that increment of options for daily activities and active area were related the increment of children's physical activities.

10.3.4 Further Study

There were several limitations in this study. One is the representativeness of data. Since this study was focused on one village, the ages of participants were not distributed uniformly, and the data for adults were lacked. It will be possible to describe Baka children's daily lives with accurately by increasing the number of participants and comparing to adults data. Second limitation is the lack of direct behavior observation. As this study was designed with indirect observations via mechanics, it is not known what children did in each activity areas. With individual tracking, detailed information will be provided about children's physical activities and time-space using. Last limitation is seasonal variety. It is known that seasonality influences children's daily time using and physical activities (Goran et al. 1998; Bénéfice and Cames 1999). For further study, it would be necessary to observe children's daily lives in rainy seasons, and compare with those of dry seasons in this present study.

10.4 Conclusion

Baka children showed a high level of physical activity and walked greater than children in developed countries. Boys tend to have vigorous physical activities as they grow, whereas girls had generally moderate physical activity since they were young. From GPS log tracking and acceleration monitoring, it was revealed that there was sex-/age- difference for daily time-space using, furthermore, it was suggested that "going out from the village" makes children's physical activity increased significantly.

References

Bénéfice E, Cames C (1999) Physical activity patterns of rural Senegalese adolescent girls during the dry and rainy seasons measured by movement registration and direct observation methods. Eur J Clin Nutr 53:636–643

FAO (2004) Human energy requirements. Report of a joint FAO/WHO/UNU expert consultation. Food and nutrition technical report series. No. 1. WHO, Rome

Goran MI, Nagy TR, Gower BA et al (1998) Influence of sex, seasonality, ethnicity, and geographic location on the components of total energy expenditure in young children: implications for energy requirements1–3. Am J Clin Nutr 68:675–682

Hagino I, Hayashi K, Kawamura K et al (2013) Adolescent growth spurt and growth pattern factors related to the short stature of Pygmy hunter-gatherers of Southeast Cameroon. Ann Hum Biol 40(1):9–14

Harold WK, Karen EH (1998) Development of physical activity behaviors among children and adolescents. Pediatrics 101:549–554

Institute of Medicine (2005) Dietary reference intakes for energy, carbohydrate, fiber, fat, fatty, acids, cholesterol, protein and amino acids. National Academy Press, Washington

Joiris DV (1998) La Chasse, La Chance, La Chant: aspects du system ritual des Baka du Cameroun. Universite Libre de Bruxelles, Brussels

Kamei N (2005) Play among Baka children in Cameroon. In: Hewlett BS, Lamb ME (eds) Hunter-gatherer childhoods: evolutionary, development & cultural perspectives. Aldine de Gruyter, New York, pp 343–359

Kamei N (2010) Little "hunters" in the forest: ethnography of hunter-gatherer children. Kyoto University Press, Kyoto (in Japanese)

Kumahara H, Schutz Y, Ayabe M et al (2004) The use of uniaxial accelerometer for the assessment of physical-activity-related energy expenditure: a validation study against whole-body indirect calorimetry. Br J Nutr 91:235–243

Munroe RH, Munroe RL, Shimin HS (1984) Children's work in four cultures: determinants and consequences. Am Anthropol 86:369–378

Ndiaye GM, Bénéfice E (2007) Patterns of daily activity and time spent in bed of adult women and adolescent and preadolescent girls from a rural community in Senegal, West Africa. Ann Hum Biol 34(4): 454–469

Owen CG, Nightingale CM, Rudnicka AR et al (2009) Ethnic and gender differences in physical activity levels among 9–10-year-old children of white European, South Asian and African–Caribbean origin: the Child Heart Health Study in England (CHASE Study). Int J Epidemiol 38:1082–1093

Pontzer H, Wrangham RW (2006) Ontogeny of ranging in wild chimpanzees. Int J Primatol 27(1):295–309

Sato H, Kawamura K, Hayashi K et al (2012) Addressing the wild yam question: how Baka hunter-gatherers acted and lived during two controlled foraging trips in the tropical rainforest of southeastern Cameroon. Anthropol Sci 120(2):129–149

Sobngwi E, Mbanya JCN, Unwin NC et al (2002) Physical activity and its relationship with obesity, hypertension and diabetes in urban and rural Cameroon. Int J Obes Relat Metab Disord 26:1009–1016

Tudor-Locke C, Pangrazi RP, Corbin CB et al (2004) BMI-referenced standards for recommended pedometer-determined steps/day in children. Prev Med 38:857–864

Tudor-Locke C, Craig CL, Beets MW et al (2011) How many steps/day are enough? for children and adolescents. Int J Behav Nutr Phys 8: 78–91

Turnbull C (1965) Wayward servants: the Two World of African Pygmies. The American Museum of National History, New York

Welk G, Differding JA, Thompson RW et al (2000) The utility of the Digi-Walker step counter to assess daily physical activity patterns. Med Sci Sports Exerc 32(9 Suppl):S481–S488

Yamauchi T, Sato H, Kawamura K (2000) Nutritional status, activity pattern, and dietary intake among the Baka hunter-gatherers in the village camps in Cameroon. Afr Study Monogr 21:67–82

Yamauchi T, Hayashi K, Kawamura K et al (2009) Nutritional status, physical activity, and dietary intake of Pygmy hunter-gatheres in Cameroon. In: Louts T, Reitenbach M, Molenbroek J (eds) Human diversity: design for life. 9th International congress of physiological anthropology proceedings. Delft University of Technology, Delft, pp 78–81

Yasuoka H (2006) Long-term foraging expeditions (Molongo) among the Baka Hunter-Gatherers in the Northwestern Congo Basin, with special reference to the "Wild Yam Question". Hum Ecol 34(2):275–296

Estimation of the Period of Childhood and Child Growth Characteristics of Pygmy Hunter-Gatherers in Southeast Cameroon

11

Taro Yamauchi and Izumi Hagino

Abstract

Data on the growth pattern of pygmy hunter-gatherers may provide key knowledge about the mechanism of human evolution. However, only few studies have compared their growth pattern with those of modern human populations. This study aims at characterizing the growth pattern of pygmy hunter-gatherers by using a mathematical method and comparing their pattern with that of other worldwide populations. Height and weight of 626 Baka children in southeast Cameroon were measured. The nutritional status was assessed using body mass index (BMI), and the Preece-Baines function was adopted for obtaining height velocity curve and assessing growth pattern. More than 80 % participants had BMI in the normal range, and their nutritional status was considered generally good. The height velocity curves and biological parameters indicated that their adolescent growth spurts were very week. However, the periods of adolescent growth spurt of Baka children were almost similar to those of previously studied five groups. Furthermore, their growth rate during the early childhood was suggested to be very slow. The periods of childhood were the same among the modern human populations. However, a great difference was observed in the linear growth rate between the Baka and other populations.

Keywords

Adolescent growth spurt • Growth pattern • Period of childhood • Pygmy hunter-gatherers

11.1 Introduction

This study aims to determine the growth pattern of Pygmy hunter-gatherers, especially the periods and the growth tempo during childhood and adolescent by using the mathematical growth model.

T. Yamauchi (✉)
Laboratory of Human Ecology, Faculty of Health Sciences, Hokkaido University, N12-W5, Kita-ku, Sapporo, Hokkaido 060-0812, Japan
e-mail: taroy@med.hokudai.ac.jp

I. Hagino
Laboratory of Human Ecology, Graduate School of Health Sciences, Hokkaido University, JPPS Research Fellow, N12-W5, Kita-ku, Sapporo, Hokkaido 060-0812, Japan
e-mail: hagino.is.me@gmail.com

Pygmy hunter-gatherers, who are known as the original inhabitants of Central African rainforest, have the smallest stature in the world (Turnbull 1965). Their short stature have attracted many anthropologists and human biologists, and the mechanism of their growth was thought as an important theme of human biology which may provide key knowledge for human evolution.

Previous studies found out that pygmy hunter-gatherers' children were shorter and lighter than rural African farmers' children for the first 5 years of life (Bailey 1991), and van de Koppel and Hewlett (1986) suggested the lack of adolescent growth spurt as the cause of short stature. However, there are many research limitations, and the growth pattern of pygmy hunter-gatherers' children have not been clarified yet.

Using mathematical methods makes it possible to compare the growth pattern among different populations. Since the last of twentieth century, many mathematical growth

T. Akazawa et al. (eds.), *Dynamics of Learning in Neanderthals and Modern Humans Volume 2: Cognitive and Physical Perspectives*, Replacement of Neanderthals by Modern Humans Series, DOI 10.1007/978-4-431-54553-8_11, © Springer Japan 2014

models were developed and employed (c.f., Largo et al. 1978; Milani 2000). Biological parameters (e.g., the age and height velocity at the onset of adolescent growth spurt) provided from the mathematical parameters of the models can be used for the comparing the growth characteristics.

11.2 Methods

11.2.1 Subjects and Data Collection

A cross-sectional survey was conducted on Baka hunter-gatherer children in southeast Cameroon. The Baka are a group of African pygmy hunter-gatherers in the rainforest. Our previous study reported on their good nutritional status and the middle range of stature among African pygmy hunter-gatherers (Yamauchi et al. 2000).

A total of 626 children (349 boys, 277 girls) participated in the study. They were from 62 Baka semi-sedentary villages ranged wide area of the East Region of Cameroon. The height and weight were measured using standard procedures (Weiner and Lounie 1981). Weight was measured for all participants to the nearest 0.1 kg using a digital scale (model TF-205, TANITA, Japan), and height was measured to the nearest 0.1 cm using a portable stadiometer (model 213, Seca, Germany). From the data, body mass index (BMI, kg/m^2) were calculated.

The ages of the participants were estimated to the nearest 0.5 year by following information obtained from: (1) birth reorder within the villages, (2) matching their birthday with local events, and (3) interviews with people from the neighbor agricultural people.

11.2.2 Assessing Nutritional Status

The nutritional status of children was assessed by BMI classification. A sex-age specific BMI cut-off reference proposed by IOTF (International Obesity Task Force) was used for the classification of children aged 2–18 years old (Cole et al. 2000, 2007). For the participants of 19–20 years old, WHO cut-offs were applied (WHO 1995). Based on the IOTF cut-off, each participant was classified into "Thin," "Normal," "Overweight," or "Obesity."

11.2.3 Applying the Mathematical Function

To analyze the growth pattern, the Preece-Baines model I function (PB-1; Preece and Baines 1978) was applied. The PB-1 function contains five mathematical parameters that are described as below:

$$Ht = H_1 - \left[2*\left(H_1 - H_\theta\right)/\left(s_0^{(t-\theta)} + s_1^{(t-\theta)}\right)\right]$$

where Ht is the height (cm) at time t (years), H_1 is final height, H_θ is the height at time θ, θ is the time constant, s_0 and s_1 are the rate constants. Height velocity curves and biological parameters were derived from the five mathematical parameters and compared with previous five growth studies from Europe, Africa, Asia, Australia, and South America (Preece and Baines 1978, Billewicz and McGregor 1982, Hauspie et al. 1980; Brown and Townsend 1982; Bogin et al. 1990). In particular, the parameters of the Baka children were compared with data from the first study to use the Preece-Baines function on British children (Preece and Baines 1978).

11.2.4 Statistical Analysis

All values are shown as mean ± SD, except for the values for the biological parameters in Tables 11.2 and 11.3 that are shown as mean ± SE. All statistical analyses and curve fitting were performed with the JMP 10.0.0 software package (SAS institute Inc.). The level of statistical significance was set at $P<0.05$

11.3 Results

The numbers and the percentages of participants in each BMI-classification group based on IOTF cut-off are provided in Table 11.1. Over 80 % of participants had normal-ranged BMI, and there was only a few person classified into "Overweight" or "Obesity."

Figures 11.1 and 11.2 show the comparison of height velocity curves derived from PB-1 function among six populations. Tables 11.2 and 11.3 contain mean values and standard errors (SE) for the biological parameters (derived from the mathematical parameters) for the Baka children as well as biological parameter results from five longitudinal studies for comparison (Preece and Baines 1978, Billewicz and McGregor 1982, Hauspie et al. 1980; Brown and Townsend 1982; Bogin et al. 1990).

The adult height (AH) was similar to the previously reported ones (Yamauchi et al. 2000; Travaglino et al. 2011), and shorter than others. Velocity at take-off (VTO) and peak height velocity (PHV) was generally lower than that of the previously reported groups. The VTO-PHV velocity increment (VTO-PHV inc) was also the lowest. Their age at take-off (ATO), considered as a marker indicating the onset of

Table 11.1 BMI classification of Baka children

	Boys		Girls	
	N	%	N	%
Thin	44	14.0	37	15.2
Normal	259	82.5	194	79.5
Overweight	10	3.2	13	5.3
Obesity	1	0.3	0	0.0
Total	314	100.0	244	100.0

Table 11.2 The biological parameters for Baka, means and (standard error) with comparison among populations (boys)

	Baka	British	India	Guatemala	Aborigine	Gambia
AH	154.11 (1.32)	174.6	165.72	177.18	172.13	170.77
ATO	10.67 (0.40)	10.75	10.62	10.05	10.80	12.20
APHV	14.98 (0.40)	14.19	14.30	13.66	14.01	16.29
VTO	3.80 (0.19)	4.52	3.95	4.57	4.34	3.66
PHV	4.88 (0.40)	8.24	8.84	9.52	10.59	6.93
VTO-PHV inc	1.08 (0.56)	3.72	4.89	4.95	6.25	3.38
HtTO	119.34 (1.77)	138.98	129.46	137.56	136.00	135.64
HtPHV	137.76 (1.48)	159.6	150.71	160.47	157.21	156.06
HtTO-AH	34.77 (2.16)	35.62	36.26	39.62	36.13	35.13
Ht inc TO-PHV	18.42 (1.10)	20.62	21.25	22.91	21.21	20.42
Ht inc PHV-AH	16.35 (2.03)	15.00	15.01	16.71	14.92	14.71

Table 11.3 The biological parameters for Baka, means and (standard error) with comparison among populations (girls)

	Baka	British	India	Guatemala	Aborigine	Gambia
AH	147.61 (0.67)	163.40	151.77	162.82	162.94	158.75
ATO	9.30 (0.37)	8.89	9.37	9.00	8.91	10.27
APHV	12.24 (0.62)	11.90	12.42	12.03	11.95	13.84
VTO	4.46 (0.16)	5.24	4.62	4.92	5.13	4.05
PHV	4.71 (0.18)	7.49	7.25	7.63	8.49	6.06
VTO-PHV inc	0.25 (0.26)	2.26	2.63	2.71	3.36	2.01
HtTO	114.26 (1.89)	129.77	121.07	129.91	128.50	127.62
HtPHV	127.68 (2.58)	148.40	138.46	148.13	148.20	145.07
HtTO-AH	33.35 (1.76)	33.63	30.67	33.57	34.44	31.13
Ht inc TO-PHV	13.42 (3.18)	18.63	17.39	18.23	19.69	17.45
Ht inc PHV-AH	19.93 (2.96)	15.00	13.31	14.67	14.74	13.68

adolescence, was similar among Baka, Indian and Guatemalan boys, and Baka and Indian girls. The age at peak height velocity (APHV) was average in girls, however, slightly delayed in boys. Compared with Gambian children, Baka children showed 1–2 years earlier ATO and APHV.

The gains in height from take-off to adult height (HtTO-AH, 34.77 cm in boys and 33.35 cm in girls) were similar among Baka children and other populations. For boys, the differences were over a range of 5.44 cm, while it was 3.76 cm for girls.

11.4 Discussion

The adolescent growth spurt of the Baka children was characterized as extremely weak compared with other populations. Figures 11.1 and 11.2 show the velocity curves for the increase in height from 1 to 20 years for the Baka children, compared with curves for British, Indian, Guatemalan, Australian aborigine, and Gambian children (Preece and Baines 1978, Billewicz and McGregor 1982, Hauspie et al. 1980; Brown and Townsend 1982; Bogin et al. 1990). The values for height growth velocity at each 0.1 year were calculated using five published mathematical parameters (H_1, $H\theta$, θ, s_0, and s_1). Figures 11.1 and 11.2 clearly demonstrate the adolescent growth spurt for the boys and girls. Height growth velocity was generally smaller than that of other populations except for the latter period of adolescence. The PHV in Baka children, 4.88 cm/year for boys and 4.71 cm/year for girls, was one of the most characteristic biological parameters in the growth of the Baka children, being only 50–80 % compared with other five populations (e.g., boys: 59.2 % and girls: 62.9 % of British children).

In contrast, the VTOs were not so low compared with other populations. Specifically, the VTOs in the Baka ranged from 76 to 102 % (84 % of British) in the boys and 85–109 % (85 % of British) in the girls. The VTO-PHV (difference between VTO and PHV) velocity increment indicated a suppressed adolescent growth spurt in the Baka children. The increment for the boys was only 1.08 cm/year, which was only one-third of Gambian boys (3.38 cm/year), the smallest in the five groups. For girls, the result was more pronounced with the VTO-PHV increment value was less than 1 cm/year, which was only one-eighth of Gambian girls (2.02 cm/year).

The ATOs (boys: 10.67 years and girls: 9.30 years) were similar to the other populations with the exception of the Gambian sample for both sexes. The ATO of the Baka girls was 0.97 years earlier than for Gambian girls, and the differences with other four populations were ranged from −0.06 to +0.44 years (+0.41 years vs. British girls). Similarly

Fig. 11.1 The height velocity curves for Baka boys with published populations

Fig. 11.2 The height velocity curves for Baka girls with published populations

for the boys, the ATO occurred 1.62 years earlier than the Gambian boys, with the differences among the other populations ranging from −0.13 to +0.40 years (−0.08 years vs. British boys). For the girls, the APHVs (boys: 14.98 years and girls: 12.24 years) had a similar tendency to the ATO. The APHV of boys slightly delayed (+0.68–+0.97 years) compared with the other populations. Adolescent duration (AD), calculated as the difference between the ATO and APHV was 4.31 years in boys and 2.93 years in girls. Compared with the other five samples, AD was longer in Baka boys (105–134 % of other boys) but shorter in Baka girls (82–97 % of other girls).

It is known that the timing of the onset of the adolescent growth spurt is related to nutritional status (Kulin et al. 1982). Previous study reported that Baka adults had normal ranged BMI and much amount of body fat (Yamauchi et al. 2000). And it is also described that energy intake and expenditure of Baka adults were well-balanced with sufficient protein obtained from game, fish, and ants (termites) in both a semi-settlement village and a forest camp (Yamauchi et al. 2009). In the present study, over 80 % of children had enough body weight for their height; that seems to support the moderate timing in the onset of puberty.

The total height gain of Baka children from take-off to adult height (boys: 34.77 cm and girls: 33.35 cm) was similar to other populations (Preece and Baines 1978, Billewicz and McGregor 1982, Hauspie et al. 1980; Brown and Townsend 1982; Bogin et al. 1990). Although the difference in adult height was 11.6–20.5 cm for boys and 4.1–15.8 cm for girls, the height gains during adolescent were similar between the Baka and the five populations for both sexes. This result suggests that the height differences in final stature is almost same as that at the period of finishing their childhood. Moreover, the height gain during early childhood is quite small in Baka. Billwicz and McGregor (1982) described that the difference in adult height between Gambian and British children was established in early childhood with the findings that the height gain from 3 years old to adult was similar between these two groups. Similarly, the rest height values for final heights of the Baka and British children were similar at 12.0 years old in boys and 7.5 years old in girls. It is also examined that the growth tempo before adolescent were slower than that of other groups' children. Even though it was certain that the birth height of pygmy hunter-gatherers (Efe in eastern D.R.C.) were shorter than that of African farmers (Lese in same area), the difference was only 1.8 cm between two population. However, there were about 7–15 cm height difference at the onset of adolescent growth spurt what meant the great difference of height gain were occurred during the same interval childhood.

There were several limitations associated with this study as below; (1) the goodness of fitting cross-sectional data for PB-1 model (Zemel and Johnson 1994), (2) the accuracy of age estimation and (3) lack of anthropometric data about early infants. In our further study, we continue our field research in the same area, it will be able to obtain the longitudinal datasets of many samples with high accuracy of information about age estimations. They will make it possible to increase the goodness of curve fitting, and to obtain the whole growth pattern of pygmy hunter-gatherers. Furthermore, we would like to elucidate the growth pattern of Neanderthals by comparing the childhood period and adolescent growth spurt characteristics using simulating methods.

11.5 Conclusion

A cross-sectional survey was conducted on a large sample of pygmy hunter-gatherer children to evaluate their growth pattern. By fitting into the PB-1 function, it was indicated that there was a weak adolescent growth spurt in Baka children, and the periods of adolescent and also childhood were similar to other modern humans. Furthermore, the height gain during early childhood is much less with the growth tempo slower than other populations.

References

Bailey RC (1991) The comparative growth of Efe pygmies and African farmers from birth to age 5 years. Ann Hum Biol 18:113–120

Billewicz WZ, McGregor IA (1982) A birth-to-maturity longitudinal study of heights and weight in two West African (Gambian) villages, 1951–1975. Ann Hum Biol 9:309–320

Bogin B, Wall M, Macvean RB (1990) Longitudinal growth of high socioeconomic status Guatemalan children analyzed by the Preece–Baines function: an international comparison. Am J Hum Biol 2:271–281

Brown T, Townsend GC (1982) Adolescent growth in height of Australian Aboriginals analysed by the Preece–Baines function: a longitudinal study. Ann Hum Biol 9:485–505

Cole TJ, Bellizzi MC, Flegal KM et al (2000) Establishing a standard definition for child overweight and obesity worldwide: international survey. Br Med J 320:1240–1243

Cole TJ, Flegal KM, Nicholls D et al (2007) Body mass index cut offs to define thinness in children and adolescents: international survey. Br Med J 335:194–197

Hauspie RC, Das SR, Preece MA et al (1980) A longitudinal study of growth in height of boys and girls of West Bengal (India) aged six months to 20 years. Ann Hum Biol 7:429–441

Kulin HE, Bwibo N, Mutie D et al (1982) The effect of chronic childhood malnutrition on pubertal growth and development. Am J Clin Nutr 36:527–536

Largo RH, Gasser T, Prader A et al (1978) Analysis of the adolescent growth spurt using smoothing spline functions. Ann Hum Biol 5:421–434

Milani S (2000) Kinetic models for normal and impaired growth. Ann Hum Biol 27:1–18

Preece MA, Baines MJ (1978) A new family of mathematical models describing the human growth curve. Ann Hum Biol 5:1–24

Travaglino P, Meazza C, Pagani S et al (2011) Secular trends in growth of African Pygmies and Bantu. Hormones (Athens) 10:144–148

Turnbull C (1965) Wayward servants: the two World of African Pygmies. The American Museum of National History, New York

van de Koppel JMH, Hewlett BS (1986) Growth of Aka Pygmies and Bangandus of the Central African Republic. In: Cavalli-Sforza LL (ed) African Pygmies. Academic, Orlando

Weiner JS, Lounie JA (1981) Practical human biology. Academic, London

World Health Organization (WHO) (1995) WHO Physical status: the use and interpretation of anthropometry. Report of a WHO Expert Committee 854

Yamauchi T, Sato H, Kawamura K (2000) Nutritional status, activity pattern, and dietary intake among the Baka hunter-gatherers in the village camps in Cameroon. Afr Study Monogr 21:67–82

Yamauchi T, Hayashi K, Kawamura K et al (2009) Nutritional status, physical activity, and dietary intake of Pygmy hunter-gatherers in Cameroon. In: Louts T, Reitenbach M, Molenbroek J (eds) Human diversity: design for life. Delft University of Technology, Delft, pp 78–81

Zemel BS, Johnson FE (1994) Application of the Preece-Baines growth model to cross-sectional data: problems of validity and interpretation. Am J Hum Biol 6:563–570

Interpretations of Practical Population Genetics Analyses of Genome-Wide SNP Data on Human Demography

12

Ryosuke Kimura

Abstract

Recent advances in DNA technologies enable researchers to investigate the genetic diversity across the whole genome within a species and to gain insight into the genetic structures of populations at an unprecedented resolution. Moreover, several recently developed statistical techniques are used to infer the demographic history of populations. However, reconstruction of a complicated demographic history of a large number of interrelated populations remains difficult. In this study, I focused on (1) phylogenetic analysis, (2) principal component analysis, and (3) model-based clustering analysis with the aim of learning by computer simulations how to interpret of a large-scale genomic data set using these methods. Such empirical understandings of these practical analyses must facilitate to set an appropriate model to be tested in the estimation of demographic parameters.

Keywords

Clustering analysis • Demography • Genome-wide SNP data • Phylogenetic analysis • Principal component analysis

12.1 Introduction

Researchers in the field in population genomics face exciting times. Because of advances in DNA technologies—DNA microarrays and next-generation DNA sequencing, in particular—researchers can investigate the genome diversity within a species and can examine genetic structures of populations at an unprecedented resolution. With genome-wide diversity data, researchers can also estimate demographic parameters assuming fairly realistic models of population history. Several recently developed statistical techniques are used to infer the demographic history of populations.

The model-based Bayesian approach has become a standard tool for reconstructing a complex population history from a genome-wide data set (Beaumont and Rannala 2004). Researchers using this approach assume some demographic model, preset parameters (including population size, divergence time, migration, strength and time of bottlenecks, and admixture events), and then explore the parameter values that provide the best-fit to the real data. When data from a small number of populations are subjected to such a Bayesian analysis, the number of possible models and parameter settings is relatively small. Therefore, it may be feasible to test and to compare all the possible models even without any prior information on population structure. However, number of possible models and parameter settings becomes very large and unmanageable when reconstruction of a demographic history for a large number of focal populations is attempted. In such reconstructions, researchers would need some prior information about the demographic history before applying a model-based estimation.

In practice, many researchers use (1) neighbor-joining (NJ) and neighbor-net (NN) methods for phylogenetic analyses (Bryant and Moulton 2004; Saitou and Nei 1987), (2) multivariate analyses such as principal component analysis (PCA) and multidimensional scaling analysis (MDS) (Patterson et al. 2006; Price et al. 2006; Purcell

R. Kimura (✉)
Graduate School of Medicine, University of the Ryukyus, Uehara 207, Nishihara-cho, Nakagami-gun, Okinawa 903-0215, Japan
e-mail: rkimura@lab.u-ryukyu.ac.jp

T. Akazawa et al. (eds.), *Dynamics of Learning in Neanderthals and Modern Humans Volume 2: Cognitive and Physical Perspectives*, Replacement of Neanderthals by Modern Humans Series, DOI 10.1007/978-4-431-54553-8_12, © Springer Japan 2014

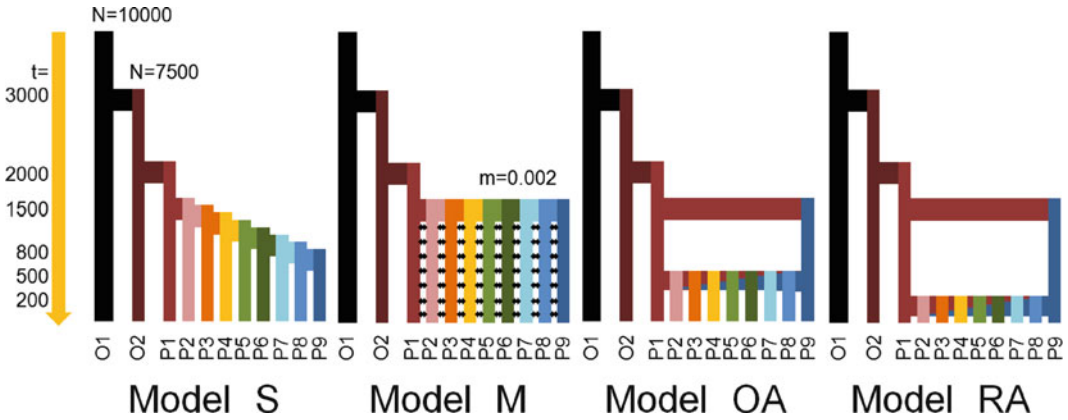

Fig. 12.1 Simulation models. An in-group consisting of nine populations (SP1-9) and two out-group populations (O1, O2) were generated and used to examine the following four models: serial splits model (S), migration model (M), old admixture model (OA), and recent admixture model (RA). Population size *N*, time of event *t* (generations ago), and migration rate *m* are shown

et al. 2007), and (3) model-based clustering analyses implemented in software including STRUCTURE, FRAPPE, and ADMIXTURE (Alexander et al. 2009; Pritchard et al. 2000; Tang et al. 2005) to understand genome diversity in multiple related populations. Although these practical genetic analyses may provide some insights into plausible demographic histories, they can neither readily provide an unambiguous demographic model nor directly estimate the demographic parameters. For example, the presence of migration or admixture between populations can distort branch lengths of a NJ tree and sometimes even changes the tree topology (Ruiz-Linares 1994). Similarly, patterns of PCA do not necessarily reflect specific large migration waves and can emerge as "mathematical artifacts" that arise generally when PCA is applied to genetic data showing continuous spatial variation (Francois et al. 2010; Novembre and Stephens 2008).

In this study, I used computer simulations in an attempt to learn how to interpret the results of practical genetic analyses for reconstructing a demographic history, and found that a specific pattern arises to each analysis depending on a simulated demographic history. Such empirical understandings of statistical methods must facilitate the reconstruction of complex demographic models of multiple populations.

12.2 Materials and Methods

12.2.1 Generation of Simulated Data Sets

Coalescent simulations that incorporated multiple models were performed using a program, msms (see Appendix for the codes) (Ewing and Hermisson 2010). Briefly, population splits/joins and demographic parameters are input, and sequence data denoted by 0 (ancestral allele) or 1 (derived allele) are output in coalescent simulations. I placed an in-group consisting of nine populations (P1–P9) and two out-group populations (O1, O2) into each of the following four models in which P1–P9 would be gradually related with each other (Fig. 12.1):

1. Serial splits model (S): in-group populations split off one by one in a temporal series.
2. Migration model (M): a population splits into nine populations at once, and continuous gene flows occur at migration rate *m* between neighboring populations as in a one-dimensional stepping-stone model.
3. Old admixture model (OA): a population had split, and the two resulting populations (P1 and P9) were separated for a time; each of seven other populations was then generated by a distant single event of population admixture with different proportions of the two parental populations (7:1, 6:2, 5:3, 4:4, 3:5, 2:6, 1:7).
4. Recent admixture model (RA): the same as the model OA but the time of admixture is more recent.

Parameters for each simulation model are described in Fig. 12.1. I assumed that the mutation rate (μ) was 1×10^{-8} (per nucleotide per generation) and the length of nucleotide sequence (L) simulated for each replication was 10,000, in which recombination did not occur. The population size (N) was constant ($N = 10{,}000$ in O1 and $N = 7{,}000$ in O2 and P1–P9). When N was set to 10,000 for the ancestral population, theta (=4 NμL) equals to 4. I sampled 20 sequences from each out-group or in-group population, and obtained 220 sequences in all. The number of replications was greater than 10,000. For each replication, I randomly collected one SNP with a minor allele frequency no less than 10 %; from 10,000 replications, I generated 220 haploids with 10,000 independent SNPs. Finally, two randomly selected haploids were paired to generate 110 diploid genomes.

12.2.2 Statistical Analyses

Nei's minimum genetic distance between each pair of populations was calculated (Nei 1987). From the resulting distance matrix, I constructed NJ trees and NN networks using SplitsTree4 (Bryant and Moulton 2004; Huson and Bryant 2006; Saitou and Nei 1987). Eigensoft 3.0 was used to perform PCA of the individual genotype data (Patterson et al. 2006; Price et al. 2006). Additionally, ADMIXTURE was used to perform a model-based clustering analysis (Alexander et al. 2009).

12.2.3 Analyses of a Real Data Set

Phylogenetic analysis, PCA, and clustering analysis were applied to data of whole-genome 50 K SNPs from the HUGO Pan-Asian SNP Consortium (The HUGO Pan-Asian SNP Consortium 2009), which consist of eight Chinese populations (sample code: CNs), fifteen Indonesian populations (IDs), nine Indian populations (INs), two Japanese populations (JPs), one Korean population (KR-KR), six Malaysian populations (MYs), nine Philippine populations (PIs), three Singaporean populations (SGs), thirteen Thai populations (THs), four Taiwanese populations (TWs, AX-AM, AX-AT), one Native American population (AX-AI), one Papua New Guinean population (AX-ME). I also used four HapMap populations (CEU, CHB, JPT, YRI). These analyses were performed to further selected data sets. Based on the frequency data in ancestries estimated from the ADMIXTURE analysis ($k=9$), NN networks were also constructed.

12.3 Results and Discussion

12.3.1 NJ Tree and NN Network

There is no doubt that, in the absence of migration and admixture, the analysis of a phylogenetic tree is a powerful tool for understanding the demographic history of a discrete population. For model S, or any model like S that lacks migration or admixture events, the shape of NJ tree directly reflects the actual demographic history (Fig. 12.2a); specifically, the tree branching patterns correspond to the patterns of population splits and the length of each branch is determined by a function of population size and divergence time (Latter 1972). However, when a demographic history includes migration or admixture, NJ trees are known to be distorted because of the incompatibilities among pairwise distances (Ruiz-Linares 1994). In models M and OA, similar tree patterns were observed (Fig. 12.2c, e), which indicated that NJ tree analysis could not discriminate between these two models; in both trees, two main lines extended toward the two end populations (P1 and P9), and intermediate (admixed) populations (P2-P8) branched off from the main lines. In the model RA, intermediate populations were just on the lines to the end populations (Fig. 12.2g), since the outer branch to each intermediate population was very short or absent.

The phylogenetic network analysis performed with the NN algorithm was very informative even when examining demography with migration and admixture. Populations without migration and admixture give rise to NN networks that do not have large reticulate structures because there is compatibility among pairwise genetic distances. Therefore, for model S, the NN network was quite similar to the NJ tree (Fig. 12.2b). NN network derived from model M, unlike the NJ tree derived from this model, had reticulate structures just like a casting net; these reticulate structures represented the connections between neighboring populations (Fig. 12.2d). Although models M and OA gave rise to undistinguishable NJ trees, these two models resulted in clearly different NN networks; in model OA, populations branched off in irregular directions, making reticulate structures (Fig. 12.2f). It is likely that this pattern reflects the independent isolation of populations after the admixture. In the model RA, the NN network had no outer branch to intermediate populations that resembled branches in the NJ tree (Fig. 12.2h).

12.3.2 PCA

PCA can be used to detect and to quantify population structure with statistical appropriateness (Patterson et al. 2006). How PCA projections relate to the underlying demographic history—which could include migration, isolation, and/or admixture—has been studied theoretically and empirically (McVean 2009; Novembre and Stephens 2008; Reich et al. 2008). In genome-wide association studies that aim to identify genetic variants involved in certain traits, PCA has become an essential tool to examine and correct population stratification between cases and controls (Price et al. 2006). However, some previous studies have also provided evidence that PCA is strongly affected by uneven sampling and that PCA generally produces mathematical artifacts when applied to genetic data showing continuous spatial variation (McVean 2009; Novembre and Stephens 2008).

When two out-groups were included in PCA, PC1 represented the differentiation between O1 and the in-group populations (Fig. 12.3a). The differentiations between O1 and O2 and within the in-group populations were projected to PC2 or PC3, with their order depending on the amount of projected variance. These results let us confirm that the amount of projected variance is affected not only by the genetic distance among populations but also by the number of individuals sampled from each population: the effect of sampling a larger number of individuals from the in-group

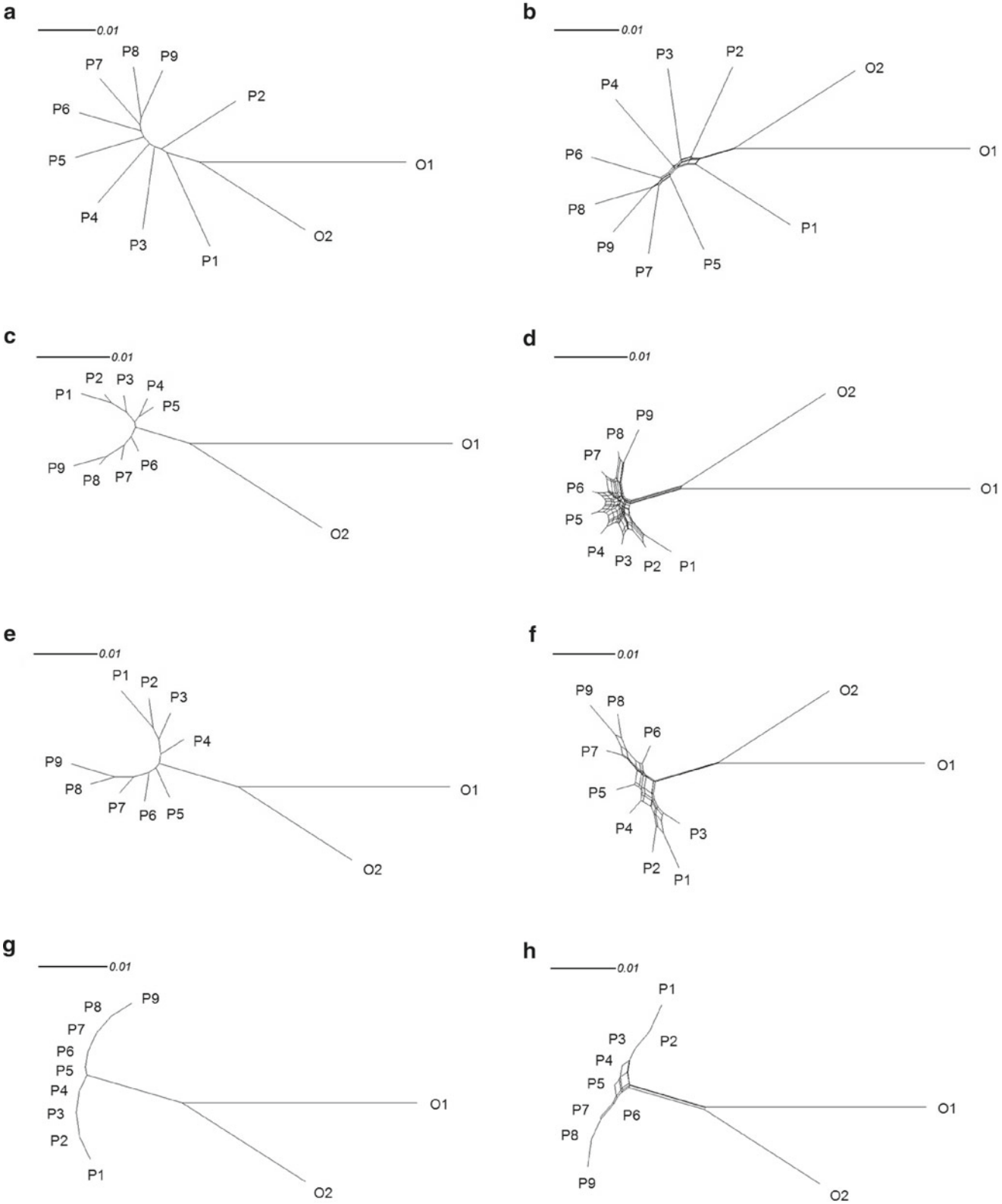

Fig. 12.2 Phylogenetic analysis of the simulated data. NJ trees (**a**, **c**, **e**, **g**) and NN networks (**b**, **d**, **f**, **h**) for the four models S (**a**, **b**), M (**c**, **d**), OA (**e**, **f**), and RA (**g**, **h**)

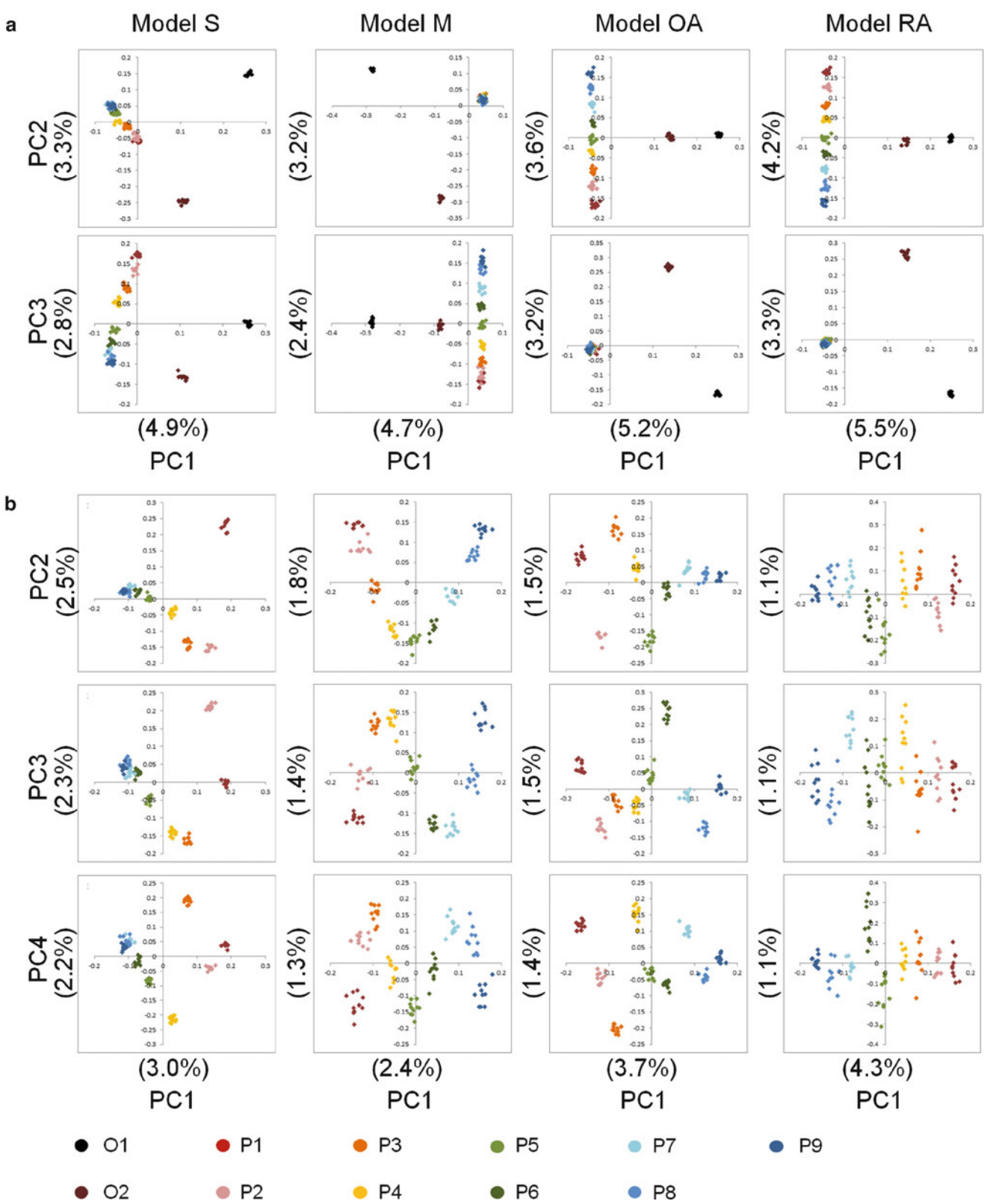

Fig. 12.3 PCA for the simulated data. PCA with the out-groups (**a**) and without the out-groups (**b**) are shown. The color coding of the population is the same as that used in Fig. 12.1. Percentage in parentheses is the contribution of each PC

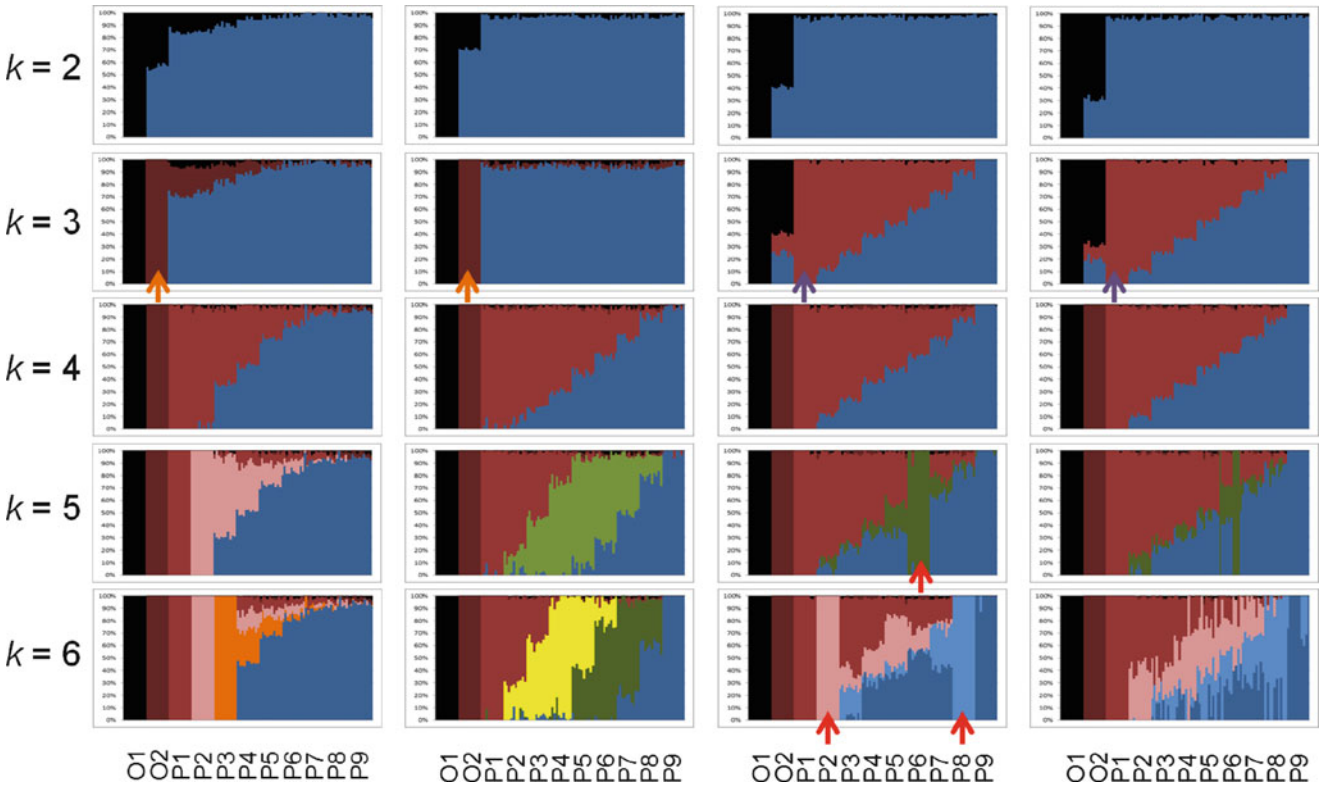

Fig. 12.4 ADMIXTURE analysis for the simulated data Results at $k=2$–6 are shown. Each individual is displayed as fractions of ancestral genetic components represented by different colors. At $k=3$, an ancestry for O2 appeared in models S and M (*orange arrows*), whereas the 2nd ancestry for the in-group appeared in models OA and RA (*purple arrows*). The analyses of model OA at $k \geq 5$ irregularly assigned specific ancestries to some populations (*red arrows*)

than from the out-groups appeared in the projected variance. In addition, all the in-group populations have the equal PC1-projected distance from O2 in model M, model OA, and model RA, but not in model S. In model S, the outer (former split) populations of the in-group seem to be closer to O2 in the PC1-PC2 biplot.

The relationships among populations in a PCA that included only in-group populations are shown in Fig. 12.3b. In all the models, PC1 represented the cline from P1 to P9. Therefore, the four models were not differentiated by PC1 as was suggested in a previous theoretical study: PCA cannot distinguish between models that lead to the same mean coalescent times (McVean 2009). However, these models showed different patterns in PC2 and higher PCs. In the case of model S, the outermost population in the divergence topology (P1) deviated from the line of the other populations in PC2, the next outermost population (P2) was then deviated in PC3, and such patterns continued. The sinusoidal patterns observed in model M were what had been observed as a mathematical artifact in a similar model previously tested by Novembre and Stephens (2008). In PC2 and higher PCs of model OA, PC scores of populations were irregularly shuffled. In model RA, individuals in each population spread widely and become sparse. These patterns observed in model OA and RA may be caused by isolation of each population after the admixture event.

12.3.3 Clustering Analysis

For the model-based clustering analysis, I used the ADMIXTURE algorithm that runs faster than STRUCTURE and FRAPPE (Alexander et al. 2009). The cluster-based and PCA-based approaches, having a close statistical relationship, are complementary to one another, and each has its particular advantages. As shown in Fig. 12.4, the results of ADMIXTURE analysis were corresponding to those of PCA. All the models showed quite similar patterns of ancestry estimation at $k=4$; intermediate populations in the in-group have two estimated ancestries even in the model S. At $k=3$, an ancestry for O2 appeared in models S and M, whereas the 2nd ancestry for the in-group appeared in models OA and RA. This clearly indicated that the order of appearance of ancestries in a clustering analysis did not necessarily reflect the history of population splits, but rather the order depended on the amount of variance among the samples as did the components of the PCA. As the number of k increased, the ancestry of the outermost population appeared in model S. In model M, the P1-to-P9 cline in the in-group was expressed by a cline of multiple ancestries. In contrast, the analyses of model OA at $k \geq 5$ irregularly assigned specific ancestries to some populations (e.g., P6 at $k=5$, P2 and P8 at $k=6$). In model RA, ancestry estimation showed an intelligible pattern at $k \geq 5$.

12.3.4 Keys to Reconstructing Past Demographic History

The three approaches—phylogenetic analysis, PCA, and clustering analysis—have their own particular weaknesses and particular strengths, but these approaches can be used together to compensate for one another. Phylogenetic analyses can reliably identify genealogical relationships among populations. In addition, NN networks are very informative for distinguishing the presence and the absence of gene flows and/or admixtures between populations. PCA can show only closeness, but not genealogy, between populations. PCA and clustering analyses may not offer conclusive evidence for the presence of admixtures. However, admixture proportions can be easily calculated if some admixture and parental populations are included in the data set. Although clustering analyses do not directly provide any relationship between ancestries at each k value, phylogenetic analyses among ancestries can be performed based on the estimated allele frequency data. In the present simulation study, even the mathematical artifacts in the analyses were demonstrably informative with regard to the past demographic history. Especially, by observing the patterns of these analyses, I could distinguish the ongoing gene flow from past gene flow that ended with population isolation.

12.3.5 Interpretation of Analyses of Real Data

Here, I used data from The HUGO Pan-Asian SNP Consortium (2009) to provide example analyses. The results of the PCA are shown in Fig. 12.5. In the analysis of all the data, PC1 and PC2 represented the Africa-Asia and Africa-Europe differentiations, respectively (Fig. 12.5a). PC3 and PC4 (data not shown) denoted genetic clines within the Asia-Pacific region. PC5 indicated the differentiation of Native Americans from the Old-world populations. Then, I reanalyzed only Asia-Pacific populations—removing YRI, CEU, the Indian populations, the Singaporean populations, the Native American population (AX-AI), the Uyghur (CN-UG), and the Mlaburi (TH-MA) (Fig. 12.5b). PC1 and PC2 in the Asia-Pacific populations were almost the same as PC3 and PC4 in the all-populations analysis. PC1 displayed a south-to-north genetic cline, which can be interpreted as the component distinguishing classical racial categories, so-called "Mongoloid (Asiatic)" and "Australoid." PC2 and PC4 showed differentiations among "Australoid" populations: insular populations vs. Malay populations (PC2) and Papuan populations vs. Philippine populations (PC4). However, the PC1-PC3 plots showed an inverted "U" shape that may be a mathematical artifact as presented in the PC1-PC2 biplot for the simulation of model M (Fig. 12.3b). When I applied PCA to Asiatic populations (Thai, Chinese, Taiwanese, Korean, and Japanese), the PC1-PC2 plots were difficult to interpret (Fig. 12.5c). Several demographic scenarios can be inferred from such a pattern. However, when I focused on PC3, a "sinusoidal" pattern was evident in the PC1-PC3 plots; such a sinusoidal pattern is considered as a signature of gene flow between neighboring populations (the PC1-PC3 biplot for model M in Fig. 12.3b). Some populations were found to drift from the sinusoidal line in the PC1-PC3 plots, suggesting that these populations were isolated from the other populations. In addition, some individuals were scattered from the cluster of the other individuals from the same population, but the reason for this is unclear.

The NJ tree and NN network constructed from the Asia-Pacific populations, YRI, and CEU populations are shown in Fig. 12.6. The NN network has reticulate structures, which indicates the presence of gene flow and/or admixtures between populations. The reticulate structures were largely divided into two parts: one is mainly for insular populations and another is for continental populations. However, as the population history in the Asia-Pacific populations seems to be complicated, dissolution into some ancestral genetic components would be required for further interpretation of these data.

The results of the ADMIXTURE analysis that included YRI, CEU, and the Asia-Pacific populations at different k values demonstrated that most of the populations and individuals have fractions of multiple ancestral genetic components (Fig. 12.7), and detailed interpretations are as follows. At $k=4$, two ancestries for the Asia-Pacific populations, which are likely to correspond to "Asiatic" and "Australoid" ancestral components, were found to form a south-to-north genetic cline. When k increased, more ancestries that represent the south-to-north cline in the continental populations appeared. These patterns resembled the simulation of model M where populations are linearly distributed and connected to each other. At $k=8$, 10, 11, and 12, ancestries for some Malaysian or Philippine populations appeared. These patterns were similar to what was observed in the simulation of model OA (Fig. 12.4). Therefore, it can be supposed that these populations became isolated after admixture between indigenous "Negrito" people and Austronesian-speaking immigrants.

ADMIXTURE analysis provides the estimated allele frequencies of SNPs in each ancestry. Therefore, phylogenetic analysis among these ancestries can be performed based on the allele frequency data. In the NN networks among the ancestries at $k=9$ (Fig. 12.8), reticulate structures, that is, the signatures of gene flow and admixtures, emerged even among the estimated ancestries. However, compared with the NN network of all the populations (Fig. 12.6b), that of the estimated ancestries can be easy to be interpreted because of a reduction in complexity. Simpler structures in the networks drawn from reduced groups also provide information about possible interactions between populations (Fig. 12.8). These procedures can be a useful technique for reconstructing the complicated history of multiple populations.

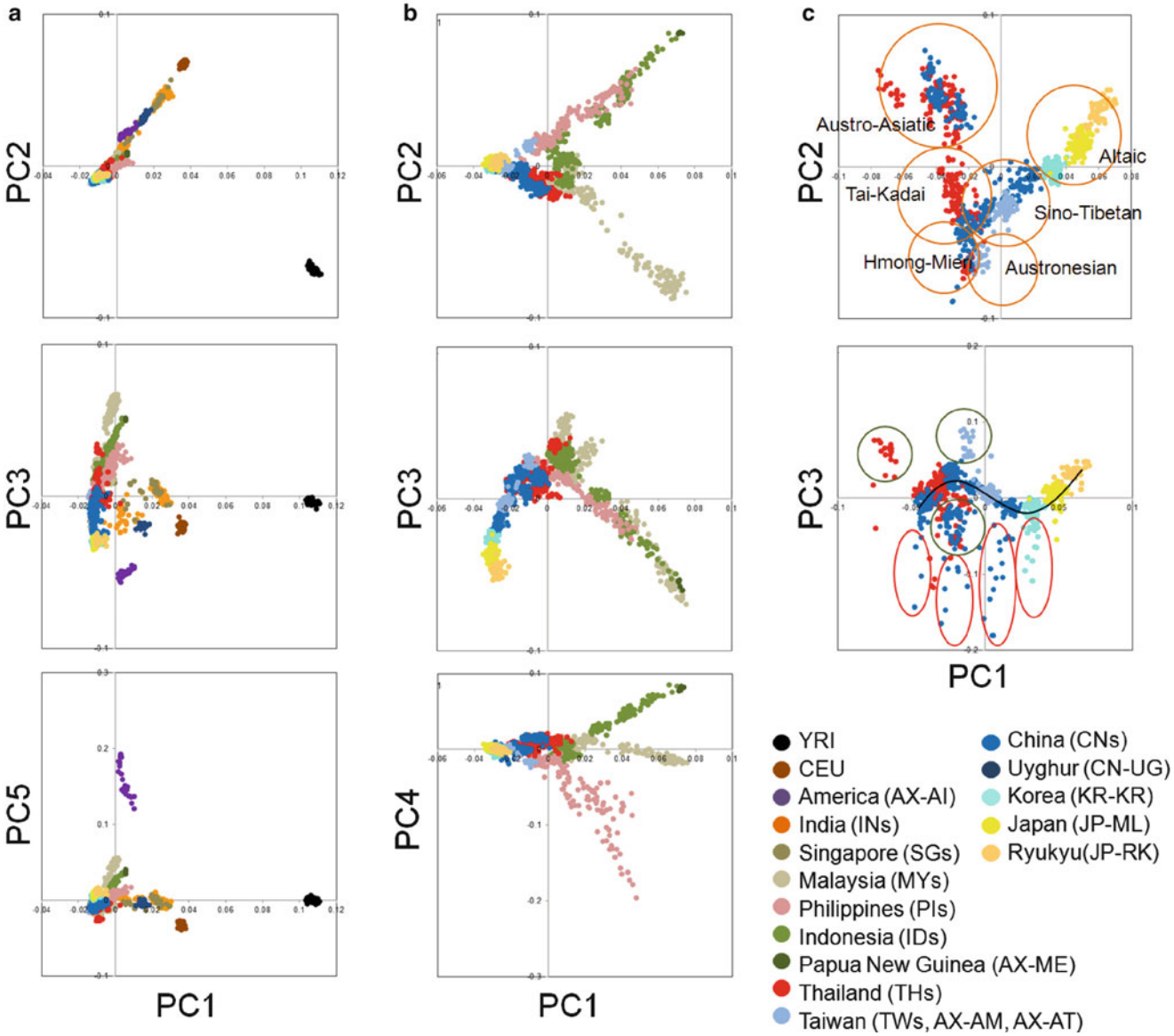

Fig. 12.5 PCA of the real data. PC plots including all the data (**a**), the Asia-Pacific populations (**b**), and the Asiatic populations (**c**). The results of the PCA of the Asiatic populations showed that people belonging to the same language group became close together (*orange circles*). In the PC1-PC3 plots for the Asiatic populations, a "sinusoidal" pattern (*black line*) was observed, but some individuals were scattered from the cluster of the other individuals from the same population (*red ellipses*). Some populations (*green circles*) were found to drift from the sinusoidal line

Through the aforementioned analyses, I can propose a model of the peopling of the Asia-Pacific region (Fig. 12.9). This model could be used for further model-based analysis to validate the model itself and to estimate demographic parameters.

12.3.6 Concluding Remarks

Phylogenetic analysis, PCA, and clustering analysis each shows some patterns depending on the demographic scenarios. In addition, I demonstrated the possibility that even mathematical artifacts in these analyses can give a cue for discriminating scenarios such as population split, migration, and admixture. Although it may be difficult to find the appropriate model to be used in a model-based Bayesian approach in case of a large number of focal populations, the practical genetic analyses, compensating each other, can play crucial roles in narrowing down the possible candidate for plausible demographic models. An empirical understanding of these statistical methods may broaden the possibilities for developing a new method for reconstruction of past demographic history.

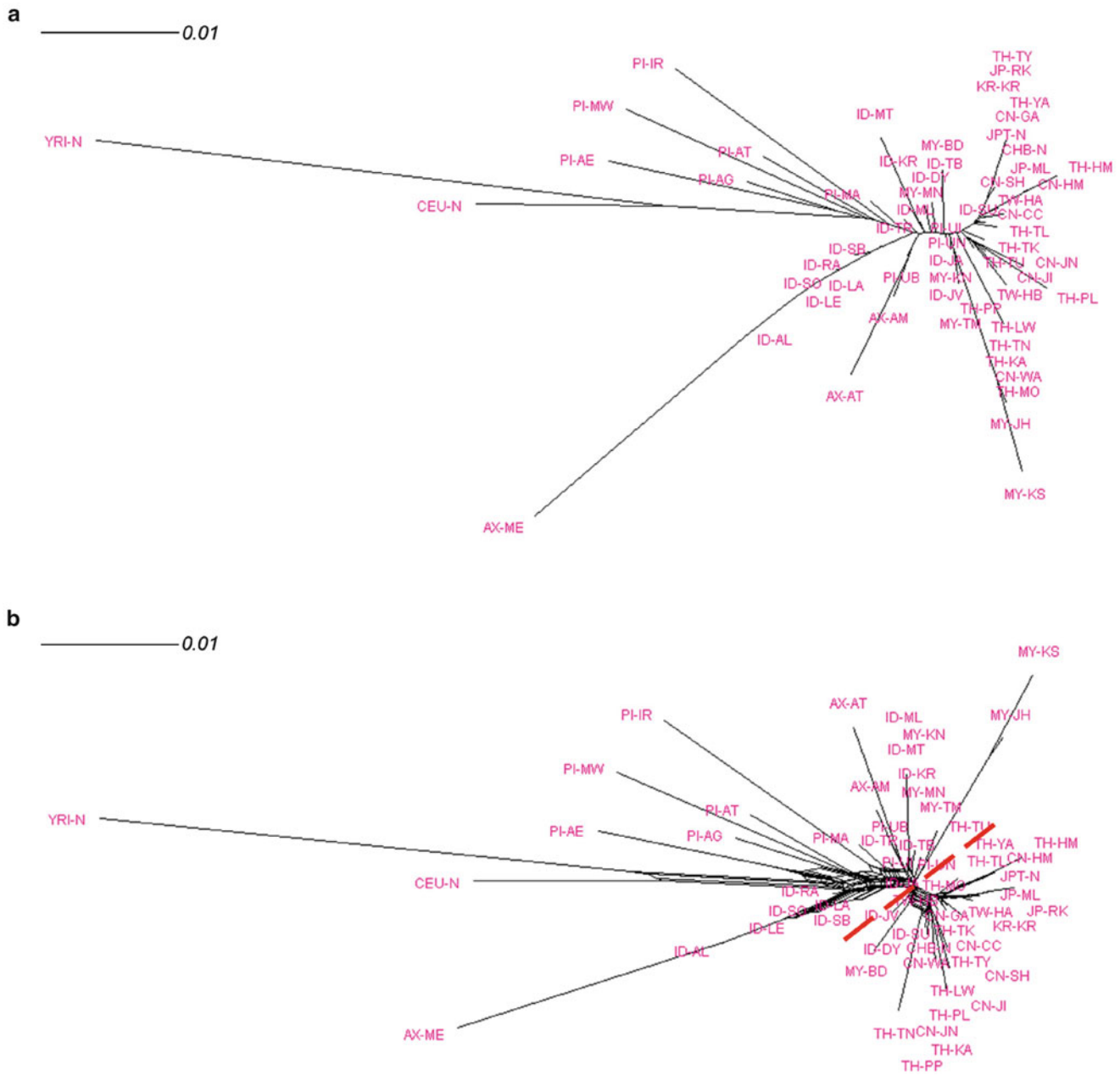

Fig. 12.6 Phylogenetic analysis of the real data. NJ tree (**a**) and NN network (**b**). Two large reticulate structures (divided by the *red dotted line*) were observed in the NN network

Acknowledgement This study was supported by a Grant-in-Aid for Scientific Research on Innovative Areas from the Ministry of Education, Culture, Sports, Science and Technology, Japan.

Appendix: Command Lines for the Simulations Operated Using msms

For Model S

msms.exe -ms 220 100000 -N 10000 -I 11 20 20 20 20 20 20 20 20 20 20 20 -t 4 -r 0 -n 2 0.75 -n 3 0.75 -n 4 0.75 -n 5 0.75 -n 6 0.75 -n 7 0.75 -n 8 0.75 -n 9 0.75 -n 10 0.75 -n 11 0.75 -ej 0.02 11 10 -ej 0.0225 10 9 -ej 0.025 9 8 -ej 0.0275 8 7 -ej 0.03 7 6 -ej 0.0325 6 5 -ej 0.035 5 4 -ej 0.0375 4 3 -ej 0.05 3 2 -ej 0.075 2 1 -oAFS >./outS.txt;

For Model M

msms.exe -ms 220 100000 -N 10000 -I 11 20 20 20 20 20 20 20 20 20 20 20 -t 4 -r 0 -n 2 0.75 -n 3 0.75 -n 4 0.75 -n 5 0.75 -n 6 0.75 -n 7 0.75 -n 8 0.75 -n 9 0.75 -n 10 0.75 -n 11 0.75 -ej 0.0375 11 10 -ej 0.0375 10 9 -ej 0.0375 9 8 -ej 0.0375 8

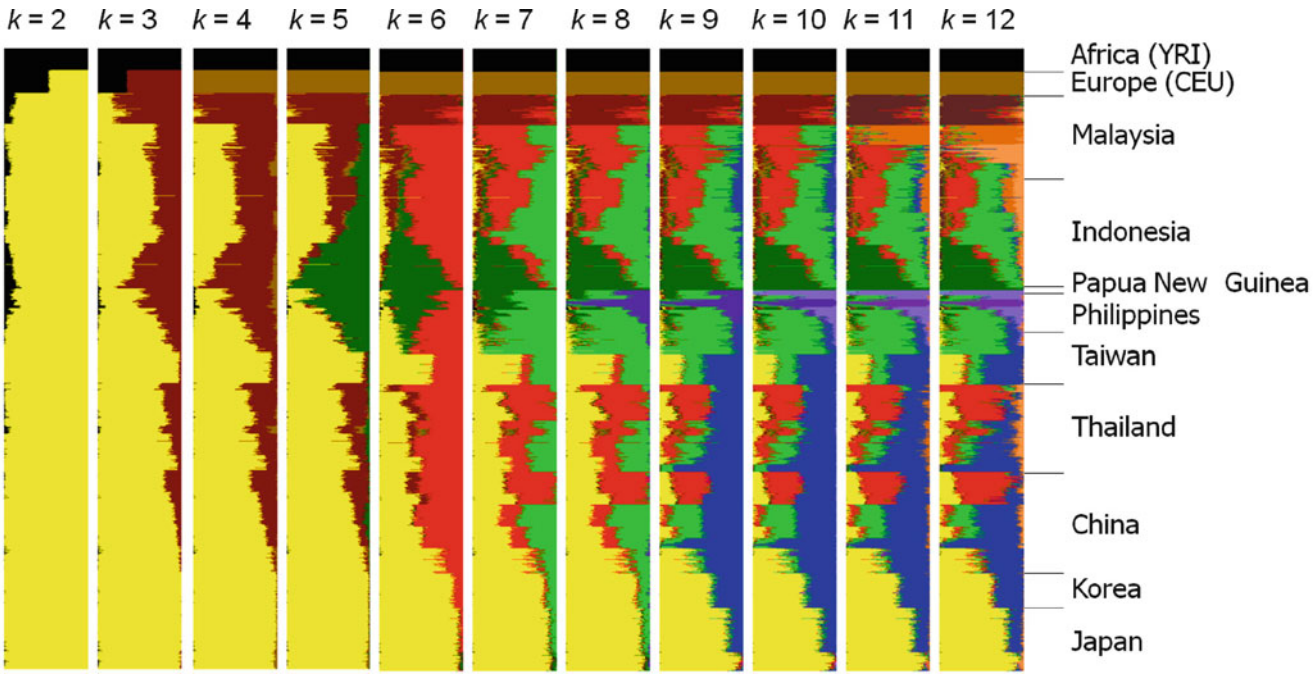

Fig. 12.7 ADMIXTURE analysis of the real data. Most of the populations and individuals have fractions of multiple ancestral genetic components. At $k=4$, two ancestries (*yellow and brawn*) are likely to correspond to "Asiatic" and "Australoid" ancestral components. At $k=9$, the south-to-north cline in the continental populations were represented with four different components (*brawn, red, blue, and yellow*). At $k=8$ (*purple*), 10 (*light purple*), 11 (*orange*), and 12 (*light orange*), ancestries for some Malaysian or Philippine populations appeared

7 -ej 0.0375 7 6 -ej 0.0375 6 5 -ej 0.0375 5 4 -ej 0.0375 4 3 -ej 0.05 3 2 -ej 0.075 2 1 -ma x 0 0 0 0 0 0 0 0 0 0 0 x 0 0 0 0 0 0 0 0 0 0 0 x 40 0 0 0 0 0 0 0 0 0 0 40 x 40 0 0 0 0 0 0 0 0 0 0 40 x 40 0 0 0 0 0 0 0 0 0 0 40 x 40 0 0 0 0 0 0 0 0 0 0 40 x 40 0 0 0 0 0 0 0 0 0 0 40 x 40 0 0 0 0 0 0 0 0 0 0 40 x 40 0 0 0 0 0 0 0 0 0 0 40 x -oAFS >./outM.txt;

For Model OA

msms.exe -ms 220 100000 -N 10000 -I 11 20 20 20 20 20 20 20 20 20 20 20 -t 4 -r 0 -n 2 0.75 -n 3 0.75 -n 4 0.75 -n 5 0.75 -n 6 0.75 -n 7 0.75 -n 8 0.75 -n 9 0.75 -n 10 0.75 -n 11 0.75 -es 0.0125 4 0.875 -es 0.0125 5 0.75 -es 0.0125 6 0.625 -es 0.0125 7 0.5 -es 0.0125 8 0.375 -es 0.0125 9 0.25 -es 0.0125 10 0.125 -ej 0.0125 10 3 -ej 0.0125 9 3 -ej 0.0125 8 3 -ej 0.0125 7 3 -ej 0.0125 6 3 -ej 0.0125 5 3 -ej 0.0125 4 3 -ej 0.0125 12 11 -ej 0.0125 13 11 -ej 0.0125 14 11 -ej 0.0125 15 11 -ej 0.0125 16 11 -ej 0.0125 17 11 -ej 0.0125 18 11 -ej 0.0375 11 3 -ej 0.05 3 2 -ej 0.075 2 1 -oAFS >./outOA.txt;

For Model RA

msms.exe -ms 220 100000 -N 10000 -I 11 20 20 20 20 20 20 20 20 20 20 20 -t 4 -r 0 -n 2 0.75 -n 3 0.75 -n 4 0.75 -n 5 0.75 -n 6 0.75 -n 7 0.75 -n 8 0.75 -n 9 0.75 -n 10 0.75 -n 11 0.75 -es 0.0025 4 0.875 -es 0.0025 5 0.75 -es 0.0025 6 0.625 -es 0.0025 7 0.5 -es 0.0025 8 0.375 -es 0.0025 9 0.25 -es 0.0025 10 0.125 -ej 0.0025 10 3 -ej 0.0025 9 3 -ej 0.0025 8 3 -ej 0.0025 7 3 -ej 0.0025 6 3 -ej 0.0025 5 3 -ej 0.0025 4 3 -ej 0.0025 12 11 -ej 0.0025 13 11 -ej 0.0025 14 11 -ej 0.0025 15 11 -ej 0.0025 16 11 -ej 0.0025 17 11 -ej 0.0025 18 11 -ej 0.0375 11 3 -ej 0.05 3 2 -ej 0.075 2 1 -oAFS >./outRA.txt;

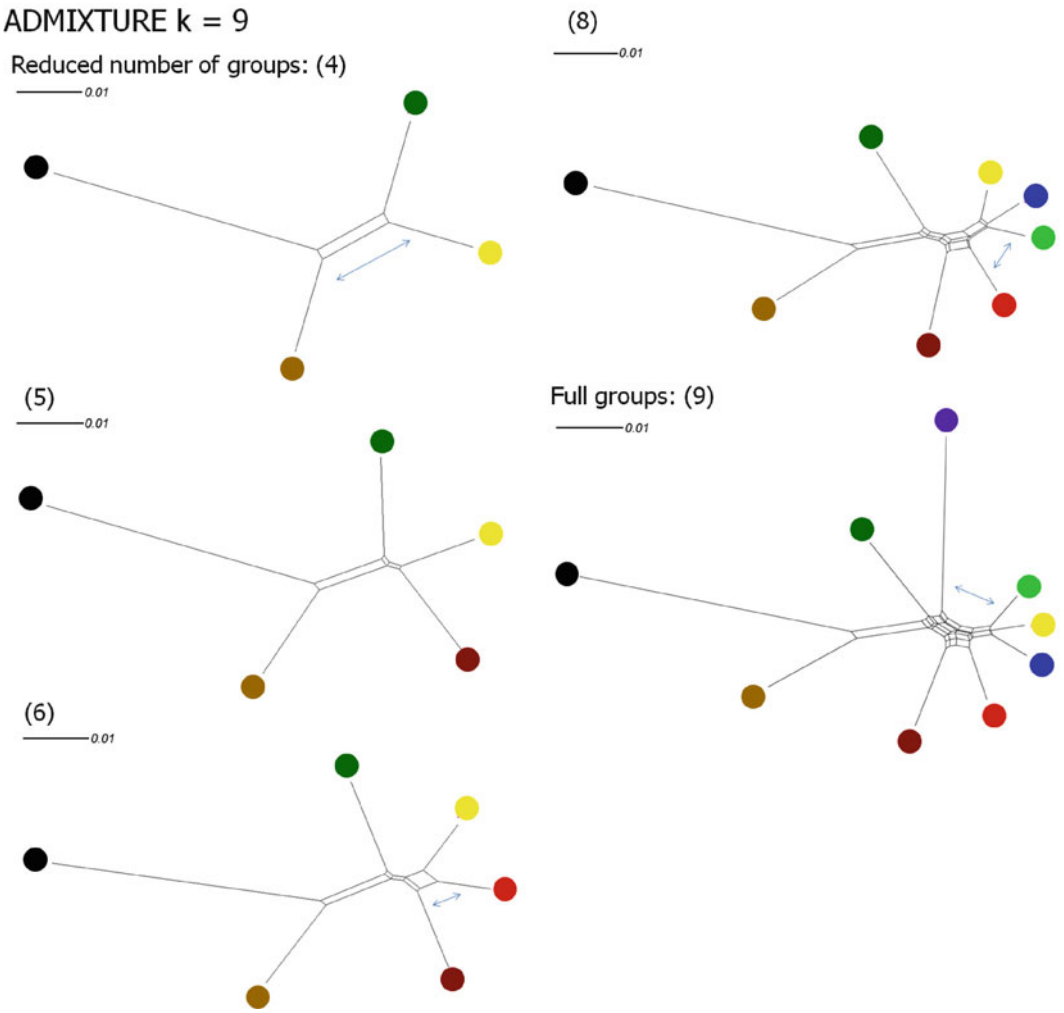

Fig. 12.8 NN networks based on the allele frequencies in ancestries estimated from the clustering analysis ($k = 9$). NN networks were constructed for all (*9*) the groups and for a reduced (*4*, *5*, *6*, *8*) number of groups. In the analyses of reduced groups, groups were selected in an ad hoc way: four groups distant to one another were firstly chosen and intermediate groups were then added. Reticulate structures suggest possible interactions between ancestral populations (*two-way arrows*)

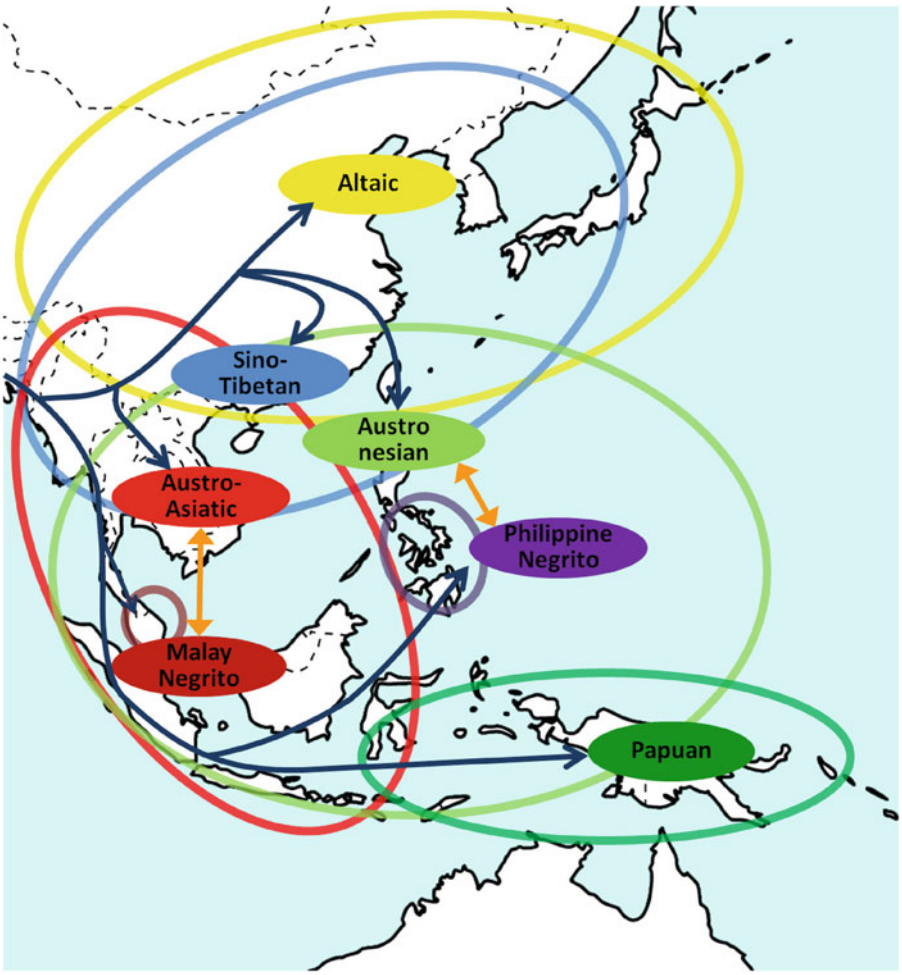

Fig. 12.9 Peopling of the Asia-Pacific region. The ancestries were named after their related language or ethnicity. *One-way arrows*: possible roots of the ancestries, *two-way arrows*: possible interactions between the ancestries, *ellipse*: expanded area of ancestries

References

Alexander DH, Novembre J, Lange K (2009) Fast model-based estimation of ancestry in unrelated individuals. Genome Res 19:1655–1664

Beaumont MA, Rannala B (2004) The Bayesian revolution in genetics. Nat Rev Genet 5:251–261

Bryant D, Moulton V (2004) Neighbor-net: an agglomerative method for the construction of phylogenetic networks. Mol Biol Evol 21:255–265

Ewing G, Hermisson J (2010) MSMS: a coalescent simulation program including recombination, demographic structure and selection at a single locus. Bioinformatics 26:2064–2065

Francois O, Currat M, Ray N, Han E, Excoffier L, Novembre J (2010) Principal component analysis under population genetic models of range expansion and admixture. Mol Biol Evol 27:1257–1268

Huson DH, Bryant D (2006) Application of phylogenetic networks in evolutionary studies. Mol Biol Evol 23:254–267

Latter BD (1972) Selection in finite populations with multiple alleles. 3. Genetic divergence with centripetal selection and mutation. Genetics 70:475–490

McVean G (2009) A genealogical interpretation of principal components analysis. PLoS Genet 5:e1000686

Nei M (1987) Molecular evolutionary genetics. Columbia University Press, New York

Novembre J, Stephens M (2008) Interpreting principal component analyses of spatial population genetic variation. Nat Genet 40:646–649

Patterson N, Price AL, Reich D (2006) Population structure and eigenanalysis. PLoS Genet 2:e190

Price AL, Patterson NJ, Plenge RM, Weinblatt ME, Shadick NA, Reich D (2006) Principal components analysis corrects for stratification in genome-wide association studies. Nat Genet 38:904–909

Pritchard JK, Stephens M, Donnelly P (2000) Inference of population structure using multilocus genotype data. Genetics 155:945–959

Purcell S, Neale B, Todd-Brown K, Thomas L, Ferreira MA, Bender D, Maller J, Sklar P, de Bakker PI, Daly MJ et al (2007) PLINK: a tool set for whole-genome association and population-based linkage analyses. Am J Hum Genet 81:559–575

Reich D, Price AL, Patterson N (2008) Principal component analysis of genetic data. Nat Genet 40:491–492

Ruiz-Linares A (1994) Analysis of classical and DNA markers for reconstructing human population history. In: Brenner S, Hanihara K (eds) The origin and past of Modern Humans as viewed from DNA. World Scientific, Singapore, pp 123–148

Saitou N, Nei M (1987) The neighbor-joining method: a new method for reconstructing phylogenetic trees. Mol Biol Evol 4:406–425

Tang H, Peng J, Wang P, Risch NJ (2005) Estimation of individual admixture: analytical and study design considerations. Genet Epidemiol 28:289–301

The HUGO Pan-Asian SNP Consortium (2009) Mapping human genetic diversity in Asia. Science 326:1541–1545

Part III

Reconstruction of Fossil Crania and Brain Morphology

Functional Craniology, Human Evolution, and Anatomical Constraints in the Neanderthal Braincase

13

Emiliano Bruner

Abstract

Neanderthals and modern humans share a similar cranial capacity but different neurocranial organization. Recently, digital anatomy and computed morphometrics have generated a revolution in functional craniology, allowing quantitative analyses to investigate integration and correlation among the anatomical elements, both in ontogeny and phylogeny. Despite some derived endocranial traits, Neanderthals display a general plesiomorph organization of the braincase. Geometrical and structural constraints between the endocranial soft and hard tissues may have induced morphogenetic limits to the growth and developmental processes. At the same time, heat production associated with a large cranial capacity and a plesiomorph vascular system may have also involved thermal limits. Although in paleontology morphogenetic and metabolic processes can only be investigated through indirect evidence, such hypotheses merit attention when considering the patterns of brain evolution in the genus *Homo*. It is tempting to wonder whether these limits may be also related to possible factors associated with the extinction of Neanderthals.

Keywords

Brain evolution • Encephalization • Neurocranial integration • Paleoneurology

13.1 Functional Craniology and Human Evolution

In the last decades, technical enhancements associated with biomedical imaging and multivariate statistics have triggered a relevant revolution in morphometrics, allowing the analysis of the anatomical variation in terms of integrated systems. Concepts like *morphological integration* and *modularity* were postulated in the early twentieth century, but only with the development of computed approaches have these topics found a proper experimental and quantitative framework. Computed tomography and magnetic resonance represent the basic tools for digital anatomy, supplying a complete and effective source of sampling procedures (Spoor et al. 2000; Zollikofer and Ponce de León 2005; Gunz et al. 2009; Weber and Bookstein 2011). Multivariate statistics, geometrical models, and landmark-based morphometrics are the most successful tools to approach variation in terms of correlation and spatial relationships between the anatomical components (Rohlf and Marcus 1993; Slice 2004). *Digital anatomy* aims to generate data, while *computed morphometrics* aims to analyze data. Together, they have renovated all the fields in anatomy, through at least three distinct processes. First, they introduced new questions and new answers. Second, they made it possible to investigate issues which couldn't be investigated before. Third (and this is very relevant) they have brought back many forgotten topics, left apart in the early twentieth century after the introduction of the brand new genetic and molecular approaches.

Complexity and non-linear dynamics are generated at three different levels. *Pleiotropy* and *poligeny* characterize reticulated networks between genes and characters, in which

E. Bruner (✉)
Centro Nacional de Investigación sobre la Evolución Humana, Paseo Sierra de Atapuerca s/n, 09002 Burgos, Spain
e-mail: emiliano.bruner@cenieh.es

T. Akazawa et al. (eds.), *Dynamics of Learning in Neanderthals and Modern Humans Volume 2: Cognitive and Physical Perspectives*, Replacement of Neanderthals by Modern Humans Series, DOI 10.1007/978-4-431-54553-8_13, © Springer Japan 2014

each gene influences several characters, and each character is influenced by several genes. *Integration* characterizes networks among genes and among characters, inducing covariation of genes and covariation of characters because of functional and structural relationships. The *environment* modulates the expression of both genes and characters, producing different variations from the same genotype-phenotype model. Such networks cannot be reduced to linear chains of causes and consequences, given that many genes and characters are linked into a single system. Multivariate statistics is clearly the only quantitative approach that can organize, reveal, and disentangle these complex correlations among functions and structures. This framework suggests that rigid linear approaches may often be misleading and counterproductive in biology and evolution. The assumption that each specific evolutionary change may be adaptive, or that selection can operate on single traits independently, are two of the worst mistakes commonly made in the last century, most of all following the reductionist approaches put forward in many molecular fields.

Anthropology and paleoanthropology, because of their legacy with both applied biomedicine and theoretical biology, were among the first disciplines to recognize the advantages of such new perspectives. Cranial integration and evolution were soon investigated by using these new toolkits (Ponce de León and Zollikofer 2001; Lieberman et al. 2002; Rosas and Bastir 2002; Bookstein et al. 2003; Richtsmeier et al. 2006). The fundamentals of such new research trends were already present decades before. Geometric morphometrics was developed upon the principles expressed much earlier by Thompson (1942). The integration between brain and braincase had been formally introduced by Moss and Young (1960) as principles of *functional craniology*. According to their view, during morphogenesis, the growth of the braincase (changes in size) is mainly due to brain pressure, while the development of the braincase (changes in shape) is associated with the biomechanical redirection of such forces according to tensions exerted by the connective endocranial components, most of all the *falx cerebri* and the *tentorium cerebelli*. The upper vault components (frontal, parietal, and occipital bones) display a quite linear response to the redistribution of forces associated with the brain pressure. On the other hand, the elements of the endocranial base are also influenced by many other non-brain factors associated with the structural and functional interaction with the rest of the skull (Lieberman et al. 2000; McCarthy 2001; Bastir and Rosas 2005; Bastir et al. 2006; Bruner and Ripani 2008). During both morphogenesis and evolution, the face strongly influences the orbital cortex, the subcortical spatial organization, and the lateral cranial base through the physical interaction with the orbits, the ethmomaxillary complex, the cranial base flexion, and the mandible (Enlow 1990; Bastir et al. 2004; Masters 2012). As a result, endocranial morphological changes in the upper vault are more likely to be associated with brain form changes, while endocranial morphological changes in the endocranial base can be associated with both neural and non-neural changes. In the latter case, the interpretation of endocranial variation is not straightforward: the final phenotype will be the result of an admixture of factors, where structural constraints of the hard tissues (bones) are likely to exert more mechanical influences than those of the soft tissues (brain).

13.2 Paleoneurology and Endocranial Constraints

For a long time, paleoneurology has dealt with changes in cranial capacity. Today we know that this variable may be really relevant, but at the same time we acknowledge that brain evolution cannot be limited to size variations. The endocranium is the mould of the brain and of its vascular and connective elements, and it can provide information on many characters imprinted on its surface, like vessels or circumvolutions. At the same time, endocranial morphology supplies information on the form of the brain, and on the spatial relationships of its components.

Since the early applications of computed morphometrics, it has been suggested that Neanderthals and modern humans have a different cranial organization, and that these differences can be recognized early in the ontogenetic pattern (Ponce de León and Zollikofer 2001). Neanderthals were large-brained hominids, with a comparable cranial capacity with modern humans and with similar gross morphology of many regions associated with relevant cognitive functions, like the Broca's area or the supramarginal gyrus (Holloway 1980, 1981; see Holloway et al. 2004 for quantitative and qualitative information on many endocranial reconstructions). The endocranial anatomy of Neanderthals shows both derived and plesiomorph traits (Fig. 13.1). Except modern humans, all the other species of the genus *Homo* display form differences which are mainly allometric: as the brain changes its size, the form adjusts accordingly to a shared system of structural and functional rules (Bruner et al. 2003). In this sense, Neanderthal brain morphology is mainly the large scaled version of a model shared by all the other extinct human taxa, and the general endocranial proportions follow the same scaling rules of their ancestors (Bruner et al. 2006). Nonetheless, they displayed also some specific traits.

Some derived features can be recognized in the frontal areas. In small-brained human species, the frontal lobes lie behind the orbital roof (Bruner and Manzi 2005), suggesting some degree of independence between the neural and facial blocks. In contrast, in modern humans and Neanderthals, the frontal lobes lie on the orbital roof (Bruner and Manzi 2008). This may suggest that in Neanderthals and modern humans,

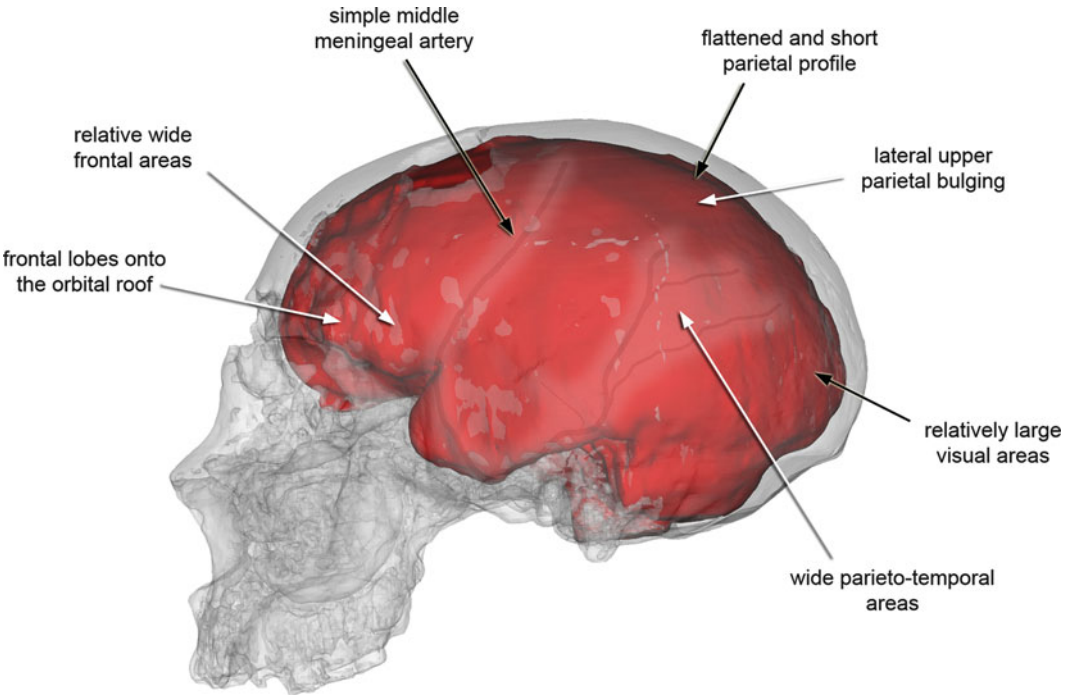

Fig. 13.1 Paleoneurological characters of Neanderthals are shown on the digital replica of the skull and endocasts of Saccopastore 1 (Bruner and Manzi 2008). Derived traits (*white arrows*) are shown as well as some plesiomorph traits (*black arrows*) which can generate constraints due to the large brain size. Large occipital areas are here interpreted as a plesiomorph trait

the constraints exerted by the upper face on the anterior endocranial fossa may be larger than in their ancestors. Furthermore, like modern humans, Neanderthals also had wider brains. Their endocranium widens at the temporo-parietal areas, at the supramarginal and angular gyri. But the widening of the prefrontal areas is even more marked, giving the endocranium of both groups a more squared appearance in upper view. Such enlargement is not strictly allometric, and it represents a discrete shift when compared with small-brained human species (Bruner and Holloway 2010). The widening of the anterior fossa is associated with a lateral expansion of the Broca's area, which is assumed to be relevant for the evolution of language. This change may be the result of a direct neural functional (cognitive) adaptation, or else the result of volumetric redistribution associated with the constraints of the underlying facial block and lateral space availability due to orbital frontation and reduction of the temporal muscle in hominids (Bruner 2004).

A mix of archaic and derived traits can be observed in the Neanderthals' parietal areas. When compared with less encephalized human species, Neanderthals display a lateral bulging in the upper parietal areas (Bruner et al. 2003). This bulging is totally absent in *Homo heildebergensis* or *Homo erectus*, resulting in the Neanderthals' brain classic "en bombe" profile in rear view. Considering the limited structural constraints in the upper parietal areas, this bulging is supposed to be the direct result of pressure exerted on the parietal bone by the underlying parietal cortex. However, when compared with modern humans, Neanderthals lack the overall bulging of the parietal surface characterizing the modern human brain globularity, in which the parietal proportions also enlarge in the longitudinal and vertical directions (Bruner 2004, 2008; Bruner et al. 2011a, b). Such geometrical dilation of the parietal areas in modern humans is associated with an early post-natal period (Neubauer et al. 2009), which is absent in chimpanzees (Neubauer et al. 2010) and in Neanderthals (Gunz et al. 2010). The spatial reorganization at the parietal areas displayed by modern humans may have been associated with important cognitive changes in visuo-spatial integration and mental experiment capabilities (Bruner 2010), but also with a vulnerability to metabolic impairments like those observed in early stages of Alzheimer's disease (Bruner and Jacobs 2013).

Concerning the cranial base, some differences in the middle cranial fossa (Bastir et al. 2008) and in the orbital regions (Bastir et al. 2011) may suggest additional differences between modern humans and Neandertals, which will deserve further attention.

Among all these features, the relative proportions of the upper vault and the morphology of the parietal areas may supply information about some characteristics of the brain vs. braincase relationships in Neanderthals. Taking into account the allometric endocranial trajectory in non-modern

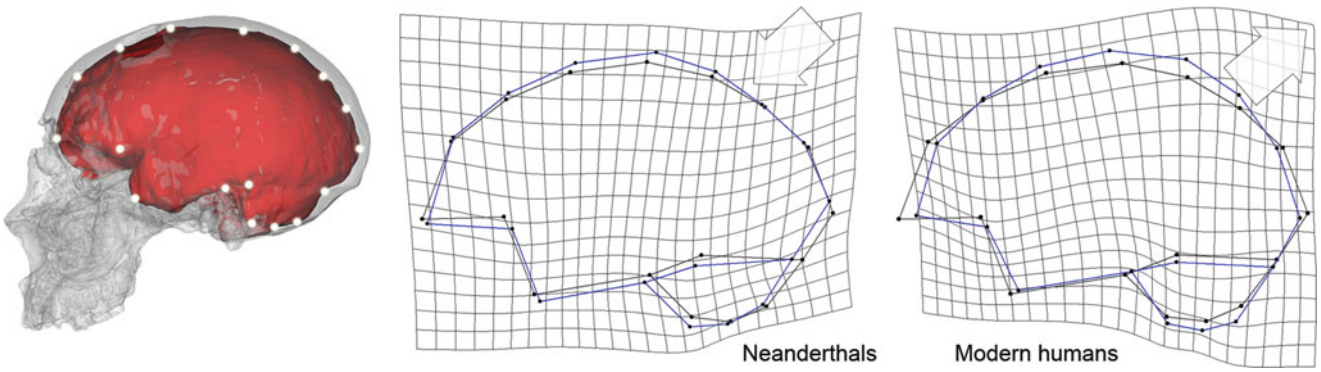

Fig. 13.2 When compared with archaic human species, Neanderthals show a relative reduction of the parietal profile, while modern humans display a geometrical dilation of the same areas. The differences are shown here after Procrustes superimposition and thin-plate spline deformation grids (data after Bruner 2004)

humans (that is in the whole genus *Homo* excluding modern humans), it has been proposed that the parietal areas underwent a relative spatial reduction during encephalization (Bruner et al. 2003): while the brain got larger, the parietal antero-posterior length became relatively shorter, with the upper brain profile bending upward. A structural hypothesis was put forward, considering the principles of functional craniology and the tensions exerted by the connective elements (Bruner 2004). According to this perspective, the parietal spatial reduction could be the results of allometric constraints between the changes in brain volume (enlarging at the power of three) and the changes in the *falx cerebri* section (enlarging at the power of two). The tension exerted by the connective sheets can limit the volumetric expansion, by direct biomechanical influence or by shared morphogenetic processes. Because the *falx cerebri* extends along the midsagittal section, it generates a tension which is mainly oriented in the longitudinal direction, constraining the neurocranial growth and development along the antero-posterior axis. Taking into account the longitudinal tensional forces and the consequent limitations on the midsagittal plane, it is worth noting that the more a species is encephalized the more the brain mass is reallocated laterally. Within this antero-posterior spatial constraint, the frontal and occipital areas are relatively free to adjust their form and position because of their location at the extremes of the hemispheric axis, while the parietal areas are forced in between them, having less spatial capacity to account for such geometric limits and readjustments. Being associated with brain size, such a pattern is stronger in the most encephalized non-modern hominids, that is in Neanderthals (Fig. 13.2).

This character seems to be relevant when one also takes into account some correspondent neurocranial traits. If the endocranial geometry is characterized by this relative parietal reduction, at the same time, on the ectocranial counterpart, Neanderthals very frequently display supernumerary

Fig. 13.3 Neanderthals often display supernumerary ossicles at the parieto-occipital boundary, suggesting hypostosis and morphogenetic unbalance. Here Wormian bones are shown on the rear view of Saccopastore 1 (photo courtesy of G. Manzi; drawing after Manzi 2003)

ossicles along the parieto-occipital boundary (Fig. 13.3). Supernumerary ossicles (Wormian bones) are additional centers of ossification, epigenetic traits whose formation can have genetic, environmental, and biomechanical components (Hauser and De Stefano 1989). In particular, Wormian bones have been assumed to be *hypostotic traits*, namely traits associated with defects in the ossification processes. Sergio Sergi (1934, 1944, 1948), an Italian paleoanthropologist, very early noticed such hypostotic characters along the lambdoid suture in Neanderthals, suggesting *morphological instability* at the parieto-occipital areas in this taxon. More recently, Giorgio Manzi hypothesized that such hypostotic traits may be associated with *ontogenetic stress*,

that is a lack of balance in the vault morphogenesis (Manzi et al. 1996; Manzi 2003). According to the principles of functional craniology, a lack of balance may follow a scarce integration between growth and development: shape changes cannot keep up with size changes. The size changes can be too fast to let the bones fill the gaps at the sutures, or else shape changes cannot accomplish the requirements associated with the suture dynamics. In both cases, additional ossification centers are supposed to be the result of biomechanical consequences, by direct physical response or else by induction exerted by the uncovered meningeal tissues (Di Ieva et al. 2013). There are clinical and experimental data confirming that cranial deformations influence suture complexity and induce supernumerary ossicles, most of all on the rear vault, probably by altering the tensile forces of the morphogenetic processes (Anton et al. 1992; White 1996; O'Laughlin 2004). Despite the fact they may be associated with pathological and syndromic conditions, many epigenetic characters like the supernumerary ossicles are generally non-pathological or sub-pathological, without functional consequences. Nonetheless, even in this case, they reveal an underlying lack of synchronization between the changes of the soft and hard tissues during the ontogenetic processes. That is, even when they are not associated with direct biological impairments, they are indicators of a lack of equilibrium in the anatomical system.

Therefore, at the same time, Neanderthals display parietal relative shortening associated with their large brain size, and parieto-occipital hypostotic traits. Putting together all this evidence, it seems reasonable to speculate that Neanderthals may have reached some structural limits in their neurocranial organization. This is even more interesting when considering that the parietal and occipital bones are strongly integrated, and the flattening of one element involves the bulging of the other (Gunz and Harvati 2007). This further emphasizes the possible relationships between the allometric reduction of the parietal chord and the expression of parieto-occipital hypostotic traits, being the lambdoid suture the hinge of this structural integration. We may therefore wonder whether a morphogenetic model largely evolved and balanced for smaller cranial capacities may have reached some intrinsic geometric limits when stretched to the Neanderthals' brain size.

13.3 Indirect Models in Paleoneurology

Recently, a different approach in paleoneurology has been proposed, based on correlation analyses and comparative morphometrics. Eiluned Pearce and colleagues found a consistent correlation in primates between orbit metrics and the size of the visual cortex (Pearce et al. 2013). When adjusting for factors like body size or other scaling parameters, Neanderthals display a larger percentage of brain visual area if compared with modern humans. The evolutionary interpretation may be debated (the authors propose climate and geography as relevant factors), but the correlation opens to new and wide perspectives in the field. Strong correlations between neural and non-neural elements may supply a reliable way to investigate paleoneurological issues beyond the limits of the endocranial casts. The hypothesis of larger visual areas matches with the raw observation of large occipital lobes in Neanderthals. Most of all, in terms of spatial balance within the parieto-occipital system, it fits also with the hypothesis of a parietal relative reduction in extinct humans, or conversely with a parietal relative dilation in *Homo sapiens*. Pearce and colleagues also use such brain proportions to estimate the average social group size in extinct taxa, by means of the correlation between these two factors among primates. This approach requires (as always) some cautions. First, such quantitative models involve necessarily a large series of adjustments and estimations, often based on variables which are scarcely known in paleontology (like body size). This chain of mathematical passages may generate risks in terms of reliability of the numerical outputs. Second, as mentioned Neanderthals and modern human may suffer some relevant structural constraints between orbits and anterior cranial fossa, introducing departures from the patterns observed in other primates. Nonetheless, the proposal of an "indirect paleoneurology" is exciting, and the results on the Neanderthals visual areas are not in contrast with other information we have on this group. It remains to be verified whether or not this cortical proportions are specific of this taxon, or else they represent a general archaic condition. Taking into account the available data on the paleoneurological variation in the human genus, I believe this second option is more likely.

13.4 Brain Metabolism and Heat Dissipation

Another trait that Neanderthals shared with small-brained hominids was a simple and scarcely reticulated middle meningeal artery, when compared with the complex and branching vascular system described in modern humans (Grimaud-Hervé 1997; Bruner et al. 2005). The meningeal vascular system can be investigated in fossils because the middle meningeal artery and the venous sinuses running into the dura mater leave imprints on the endocranial surface (Falk 1993). Although the course of these vessels can be altered by cranial deformations (O'Loughlin 1996), in normal variation the influence of the neurocranial shape on the general appearance of their imprints seems absent or negligible (Bruner et al. 2009). Hence, the traces left on the endocranial wall can be assumed to be a reliable proxy of the distribution of the vessels themselves. Although this is a

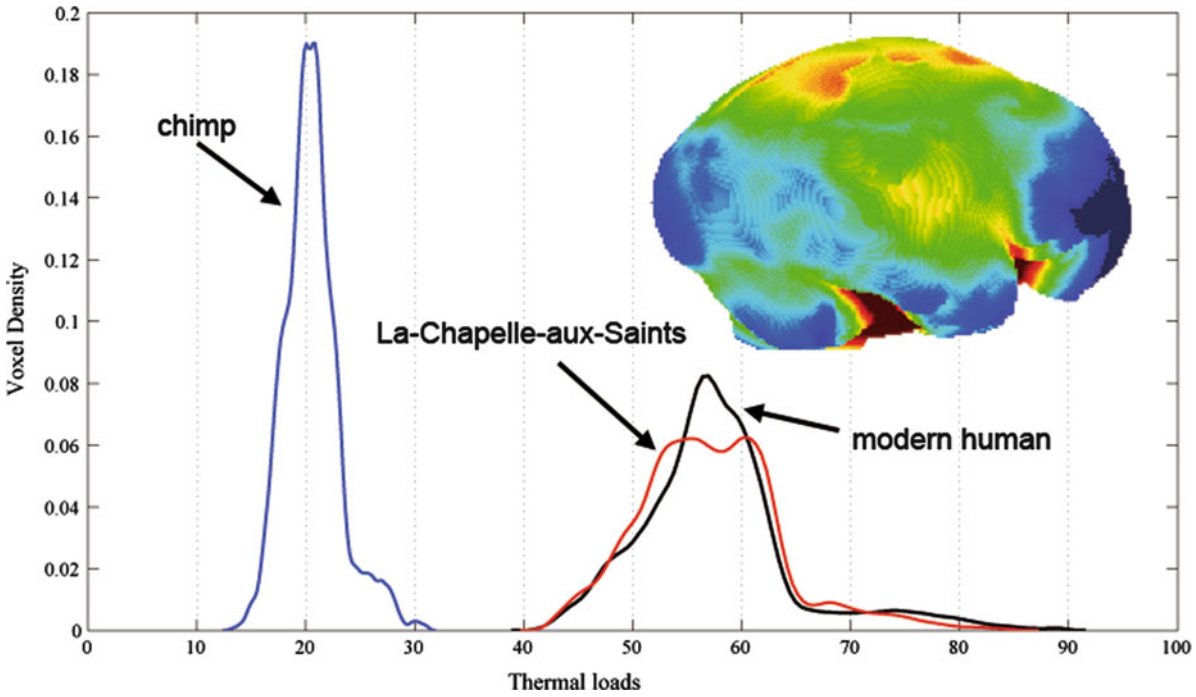

Fig. 13.4 The heat dissipation is influenced by the size and shape of an object. Thermal distribution can be therefore modelled on an endocast to display the patterns of heat distribution and to quantify the heat accumulation (Bruner et al. 2013). Here the thermal spectrum of one chimpanzee, one Neanderthal (La Chapelle-aux-Saints), and one modern human are compared through normalized curves (density function). Neanderthals and modern humans show differently shaped curves (pattern of heat distribution) due to the different endocranial shape, but similar amounts of heat production because of the comparable brain size. The thermal map shows the heat distribution on the endocast of La Chapelle-aux-Saints (*blue*: cooler areas; *red*: warmer areas)

relevant topic both in paleoanthropology and biomedicine, the morphogenetic factors, intra and inter-group variation, and functions of these vessels are still largely unknown (Bruner and Sherkat 2008). The middle meningeal artery in modern adult individuals at rest can present a modest or even absent blood flow, suggesting that its function may be mainly limited to younger ages (early ontogenetic stages), to exercise or "emergency" situations (hyperthermic conditions such as intense physical activity, fever, etc.), or to non-metabolic biomechanical factors (hydrostatic support or protection) (Bruner et al. 2011b).

One of the most interesting issues concerns its possible role in thermoregulation. Because of the cold climate associated with Neanderthal presence in Europe, thermoregulation and metabolic variables have often been addressed to interpret the Neanderthals' anatomical and behavioral characters (Churchill 1998, 2006).

The energetic management of the brain is characterized by physiological processes (Karbowski 2009), anatomical components (Zenker and Kubik 1996; Zhu et al. 2006), and evolutionary factors (Leonard et al. 2007). Despite the large energy expenditure of the human brain and its sensitivity to heat stress, there is still no agreement on whether or not the human brain needs some specific cooling system (see Brengelmann 1993; Cabanac 1993; Rango et al. 2012). Once more, these issues are relevant in both evolutionary and clinical contexts (Bertolizio et al. 2011). The venous channels may have had also some role during hominid evolution in this sense, and their variations are associated with relative changes of brain size (Falk 1990). Although there are important difficulties in analyzing the thermal processes in living humans, heat distribution can be modeled according to brain morphology, heat production and dissipation, and physical properties associated with physiological functions (Van Leeuwen et al. 2000; Sukstanskii and Yablonskiy 2006; Bruner et al. 2012).

Because of the large cranial capacity but different endocranial shape, Neanderthals had a different endocranial heat dissipation pattern when compared with modern humans, but a comparable amount of heat production (Fig. 13.4). It remains to be evaluated whether or not the middle meningeal vessels are involved in brain thermoregulation. Nonetheless, the fact that modern humans have a patent increase in vascular complexity for this system suggests that similar changes may have also occurred in the other vascular districts. Actually, the vascular differences we can detect for the middle meningeal vessels may be just a part of a more generalized vascular increase in modern humans. Brain thermoregulation is mainly based on blood input and output managed through exchange among cerebral, meningeal,

diploic, and pericranial systems. Through the head vascular system, the brain is supposed to rely onto the whole body thermal adjustment to perform heat regulation. According to indirect paleontological evidence, we may then speculate that Neanderthals may have had a comparable heat production with modern humans, but a simpler vascular network, with limited capacity of thermal adjustments. It is hence tempting to hypothesize that a plesiomorph vascular system and a derived brain size may have therefore represented another limit for such a large thermal load.

13.5 A Neanderthal's Lineage

Despite the morphological homogeneity of this taxon when compared with other hominid species, and despite the abundance of the fossil record when compared with other fossil groups, we must take into consideration that "Neanderthals" may have had a remarkable and relevant variation, which we largely ignore. Although the linkage with the European species *Homo heidelbergensis* as ancestor seems reasonable, Neanderthals prospered for at least 130 thousand years throughout Europe and West Asia, in many different environments, undergoing local variations and possibly different genetic influences (Vandermeersch and Garralda 2011). It is for example worth noting that the Eastern specimens display a less bulging occipital bone and higher and more rounded vault, suggesting a tendency toward the opposite direction along the parieto-occipital integration pattern, when compared with their European counterpart. Adaptations and genetic drifts have probably both contributed to the Neanderthal phenotype (Weaver 2009). Whatever the processes involved the available information suggests that, compared to modern humans, Neanderthals had a very different cranial organization, which evolved according to different morphogenetic schemes. Neanderthals and modern humans represent the two hominid taxa with largest absolute cranial capacity and with the largest relative brain size. These two lineages are characterized by different ontogenetic and phylogenetic neurocranial organization (Ponce de León and Zollikofer 2001). The "Neanderthal model" could have been fixed after climatic bottlenecks associated with Oxygen Isotopic Stage 6 (Bruner and Manzi 2006) and involving distinct morphological changes (Rosas et al. 2006). Alternatively, it could have been the result of a more gradual change during Middle Pleistocene (Dean et al. 1998; Hublin 2009). In any case, differences and discontinuities in morphology, ecology, and biogeography are often regarded as enough to support a species-specific distinction between Neanderthals and modern humans (Tattersall 2007). Despite the fact the possibility of interbreeding is frequently used as a biological threshold for the identification of species, breeding potentiality does not necessarily impede the formation of independent and isolated lineages, which are the actual evolutionary units in terms of adaptations and biological models (Bruner 2013). In fact, Neanderthals and modern humans could have been interfertile and at the same time evolutionarily independent, taking into account the patterns of variation characterizing the genetic barriers in primates (Holliday 2006). Furthermore, we must recognize that the complicated biogeographic history associated with the origin of *Homo sapiens* may rely on a more intricate scenario, difficult to interpret through the limited information available from the fossil record. Specimens like those of Jebel Irhoud, probably belonging to the modern lineage but with a "Neanderthal-like" endocranial form, suggest that maybe the evolutionary origin of modern humans did not coincide with the origin of a modern human brain (Bruner and Pearson 2013).

Since the earliest studies on Neanderthals, their large cranial dimensions have been one of their most outstanding traits. Allometric variations may facilitate or constrain evolutionary changes, allowing adaptive changes along preferred directions by channeling the ontogenetic and phylogenetic pathways, but also forcing and confining the biological potential of a taxon according to a given set of structural and functional rules (Gould 1966; Shea 1992). Size and allometry are the main factors characterizing the actual limits of variation of a biological model (Simpson 1944; McGhee 2006). Because of the complex nature of the genotype-phenotype systems, environmental changes or contrasting selective forces can lead a species toward extremes of its functional or structural range. Once such limits have been reached, or the model undergoes a radical change altering its general biological plan, or it enters a blind evolutionary alley. The general morphology of the Neanderthal brain can be recognized since the earliest specimens, such as Saccopastore 1, dated around 120 ka (Bruner and Manzi 2008). The Neanderthal lineage probably underwent a further process of encephalization in the following period, reaching the largest cranial capacity values around 50 ka. Despite the many derived and relevant features (some of them shared with modern humans), they display many pleisiomorph characters, and generally the overall model of neurocranial growth and development is rather similar to the other non-modern species, just scaled at a larger size. This allometric model can be traced back at least to the earliest human taxa. Structural limits associated with the endocranial geometrical organization and the system of forces linking brain pressure and connective tensors may have induced constraints in the parieto-occipital area. Similarly, functional constraints may have been related to limits associated with the endocranial vascular network and increased brain heat storage. Independently on the relationships of such factors with cognitive functions, such constraints must be carefully

considered when providing hypotheses on the Neanderthal paleoneurology. Their contribution to the Neanderthals' extinction remains to be evaluated.

Acknowledgements I am grateful to Naomichi Ogihara for inviting me to join his team on Neanderthal brain evolution, and to Takeru Akazawa for coordinating this project. Thanks to Osamu Kondo, Hideki Amano, Yasushi Kobayashi, Hiroki Tanabe, and Daisuke Kubo, for their contribution and involvement. Thanks to José Manuel de la Cuétara for his collaboration on the study of the endocranial heat dissipation patterns and for his comments on this manuscript, to Giorgio Manzi for his help on the epigenetic traits, and to Shahram Sherkat and Simone Mantini for their participation in the study of the middle meningeal vessels. This paper is supported by the Proyecto Atapuerca (Spain) and by the Italian Institute of Anthropology (Italy).

References

Anton SC, Jaslow CR, Swartz SM (1992) Sutural complexity in artificially deformed human (*Homo sapiens*) crania. J Morphol 214:321–332

Bastir M, Rosas A (2005) Hierarchical nature of morphological integration and modularity in the human posterior face. Am J Phys Anthropol 128:26–34

Bastir M, Rosas A, Kuroe K (2004) Petrosal orientation and mandibular ramus breadth: evidence for an integrated petroso-mandibular developmental unit. Am J Phys Anthropol 123:340–350

Bastir M, Rosas A, O'Higgins P (2006) Craniofacial levels and the morphological maturation of the human skull. J Anat 209: 637–654

Bastir M, Rosas A, Lieberman DE, O'Higgins P (2008) Middle craneal fossa and the origin of modern humans. Anat Rec 291:130–140

Bastir M, Rosas A, Gunz P, Peña-Melian A, Manzi G, Harvati K, Kruszynski R, Stringer C, Hublin JJ (2011) Evolution of the base of the brain in highly encephalized human species. Nat Commun 2:588

Bertolizio G, Mason L, Bissonnette B (2011) Brain temperature: heat production, elimination and clinical relevance. Paediatr Anaesth 21:347–358

Bookstein FL, Gunz P, Mitteroecker P, Prossinger H, Schaefer K, Seidler H (2003) Cranial integration in *Homo*: singular warps analysis of the midsagittal plane in ontogeny and evolution. J Hum Evol 44:167–187

Brengelmann GL (1993) Specialized brain cooling in humans? FASEB J 7:1148–1153

Bruner E (2004) Geometric morphometrics and paleoneurology: brain shape evolution in the genus *Homo*. J Hum Evol 47:279–303

Bruner E (2008) Comparing endocranial form and shape differences in modern humans and Neandertal: a geometric approach. PaleoAnthropology 2008:93–106

Bruner E (2010) Morphological differences in the parietal lobes within the human genus: a neurofunctional perspective. Curr Anthropol 51:S77–S88

Bruner E (2013) The species concept as a cognitive tool for biological anthropology. Am J Primatol 75:10–15

Bruner E. Manzi G (2006) Saccopastore 1: the earliest Neanderthal? A new look at an old cranium. In: Harvati K, Harrison T (eds) Neanderthals revisited: new approaches and perspectives. Springer, The Netherlands, pp 23–36

Bruner E, Holloway R (2010) Bivariate approach to the widening of the frontal lobes in the genus *Homo*. J Hum Evol 58:138–146

Bruner E, Jacobs HIL (2013) Alzheimer's Disease: the downside of a highly evolved parietal lobe? J Alzheimer's Disease 35:227–240

Bruner E, Manzi G (2005) CT-based description and phyletic evaluation of the archaic human calvarium from Ceprano, Italy. Anat Rec 285A:643–658

Bruner E, Manzi G (2008) Paleoneurology of an early Neanderthal: endocranial size, shape, and features of Saccopastore 1. J Hum Evol 54:729–742

Bruner E, Pearson O (2013) Neurocranial evolution in modern humans: the case of Jebel Irhoud 1. Anthropol Sci 121:31–41

Bruner E, Ripani M (2008) A quantitative and descriptive approach to morphological variation of the endocranial base in modern humans. Am J Phys Anthropol 137:30–40

Bruner E, Sherkat S (2008) The middle meningeal artery: from clinics to fossils. Childs Nerv Syst 24:1289–1298

Bruner E, Manzi G, Arsuaga JL (2003) Encephalization and allometric trajectories in the genus *Homo*: evidence from the Neanderthal and modern lineages. Proc Natl Acad Sci U S A 100:15335–15340

Bruner E, Mantini S, Perna A, Maffei C, Manzi G (2005) Fractal dimension of the middle meningeal vessels: variation and evolution in *Homo erectus*, Neanderthals, and modern humans. Eur J Morphol 42:217–224

Bruner E, Manzi G, Holloway RL (2006) Krapina and Saccopastore: Endocranial morphology in the pre-Wurmian Europeans. Period Biolog 108:433–441

Bruner E, Mantini S, Ripani M (2009) Landmark-based analysis of the morphological relationship between endocranial shape and traces of the middle meningeal vessels. Anat Rec 292:518–527

Bruner E, de la Cuétara JM, Holloway R (2011a) A bivariate approach to the variation of the parietal curvature in the genus *Homo*. Anat Rec 294:1548–1556

Bruner E, Mantini S, Musso F, de la Cuétara JM, Ripani M, Sherkat S (2011b) The evolution of the meningeal vascular system in the human genus: from brain shape to thermoregulation. Am J Hum Biol 23:35–43

Bruner E, De la Cuétara M, Musso F (2012) Quantifying patterns of endocranial heat distribution: brain geometry and thermoregulation. Am J Hum Biol 24:753–762

Cabanac M (1993) Selective brain cooling in humans: 'fancy' or fact? FASEB J 7:1143–1146

Churchill SE (1998) Cold adaptation, heterochrony, and Neandertals. Evol Anthropol 7:46–60

Churchill SE (2006) Bioenergetic perspectives on Neanderthal thermoregulatory and activity budgets. In: Harvati K, Harrison T (eds) Neanderthals revisited: new approaches and perspectives. Springer, Dordrecht, pp 113–134

D'AW T (1942) On growth and form. Cambridge University Press, Cambridge

Dean D, Hublin JJ, Holloway R, Ziegler R (1998) On the phylogenetic position of the pre-Neandertal specimen from Reilingen, Germany. J Hum Evol 34:485–508

Di Ieva A, Bruner E, Davidson J, Pisano P, Haider T, Stone SS, Cusimano MD, Tschabitscher M, Grizzi F (2013) Cranial sutures: a multidisciplinary review. Childs Nerv Syst 29:893–905

Enlow DH (1990) Facial Growth. WB Saunders Company, Philadelphia

Falk D (1990) Brain evolution in *Homo*: the "radiator" theory. Behav Brain Sci 13:333–344

Falk D (1993) Meningeal arterial pattern in great apes: implication for hominoid vascular evolution. Am J Phys Anthropol 92:81–97

Gould SJ (1966) Allometry and size in ontogeny and phylogeny. Biol Rev 41:587–640

Grimaud-Hervé D (1997) L'évolution de l'encéphale chez l'*Homo erectus* et l'*Homo sapiens*. CNRS Eds, Paris

Gunz P, Harvati K (2007) The Neanderthal "chignon": variation, integration, and homology. J Hum Evol 52:262–274

Gunz P, Mitteroecker P, Neubauer S, Weber GW, Bookstein FL (2009) Principles for the virtual reconstruction of hominin crania. J Hum Evol 57:48–62

Gunz P, Neubauer S, Maureille B, Hublin JJ (2010) Brain development after birth differs between Neanderthals and modern humans. Curr Biol 20:R921–R922

Hauser G, De Stefano GF (1989) Epigenetic variants of the human skull. Schweizerbart, Stuttgart

Holliday TW (2006) Neanderthals and modern humans: an example of mammalian syngameon. In: Harvati K, Harrison T (eds) Neanderthals revisited: new approaches and perspectives. Springer, The Netherlands, pp 281–298

Holloway RL (1980) Indonesian "Solo" (Ngandong) endocranial reconstructions: some preliminary observations with Neanderthal and *Homo erectus* groups. Am J Phys Anthropol 53:285–295

Holloway RL (1981) Volumetric and asimmetry determinations on recent hominid endocasts: Spy I and Spy II, Djebel Ihroud I, and the Sale´ *Homo erectus* specimen. With some notes on Neandertal brain size. Am J Phys Anthropol 55:385–393

Holloway RL, Broadfiled DC, Yuan MS (2004) The human fossil record, vol 3: brain endocast. Wiley, Hoboken

Hublin JJ (2009) The origin of Neandertals. Proc Natl Acad Sci U S A 106:16022–16027

Karbowski J (2009) Thermodynamic constraints on neural dimensions, firing rates, brain temperature and size. J Comput Neurosci 27:415–436

Leonard WR, Snodgrass JJ, Robertson ML (2007) Effects of brain evolution on human nutrition and metabolism. Annu Rev Nutr 27:311–327

Lieberman DE, Ross C, Ravosa M (2000) The primate cranial base: ontogeny function and integration. Yearb Phys Anthropol 43:117–169

Lieberman DE, McBratney BM, Krovitz G (2002) The evolution and development of cranial form in *Homo sapiens*. Proc Natl Acad Sci U S A 99:1134–1139

Manzi G (2003) "Epigenetic" cranial traits, Neandertals and the origin of *Homo sapiens*. Riv Antropol 81:57–68

Manzi G, Vienna A, Hauser G (1996) Developmental stress and cranial hypostosis by epigenetic trait occurrence and distribution: an exploratory study on the Italian Neandertals. J Hum Evol 30:511–527

Masters MP (2012) Relative size of the eye and orbit: an evolutionary and craniofacial constraint model for examining the etiology and disparate incidence of juvenile-onset myopia in humans. Med Hypotheses 78:649–656

McCarthy RC (2001) Anthropoid cranial base architecture and scaling relationships. J Hum Evol 40:41–66

McGhee GR (2006) The geometry of evolution: adaptive landscapes and theoretical morphospaces. Cambridge University Press, New York

Moss ML, Young RW (1960) A functional approach to craniology. Am J Phys Anthropol 18:281–292

Neubauer S, Gunz P, Hublin JJ (2009) The pattern of endocranial ontogenetic shape changes in humans. J Anat 215:240–255

Neubauer S, Gunz P, Hublin JJ (2010) Endocranial shape changes during growth in chimpanzees and humans: a morphometric analysis of unique and shared aspects. J Hum Evol 59:555–566

O'Laughlin VD (2004) Effects of different kinds of cranial deformation on the incidence of Wormian bones. Am J Phys Anthropol 123:146–155

O'Loughlin VD (1996) Comparative endocranial vascular changes due to craniosynostosis and artificial cranial deformation. Am J Phys Anthropol 101:369–385

Pearce E, Stringer C, Dunbar RIM (2013) New insights into differences in brain organization between Neanderthals and anatomically modern humans. Proc R Soc B 280:20130168

Ponce de León MS, Zollikofer CPE (2001) Neanderthal cranial ontogeny and its implications for late hominid diversity. Nature 412:534–538

Rango M, Arighi A, Bresolin N (2012) Brain temperature: what do we know? Neuro Report 23:483–487

Richtsmeier JT, Aldridge K, de Leon VB, Panchal J, Kane AA, Marsh JL, Yan P, Cole TM (2006) Phenotypic integration of neurocranium and brain. J Exp Zool 306B:360–378

Rohlf FJ, Marcus LF (1993) A revolution in morphometrics. Trends Ecol Evol 8:129–132

Rosas A, Bastir M (2002) Thin-plate spline analysis of allometry and sexual dimorphism in the human craniofacial complex. Am J Phys Anthropol 117:236–245

Rosas A, Bastir M, Martínez-Maza C, García-Tabernero A, Lalueza-Fox C (2006) Inquires into Neandertal craniofacial development and evolution: "accretion" versus "organismic" models. In: Harvati K, Harrison T (eds) Neanderthals revisited: new approaches and perspectives. Springer, The Netherlands, pp 37–70

Sergi S (1934) Ossicini fontanellari della regione del lambda nel cranio di Saccopastore e nei crani neandertaliani. Riv Antropol 30:101–112

Sergi S (1944) Craniometria e craniografia del primo paleantropo di Saccopastore. Ricerche di Morfologia 20–21:733–791

Sergi S (1948) L'uomo di Saccopastore. Paleontographia Italica XLII:25–164

Shea BT (1992) Developmental perspective on size change and allometry in evolution. Evol Anthropol 1:125–134

Simpson GG (1944) Tempo and mode in evolution. Columbia University Press, New York

Slice DE (2004) Modern morphometrics in physical anthropology. Kluwer Academic/Plenum, New York

Spoor F, Jeffery N, Zonneveld F (2000) Using diagnostic radiology in human evolutionary studies. J Anat 197:61–76

Sukstanskii AL, Yablonskiy DA (2006) Theoretical model of temperature regulation in the brain during changes in functional activity. Proc Natl Acad Sci U S A 103:12144–12149

Tattersall I (2007) Neanderthals, *Homo sapiens*, and the question of species in paleoanthropology. J Anthropol Sci 85:139–146

Van Leeuwen GM, Hand JW, Lagendijk JW, Azzopardi DV, Edwards AD (2000) Numerical modeling of temperature distributions within the neonatal head. Pediatr Res 48:351–356

Vandermeersch B, Garralda MD (2011) Neanderthal geographical and chronological variation. In: Condemi S, Weniger GC (eds) Continuity and discontinuity in the peopling of Europe. Springer, Dordrecht, pp113–125

Weaver TD (2009) The meaning of the Neandertal skeletal morphology. Proc Natl Acad Sci U S A 106:16028–16033

Weber GW, Bookstein FL (2011) Virtual anthropology: a guide to a new interdisciplinary field. Springer, Wien

White CD (1996) Sutural effects of fronto-occipital cranial modification. Am J Phys Anthropol 100:397–410

Zenker W, Kubik S (1996) Brain cooling in humans – anatomical considerations. Anat Embryol 193:1–13

Zhu M, Ackerman JJH, Sukstanskii AL, Yablonskiy DA (2006) How the body controls brain temperature: the temperature shielding effect of cerebral blood flow. J Appl Physiol 101:1481–1488

Zollikofer CPE, Ponce de León MS (2005) Virtual reconstruction: a primer in computer-assisted paleontology and biomedicine. Wiley, New York

Cerebral Sulci and Gyri Observed on Macaque Endocasts

14

Yasushi Kobayashi, Toshiyasu Matsui, Yoshinori Haizuka, Naomichi Ogihara, Naoki Hirai, and George Matsumura

Abstract

In order to evaluate the extent of the subdivisions of Neanderthal brains, we explored methods to determine the extent of subdivisions of brains in extant primate species. In the present study, we analyzed skulls and brains of macaque monkeys (*Macaca fascicularis*). Under deep anesthesia, five aged monkeys were perfused transcardially with phosphate-buffered 10 % formalin. The heads were scanned using a Toshiba Asterion CT scanner, and the reconstructed skulls and endocasts were compared with the convolutional patterns of the brain. In contrast to adult humans, which barely exhibit impressions in the upper part of the calvaria, the endocasts of the monkey skulls showed marked impressions of the cerebral sulci and gyri through the entire surface. On the dorsolateral surface, we identified most of the major sulci including the principal, arcuate, central, intraparietal, lunate, lateral, and superior temporal sulci, as well as the gyri in-between. On the ventral surface, we identified the medial and lateral orbital sulci, and the anterior middle temporal sulcus. Some of the individual differences in sulcal patterns were also observed on the endocast surface. We can thus infer the extent of major subdivisions of the macaque cerebral cortex by creating endocasts.

Keywords

Cerebral cortex • Endocast • Gyrus • Primate • Sulcus

Y. Kobayashi (✉) • T. Matsui
Department of Anatomy and Neurobiology, National Defense Medical College, 3-2 Namiki, Tokorozawa, Saitama 359-8513, Japan
e-mail: yasushi@ndmc.ac.jp; matsuto@ndmc.ac.jp

Y. Haizuka • G. Matsumura
Department of Anatomy, Kyorin University School of Medicine, 6-20-2 Shinkawa, Mitaka-shi, Tokyo 181-8611, Japan
e-mail: haiduka@ks.kyorin-u.ac.jp; george@ks.kyorin-u.ac.jp

N. Ogihara
Department of Mechanical Engineering, Faculty of Science and Technology, Keio University, 3-14-1 Hiyoshi, Kohoku-ku, Yokohama, Kanagawa 223-8522, Japan
e-mail: ogihara@mech.keio.ac.jp

N. Hirai
Department of Integrative Physiology, Kyorin University School of Medicine, 6-20-2 Shinkawa, Mitaka-shi, Tokyo 181-8611, Japan
e-mail: hirain@ks.kyorin-u.ac.jp

14.1 Introduction

Understanding the brain structures and cognitive capabilities of fossil hominids is a major goal of anthropological research. Approaches to this issue based on skull morphology comprise the field of paleoneurology, which has been rapidly progressing by incorporating computed tomography and other imaging techniques (see detailed review by Bruner (2003)). However, characterizing the size of neural structures in fossil species is problematic, given that only skulls and other bone fragments are available for measurement. To address this problem, we investigated the characteristics of skulls that reliably indicate the borders of cortical areas. We evaluated the relationship between the skull and brain morphology in extant primate species. Understanding this relationship will

T. Akazawa et al. (eds.), *Dynamics of Learning in Neanderthals and Modern Humans Volume 2: Cognitive and Physical Perspectives*, Replacement of Neanderthals by Modern Humans Series, DOI 10.1007/978-4-431-54553-8_14, © Springer Japan 2014

allow us to estimate the location of cortical subdivisions in fossil hominids based on skull morphology.

A number of previous morphological studies on the skulls of fossil hominids showed some convolutional patterns on the inner surface of the skulls or on the endocasts (Holloway et al. 2004). In some cases, these patterns are too faint or too often interrupted by ridges caused by sutures and meningeal arteries to show any correspondence to cerebral sulci and gyri. However, in other cases, the convolutional patterns are so marked that the locations of cerebral sulci can be easily identified. For example, Dart demonstrated the locations of major cerebral sulci on the endocast of the Taung child (Dart 1925, 1940), and a recent study on *Australopithecus sediba* showed a more distinct convolutional pattern on the inner surface of the frontal bone (Carlson et al. 2011). However, even in such cases, there are sometimes discrepancies between interpretations by different researchers; for example, regarding the location of the lunate sulcus in the Taung child (Falk 1980; Holloway 1980; Falk 1983).

Le Gros Clark et al. (1936) examined the skulls and brains of chimpanzees, and reached the conclusion that very little information could be extracted in regard to sulcal pattern from the majority of the endocranial casts of their specimens. The same author, however, described marked convolutional patterns in lemuroid endocasts in another paper (Le Gros Clark 1945). Radinsky (1974) also analyzed a number of fossil and extant primate skulls and demonstrated distinct imprints possibly corresponding to cerebral sulci. We thus put forward a hypothesis that smaller primates with simpler sulcal patterns show clearer correspondence between the impressions on the endocasts and cerebral sulci and gyri. If this holds true, we will have a secure starting point for inference of sulcal patterns using endocasts. In the first of our series of studies, we used macaque monkeys to compare the morphological characteristics of the inner surface of the skull and the brain of the same animal.

14.2 Materials and Methods

We used five aged monkeys (*Macaca fascicularis*; See Table 14.1 for details) that had long been used for studies on the gastrointestinal tract and were scheduled to be euthanized. All the experimental procedures were approved by the animal ethics committee at Kyorin University School of Medicine. After being sedated by intramuscular injection of atropine (0.1 mg/kg body weight; BW), xylazine (3.0 mg/kg BW), and ketamine (13 mg/kg BW), the animals were deeply anesthetized by intraperitoneal injection of sodium pentobarbital (70 mg/kg BW), and were perfused transcardially with 2.5 % formalin in phosphate buffer (pH 7.4) for 2 min (200 mL/min), followed by 10 % formalin in the same buffer solution for 50 min (200 mL/min for the initial 10 min, followed by 100 mL/min for the remaining 40 min). The first 2 cervical vertebrae were laminectomized, and the spinal cords were cut at the C2-C3 junction. The heads were subsequently separated from the neck at approximately the same level and stored in phosphate-buffered 2.5 % formalin solution at room temperature. The heads were then scanned using an Asterion CT scanner (Toshiba; Tokyo, Japan) at the Laboratory of Evolutionary Biomechanics, Department of Mechanical Engineering, Keio University. We obtained full three-dimensional image stacks consisting of 253–281 contiguous, 0.5-mm-thick slices. The images consisted of a 512×512 pixel matrix, with a pixel size of 0.351×0.351 mm.

CT images were analyzed using either the Amira 5.4 software package (Visage Imaging; Berlin, Germany) on a Z620 workstation (Hewlett-Packard Japan; Tokyo, Japan) or the OsiriX image processing software (Pixmeo; Geneva, Switzerland) on a MacPro computer (Apple; Cupertino, CA, USA). To create virtual endocasts, we selected pixels inside the skull in each slice based on their density, reconstructed the surfaces of the endocasts, and measured parameters of the virtual endocasts in Amira 5.4.

The skulls and brains were next analyzed macroscopically at the National Defense Medical College. After removing the scalp, fascia, and temporalis muscles, we mounted the heads on a stereotaxic frame, and photographically recorded the surface of the calvaria. We then removed the calvaria and the dura mater, and recorded the surface of the brains. The brains were coronally cut at the level of the ear bars and at 24 mm or 30 mm anterior to it. The brain blocks were stored at −80 °C for further histological analysis.

14.3 Results

14.3.1 General Morphology of the Skulls

The body weights ranged from 3.0 kg in M17 to 7.3 kg in M18 (Table 14.1). Male monkeys weighed almost twice as much (mean = 6.27 kg) as did female monkeys (mean = 3.3 kg). Although surface-rendered reconstructions of the skulls showed clear sexual dimorphism, the cranial cavity showed very similar morphology between the sexes (Fig. 14.1). The average endocranial volume was 63.0 cm^3 in male monkeys and 61.9 cm^3 in female monkeys. The macroscopically observed shape and major endocranial parameters had hardly any differences between sexes (Table 14.1).

14.3.2 Correspondence of Impressions on the Endocasts to Cerebral Sulci

In contrast to adult human skulls, the virtual endocasts of the macaques showed clearly discernible convolutional patterns both on the dorsolateral and ventral surfaces.

Table 14.1 Body weight and endocranial parameters of the monkeys

Animal ID	M15	M16	M18	M17	M19
Sex	M	M	M	F	F
Body weight (kg)	5.5	6.0	7.3	3.0	3.6
Endocast volume (mL)	62.4	62.8	63.7	63.0	60.8
Maximum length (mm)	63.9	66.1	65.4	62.9	62.9
Maximum width (mm)	49.9	50.2	51.2	51.6	50.8
Frontal width (mm)	46.0	46.9	47.1	46.0	46.4
Basion–Bregma height (mm)	48.6	46.3	45.1	41.7	45.1
Vertex to lowest temporal depth (mm)	4.25	4.26	4.22	4.14	4.25

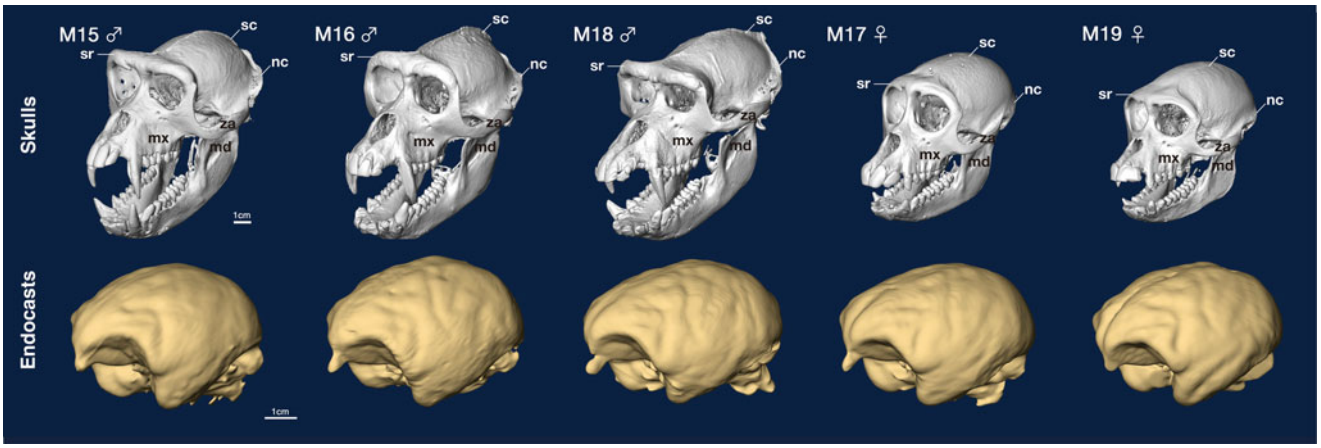

Fig. 14.1 Surface-rendered images of the skulls (*upper panels*) and virtual endocasts (*lower panels*). Sexual dimorphism was clearly observed in skull size and morphology. Male monkeys (M15, 16, 18) had more robust skulls with more marked supraorbital ridges (sr), sagittal (sc) and nuchal (nc) crests, and longer maxillae (mx), as well as wider zygomatic arches (za) and ascending rami of mandible (md) than females (M17, 19). In contrast to the skulls, virtual endocasts showed hardly any difference in size and morphology between males and females. The surface of the endocasts exhibited grooves that resembled cerebral sulci

Each endocast was compared with the brain of the same monkey. In the lateral views of the endocasts (Fig. 14.2), we observed several shallow grooves. Comparisons with the brains showed that they corresponded to the principal sulcus, the arcuate sulcus, the central sulcus, the intraparietal sulcus, the lunate sulcus, the lateral sulcus (Sylvian fissure), and the superior temporal sulcus.

The principal sulcus is regarded as the homologue of the inferior prefrontal sulcus in humans and comprises area 46 in its banks and the surrounding region. We traced the principal sulcus almost through its entire length on the endocasts, from 2 to 3 mm caudal to the frontal pole to about 2–3 mm rostral to the lower limb of the arcuate sulcus (Figs. 14.2 and 14.3).

The arcuate sulcus is divided into the upper and lower limbs. The upper limb is regarded as the homologue of the superior frontal sulcus, and the lower limb as the lower half of the precentral sulcus. The depression corresponding to the arcuate sulcus can also be easily observed on the endocast through the entire length of the sulcus in all the cases.

The central sulcus demarcates the frontal lobe and the parietal lobe and lies between the primary motor area rostrally and the primary somatosensory areas caudally. In contrast to humans, its medial end does not extend into the medial surface of the cortex, while its ventral end resembles the human central sulcus and does not join the lateral sulcus. We also observed these characteristics on the endocasts.

The macaques lack a postcentral sulcus. The only sulcus consistently observed on the parietal lobe is the intraparietal sulcus. Its most rostral part seemed to correspond to part of the human postcentral sulcus. The intraparietal sulcus runs between the superior and inferior parietal lobules, and the latter is deeply involved in spatial cognition and some aspects of language in humans. On the endocasts, the intraparietal sulcus in macaques was more clearly observed in the rostral part than the caudal part. The caudal half was also clearly identified in M17 and M18, but was obscured in the other monkeys.

The lunate sulcus is one of the most frequently referred sulcus in fossil hominids, since it demarcates the rostral border of the primary visual area in most of the primates. The lunate sulcus of macaques was also identified on the endocasts, but the depth of the depression was shallower than those of the sulci in the frontal lobe. Its dorsal and ventral ends were not clearly observed on the endocasts.

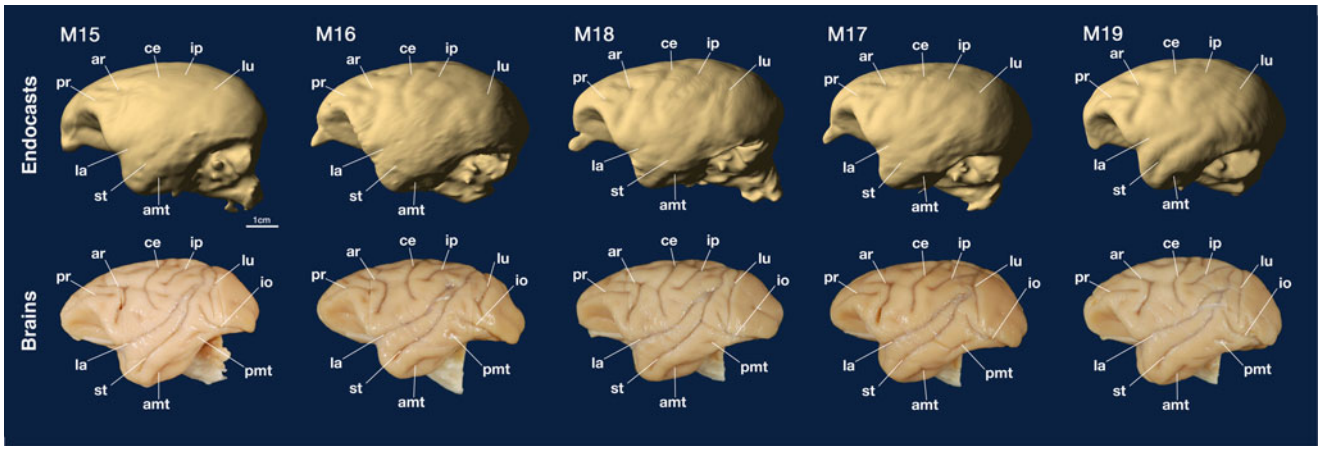

Fig. 14.2 Comparisons between endocasts and brains viewed from the *left side*. Abbreviations: *amt* anterior middle temporal sulcus, *ar* arcuate sulcus, *ce* central sulcus, *io,* inferior occipital sulcus, *ip* intraparietal sulcus, *la* lateral sulcus, *lu* lunate sulcus, *pmt* posterior middle temporal sulcus, *pr* principal sulcus, *st* superior temporal sulcus

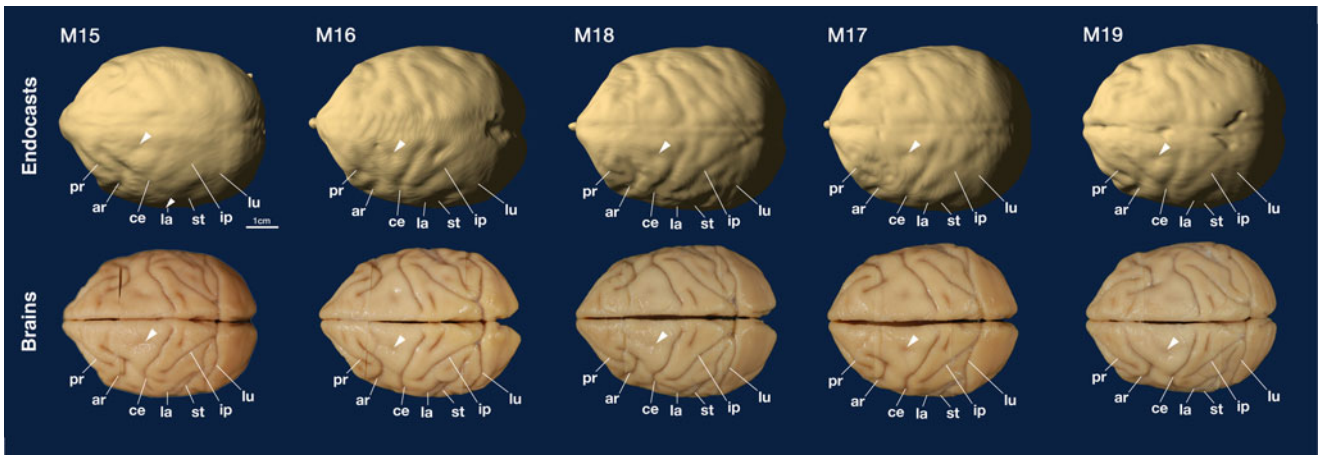

Fig. 14.3 Comparisons between endocasts and brains viewed from the *top*. *Arrowheads* indicate superior prefrontal dimples. Abbreviations: *ar* arcuate sulcus, *ce* central sulcus, *ip* intraparietal sulcus, *la* lateral sulcus, *lu* lunate sulcus, *pr* principal sulcus, *st* superior temporal sulcus

The lateral sulcus, also called Sylvian fissure, is one of the deepest and most marked sulci in monkey brains. The rostral end of the sulcus forms a deep notch between the frontal and temporal lobes, which faces the orbitosphenoidal ridge of the skull. Ventral to the lateral sulcus is the superior temporal sulcus. The depression corresponding to the lateral sulcus on the macaque endocasts was always marked in its rostral part, but the caudal part was less obvious, particularly in M15. In the other four monkeys, the depression was merged with that of the superior temporal sulcus as they approached caudally. The depression of the superior temporal sulcus was most clearly observed in the middle portion and less obvious in its rostral end, except that the rostral part was very distinct in M19.

Surprisingly, very shallow dents on the dorsal aspects, such as the superior precentral dimples, were identified on the endocasts, in addition to the typical sulci described above. They were consistently observed on the endocasts of all five monkeys.

On the ventral surface of the temporal lobe, we observed only a depression corresponding to the anterior middle temporal sulcus (Fig. 14.4). This is a short sulcus located in the rostral third of the temporal lobe. We observed the depression on the endocasts of all monkeys, with various degrees of clarity. Other sulci on the ventral surface of the temporal lobe were not detected on the endocasts. We did not observe a depression corresponding to the posterior middle temporal sulcus, even though it faced the internal surface of the cranial cavity. The other sulci were not identified, since they did not face the skull, but were instead facing the cerebellar tentorium or other parts of the brain.

The orbital surface of the macaque frontal lobe has two sulci, the medial and lateral orbital sulci, and the depressions

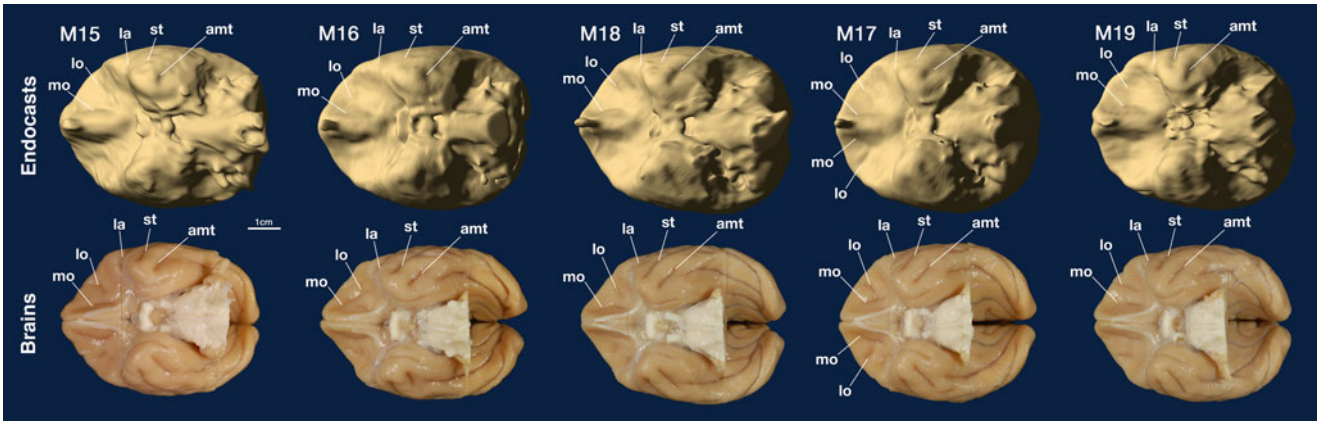

Fig. 14.4 Comparisons between endocasts and brains viewed from the *bottom*. Abbreviations: *amt* anterior middle temporal sulcus, *la* lateral sulcus, *lo* lateral orbital sulcus, *mo* medial orbital sulcus, *st* superior temporal sulcus

corresponding to them were consistently observed on the endocasts. The human orbitofrontal cortex has a larger number of (and more variable) orbital sulci and a straight sulcus, and it is the part of the cerebral cortex that leaves the most marked impressions on the skull.

14.3.3 Individual Difference in Sulcal Patterns Observed on the Endocasts

Besides identifying the depressions corresponding to the sulci, we also detected some individual differences in sulcal pattern on the macaque endocasts. From the medial end, the central sulcus follows a course rostroventrally in its dorsal portion, while in its ventral portion it curves more or less caudally as it approaches the lateral sulcus. The curve showed obvious individual differences in the macaques we analyzed: the ventral portion ran still slightly rostrally in M17, and slightly caudally in M18; whereas, M15, 16, and 19 exhibited a sharper bend caudally. These differences were well preserved on the endocasts.

The sulcal pattern of the medial and lateral orbital sulci also showed marked individual differences. The two sulci were almost parallel in M19, and gradually ran away from each other caudally in M16. In contrast, the two sulci in the other three monkeys approached each other caudally and merged to form a single sulcus. These differences were also observed on the endocasts.

14.4 Discussion

In the present study, we scanned monkey heads using a CT scanner, then reconstructed their skulls and created virtual endocasts. We compared the convolutional patterns observed on the endocasts with the sulcal patterns of the brains dissected out from the same monkeys. Although the skulls exhibited very marked sexual dimorphism, the endocasts showed only slight sexual differences in their volumes and hardly any differences in their surface morphology.

The convolutional patterns of the endocasts were so obvious that we were able to determine the locations of most of the major sulci that faced the inner surface of the skulls. We unambiguously identified the depressions corresponding to the following sulci:

Principal sulcus
Arcuate sulcus
Central sulcus
Intraparietal sulcus
Lunate sulcus
Lateral sulcus
Superior temporal sulcus
Anterior middle temporal sulcus
Medial and lateral orbital sulci
Superior precentral and postcentral dimples

We also observed individual differences in the course of the central sulcus, as well as that of the medial and lateral orbital sulci on the endocasts. The sulci observed on the dorsolateral surface of the endocasts were highly consistent with the findings reported by Radinsky (1974). In the panels showing an endocast of a rhesus monkey, he illustrated not only sulci, but also superior precentral and postcentral dimples, although he did not refer to them. The extent of each sulcus depicted on his illustrations agreed well with the present findings. According to Radinsky's observation, the presence of marked convolutional patterns on the endocasts is a common feature among New World and Old World monkeys, both fossil and extant. The present study clearly showed a close relationship between these patterns and the cerebral sulci and gyri.

There is a long history of discussion on the correspondence of endocranial impressions to cerebral sulci and gyri. Several of the earliest studies done on hominid skulls showed convolutional patterns on the inner surface of their skulls, or on the endocasts, and identified the corresponding cerebral sulci; for example, in "*Pithecanthropus erectus*" (Dubois 1937), La Chapelle aux Saints (Boule 1917), La Quina (Anthony 1913), and "Sinanthropus" (Shellshear and Smith 1934). In terms of the validity of those inferences, Symington (1916) criticized the simple assumption of the correspondence of endocranial morphology to cerebral convolutions and stated that "the simplicity or complexity of the cerebral fissures and convolutions cannot be determined with any degree of accuracy from endocranial casts." Le Gros Clark et al. (1936) generally supported Symington's view in his paper on the comparison of endocasts and brains of chimpanzees, and Ogawa et al. (1970) also stated that Symington's explanations were more plausible in their study on the Amud endocast. Smith-Agreda (1955) examined more than 300 modern human skulls and found that impressions corresponding to cerebral gyri were observed typically in the anterior and middle cranial fossa, and to a lesser extent on the inner surface of the lateral wall of the skull. Only a few abnormal cases showed convolutional patterns up to the vertex. These findings indicate that the inference of the cerebral gyri and sulci using the skull might be reliable in the basal portion of the skull, but is increasingly difficult towards the vertex.

On the other hand, Le Gros Clark (1945) reported that the convolutional pattern of the cerebral cortex could be estimated using endocasts in fossil lemuroids, which had much smaller skulls and brains than chimpanzees. Moreover, in hominids, an *Australopithecus*, Taung child, exhibited marked convolutional patterns that resembled cerebral sulci and gyri (Dart 1925, 1940). However, the identification of the locations of sulci and gyri was problematic, since it is impossible to evaluate the reliability of the inference because fossil skulls lack brains. Indeed, the location of the lunate sulcus of the Taung child's skull raised considerable controversy (Falk 1980; Holloway 1980; Falk 1983).

We, therefore, planned to analyze the relationship between the skull and the brain using extant primates, in order to determine the validity and limitations of the inference of the locations of the sulci and gyri using endocasts. In adult modern humans, we can only observe marked convolutional patterns on the orbital plate of the frontal bone and the orbitosphenoidal ridge. On the other parts of the skull, there is sometimes a hint of convolutional patterns, but they are usually faint and disrupted by thin ridges corresponding to sutures and branches of the middle meningeal artery. Le Gros Clarke et al. (1936) analyzed the skulls and the brains belonging to the same chimpanzees and concluded that, except for parts of some sulci, it is difficult to infer the location and the length of the sulci using endocasts. We thus started the analysis using the macaque monkey as a representative of species that have smaller bodies and skulls.

Our findings clearly show that we can infer the locations of most of the cerebral sulci facing the inner surface of the skull. Moreover, even shallow dimples and individual differences in sulcal pattern were identified in our study. At the same time, some of the sulci were partly obscured on the endocast. The reason is not yet clear, but one possible reason could be the thickness of the connective tissues, blood vessels, and cerebrospinal fluid between the brain and the skull as discussed by Symington (1916).

The posterior middle temporal sulcus was not identified on the endocasts, probably because it was located near the transition between the inner surface of the skull and the cerebellar tentorium. In this region, the thickness of the dura mater increased, and the inferior cerebral veins joined the transverse sinus. The same was true for the portion of the endocasts close to the caudal half of the superior sagittal sinus where the superior cerebral veins join the sinus. The intraparietal sulcus and the dorsal part of the lunate sulcus were indistinct, probably due to connective tissues, blood vessels, and cerebrospinal fluid.

The issue now is how we can apply the methods of inference to Neanderthals and modern humans, who have much larger skulls and brains. A key to the solution may lie in the infant skull. Balzeau et al. (2005) analyzed the skull of a child fossil of Mojokerto and identified several of the major cerebral sulci and gyri on its endocast. Developing brains may exert more influence on the adjacent parts of the skull. We are now planning to analyze other primate skulls to confirm our findings in macaques and human infant skulls to examine whether smaller but developing skulls and brains of infants have different characteristics from those of adults in terms of the correspondence between endocranial surface morphology and the sulcal pattern of the brain.

Acknowledgments We thank Dr. Fuhito Hojo at the Animal Research Facilities, Kyorin University School of Medicine, for his valuable advice regarding animal experimental procedures. This study was partly supported by a Grant-in-Aid for Scientific Research on Innovative Areas (Grant No. 23101509) from the Japanese Ministry of Education, Science, Culture, and Technology.

References

Anthony R (1913) L'encéphale de l'homme fossile de la Quina. Bulletins et Mémoires de la Société d'anthropologie de Paris 4:117–195

Balzeau A, Grimaud-Herve D, Jacob T (2005) Internal cranial features of the Mojokerto child fossil (East Java, Indonesia). J Hum Evol 48:535–553

Boule M (1917) Neopallial morphology of fossil men as studied from endocranial casts. J Anat 51:95–102

Bruner E (2003) Fossil traces of the human thought: paleoneurology and the evolution of the genus Homo. Rivista di Antropologia 81:29–56

Carlson KJ, Stout D, Jashashvili T, de Ruiter DJ, Tafforeau P, Carlson K, Berger LR (2011) The endocast of MH1, *Australopithecus sediba*. Science 333:1402–1407

Dart RA (1925) *Australopithecus africanus*: The Man-Ape of South Africa. Nature 115:195–199

Dart RA (1940) The status of *Australopithecus*. Am J Phys Anthropol 26:167–186

Dubois E (1937) On the fossil human skulls recently discovered in Java and *Pithecanthropus erectus*. Man 37:1–7

Falk D (1980) A reanalysis of the South African australopithecine natural endocasts. Am J Phys Anthropol 53:525–539

Falk D (1983) The Taung endocast: a reply to Holloway. Am J Phys Anthropol 60:479–489

Holloway RL (1980) Revisiting the South African Taung australopithecine endocast: the position of the lunate sulcus as determined by the stereoplotting technique. Am J Phys Anthropol 56:43–58

Holloway RL, Broadfield DC, Yuan MS (2004) The human fossil record. Schwartz JH, & Tattersall I (eds). Brain Endocasts - The Paleoneurological Evidence. Wiley, New York, Vol. 3,

Le Gros Clark WE (1945) Note on the palaeontology of the lemuroid brain. J Anat 79:123–126

Le Gros Clark WE, Cooper DM, Zuckerman S (1936) The endocranial cast of the chimpanzee. J R Anthropol Inst 66:249–268

Ogawa T, Kamiya T, Sakai S, Hosokawa H (1970) Some observation on the endocranial cast of the Amud man. In: Suzuki H, Takai F (eds) The Amud Man and his Cave Site. The University of Tokyo Press, Tokyo, pp 411–424

Radinsky L (1974) The fossil evidence of anthropoid brain evolution. Am J Phys Anthropol 41(1):15–27

Shellshear JL, Smith GE (1934) A Comparative Study of the Endocranial Cast of Sinanthropus. Philos Trans R Soc Lond B Biol Sci 223:469–487

Smith-Agreda V (1955) Über die Verteilung der Impressiones gyrorum an der Innenseite des Gehirnschädels des Menschen. Mit Benützung von Endokranialausgüssen. Deutsche Zeitschrift für Nervenheilkunde 173:37–68

Symington J (1916) Endocranial casts and brain form: a criticism of some recent speculations. J Anat Physiol 50:111–130

The Coronal Suture as an Indicator of the Caudal Border of the Macaque Monkey Prefrontal Cortex

15

Yasushi Kobayashi, Toshiyasu Matsui, Yoshinori Haizuka, Naomichi Ogihara, Naoki Hirai, and George Matsumura

Abstract

In order to estimate the extent of cortical subdivisions in the now extinct Neanderthals, we explored the relationship between skull and brain morphology in extant primate species, including humans. In this study, we used macaque monkeys (*Macaca fascicularis*) to determine the relationship between the location of sutures and the location of major sulci of the brain. Among the sulci examined, the inferior limb of the arcuate sulcus showed a close spatial relationship with the ventral portion of the coronal suture. The inferior limb of the arcuate sulcus is homologous to the ventral part of the precentral sulcus in modern humans, and it defines the caudal border of the prefrontal association cortex. These findings prompted us to examine whether a similar relationship could be observed in Neanderthals and modern humans, in order to obtain a more accurate inference of the extent of prefrontal cortical development in Neanderthals.

Keywords

Arcuate sulcus • Coronal suture • Precentral sulcus • Primate

15.1 Introduction

In the first of our series of reports (Kobayashi et al. 2014), we showed that the locations of major cerebral sulci could be determined based on virtual endocasts of macaque monkeys. This correspondence is useful, since it means that the extent of cortical subdivisions can be determined directly from the surface morphology of the endocasts; however, it is increasingly difficult to apply to larger primate species such as greater anthropoids or modern humans. As an alternative approach to the inference of the extent of cortical subdivisions, we investigated the correlation between the locations of cranial sutures and cerebral sulci.

Among the many cortical regions, the prefrontal cortex is of particular interest because it is the most rapidly developing cortical region during primate evolution, and it is associated with important higher-order cognitive functions. The ventral border between the prefrontal cortex and the temporal lobe is marked by the lateral sulcus (Sylvian fissure). The lateral sulcus is one of the deepest cerebral sulci, and its rostral end opens widely between the orbital aspect of the frontal lobe and

Y. Kobayashi (✉) • T. Matsui
Department of Anatomy and Neurobiology, National Defense Medical College, 3-2 Namiki, Tokorozawa, Saitama 359-8513, Japan
e-mail: yasushi@ndmc.ac.jp; matsuto@ndmc.ac.jp

Y. Haizuka • G. Matsumura
Department of Anatomy, Kyorin University School of Medicine, 6-20-2 Shinkawa, Mitaka-shi, Tokyo 181-8611, Japan
e-mail: haiduka@ks.kyorin-u.ac.jp; george@ks.kyorin-u.ac.jp

N. Ogihara
Department of Mechanical Engineering, Faculty of Science and Technology, Keio University, 3-14-1 Hiyoshi, Kohoku-ku, Yokohama, Kanagawa 223-8522, Japan
e-mail: ogihara@mech.keio.ac.jp

N. Hirai
Department of Integrative Physiology, Kyorin University School of Medicine, 6-20-2 Shinkawa, Mitaka-shi, Tokyo 181-8611, Japan
e-mail: hirain@ks.kyorin-u.ac.jp

T. Akazawa et al. (eds.), *Dynamics of Learning in Neanderthals and Modern Humans Volume 2: Cognitive and Physical Perspectives*, Replacement of Neanderthals by Modern Humans Series, DOI 10.1007/978-4-431-54553-8_15, © Springer Japan 2014

the dorsal surface of the temporal lobe. Corresponding to this opening, the inner surface of the skull forms a so-called "orbitosphenoidal crest." The caudal extension of the crest was designated as "crista Sylvii" by Schwalbe (Weidenreich 1947).

On the lateral surface of the cerebrum, the prefrontal cortex caudally borders the premotor cortex. The ventral half of this border approximately corresponds to the ventral portion of the precentral sulcus. However, no cranial landmark has been established as the caudal border of the prefrontal cortex. Concerning the caudal border of the frontal lobe, several reports described a ridge corresponding to the central sulcus in some fossil hominids (See Kochetkova 1978 for a review). However, this ridge is barely discernible in adult skulls of modern humans.

To estimate the caudal border of the prefrontal cortex, we surveyed the literature and found a possible correlation between a cranial suture and a cerebral sulcus. Flatau and Jacobsohn (1899) illustrated the morphology of the skull and the brain in several mammalian species. In their figures, the ventral portion of the coronal suture and the ventral portion of the precentral sulcus were closely located to each other in primate species, including macaques, chimpanzees, and humans. Even in lemurs, which lack a homologue of the precentral sulcus, the cytoarchitectonic border, identified in later studies (Brodmann 1909), lies close to the coronal suture.

In fossil hominids such as *Australopithecus sediba* (Carlson et al. 2011), the precentral sulcus is located close to the coronal suture; whereas, the inferior precentral sulcus in the Taung endocast was located far more rostrally (Falk 1980). However, to confirm that an indentation truly corresponds to a specific sulcus, further studies are necessary in extant species, in which we can analyze both skull and brain morphology. Thus, we evaluated the correlation between the locations of the coronal suture and the precentral sulcus using modern imaging techniques. As the first step of our analysis, we examined these spatial relationships in macaques.

15.2 Materials and Methods

We used five aged monkeys (*Macaca fascicularis;* See Table 15.1 for details) that had long been used for studies on the gastrointestinal tract and were scheduled to be euthanized. All the experimental procedures were approved by the animal ethics committee at Kyorin University School of Medicine. After being sedated by intramuscular injection of atropine (0.1 mg/kg body weight; BW), xylazine (3.0 mg/kg BW), and ketamine (13 mg/kg BW), the animals were deeply anesthetized by intraperitoneal injection of sodium pentobarbital (70 mg/kg BW), and were perfused transcardially with 2.5 % formalin in phosphate buffer (pH 7.4) for 2 min (200 mL/min), followed by 10 % formalin in the same buffer solution for 50 min (200 mL/min for the initial 10 min, followed by 100 mL/min for the remaining 40 min).

Table 15.1 Monkeys used in this study

Animal ID	Sex	Body weight (kg)
M15	M	5.5
M16	M	6.0
M17	F	3.0
M18	M	7.3
M19	F	3.6

The first 2 cervical vertebrae were laminectomized, and the spinal cords were cut at the C2-C3 junction. The heads were subsequently separated from the neck at approximately the same level and stored in phosphate-buffered 2.5 % formalin solution at room temperature. The heads were then scanned using an Asterion CT scanner (Toshiba; Tokyo, Japan) at the Laboratory of Evolutionary Biomechanics, Department of Mechanical Engineering, Keio University. We obtained full three-dimensional image stacks consisting of 253–281 contiguous, 0.5-mm-thick slices. The images consisted of a 512×512 pixel matrix, with a pixel size of 0.351×0.351 mm. CT images were analyzed using either the Amira 5.4 software package (Visage Imaging; Berlin, Germany) on a Z620 workstation (Hewlett-Packard Japan; Tokyo, Japan) or the OsiriX image processing software (Pixmeo; Geneva, Switzerland) on a MacPro computer (Apple; Cupertino, CA, USA).

The skulls and brains were next analyzed macroscopically and histologically at the National Defense Medical College. After removing the scalp, fascia, and temporalis muscles, we mounted the heads on a stereotaxic frame, and photographically recorded the surface of the calvaria. We then removed the calvaria and the dura mater, and recorded the surface of the brains. The brains were coronally cut at the level of the ear bars and at 24 or 30 mm anterior to it. The brain blocks were stored at −80 °C for further histological analysis.

The location of the arcuate sulcus and the coronal sutures were quantitatively analyzed using CT images of the skull and macroscopic photographs of the brain. The lateral view of each skull was created by volume rendering of the bones. The locations of the coronal suture were determined either using CT data (Fig. 15.1) or macroscopic photographs, and were marked on the lateral view. The macroscopic photographs of the brains were superimposed on the lateral view of the skulls after adjusting the magnification of the brain images to fit in the cranial cavity of CT images (Fig. 15.2).

For the quantitative analysis of the location of the suture and the sulcus, we drew a line connecting the frontal and occipital poles (F-O line), and a line that was parallel to the F-O line and passed through the vertex of the brain. The space between the 2 lines was divided by 9 lines with equal intervals. Using these 11 lines, we determined the relative dorsoventral levels: from DV0 on the F-O line to DV10 on the line through the vertex. In this analysis, we call the direction of these lines horizontal.

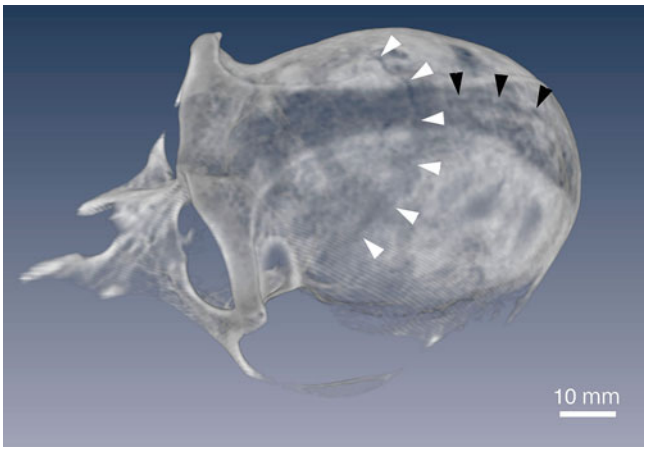

Fig. 15.1 Volume-rendered image of the calvaria of Monkey 17. The coronal suture was identified as a curved line of low density between the frontal and parietal bones (*white arrowheads*). The sagittal suture (*black arrowheads*) was observed in the midline posterior to the coronal suture

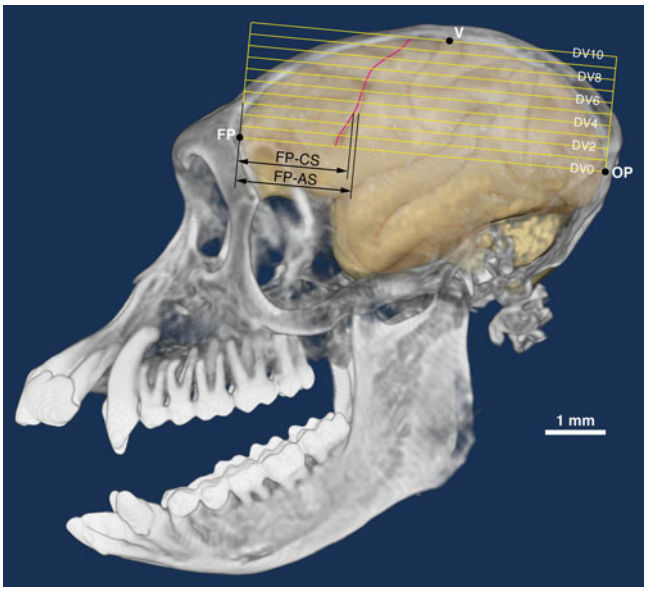

Fig. 15.2 Lateral view of a photographic image of the brain superimposed on the volume-rendered image of the skull of Monkey 19. The horizontal line (F–O line) was defined as the line connecting the frontal and occipital poles (FP, OP). For analysis of the location of the coronal suture and the arcuate sulcus, the horizontal distances from the frontal pole were measured at 11 dorsoventral levels between the vertex of the brain and the F–O line. FP–CS shows the distance of the coronal suture from the frontal pole, while FP–AS shows that of the arcuate sulcus

We recorded intersections of the coronal suture and the arcuate sulcus with these horizontal lines and measured their horizontal distance from the frontal pole at each DV level.

To normalize the differences in absolute size of the skulls and brains, we also calculated the distances in proportion to the distance of the frontal and occipital poles. Statistical analysis was performed using JMP software (SAS Institute Inc.; Cary, NC, USA).

Table 15.2 Horizontal distance (in millimeters) of the coronal suture and the arcuate sulcus from the frontal pole

	Coronal suture		Arcuate sulcus		AS-CS	
	Mean	SD	Mean	SD	Mean	SD
DV10	29.0	2.4				
DV 9	26.2	2.9				
DV 8	24.1	2.7				
DV 7	22.2	2.6				
DV 6	21.1	2.6				
DV 5	20.3	2.5	18.6	1.4	−1.7	1.5
DV 4	19.6	2.3	19.1	1.7	−0.5	0.9
DV 3	18.8	2.4	18.8	1.9	0.0	0.7
DV 2	18.1	2.6	18.1	2.0	0.0	1.1
DV 1	17.7	3.0	17.1	2.0	−0.5	1.5
DV 0	17.4	3.5	16.5	1.9	−0.9	2.0

AS–CS represents the distance between the coronal suture and the arcuate sulcus. Positive numerals indicate that the sulcus was located posterior to the suture. Average fronto-occipital distance was 62.5 mm

15.3 Results

We observed the coronal, sagittal, lambdoid, and squamous sutures on the macaque calvaria. The sagittal suture was located in the midline between the right and left parietal bones immediately on top of the superior sagittal sinus and the cerebral longitudinal fissure. The lambdoid suture was located on top of the occipital cortex but its location did not correspond to any particular sulcus. The squamous suture was located lateral to the rostral portion of the temporal lobe. Its course did not match any sulci, although it crossed the rostral part of the superior temporal sulcus.

In contrast to the above-mentioned sulci, the ventral portion of the coronal suture followed a course very close to the inferior limb of the arcuate sulcus. For quantitative analysis, the coronal sutures were identified in volume-rendered images of the skull (Fig. 15.1). The sutures were not always obvious in their entire length, but were partly obscured due to complete fusion of the frontal and parietal bones with ossification. We also examined the skulls and their photographic images and confirmed the location of the coronal suture. In three-dimensional reconstruction, we then placed markers on the suture where it was clearly visible, and connected the markers using a smoothly curved line (Fig. 15.2).

First, we compared the horizontal distances of the coronal suture from the frontal pole at DV0-5 between left and right sides. Since a paired t-test (n = 30) did not show a significant difference (P = 0.17), we analyzed the locations on both sides together, and the results were illustrated so that all data were projected onto the left side.

Table 15.2 shows the mean distances and their standard deviations in millimeters (n = 10). The arcuate sulcus crossed the horizontal lines at DV0 through DV5. Only in Monkey 19, the superior limb of the arcuate sulcus crossed also at

Table 15.3 Horizontal distance (as a percentage of the fronto-occipital distance) of the coronal suture and the arcuate sulcus from the frontal pole

	Coronal suture		Arcuate sulcus		AS-CS	
	Mean	SD	Mean	SD	Mean	SD
DV10	46.3	2.6				
DV 9	41.9	3.2				
DV 8	38.4	3.0				
DV 7	35.4	2.8				
DV 6	33.8	3.0				
DV 5	32.5	3.0	29.8	1.8	−2.7	2.2
DV 4	31.3	2.8	30.5	2.2	−0.8	1.3
DV 3	30.1	3.0	30.1	2.4	0.0	1.1
DV 2	29.0	3.3	29.0	2.6	0.0	1.7
DV 1	28.2	3.8	27.4	2.5	−0.8	2.3
DV 0	27.7	4.6	26.4	2.3	−1.4	3.0

AS–CS represents the distance between the coronal suture and the arcuate sulcus. Positive numerals indicate that the sulcus was located posterior to the suture

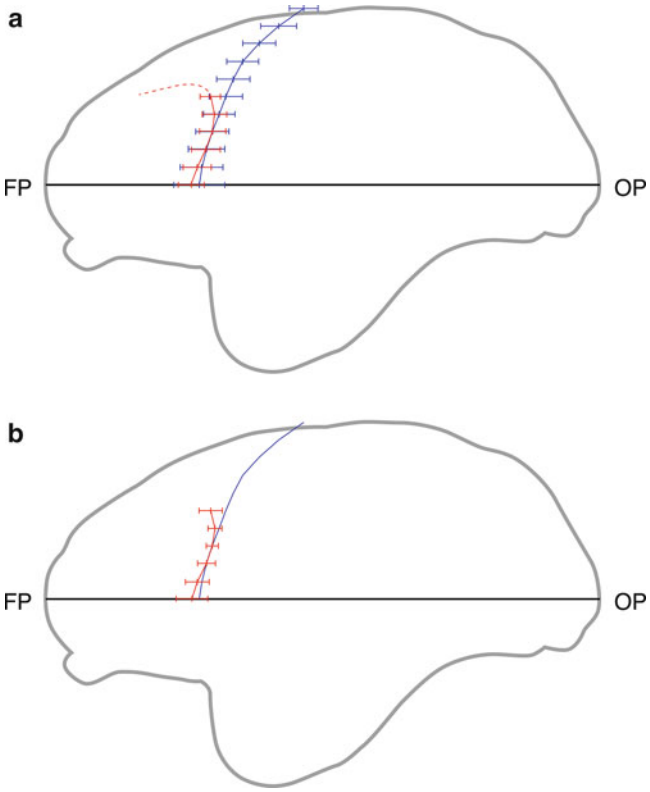

Fig. 15.3 Average location of the coronal suture and the arcuate sulcus. The data are shown on the contour of the brain of Monkey 19 (*gray line*). In Panel A, the coronal suture (*blue curved line*) and the inferior limb of the arcuate sulcus (*red curved line*) were shown based on the average horizontal distance from the frontal pole. *Horizontal bars* indicate the standard deviation. In Panel B, the inferior limb of the arcuate sulcus is illustrated based on the horizontal distance from the coronal suture. Once the location of the coronal suture is determined in each skull, the inferior limb of the arcuate sulcus is expected to be located on the red curved line. *Horizontal bars* indicate the 95 % confidence intervals

DV6, but this was not included in the statistics. The coronal suture and arcuate sulcus were located at fairly constant distances from the frontal pole at each dorsoventral level. The standard deviations were typically less than 2 mm both rostrally and caudally. Since the size of the skulls and brains varied considerably, depending on body size, part of the deviations arose due to differences in the absolute size of the skulls. To normalize these differences, we also calculated the distances proportional to the F-O distance (Table 15.3). The table shows that the ventral portion of the inferior limb of the arcuate sulcus ran almost parallel to the coronal suture. Figure 15.3a illustrates the average location of the coronal suture and the inferior limb of the arcuate sulcus projected onto the left hemisphere of M19.

When we calculated the distance between the coronal suture and the arcuate sulcus, the data were even more consistent. The average distance was about 1 % of the F-O distance. The 95 % confidence interval was less than 2 % of F-O distance on both sides of the average at levels between DV1 and DV5 (Table 15.4). Consequently, once the location of the coronal suture was determined in a given skull, we could infer the average location of the inferior limb of the arcuate sulcus with 95 % certainty within this range (Fig. 15.3b).

Table 15.4 Confidence interval (95 %) of the average location of the arcuate sulcus (as a percentage of the fronto-occipital distance)

	95 % Confidence limits of the mean	
	Lower	Upper
DV 5	28.18	31.34
DV 4	29.55	31.45
DV 3	29.27	30.91
DV 2	27.75	30.19
DV 1	25.76	28.99
DV 0	24.20	28.51

15.4 Discussion

In the present study, we have quantitatively analyzed the locations of the coronal suture and the arcuate sulcus of macaque monkeys for the first time using modern imaging techniques. The results showed a reliable spatial relationship between the coronal suture and the inferior limb of the arcuate sulcus. The findings indicate that we can determine the location of the arcuate sulcus (that is, the caudal border of the prefrontal association cortex) by analyzing skulls alone.

The expansion of the prefrontal cortex during primate evolution was first evaluated quantitatively by Brodmann (1912). He measured the surface areas of cortical regions and reported that the prefrontal cortex (his “Regio frontalis”) occupied only 2.2 % of the total cortical area in the rabbit,

3.4 % in the cat, and 6.9 % in the dog, but grew rapidly during primate evolution (8.9 % in lemur, 9.2 % in cebus, 11.3 % in macaque, 11.1 % in gibbon, 16.9 % in chimpanzee), and reached 29.0 % in the human. Although a recent volumetric study using MRI revealed fairly constant proportion of the frontal cortex (including precentral gyrus) among great apes and humans (Semendeferi et al. 2002), the proportion of the prefrontal cortex in humans is still larger than that of apes.

Endocasts of some hominids exhibit distinctly marked patterns of cerebral convolutions that allow several cerebral sulci and gyri to be distinguished (Carlson et al. 2011; Falk 1980). If the pattern would match the gyri and sulci of the cerebral cortex, the analysis of the extent of the prefrontal cortex would be straightforward. However, even in such cases with marked convolutional pattern on the endocasts, the identification of the sulci is problematic because of individual differences, poor preservation, and lack of any brain in fossil hominid species. Le Gros Clark compared the brains and endocasts of chimpanzees and showed that depressions on the endocasts did not always correspond to the location of the cerebral sulci (Le Gros Clark et al. 1936). In his specimens, some depressions on endocasts were interrupted, while others were connected to depressions that corresponded to different sulci. The depression corresponding to the precentral sulcus is often obscured by the coronal suture even in the species with marked convolutional pattern on the endocast. This occurs because the shallow groove corresponding to the precentral sulcus is often buried by a sharp ridge corresponding to the suture. Therefore, we need to accumulate quantitative data on the location of sutures and sulci in extant primate species, in order to statistically evaluate the data from fossil hominids.

Moreover, the convolutional pattern on the endocast is not apparent in adult modern humans. This is likely also true in adult Neanderthals, with the exception of the orbital plate of the frontal bone. The spatial correlation between the arcuate sulcus with the coronal suture, therefore, provides valuable information in this regard.

In macaques, the inferior limb of the arcuate sulcus represents only the ventral portion of the caudal border of the prefrontal cortex. Its dorsal portion needs to be determined using histological sections of the cortex. We are currently planning to analyze cytoarchitectonic areas of the macaque cerebral cortex, and evaluate the relationship between the location of the coronal suture and the dorsal portion of the caudal prefrontal border. We are also analyzing the relationship of the coronal suture and the precentral sulcus in modern humans. If a similar relationship is confirmed in modern humans and other primates, it will allow us to make even more accurate and informed estimates of the extent of prefrontal cortical development in Neanderthals.

Acknowledgments We thank Dr. Fuhito Hojo at the Animal Research Facilities, Kyorin University School of Medicine for his valuable advice regarding animal experimental procedures. This study was partly supported by a Grant-in-Aid for Scientific Research on Innovative Areas (Grant No. 23101509) from the Japanese Ministry of Education, Science, Culture, and Technology.

References

Brodmann K (1909) Vergleichende Lokalizationslehre der Grosshirnrinde in ihren Prinzipien dargestellt auf Grund des Zellenbaues. Barth, Leipzig

Brodmann K (1912) Neue Ergebnisse über die vergleichende histologische Lokalisation der Grosshirnrinde mit besonderer Berücksichtigung des Stirnhirns. Anat Anz 41:157–216

Carlson KJ, Stout D, Jashashvili T, de Ruiter DJ, Tafforeau P, Carlson K, Berger LR (2011) The endocast of MH1, *Australopithecus sediba*. Science 333(6048):1402–1407

Falk D (1980) A reanalysis of the South African australopithecine natural endocasts. Am J Phys Anthropol 53(4):525–539

Flatau E, Jacobsohn L (1899) Handbuch der Anatomie und vergleichenden Anatomie des Centralnervensystem der Säugetiere. 1. Makroskopischer Teil. Karger, Berlin

Kobayashi Y, Matsui T, Haizuka Y, Ogihara N, Hirai N, Matsumura G (2014) Cerebral sulci and gyri observed on macaque endocasts. In: Akazawa T, Ogihara N, Tanabe HC, Terashima H (eds) Dynamics of Learning in Neanderthals and Modern Humans Volume 2: Cognitive and Physical Perspectives 2:131–137, Springer, Tokyo

Kochetkova VI (1978) Paleoneurology. Wiley, New York

Le Gros Clark WE, Cooper DM, Zuckerman S (1936) The endocranial cast of the chimpanzee. J R Anthropol Inst 66:249–268

Semendeferi K, Lu A, Schenker N, Damasio H (2002) Humans and great apes share a large frontal cortex. Nat Neurosci 5(3):272–276

Weidenreich F (1947) Some particulars of skull and brain of early hominids and their bearing on the problem of the relationship between man and anthropoids. Am J Phys Anthropol 5(4):387–428

Application of Sliding Landmark Method for Morphological Analysis of Modern Japanese Neurocranial Shape

16

Naomichi Ogihara, Yusuke Morita, Hideki Amano, Osamu Kondo, Hiromasa Suzuki, and Masato Nakatsukasa

Abstract

We apply the sliding semi-landmark method for the analysis of morphological variability in the modern Japanese population. Specifically, we prepare two kinds of template landmark configurations that will be projected onto and slid along each of the samples. We then analyze the variability in the neurocranial shape in the modern Japanese population by means of a landmark-based geometric morphometric method. We also analyze the differences in the patterns of extracted morphological variances due to different landmark configurations. Our results demonstrate that the morphological variabilities extracted by the two different template configurations generally correspond to each other, and indicate that if a sufficient number of semi-landmarks are evenly distributed across the neurocranial surface, the global tendency of the morphological variability to be extracted may not be affected by the choice of template configurations. Furthermore, the most predominant shape variability found in the cranial vault in the modern Japanese population is the brachycephalic/dolichocephalic tendency. The present semi-landmark-based approach will serve as a basis for detailed quantification and comparisons of the human neurocranial shape.

Keywords

Craniometry • Geometric morphometrics • Semi-landmark • Skull

N. Ogihara (✉) • Y. Morita • H. Amano
Department of Mechanical Engineering, Faculty of Science and Technology, Keio University, 3-14-1 Hiyoshi, Kohoku-ku, Yokohama, Kanagawa 223-8522, Japan
e-mail: ogihara@mech.keio.ac.jp; ogilab_morita10@yahoo.co.jp; ogilab_amano11@yahoo.co.jp

O. Kondo
Department of Biological Sciences, Graduate School of Science, University of Tokyo, 7-3-1 Hongo, Bunkyo-ku, Tokyo 113-0033, Japan
e-mail: kondo-o@biol.s.u-tokyo.ac.jp

H. Suzuki
Research Center for Advanced Science and Technology, University of Tokyo, Komaba 4-6-1, Meguro-ku, Tokyo 153-8904, Japan
e-mail: suzuki@den.rcast.u-tokyo.ac.jp

M. Nakatsukasa
Laboratory of Physical Anthropology, Graduate School of Science, Kyoto University, Kitashirakawa-Oiwakecho, Sakyo, Kyoto 606-8502, Japan
e-mail: nakatsuk@anthro.zool.kyoto-u.ac.jp

16.1 Introduction

In recent years, three-dimensional (3D) geometric morphometrics have been extensively utilized for the analyses of morphological variability in the human crania. Geometric morphometrics is a statistical method to analyze shape variations based on biological landmark coordinates (Bookstein 1991; O'Higgins 2000; Adams et al. 2004; Slice 2005; Mitteroecker and Gunz 2009). Homologous landmarks were digitized on the surface of each specimen to describe the biological shape. The landmark coordinates were then normalized and registered using the centroid size and the Generalized Procrustes Analysis (superimposition of landmark coordinates based on a least squares method), respectively, and the shape variations among the specimens were quantified based on Procrustes residuals (deviation of landmark coordinates from the average landmark configuration of all the specimens).

T. Akazawa et al. (eds.), *Dynamics of Learning in Neanderthals and Modern Humans Volume 2: Cognitive and Physical Perspectives*, Replacement of Neanderthals by Modern Humans Series, DOI 10.1007/978-4-431-54553-8_16, © Springer Japan 2014

On the human cranial vault, however, only a few definable landmarks exist, and the application of such landmark-based morphological techniques is quite difficult.

Semi-landmarks are introduced to capture and analyze curves or surfaces that have few or no landmarks. Specifically, landmarks are placed by sliding a "template" landmark structure along the curves or surfaces so as to minimize a certain criterion function, such as bending energy (Bookstein 1997; Gunz et al. 2005; Perez et al. 2006). Because the semi-landmark method allows for quantification of the overall shape of the human cranial vaults, more research on cranial morphology now utilizes this new technique (e.g., Gunz et al. 2009; Bastir et al. 2011).

In the present study, we apply the sliding semi-landmark method for the analysis of morphological variability in the modern Japanese population. Specifically, we prepare two kinds of template landmark configurations that will be projected onto and slid along each of the samples. We then analyze the variability in the neurocranial shape in the modern Japanese population by means of the landmark-based geometric morphometric method. We also analyze the differences in the patterns of extracted morphological variances due to different landmark configurations.

16.2 Materials and Methods

16.2.1 Specimens

We used a total of 22 crania (9 female and 13 male crania) from the modern Japanese population housed at Kyoto University to investigate neurocranial shape variability (Makishima and Ogihara 2009; Ogihara et al. 2009). Each cranium was scanned using a helical computed tomography (CT) scanner (TSX-002A/4I; Toshiba Medical Systems, Japan) in the Laboratory of Physical Anthropology at Kyoto University. Tube voltage, current, and slice thickness were set at 120 kV, 100 mA, and 2.0 mm, respectively. Cross-sectional images were reconstructed at 0.5-mm intervals, with a pixel size of 0.5 mm. The images were then transferred to medical imaging software (Analyze 9.0; Mayo Clinic, USA), and the 3D surface of the cranium was generated as a triangular mesh model using the marching cube method. The mesh structure was then regenerated based on its curvature flow using reverse engineering software (RapidForm 2006; INUS Technology, Korea). The size of a triangular mesh is about 0.5 mm and the number of total mesh for one cranium is about two millions. The 3D coordinates of six midsagittal landmarks and the midpoints of five bilateral landmarks were extracted by pointing to their locations on the 3D surface model using a virtual probe incorporated in the software, and the medial sagittal plane was calculated based on a least squares method.

16.2.2 Landmarks

The anatomical landmarks on the surface of each cranium were digitized, as shown in Fig. 16.1 by pointing to their locations on the 3D surface model using a virtual probe incorporated in the software. Landmarks #1–#10 are conventional anatomical landmarks (Table 16.1). Landmarks #11–#13 and #14–#15 are equally spaced points along the superior nuchal curve between the inion (#2) and the intersection of the superior nuchal line and occipitomastoid suture (#10), and the temporal curve between the frontomalare temporale (#5) and stephanion (#6), respectively. Each curve was fitted by a seventh-order Bezier curve, and equally spaced points (#11–13 and #14–15) were calculated as non-sliding landmarks along curves (Morita et al. 2013). Therefore, a total of 27 landmarks were obtained as conventional non-sliding landmarks for all 22 crania.

In the present study, two kinds of sliding semi-landmark configurations were constructed for comparisons of the neurocranial shape. Sliding semi-landmarks are landmarks on a smooth surface calculated by sliding a "template" landmark structure along a target surface so as to minimize a certain criterion function such as bending energy or Procrustes distance between the template and the target. The sliding semi-landmark coordinates were obtained using the following two methods. In the first method, the semi-landmark coordinates were calculated based on the shortest paths connecting pairs of anatomical landmarks (Morita et al. 2013). The above 27 non-sliding landmarks as well as 14 equally spaced points along the midsagittal curve [between the nasion (#1) and inion (#2)] were used to calculate the shortest paths as shown in Fig. 16.2a. The equally spaced points along the paths were then computed and designated as sliding semi-landmarks. Including the 14 midsagittal equally spaced points, 83 sliding (semi-) landmarks were obtained, as shown in Fig. 16.2a. See Morita et al. (2013) for more details about the shortest path calculation. In the second method, 102 sliding landmarks are obtained in a lattice pattern, as shown in Fig. 16.2b. Specifically, planar grid patterns of 22.5 mm from the origin (centroid) that are parallel to the x-y, y-z, x-z planes were prepared. The intersection points of the planes and the neurocranial surface were defined as sliding landmarks. Therefore, a total of 110 and 129 landmarks were obtained for the shortest path (SP) template and the lattice (L) template, respectively.

16.2.3 Sliding Semi-Landmark Method

The defined template configurations were then used to determine the semi-landmarks on the other crania. Specifically, the coordinates of the 27 non-sliding landmarks were used to define a thin-plate spline function

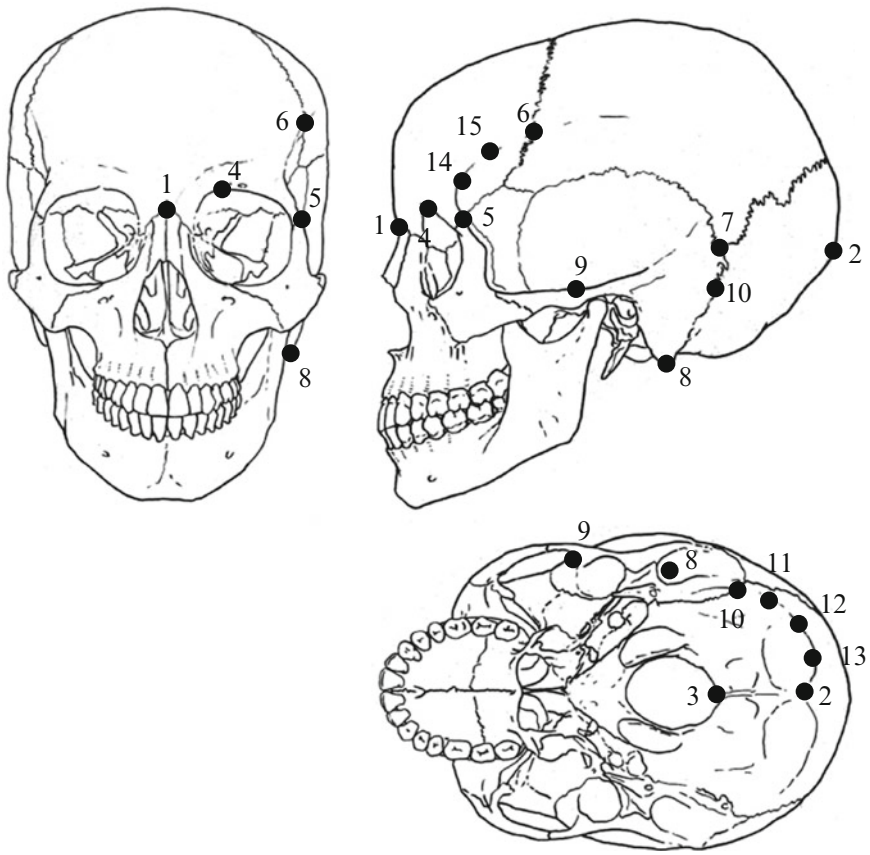

Fig. 16.1 The non-sliding landmarks used in the present study

Table 16.1 Descriptions of the landmarks used in the present study

Number	Landmark name	Type
1	Nasion	m
2	Inion	m
3	Opisthion	m
4	Uppermost of the orbital margin	b
5	Front om alare temporale	b
6	Stephanion	b
7	Asterion	b
8	Mastoidale	b
9	Posterior end of the margin of temporal fossa	b
10	Intersection of nuchal line and occipitomastoid suture	b
11–13	Equally spaced points along nuchal line	b
14–15	Equally spaced points along temporal line	b

m = midsagittal landmark, b = bilateral landmark

describing a mapping from each of the template configurations to a target specimen. The sliding landmarks from the templates were first deformed to the target specimen using this mapping function (Fig. 16.3a). The sliding landmarks were then projected onto (Fig. 16.3b) and slid along (Fig. 16.3c) the neurocranial surface of the target specimen so as to minimize the bending energy of the thin-plate spline method. This process is iterated until the solution converges. As each of the landmarks slide, they move along a plane tangential to the surface; therefore, an offset exists from the surface as each landmark slides and thus it is projected back to the surface after each iteration. See Gunz et al. (2005) for more details on the calculation method.

In the present study, Templand in the EVAN Toolbox (www.evan-society.org) is used to calculate the positions of the sliding landmarks corresponding to the two template configurations.

16.2.4 Morphological Analysis

The coordinates of the non-sliding and sliding landmarks were then analyzed using Morphologika geometric morphometric software, version 2.3.1 (O'Higgins and Jones 2006). First, landmark coordinates were symmetrized, as shape variance due to asymmetry was not considered in the present study (Zollikofer and Ponce de León 2002). Then, for size-independent shape analysis, the symmetrized landmark coordinates were normalized by centroid size and registered using the Generalized Procrustes Analysis. Principal components (PCs) of shape variations among the specimens were then calculated using the variance-covariance matrix of the Procrustes residuals of all crania. See O'Higgins and Jones (1998) and O'Higgins (2000) for more details on the calculation method.

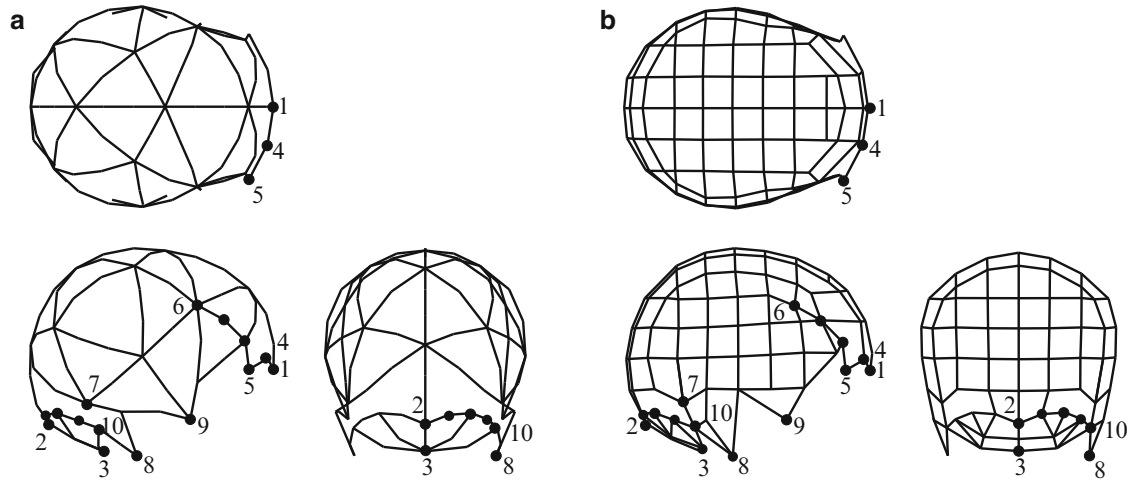

Fig. 16.2 Template configurations. (**a**) Shortest path template configuration; (**b**) Lattice template configuration. *Labels* indicate anatomical landmarks in Table 16.1. *Black dots* indicate the non-sliding landmarks

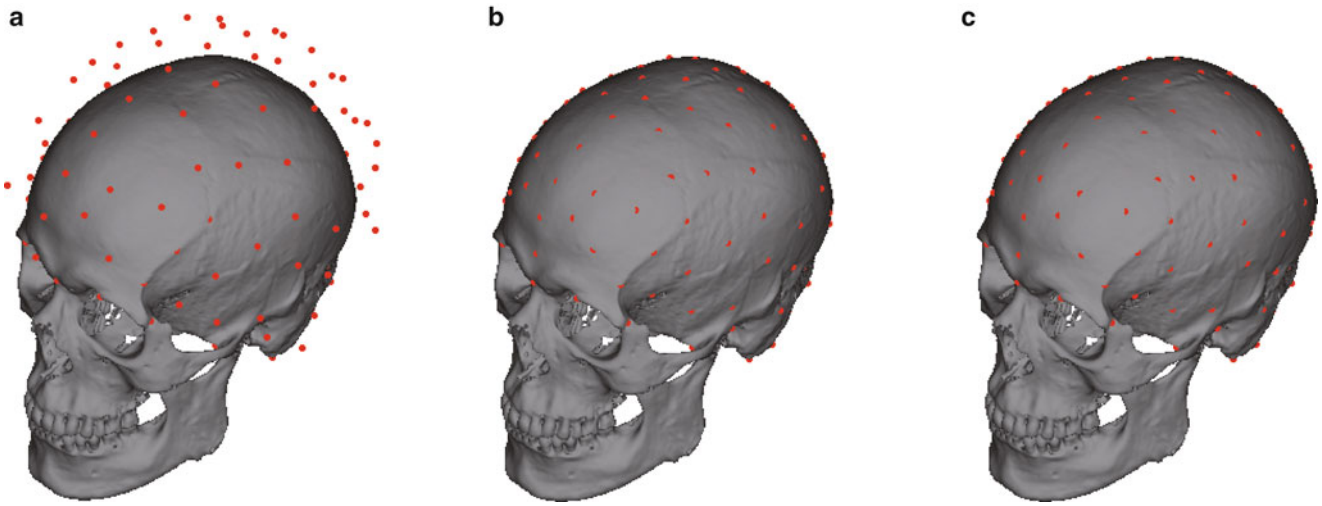

Fig. 16.3 Sliding semi-landmarks. (**a**) The sliding landmarks from the templates were firstly warped to the target specimen using the thin-plate spline function. (**b**) The landmarks are projected onto the surface. (**c**) The landmarks are slid along the surface to minimize the bending energy

16.3 Results

The results of a principal component analysis (PCA) of morphological variability in the cranial vault of the modern Japanese based on the two kinds of template configurations are presented in Fig. 16.4 as plots of the first principal component (PC1) versus PC2 and PC3 versus PC4. The first four PCs accounted for 69.2 % (30.8 %, 14.4 %, 13.3 %, and 10.7 % for PC1, PC2, PC3, and PC4, respectively) for the SP template and 71.5 % (31.9 %, 15.9 %, 12.2 %, and 11.5 % for PC1, PC2, PC3, and PC4, respectively) for the L template. The plots are labeled with the specimen number. As shown in Fig. 16.4, the scatter plots of the PC scores are very similar between the SP and L template analyses.

Figures 16.5 and 16.6 show the variations in the 3D shape along PC1, PC2, PC3, and PC4 (other PCs = 0) by warping the neurocranial shape represented by the wireframe connecting the landmarks. We observed that the morphological variability extracted along the first four PCs by the two different template configurations generally resembled each other as in the scatter plots of the PC scores (Fig. 16.4).

As illustrated in Fig. 16.5, with increasing PC1, a relative contraction of the cranial length and relative elongation of the cranial breadth were observed. Particularly, the forehead and occipital region had receded and the nuchal lines were located relatively more inferiorly with an increase in PC1.

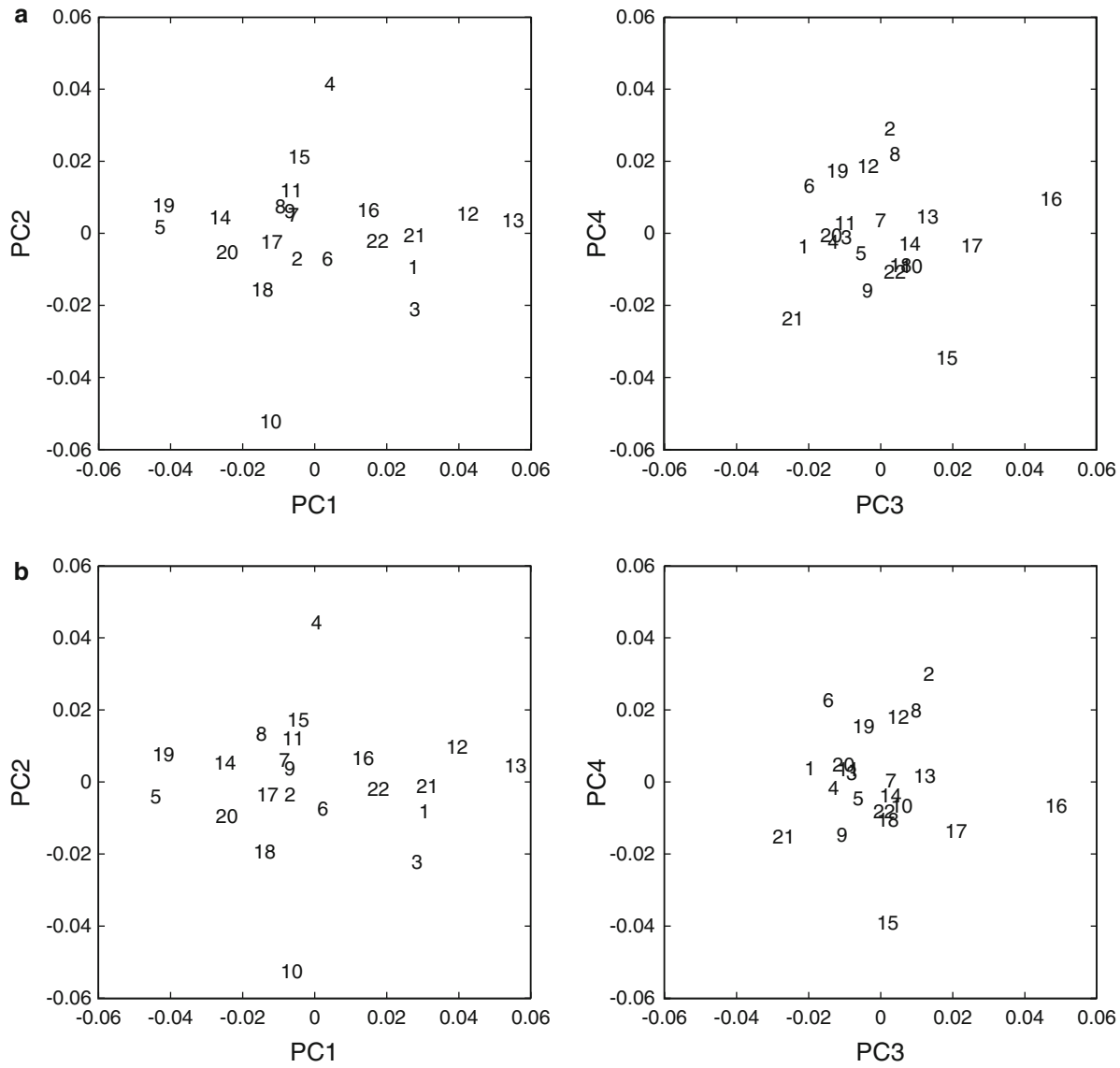

Fig. 16.4 The results of principal component analysis PC1 (x-axis) versus PC2 (y-axis) and PC3 (x-axis) versus PC4 (y-axis). (**a**) Results based on the shortest path template. (**b**) Results based on the lattice template. The plots are labeled with the specimen number

With increasing PC2, a relative decrease in the cranial breadth but relative increase in the cranial height were observed (Fig. 16.5). There were also large differences in the positions of the inion and the nuchal line, which were located relatively more inferiorly with an increase in PC2.

As illustrated in Fig. 16.6, PC3 described the relative retraction of the parieto-occipital region and relative downward displacement of the mastoid process and the lower part of the squama of the occipital bone with an increase in PC3, although the relative position of the inion was unaltered.

PC4 described the relative downward displacement of the nasion, the frontomalare temporale, and the supraorbital margin with increasing PC4 (Fig. 16.6). The stephanion was located relatively more superiorly with an increase in PC4.

16.4 Discussion

In the present study, we attempted to extract the morphological variability in the cranial vault shape in the modern Japanese population by means of the sliding landmark method. Comparisons of the results of the geometric morphometric analyses demonstrated that the morphological variabilities extracted by the two different template configurations (SP and L template configurations) generally correspond to each other. This indicates that if a sufficient number of semi-landmarks are evenly distributed across the neurocranial surface, the global tendency of the morphological variability to be extracted may not be affected by the choice of template configurations.

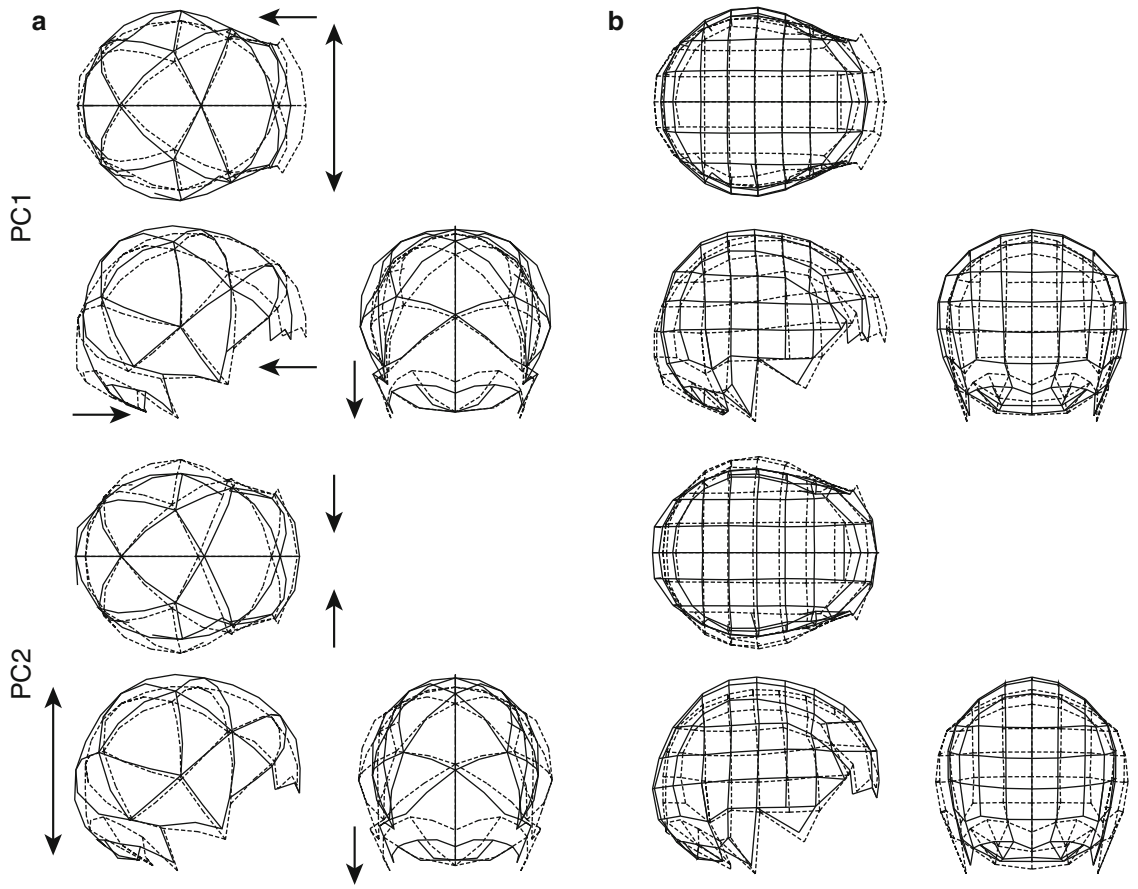

Fig. 16.5 The variation in neurocranial shape represented by PC1 and PC2. Shape variations are visualized with 3D deformation of the wire-frame connecting landmarks. (**a**) Results based on the shortest path template. (**b**) Results based on the lattice template. *Solid line*: PC1 and PC2 = 0.06, *Dotted line*: PC1 and PC2 = −0.06

Here we used only the sample of the modern Japanese crania, but the morphological variabilities extracted by the two methods would be more similar if the dataset included the crania of other populations in addition to the Japanese crania. However, the pattern of morphological variations represented by higher order PCs are certainly affected by the template configuration, as the higher order PCs deal with smaller, local variabilities in shape. Special attention thus seems necessary when dealing with the morphological variabilities represented by higher order PCs.

In the present study, we, for the first time, clarified the 3D shape variability in the neurocranial shape in the modern Japanese population by successfully applying the semi-landmark method. As a result, we demonstrated that the most predominant shape variability in the cranial vault in the modern Japanese population is the brachycephalic/dolichocephalic tendency. In a dolichocephalic cranial vault, the forehead tends to be relatively more elongated than the occipital bone, and the inion tends to project superoposteriorly. The next major morphological variability was that the narrow cranial vault tends to have a larger cranial height with its parietal region protruded upward (PC2). Interestingly, however, the inion and the nuchal line tend to be located relatively more inferiorly. Furthermore, it was demonstrated that if the mastoid process and the occipital region are located inferiorly, the parieto-occipital region tends to be flatter and recede further (PC3), and if the orbital region is located inferiorly, the stephanion region tends to move upward (PC4). Mechanisms underlying the existence of such patterns in the morphological variability in the neurocranial shape are obscure, but this could possibly be an area of future research.

In the present study, only 22 samples were preliminarily studied to extract the 3D variability in the neurocranial shape in the modern Japanese population using the semi-landmark method. However, more samples should be included in the future to confirm our present findings in a larger number of cases. Nevertheless, the present semi-landmark-based approach seems to serve as a basis for detailed quantification and comparisons of the human neurocranial shape.

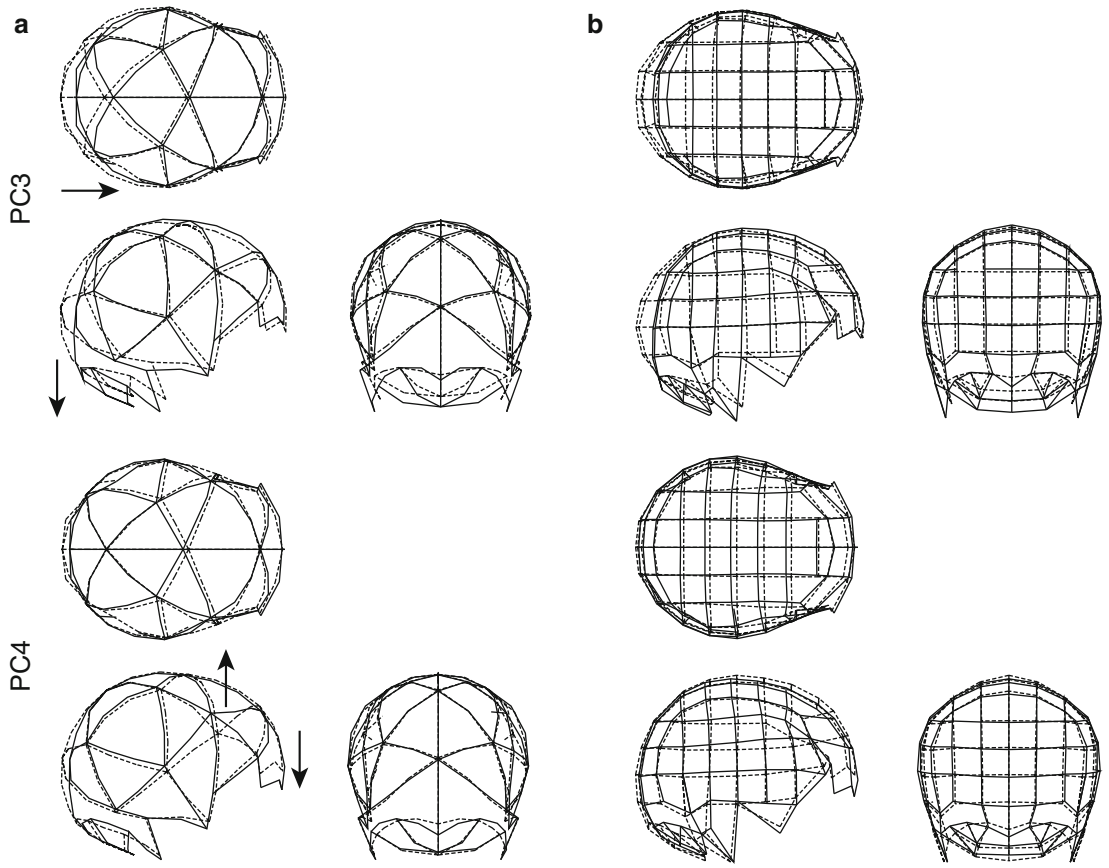

Fig. 16.6 The variation in neurocranial shape represented by PC3 and PC4. (**a**) Results based on the shortest path template. (**b**) Results based on the lattice template. *Solid line*: PC3 and PC4 = 0.04, *Dotted line*: PC3 and PC4 = −0.04

We will use this approach to construct a morphological database of human cranial shape, which will be indispensable for the anatomically accurate assembly of fossil cranial fragments as well as the statistical interpolation of missing parts in such assembled fossil crania.

Acknowledgement We wish to express our sincere gratitude to Prof. Takeru Akazawa (Kochi Institute of Technology) for giving us an opportunity to participate in this research project and for his continuous guidance and support throughout the course of the present study. This study was supported by a Grant-in-Aid for Scientific Research on Innovative Areas "Replacement of Neanderthals by Modern Humans: Testing Evolutionary Models of Learning" from the Japanese Ministry of Education, Culture, Sports, Science and Technology.

References

Adams DC, Rohlf FJ, Slice DE (2004) Geometric morphometrics: ten years of progress following the 'revolution'. Ital J Zool 71:5–16

Bastir M, Rosas A, Gunz P, Pena-Melian A, Manzi G (2011) Evolution of the base of the brain in highly encephalized human species. Nat Commun 2:1–8

Bookstein FL (1991) Tools for landmarks data: geometry and biology. Cambridge University Press, Cambridge

Bookstein FL (1997) Landmark methods for forms without landmarks: localizing group differences in outline shape. Med Image Anal 1:225–243

Gunz P, Mitteroecker P, Bookstein FL (2005) Semilandmarks in three dimensions. In: Slice DE (ed) Modern morphometrics in physical anthropology. Kluwer/Plenum, New York

Gunz P, Mitteroecker P, Neubauer S, Weber GW, Bookstein FL (2009) Principles for the virtual reconstruction of hominin crania. J Hum Evol 57:48–62

Makishima H, Ogihara N (2009) Three-dimensional geometric morphometric study of craniofacial variations in Jomon populations. Anthropol Sci (Jpn Ser) 117:11–21

Mitteroecker P, Gunz P (2009) Advances in geometric morphometrics. Evol Biol 36:235–247

Morita Y, Ogihara N, Kanai T, Suzuki H (2013) Quantification of neurocranial shape variation using shortest paths connecting pairs of anatomical landmarks. Am J Phys Anthropol 151:658–666

O'Higgins P (2000) The study of morphological variation in the hominid fossil record: biology, landmarks and geometry. J Anat 197: 103–120

O'Higgins P, Jones N (1998) Facial growth in *Cercocebus torquatus*: an application of three-dimensional geometric morphometric techniques to the study of morphological variation. J Anat 193: 251–272

O'Higgins P, Jones N (2006) Tools for statistical shape analysis. Hull York Medical School. http://hyms.fme.googlepages.com/resources

Ogihara N, Makishima H, Ishida H (2009) Geometric morphometric study of temporal variations in human crania excavated from the Himrin Basin and neighboring areas, northern Iraq. Anthropol Sci 117:9–17

Perez SI, Bernal V, Gonzalez PN (2006) Differences between sliding semi-landmarks methods in geometric morphometrics with an application to human craniofacial and dental variation. J Anat 208:769–784

Slice DE (2005) Modern morphometrics. In: Slice DE (ed) Modern morphometrics in physical anthropology. Kluwer/Plenum, New York

Zollikofer CPE, Ponce de León MS (2002) Visualizing patterns of craniofacial shape variation in *Homo sapiens*. Proc R Soc B 269:801–807

A Geometric Morphometric Study of Neurocranial Shape Variations in the Crania of Modern Japanese

17

Yusuke Morita, Hideki Amano, Masato Nakatsukasa, Osamu Kondo, and Naomichi Ogihara

Abstract

We analyzed the morphological variability of the cranial shape among the modern Japanese population using landmark-based geometric morphometrics. The sample comprised 56 cranial specimens of the modern Japanese population (23 female and 33 male) housed at Kyoto University. Computed tomography images of the crania were created and virtual models were generated. Variability in cranial shape was examined using a geometric morphometric technique based on a total of 161 anatomical and semi-sliding landmarks distributed across the entire cranial surface. Semi-landmarks were defined on the neurocranium using equally-spaced points along the shortest paths connecting pairs of landmarks. The results show that the most noticeable shape variance observed in the modern Japanese crania is the brachycephalic/dolichocephalic tendency. Multivariate analyses of variance indicate that significant sexual differences exist in the cranial morphology among the modern Japanese population.

Keywords

Craniometry • Geometric morphometrics • Semi-landmark • Sexual dimorphism

17.1 Introduction

Geometric morphometrics have been widely used for the analyses of morphological variation in human crania. For instance, geographic variations (e.g., Hennessy and Stringer 2002; Badawi-Fayad and Cabanis 2007), temporal variations (e.g., Gonzalez-Jose et al. 2008; Ogihara et al. 2009), ontogenetic changes (e.g., Viðarsdóttir and Cobb 2004; Morimoto et al. 2008; Neubauer et al. 2009) and sexual dimorphism (e.g., Rosas and Bastir 2002; Franklin et al. 2006; Bigoni et al. 2010) of human craniofacial morphology have all been analyzed based on geometric morphometrics, demonstrating the effectiveness of the technique. However, although analyses of anthropological characteristics and morphological variance in the modern Japanese crania are important for better understanding of the formation of the Japanese population, no detailed morphological analyses using geometric morphometric techniques have been conducted until now.

In the present study, therefore, we analyzed the morphological variability of cranial shape among the modern Japanese population using landmark-based geometric morphometrics. On the cranial vault, however, only a few morphologically-definable landmarks exist. To quantify the overall shape of the human cranial vault, therefore, semi-landmarks were defined on the neurocranial surface by using

Y. Morita • H. Amano • N. Ogihara (✉)
Department of Mechanical Engineering, Faculty of Science and Technology, Keio University, 3-14-1 Hiyoshi, Kohoku-ku, Yokohama, Kanagawa 223-8522, Japan
e-mail: ogilab_morita10@yahoo.co.jp; ogilab_amano11@yahoo.co.jp; ogihara@mech.keio.ac.jp

M. Nakatsukasa
Laboratory of Physical Anthropology, Graduate School of Science, Kyoto University, Kitashirakawa-Oiwakecho, Sakyo, Kyoto 606-8502, Japan
e-mail: nakatsuk@anthro.zool.kyoto-u.ac.jp

O. Kondo
Department of Biological Sciences, Graduate School of Science, University of Tokyo, 7-3-1 Hongo, Bunkyo-ku, Tokyo 113-0033, Japan
e-mail: kondo-o@biol.s.u-tokyo.ac.jp

T. Akazawa et al. (eds.), *Dynamics of Learning in Neanderthals and Modern Humans Volume 2: Cognitive and Physical Perspectives*, Replacement of Neanderthals by Modern Humans Series, DOI 10.1007/978-4-431-54553-8_17, © Springer Japan 2014

equally-spaced points along the shortest paths connecting pairs of landmarks. The landmark coordinates were then analyzed based on geometric morphometrics to describe variations in craniofacial shape among the modern Japanese.

17.2 Materials and Methods

17.2.1 Specimens

We used a total of 56 crania (23 female and 33 male) from the modern Japanese population housed at Kyoto University to construct the reference database of human cranial shape. Each cranium was scanned using a CT scanner and cross-sectional images were reconstructed at 0.5 mm intervals, with a pixel size of 0.5 mm or 0.468 mm. The images were then transferred to medical imaging software (Analyze 9.0; Mayo Clinic, USA) and the 3D surface model of the cranium was generated as a triangular mesh model using the marching cube method. The mesh structure was then regenerated using its curvature flow in conjunction with reverse engineering software (RapidForm 2006; INUS Technology, Korea). The 3D coordinates of midsagittal landmarks and midpoints of bilateral landmarks were digitized using the same software and the midsagittal plane was calculated using the least squares method.

17.2.2 Landmarks

To capture the cranial morphology of each specimen, we firstly digitized the 62 anatomical landmarks listed in Table 17.1 (#1-#36) on the surface of each cranium (Fig. 17.1). In addition, the superior nuchal, temporal and supraorbital curves were approximated using a seventh-order Bezier curve and a total of 14 equally-spaced points along the curves were also defined as landmarks (#37-#43). Therefore, a total of 76 landmarks were extracted for each cranium as non-sliding landmarks.

On one specimen that was chosen as a template, we defined semi-landmarks based on the shortest paths connecting pairs of anatomical landmarks (Morita et al. 2013). Specifically, the above 76 non-sliding landmarks as well as 14 equally-spaced points along the midsagittal curve (between the nasion and inion) were used to calculate the shortest paths, and the equally-spaced points along the paths were then computed as shown in Fig. 17.2. A total of 85 landmarks, including the 14 midsagittal equally-spaced points were designated as sliding semi-landmarks.

This template configuration was then used to determine the locations of the semi-landmarks on the other crania. The coordinates of the 76 non-sliding landmarks were used to define a thin-plate function describing a mapping from the template configuration to a target specimen. The sliding landmarks from the template were deformed to the target specimen using this mapping function. The sliding landmarks were then projected onto and slid along the cranial surface of the target specimen so as to minimize the bending energy of the thin-plate spline method. This process was iter-

Table 17.1 Descriptions of the landmarks used in the present study

Number	Landmark name	Type
1	Nasion	m
2	Glabella	m
3	Inion	m
4	Opisthion	m
5	Maxillonasofrontale	b
6	Uppermost point on the orbital margin	b
7	Frontomalare-orbitale	b
8	Frontomalare-temporale	b
9	Stephanion	b
10	Asterion	b
11	Intersection of nuchal line and occipitomastoid suture	b
12	Mastoidale	b
13	Posterior end of the margin of temporal fossa	b
14	Porion	b
15	Rhinion	m
16	Akathion	m
17	Prosthion	m
18	Alveolon	m
19	Sphenobasion	m
20	Basion	m
21	Alare	b
22	Zygoorbitale	b
23	Orbitale	b
24	Zygomaxillare	b
25	Ektomolare	b
26	Jugale	b
27	Most inferior point of the temporozygomatic suture	b
28	Most anterior point of the posteior margin of the palate	b
29	Most lateral point of the margin of the foramen magnum	b
30	Infratemporale	b
31	Stenion	b
32	Midpoint of the labial margin of the canine alveolar foramen	b
33	Midpoint of the labial margin of the second premolar alveolar foramen	b
34	Most medial point of the margin of the lacerated foramen	b
35	Most medial point of the margin of the carotid canal	b
36	Posterior root of the styloid process	b
37–39	Equally spaced points along the nuchal line	b
40–41	Equally spaced points along the temporal line	b
42–43	Equally spaced points along the supraorbiral line	b

Note: m = midsagittal landmark; b = bilateral landmark

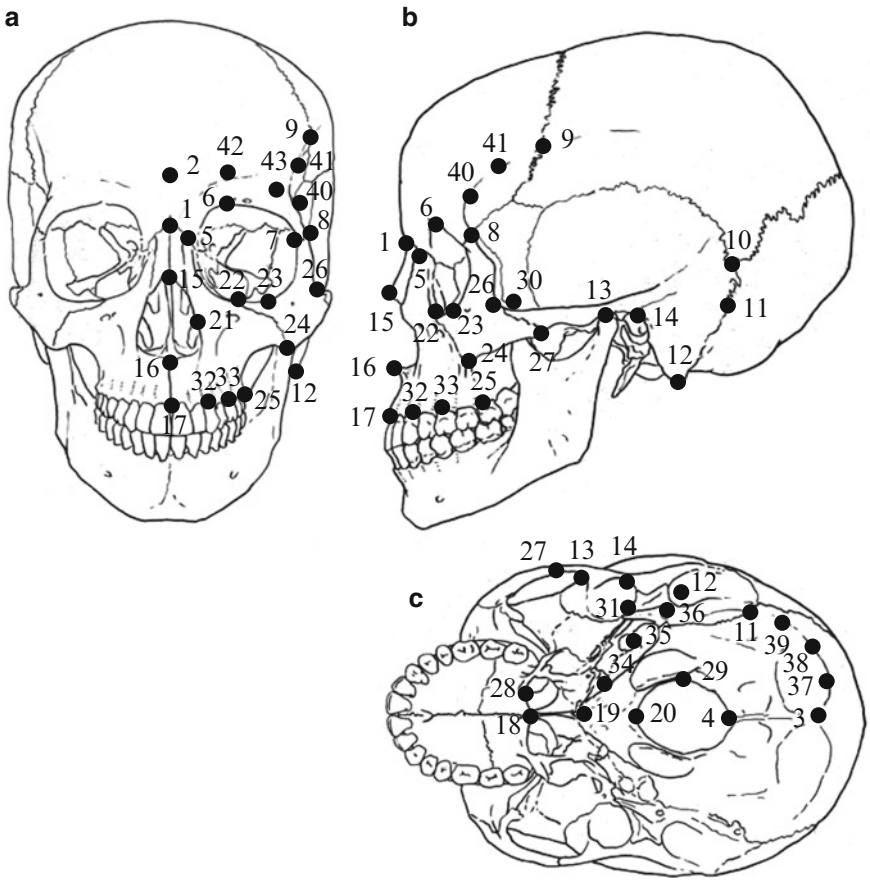

Fig. 17.1 The non-sliding landmarks used in the present study. (**a**) *Anterior view*, (**b**) *lateral view*, (**c**) *bottom view*

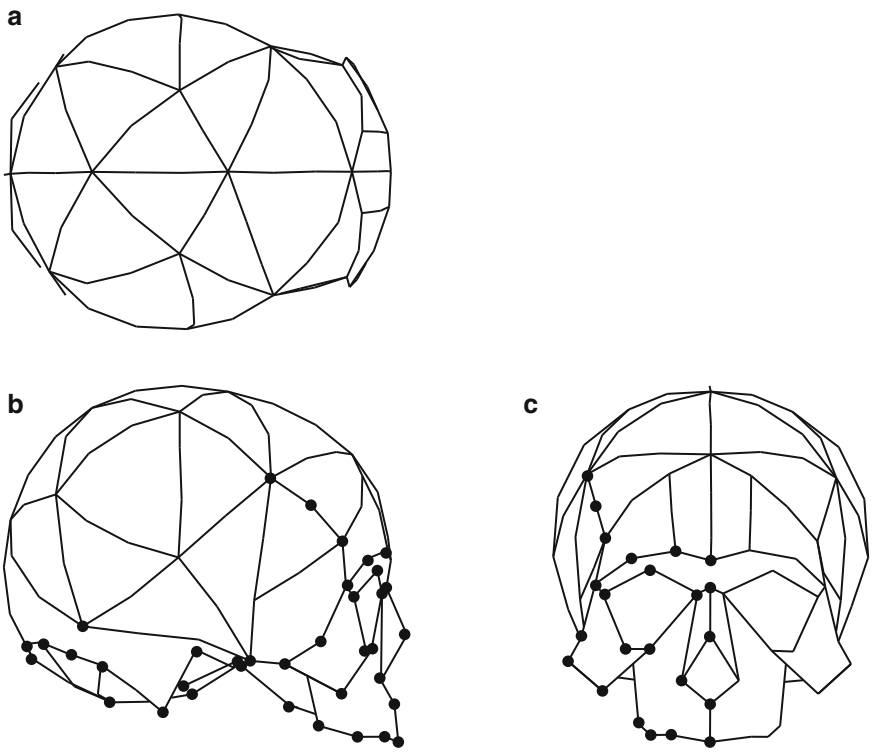

Fig. 17.2 Sliding and non-sliding landmarks used in the present study. The entire cranial shape represented by the *wireframe* connecting the landmarks. (**a**) *Top view*, (**b**) *lateral view*, (**c**) *anterior view*. *Black dots* indicate the non-sliding landmarks

ated until the solution converged. In the present study, Templand in the EVAN Toolbox (www.evan-society.org) was used to calculate the positions of the sliding landmarks corresponding to the two template configurations. The morphology of each cranium was therefore represented by a total of 161 landmark coordinates that were evenly distributed across the cranial surface.

17.2.3 Morphological Analysis

The coordinates of the non-sliding and sliding landmarks were analyzed using Morphologika geometric morphometric software, version 2.3.1 (O'Higgins and Jones 2006). For each analysis, the landmark coordinates were firstly normalized using centroid size (the square root of the sum of squared distances of landmarks from the centroid) for size-independent shape analysis. The normalized coordinates were then registered using the Generalized Procrustes Analysis (a least-squares method for superimposing a set of landmark configurations by translation, rotation and re-scaling). The principal components (PCs) of shape variations among the specimens were then calculated using the variance-covariance matrix of the Procrustes residuals of all crania used in the present study (see O'Higgins and Jones 1998; O'Higgins 2000 for more details about the calculation method).

In order to test for significant differences in PC scores between female and male crania, multivariate analyses of variance (MANOVA) were conducted using Statistica 10 (Statsoft Inc, Tulsa, USA). Significance levels for all multiple comparison tests were adjusted using the Bonferroni correction.

17.3 Results

The results of a principal component analysis (PCA) of morphological variability in the modern Japanese crania are presented in Fig. 17.3 as plots of the first principal component (PC1) versus PC2, and PC3 versus PC4. The first four PCs accounted for 50.5 % (21.0 %, 12.4 %, 10.7 % and 6.4 % for PC1, PC2, PC3 and PC4, respectively), and approximately 90 % of variance was incorporated into the first 24 PCs. The PC scores of the first three PCs showed large superposition of female and male crania. However, along the PC4 axis the female crania were slightly separated from the male crania, suggesting that shape variation represented by PC4 corresponds to a sexually-dimorphic structure of the cranial shape among the modern Japanese. MANOVA testing indicated that the overall difference between the sexes was statistically significant (Wilks' lambda = 0.273, $F = 3.440$, $p = 0.001$). The Bonferroni multiple comparison tests showed that PC4, PC8 and PC11 scores differed significantly between the sexes ($p = 0.032$, 0.018 and 0.021, respectively). PC8 and PC11 accounted for 3.3 % and 2.2 %, respectively.

Figures 17.4, 17.5, and 17.6 display the variations in the 3D shape along PC1, PC2 and PC3, respectively, (other PCs = 0) by warping the entire cranial shape represented by the wireframe connecting the landmarks. With increasing PC1, a relative contraction of the cranial length, relative elongation of the cranial breadth and relative increase of the cranial height were observed. It was also observed that the forehead, facial and occipital regions had receded, the maxilla breadth was narrower and the nuchal lines were more inferiorly located with an increase in PC1. With increasing PC2, downward displacement of the orbits and shortening of the nasal height were observed, although the relative position of the palate and parietal and the bizygomatic breadth were virtually unchanged. In addition, the cranial base tended to be located more superiorly, and the maxilla was less protruding with an increase in PC2. With increasing PC3, relative contraction of the cranial length and relative elongation of the cranial breadth were again observed as in PC1. However, relative contraction of the cranial length occurred in the parieto-occipital region, but not in the forehead. Furthermore, the cranial height remained unchanged.

Figures 17.7 and 17.8 show the variations in 3D shape along PC4 and PC8, respectively, (other PCs = 0) that are significantly different between the sexes. The PC4 and 8 scores were negative and positive in male crania, respectively. In male crania (with decreasing PC4) it was observed that the superior surface of the frontal bone was more superiorly positioned and the posterior surface of the parietal and occipital bones had receded. The mastoid process and the squama of the occipital bone were also more inferiorly projected along with decreasing PC4. Conversely, the maxilla (prosthion) was less projected and the palate was less inferiorly located. With increasing PC8, the neurocranium differed only slightly. However, in the viscerocranium, the orbits got narrower with an increase in PC8. It was also observed that the nasal bones (rhinion) were more prominent, the maxilla was less projected and the palate was more inferiorly located with an increase in PC8.

17.4 Discussion

In the present study, we tried to extract the 3D shape variability of the complete cranial shape among the modern Japanese population using landmark-based geometric morphometrics. Using this methodology, the morphological variability of the cranial shape among modern Japanese populations could be successfully extracted and visualized. The most predominant shape variability in modern Japanese crania was found to be the brachycephalic/dolichocephalic tendency (PC1).

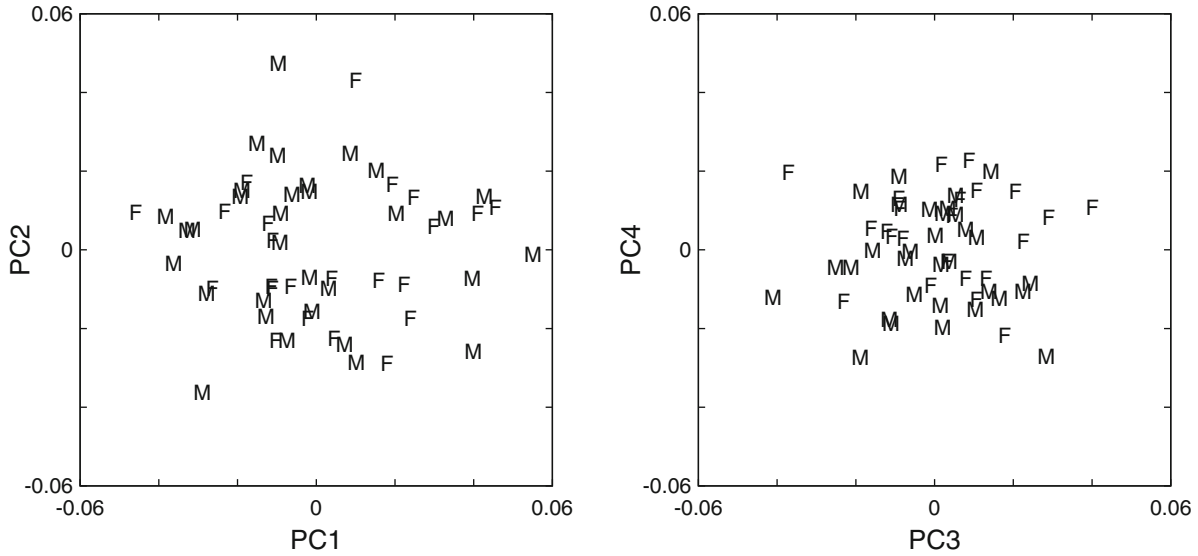

Fig. 17.3 The results of principal component analysis: PC1 (x-axis) versus PC2 (y-axis) and PC3 (x-axis) versus PC4 (y-axis). F = female, M = male

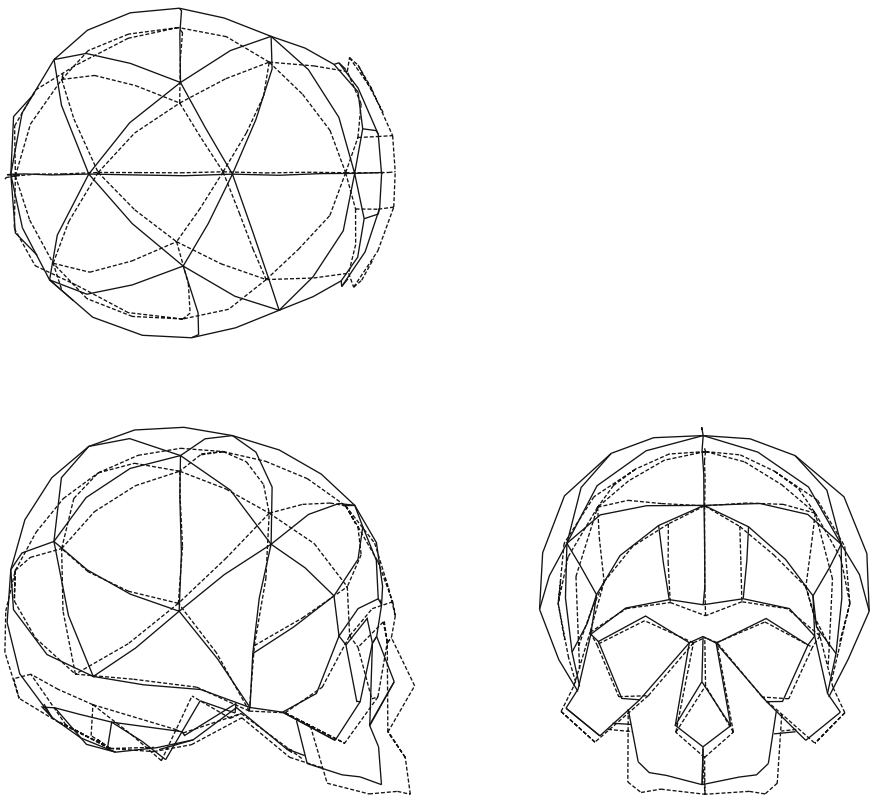

Fig. 17.4 The variation in cranial shape represented by PC1. Shape variations are visualized with 3D deformation of the wireframe connecting landmarks. *Solid line*: PC1 = 0.06, *Dotted line*: PC1 = −0.06

It was observed that the forehead and face are relatively forward-protruding and the cranial height is smaller in a dolichocephalic cranium, and vice versa in a brachycephalic cranium. Interestingly, the shape variability represented by PC3 was also the brachycephalic/dolichocephalic tendency. However, while the forehead is relatively more forward-protruding along PC1, this is not the case along PC3 and the parieto-occipital region is projected relatively more in the

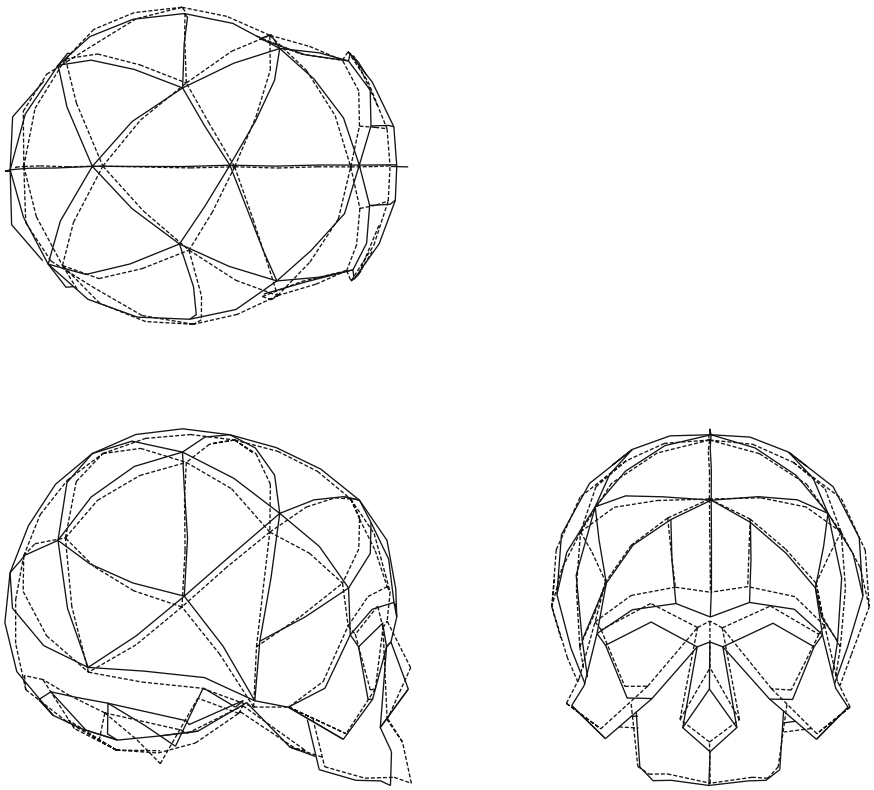

Fig. 17.5 The variation in cranial shape represented by PC2. *Solid line*: PC2 = 0.04, *Dotted line*: PC2 = −0.04

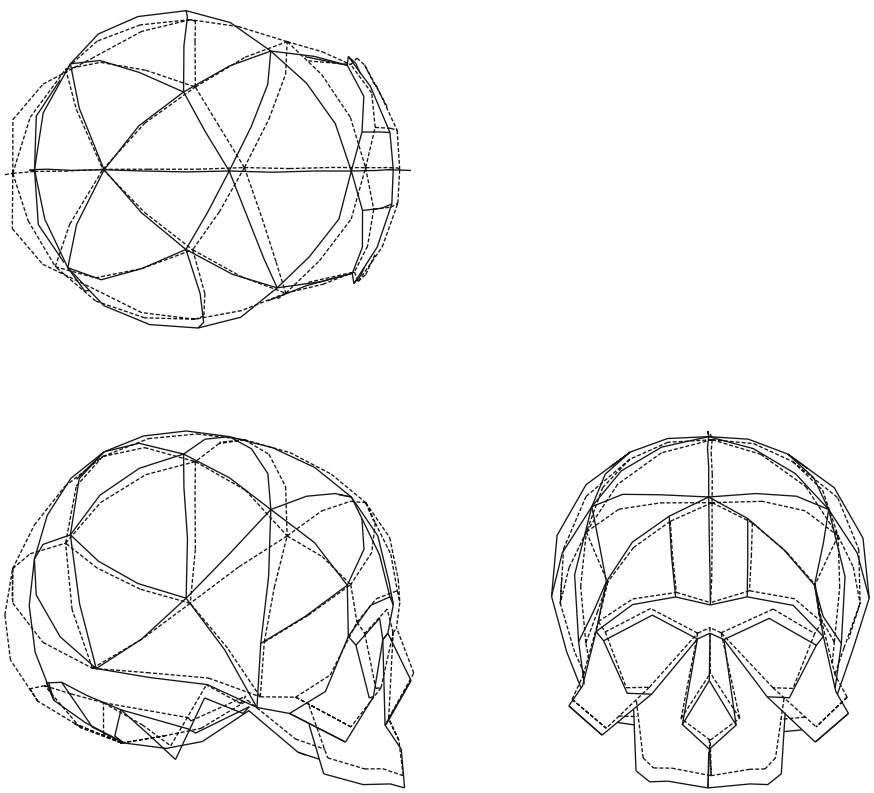

Fig. 17.6 The variation in cranial shape represented by PC3. *Solid line*: PC3 = 0.04, *Dotted line*: PC3 = −0.04

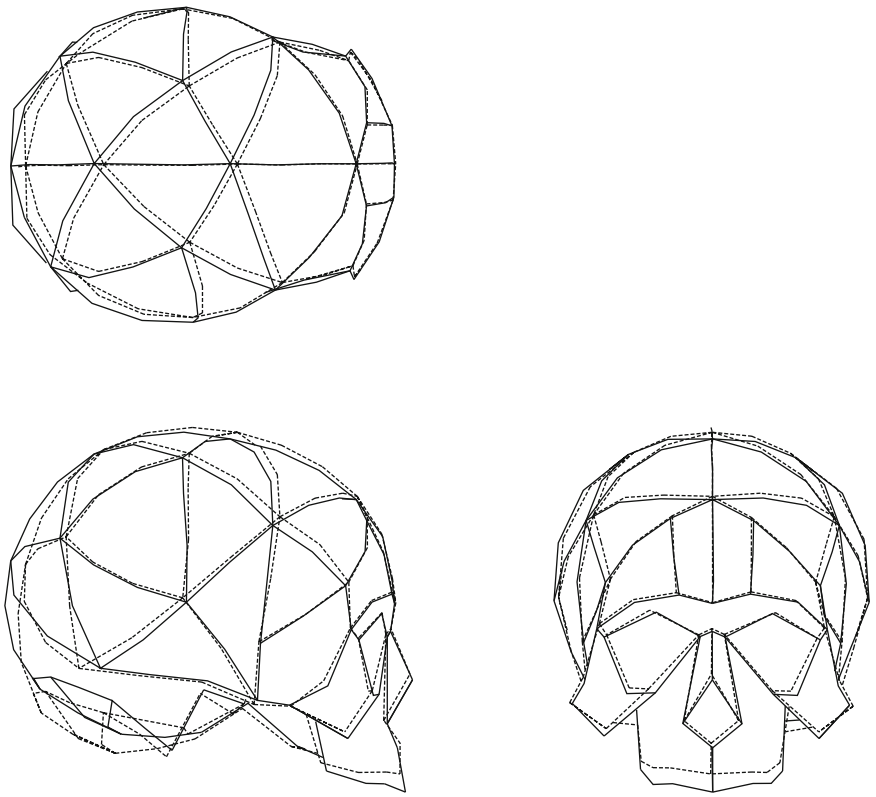

Fig. 17.7 The variation in cranial shape represented by PC4. PC4 separates the two sexes. *Solid line*: PC4 = 0.03 (female), *Dotted line*: PC4 = −0.03 (male)

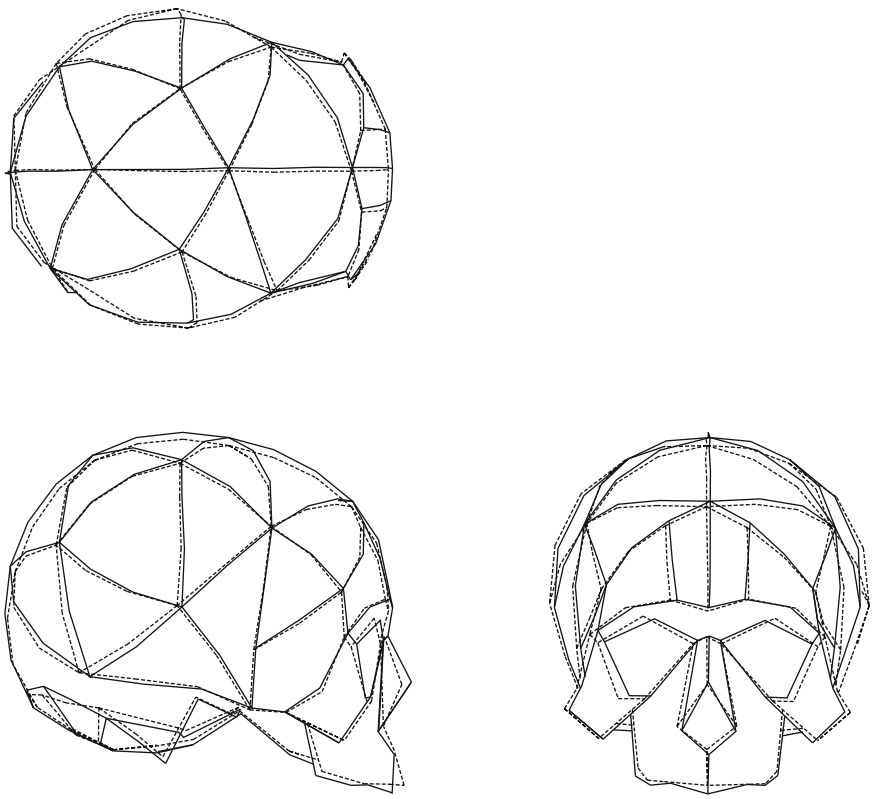

Fig. 17.8 The variation in cranial shape represented by PC8. PC8 separates the two sexes. *Solid line*: PC8 = 0.02 (male), *Dotted line*: PC8 = −0.02 (female)

backward direction. Therefore, there seems to be mainly two types of dolichocephaly among modern Japanese; one with the forehead and face protruding relatively forward and the other with the parieto-occipital region projected relatively backward.

The next predominant shape variability was the euryenic/leptenic tendency along PC2, often represented by the upper facial index. It was also demonstrated that if the face is broader (the upper facial height is shorter), the cranial base tends to be located more superiorly and the maxilla tends to be less protuberant, and vice versa. Such interrelationships among the cranial parts extracted in the present study have not been reported previously. Further studies are necessary to confirm these first results, possibly using samples from other population groups.

In the present study, statistically significant sexual differences in the cranial morphology were also extracted. Franklin et al. (2006) demonstrated that, in male African crania, the forehead is less vertical and rounded; the glabella region is larger and more convexly protuberant; the cranial vault is shorter; the mastoid process is larger and more antero-inferiorly projected; and the occipital bone is more posteriorly projected. Regarding the sexually-dimorphic characteristics in the facial region, Bigoni et al. (2010) have noted that, in male European crania, the face and the zygomatic arches are relatively wider; the orbit is relatively less round (lower and wider); the lateral landmarks of the orbit are shifted more posteriorly; the nasal aperture is relatively narrower; the nasal bones (rhinion) are more prominent; the maxilla (prosthion) is less projected; and the palate is lower. Although direct comparisons between the results of the present study and those of other published studies are generally difficult as landmarks used to represent morphology are different, the sexually-dimorphic morphological characteristics extracted in the present study are generally in agreement with those of previous morphometric studies.

The results in the present study will serve as a reference database of the cranial morphology for the modern Japanese population. Such a database is indispensable for the anatomically-accurate assembly of fossil cranial fragments as well as the statistical interpolation of missing parts in assembled fossil crania. As a morphological database, the number of specimens may be rather small. However, the number of intact cranial specimens, particularly those of females, is actually quite limited because many of the cranial specimens housed at Kyoto University (and the University of Tokyo as well) have been cut transversely for removal of brains. Hence the number of samples is limited to 56, even though we have tried to include as many specimens as possible in our analysis. Therefore, the present database is currently the most complete 3D cranial database for the modern Japanese population. Nevertheless, the database certainly includes regional variations. We would like to increase the number of cranial specimens from different population groups when the opportunity arises in future.

Acknowledgements We wish to express our sincere gratitude to Prof. Takeru Akazawa (Kochi Institute of Technology) for giving us an opportunity to participate in this research project and for his continuous guidance and support throughout the course of the present study. This study was supported by a Grant-in-Aid for Scientific Research on Innovative Areas, "Replacement of Neanderthals by Modern Humans: Testing Evolutionary Models of Learning," (No. 22101006) from the Japanese Ministry of Education, Culture, Sports, Science and Technology.

References

Badawi-Fayad J, Cabanis EA (2007) Three-dimensional procrustes analysis of modern human craniofacial form. Anat Rec Adv Integr Anat Evol Biol 290:268–276

Bigoni L, Veleminska J, Bruzek J (2010) Three-dimensional morphometric analysis of cranio-facial sexual dimorphism in a Central European sample of known sex. Homo 61:16–32

Franklin D, Freedman L, Milne N, Oxnard CE (2006) A geometric morphometric study of sexual dimorphism in the crania of indigenous southern Africans. S Afr J Sci 102:229–238

Gonzalez-Jose R, Bortolini MC, Santos FR, Bonatto SL (2008) The peopling of America: craniofacial shape variation on a continental scale and its interpretation from an interdisciplinary view. Am J Phys Anthropol 137:175–187

Hennessy RJ, Stringer CB (2002) Geometric morphometric study of the regional variation of modern human craniofacial form. Am J Phys Anthropol 117:37–48

Morimoto N, Ogihara N, Katayama K, Shiota K (2008) Three-dimensional ontogenetic shape changes in the human cranium during the fetal period. J Anat 212:627–635

Morita Y, Ogihara N, Kanai T, Suzuki H (2013) Quantification of neurocranial shape variation using shortest paths connecting pairs of anatomical landmarks. Am J Phys Anthropol 151:658–666

Neubauer S, Gunz P, Hublin JJ (2009) The pattern of endocranial ontogenetic shape changes in humans. J Anat 215:240–255

O'Higgins P (2000) The study of morphological variation in the hominid fossil record: biology, landmarks and geometry. J Anat 197: 103–120

O'Higgins P, Jones N (1998) Facial growth in Cercocebus torquatus: an application of three-dimensional geometric morphometric techniques to the study of morphological variation. J Anat 193: 251–272

O'Higgins P, Jones N (2006) Tools for statistical shape analysis. Hull York Medical School. http://hyms.fme.googlepages.com/resources

Ogihara N, Makishima H, Ishida H (2009) Geometric morphometric study of temporal variations in human crania excavated from the Himrin Basin and neighboring areas, northern Iraq. Anthropol Sci 117:9–17

Rosas A, Bastir M (2002) Thin-plate spline analysis of allometry and sexual dimorphism in the human craniofacial complex. Am J Phys Anthropol 117:236–245

Viðarsdóttir US, Cobb S (2004) Inter- and intra-specific variation in the ontogeny of the hominoid facial skeleton: testing assumptions of ontogenetic variability. Ann Anat/Anat Anz 186:423–428

Statistical Interpolation of Missing Parts in Human Crania Using Regularized Multivariate Linear Regression Analysis

18

Hideki Amano, Yusuke Morita, Hiroyasu Nagano, Osamu Kondo, Hiromasa Suzuki, Masato Nakatsukasa, and Naomichi Ogihara

Abstract

Anatomically-accurate interpolation of missing parts in fossil crania is important for correct estimation of brain morphology based on cranial shape information. In the present study, we attempted to establish a method to mathematically interpolate missing coordinates of crania based on a reference database of cranial morphology. Specifically, a total of 151 landmarks were acquired for each specimen using anatomical and sliding landmarks, and a reference database of human cranial shape was constructed. Based on the sample of complete specimens as reference data, multivariate regressions were calculated with the missing coordinates as dependent variables, and other remaining coordinates as independent variables. We used a Moore-Penrose pseudo-inverse matrix to solve for the under-constrained linear algebraic regression equations. In order to examine the efficacy of the proposed interpolation method, we virtually created crania with missing portions, and the missing landmarks in the crania were then re-estimated for comparisons with their true values. The computed positions of the missing landmarks are located reasonably close to the corresponding landmarks on the original cranium, indicating that the present interpolation method may be effective for subjective estimation of missing parts in fossil crania. However, this estimation method seems not to be applicable to the estimation of missing landmarks in the basicranial region, possibly because of the low correlation between the shape of the basicranium and the rest of the cranium.

Keywords

Fossil • Reconstruction • Surface approximation • Surface interpolation

H. Amano • Y. Morita • H. Nagano • N. Ogihara (✉)
Department of Mechanical Engineering, Faculty of Science and Technology, Keio University, 3-14-1 Hiyoshi, Kohoku-ku, Yokohama, Kanagawa 223-8522, Japan
e-mail: ogilab_amano11@yahoo.co.jp; ogilab_morita10@yahoo.co.jp; ogilab_nagano12@yahoo.co.jp; ogihara@mech.keio.ac.jp

O. Kondo
Department of Biological Sciences, Graduate School of Science, University of Tokyo, 7-3-1 Hongo, Bunkyo-ku, Tokyo 113-0033, Japan
e-mail: kondo-o@biol.s.u-tokyo.ac.jp

H. Suzuki
Research Center for Advanced Science and Technology, University of Tokyo, Komaba 4-6-1, Meguro-ku, Tokyo 153-8904, Japan
e-mail: suzuki@den.rcast.u-tokyo.ac.jp

M. Nakatsukasa
Laboratory of Physical Anthropology, Graduate School of Science, Kyoto University, Kitashirakawa-Oiwakecho, Sakyo, Kyoto 606-8502, Japan
e-mail: nakatsuk@anthro.zool.kyoto-u.ac.jp

T. Akazawa et al. (eds.), *Dynamics of Learning in Neanderthals and Modern Humans Volume 2: Cognitive and Physical Perspectives*, Replacement of Neanderthals by Modern Humans Series, DOI 10.1007/978-4-431-54553-8_18,

18.1 Introduction

During fossilization, crania are often fractured and all of the component fragments are rarely recovered. To restore the antemortem appearance of a fossil cranium, it is necessary to correctly assemble the fragments, eliminate distortions, and compensate for missing parts. In the present paper, we consider the interpolation of the missing parts in the process of cranial reconstruction. Establishing an anatomically-accurate interpolation of the missing parts of fossil crania is of crucial importance for the correct estimation of brain morphology based on cranial shape information.

Conventionally, such interpolation is created manually using plaster as filler based on the knowledge and experience of skilled anthropologists. However, in order to more precisely interpolate missing parts in fossil crania, researchers have recently attempted to digitally interpolate missing parts in a virtual space using a composite technique involving X-ray computed tomography (CT) and computer-assisted morphology. Mainly two methods have been proposed for such interpolation: geometric interpolation using a spline function, and statistical interpolation using multivariate regression (Gunz et al. 2009).

Geometric interpolation interpolates a missing part based on data mapped from a complete reference specimen using a spline function. Specifically, the existing portion of the specimen to be interpolated is used to define the mapping function, and the corresponding portion of the complete specimen is mapped to the partial specimen in order to reconstruct the missing parts. For example, using modern human and ape crania as referfences, Gunz et al. (2009) attempted to reconstruct the cranial morphology of *Homo erectus* KNM-WT-15000 (Turkana Boy). This method yields anatomically natural, morphologically consistent interpolation of the missing parts, but the reconstructed results vary depending on the reference specimen used.

On the other hand, statistical interpolation based on multivariate regression is a method to estimate missing coordinates based on a sample of complete specimens as a reference dataset. Multivariate regressions are calculated with the missing coordinates as dependent variables and other coordinates as independent variables. These equations are then applied to predict the missing coordinates. Weaver and Hublin (2009), for example, used this technique to restore the position of the sacrum in a Neanderthal pelvis (Tabun 1) based on a human pelvis specimen using the Expectation Maximization Algorithm for the estimation of regression coefficients.

To compute a multivariate regression analysis, the number of the samples in the reference dataset has to exceed the number of landmark coordinates used as independent variables. However, the number of reference specimens that can be used for analysis is often limited, although more landmark coordinates are certainly necessary to precisely capture the morphological characteristics of each cranial specimen. Previously, Neeser et al. (2009) employed the principal component analysis to reduce the number of independent variables used in the estimation of missing landmarks. However, a certain amount of morphological variance is certainly lost in such data reduction.

In the present study, we propose a method to statistically interpolate missing coordinates of human crania based on a multivariate regression analysis using a small number of cranial specimens. In a multivariate regression analysis, values of the regression coefficients that best fit the reference data are uniquely calculated by minimizing the summed squared error. However, if the number from the reference dataset is smaller than the number of landmarks, the problem becomes under-constrained, hindering the use of the multivariate regression analysis for the interpolation of missing parts in fossil crania. Nevertheless, such ill-posed problems can be made well-posed if the problem is regularized by introducing an additional constraint. Here we introduced a norm-minimization criterion to solve for the under-constrained linear algebraic equations to compute the regression coefficients. To evaluate the performance of the proposed interpolation method, we virtually created crania with missing portions and the missing landmarks were re-estimated by the proposed method.

18.2 Materials and Methods

18.2.1 Specimens

We used a total of 56 crania (23 female and 33 male) from the modern Japanese population housed at Kyoto University to construct the reference database of human cranial shape. Each cranium was scanned using a CT scanner and cross-sectional images were reconstructed at 0.5 mm intervals, with a pixel size of 0.5 mm or 0.468 mm. The images were then transferred to medical imaging software (Analyze 9.0; Mayo Clinic, USA) and the 3D surface model of the cranium was generated as a triangular mesh model using the marching cube method. The mesh structure was then regenerated using its curvature flow in conjunction with reverse engineering software (RapidForm 2006; INUS Technology, Korea). The 3D coordinates of midsagittal landmarks and midpoints of bilateral landmarks were digitized using the same software and the medial sagittal plane was calculated using the least square method.

18.2.2 Landmarks

To capture the cranial morphology of each specimen, we applied the sliding semi-landmark method (Bookstein 1997), and the variability in the cranial shape was represented by means of the landmark-based geometric morphometric method.

Table 18.1 Descriptions of the landmarks used in the present study

Number	Landmark name	Type
1	Nasion	m
2	Glabella	m
3	Inion	m
4	Opisthion	m
5	Maxillonasofrontale	b
6	Uppermost point on the orbital margin	b
7	Frontomalare-orbitale	b
8	Frontomalare-temporale	b
9	Stephanion	b
10	Asterion	b
11	Intersection of nuchal line and occipitomastoid suture	b
12	Mastoidale	b
13	Posterior end of the margin of temporal fossa	b
14	Porion	b
15	Rhinion	m
16	Akathion	m
17	Prosthion	m
18	Alveolon	m
19	Sphenobasion	m
20	Basion	m
21	Alare	b
22	Zygoorbitale	b
23	Orbitale	b
24	Zygomaxillare	b
25	Ektomolare	b
26	Jugale	b
27	Most inferior point of the temporozygomatic suture	b
28	Most anterior point of the posteior margin of the palate	b
29	Most lateral point of the margin of the foramen magnum	b
30	Infratemporale	b
31	Stenion	b
32–34	Equally spaced points along the nuchal line	b
35–36	Equally spaced points along the temporal line	b
37–38	Equally spaced points along the supraorbiral line	b

Note: m = midsagittal landmark; b = bilateral landmark

Firstly, the 52 anatomical landmarks listed in Table 18.1 (#1-#31) were digitized on the surface of each cranium (Fig. 18.1). In addition, the superior nuchal, temporal and supraorbital curves were approximated using a seventh-order Bezier curve and a total of 14 equally-spaced points along each of the curves were also defined as landmarks (#32-#38). Therefore, a total of 66 landmarks were extracted for each cranium as non-sliding landmarks.

On one specimen chosen as a template from the reference database, we defined semi-landmarks based on the shortest paths connecting pairs of anatomical landmarks (Morita et al. 2013). Specifically, the above 66 non-sliding landmarks, as well as 14 equally-spaced points along the midsagittal curve (between the nasion and inion), were used to calculate the shortest paths connecting pairs of landmarks. The equally-spaced points along the paths were then computed (Fig. 18.2). A total of 85 landmarks including the 14 midsagittal equally-spaced points were designated as sliding semi-landmarks.

This template configuration was then used to determine the locations of the semi-landmarks on the other crania. For this, the coordinates of the 66 non-sliding landmarks were used to define a thin-plate function describing a mapping from the template configuration to a target specimen. The sliding landmarks from the template were deformed to the target specimen using this mapping function. The sliding landmarks were then projected onto and slid along the cranial surface of the target specimen so as to minimize the bending energy of the thin-plate spline method. This process is iterated until the solution converges. In the present study, Templand in the EVAN Toolbox (www.evan-society.org) is used to calculate the positions of the sliding landmarks corresponding to the two template configurations.

The morphology of each cranium was therefore represented by a total of 151 landmark coordinates that were evenly distributed across the cranial surface. In order to represent cranial shape variability, the landmark coordinates were normalized for centroid size and registered using the Generalized Procrustes Analysis using Morphologika geometric morphometric software (O'Higgins and Jones 2006). See O'Higgins and Jones (1998) and O'Higgins (2000) for more details about the calculation method.

18.2.3 Estimation of Missing Landmark Coordinates

Based on the sample of 56 complete specimens with 151 landmark coordinates, multivariate regressions are calculated with the missing coordinates as dependent variables and the other remaining coordinates as independent variables. Let $\Delta\mathbf{p}_i$ (i = 1..N) be the (3 × 1) position vector of the i-th missing landmark from the corresponding landmark on the averaged cranium (Procrustes consensus configuration), N be the number of missing coordinates and $\Delta\mathbf{x}$ be the ({3(151-N)} × 1) vector representing the deviations of the remaining landmark coordinates from the consensus configuration. The regression equations can be written as:

$$\Delta\mathbf{p}_i = \mathbf{A}_i \begin{bmatrix} \Delta\mathbf{x} \\ 1 \end{bmatrix}, \tag{18.1}$$

where $\mathbf{A}_i$ is the (3 × {3(151-N) + 1}) matrix of the regression coefficients for $\Delta\mathbf{p}_i$. Therefore, $\Delta\mathbf{p}_i$ corresponds to the dependent variables while $\Delta\mathbf{x}$ corresponds to the independent (explanatory) variables. To solve for $\mathbf{A}_i$, we exploited correspondence between $\Delta\mathbf{p}_i$ and $\Delta\mathbf{x}$ in the complete specimens. Specifically we solved the following simultaneous linear algebraic equations for $\mathbf{A}_i$.

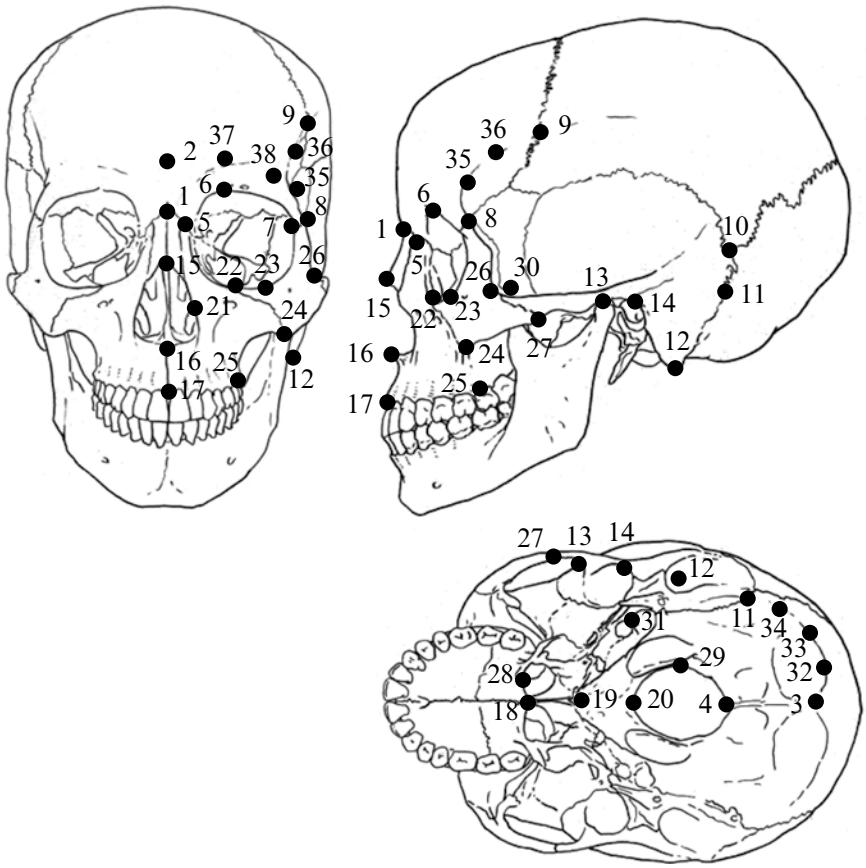

Fig. 18.1 The non-sliding landmarks used in the present study

$$\begin{aligned} &\mathbf{P} - \mathbf{A}_i \mathbf{X} = \mathbf{0} \\ &\mathbf{P} = \left[\Delta\mathbf{p}_{i,1} \quad \Delta\mathbf{p}_{i,2} \quad \cdots \quad \Delta\mathbf{p}_{i,S} \right] \\ &\mathbf{X} = \begin{bmatrix} \Delta\mathbf{x}_1 & \Delta\mathbf{x}_2 & \cdots & \Delta\mathbf{x}_S \\ 1 & 1 & \cdots & 1 \end{bmatrix} \end{aligned} \tag{18.2}$$

where $\Delta\mathbf{p}_{i,j}$ and $\Delta\mathbf{x}_j$ (j = 1..S) are $\Delta\mathbf{p}_i$ and $\Delta\mathbf{x}$ of the j-th complete specimen, respectively, and S is the number of reference specimens (=56).

As the number of equations ($3 \times 56 = 168$) is much less than the number of unknown coefficients ($3 \times \{3 \times (151 - 56) + 1\} = 858$), the problem is under-constrained and therefore no unique solution can be obtained. However, such an ill-posed problem can be made well-posed if the problem is regularized by introducing an additional constraint. Here we introduced a norm-minimization criterion to solve for the under-constrained linear algebraic equations to compute the regression coefficients. Using the Moore-Penrose pseudo-inverse matrix, the norm-minimizing solution for $\mathbf{A}_i$ can be computed as:

$$\begin{aligned} &\mathbf{A}_i^{\mathrm{T}} = \mathbf{X}^{+}\mathbf{P} \\ &\mathbf{X}^{+} = \mathbf{X}^{\mathrm{T}}\left(\mathbf{X}\mathbf{X}^{\mathrm{T}}\right)^{-1}, \end{aligned} \tag{18.3}$$

where $\boldsymbol{X}^{+}$ is the Moore-Penrose pseudo-inverse matrix of $\boldsymbol{X}$.

18.2.4 Virtual Crania with Missing Portions

In order to examine the efficacy of the proposed interpolation method, we virtually created two crania with missing portions. The missing landmarks in the crania were re-estimated using Eq. (18.1). Figure 18.3 shows the landmarks of the virtually-generated crania based on one specimen (KUMA554). For each specimen, we virtually created holes (missing portions) on the parietal, frontal and basicranial regions of each at two different sizes: small and large holes corresponding to 5 and 20 landmarks, respectively. The estimated coordinates of the missing landmarks were compared with their true values. The same coordinate estimations were also obtained based on the conventional geometric interpolation, i.e., the interpolation by deformation of the consensus cranium based on the thin-plate spline function defined using the existing portion of the crania.

18.3 Results

Figure 18.4 compares the estimated positions of the missing landmarks on the parietal region of the two crania with the true values of the corresponding landmarks. Here the cranial shape is represented by the wireframe connecting

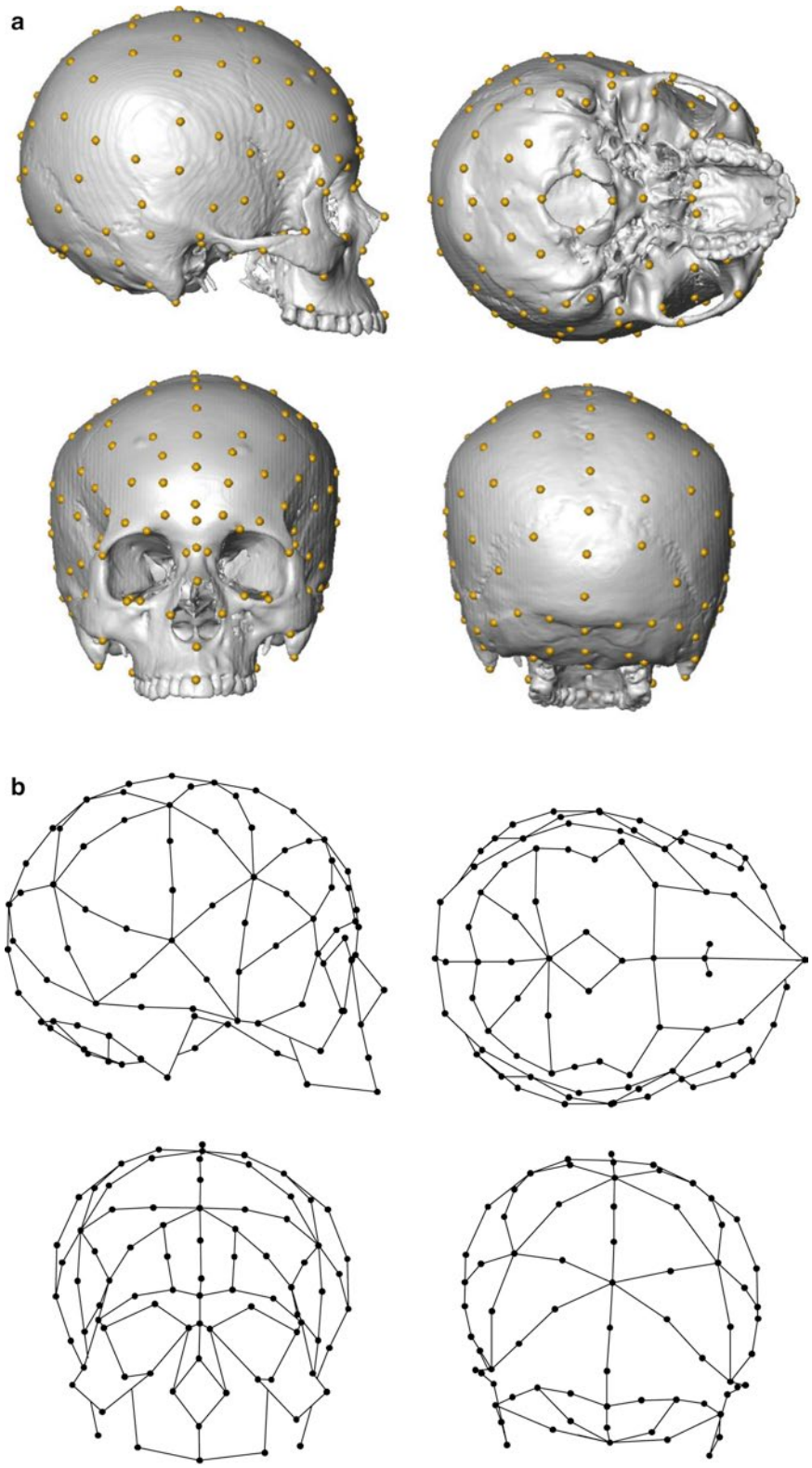

Fig. 18.2 (**a**) Sliding and non-sliding landmarks used in the present study. (**b**) Wireframe connecting landmarks for visualization of variation in cranial shape

the landmarks. Figures 18.5 and 18.6 compare the estimated and true positions of the missing landmarks on the frontal and basicranial regions, respectively. As illustrated, the estimated positions of the missing landmarks are located reasonably close to the corresponding landmarks on the original crania.

The mean prediction errors (± standard deviation) were 1.1 ± 0.3 mm and 1.6 ± 0.5 mm for the small and large parietal

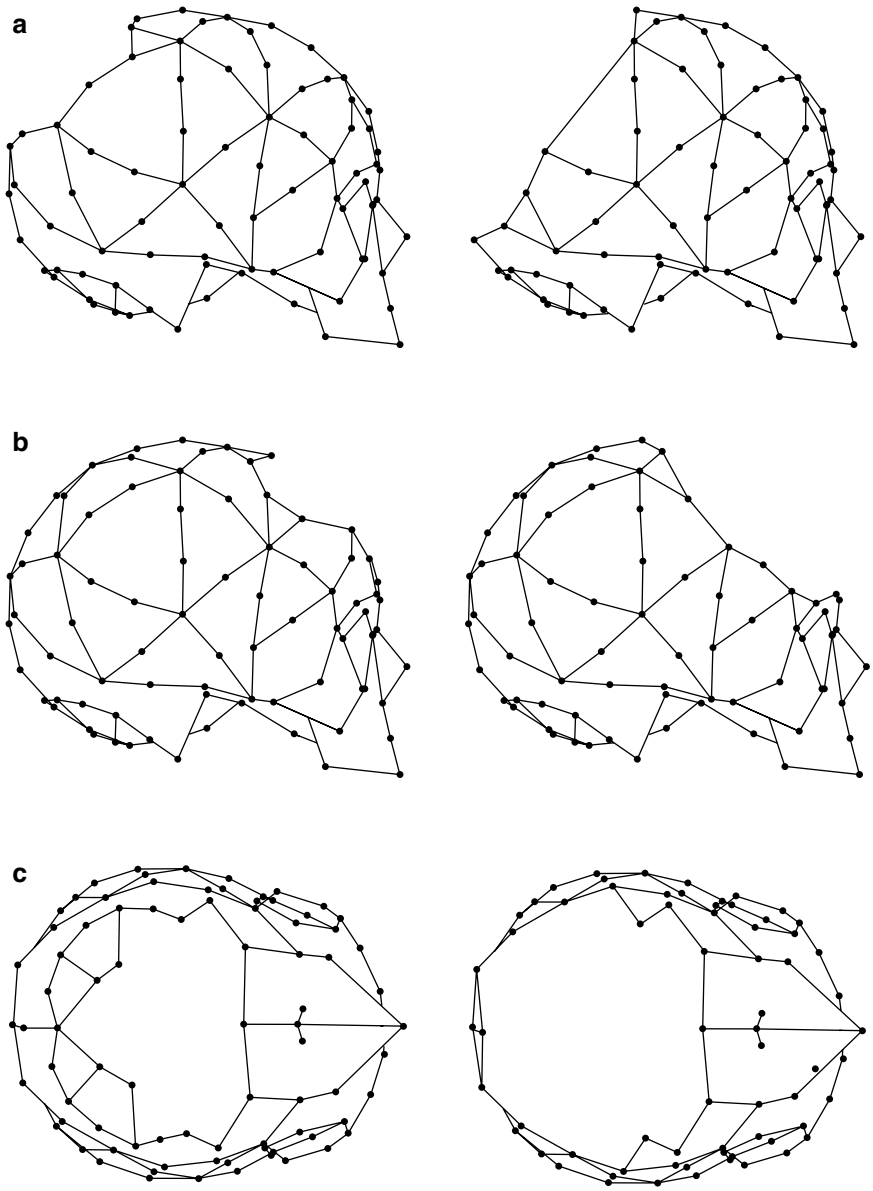

Fig. 18.3 Virtually generated crania with missing parts. (**a**) parietal, (**b**) frontal and (**c**) basicranial regions are missing. *Left* and *right columns* represent crania with small and large holes, respectively

holes on KUMA554, respectively, and 0.6±0.4 mm and 1.3±0.7 mm, respectively on KUMA1421. The maximum errors were 1.4 mm and 3.2 mm for the small and large parietal holes, respectively.

The mean prediction errors of the small and large holes on the frontal bone were 1.0±0.6 and 1.4±0.7 mm on KUMA554, respectively, and 0.7±0.3 and 1.1±0.6 mm, respectively on KUMA1421. The maximum errors were 1.8 mm and 3.1 mm for the small and large frontal holes, respectively.

The mean prediction errors of the small and large basicranial holes were 3.2±1.1 and 4.0±1.5 mm on KUMA554, respectively, and 2.5±1.3 and 4.1±1.8 mm, respectively on KUMA1421. The maximum errors were 4.3 and 9.0 mm for the small and large basicranial holes, respectively.

Figure 18.7 compares the mean prediction errors of the present method with those of the conventional geometric interpolation method. The results indicate that the prediction errors of the parietal and frontal holes in the present interpolation method are generally smaller than or equal to those of the geometric interpolation method. It was also observed that the predictive errors of the present method are significantly smaller than those of the conventional geometric method for the interpolation of large holes. However, much larger prediction errors were observed in the estimation of the basicranial region by both methods.

18.4 Discussion

In the present study, we attempted to interpolate missing portions of the human cranium based on a statistical interpolation method with a small number of specimens.

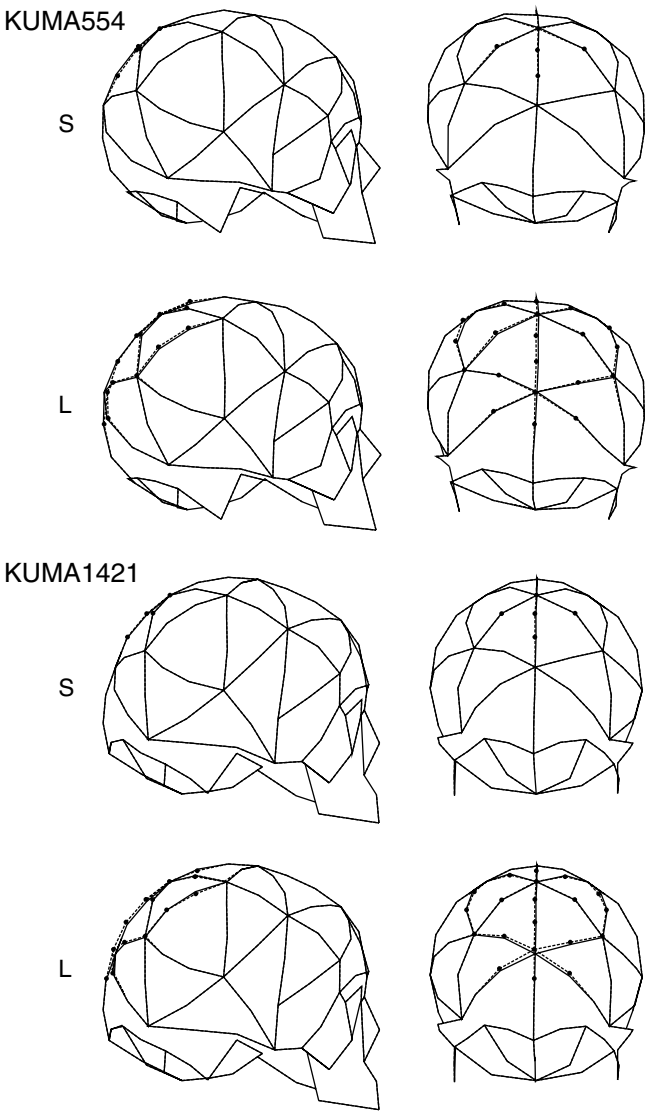

Fig. 18.4 Estimated positions of the missing landmarks in the parietal region. *Dots* represent the estimated coordinates. *S* and *L* indicate crania with small and large holes, respectively. *Dotted wireframe* = estimated. *Solid wireframe* = original

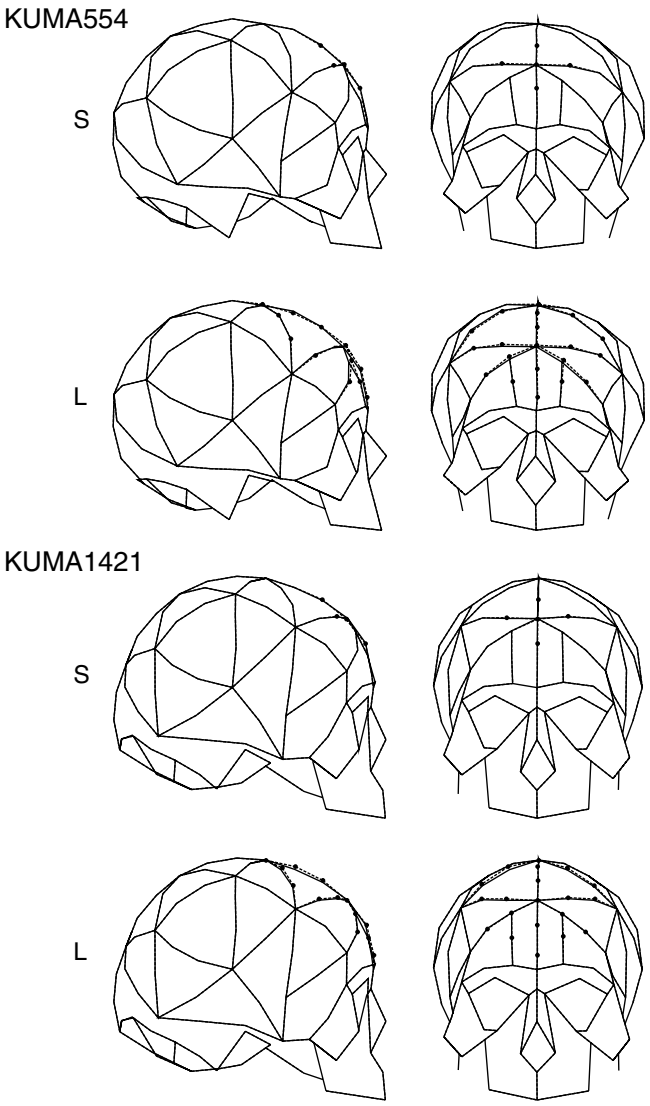

Fig. 18.5 Estimated positions of the missing landmarks in the frontal region. *Dots* represent the estimated coordinates. *S* and *L* indicate crania with small and large holes, respectively. *Dotted wireframe* = estimated. *Solid wireframe* = original

The mean prediction errors were found to be smaller than 2 mm, a magnitude of accepted error in estimation of missing landmarks (Neeser et al. 2009), in the frontal and parietal areas, indicating that the estimates are reasonably accurate. The present study also showed that the prediction errors were generally smaller than or equal to those of the conventional geometric interpolation method. The present method can therefore be used as a tool to estimate missing parts in human crania. In particular, if the missing portion is large, the performance of the present method tends to be much better than that of the conventional geometric method. This is consistent with Neeser et al. (2009) who noted that the thin-plate splines show comparatively larger errors in estimating landmarks over large areas.

However, it must be noted that the mean prediction errors were found to be much worse in the basicranial area. The cause of this discrepancy is currently obscure, but this fact may indicate that the shape of the basicranial region is correlates less with other parts of the cranium. Actually, it was suggested that the morphological relationship among various regions of the cranial base is poorly integrated (Bruner and Ripani 2008) possibly due to differential maturation of these structures (Bastir et al. 2006; Lieberman et al. 2000). This issue should be addressed in future studies. In any case, this estimation method seems not to be applicable to the estimation of missing landmarks in the basicranial region.

In the multivariate regression analysis, the relationship between dependent variables and independent variables are

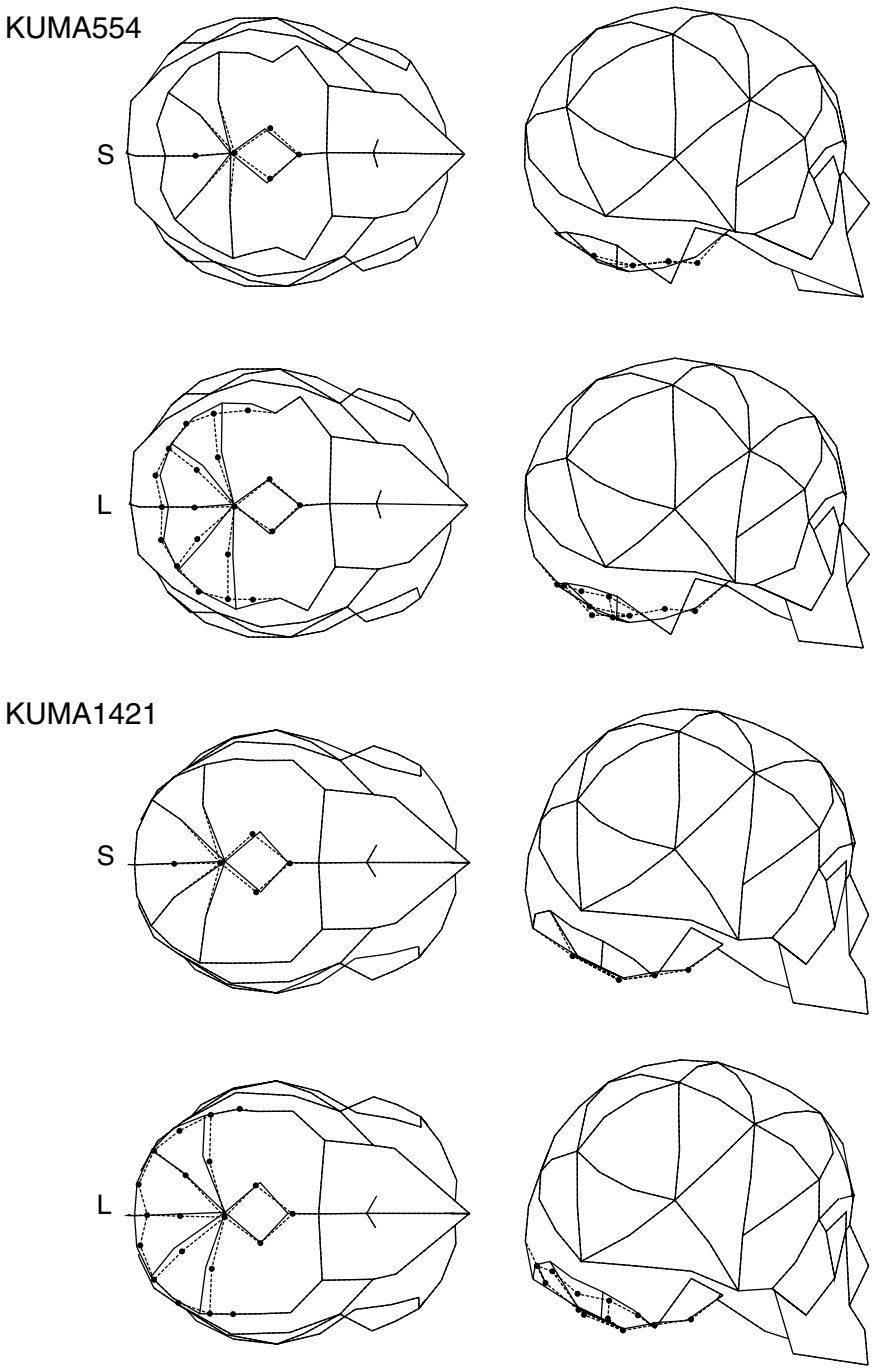

Fig. 18.6 Estimated positions of the missing landmarks in the basicranial region. *Dots* represent the estimated coordinates. *S* and *L* indicate crania with small and large holes, respectively. *Dotted wireframe* = estimated. *Solid wireframe* = original

generally determined based on the minimization of the least mean square error of the regression equations. For this, there must be more samples (equations) than unknown regression coefficients. However, if the number of landmarks representing the cranial morphology becomes large, accumulating a number of specimens larger than the number of landmarks becomes extremely difficult. In the present study, we introduced a norm-minimization criterion to solve for the regression equations with a small number of specimens that can be used for the multivariate regression analysis. What we have aimed for here is to minimize the norm of matrix $\mathbf{A}_i$ or, more precisely, the sum of the norms of the column vectors constituting $\mathbf{A}_i$. If the elements of $\mathbf{A}_i$ are all zero, $\Delta\mathbf{p}_i$ in Eq. (18.1) becomes zero and the estimated coordinates of the missing landmarks always correspond to those of the consensus configuration. Therefore, the regression equations solved based on the norm-minimization criterion would provide an estimation of the missing landmark coordinate that is closest to the corresponding landmark coordinate in the consensus configuration (where $\Delta\mathbf{p}_i = \mathbf{0}$). This may explain why

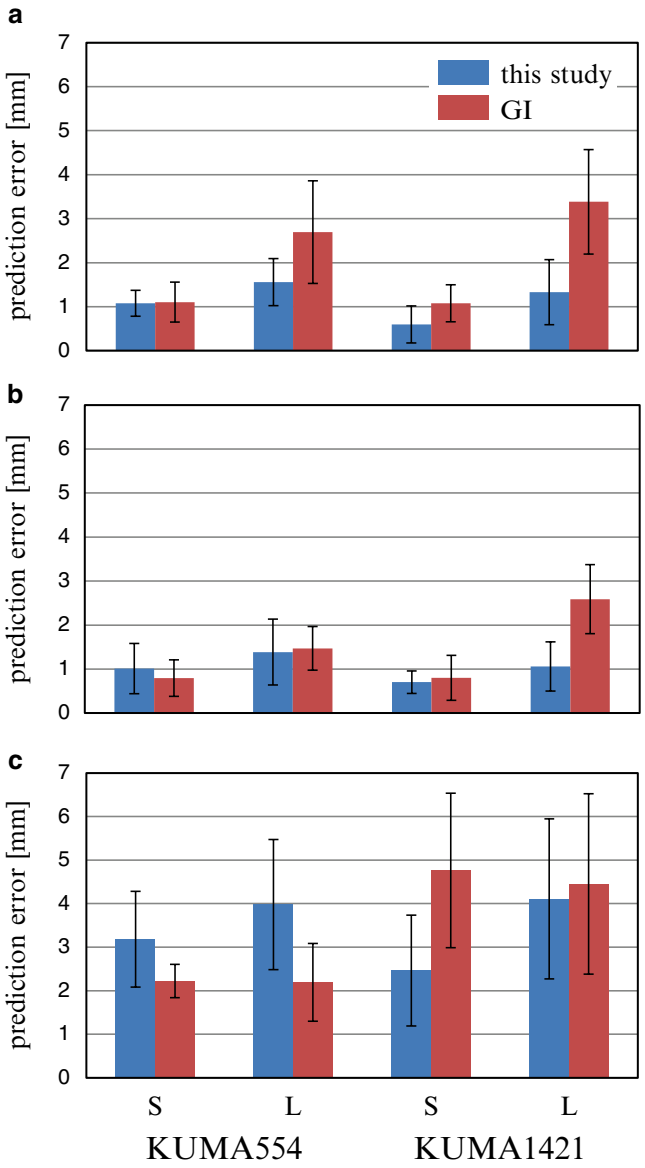

Fig. 18.7 Comparisons of the prediction errors of the missing landmark coordinates between the present method and the conventional geometric interpolation (GI). *S* and *L* indicate the prediction errors of the small and large holes, respectively. The *error bars* represent one standard deviation. (**a**) parietal, (**b**) frontal and (**c**) basicranial regions

the proposed method shows a good predictive performance. However, the predictive performance must be further tested with a larger number of datasets.

In future, we plan to apply the proposed method for reconstruction to Neanderthal fossil crania. However, this will be a challenge since the shape of the modern human crania is certainly very different from that of Neanderthals, and the specificity of the sample must be taken into account when using reference populations. A practical application of the proposed method to actual fossil crania should be investigated in future studies.

Acknowledgements We wish to express our sincere gratitude to Prof. Takeru Akazawa (Kochi Institute of Technology) for giving us an opportunity to participate in this research project and for his continuous guidance and support throughout the course of the present study. This study was supported by a Grant-in-Aid for Scientific Research on Innovative Areas, "Replacement of Neanderthals by Modern Humans: Testing Evolutionary Models of Learning," from the Japanese Ministry of Education, Culture, Sports, Science and Technology.

References

Bastir M, Rosas A, O'Higgins P (2006) Craniofacial levels and the morphological maturation of the human skull. J Anat 209:637–654

Bookstein FL (1997) Landmark methods for forms without landmarks: morphometrics of group differences in outline shape. Med Image Anal 1:225–243

Bruner E, Ripani M (2008) A quantitative and descriptive approach to morphological variation of the endocranial base in modern humans. Am J Phys Anthropol 137:30–40

Gunz P, Mitteroecker P, Neubauer S, Weber GW, Bookstein FL (2009) Principles for the virtual reconstruction of hominin crania. J Hum Evol 57:48–62

Lieberman DE, Ross C, Ravosa M (2000) The primate cranial base: ontogeny function and integration. Yrbk Phys Anthropol 43:117–169

Morita Y, Ogihara N, Kanai T, Suzuki H (2013) Quantification of neurocranial shape variation using shortest paths connecting pairs of anatomical landmarks. Am J Phys Anthropol 151:658–666

Neeser R, Ackermann RR, Gain J (2009) Comparing the accuracy and precision of three techniques used for estimating missing landmarks when reconstructing fossil hominin crania. Am J Phys Anthropol 140:1–18

O'Higgins P (2000) The study of morphological variation in the hominid fossil record: biology, landmarks and geometry. J Anat 197: 103–120

O'Higgins P, Jones N (1998) Facial growth in *Cercocebus torquatus*: an application of three-dimensional geometric morphometric techniques to the study of morphological variation. J Anat 193: 251–272

O'Higgins P, Jones N (2006) Tools for statistical shape analysis. Hull York Medical School. http://hyms.fme.googlepages.com/resources

Weaver TD, Hublin JJ (2009) Neandertal birth canal shape and the evolution of human childbirth. Proc Natl Acad Sci U S A 106: 8151–8156

Transferring Semi-Landmarks by Minimizing Bending Energy on Surfaces

19

Masaki Moriguchi, Hiromasa Suzuki, Takashi Michikawa, Naomichi Ogihara, and Osamu Kondo

Abstract

Semi-landmarks play an important role in the analysis of the fossil crania. While anatomical landmarks can be located reliably, locating semi-landmarks consistently is difficult because they are generally distributed around featureless regions and cannot be located using local shape descriptors.

We consider the problem of semi-landmark transfer in this research: given a surface mesh A (with landmarks P_A and semi-landmarks Q_A) and a surface mesh B (with landmarks P_B), transfer the semi-landmarks of A onto B. In other words, compute the positions of semi-landmarks Q_B of B using P_A, Q_A and P_B. We solve this problem using a surface-based deformation technique: we minimize the bending energy of the deformation *over the surface* rather than over the whole 3D space (which is the case of sliding semi-landmarks).

Keywords

Crania • Semi-landmarks • Surface-based deformation

19.1 Introduction

Estimating the positions of semi-landmarks is important in the analysis of the fossil crania (Gunz et al. 2009). While anatomical landmarks can be located reliably, locating semi-landmarks consistently is difficult task because they are generally distributed around featureless regions and cannot be located them using local shape descriptors.

To estimate the positions of semi-landmarks, the problem of semi-landmark transfer is considered in this research. Given a surface mesh A (the source model with landmarks P_A and semi-landmarks Q_A) and a surface mesh B (the target model with landmarks P_B), the semi-landmarks of A are transferred onto B. In other words, the positions of B's semi-landmarks Q_B are computed using P_A, Q_A and P_B. It is assumed that landmarks $P_A = \left\{p_A^i\right\}_{i=1}^k$ and $P_B = \left\{p_B^i\right\}_{i=1}^k$ have the same size, and that each landmark p_A^i on A has a corresponding landmark p_B^i on B ($i=1,\cdots,k$). Similarly, semi-landmarks $Q_A = \left\{q_A^i\right\}_{i=1}^l$ and $Q_B = \left\{q_B^i\right\}_{i=1}^l$ have the same size, and each semi-landmark q_A^i on A corresponds to the semi-landmark q_B^i on B ($i=1,\cdots,l$). Figure 19.1 shows input for the semi-landmark transfer problem.

The sliding semi-landmark method (Bookstein 1997) is the standard approach to semi-landmark transfer. With this technique, semi-landmarks are transferred to minimize the bending energy of the thin-plate spline warp (Bookstein 1989) between $P_A \cup Q_A$ and $P_B \cup Q_B$. This minimization problem is

M. Moriguchi (✉)
Department of Information and System Engineering, Chuo University, 1-13-27 Kasuga, Bunkyo-ku, Tokyo 112-8551, Japan
e-mail: moriguchi@ise.chuo-u.ac.jp

H. Suzuki • T. Michikawa
Research Center for Advanced Science and Technology, University of Tokyo, Komaba 4-6-1, Meguro-ku, Tokyo 153-8904, Japan
e-mail: suzuki@den.rcast.u-tokyo.ac.jp; michi@den.rcast.u-tokyo.ac.jp

N. Ogihara
Department of Mechanical Engineering, Faculty of Science and Technology, Keio University, 3-14-1 Hiyoshi, Kohoku-ku, Yokohama, Kanagawa 223-8522, Japan
e-mail: ogihara@mech.keio.ac.jp

O. Kondo
Department of Biological Sciences, Graduate School of Science, University of Tokyo, 7-3-1 Hongo, Bunkyo-ku, Tokyo 113-0033, Japan
e-mail: kondo-o@biol.s.u-tokyo.ac.jp

T. Akazawa et al. (eds.), *Dynamics of Learning in Neanderthals and Modern Humans Volume 2: Cognitive and Physical Perspectives*, Replacement of Neanderthals by Modern Humans Series, DOI 10.1007/978-4-431-54553-8_19, © Springer Japan 2014

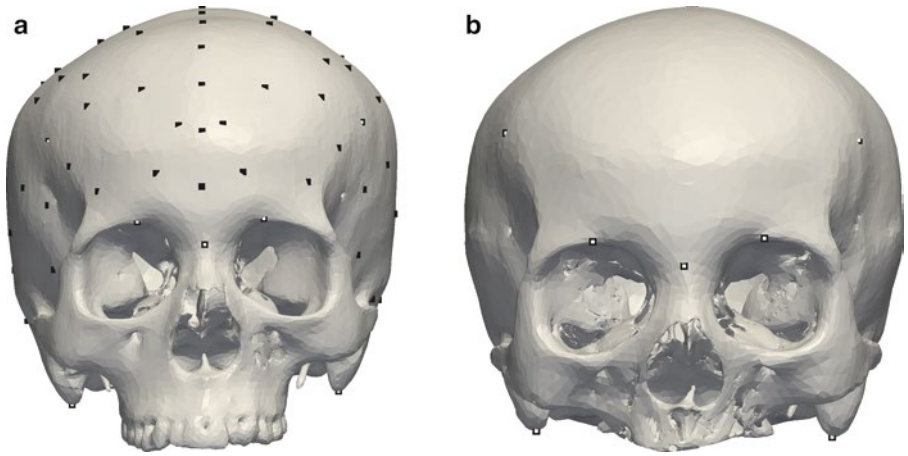

Fig. 19.1 Input of semi-landmark transfer: (**a**) source model with landmarks and semi-landmarks; (**b**) target model with landmarks. *White dots* indicate landmarks and *black dots* indicate semi-landmarks

solved by applying the following procedures iteratively (Gunz et al. 2005):

1. Tangential optimization: under the constraint that each semi-landmark is allowed to move only along the tangent plane, semi-landmark positions are updated by minimizing the bending energy of the thin-plate spline warp.
2. Projection: the optimized semi-landmarks are projected onto the closest points on the surface.

As the semi-landmarks deviate from the surface after tangential optimization, they need to be projected back onto the surface. The thin-plate spline deformation technique is a fundamental tool in the sliding method, but has the following disadvantages:

- The bending energy over the whole 3D space is considered and minimized; however, we are only interested in a region around the surface of the cranium.
- When a thin-plate spline deformation function is determined, only a small set of discrete points on the surface (i.e. landmarks and semi-landmarks in this case) is considered and other points on the surface are ignored.

Although the latter problem is alleviated to some degree by tangential optimization and projection, the sliding method has the same disadvantages.

The proposed method for semi-landmark transfer is also based on an energy minimization approach, but involves the minimization of the bending energy *over the surface* rather than over the whole 3D space (which is the case of the sliding method). The proposed approach has the following characteristics in contrast to those of the sliding method:

- Only bending energy over the surface of the cranium is considered and minimized.
- When a deformation function is determined, all the vertices and triangles on the surface mesh are considered (via the use the Laplace–Beltrami operator).

As more surface information is used in this technique than in the sliding method, more accurate transfer results can be expected. The minimization leads to a bi-Laplace equation, which can be solved discretely as a sparse linear system.

19.2 Method

19.2.1 Overview

While the sliding method involves the deformation of the whole 3D space, only the surface is deformed in the proposed approach via a technique called *surface-based deformation* (Botsch and Sorkine 2008). Such deformation (or more specifically Laplacian mesh deformation) is computed by minimizing the bending energy over the surface. In this work, we assume that the surface is discretized and represented as a triangle mesh. Minimizing the bending energy over the surface mesh is equivalent to solving the bi-Laplacian system:

$$L^2 \boldsymbol{x} = \boldsymbol{0}, \tag{19.1}$$

where L is a Laplacian matrix (a discretization of the Laplace-Beltrami operator) and x is a variable vector.

Additionally the interpolation condition is enforced (i.e. the landmarks on the source model are transformed to the landmarks on the target model) and a constrained optimization is solved, minimizing

$$\boldsymbol{x}^{\mathrm{T}} L^{\mathrm{T}^2} L^2 \boldsymbol{x}, \tag{19.2}$$

subject to the interpolation condition. Suppose that the constraint is expressed as

$$Cx = b, \tag{19.3}$$

for a constraint matrix C. Then, using the Lagrange multiplier method, the following linear system is obtained:

$$\begin{pmatrix} L^{T^2} L^2 & C^T \\ C & O \end{pmatrix} \begin{pmatrix} x \\ \lambda \end{pmatrix} = \begin{pmatrix} 0 \\ b \end{pmatrix}, \tag{19.4}$$

where λ is the vector of the Lagrange multipliers.

19.2.2 The Linear System

As in Allen et al. (2003), we assign an Affine transformation to each vertex of the mesh and compute it by minimizing the bending energy. Since the landmarks P_A on A corresponds to the landmarks P_B on B, we set hard constraints: P_A is transformed to P_B. This constrained optimization can be solved by the Lagrange multiplier method and it reduces to the linear system as shown in Welch and Witkin (1992).

Let

$$\begin{pmatrix} a^i_{1,x} & a^i_{2,x} & a^i_{3,x} & a^i_{4,x} \\ a^i_{1,y} & a^i_{2,y} & a^i_{3,y} & a^i_{4,y} \\ a^i_{1,z} & a^i_{2,z} & a^i_{3,z} & a^i_{4,z} \\ 0 & 0 & 0 & 1 \end{pmatrix} \tag{19.5}$$

be the Affine transformation assigned to the ith vertex of the surface mesh A. Then, for x-coordinates, we solve the following linear system:

$$\begin{pmatrix} L^{T^2} L^2 \otimes I_4 & C^T \\ C & O \end{pmatrix} \begin{pmatrix} a_x \\ \lambda_x \end{pmatrix} = \begin{pmatrix} 0 \\ b_x \end{pmatrix}, \tag{19.6}$$

where L is a Laplacian matrix, $\otimes$ denotes the Kronecker product, I_4 is the identity matrix of size 4, a_x is a variable corresponding to the Affine transformations, $Ca_x = b_x$ is the set of the hard constraints, and $\boldsymbol{\lambda}_x$ is the vector of the Lagrange multipliers. Specifically,

$$a_x = \left(a^1_{1,x} \;\; a^1_{2,x} \;\; a^1_{3,x} \;\; a^1_{4,x} \;\; a^2_{1,x} \;\; a^2_{2,x} \;\; a^2_{3,x} \;\; a^2_{4,x} \;\; \cdots \right).$$

$L^{T^2} L^2$ corresponds to the bi-Laplacian system, and the ith row of $Ca_x = b_x$ corresponds to the constraint by which p^i_A is transformed into p^i_B $(i = 1, \cdots, k)$. The linear system is large and sparse, and its size is $(4n+k) \times (4n+k)$, where n is the number of the vertices of the surface mesh A and k is the number of the landmarks. There are similar linear systems for y- and z-coordinates. Solving these three linear systems gives the Affine transformations of the vertices.

It should be noted that, since the coefficient matrices of the linear system for y- and z-coordinates are the same as that of the linear system for x-coordinates, the decomposition results can be reused to save the computational time of the linear solves.

19.2.3 Numerical Stability

The area-normalized cotangent weighting is a better discretization of the Laplace–Beltrami operator. However, its Laplacian matrix is asymmetric and it causes numerical stability issues for the problem at hand (i.e. the linear system that contains $L^{T^2} L^2$). Accordingly, the unnormalized cotangent weighting is used for the discretization of the Laplace-Beltrami operator. For a linear solver, we use UMFPACK (Davis 2004).

19.3 Experimental Results

We applied the proposed method to two modern Japanese crania (housed at Kyoto University), which are represented as triangle meshes. One is used as a source model and the other is used as a target model. The target model has missing parts on maxilla, where neither landmarks nor semi-landmarks are located. The source model has 13 landmarks (anatomical landmarks) and 93 semi-landmarks as shown in Fig. 19.2, and the target model has 13 landmarks as shown in Fig. 19.3. The semi-landmarks were placed at equally spaced points along the shortest paths between landmarks (Morita et al. 2011). The semi-landmarks on the source model were transferred onto the target model via the surface-based deformation.

Before applying the surface-based deformation, we first simplified the models into meshes with 100,000 faces to reduce the computational time and space, and to increase the numerical stability. Then we start performing semi-landmark transfer by minimizing the bending energy over the surface. As a comparison, we also applied the sliding method to the same input. The results of transfer using the both methods are shown in Fig. 19.4. In this figure, we can see that many of the semi-landmarks computed using the proposed method are positioned to the right of those computed using the sliding method. Because the source model has a bump at the left side, the deformation from the source model to the target model should pull back the bump (i.e. move it to the right). We estimate that the influence of this pull-back effect is stronger in the surface-based deformation and that this is the reason for the differences in the results.

19.4 Conclusions

In this research, we propose a method for semi-landmark transfer using surface-based deformation. By minimizing the bending energy of the deformation over the surface, we can transfer the semi-landmarks on the source model into the target model. This minimization problem reduces to a large sparse linear system. The preliminary experiments indicated

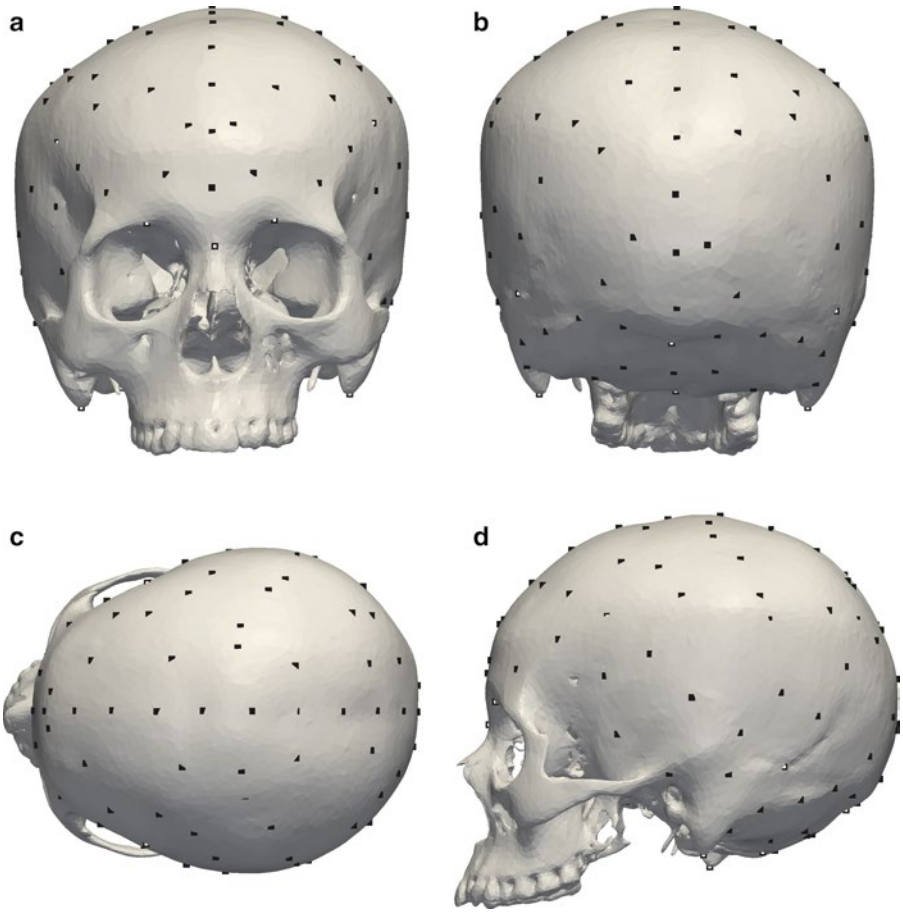

Fig. 19.2 Source model with landmarks and semi-landmarks: (**a**) frontal view; (**b**) posterior view; (**c**) superior view; (**d**) lateral view. *White dots* indicate landmarks and *black dots* indicate semi-landmarks

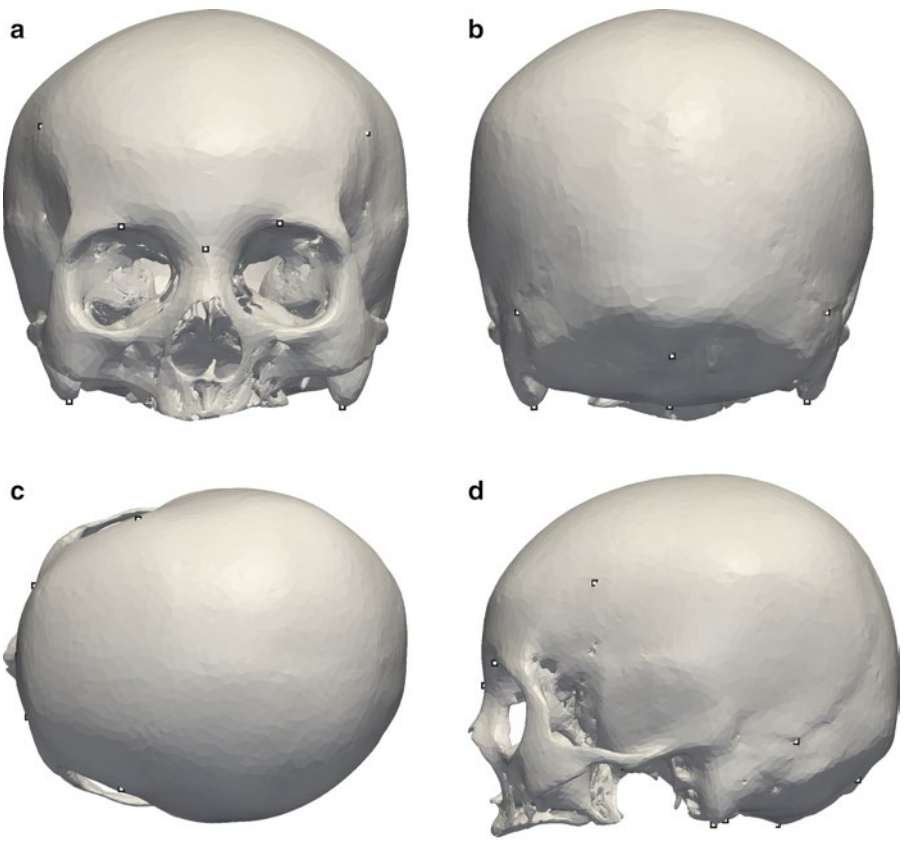

Fig. 19.3 Target model with landmarks: (**a**) frontal view; (**b**) posterior view; (**c**) superior view; (**d**) lateral view. *White dots* indicate landmarks

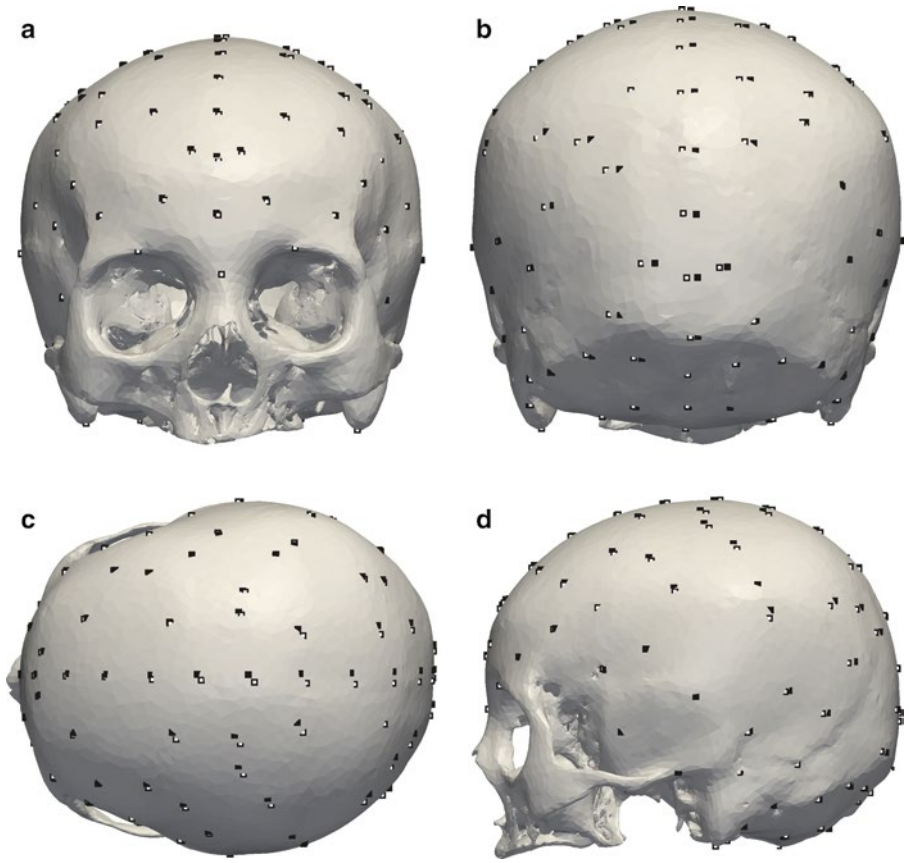

Fig. 19.4 Transferred semi-landmarks on the target model: (**a**) frontal view; (**b**) posterior view; (**c**) superior view; (**d**) lateral view. *White dots* indicate the results of the sliding method and *black dots* indicate the results of the proposed method

that the proposed method is more sensitive to the geometric differences between the source model and the target model than the sliding method.

As a future research, we plan to improve the transfer results by adding positional soft-constraints to the linear system to enable better alignment of the vertices (other than the landmarks) for higher-quality results.

Acknowledgements The authors would like to thank the anonymous reviewers for their valuable comments. This work was supported by MEXT Grant-in-Aid for Scientific Research on Innovative Areas (No. 22101006).

References

Allen B, Curless B, Popovic Z (2003) The space of human body shapes: reconstruction and parameterization from range scans. In: Proceedings of SIGGRAPH, San Diego, pp 587–594

Bookstein FL (1989) Principal warps: thin-plate splines and the decomposition of deformations. IEEE Trans Pattern Anal Mach Intell 11:567–585

Bookstein FL (1997) Landmark methods for forms without landmarks: morphometrics of group differences in outline shape. Med Image Anal 1:225–243

Botsch M, Sorkine O (2008) On linear variational surface deformation methods. IEEE Trans Vis Comput Graph 14:213–230

Davis TA (2004) A column pre-ordering strategy for the unsymmetric-pattern multifrontal method. ACM Trans Math Softw 30:165–195

Gunz P, Mitteroecker P, Bookstein FL (2005) Semilandmarks in three dimensions. In: Slice DE (ed) Modern morphometrics in physical anthropology. Springer, New York

Gunz P, Mitteroecker P, Neubauer S, Weber GW, Bookstein FL (2009) Principles for the virtual reconstruction of hominin crania. J Hum Evol 57:48–62

Morita Y, Kikuchi T, Ogihara N, Kanai T, Suzuki H (2011) A method to quantify neurocranial shape variation based on calculation of shortest paths connecting anatomical landmarks. Anthropol Sci 119:300

Welch W, Witkin A (1992) Variational surface modeling. In: Proceedings of SIGGRAPH, Chicago, pp 157–166

CT Image Segmentation for Bone Structures Using Image-Based FEM

20

Hiromasa Suzuki, Hiroyuki Hishida, Takashi Michikawa, Yutaka Ohtake, Satoshi Oota, Naomichi Ogihara, and Osamu Kondo

Abstract

We propose a CT image segmentation method using structural analysis. The aim of our research is to decompose assembled fossil of skeletons and crania into fragments in the area of fossil reconstruction. One challenge specific to this type of segmentation procedure is the separation of fragments where their gaps are not necessarily clear. We previously proposed a method of segmenting CT images using structural analysis. This technique is based on the assumption that the interference area (joint) between components (bones) is structurally weak. We compute strain, which tends to be large in structurally weak areas and segment the image in the region of high strain. With this approach, there is a need to specify boundary conditions for the structural analysis, namely, loading conditions (loading forces and their positions) and locations of fixed boundaries. In our previous work, we proposed a method of optimizing loading forces given loading positions and fixed boundary positions. In this study, we propose a method to find both of those positions to automate the segmentation procedure. Some segmentation results generated by our prototype software demonstrate applicability of the proposed method.

Keywords

Fossil reconstruction • Image processing • Segmentation • Structural analysis

H. Suzuki (✉) • H. Hishida • T. Michikawa
Research Center for Advanced Science and Technology, University of Tokyo, Komaba 4-6-1, Meguro-ku, Tokyo 153-8904, Japan
e-mail: suzuki@den.rcast.u-tokyo.ac.jp; hiroyuki_hishida@ihi.co.jp; michi@den.rcast.u-tokyo.ac.jp

Y. Ohtake
Department of Precision Engineering, University of Tokyo, Komaba 4-6-1, Meguro-ku, Tokyo 153-8904, Japan
e-mail: yu-ohtake@den.rcast.u-tokyo.ac.jp

S. Oota
RIKEN BioResource Center, 3-1-1 Koyadai, Tsukuba, Ibaraki 305-0074, Japan
e-mail: oota@riken.jp

N. Ogihara
Department of Mechanical Engineering, Faculty of Science and Technology, Keio University, 3-14-1 Hiyoshi, Kohoku-ku, Yokohama, Kanagawa 223-8522, Japan
e-mail: ogihara@mech.keio.ac.jp

O. Kondo
Department of Biological Sciences, Graduate School of Science, University of Tokyo, 7-3-1 Hongo, Bunkyo-ku, Tokyo 113-0033, Japan
e-mail: kondo-o@biol.s.u-tokyo.ac.jp

T. Akazawa et al. (eds.), *Dynamics of Learning in Neanderthals and Modern Humans Volume 2: Cognitive and Physical Perspectives*, Replacement of Neanderthals by Modern Humans Series, DOI 10.1007/978-4-431-54553-8_20, © Springer Japan 2014

20.1 Introduction

We propose a CT image segmentation method using structural analysis. The aim of our research is to decompose assembled fossil of skeletons and crania into fragments in the area of fossil reconstruction. X-ray CT is used to scan an assembly, then its image is manually segmented into bone pieces. Figure 20.1a, b show the CT image of the fossil cranium and the segmentation results respectively. Considering the number of fragments involved, it is desirable for this segmentation procedure to be automatic. A challenge specific to this segmentation procedure is the separation of fragments where their gaps are not necessarily clear. Various image segmentation methods are available, such as approaches based on active contour (Kass et al. 1988; Pardo et al. 2001; Sebastian et al. 2003), region growing method (Adams and Bischof 1994; Joliot and Mazoyer 1993; Mat-Isa et al. 2005), watershed method (Vincent and Soille 1991; Grau et al. 2004; Hahn et al. 2006), and graph-cut method (Boykov and Funka-Lea 2006). However, none of these match our objectives.

For this reason, we previously proposed a method of segmenting CT images using structural analysis (Hishida 2013). The technique is based on the assumption that the interference area (joint) between components (bones) is structurally weak. Figure 20.2 shows the flow of computation of this method. Figure 20.2a shows the input image of the bone pieces with their joints indicated in red. (b) shows white ROIs (region of interest) which are specified by the user. Then loading forces shown in (c) and (d) are applied to these ROIs. We compute strain using image-based FEM (finite element method) analysis (Bendsoe and Kikuchi 1988), where each pixel (or voxel in 3D) is used as a structural element of FEM (Rao 2005). As the strain tends to be large in structurally weak areas, we remove such pixels in the regions of high strain. We iterate strain calculation and removal until the input image is decomposed into multiple fragments. Figure 20.2e shows the decomposed image and (f) shows segmented regions. The method can be used to segment low-contrast CT images—a task that is difficult with conventional methods.

The main advantage of the proposed approach is its reliability; because it involves structural analysis, appropriate object segmentation in structurally weak areas is guaranteed.

20.2 Methods

20.2.1 Strain Computation Using FEM

Our method is based on the computation of strain over the image using image-based FEM. First region of an object in the image is selected by a standard thresholding method. In Fig. 20.3, each cube corresponds to a pixel p of an object in an image and also acts as a finite element of FEM. The corners of these cubic elements are nodal points which have freedom of displacement $\boldsymbol{x}$. We specify fixed boundaries and loading forces to those nodes. At the fixed nodes, their displacements are restricted. The loading forces applied to these nodes are represented as a vector $\boldsymbol{f}$. For each element, we specify material properties such as Young's modulus and Poisson ratio based on its pixel value (CT value). Then we can compute stiffness matrix $\boldsymbol{K}$ of the system which relate the displacement $\boldsymbol{x}$ and loading forces $\boldsymbol{f}$ as follows:

$$\boldsymbol{K}\boldsymbol{x} = \boldsymbol{f}. \tag{20.1}$$

By solving this equation, we can obtain the displacement of the nodes from which von Mises strain $\epsilon(p)$ is computed at each pixel p.

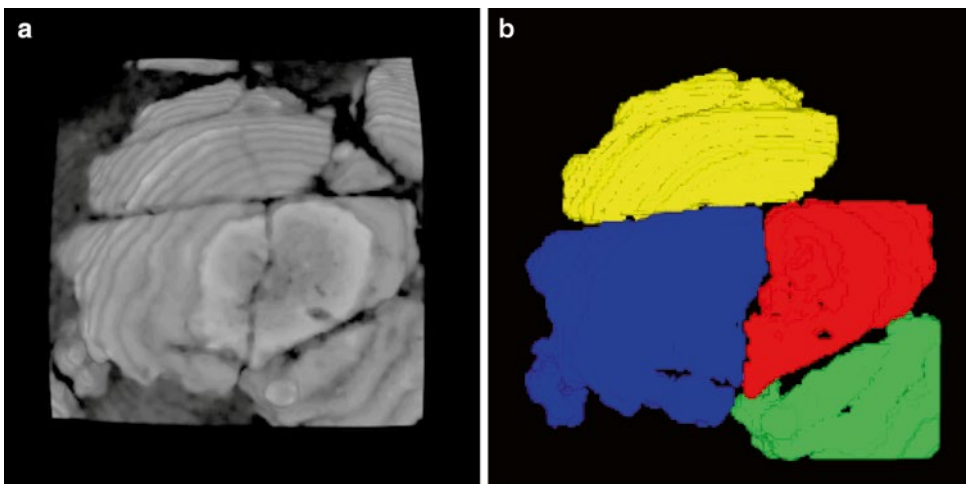

Fig. 20.1 CT image of fossil cranium with assembled fragments (**a**). Segmentation results (**b**)

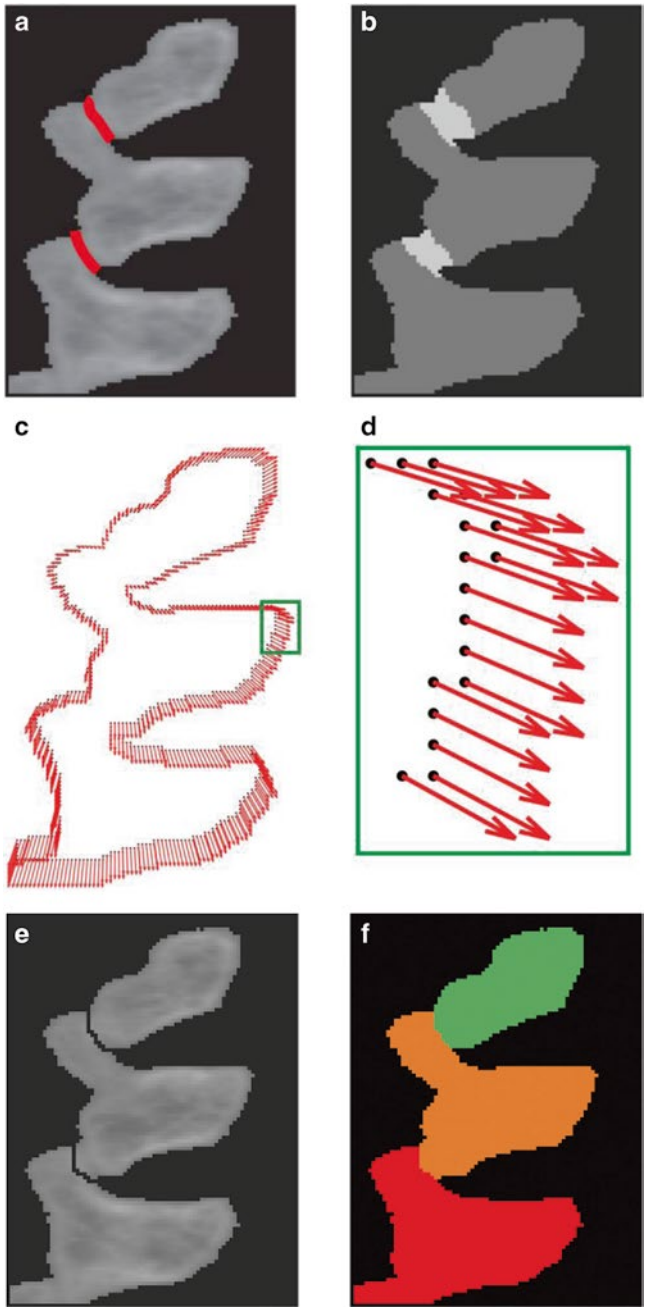

Fig. 20.2 Flow of proposed segmentation procedures. Desired segmentation boundaries in CT image (**a**). ROI (region of interest) involving the boundaries (**b**). Estimated loading forces on the boundaries (**c**) and zoomed in view (**d**). Removed pixels on the boundaries (**e**) and segmentation results (**f**)

20.2.2 Estimation of Loading Forces

Our aim is to minimize efforts required for data input by the user. In our previous paper (Hishida et al. 2012), we proposed a method to automatically estimate $\boldsymbol{f}$, that is, the directions and strengths of the loading forces. After specifying the nodes of loading forces, fixed points and ROI which roughly surround the desired segmentation boundaries, the directions and strengths of the loading forces are estimated by solving an optimization problem. We introduce the following objective function to maximize to find $\boldsymbol{f}$:

$$F(\boldsymbol{f}) = \sum_{p \in ROI} \varepsilon(p)^2 \rightarrow \max. \tag{20.2}$$

The purpose of this function is to maximize the sum of squared strain of pixels in the ROI. The gradient ascent method is used to find a maximum of the function.

$$\boldsymbol{f} = \boldsymbol{f} + \lambda \nabla F(\boldsymbol{f}), \tag{20.3}$$

where λ is a step size. The loading forces shown in Fig. 20.2b, c are computed by this method.

20.2.3 Estimation of Positions of Fixed Nodes and Loading Nodes

It is tedious for the user to specify all the fixed and loading nodes, particularly in the case of 3D image segmentation. As each node can be fixed or loaded, the number of their combinations is exponential to the number of nodes. It is impossible, in practice, to find the optimal boundary condition of fixed and loading nodes, so we separate the boundary nodes into several groups as shown in Fig. 20.4. We call these fragments. A fragment consists of three types; fixed, loaded, and free. The nodes in a fragment are set to be fixed, loaded, or freed according to its fragment type.

In 2D images, given some initial number of fragments, we uniformly decompose the boundary to define segments. Then, we specify the fragment type to compute the distribution of the strain using the method described in the previous subsection. We check all possible fragment type assignments to find the best one which maximizes the objective function $F(\boldsymbol{f})$ (see Fig. 20.5). In case the value of the function is below the user- specified threshold, the number of the fragments is increased and the above procedure is repeated. For 3D images, we use the Lloyd clustering method to define fragments. First, we randomly select the given number of boundary nodes as *sites*. Then, we group all the other nodes to their nearest site. Finally, we move the sites to the center of the group. This process is iterated until the sites are stable.

20.3 Results

We developed a prototype software based on the methods described in the previous section and applied it to the CT images of bone structures. Figure 20.6 shows a 2D example. (a) is the input image and (b) is the segmentation results. In Fig. 20.2a the boundary between the bone fragments is not

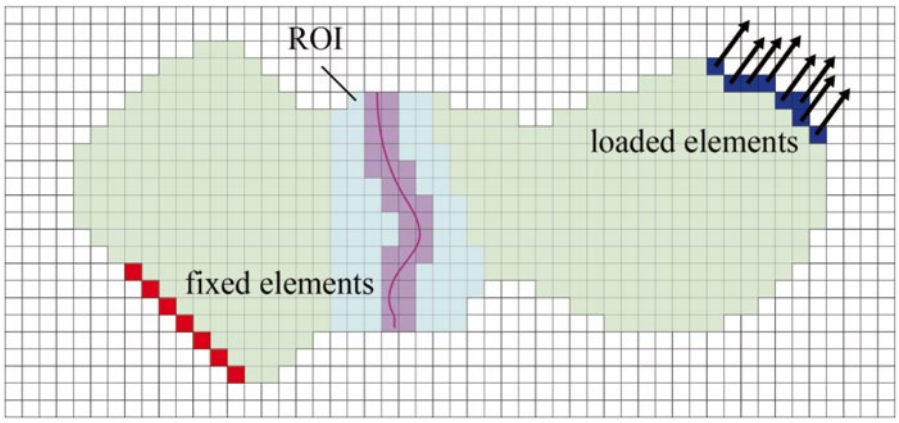

Fig. 20.3 Image-based FEM. Fixed elements, loaded elements and elements in ROI

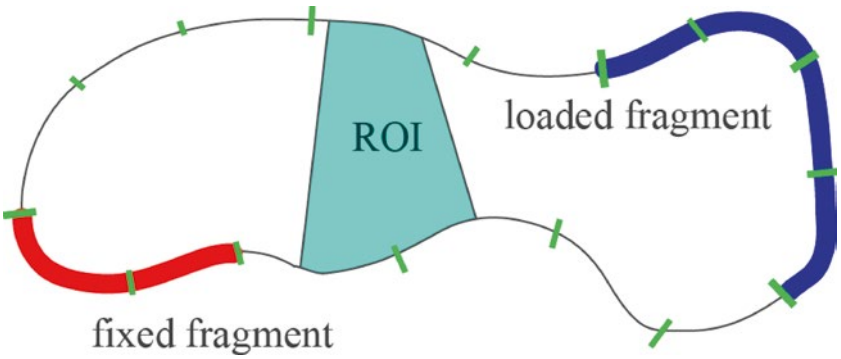

Fig. 20.4 Decomposition of boundary into fragments. Fragments consist of three types; fixed, loaded and free

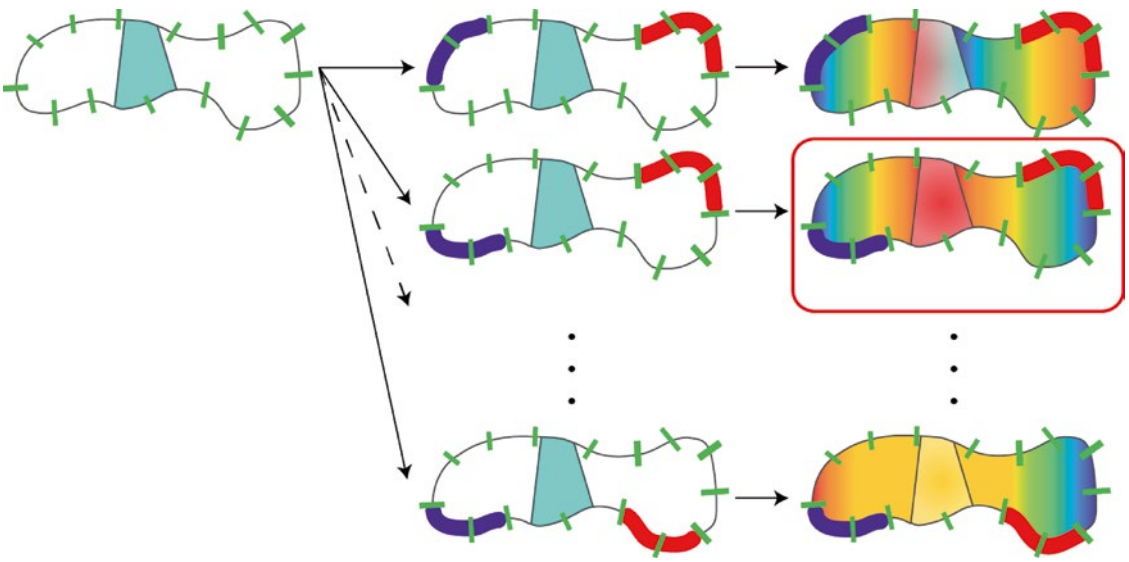

Fig. 20.5 To assign types to fragments, strain distribution is evaluated. The type assignment with highest strain concentration is chosen for image segmentation

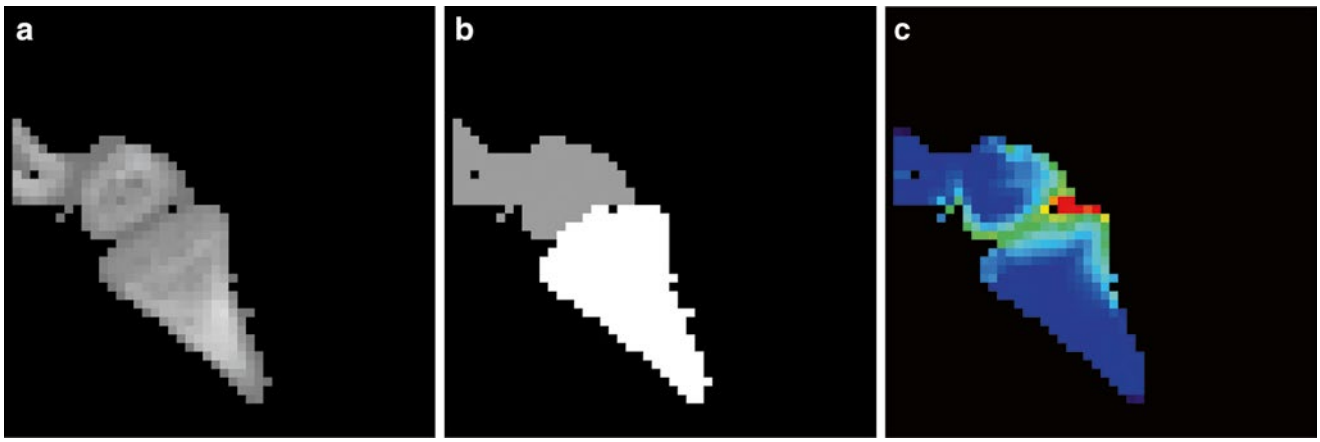

Fig. 20.6 2D examples of segmentation. Input CT image (**a**), segmentation result (**b**) and strain distribution (**c**)

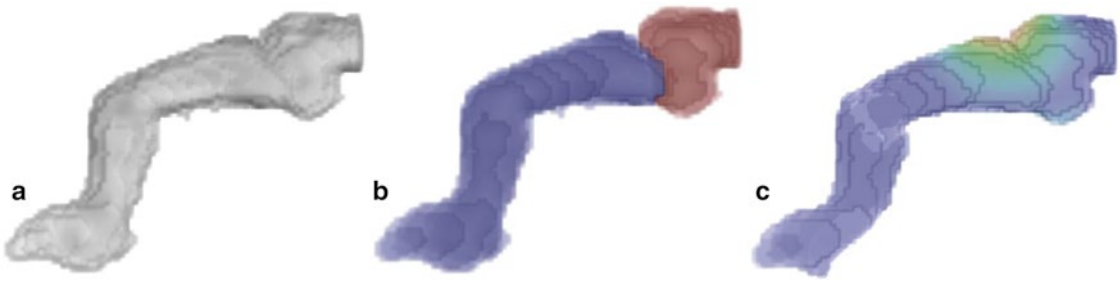

Fig. 20.7 3D examples of segmentation. Input CT image (**a**), segmentation result (**b**) and strain distribution (**c**)

very clear but it was successfully recognized. In the stress distribution shown in (c), a region of high strain spreads along the boundary. It indicates that our method works properly for setting boundary conditions. Figure 20.7 shows a 3D example. (a)–(c) are the input 3D image, segmentation results, and strain distribution respectively. The size of the 3D image is $90 \times 90 \times 90$ voxels and the computation takes about 20 h on a standard desktop PC. Our method is still computationally expensive for application to more complex 3D images.

20.4 Conclusions

We proposed a CT image segmentation method using FEM based structural analysis for the CT images of a skeleton of bone pieces contacting each other at the interface region where the contrast of the image is usually weak. By computing the strain distribution of a structure in the image, pixels with high level of strain are removed to segment the image along these pixels. To compute the strain distribution, we use the image-based FEM method. In order to automatize the procedure, we introduce methods to derive boundary conditions so as to bring high strain to the pixels in user-defined ROI. From the experimental results, we demonstrate that the proposed algorithm works well with CT images with large or ambiguous interference regions. Our most important future work is to improve computation efficiency to enable application of our method to 3D problems of assembled fossil.

References

Adams R, Bischof L (1994) Seeded region growing. IEEE Trans Pattern Anal Mach Intell 16:641–647

Bendsoe M, Kikuchi N (1988) Generating optimal topologies in structural design using a homogenization method. Comput Methods Appl Mech Eng 71:197–224

Boykov Y, Funka-Lea G (2006) Graph cuts and efficient N-D image segmentation. Int J Comput Vis 70:109–131

Grau V, Mewes A, Alcaniz M, Kikinis R, Warfield S (2004) Improved watershed transform for medical image segmentation using prior information. IEEE Trans Med Imaging 23:447–458

Hahn H, Wenzel M, Konrad-Verse O, Peitgen H (2006) A minimally-interactive watershed algorithm designed for efficient CTA bone removal. Comput Vis Approaches Med Image Anal 178–189

Hishida H, Suzuki H, Michikawa T, Ohtake Y, Oota S (2012) CT image segmentation using FEM with optimized boundary condition. PLoS One 7:2–1

Joliot M, Mazoyer B (1993) Three-dimensional segmentation and interpolation of magnetic resonance brain images. IEEE Trans Med Imaging 12:269–277

Kass M, Witkin A, Terzopoulos D (1988) Snakes: active contour models. Int J Comput Vis 1:321–331

Mat-Isa N, Mashor M, Othman N (2005) Seeded region growing features extraction algorithm; its potential use in improving screening for cervical cancer. Int J Comput Internet Manag 13:61–70, ISSN No: 0858-7027

Pardo X, Carreira M, Mosquera A, Cabello D (2001) A snake for CT image segmentation integrating region and edge information. Image Vis Comput 19:461–475

Rao SS (2005) The finite element method in engineering, 4th edn. Elsevier Butterworth Heinemann, Oxford. ISBN 978-0-7506-7828-5

Sebastian T, Tek H, Crisco J, Kimia B (2003) Segmentation of carpal bones from CT images using skeletally coupled deformable models. Med Image Anal 7:21–45

Vincent L, Soille P (1991) Watersheds in digital spaces: an efficient algorithm based on immersion simulations. IEEE Trans Pattern Anal Mach Intell 13(6):583–598

Virtual Endocast of Qafzeh 9: A Preliminary Assessment of Right-Left Asymmetry

21

Osamu Kondo, Daisuke Kubo, Hiromasa Suzuki, and Naomichi Ogihara

Abstract

We performed a semi-virtual reconstruction of the endocast for Qafzeh 9, a representative of early anatomically modern humans in the Near East, by using sequential CT images of the present cranial reconstruction with manual clay infilling of the gap and missing portions in the inner cranial surface. After assessing the reconstructed virtual endocast in terms of right-left (R-L) asymmetry, we morphed it in such a manner that the observed asymmetry reduced and fit into the range of variation observed in recent humans. The assessment suggests that the present reconstruction of the Qafzeh 9 cranium, possessing a significant degree of R-L asymmetry, suffers from distortion. Directly measured endocranial volumes (1411 cc for the original reconstruction and 1477 cc for the morphed version) were smaller than previously published data (1531 cc) using least-square regression equations. After morphing, the endocast was higher at the middle cranial fossa and narrower at the frontal lobe, both characteristics falling within the range of recent human variation. Although the reconstructed Qafzeh 9 endocasts of both the original and morphed versions fit into the endocranial evolution among lineages of the genus *Homo*, many fossil crania may have undergone a substantial degree of taphonomic deformation. Therefore, application of possible corrections or hypothesis of plausible taphonomic scenarios should be part of a reasonable assessment of a single precious fossil specimen.

Keywords

Endocranial volume (ECV) • *Homo sapiens* • Right-left asymmetry

21.1 Introduction

The field of paleoneurology is valuable to the study of human evolution because it contributes important information to other areas of paleoanthropology. Variations in the size and shape of endocasts help in differentiating among fossil species. Moreover, comparisons of the size and shape of fossil endocasts link morphological evidence to behavioral and cognitive differences among fossil species, which might have driven the speciation between taxa.

We aim to perform reasonable reconstructions of fossil hominids in order to visualize the endocasts and to estimate their brain sizes. We also aim to obtain possible inferences for behavioral and cognitive differences between Neanderthals

O. Kondo (✉) • D. Kubo
Department of Biological Sciences, Graduate School of Science, University of Tokyo, 7-3-1 Hongo, Bunkyo-ku, Tokyo 113-0033, Japan
e-mail: kondo-o@biol.s.u-tokyo.ac.jp; dkubo@biol.s.u-tokyo.ac.jp

H. Suzuki
Research Center for Advanced Science and Technology, University of Tokyo, Komaba 4-6-1, Meguro-ku, Tokyo 153-8904, Japan
e-mail: suzuki@den.rcast.u-tokyo.ac.jp

N. Ogihara
Department of Mechanical Engineering, Faculty of Science and Technology, Keio University, 3-14-1 Hiyoshi, Kohoku-ku, Yokohama, Kanagawa 223-8522, Japan
e-mail: ogihara@mech.keio.ac.jp

T. Akazawa et al. (eds.), *Dynamics of Learning in Neanderthals and Modern Humans Volume 2: Cognitive and Physical Perspectives*, Replacement of Neanderthals by Modern Humans Series, DOI 10.1007/978-4-431-54553-8_21, © Springer Japan 2014

and modern humans based on the estimated endocasts and brain sizes.

Fossil hominids have been reconstructed both manually and digitally from a series of original fragments of the skull (Zollikofer et al. 1998; Gunz et al. 2009b). Because fossil skull reconstruction defines the size and shape of the endocasts, the validity or reliability of endocasts depends on the quality of cranial reconstruction. Therefore, many fossil endocasts have been produced after selection of relatively well-preserved fossil crania based on better preservation or minimal distortion of the original fossils (Holloway et al. 2004).

In line with this consideration, we assessed the original status of the fossil cranium of Qafzeh 9 at the time of endocast production. In this preliminary assessment, we focused on the degree of deformation or distortion. Deformation denotes all morphological changes including size, whereas distortion often refers to changes in shape or partial deformation from symmetry. In this study, we assessed the degree of distortion of the Qafzeh 9 cranium by comparing the degree of right-left asymmetry against a hypothetical midsagittal plane. We then tried to correct the degree of observed distortion and applied it to the endocast. The Qafzeh 9 specimen is a fossil representative of early modern *Homo sapiens* and is important for studying the expansion of *H. sapiens* and the extinction of *Homo neanderthalensis*. However, until now, an endocast of Qafzeh 9 has not been produced.

21.2 Materials and Methods

21.2.1 Virtual Reconstruction of the Qafzeh 9 Endocast

Qafzeh 9 was discovered and excavated by Bernard Vandermeersch in 1969 from the Qafzeh Cave in Israel. It was associated with Middle Paleolithic assemblages of the Levallois–Mousterian culture (Vandermeersch 1981). In spite of a chronological age of more than 90,000 years BP (Schwarcz et al. 1988; Valladas et al. 1988) and an older type of associated lithic assemblage (Tabun C type in the Middle Paleolithic), human skeletal morphology from the Qafzeh Cave fossils is quite modern and in contrast to contemporary or even younger classic Neanderthals. According to the first description, the Qafzeh 9 individual is an adult female whose cranial bones were crushed and heavily fragmented. The whole cranium has since been restored and reconstructed (Vandermeersch 1981). The endocranial features were only described for the parietal meningeal vessels because no endocasts had been created for this specimen. The degree of distortion was unknown, although the present reconstruction exhibits possible mediolateral compression and irregular distortions both in the neurocranium and the face (Fig. 21.1). In spite of this, the endocranial capacity was calculated to be between 1508 and 1554 cc using several regression equations of the linear measurements (Vandermeersch 1981), and a mean value of 1531 cc has been reported in textbooks (e.g., Holloway et al. 2004).

We conducted a virtual reconstruction of the endocast from CT images of the specimen with a planar resolution of 0.41 mm/pixel and a slice thickness of 0.5 mm. Because the inner surface of the original cranium was partially damaged, the reconstruction process included both digital and manual restoration, consistent with the method reported by Kubo and Kono (2011). We extracted the cranial model from the CT images using a threshold between the bone and air and prepared a physical mold of the endocranium using a 3D printer. Then, we filled the gap and repaired the missing portions of the inner cranial surface with clay (Fig. 21.2). Although the potential error due to clay restoration cannot be precisely estimated, the smaller portion of clay may support an error of less than 10–20 cc; this value has been speculated for the larger clay restoration of Minatogawa IV (Kubo and Kono 2011).

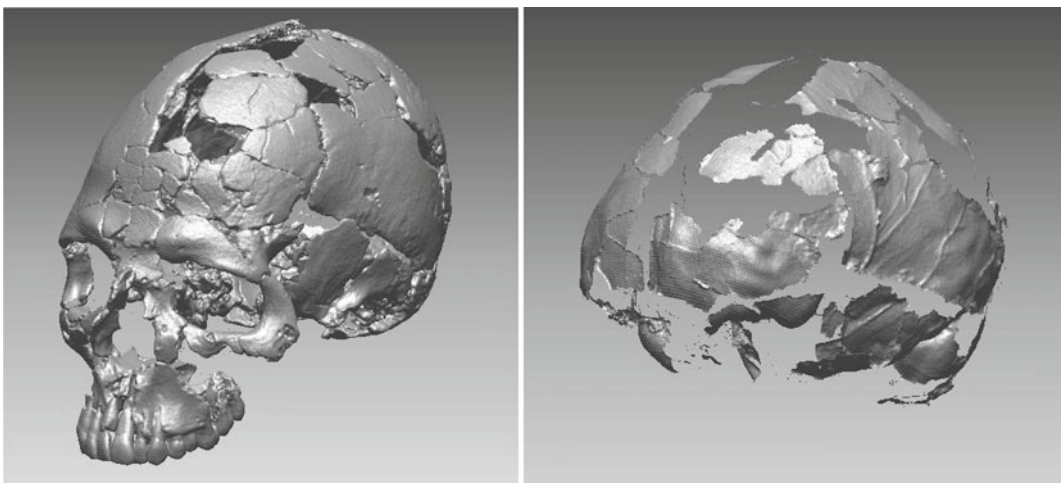

Fig. 21.1 Qafzeh 9 cranium and endocast model

Fig. 21.2 Physical mold of Qafzeh 9 endocranium with infilled clay

A more complete surface model of the endocast was produced by rescanning CT images of the repaired mold.

21.2.2 Assessment of Right-Left Asymmetry and Correction of Distortion

We used landmark-based geometric morphometrics for assessment of right-left asymmetry. The human skull is considered as a typical example of "object symmetry," which is the symmetry of objects that are symmetric in themselves. This means that the axis or plane of symmetry passes through the landmark configuration of the object. Some landmarks may lie in the midline or mid-plane, whereas others exist as corresponding pairs on the left and right sides (Klingenberg et al. 2002). After a normal procedure of Procrustes superimposition, the variance and covariance for each individual landmark is decomposed into symmetric and asymmetric components based on the pre-setting midsagittal plane. Each component is then analyzed using principal component analysis (PCA). The symmetric components exhibit individual variation under the assumption of full symmetric configuration, whereas the asymmetric components express variation in terms of right-left asymmetry for each individual.

For this assessment, we digitized 3D coordinate data of anatomical landmarks on CT data from 20 recent Japanese skulls (ten males and ten females) plus two prehistoric Jomon skulls (one male and one female), both of which are stored at the University Museum, The University of Tokyo. The former recent Japanese skulls are cadaveric specimens from the anatomical collection, presenting normal asymmetric variation without taphonomic distortion. The latter two skulls are archaeological samples that are assumed to be fossil representatives with a degree of deformation due to taphonomic factors. The degree of right-left asymmetry of Qafzeh 9 can be compared with that of the two Jomon specimens in terms of normal variation in the recent Japanese skulls.

Table 21.1 Landmarks used in this study

1	pr	Prosthion
2	o	Opisthion
3	fi	Foramina incisiva
4	l	Lambda
5	fmoR	Right frontomalare orbitale
6	fmoL	Left
7	ccR	Right crus commune
8	ccL	Left
9	poR	Right porion
10	poL	Left
11	astR	Right asterion
12	astL	Left

While digitizing anatomical landmarks on sequential CT images, we established four landmarks to define a midsagittal plane: prosthion (pr), opisthion (o), foramen incisiva (fi), and lambda (l); we also established another four pairs of bilateral landmarks: fontomalare orbitale (fmoR, fmoL), crus commune (ccR, ccL), porion (poR, poL), and asterion (astR, astL) (Table 21.1). The captured 3D coordinates were then imported into software (MophoJ) and processed through a geometric morphometric analysis (Klingenberg 2011), where Procrustes superimposition and decomposition of the variance and covariance were performed for each landmark. The asymmetric components were then analyzed using PCA; the PCA plot expressed the variation in terms of right-left asymmetry. This enabled us to assess the degree of distortion for Qafzeh 9 among the distribution of the 20 recent and two Jomon specimens.

In the final step, we corrected the observed asymmetry by morphing the Qafzeh 9 skull into a version that falls into the range of variation of recent specimens in terms of the asymmetric components. For this step, we used a "3D morphing" procedure in the software "Landmark" (http://graphics.idav.ucdavis.edu/research/EvoMorph), which enables thin-plate spline warping of a 3D surface object to another based on the homological correspondence between anatomical landmarks of the two objects. We could do this by calculating target coordinates for the landmarks of Qafzeh 9 using the observed principal axis in the asymmetric components.

21.2.3 Comparison of the Original and Morphed Versions of the Qafzeh 9 Endocast with Those of Recent Humans

Both the original and morphed versions of endocasts for Qafzeh 9 were metrically compared and assessed using previous datasets (Kubo et al. 2012), which include the specimens

Table 21.2 Endocranial metrics used in this study

Name	Abbreviation	Definition
Cerebral length = telencephalon length	TL	Length between "fp" (frontal pole), the most rostral point on the frontal surface, and "op" (occipital pole), the most caudal point on the occipital surface
Frontal width	FW	Width across the lateral surface of the two frontal caps
Maximum width	MW	Maximum width on the ventral part to the presumable Sylvian impression
Cerebral height	CH	Height from the bottom of the middle cranial fossa (both side mean) to vertex
Endocranial height	EH	Height from the bottom of the cerebellar surface (both side mean) to vertex
Endocranial volume (cc)	ECV	Volume measured by counting the total voxels

in the asymmetric assessment and comprise 52 Japanese, 19 Jomon, and 6 Australian aborigines. All samples were captured as 3D surface objects in the software "Rapidform XOS," rearranged in correct anatomical direction, and measured on five basic linear metrics and one endocranial volume (ECV) (Table 21.2). The difference in the metrics of the original and morphed versions of Qafzeh 9 was statistically assessed using a *T*-test based on variation among the recent humans.

21.3 Results

The first version of the endocast was captured from the intact (original) reconstruction (Fig. 21.3). This version fits the general morphology of a recent human endocranium, including a high and voluminous cerebrum with a round contour of the frontal lobe. In addition, it exhibits a degree of asymmetry in the parieto-temporal contours from the superoinferior or anteroposterior views, or in the orbit-frontal development, temporal convolution, and petrous depression from the inferior view.

Assessment of the degree of right-left asymmetry in the present Qafzeh 9 reconstruction is depicted in Figs. 21.4 and 21.5. Figure 21.4 exhibits the asymmetric components of variation from the consensus configuration along the PC1 and PC2. The position of Qafzeh 9 falls far outside of the recent range of variation, deviating along the negative direction of PC1, whereas the two Jomon specimens fall within it. This suggests that the present reconstruction of Qafzeh 9 should be regarded as significantly distorted over a normal range of variation in the recent individuals. Figure 21.5 depicts the directions and degrees of asymmetry for Qafzeh 9 along the PC1. Although the deviation vectors are exaggerated by approximately four times the actual value (−0.045), the right-left asymmetry is conspicuous. The posterior neurocranium is skewed with right-anterior and left-posterior warping. The face deviates toward the right as a whole and skews with the right-upper and the left-lower shift.

The second version of the corrected endocast was produced by morphing the original (first) endocast (Fig. 21.6). The warping direction and value were obtained from the PCA of the asymmetric variation components based on anatomical landmarks on the skull, where the absolute value along the PC1 (0.045) was corrected for the right-left asymmetry in the Qafzeh 9 skull. Thin-plate spline functions implemented with the software "Landmark" were used to morph the original endocast into the corrected version with warping of corresponding anatomical landmarks. The correction of asymmetry can be confirmed in the morphed version of the endocast (Fig. 21.6, right), which gains a higher degree of symmetry from the inferior view.

The two versions of the endocast were compared with each other and with the recent human standards using some selected metrics (Table 21.3). The ECV estimates were 1411 cc for the original and 1477 cc for the morphed version of the Qafzeh 9 endocast. Both these values are greater than the recent average and within the range of one standard deviation. They are smaller than the previously published mean value (1531 cc) (Vandermeersch 1981; Holloway et al. 2004). The morphing added to the volume by 66 cc, which is statistically significant but less than one-half a standard deviation of the combined recent sample. Morphological change after morphing was detected in a few metrics. The frontal width, i.e., the length between the bilateral frontal caps, was shortened by 6 mm. The cerebral height from the middle cranial fossa was expanded by 10 mm. Both changes were statistically significant, but the respective absolute values were well within the range of the recent specimens. Although the correction of right-left asymmetry by morphing caused a significant degree of change in size and shape of the endocast, the general morphology of the Qafzeh 9 endocast still fit with those of the recent humans.

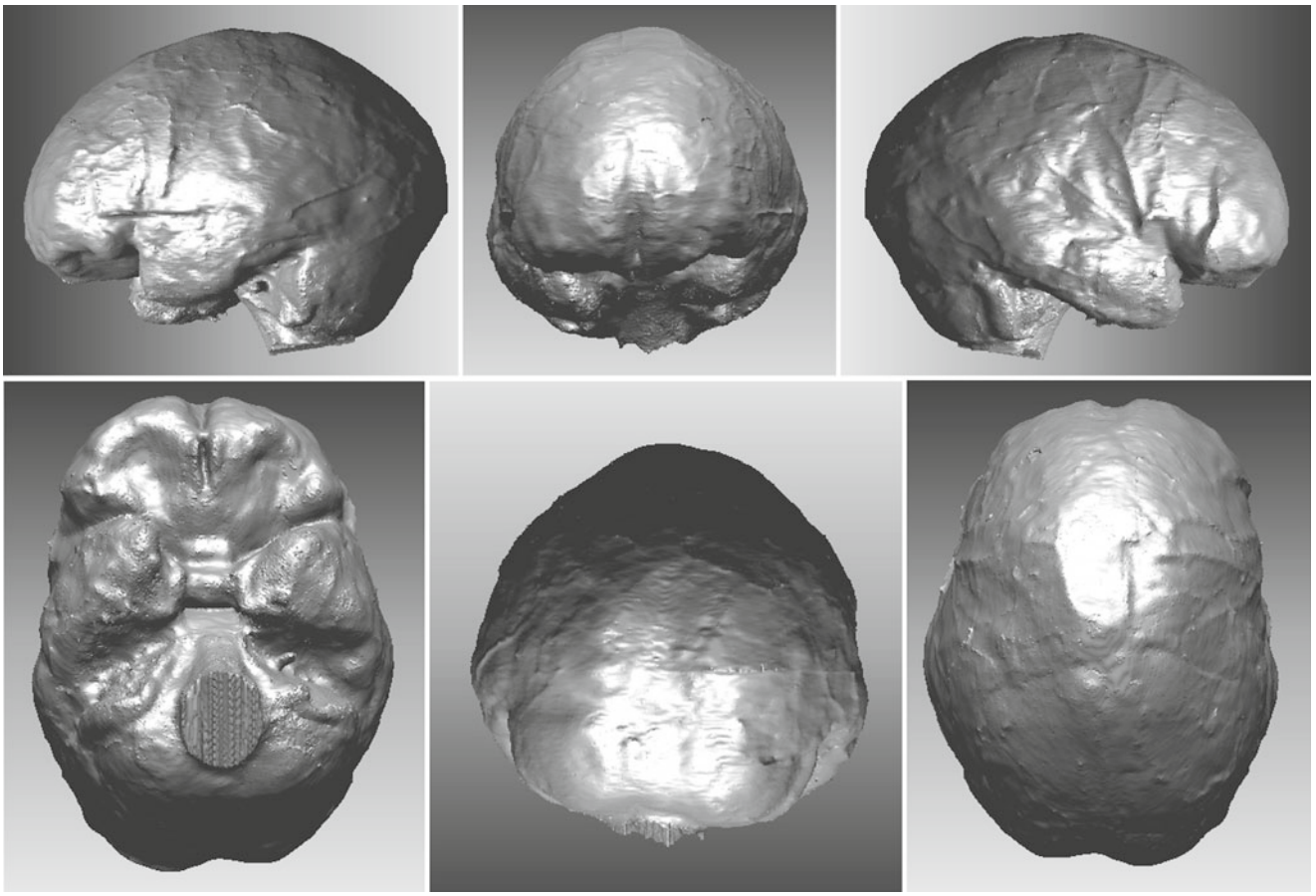

Fig. 21.3 Qafzeh 9 endocast based on original reconstruction

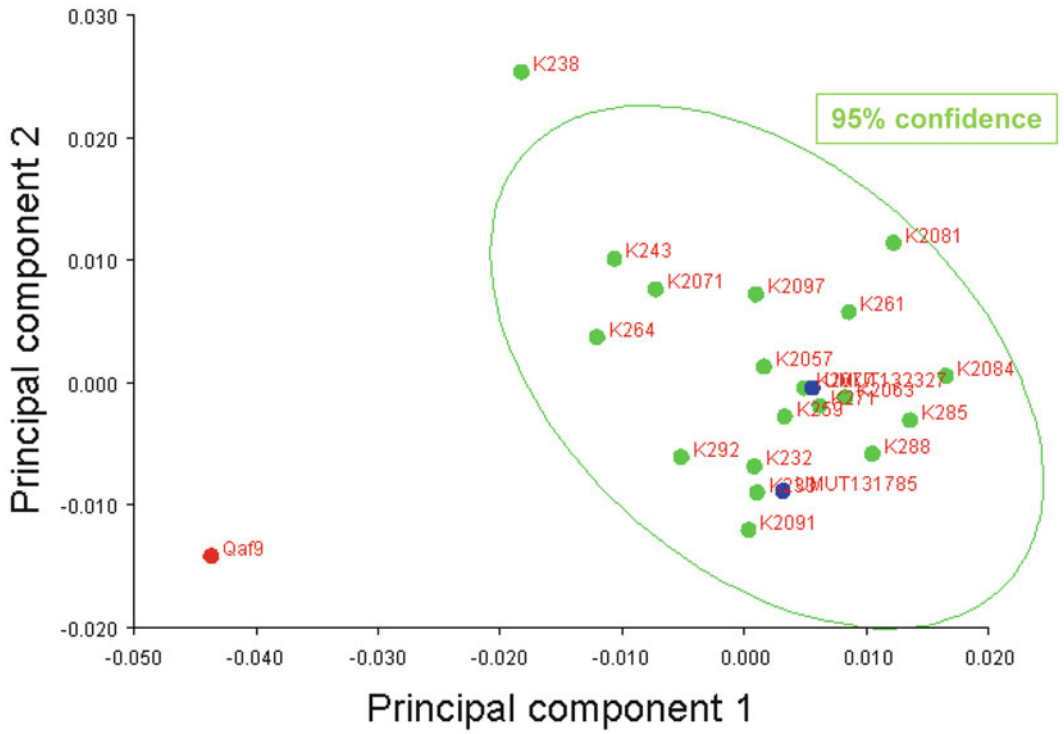

Fig. 21.4 Principal component analysis of the asymmetric component of the variation. 95 % confidence limit is drawn for the recent specimens. *Green*, recent Japanese; *blue*, Jomon; *red*, Qafzeh 9

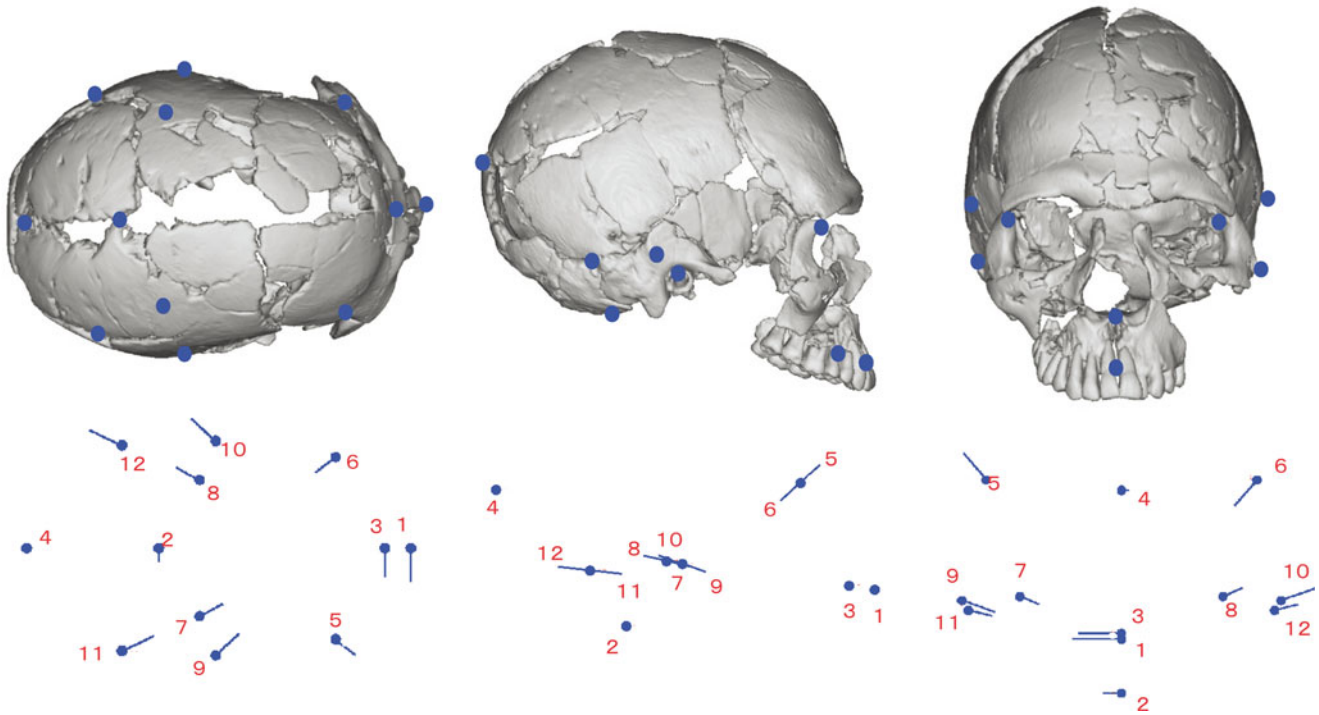

Fig. 21.5 PC1 deviation vectors of Qafzeh 9 based on the asymmetric variation (scale factor = −0.2). The landmark numbers are the same as in Table 21.1

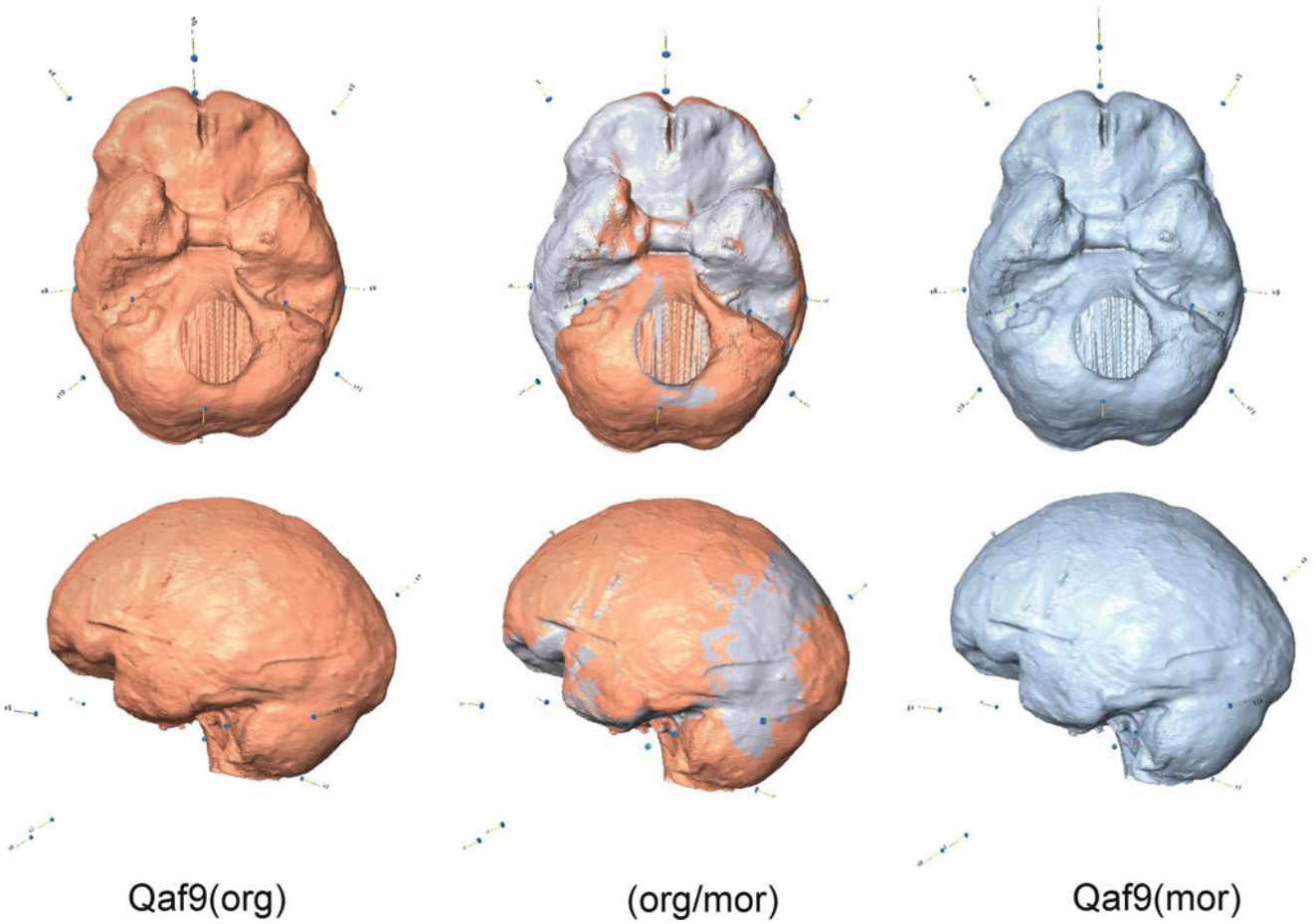

Fig. 21.6 Morphing the Qafzeh 9 endocast (*left*; org) into a modified version (*right*; mor) along the PC1 of the asymmetric variation. The *center* (org/mor) is a half-morphed version (50 % original plus 50 % modified)

Table 21.3 Comparisons of endocranial metrics from Qafzeh 9 original (org) and morphed (mor) versions with combined recent samples

				Combined recent sample (n = 77)	
(mm, cc)	Qaf9 (org)	Qaf9 (mor)	Difference	Mean	s.d.
TL	175	176	+1	167.9	6.1
FW	103	99	−6[a]	99.3	3.8
MW	133	132	−1	131	6
CH	113	123	+10[a]	115.8	6.1
EH	131	133	+2	126	5.2
ECV (cc)	1,411	1,477	+66[a]	1384.5	137.8

[a]Significance < 0.1 %

21.4 Discussion and Conclusions

Virtual reconstruction of fossil hominid crania has become a popular and widely used method in paleoanthropology (Zollikofer and Ponce de León 2005; Gunz et al. 2009b). It is advantageous as a non-invasive, trial-free approach to reconstructing precious fossil specimens and a new tactic for recovering missing portions and correcting deformations using digital toolkits, including geometric morphometrics. However, it should be cautioned that no "all-purpose" reconstruction method exists because every estimation reconstruction should start from different assumptions and then use different algorithms.

For correction of deformation or distortion, it is necessary to consider and hypothesize about the process and context of the specimen. The main sources of detectable morphological deformation are presumed to be postmortem, due to geophysical diagenetic changes during taphonomic processes. The taphonomic deformation has been categorized in terms of its taphonomic scenarios into "fracturing deformation," "plastic deformation," and "expanding matrix deformation" (Ponce De León and Zollikofer 1999; White 2003). Among these, plastic deformation has been detected and corrected mathematically or digitally in virtual space under the principle of "symmetric restoration," which hypothesizes the human skull as a typical example of "object symmetry." Most cases of virtual re-deformation have been accomplished with this "symmetric" scheme (Ogihara et al. 2006; Zollikofer and Ponce de León 2005; Gunz et al. 2009b). However, from the paleoneurological viewpoint, completely symmetric restoration eliminates the opportunity to track right-left asymmetry in the endocast or brain morphology. For retaining the asymmetry signal, other approaches such as reflection using thin-plate spline (Gunz et al. 2009b) should be considered.

Our tentative approach for endocranial reconstruction of Qafzeh 9 started with assessment of right-left asymmetry among recent counterparts represented by non-deformed cadavers and two prehistoric specimens with possible taphonomic alterations. The significantly isolated position of Qafzeh 9 in the asymmetric assessment emphasizes the importance of correcting distortion in the present cranial reconstruction. Our correction strategy using asymmetric variation eliminates major portions (but not all) of the entire asymmetry, which shifts the position of Qafzeh 9 into the peripheral range of variation among recent humans. This suggests that our morphed version of the endocast retains a degree of the asymmetric signal characteristic of this individual. However, because all taphonomic effects are untraceable, it is not possible to determine the correct division between the inherent and taphonomic factors in the observed asymmetry. To overcome this unsolvable issue to some degree, multiple, possible versions with different assumptions should be presented, and a plausible cloud should be created for the reconstruction. For example, a large-scale affine transformation can be estimated by averaging the directions of bilateral anatomical landmarks (Ponce de León and Zollikofer 1999). Alternatively, "geometrical reconstruction" can be performed using thin-plate spline interpolation (Bookstein 1997) from the average or individual recent reference specimens, because the assignment of Qafzeh 9 to *H. sapiens* ensures similarity of cranial shape between the two groups (Grine et al. 2010).

As previously mentioned, Qafzeh 9 is an early representative of anatomically modern *H. sapiens*, which evolved in Africa and then dispersed into Eurasia. The cranium of Qafzeh 9 has been analyzed repeatedly by various scholars, ranging from multivariate analysis of linear measurements (Turbon et al. 1997; Pearson 2008) to geometric morphometrics of 3D landmarks (Gunz et al. 2009a; Gunz et al. 2009b; Harvati et al. 2010). Our assessment of right-left asymmetry clearly indicates that the present reconstruction of the Qafzeh 9 cranium possesses an inevitable and significant degree of deviation from symmetry, far more than recent variation. This specimen may have undergone heavier deformation or distortion due to taphonomic processes. Because of these limitations, any morphological quantification should be regarded with caution.

In evolutionary contexts of brain or endocast morphology, it is easy to assume that Qafzeh 9 should correspond to modern *H. sapiens*, even after considering and repairing any taphonomic alterations. From a broader phylogenetic perspective, it has been suggested that the genus *Homo* experienced a non-allometric widening of the brain at the parieto-temporal area and at the Broca's cap in the frontal lobe; this widening is more prominent in Neanderthals than in modern humans (Bruner and Holloway 2010). In addition, although asymmetry in regional brain surfaces does not exhibit different patterns between fossil *Homo* specimens and modern *H. sapiens*, Neanderthals may have possessed different proportional areas of frontal, parieto-temporal, and occipital lobes compared to those of anatomically modern *H. sapiens* (Balzeau et al. 2012). Our refined approach to the

Qafzeh 9 endocast will contribute to the progress of interpreting endocast morphology and variation among anatomically modern *H. sapiens*.

Acknowledgements CT data for Qafzeh 9 were scanned and are owned by Profs. Yoel Rak, Christoph Zollikofer, and Ponce de Léon, who kindly provided them for our project. We express our sincere gratitude to them. This study was supported by a Grant-in-Aid for Scientific Research on Innovative Areas "Replacement of Neanderthals by Modern Humans: Testing Evolutionary Models of Learning" from the Japanese Ministry of Education, Culture, Sports, Science and Technology (No. 22101006).

References

Balzeau A, Holloway RL, Grimaud-Hervé D (2012) Variations and asymmetries in regional brain surface in the genus *Homo*. J Hum Evol 62:696–706

Bookstein FL (1997) Morphometric tools for landmark data: geometry and biology. Cambridge University Press, Cambridge

Bruner E, Holloway RL (2010) A bivariate approach to the widening of the frontal lobes in the genus homo. J Hum Evol 58:138–146

Grine FE, Gunz P, Betti-Nash L, Neubauer S, Morris AG (2010) Reconstruction of the late Pleistocene human skull from Hofmeyr, South Africa. J Hum Evol 59:1–15

Gunz P, Bookstein FL, Mitteroecker P, Stadlmayr A, Seidler H, Weber GW (2009a) Early modern human diversity suggests subdivided population structure and a complex out-of-Africa scenario. Proc Natl Acad Sci U S A 106:6094–6098

Gunz P, Mitteroecker P, Neubauer S, Weber GW, Bookstein FL (2009b) Principles for the virtual reconstruction of hominin crania. J Hum Evol 57:48–62

Harvati K, Hublin JJ, Gunz P (2010) Evolution of middle-late Pleistocene human cranio-facial form: a 3-D approach. J Hum Evol 59:445–464

Holloway RL, Broadfield D, Yuan M (2004) The human fossil record, volume 3, Brain endocasts-the paleoneurological evidence. Wiley-Liss, Hoboken

Klingenberg CP (2011) MorphoJ: an integrated software package for geometric morphometrics. Mol Ecol Resour 11:353–357

Klingenberg CP, Barluenga M, Meyer A (2002) Shape analysis of symmetric structures: quantifying variation among individuals and asymmetry. Evolution 56:1909–1920

Kubo D, Kono RT (2011) Endocranial restoration and volume estimation of the minatogawa IV cranium using micro-CT and 3D printer systems. Anthropol Sci 119:203–209

Kubo D, Kono RT, Suwa G (2012) Endocranial proportions and postorbital morphology of the Minatogawa I and IV Late Pleistocene *Homo sapiens* crania from Okinawa Island, Japan. Anthropol Sci 120:179–194

Ogihara N, Nakatsukasa M, Nakano Y, Ishida H (2006) Computerized restoration of nonhomogeneous deformation of a fossil cranium based on bilateral symmetry. Am J Phys Anthropol 130:1–9

Pearson OM (2008) Statistical and biological definitions of "anatomically modern" humans: suggestions for a unified approach to modern morphology. Evol Anthropol Issues News Rev 17:38–48

Ponce De León MS, Zollikofer CPE (1999) New evidence from Le Moustier 1: computer-assisted reconstruction and morphometry of the skull. Anat Rec 254:474–489

Schwarcz H, Grün R, Vandermeersch B, Bar-Yosef O, Valladas H, Tchernov E (1988) ESR dates for the hominid burial site of Qafzeh in Israel. J Hum Evol 17:733–737

Turbon D, Pérez-Pérez A, Stringer C (1997) A multivariate analysis of Pleistocene hominids: testing hypotheses of European origins. J Hum Evol 32:449–468

Valladas H, Reyss J, Joron J, Valladas G, Bar-Yosef O, Vandermeersch B (1988) Thermoluminescence dating of Mousterian 'Proto-Cro-Magnon' remains from Israel and the origin of modern man. Nature 331:614–616

Vandermeersch B (1981) Les hommes fossiles de Qafzeh (Israël). Editions du CNRS, Paris

White T (2003) Early hominids–diversity or distortion? Science 299:1994–1997

Zollikofer CPE, Ponce de León MS (2005) Virtual reconstruction: a primer in computer-assisted paleontology and biomedicine. Wiley-Interscience, Hoboken

Zollikofer CPE, Ponce De León MS, Martin RD (1998) Computer-assisted paleoanthropology. Evol Anthropol Issues News Rev 6:41–54

Reconstruction of the Brain from Skull Fossils Using Computational Anatomy

22

Takanori Kochiyama, Hiroki C. Tanabe, and Naomichi Ogihara

Abstract

We investigated the presumed differences in learning abilities between Neanderthals and modern humans by combining evidence from the morphological analysis of fossil brains and functional mapping of modern human brain functions. To achieve this, we established a method for extrapolating to human brain functions from skull anatomy data, which are the only data available to compare modern humans and Neanderthals. Over the last three years, we have developed a skull-based image analysis method based on the computational anatomy technique, which is a standard method used in neuroimaging research, such as functional magnetic resonance imaging (fMRI) and voxel-based morphometry (VBM). In this report, we introduce the concept and practice of our method, and also present some prototype studies to investigate the performance of the proposed approach.

Keywords

Brain anatomy • Computational anatomy • Fossil brain • Neuroimaging • Skull

22.1 Purpose of Our Research

We examine the working hypothesis that there are differences in learning ability between modern and ancient humans, Neanderthals. We conduct functional brain mapping studies of modern humans in order to localize the different learning strategies: social and individual learning. The results from functional brain mapping studies are combined with the morphological differences between fossil brains of Neanderthals and living brains of humans to extrapolate the functional distinctions between them. By assuming that morphological differences observed in the brains reflect functional differences between Neanderthals and humans, we investigate the presumed gaps in learning ability between them in light of anatomical evidence. This report comprises three sections. In the first, we review the computational anatomy approach (Ashburner and Friston 2007) with a special focus on two important methodologies: image registration and computational morphometry. The second section uses two key methods of the computational anatomy approach to conduct prototype analyses using modern human MRI data instead of Neanderthal data.

T. Kochiyama (✉)
The Hakubi Project, Primate Research Institute, Kyoto University, Inuyama, Aichi 484-8506, Japan

Brain Activity Imaging Center, Advanced Telecommunications Research Institute International, 2-2-2 Hikaridai, Seika-cho, Soraku-gun, Kyoto 619-0288, Japan
e-mail: kochiyama.takanori.8r@kyoto-u.ac.jp; kochiyam@atr.jp

H.C. Tanabe
Department of Social and Human Environment, Graduate School of Environmental Studies, Nagoya University, Furo-cho, Chikusa-ku, Nagoya, Aichi 464-8601, Japan

Division of Cerebral Integration, Department of Cerebral Research, National Institute for Physiological Sciences, 38 Nishigo-naka, Myodaiji, Okazaki, Aichi 444-8585, Japan
e-mail: htanabe@lit.nagoya-u.ac.jp

N. Ogihara
Department of Mechanical Engineering, Faculty of Science and Technology, Keio University, 3-14-1 Hiyoshi, Kohoku-ku, Yokohama, Kanagawa 223-8522, Japan
e-mail: ogihara@mech.keio.ac.jp

T. Akazawa et al. (eds.), *Dynamics of Learning in Neanderthals and Modern Humans Volume 2: Cognitive and Physical Perspectives*, Replacement of Neanderthals by Modern Humans Series, DOI 10.1007/978-4-431-54553-8_22, © Springer Japan 2014

In the final section, we briefly summarize our proposed methods and future plans for application to Neanderthal data.

22.2 Computational Anatomy

22.2.1 Introduction to Computational Anatomy

Computational anatomy is a method focusing on quantitative analysis of the variability of biological shapes including the brain. It involves many computerized methods to process and analyze medical images including CT and MRI. It can be performed with software such as Statistical Parametric Mapping (SPM; www.fil.ion.ucl.ac.uk/spm/) and FMRIB Software Library (FSL; www.fmrib.ox.ac.uk/fsl/). In this study, we mainly use SPM.

There are many advantages of using SPM software. There are many functions for anatomical image processing, including multimodal image registration or coregistration (cf. Collignon et al. 1995; Zuk and Atkins 1996; Hill et al. 2001), and linear and nonlinear image transformation (cf. Friston et al. 1995; Ashburner and Friston 1999). The functions for analyzing multi-modality images are essential for our study because a reconstructed fossil brain is a CT image and a modern human brain is usually scanned by MRI to prevent radiation exposure. Using coregistration, we can align the image position between CT and MRI. We can also change the brain shape from one subject to another (or Neanderthals) using linear and nonlinear image transformation. In addition, we can perform quantitative statistical evaluation to obtain whole brain anatomical as well as functional data. Using SPM, we can test where the brain has changed in shape between populations or even different species.

There are the two main tools in computational anatomy: image registration involves spatially transforming the source image to align with the target/reference image (Friston et al. 1995; Ashburner and Friston 1999); computational morphometry is a neuroimaging analysis technique that can be used to investigate focal differences in brain anatomy using a statistical approach (e.g. VBM; Ashburner and Friston 2000; Good et al. 2001a). Quantitative volumetric analysis of anatomical changes has been carried out by, for example, manually tracing specific regions of interest. In contrast, computational morphometry is a fully automated technique that allows examination of the whole brain on a voxel-by-voxel basis. Each method is described in detail in the following subsection.

22.2.2 Spatial Transformation

We illustrate the types of spatial transformation in Fig. 22.1. The goal of spatial transformation is to fit the source image to a target image using various image transformations. Translation makes the image shift up and down, left and right, and back and forth. Rotation adjusts the yaw, pitch, and roll of the image, which means the rotation about x, y, and z axes, respectively. Rigid body transformation consists of translation and rotation. Scaling makes the image expand or contract along x, y, and z axes. The effect of shear transformation is

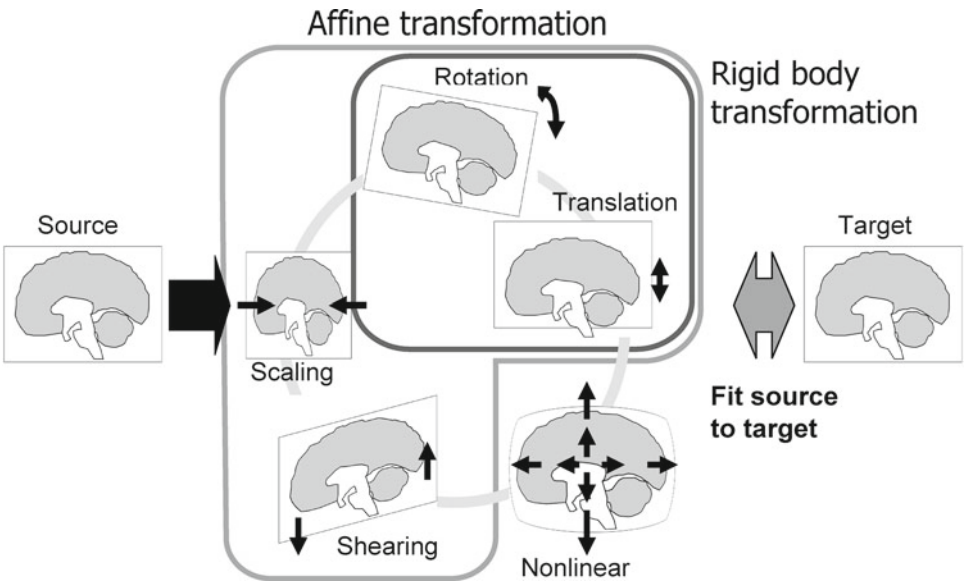

Fig. 22.1 Types of spatial transformation

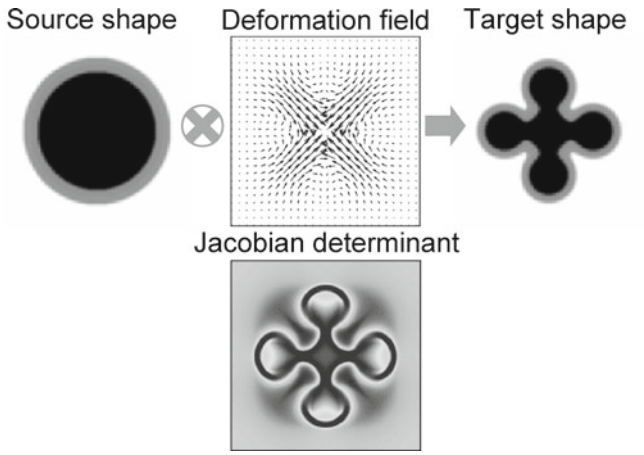

Fig. 22.2 Example of deformation field

like pushing an image along a coordinate axis. Affine transformation comprises translation, rotation, scaling, and shearing in x, y, and z dimensions. The other important type of spatial transformation is nonlinear spatial transformation, including locally deforming the image. Nonlinear spatial transformation plays an important role in our study.

Affine and nonlinear spatial transformations are associated with the deformation field, which contain anatomically relevant information (cf. Ashburner et al. 1998). The deformation field is a vector field that can be thought of as small vectors at each position in space showing how that particular location has been deflected. In Fig. 22.2, we illustrate a typical nonlinear transformation involving a local shape change. For example, we want to transform an image containing two concentric circles (Left) into a 4-leaf-clover-like, more complex shape (Right) (cf. Ashburner and Friston 2011; Note that we used a script for the demonstration provided by them). In the deformation field of this transformation (Middle), many small blue arrows indicate that the four corners of the image are distorted toward the center of the circle. You can easily see that the left circle becomes the complex right shape if the deformation field of the middle image is applied to the left circle. One more useful measure associated with the deformation is the Jacobian determinant of the deformation field (Fig. 22.2). Technically, it is the determinant of the Jacobian matrix which encodes the local stretching, shearing, and rotating of the deformation field. The Jacobian determinant of the deformation field, or just Jacobian, indicates relative volumes before and after spatial transformation. Unlike the deformation field, this measure is a scalar value at each voxel. Jacobian is mainly used to detect local volumetric changes (Gaser et al. 1999; Hua et al. 2008a, 2008b; Lee et al. 2007 for clinical applications).

At the end of the overview of image registration, we introduce one of the promising spatial transformations that have recently been developed, which is Large Deformation Diffeomorphic Metric Mapping, or the LDDMM approach (Avants and Gee 2004; Miller et al. 2005; Miller et al. 2006; Ashburner 2007; Wang et al. 2007; Ashburner and Friston 2011). The LDDMM approach of high-dimensional nonlinear transformation has several million degrees of freedom, as opposed to one thousand in normal non-linear transformation. During the optimization, LDDMM minimizes the two metrics: the image intensity difference between the target and source image and the squared distance measure of the deformations are called the geodesic distance. Minimizing metric distances between anatomical shapes is a marked feature of this high-quality registration method. Diffeomorphic mappings like LDDMM are smooth and topology-preserving. In short, using LDDMM, we can perform precise, smooth, and well-behaved transformation. We can use two types of LDDMM in SPM software: the DARTEL toolbox (Ashburner 2007) and Geodesic shooting toolbox (Ashburner and Friston 2011).

We provide practical examples of image registration. Image registration has been used in spatial preprocessing for fMRI data analysis. Spatial preprocessing is one of the stages in fMRI data analysis to improve the sensitivity of detecting brain activation. We present two examples where computational anatomy plays an important role in solving the technical issues in fMRI experiments.

The first example is realignment. Realignment is commonly used in fMRI experiments to reduce head motion artifacts during scanning. We instruct the subject not to move during scanning. However, head movements by a few millimeters are often observed. Even small head movements can be a major problem, increasing noise variance and decreasing the statistical power of detecting the brain activation. The realignment function re-aligns each subject's head position in image time-series using rigid-body transformation which assumes that the brain shape does not change (Fig. 22.3a).

Normalization is also important spatial preprocessing in fMRI analysis. Subjects participating in an fMRI experiment have different brain shapes. Through normalization, individual brains can be transformed into a common standard space. Normalization enables inter-subject averaging to increase the statistical power above that obtained with a single subject, and extrapolate findings to the population as a whole. Normalization also makes results from different studies comparable in a standard space.

During normalization, individual images are fitted to the same template image. An ideal template consists of the average of a large number of MR images that have been registered in the same standard space. Spatial normalization is achieved in two steps: the first step involves estimating the affine transformation including translations, rotations, scalings, and shears to fit the overall size and shape of the individual images to the template; the second step accounts for global, nonlinear shape differences,

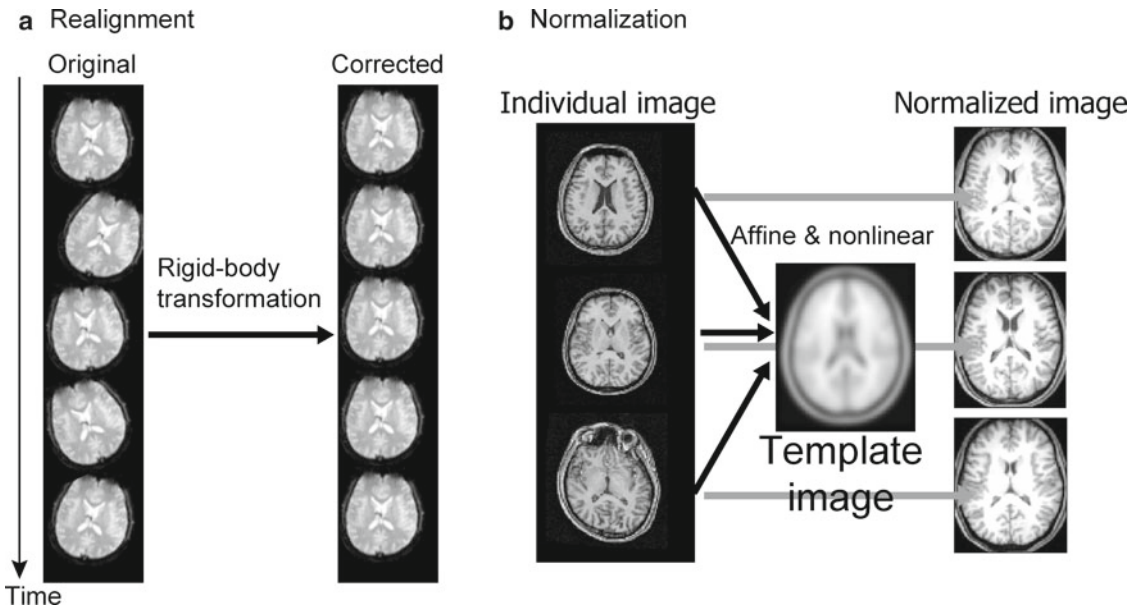

Fig. 22.3 Realignment (**a**) and spatial normalization (**b**)

which are modeled by a nonlinear deformation. After normalization, individual images have the same shape as the template image (Fig. 22.3b).

22.2.3 Computational Morphometry

We illustrate two specific examples of computational morphometry. One of the methods for investigating neuroanatomical differences is to use voxel-based morphometry (VBM) (Ashburner and Friston 2000; Good et al. 2001a). VBM analysis can be used to study the variability in the form, shape, and size of the brain. The basic idea of VBM analysis is to detect differences in the regional volume of grey matter, white matter, and so on while discounting global brain shape differences. VBM analysis is whole-brain analysis that does not require a priori assumptions about regions of interest (ROIs).

VBM analysis is a simple, fully automated protocol that involves several processing steps, mainly spatial normalization, segmentation, and statistical analysis. The results of statistical analysis, specifically statistical parametric maps, show the regions where tissue types differ significantly between groups.

One of the critical processing steps in VBM is segmentation (Ashburner and Friston 2005). Each brain tissue in MRI has a different signal intensity distribution. For example, the gray matter (GM) is darker than the white matter (WM), and the cerebrospinal fluid (CSF) and water are dark and the skull is almost black in T1-weighted MR images. Using this information as well as prior knowledge on the spatial distribution of tissue classes, every voxel can be classified as either GM, WM, CSF, skull, or scalp in a fully automated segmentation routine, for example, a unified segmentation-normalization approach implemented in SPM.

Another type of computational morphometry is deformation-based morphometry (DBM) (Ashburner et al. 1998; Chung et al. 2001; Chung et al. 2003). In DBM analysis, statistical analyses are performed on the deformation fields used for spatial transformation. In contrast to VBM using univariate statistics, DBM analysis requires multivariate statistics because the deformation field is a vector field; specifically, there are three data at every position (Worsley et al. 2004; Chung et al. 2010). DBM analysis is also useful for analyzing the brain anatomy since DBM can not only detect where the anatomy has changed, but it can also show how the anatomy has moved, in other words, the direction of the changes, as indicated by the small yellow arrow in this figure.

22.3 Studies on Modern Human Brain Data

In this section, we demonstrate some results from prototype analyses for the application of computational anatomy to fossil brain research. The purpose of our research is to develop a method for extrapolation of the Neanderthal brain from the modern human brain by matching their skulls and to examine quantitative morphological differences between Neanderthal and modern human skulls to improve skull-based brain reconstruction. To achieve this, we conducted three prototype analyses using modern human MRI data.

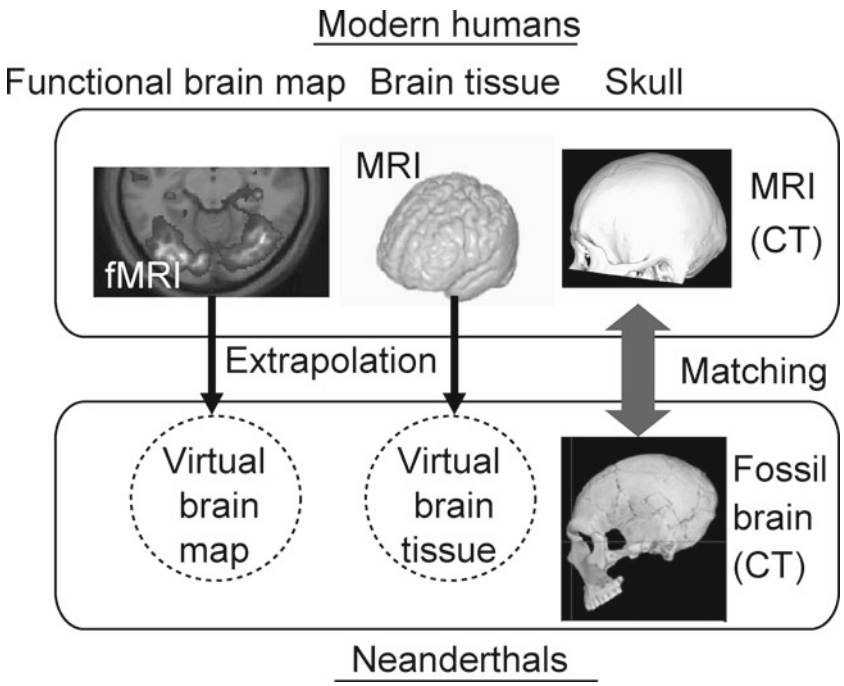

Fig. 22.4 Available data in our study

In the first analysis, we replaced the effects of species with those of individual variability in modern humans. We tried to extrapolate one modern human brain from another's brain by matching their skulls. In the second and third analyses, we replaced the effects of species with those of gender in modern humans. We examined quantitative morphological differences in the skull shape between males and females in this study.

22.3.1 Brain Reconstruction with Skull Shape Matching

Figure 22.4 shows the available data in our study and also clarifies what we need to extrapolate from this data. In modern humans, all data are available. A functional brain map is constructed from fMRI data. The brain tissue and skull are obtained by segmentation of MR or CT images. In contrast, only skull data are available for Neanderthals. Thus, to create a virtual Neanderthal brain, we extrapolate functional brain maps and brain tissue from modern human data. This extrapolation is essentially image registration in computational anatomy while matching the skull shape or the endocast (i.e., inner skull shape) between the two populations.

To create a protocol for image registration, we analyzed modern human MRI by simulating a similar situation to the fossil brain case: one individual human brain was extrapolated from another by matching their skulls. In other words, we investigate whether the brain can be exchanged between two modern human individuals if exactly aligning their skull shape.

The analysis protocol is shown in Fig. 22.5. It is divided into two parts: Step 1 is segmentation. An MR image of a modern human subject is divided into tissue classes: gray matter, white matter, and skull. Step 2 is nonlinear image transformation based on LDDMM. We estimate the deformation field for each subject to allow the nonlinear transformation from the individual skull to an average skull shape. After that, the estimated deformation field is applied to subject 1's brain to transform it to an average shaped brain. Next, an inverse deformation field that allows transformation from the average skull shape to subject 2's skull shape is applied to subject 1's average shaped brain to obtain subject 2's brain. We compare the accuracy of the skull-based brain exchange with the gray and white matter-based exchanges.

The results of skull and GM & WM-based brain exchange are shown in Figs. 22.6 and 22.7. The axial sections of MR images with the same z level are shown. Figure 22.6a shows the results of gray and white matter-based analyses. Figure 22.6b shows those of skull-based analysis. The upper and lower rows show subject 1's and 2's brains, respectively. The left and right columns show subject 1's and 2's brain shapes, respectively. Therefore, the figures on the diagonal are the original MR images for each subject. The figures on the off-diagonal part are the transformed brain from another subject. In the case of gray and white matter-based brain exchange, visual inspection of the overall appearance indicates that the accuracy of transformation was very high. Not only the global skull and brain shape, but also the structures within the brain tissues such as the lateral ventricle, circled by a dotted line, were well-matched between the original and transformed brains. Since LDDMM preserves the topology of objects, the thick bone marrow of subject 1, as indicated by the arrow, remained after transformation. In the case of skull-based brain

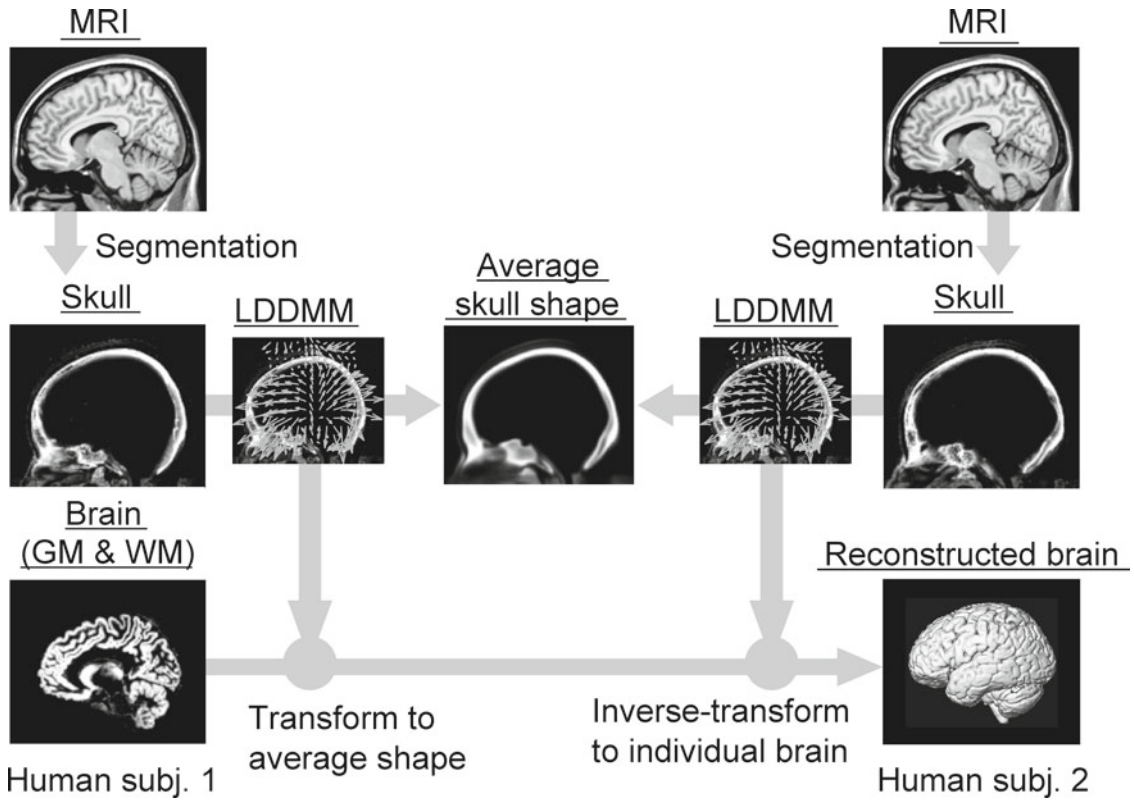

Fig. 22.5 Protocol of brain exchange

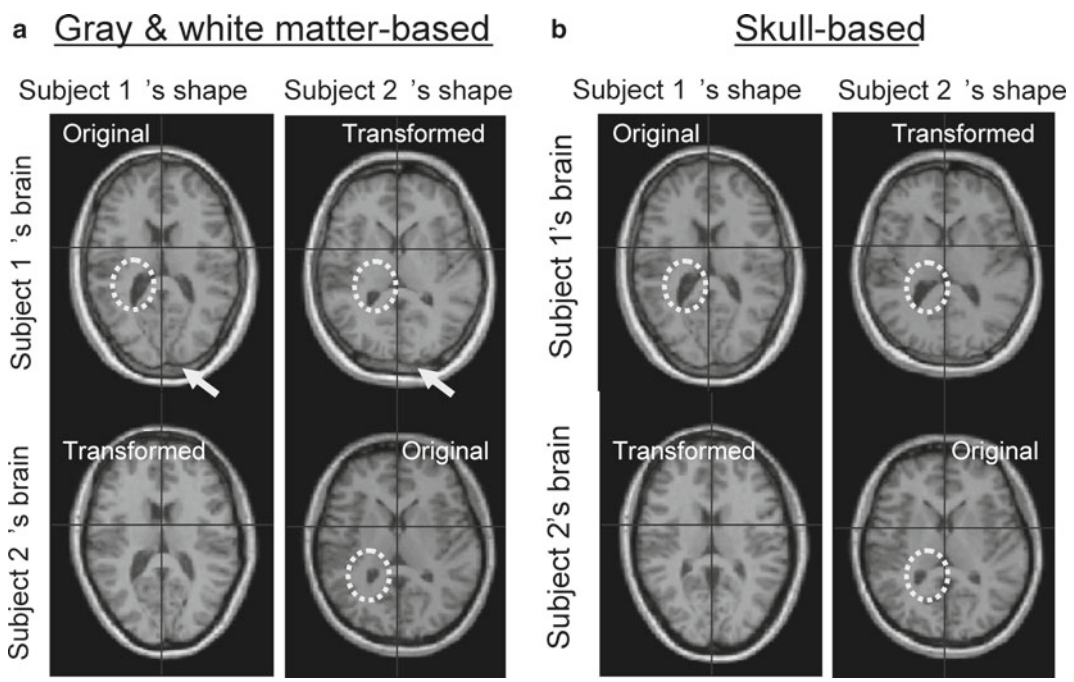

Fig. 22.6 Results of brain exchange. Gray and white matter-based (**a**) and skull-based (**b**) analyses

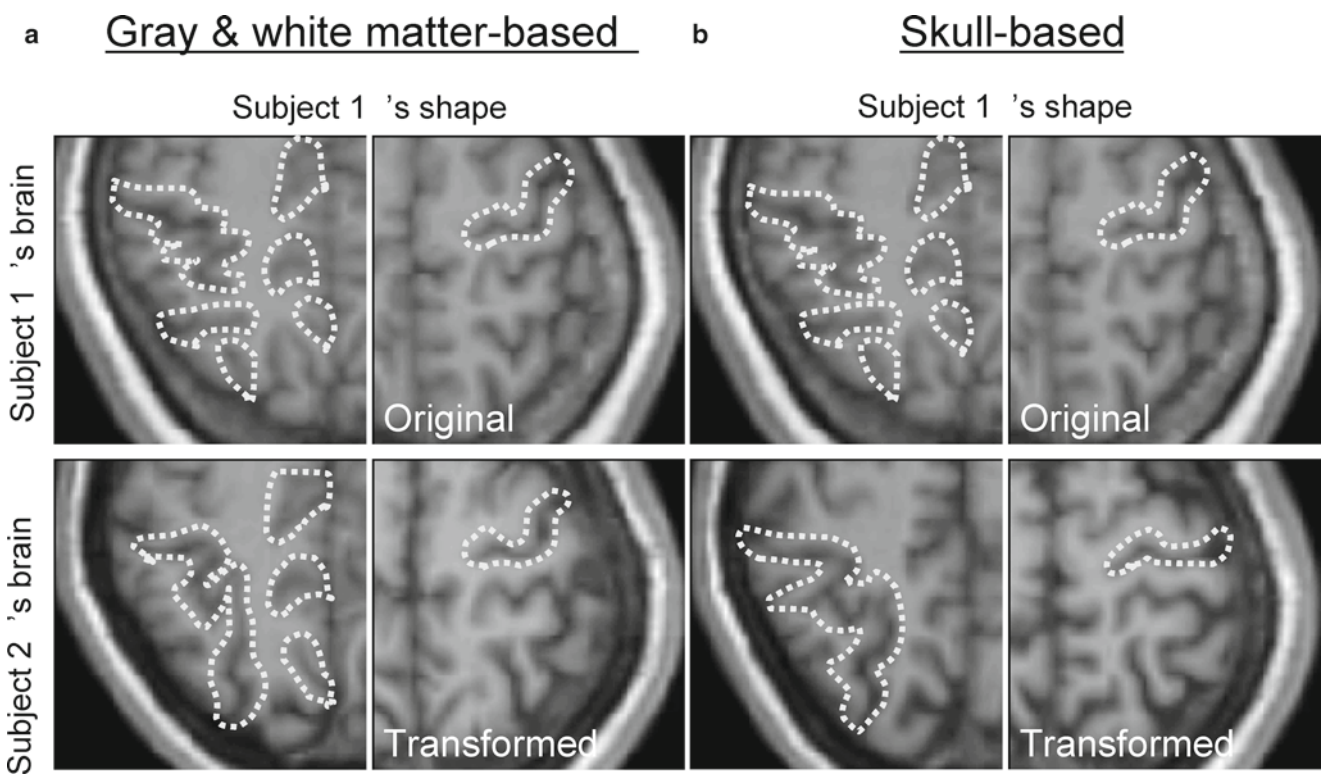

Fig. 22.7 Results of brain exchange (details). Gray and white matter-based (**a**) and skull-based (**b**) analyses

exchange, although the global skull shape and brain outline were well-matched between the original and transformed brains, there were clear failures in the registration over brain tissues, as expected. For example, the shape of subject 1's lateral ventricle did not change between before and after transformation, and it did not fit subject 2's structure at all.

If we focus on details, we can see that a high level of accuracy for aligning gyri and sulci across subjects is also achieved. Figure 22.7 has the same format as the previous one except it includes subject 1's shape only. The left and right columns in Fig. 22.7a, b are close-ups of the parietal and hand motor regions, respectively. In the case of gray and white matter-based analysis, the position and sulcal shape of the hand motor area in the transformed brain were very similar to those of subject 1's original data. The intra-parietal sulcus in the transformed brain was also similar in appearance to that of the original. By the law of topology preservation, if a sulcus is a single connected structure in the original brain, it will have the same topology even with a different appearance in the transformed brain (i.e., it is not divided into two parts and does not disappear). In the case of skull analysis, the sulcus shape and its position varied between the original and transformed brain. They seemed to be proportionally scaled according to the transformation of the skull when reviewing the deformation field.

These results suggest that brain exchange is technically possible; however, there is a limitation in that the accuracy of registration remains at the level of the overall brain shape if only anatomical information on the skull is used. That is exactly the case for the fossil brain analysis and problematic. We are working to improve the accuracy of skull-based analysis. It may be effective to combine global shape matching with the use of some landmarks extracted from the skull.

22.3.2 Quantitative Whole-Brain Morphometric Analysis

We test whether we can detect gender differences in the skull shape using quantitative whole-brain morphometric analysis. Previous studies reported that there were some regionally specific differences in gray matter over and above global brain shape differences using VBM (Good et al. 2001b; Im et al. 2006). However, no research has compared the skull shape between males and females using the automated analysis protocol such as VBM or DBM. In addition to the morphometric research interests, this analysis is supposed to the prototype analysis for future application of the fossil brain analysis.

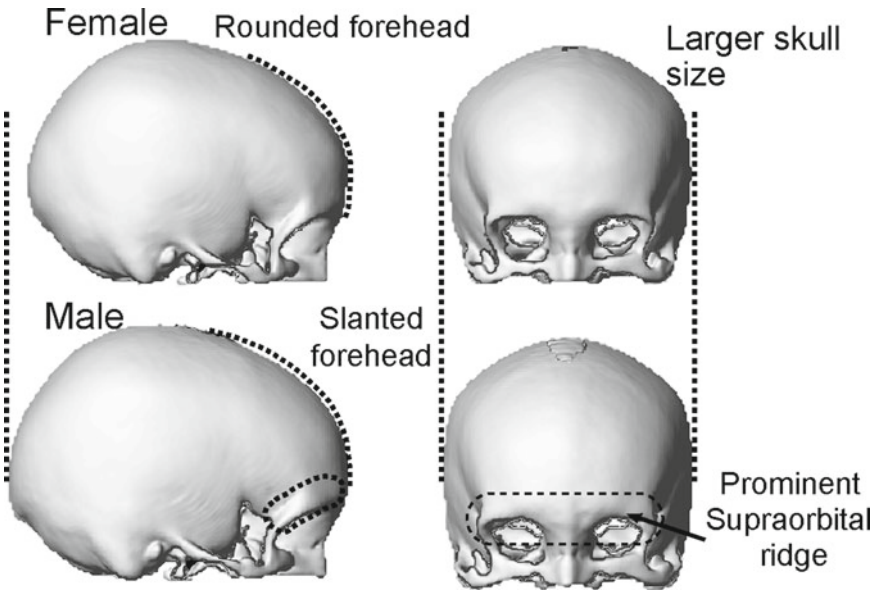

Fig. 22.8 Gender differences in skull shape

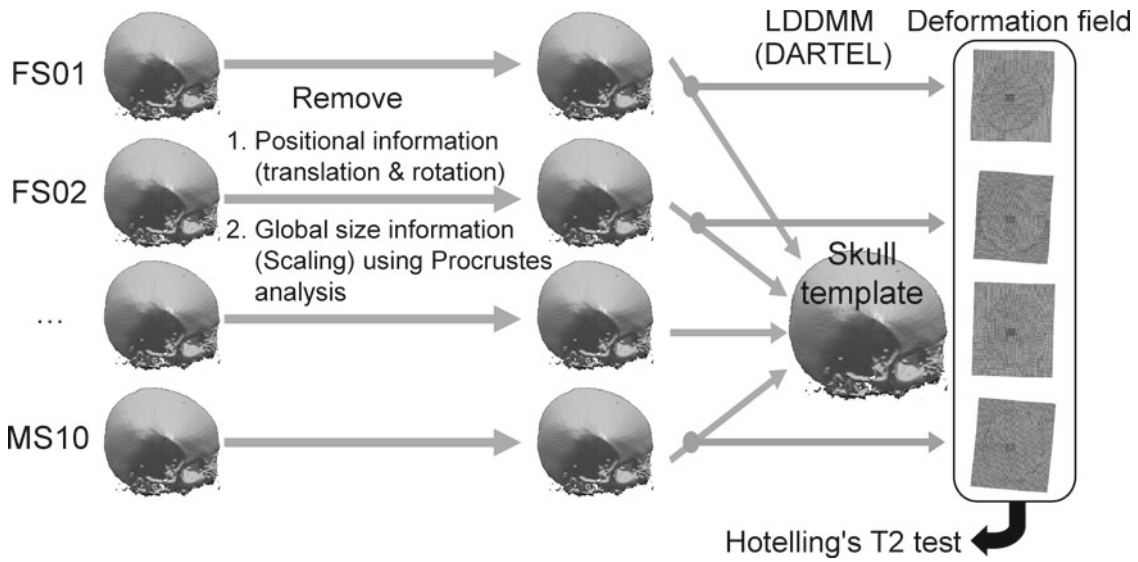

Fig. 22.9 Protocol of skull shape analysis

Before the analysis, we confirmed the well-known gender differences in skull features (cf. Bass 1995). Figure 22.8 shows average shaped skulls created from our MRI data using segmentation. When we compared male and female skulls, the female skull appeared smaller and more gracile, and the male skull was usually larger and more rugged. There were also some local differences. The supraorbital ridge, which is the region directly above the orbit and nose, was more marked in males. In contrast, in females, it was less pronounced. The frontal bone or forehead of males tended to be slanted back or sloping. In females, it tended to be more rounded. The goal of the following analysis is to detect these gender differences using computational morphometry. We perform DBM analysis of skull data to evaluate the location and direction of the changes in shape. We try to not only detect but also statistically evaluate the shape differences between males and females.

Figure 22.9 shows the DBM analysis protocol. First, we conducted skull extraction from individual MR images using a segmentation tool. Next, positional information, translation and rotation, was removed from the skull image. This process was required to set the initial condition for LDDMM estimation.

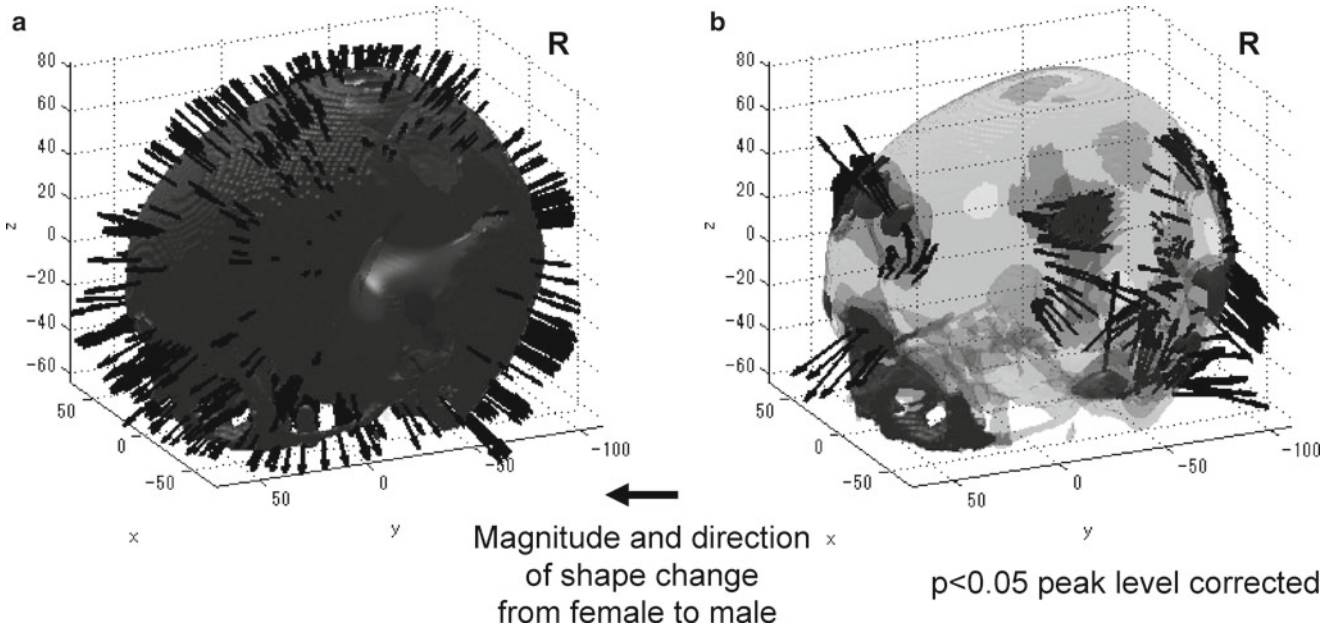

Fig. 22.10 Results of skull shape analysis. With (**a**) and without (**b**) global size effects

To evaluate local changes in the shape, global size effects, or expanding and contracting in x, y, and z directions, were removed from the deformation fields using Procrustes analysis (Bookstein 1997). For this, we compared the results with and without global size effects. Finally, the overall size and shape of the individual skull images were fitted to the averaged skull image as a template. The LDDMM approach, the DARTEL method in this case, was used to estimate the deformation field of this transformation. Resulting deformation fields were entered into Hotelling's T square statistics, which is the standard multivariate test for single comparison and can be used to visualize significant changes in the skull shape between males and females. We used the Surfstat toolbox (http://www.math.mcgill.ca/keith/surfstat/) because it can perform correction for multiple comparison on statistical parametric maps based on the random field theory (Cao and Worsley 1999; Worsley et al. 2004; Chung et al. 2010).

The MRI data used here were selected from the freely accessible image repository for the 1000 Functional Connectomes Project (http://www.nitrc.org/projects/fcon_1000/). These data consists of forty one males and forty five females MRI images were scanned at the MRI center for International Consortium for Brain Mapping (ICBM). Freely publishing any portion of the data in the web-based repository is approved by the 1000 Functional Connectomes Project.

The results of DBM analysis with and without the global size effects are shown in Fig. 22.10a, b, respectively. Red blobs indicate the regions with significant changes in shape between females and males at a significance level of less than 5 % under correction for multiple comparison over the whole brain. Yellow arrows indicate the magnitude and direction of the shape change from females to males. There were clear differences between the blob patterns with and without global size effects. With the global size effects (Fig. 22.10a), all arrows point outward, meaning that almost all regions had expanded from females to males, particularly the frontal, temporal, and occipital regions. This is consistent with the general appearance; however, it failed to detect local differences, such as in the supraorbital area. Without the global size effects (Fig. 22.10b), DBM succeeded in detecting local differences between males and females. We can see some diffuse blobs in the skull that indicate regions showing a significant difference between males and females and those undergoing multiple comparison correction. The blobs were located in supraorbital areas, the forehead, and inferior occipital regions. When we focused on the direction of transformation for each blob, the blob on supraorbital ridges expanded in an anterior direction. This is consistent with the evidence that supraorbital ridges are more marked in males. The blob on the lateral forehead shrank slightly in superior and posterior directions from females to males. This result can be explained by the vector sum of the two deformation fields provided by the males and females to average transformation. Because female foreheads tended to be more vertical and prominent, male foreheads were more slanted back when viewed from the shape of a female forehead. We also found that the occipital regions in the right hemisphere expand in a posterior or postero-inferior direction. Overall, the results of multivariate analysis are consistent with prior observations of the general appearance.

22.4 Summary and Future Plans

In this study, we examined the application of computational anatomy to fossil brain research. Two principle analysis protocols were developed. First is brain reconstruction with skull shape matching. Using this method, one individual brain can be extrapolated from another with matching of their skull shape. Second is whole-brain morphometric analysis for fossil brain research. DBM analysis can be used to evaluate the location and direction of changes in the skull shape among different populations. Prototype analysis using modern human MRI data indicates that brain reconstruction based on skull shape matching is possible, and whole-brain morphometric analysis reveals gender differences in the skull shape at local and global levels. These methods can be a prototype for future research using Neanderthal skulls.

As our next step, we plan to extend the proposed method to analyze Neanderthal fossil skulls. We will extrapolate the Neanderthal brain from the modern human brain by matching their skulls and investigate the morphological differences and similarities between them. By integrating these morphological analyses with functional mapping of the modern human brain, we can identify the brain regions causing the differences in learning ability between Neanderthals and modern humans.

References

Ashburner J (2007) A fast diffeomorphic image registration algorithm. Neuroimage 38:95–113

Ashburner J, Friston KJ (1999) Nonlinear spatial normalization using basis functions. Hum Brain Mapp 7:254–266

Ashburner J, Friston KJ (2000) Voxel-based morphometry—the methods. Neuroimage 11:805–821

Ashburner J, Friston KJ (2005) Unified segmentation. Neuroimage 26: 839–851

Ashburner J, Friston KJ (2007) Computational anatomy (part2). In: Friston KJ, Ashburner J, Kiebel SJ, Nichols TE, Penny WD (eds) Statistical parametric mapping: the analysis of functional brain images. Academic, New York

Ashburner J, Friston KJ (2011) Diffeomorphic registration using geodesic shooting and Gauss-Newton optimisation. Neuroimage 55:954–967

Ashburner J, Hutton C, Frackowiak R, Johnsrude I, Price C, Friston K (1998) Identifying global anatomical differences: deformation-based morphometry. Hum Brain Mapp 6:348–357

Avants B, Gee JC (2004) Geodesic estimation for large deformation anatomical shape averaging and interpolation. Neuroimage 23(Suppl 1): S139–150

Bass WM (1995) Human osteology: a laboratory and field manual, 4th edn. Missouri Archaeological Society, Columbia

Bookstein FL (1997) Landmark methods for forms without landmarks: morphometrics of group differences in outline shape. Med Image Anal 1:225–243

Cao J, Worsley KJ (1999) The detection of local shape changes via the geometry of Hotelling's T2 field. Ann Statist 27:925–942

Chung MK, Worsley KJ, Paus T, Cherif C, Collins DL, Giedd JN, Rapoport JL, Evans AC (2001) A unified statistical approach to deformation-based morphometry. Neuroimage 14:595–606

Chung MK, Worsley KJ, Robbins S, Paus T, Taylor J, Giedd JN, Rapoport JL, Evans AC (2003) Deformation-based surface morphometry applied to gray matter deformation. Neuroimage 18: 198–213

Chung MK, Worsley KJ, Nacewicz BM, Dalton KM, Davidson RJ (2010) General multivariate linear modeling of surface shapes using SurfStat. Neuroimage 53:491–505

Collignon A, Maes F, Delaere D, Vandermeulen D, Suetens P, Suetens P, Marchal G (1995) Automated multi-modality image registration based on information theory. In: Bizais Y, Barillot C, Paola PD (eds) Proceedings of information processing in medical imaging, Lecture notes in computer science. Kluwer Academic, Dordrecht

Friston KJ, Ashburner J, Frith CD, Poline JB, Heather JD, Frackowiak RSJ (1995) Spatial registration and normalization of images. Hum Brain Mapp 2:165–189

Gaser C, Volz HP, Kiebel S, Riehemann S, Sauer H (1999) Detecting structural changes in whole brain based on nonlinear deformations—application to schizophrenia research. Neuroimage 10:107–113

Good CD, Johnsrude IS, Ashburner J, Henson RN, Friston KJ, Frackowiak RSJ (2001a) A voxel-based morphometric study of ageing in 465 normal adult human brains. Neuroimage 14:21–36

Good CD, Johnsrude I, Ashburner J, Henson RN, Friston KJ, Frackowiak RSJ (2001b) Cerebral asymmetry and the effects of sex and handedness on brain structure: a voxel-based morphometric analysis of 465 normal adult human brains. Neuroimage 14:685–700

Hill DL, Batchelor PG, Holden M, Hawkes DJ (2001) Medical image registration. Phys Med Biol 46:R1–45

Hua X, Leow AD, Lee S, Klunder AD, Toga AW, Lepore N, Chou YY, Brun C, Chiang MC, Barysheva M, Jack CR Jr, Bernstein MA, Britson PJ, Ward CP, Whitwell JL, Borowski B, Fleisher AS, Fox NC, Boyes RG, Barnes J, Harvey D, Kornak J, Schuff N, Boreta L, Alexander GE, Weiner MW, Thompson PM, Alzheimer's Disease Neuroimaging I (2008a) 3D characterization of brain atrophy in Alzheimer's disease and mild cognitive impairment using tensor-based morphometry. Neuroimage 41:19–34

Hua X, Leow AD, Parikshak N, Lee S, Chiang MC, Toga AW, Jack CR Jr, Weiner MW, Thompson PM, Alzheimer's Disease Neuroimaging I (2008b) Tensor-based morphometry as a neuroimaging biomarker for Alzheimer's disease: an MRI study of 676 AD, MCI, and normal subjects. Neuroimage 43:458–469

Im K, Lee JM, Lee J, Shin YW, Kim IY, Kwon US, Kima SI (2006) Gender difference analysis of cortical thickness in healthy young adults with surface-based methods. Neuroimage 31:31–38

Lee AD, Leow AD, Lu A, Reiss AL, Hall S, Chiang MC, Toga AW, Thompson PM (2007) 3D pattern of brain abnormalities in Fragile X syndrome visualized using tensor-based morphometry. Neuroimage 34:924–938

Miller MI, Beg MF, Ceritoglu C, Stark C (2005) Increasing the power of functional maps of the medial temporal lobe by using large deformation diffeomorphic metric mapping. Proc Natl Acad Sci U S A 102:9685–9690

Miller MI, Trouve A, Younes L (2006) Geodesic shooting for computational anatomy. J Math Imaging Vis 24:209–228

Wang L, Beg F, Ratnanather T, Ceritoglu C, Younes L, Morris JC, Csernansky JG, Miller MI (2007) Large deformation diffeomorphism and momentum based hippocampal shape discrimination in dementia of the Alzheimer type. IEEE Trans Med Imaging 26:462–470

Worsley KJ, Taylor JE, Tomaiuolo F, Lerch J (2004) Unified univariate and multivariate random field theory. Neuroimage 23(Suppl 1):S189–195

Zuk TD, Atkins MS (1996) A comparison of manual and automatic methods for registering scans of the head. IEEE Trans Med Imaging 15:732–744

Part IV

Neuroscience

Integrated Analytical Scheme for Comparing the Neanderthal Brain to Modern Human Brain Using Neuroimaging Techniques

23

Hiroki C. Tanabe, Takanori Kochiyama, Naomichi Ogihara, and Norihiro Sadato

Abstract

To investigate the differences in learning abilities between *Homo neanderthalensis* and *Homo sapiens* based on the morphology of the brain, we constructed an integrated analytical system for (1) estimating Neanderthal's brain based on the reconstructed skull, (2) identifying local regions that correspond to leaning abilities in modern humans, (3) comparing the estimated Neanderthal brain to the averaged modern human brain based on our functional MRI results and meta-analytical data, using a neuro-computational and functional neuroimaging framework. First, we introduce the strategy of analyzing functional neuroimaging data, especially spatial normalization. Second, we describe the brain functions essential for learning ability in modern humans. We assume that formation of an innovative society is strongly correlated with the two components of cognitive ability; 'intrinsic drive (internal motivation and perspective) to produce creative activity' and 'social brain'. Here, an example of our functional MRI research regarding the social brain is presented. Finally, we provide a brief summary of our integrated scheme.

Keywords

Computational neuroanatomy • fMRI • Functional map • Reconstruction • Social brain

H.C. Tanabe (✉)
Department of Social and Human Environment, Graduate School of Environmental Studies, Nagoya University, Furo-cho, Chikusa-ku, Nagoya, Aichi 464-8601, Japan

Division of Cerebral Integration, Department of Cerebral Research, National Institute for Physiological Sciences, 38 Nishigo-naka, Myodaiji, Okazaki, Aichi 444-8585, Japan
e-mail: htanabe@lit.nagoya-u.ac.jp

T. Kochiyama
The Hakubi project, Primate Research Institute, Kyoto University, Inuyama, Aichi 484-8506, Japan

Brain Activity Imaging Center, Advanced Telecommunications Research Institute International, 2-2-2 Hikaridai, Seika-cho, Soraku-gun, Kyoto 619-0288, Japan
e-mail: kochiyama.takanori.8r@kyoto-u.ac.jp; kochiyam@atr.jp

N. Ogihara
Department of Mechanical Engineering, Faculty of Science and Technology, Keio University, 3-14-1 Hiyoshi, Kohoku-ku, Yokohama, Kanagawa 223-8522, Japan
e-mail: ogihara@mech.keio.ac.jp

N. Sadato
Division of Cerebral Integration, Department of Cerebral Research, National Institute for Physiological Sciences, 38 Nishigo-naka, Myodaiji, Okazaki, Aichi 444-8585, Japan
e-mail: sadato@nips.ac.jp

T. Akazawa et al. (eds.), *Dynamics of Learning in Neanderthals and Modern Humans Volume 2: Cognitive and Physical Perspectives*, Replacement of Neanderthals by Modern Humans Series, DOI 10.1007/978-4-431-54553-8_23, © Springer Japan 2014

23.1 Background

We adopted cognitive neuroscientific and comparative neuroanatomical approaches to examine our hypothesis that the replacement of *Homo neanderthalensis* by *Homo sapiens* was promoted by the differences in their learning abilities (learning hypothesis). By assuming that morphological changes in fossil skulls reflect functional differences between the brains of modern humans versus Neanderthals, we examined for gaps in learning abilities based on differences in cerebral morphology and region-specific activities. Herein, we introduce a scheme for comparing the Neanderthal brain to the modern human brain using neuro-computational and functional neuroimaging techniques. This scheme involves three parts: (1) estimating Neanderthal brain from the reconstructed skull, (2) specifying which brain functions have distinguished their fates, generating maps regarding these functions, and identifying local regions that correspond to those functions in modern humans, (3) comparing the estimated Neanderthal brain to the averaged modern human brain and determining the morphological differences, while taking account of functional MRI results.

23.2 Strategy of Human Neuroimaging Analysis

Progress in magnetic resonance imaging (MRI) techniques has accelerated non-invasive functional brain imaging and direct measurement of living human brain activities (i.e., functional MRI) (Ogawa et al. 1990; Kwong et al. 1992; reviewed by Huttel et al. 2009). These techniques have enabled mapping of the specific functions of the modern human brain (Friston 1997). Statistical parametric mapping (SPM) is used to identify functionally specialized brain responses and areas, and is the most prevalent approach to characterizing functional anatomy (Friston 1997).

The analysis of functional neuroimaging data involves multiple steps (Fig. 23.1), although can be divided into four main parts: (1) spatial (and temporal) processing, (2) estimating the parameters of a statistical model, (3) making inferences about those parameter estimates in each individual data set, and (4) making group inferences with the effect of interests from the individual analysis (Friston et al. 2007). Friston et al. developed a statistical analysis package that included all these steps (Friston 1997), which we consider will be applicable to our analytical scheme, especially the first step. Herein, we describe this pre-processing in detail, which involves removal of noise, correcting for sampling errors, and spatial transformation of both

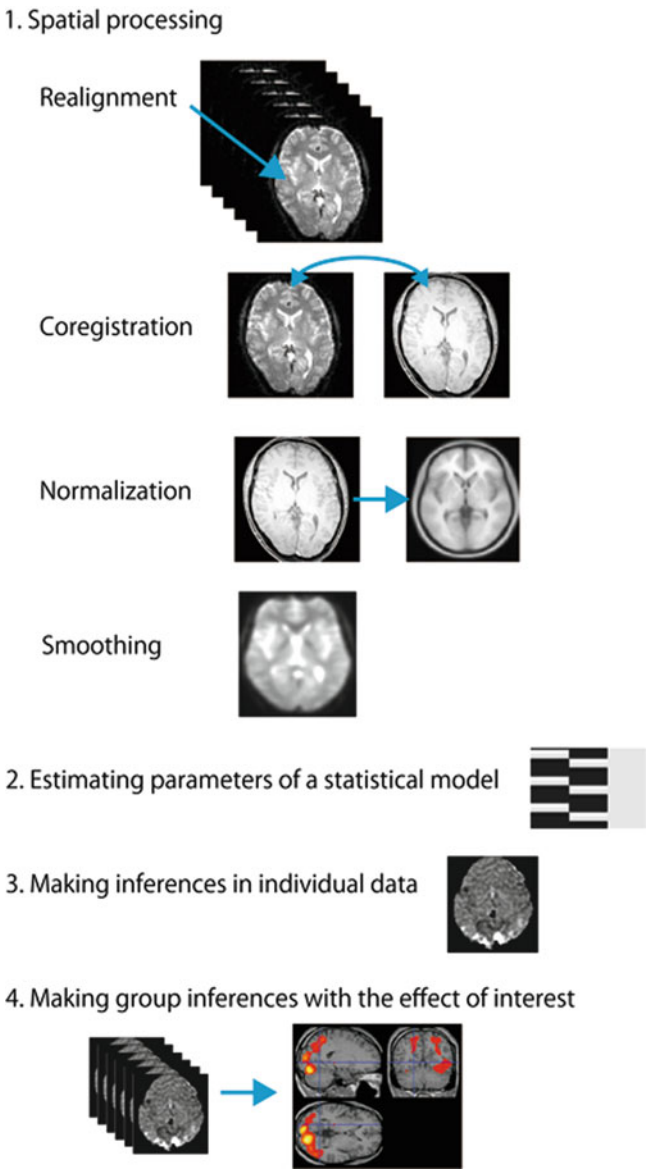

Fig. 23.1 Stream of the functional MRI data analysis

functional and anatomical images. This process includes four small steps: (1) realignment of the functional images (time series data), (2) co-registration between functional and anatomical images, (3) spatial normalization of both images, and (4) spatial smoothing for functional images. The first step is to realign the functional data to reduce unwanted variance components in the voxel time-series that are induced by head movement during the acquisition of the data or shape differences among a series of scans based on head movement. After realigning the data, a mean image of the time-series functional images is co-registered to an anatomical image such as T1-weighted

image. This enables us to map the results of brain activation onto a fine structured anatomical image. The third step involves spatial normalization, which is necessary because functional neuroimaging studies usually involve approximately 20–30 subjects, and although all subjects are likely to have the same gross anatomy, there are often minor differences in overall brain size and individual variation in the topography of the gyri and sulci of the cerebral cortex (Ashburner and Friston 2003; Friston et al. 2007). In the spatial normalization step, the anatomical and functional images are transformed into a standard anatomical space such as the Talairach-Tournoux (Talairach and Tournoux 1988) or templates from the Montréal Neurological Institute (MNI) to allow the data to be summarized to compare to previous studies. The last step of the preprocessing involves spatial smoothing the functional data, which is required because: (1) the optimum smoothing kernel corresponds to the anticipated size of the effect (matched filter theorem), (2) smoothing the data reduces errors (central limit theorem), (3) to fulfill the assumption of random field theory (for the correction of multiple comparisons), and (4) to reduce the individual anatomical differences for performing group level analysis. This pre-processing stage is able to be applied our scheme, especially in the spatial normalization process.

23.3 Spatial Normalization to Our Scheme

There are two main categories of normalization methods developed to transform images: the small-deformation framework, which does not necessary to preserve topology, and the large-deformation framework, which generates deformations that have a number of elegant mathematical properties (Ashburner 2007). Because of the simplicity and lower computational demands, many normalization approaches utilize a small-deformation strategy. However, this approach is only a very approximate inverse, and fails badly for large deformations. By contrast, large-deformation involves global one-to-one smoothing and continuous mapping with derivatives that are invertible, and is thus suitable for normalization of functional neuroimaging data. Recently, Ashburner (2007) developed a new large-deformation approach for normalization in human neuroimaging research, termed DARTEL (i.e., Diffeomorphic Anatomical Registration using Exponentiated Lie algebra). This method is useful in our scheme as: (1) DARTEL provides global one-to-one mapping that enables us to transform the data back and forth, (2) this method is in the pre-processing of the SPM package used in our neuroimaging study, and (3) standardized stereotaxic space is available (i.e., can be transformed with addition of a few steps). Therefore, we can easily integrate the estimation and the creation of the 'fossil brain' of the Neanderthal with a functional neuroimaging study of modern humans.

23.4 Which Function Do We Examine?

To create maps of differences of 'learning abilities' between *Homo neanderthalensis* and *Homo sapiens*, we need to select the brain function to examine. According to Tomasello (1999), in *Homo sapiens* history some individuals or group of individuals first invented a primitive version of an artifact or practice (i.e., creative or innovative activity; termed individual learning ability), while later users made a modification or accepted the practice without any change for many generations (i.e., learnt and used by others over time; termed social learning ability). The important point is that the *Homo sapiens* were able to pool their cognitive resources, suggesting that they could understand conspecifics as beings like themselves who have intentional and mental lives like their own (Tomasello et al. 1993). As such, we assume that formation of the innovative society is strongly correlated with the two components of cognitive ability: 'intrinsic drive (internal motivation and perspective) to produce creative activity' and 'social brain'. *Homo sapiens* are superior in these abilities compared to *Homo neanderthalensis*, and this difference may have distinguished their fate.

23.5 Social Brain and Its Neural Basis: Example of the Neuroimaging Study

'Social brain' is a circumscribed set of brain regions that are dedicated to the social cognition and interaction (Brothers 1990). The most important attribute of the social brain is to make predictions about the actions of others on the basis of their mental states, an ability which has developed from the early stage of human life. As an example of these social cognitive abilities, in neuroimaging studies we previously investigated the neural substrates of 'eye contact' and 'joint attention' (Saito et al. 2010; Tanabe et al. 2012), which are both the merkmal of the social cognitive abilities during the early development of humans. Eye contact allows establishment of a communicative link between humans and prompts joint attention. Joint attention is an ability to coordinate interactive attention between two persons regarding objects or events. The impaired development of joint attention is a key feature of autism spectrum disorder (ASD). As eye contact is implicated in the sharing of various psychological states, it might provide a communicative context in which joint attention can be initiated. To elucidate the neural mechanisms of

inter-subjective sharing during eye contact and joint attention, we conducted a hyper-scanning functional MRI experiment while subjects were engaged in joint attention tasks (to elucidate task-related brain activity) with eye contact as the baseline (to reveal state-related brain activity). We assumed that the eye contact-based psychologically-shared mental states are neurally represented by the subjects' synchronization of the 'state' of brain activity, which is obtained by the elimination of the task-related brain activity component. By contrast, we detected brain regions related to joint attention in terms of task-related activity. Moreover, to compare the neural mechanisms during eye contact and joint attention between typically-developed young adult individuals and those with high-functioning autism (HFA), we examined the brain regions involved in social cognition during eye-based communication. Our findings suggest that the right inferior frontal gyrus (IFG) plays an important role for shared intention during eye contact that provides the context for joint attention (for details see Saito et al. 2010 and Tanabe et al. 2012). Taken with other neuroimaging studies, we consider that the right IFG is specifically involved in social interaction, and is a candidate region for the difference between the brain of *Homo sapiens* and that of *Homo neanderthalensis*.

23.6 Meta-analysis: A Method for Summarizing Results Across Multiple Neuroimaging Studies

A potential limitation of neuroimaging studies is that each result only shows the statistically significant correlation between the specific experiment task and regional brain activation. From the results of one experiment, it is difficult to establish the relationship between psychological process (function) and specific brain region(s). Moreover, interpreting results from a limited set of studies is flawed. Therefore, it is necessary to integrate research findings across multiple laboratories and using a variety of scanning procedures. The tool of meta-analysis can achieve this requirement (Warger et al. 2007). The goal of the meta-analysis is to determine consistently activated regions in a set of studies related to the same psychological process in a quantitative or statistical manner (Warger et al. 2007). As many neuroimaging studies use the same stereotaxic coordinates (e.g., MNI), it is relatively easy to integrate the results. Meta-analysis tools are also being further developed (for example, Yarkoni et al. 2011), and we have been able to access and use them. Therefore, if we determine a specific function to focus on, meta-analysis would be powerful tool to accomplish our goal.

23.7 Integrated System for Estimating and Creating Neanderthal's Brain, Neuroimaging Studies of Modern Humans, and Comparison Between Neanderthal and Modern Human Brains

Our final goal is to examine the differences in learning abilities between *Homo neanderthalensis* and *Homo sapiens* by integrating morphological analysis of fossilized brains with functional mapping of the modern human brain. As described above, we have established an integrated analytical system for elucidating the difference between the Neanderthal brain and the modern human brain (Fig. 23.2). In this scheme, modern human MR head images (i.e., both skull and brain) are segmented into skull, grey matter, and white matter. The skull images and the reconstructed skull CT image of Neanderthals are then transformed to the averaged skull shape using the DARTEL method. The constraints and priors can be added to the transformation. The parameters are applied to the MR brain of the modern human to create an averaged brain shape. To create the fossil brain of the Neanderthal, the averaged brain is transformed inversely using parameters from Neanderthal's reconstructed skull to the averaged skull shape. The key feature of this analytical scheme is that all images are transformed into the same stereotaxic space to allow comparison between the different types of images, even if the image is estimated from the Neanderthal's reconstructed skull. We can also compare the results of functional MRI research as these data can be transformed into the same stereotaxic space.

The advantages of this system are: (1) the ability to add constraints and priors to precisely estimate the Neanderthal brain, (2) to allow improved estimation if the sample size is increased, (3) the ability to add the comparisons with different types of fossil brains such as early modern humans (e.g., Qafzeh), (4) the ability to perform quantitative statistical volume analysis based on the brain morphology, and (5) the ability to refer to functional maps (regarding the learning ability) of our functional MRI results and also results of meta-analysis of previous functional neuroimaging studies. We also recognize are some assumptions and limitations in our approach, although we try to minimize their effects. In the near future, we will attempt to elucidate a possible difference in learning abilities between *Homo neanderthalensis* and *Homo sapiens* based on this scheme.

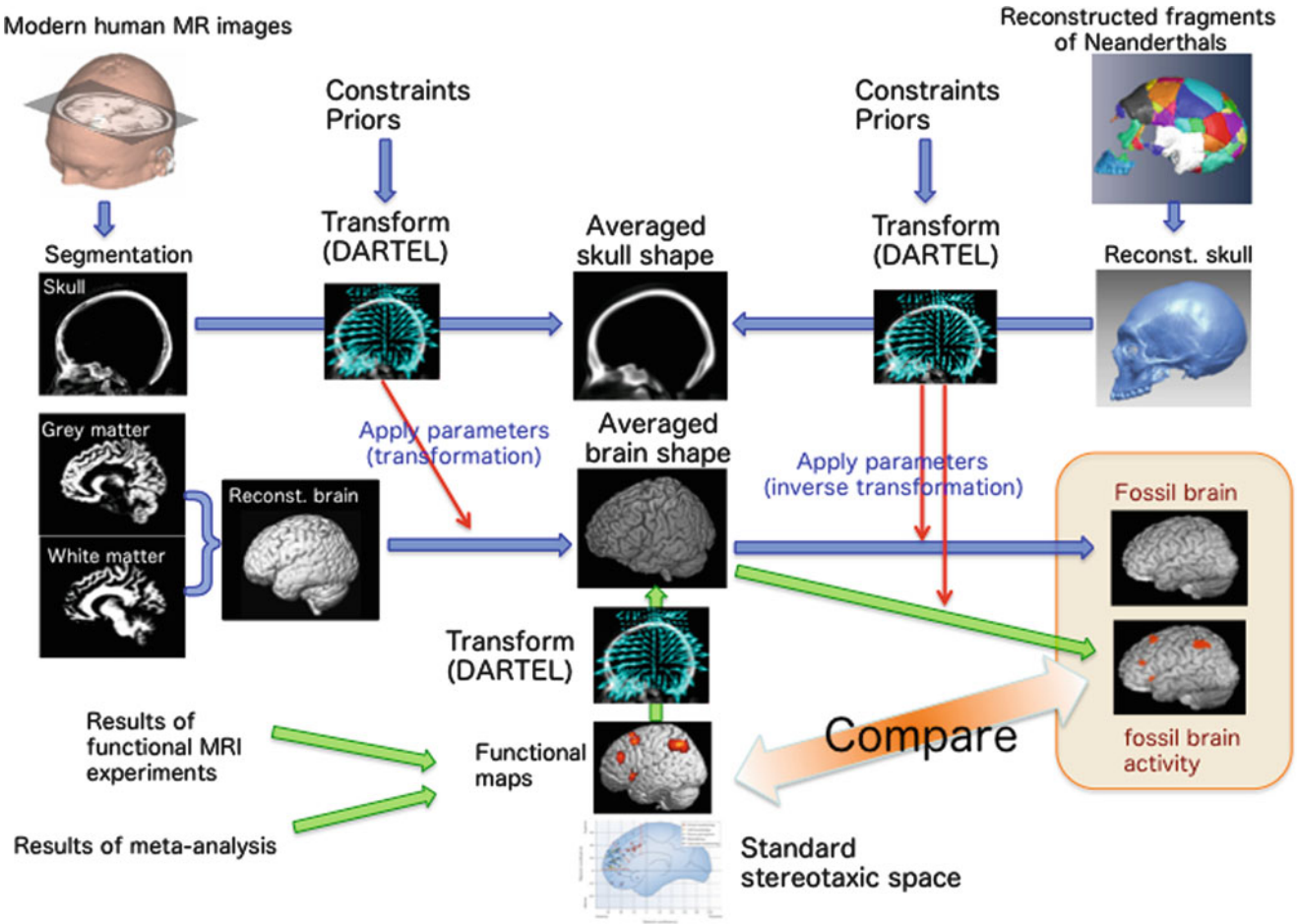

Fig. 23.2 Integrated analytical scheme

Acknowledgements This study was supported by Grant-in-Aid for Scientific Research on Innovative Areas (Grand No. 22101007) from the Ministry of Education, Culture, Sports, Science, and Technology of Japan (MEXT).

References

Ashburner J (2007) A first diffeomorphic image registration algorithm. Neuroimage 38:95–113

Ashburner J, Friston KJ (2003) Spatial normalization using basis functions. In: Frackowiak RSJ, Friston KJ, Frith CD, Dolan RJ, Price CJ, Zeki S, Ashburner JT, Penny WD (eds) Human brain function, 2nd edn. Academic, Waltham

Brothers L (1990) The social brain: A project for integrating primate behaviour and neurophysiology in a new domain. Concepts Neurosci 1:27–251

Friston KJ (1997) Analyzing brain images: principles and overview. In: Frackowiak RSJ, Friston KJ, Frith CD, Dolan RJ, Mazziotta JC (eds) Human brain function, 1st edn. Academic, Waltham

Friston KJ, Ashburner JT, Kiebel SJ, Nichols TE, Penny WD (2007) Statistical parametric mapping. Academic, London

Huttel S, Song AW, McCarthy G (2009) Functional magnetic resonance imaging, 2nd edn. Sinauer Associates, Wlatham

Kwong KK, Bellibeau JW, Chesler DA, Goldberg IE, Weisskoff RM, Poncelet BP, Kennedy DN, Hoppel BE, Cohen MS, Turner R (1992) Dynamic magnetic resonance imaging of human brain activity during primary sensory stimulation. Proc Natl Acad Sci U S A 89: 5675–5679

Ogawa S, Lee TM, Kay AR, Tak DW (1990) Brain magnetic resonance imaging with contrast dependent on blood oxygenation. Proc Natl Acad Sci U S A 87:9868–9872

Saito DN, Tanabe HC, Izuma K, Hayashi MJ, Morito Y, Komeda H, Uchiyama H, Kosaka H, Okazawa H, Fujibayashi Y, Sadato N (2010) "Stay tuned": Inter-individual neural synchronization during mutual gaze and joint attention. Front Integ Neurosci 4:127

Talairach J, Tournoux P (1988) Co-planar stereotaxic atlas of the human brain. Thieme Medical Publishers, New York

Tanabe HC, Kosaka H, Saito DN, Koike T, Hayashi MJ, Izuma K, Komeda H, Ishitobi M, Omori M, Munesue T, Okazawa H, Wada Y, Sadato N (2012) Hard to "tune in": Neural mechanisms of live face-to-face interaction with high-functioning autism spectrum disorder. Front Hum Neurosci 6:268

Tomasello M (1999) The cultural origins of human cognition. Harvard University Press, Cambridge

Tomasello M, Kruger AC, Ratner HH (1993) Cultural learning. BehavBrain Sci 16:495–552

Warger TD, Lindquist M, Kaplan L (2007) Meta-analysis of functional neuroimaging data: current and future directions. Soc Cogn Affect Neurosci 2:150–158

Yarkoni T, Poldrack RA, Nichols TE, van Essen DC, Wager TD (2011) Large-scale automated synthesis of human functional neuroimaging data. Nat Methods 8:665–670

Cerebellar Size Estimation from Endocranial Measurements: An Evaluation Based on MRI Data

24

Daisuke Kubo, Hiroki C. Tanabe, Osamu Kondo, Naomichi Ogihara, Akira Yogi, Sadayuki Murayama, and Hajime Ishida

Abstract

Cerebellar volume (CBV) estimation of fossil hominins can help in understanding the evolution of modern behavior, considering that recent neurological studies suggest significant contribution of the cerebellum to high cognitive abilities of modern humans. However, there has been no reliable methods to estimate the CBV from the endocranial cavity. In order to develop the method, the correlation between CBV and the volume and linear measurements of the posterior cranial fossa (PCF), which were taken from MRI data of thirty-two Japanese subjects, was examined. Estimation equations were then obtained from the bivariate relationships and the validity were evaluated based on prediction intervals. We found that, among the PCF metrics we examined, PCF volume was most highly correlated with CBV ($r=0.88$), and the estimation equation provides CBV estimates with the error of about ±12 cc for specimens from the reference population sample. This result could offer a promising prospect for CBV estimation of fossil hominins including Neanderthal examples.

Keywords

Cerebellar volume • Endocast • MRI • Neanderthals • Posterior cranial fossa

D. Kubo (✉) • O. Kondo
Department of Biological Sciences, Graduate School of Science, University of Tokyo, 7-3-1 Hongo, Bunkyo-ku, Tokyo 113-0033, Japan
e-mail: dkubo@biol.s.u-tokyo.ac.jp; kondo-o@biol.s.u-tokyo.ac.jp

H.C. Tanabe
Department of Social and Human Environment, Graduate School of Environmental Studies, Nagoya University, Furo-cho, Chikusa-ku, Nagoya, Aichi 464-8601, Japan

Division of Cerebral Integration, Department of Cerebral Research, National Institute for Physiological Sciences, 38 Nishigo-naka, Myodaiji, Okazaki, Aichi 444-8585, Japan
e-mail: htanabe@lit.nagoya-u.ac.jp

N. Ogihara
Department of Mechanical Engineering, Faculty of Science and Technology, Keio University, 3-14-1 Hiyoshi, Kohoku-ku, Yokohama, Kanagawa 223-8522, Japan
e-mail: ogihara@mech.keio.ac.jp

A. Yogi • S. Murayama
Department of Radiology, Graduate School of Medicine, University of the Ryukyus, 207 Uehara, Nishihara, Okinawa 903-0215, Japan
e-mail: jxo98ayg@med.u-ryukyu.ac.jp; sadayuki@med.u-ryukyu.ac.jp

H. Ishida
Department of Human Biology and Anatomy, Graduate School of Medicine, University of the Ryukyus, 207 Uehara, Nishihara, Okinawa 903-0215, Japan
e-mail: ishidaha@med.u-ryukyu.ac.jp

T. Akazawa et al. (eds.), *Dynamics of Learning in Neanderthals and Modern Humans Volume 2: Cognitive and Physical Perspectives*, Replacement of Neanderthals by Modern Humans Series, DOI 10.1007/978-4-431-54553-8_24, © Springer Japan 2014

24.1 Introduction

To what extent Neanderthal cognitive abilities were similar to or different from those of modern humans is currently under intensive debate (Nowell 2010; Zilhão et al. 2010). While there is a broad consensus that higher cognitive functions in modern humans are associated with the well-developed cerebral system (e.g. Beaumont 2008), an increasing number of neuroanatomical, clinical, and functional neuroimaging studies suggest that the cerebellum also contributes to higher cognitive abilities, including language competence (Murdoch 2010; Stoodley and Schmahmann 2010). Therefore, reliable data of cerebellar volume (CBV) estimates of extinct hominins, as with that of the whole brain size, may help to clarify when and how the neural bases of cognitive abilities evolved and enabled modern behaviors.

Anatomically, a substantial volume of the cerebellum is housed in the posterior cranial fossa (PCF): a bowl-shaped depression occupying a posteroinferior region of the endocranial cavity (in Fig. 24.1, the location of the PCF is shown). Researchers have hence tentatively used the PCF measures of fossil endocasts as alternatives of the cerebellar size (e.g. Holloway and Yuan 2004). However, the spatial correspondence between the PCF and cerebellum is actually not so straightforward; the PCF does not house an upper portion of the cerebellum, while the former houses some other soft tissues (e.g. the brain stem, cerebrospinal fluid, sinuses, and dura mater). Thus, quantitative evaluation is necessary to substantiate the presumed correspondence between the PCF and the cerebellum.

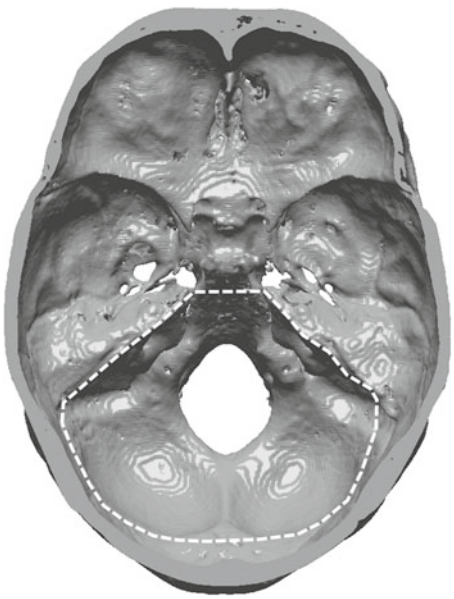

Fig. 24.1 Endocranial cavity of a modern human skull (superior view of the *lower half*). The region surrounded by a *dashed line* is the PCF. The image was reconstructed from CT data

The correlation between the cerebellar and PCF volumes can be examined based on cadaver materials or by using MRI data of living subjects. As far as we know, Weaver (2001) is the only work aiming at this problem, in which she examined the relationship based on T1-weighted MRI data of a mixed hominoid sample and found a high correlation between these volumes: $r^2 = 0.89$. However, this is probably overestimated due to a large range of variation in size from gibbons to humans and does not secure that the CBV can be estimated accurately from the PCF. In fact, the correlation within the human sample (n = 17) of Weaver's dataset is actually weak ($r^2 = 0.16$) and not significant (Kubo et al. 2011). Besides, the estimation equation of CBV devised by Weaver (2001) may have considerable systematic errors stemming from the measurement and calibration procedures, as we will see in the Discussion and Prospects section.

Difficulties inherent in MRI data-based volumetric studies are worthy of consideration. We cannot directly verify the accuracy of CBV obtained from MRI data of living humans since the true value can be determined only by dissection. The best we can do is to validate it by referring some postmortem data. On the other hand, we can evaluate the accuracy of the PCF volume (PCFV) obtained from MRI data with reference to the value obtained from CT data of the same individuals. The latter validation is important not only because the MRI data is less frequently used for segmentation of bone structure than CT data, but also because endocasts of fossil specimens are often obtained from the CT images.

The purpose of this study is to develop estimation methods of the CBV and clarify the limitation. After validation of our measurements, we examine the correlations between CBV and some PCF metrics (PCFV and linear metrics), which were taken from MRI data of Japanese subjects. We then provide estimation equations of the CBV based on the PCF metrics, and finally evaluate the possible error of the estimated values.

24.2 Materials and Methods

24.2.1 Data Acquisition and Some Steps of Preparation

Head MR images of thirty-two healthy Japanese subjects (18–22 years-old; 16 male and 16 female) were used for correlation and regression analyses. Their stature and body weight are summarized in Table 24.1. The MR images were acquired using a 3-Tesla MR scanner (Verio, Siemens, Erlangen, Germany) at National Institute for Physiological Sciences, Okazaki, Japan. To acquire fine structural whole-brain images, we used T1-weighted MP-RAGE axial sequence. The parameters of each protocol are listed below: TR, 1,800 ms; TE, 2.97 ms; TI, 800 ms; flip angle, 9°,

Table 24.1 Stature (cm) and body weight (kg) of subjects

	Male (n = 16)	Female (n = 16)	Total (n = 32)
Stature	172.2 ± 4.4	156.4 ± 6.3	164.3 ± 9.7
Body weight	61.0 ± 7.3	49.0 ± 10.5	55.0 ± 10.8

FoV, 250 mm, number of slices per slab = 192; voxel dimensions = 0.976563 × 0.976563 × 1 mm.

Pairs of head MR and CT images of three healthy Japanese subjects (29–40 years-old) were used for validation of PCF segmentation. The MR images were acquired by the above noted system with T1-weighted MP-RAGE sagittal sequence. The parameters of each protocol are listed below: TR, 1,800 ms; TE, 1.98 ms; TI, 800 ms; flip angle, 9°, FoV, 256 mm, number of slices per slab = 176; voxel dimensions = 1 × 1 × 1 mm. The CT images were acquired using a 320-detector row MDCT scanner (Aquilion One, Toshiba, Tokyo, Japan) at the Hospital in University of the Ryukyus. The reconstructed voxel resolution is ~0.45 × ~0.45 × 0.5 mm or ~0.45 × ~0.45 × 1 mm.

All acquired MR images were initially corrected to remove artifactual intensity gradient by using SPM8 (Wellcome Trust Centre for Neuroimaging, London, UK). Anisotropic voxel data were converted into the isotropic voxel data by using Analyze 10.0 (Mayo Clinic, MN, USA), and then realigned to a standard anatomical orientation with reference to the AC-PC line and the interhemispheric fissure by using Mayo 3D Brain Atlas of the Analyze 10.0 software.

24.2.2 Measurement of CBV, PCFV, and Some Linear Metrics

In Fig. 24.2, the flow chart of cerebellar and PCF segmentation from MR images is shown.

Extraction of cerebellar region from MR images was done by the following three steps: (1) automated skull stripping using BET2 in the FSL package (FMRIB Analysis Group, Oxford, UK), in which the parameters were set at -R, -f 0.5, -g 0; (2) automated segmentation of cerebellar portion using the BrainSuite software (Shattuck and Leahy 2002), in which the threshold of Grey matter/CSF (cerebrospinal fluid) interface was set at 35 %; (3) slice-by-slice manual correction of the cerebellar portion extracted by the above two steps, using Amira 5.3 (Visage Imaging, Inc., CA, USA). Finally, the CBV was obtained as the product of the number of voxels assigned to cerebellum and the voxel size. In Fig. 24.3, a reconstructed model of the cerebellum thus extracted is shown.

Extraction of PCF region from MR images was done by the following two steps: (1) Semi-automated segmentation of PCF region using the Amira 5.3 software. Non-endocranial portions which exhibit similar intensities to endocranial contents (e.g. diploe regions) hamper fully automated segmentation.

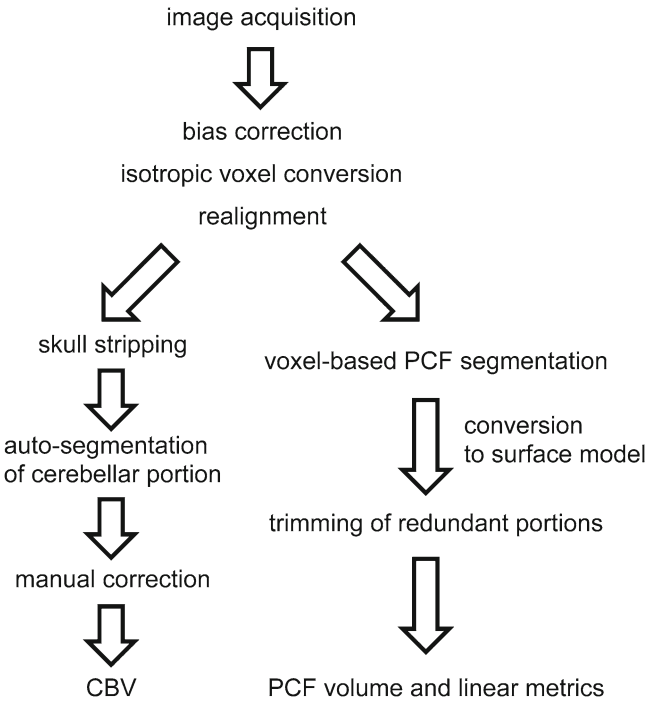

Fig. 24.2 Flow chart of cerebellar and PCF segmentation from MR images

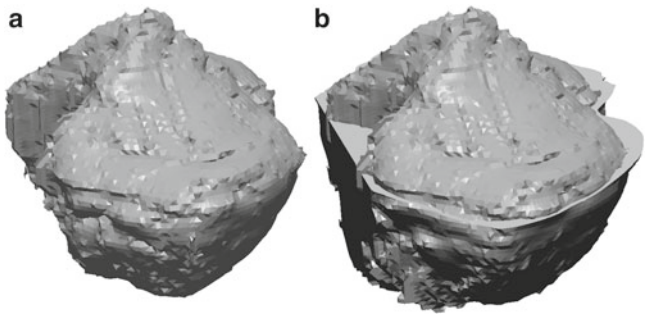

Fig. 24.3 A polygon surface model of the cerebellum, which was extracted from MRI data. An oblique view (**a**), and the same view with the PCF model superimposed (**b**). See also Fig. 24.4 for the PCF model

To resolve this, slice-by-slice manual masking of these regions was firstly done, and then threshold-based auto-segmentation was performed to detect dura mater/bone interface (see Meltzer et al. 1996 for visualization of the dura mater in MRI). Since it is difficult to delineate the anterior and superior limits of the PCF on the volume data properly, these were temporarily set outside it proper position. (2) Determination of the anterior and superior limits of the PCF based on anatomical landmarks. The PCF region extracted from the volume data was converted to a polygon surface model. By using Rapidform XOS3 (INUS Technology, Inc., Seoul, South Korea), the anterior and superior margins of the PCF model were trimmed by three planes defined by seven anatomical landmarks (Table 24.2), and the remaining volume is calculated as PCFV. In Fig. 24.4, these anatomical landmarks and planes as well as a surface model of

Table 24.2 Anatomical landmarks and planes used to define the PCF in this study

	Definition
Bilateral landmarks	
L1, R1	The intersection between the petrous superior margin and the parasagittal plane where the posterior edge of the opening of the internal acoustic meatus is located
L2, R2	The meeting point between the petrous superior margin and the medial edge of the sigmoid sinus groove
Midsagittal landmarks	
M1	Basion
M2	The midpoint of L1 and R1
M3	A representative point of the internal occipital protuberance. This is located in the mid-height level between the inferior edge of the occipital bulge and the superior edge of the cerebellar bulge
Planes	
Plane 1	Plane including L1, R1, and M1.
Plane 2	Plane including L2, R2, and M2.
Plane 3	Plane including L2, R2, and M3.

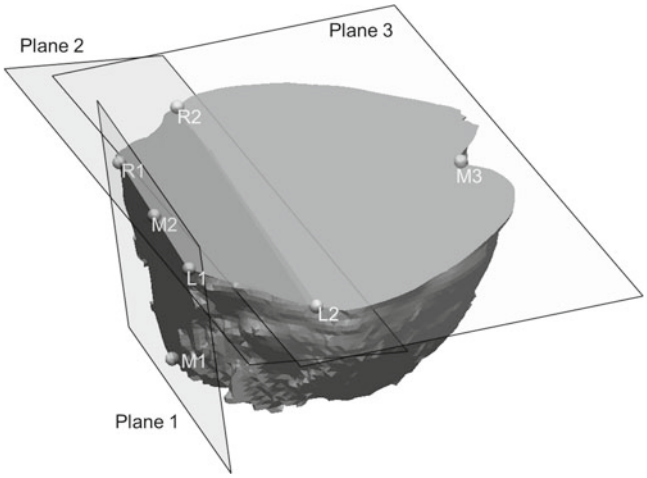

Fig. 24.4 A polygon surface model of the PCF with the anatomical landmarks and planes, which were used to define the anterior and superior limits of the PCF. See Table 24.2 for the details of the definition. The PCF model was reconstructed from MRI data

the trimmed PCF are shown. In addition, some width and height measurements of the PCF (Table 24.3) were taken on the polygon surface model in order to examine the relationship between these and CBV. In Fig. 24.5, diagrammatic representation of the linear measurements is shown.

Extraction of PCF region from CT images was done by use of a threshold value to detect endocranial contents/bone interface. The anterior and superior limits of the PCF region was defined following the same procedure as above.

24.2.3 Validation of the Reliability of MRI Data-Based Measurement

The volumetric error attributed to the voxel size accuracy of our MRI data was estimated to be 1 % at best with reference to MR images of a known size phantom (D170, Siemens, Erlangen, Germany).

Table 24.3 Definition of metrics used in this study

	Definition
PCFV	Volume of the PCF bordered by Plane 1–3
CW1	Maximum width of the PCF including the sinus
CW2	Maximum width of the PCF excluding the sinus
CW3	Maximum chord distance across the cerebellar hemisphere (both side mean). The one side of the chord is set at L2 or R2
PCFH	Perpendicular distance from Plane 3 to the bottom of the cerebellar hemisphere (both side mean)
GMM	Geometric mean of CW2, CW3, and PCFH

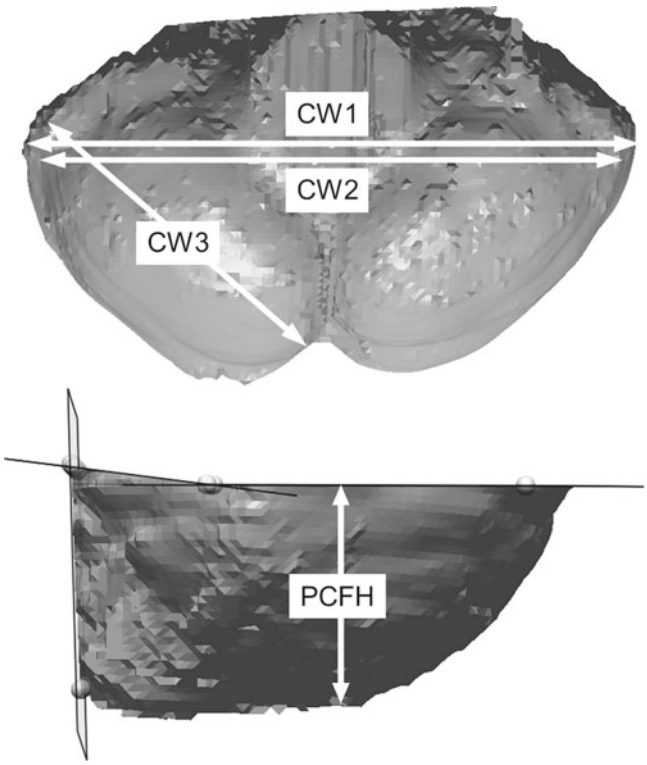

Fig. 24.5 PCF linear metrics, whose definitions are provided in Table 24.3. The PCF model was reconstructed from MRI data

As already noted, we cannot directly verify the accuracy of CBV obtained from MRI data. Instead, we examined whether the obtained CBVs are not far from the expected values with reference to two previous studies based on Japanese cadaver materials (Hoshi 1929; Shimada 1939). In order to validate the reliability of MRI-based PCF measurements, we compared the PCFV obtained from MR data with that from CT data of the same individuals.

24.2.4 Correlation and Regression Analysis

The Pearson's product moment correlation coefficient r was calculated to evaluate the strength of the correlation between CBV and each PCF metric for the male, female, and sex-combined (total) samples, respectively. For the cases where the correlation was significant, the least squares regression was calculated to obtain the estimation equation of the CBV based on the PCF metric. The analysis of covariance (ANCOVA) was performed to test the sex difference under the null hypothesis 'the male and female samples share the common CBV–PCF relationship'. After confirmation the null hypothesis is not rejected, the possible error of the estimated values based on each equation for the sex-combined sample was evaluated by the 95 % prediction intervals. These statistical analyses were performed using R software (R Core Team 2012).

24.3 Results

The CBVs measured in this study are 2–14 % larger than those reported by the studies based on cadaver materials (Table 24.4). Brains of cadaver materials shrink owing to fixation by about 10 % (Pickering 1930) or more (Quester and Schröder 1997). In addition, the head breadth of Japanese rapidly increased during the last century while the head length was stable (Kouchi 2004). Considering these, the CBVs obtained from MRI data in this study may largely represent the actual volumes. PCFVs obtained from MRI data were well consistent with those from CT data of the same individuals: the differences were less than 4 cc (Table 24.5).

Table 24.6 shows statistical summary of measurements used for correlation and regression analyses. Table 24.7 shows the correlation coefficients between CBV and each PCF metric and the results of the least squares regression of CBV on each PCF metric. Significant correlations for both the male and female samples were found only between CBV and PCFV. ANCOVA showed that there is no significant sex difference for the regression slope or intercept. This means that the regression lines for the male and female samples can be considered as identical, indicating a common relationship between CBV and PCFV. In Fig. 24.6, bivariate plots of CBV and each PCF metric are shown, with the least squares regression line of the former on the latter for the total sample and the 95 % confidence and prediction intervals in addition. Among the PCF measures, PCFV is most highly correlated with CBV ($r = 0.88$), explaining 78 % of the whole variance of the latter. A geometric mean of three PCF linear measurements (GMM) exhibits the second highest correlation with the CBV ($r = 0.74$), explaining 55 % of the whole variance. Using the least squares regression equation based on PCFV (or GMM), the 95 % prediction intervals suggest that the CBV of a specimen from the reference population can be estimated with the error of about ±12 cc (or ±18 cc). The equations based on each single linear metric provide the CBV with the error of about ±21 to ±28 cc.

Table 24.4 Mean of CBV in the present and previous studies

	Sample	Sex	N	CBV (cc)	Ratio[a]
This study	Japanese (18–22 years), MRI	M	16	147.1	–
		F	16	130.4	–
Hoshi (1929)	Japanese (17 years and older), cadaver, not stated for fixation	M	101	140.2[b]	1.05
		F	78	127.7[b]	1.02
Shimada (1939)	Japanese (17–81 years-old), cadaver, formalin fixed	M	50	128.6	1.14
		F	50	117	1.11

[a]CBV of this study/CBV of the previous study
[b]calculated from the percentage of CBV in the total brain volume: 10.57 % in male; 10.67 % in female (Shimada 1939)

Table 24.5 PCF volumes (cc) measured from CT and MRI data for the same individuals

	PCFV (CT)	PCFV (MRI)	Difference	Ratio
Subject 1	134.2	134.9	0.7	0.994
Subject 2	114.7	116.2	1.5	0.987
Subject 3	148.7	145.2	3.5	1.024

Table 24.6 Mean and S.D. of measured variables based on MR images

	Male (n = 16)	Female (n = 16)	Total (n = 32)
CBV (cc)	147.1 ± 10.4	130.4 ± 7.4	138.8 ± 12.3
PCFV (cc)	139.4 ± 12.7	116.2 ± 8.3	127.8 ± 15.8
CBV/PCFV ratio	1.059 ± 0.055	1.125 ± 0.063	1.092 ± 0.067
CW1 (mm)	118.0 ± 4.2	112.0 ± 4.9	115.0 ± 5.4
CW2 (mm)	107.1 ± 3.3	101.1 ± 3.3	104.1 ± 4.5
CW3 (mm)	62.6 ± 2.5	61.6 ± 2.8	62.1 ± 2.7
PCFH (mm)	31.6 ± 2.4	29.4 ± 1.7	30.5 ± 2.4
GMM	59.5 ± 2.0	56.7 ± 1.5	58.1 ± 2.3

Table 24.7 Summary of correlation with CBV and least squares regression of CBV on each variable

	Male (n = 16)			Female (n = 16)			Total (n = 32)		
	r	Intercept	Slope	*r*	Intercept	Slope	*r*	Intercept	Slope
PCFV	0.83**	52.2	0.68	0.64*	64.5	0.57	0.88**	50.9	0.69
CW1	–	–	–	–	–	–	0.54*	−1.4	1.22
CW2	–	–	–	–	–	–	0.58**	−27.4	1.60
CW3	–	–	–	0.66*	24.3	1.72	0.44+	12.3	2.04
PCFH	0.60+	66.8	2.54	–	–	–	0.55*	51.2	2.87
GMM	0.67*	−55.7	3.41	–	–	–	0.74**	−96.4	4.05

Symbols **, *, and + represent significance level at $p < 0.001$, $p < 0.01$, and $p < 0.05$, respectively. Dashes mean that the correlation with CBV is not significant

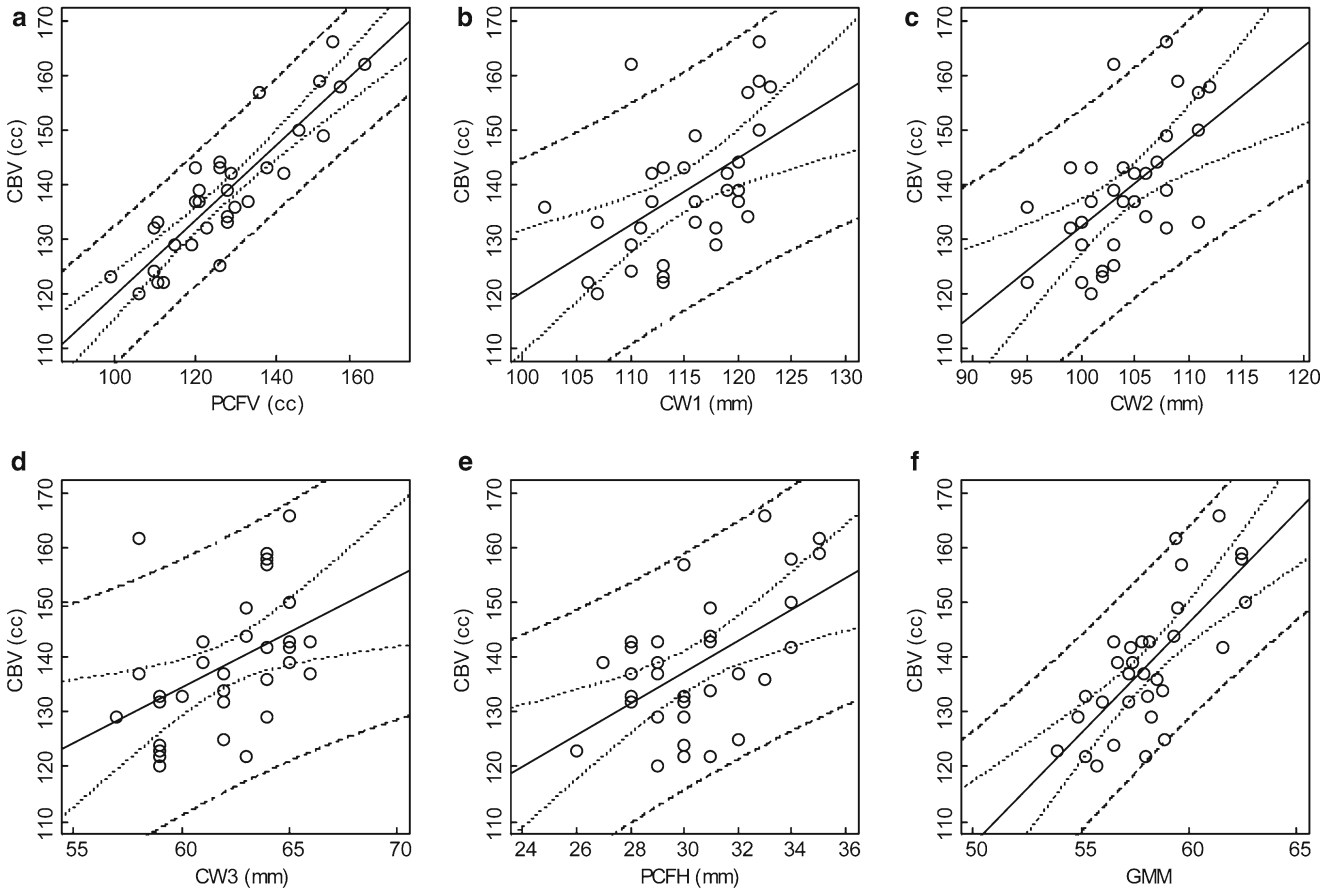

Fig. 24.6 Bivariate plots of PCF metrics and CBV, with the least squares regression lines of CBV on PCF metric for the total sample (*solid line*) and the 95 % confidence and prediction intervals (*dotted* and *dashed lines*). PCFV and CBV (**a**), CW1 and CBV (**b**), CW2 and CBV (**c**), CW3 and CBV (**d**), PCFH and CBV (**e**), and GMM and CBV (**f**). See Table 24.3 for abbreviations

24.4 Discussion and Prospects

We confirmed that the PCFV is highly correlated with the CBV in a modern Japanese sample, in contrast to the result based on the human MRI sample from Weaver's dataset (see above). This might be partly due to difference of the definition of the PCFV. Weaver (2001, p.135) defined the PCF region on MR images by consulting some soft tissue landmarks that cannot be available from fossil skulls, which is a possible source of systematic error. On the other hand, we define the PCF using anatomical landmarks that can be applicable to fossil skulls, and also exclude a volume of the anterior PCF part that houses the brain stem, which could probably contribute to the higher correlation.

We also note another possible error involved in the estimation method devised by Weaver (2001). Weaver (2001) noted that her MRI-based measurement underestimates CBV compared to her Laser-scan-based or CT-based measurements, and thus introduced a calibration coefficient of 0.68 for the CBV

estimation equation; this calibration value was determined by comparing the CBV estimate of a chimpanzee endocast, which was obtained by applying the MRI-based equation to the Laser-scan-based PCFV, with the mean value of CBV for *Pan troglodytes* from literature (Weaver 2001, pp. 151–152). Therefore, the calibration value can be inherently a source of systematic errors. Based on the CBV estimates for a few Neanderthal and early European (Cro-Magnon 1) specimens, which were reported to be relatively smaller than those for recent human samples, Weaver (2001, 2005) suggested that reorganization of neural system with cerebellar expansion may have occurred around the terminal Pleistocene. However, we think it possible that the CBVs of these fossil specimens are underestimated partly due to the above noted errors.

On the other hand, we tested the accuracy of our MRI-based measurements by comparing (1) population mean values for CBV with those from cadaver data with similar ethnicity, and (2) PCFV measures from MRI with those from the CT data of the same individuals, although based on a small sample. The two series of validation provided reasonable reliability for our measurements. Conclusively, our results could offer a promising prospect for CBV estimation of fossil hominins including Neanderthals.

The neural bases underlying cognitive abilities in modern humans, such as language competence (Mithen 2005) and enhanced working memory (Wynn and Coolidge 2010), are presumably associated with various parts of cerebral and cerebellar regions. For instance, working memory is likely associated with the frontal and parietal cerebral regions (Nee et al. 2013). Associations between the left frontal/temporal regions and language ability are well known (e.g. Friederici 2012), and recently, some contribution of cerebellar regions to language competence is also pointed out (Murdoch 2010; Stoodley and Schmahmann 2010). These leads to a possible hypothesis that the evolution of neural bases underlying cognitive abilities of modern humans may have caused not only whole brain size increase but also unproportional volumetric changes of cerebrum and cerebellum. The present study provides an essential first step for assessing the cerebral–cerebellar volumetric proportion of fossil hominins.

Acknowledgement This work was supported by a grant from MEXT, Japan (No.22101006).

References

Beaumont JG (2008) Introduction to neuropsychology, 2nd edn. The Guilford, New York

Friederici AD (2012) The cortical language circuit: from auditory perception to sentence comprehension. Trends Cogn Sci 16:262–268. doi:10.1016/j.tics.2012.04.001

Holloway RL, Yuan MS (2004) Endocranial morphology of A.L. 444-2. In: Kimbel WH, Rak Y, Johanson DC (eds) The skull of *Australopithecus afarensis*. Oxford University Press, New York, pp 123–135

Hoshi S (1929) A study of brain volume. Neurologia (Shinkeigaku Zasshi) 30:497–499 (in Japanese)

Kouchi M (2004) Secular changes in the Japanese head form viewed from somatometric data. Anthropol Sci 112:41–52. doi:10.1537/ase.00071

Kubo D, Kono RT, Suwa G (2011) A micro-CT based study of the endocranial morphology of the Minatogawa I cranium. Anthropol Sci 119:123–135. doi:10.1537/ase.100120

Meltzer CC, Fukui MB, Kanal E, Smirniotopoulos JG (1996) MR imaging of the meninges: part I. normal anatomic features and non-neoplastic disease. Radiology 201:297–308

Mithen S (2005) The singing Neanderthals: the origins of music, language, mind, and body. Wiedenfeld and Nicolson, London

Murdoch BE (2010) The cerebellum and language: historical perspective and review. Cortex 46:858–868. doi:10.1016/j.cortex.2009.07.018

Nee DE, Brown JW, Askren MK, Berman MG, Demiralp E, Krawitz A, Jonides J (2013) A meta-analysis of executive components of working memory. Cereb Cortex 23:264–282. doi:10.1093/cercor/bhs007

Nowell A (2010) Defining behavioral modernity in the context of Neandertal and anatomically modern human populations. Annu Rev Anthropol 39:437–452. doi:10.1146/annurev.anthro.012809.105113

Pickering SP (1930) Correlation of brain and head measurements, and relation of brain shape and size to shape and size of the head. Am J Phys Anthropol 15:1–52

Quester R, Schröder R (1997) The shrinkage of the human brain stem during formalin fixation and embedding in paraffin. J Neurosci Methods 75:81–89. doi:10.1016/S0165-0270(97)00050-2

R Core Team (2012) R: a language and environment for statistical computing. R Foundation for Statistical Computing, Vienna, Austria. http://www.R-project.org/. Accessed 6 Dec 2012

Shattuck DW, Leahy RM (2002) BrainSuite: an automated cortical surface identification tool. Med Image Anal 8:129–142. doi:10.1016/S1361-8415(02)00054-3

Shimada K (1939) The brain of Japanese. In: Nagasaka K (ed) Lectures on anthropology and archaeology, vol 7. Yuzankaku, Tokyo, pp 1–188 (in Japanese)

Stoodley CJ, Schmahmann JD (2010) Evidence for topographic organization in the cerebellum of motor control versus cognitive and affective processing. Cortex 46:831–844. doi:10.1016/j.cortex.2009.11.008

Weaver AGH (2001) The cerebellum and cognitive evolution in Pliocene and Pleistocene hominids. Dissertation, University of New Mexico.

Weaver AH (2005) Reciprocal evolution of the cerebellum and neocortex in fossil humans. Proc Natl Acad Sci U S A 102:3576–3580. doi:10.1073/pnas.0500692102

Wynn T, Coolidge FL (2010) Beyond symbolism and language: an introduction to supplement 1, working memory. Curr Anthropol 51(suppl 1):S5–16. doi:10.1086/650526

Zilhão J, Angelucci DE, Badal-García E, d'Errico F, Daniel F, Dayet L, Douka K, Higham TFG, Martínez-Sánchez MJ, Montes-Bernárdez R, Murcia-Mascarós S, Pérez-Sirvent C, Roldán-García C, Vanhaeren M, Villaverde V, Wood R, Zapata J (2010) Symbolic use of marine shells and mineral pigments by Iberian Neandertals. Proc Natl Acad Sci U S A 107:1023–1028. doi:10.1073/pnas.0914088107

Sense of Acceptance: Key Factor of Social Learning

25

Hiroaki Kawamichi, Kazufumi Yoshihara, Ryo Kitada, Masahiro Matsunaga, Akihiro Sasaki, Yumiko Yoshida, Haruka Takahashi, and Norihiro Sadato

Abstract

In addition to individual learning abilities, the social learning abilities of modern humans likely played a key role in the replacement of Neanderthals by modern humans. In terms of social learning, acceptance from skilled members might facilitate the promotion of social learning processes. Accordingly, a sense of acceptance is one of major functions of social abilities underlying social learning. Thus, a sense of acceptance should be investigated for clarifying neural mechanisms underlying social learning. We propose two viewpoints for investigating the neural correlates underlying the sense of acceptance. Because a sense of acceptance promotes social behaviors, including social learning, through emotional changes, the neural correlates underlying the link between a sense of acceptance and the enhancement of social behavior and between a sense of acceptance and psychological effects should be explored.

Keywords

Sense of acceptance • Social learning

25.1 Introduction

Cognitive and behavioral capabilities of modern humans, such as creativity, likely played a key role in the demise of Neanderthals. Both individual and social learning contribute to this creativity. For instance, in regards to individual learning, humans acquire new skills through trial and error processes; thus, this learning ability facilitates the invention of new skills and technologies. In social learning, on the other hand, humans acquire new skills by observing (Bandura 1965) and imitating (Field and Walden 1982) the behaviors of others. Social learning ability thus promotes the spread of the new skills and technologies invented by individual learning.

Modern humans have enhanced social abilities compared with other animal species (Dunbar 1998); indeed, the capacity for social learning is one of the major characteristics of modern humans. There are four necessary conditions of social learning processes: paying attention to a target, the retention and reproduction of a target's behavior, and motivation for imitation (Badura 1977). Acceptance from others, i.e., approval, enhances the motivation to imitate behaviors (Badura 1977). Thus, sensing acceptance from others might facilitate processes of social learning. Because they can perceive a sense of acceptance, modern humans might tend to spread new skills in comparison to Neanderthals. In this sense, the spread of new skills, motivated by sense of acceptance, could play a key role in the replacement of Neanderthals by modern humans.

H. Kawamichi (✉) • R. Kitada • M. Matsunaga • A. Sasaki
Y. Yoshida • H. Takahashi • N. Sadato
Division of Cerebral Integration, Department of Cerebral Research, National Institute for Physiological Sciences, 38 Nishigo-naka, Myodaiji, Okazaki, Aichi 444-8585, Japan
e-mail: kawami@nips.ac.jp; kitada@nips.ac.jp; mmatsu@nips.ac.jp; akihiro.sasaki@riken.jp; yyumiko@nips.ac.jp; tharuka@nips.ac.jp; sadato@nips.ac.jp

K. Yoshihara
Department of Psychosomatic Medicine, Graduate School of Medical Sciences, Kyushu University, 3-1-1 Maidashi, Higashi-ku, Fukuoka-shi, Fukuoka 812-8582, Japan
e-mail: kyoshiha@cephal.med.kyushu-u.ac.jp

T. Akazawa et al. (eds.), *Dynamics of Learning in Neanderthals and Modern Humans Volume 2: Cognitive and Physical Perspectives*, Replacement of Neanderthals by Modern Humans Series, DOI 10.1007/978-4-431-54553-8_25, © Springer Japan 2014

Recent advances of neuroimaging techniques, such as functional magnetic resonance imaging (fMRI), have revealed the neural correlates underlying a wide range of social abilities, including a sense of acceptance. In this paper, we will review research related to the sense of acceptance, including the modulation of brain activation. Finally, we will introduce our future experimental plan.

25.2 Sense of Acceptance

Sociometer theory has suggested that social acceptance from other people enhances self-esteem (Leary et al. 1995), and furthermore, self-esteem is a consequence of the degree to which people receive acceptance from other people. As proposed in person-centered therapy, a sense of acceptance can influence social behaviors through psychological contact (Rogers 1957). Congruence, unconditional positive regard, and an empathic attitude of the therapist are the most important factors in person-centered therapy. Within successful therapy, the client has changed his/her way of thinking. This change in thinking promotes new social behaviors. Thus, perceiving a sense of acceptance contributes to new social behaviors through changes in mindset.

Functional MRI studies have shown that acceptance (praise) from others activates the striatum, which is part of the reward system (Izuma et al. 2008). On the other hand, rejection from others shows activation in the dorsal anterior cingulate cortex (ACC), part of the pain matrix (Eisenberger et al. 2003), and is accompanied by a self-esteem decrease (Eisenberger et al. 2011a). Interestingly, social support has been shown to decrease psychological pain-related activation in the ACC during social exclusion (Onoda et al. 2009). Thus, social acceptance from others modulates brain activation in two ways: enhancement for reward-related activation and attenuation for pain-related activation.

Humans can also perceive a sense of acceptance even without the explicit words of others (Rogers 1957), which likely stems from their nonverbal attitude. Perceived social support can come in the form of interpersonal touch (Coan et al. 2006). For instance, hand-holding with a spouse or stranger decreases the neural response to pain threat in the right anterior insula, superior frontal gyrus, and hypothalamus, including the affective pain matrix (Coan et al. 2006). In addition, a photo of romantic partner also decreases pain-related responses (Eisenberger et al. 2011b). Therefore, a sense of acceptance stemming from the nonverbal and verbal behaviors of others can modulate emotion-related responses during social behaviors.

25.3 Suggested Experiment for the Sense of Acceptance and Social Learning

25.3.1 Missing Link Between Social Behavior and Sense of Acceptance

Despite the progress in research on the sense of acceptance, there are still issues that need to be resolved. First, as mentioned in the introduction, a sense of acceptance enhances social behavior. However, the neural correlates underlying the link between the sense of acceptance and the enhancement of social behavior is unresolved. Second, the motives for social behavior mainly consist of psychological factors; i.e., the enhancement of social behavior might be caused by emotional changes elicited by a sense of acceptance. Thus, the link between negative feelings stemming from psychological factors and a sense of acceptance warrants further investigation (Fig. 25.1).

25.3.2 Example of Experimental Design

In this article, we suggest a potential experimental design regarding the link between negative feelings stemming from psychological factors and a sense of acceptance. In this type of experiment, empathic pain, the negative feeling aroused by seeing others in pain (Singer et al. 2004), can be treated as psychological pain. Other conditions in the

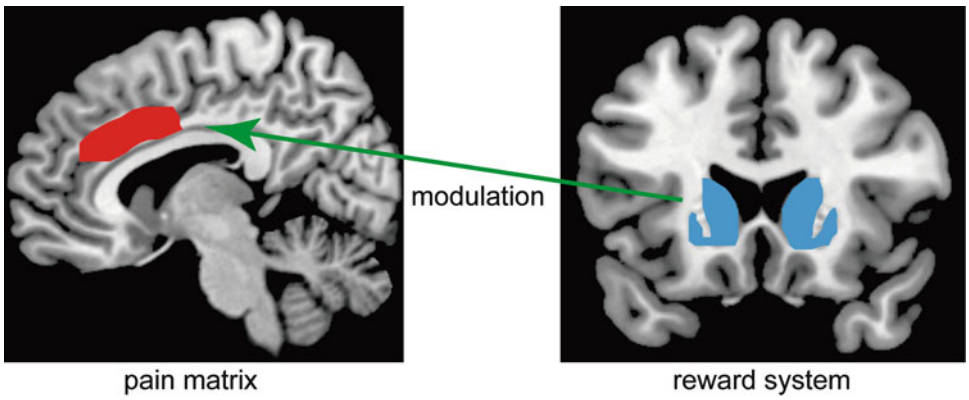

Fig. 25.1 Time chart example of visual stimuli presentation. In the stimulus presentation, two types of stimuli (painful and no painful) are presented

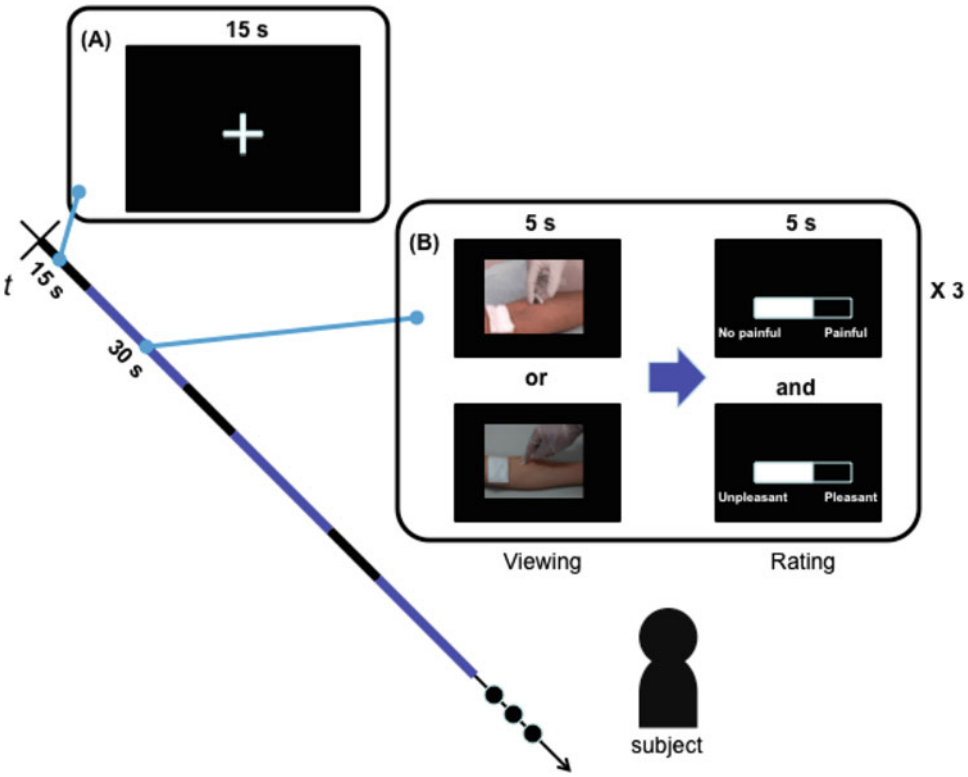

Fig. 25.2 Potential neural correlates underlying sense of acceptance

experiment include supportive words or hand holding as a sense of acceptance. For this experiment, each subject observes painful or non-painful visual stimuli throughout the session. They then evaluate the stimuli while the left hand of a familiar person is placed on their hand (human hand condition). Alternatively, the control condition is when a non-human (e.g., rubber) hand or no hand (non-hand condition) is used.

As hand holding is a gesture that imparts a sense of acceptance, we anticipate that hand holding will be perceived as reward. Thus, we expect that activation of the reward circuit, including ventral striatum, will be enhanced by hand holding. Furthermore, reward system activation is expected to modulate pain-related activation aroused by painful stimuli (Fig. 25.2).

25.4 Conclusion

In this paper, we have indicated the importance of a sense of acceptance for promoting social learning. The sense of acceptance has been investigated in wide range of studies including its underlying neural mechanisms in regards to social behavior or psychological factor effects. However, there is a missing link at the mechanistic level among social behavior, psychological factors, and sense of acceptance. Our proposed experiment may help clarify the neural mechanisms underlying social learning.

Acknowledgement This study was partly supported by Scientific Research on Innovative Areas (grant no. 23101507 to H.K.) and by a Grant-in-Aid for Scientific Research on Innovative Areas (grant no. 25135734 to R.K.).

References

Badura A (1977) Social learning theory. General Learning, New York

Bandura A (1965) Influence of models' reinforcement contingencies on the acquisition of imitative response. J Pers Soc Psychol 1: 589–595

Coan JA, Schaefer HS, Davidson RJ (2006) Lending a hand: social regulation of the neural response to threat. Psychol Sci 17: 1032–1039

Dunbar RIM (1998) The social brain hypothesis. Evol Anthropol 6:178–190

Eisenberger NI, Lieberman MD, Williams KD (2003) Does rejection hurt? An fMRI study of social exclusion. Science 302: 290–292

Eisenberger NI, Inagaki TK, Muscatell KA, Haltom KEB, Leary MR (2011a) The neural sociometer: brain mechanisms underlying state self-esteem. J Cogn Neurosci 23:3448–3455

Eisenberger NI, Master SL, Inagaki TK, Taylor SE, Shirinyan D, Lieberman MD, Naliboff BD (2011b) Attachment figures activate a safety signal-related neural region and reduce pain experience. Proc Natl Acad Sci U S A 108:11721–11726

Field TM, Walden TA (1982) Production and perception of facial expressions in infancy and early childhood. Adv Child Dev Behav 16:169–211

Izuma K, Saito DN, Sadato N (2008) Processing of social and monetary rewards in the human striatum. Neuron 58:284–294

Leary MR, Tambor ES, Terdal SK, Downs DL (1995) Self-esteem as an interpersonal monitor: the sociometer hypothesis. J Pers Soc Psychol 68:518–530

Onoda K, Okamoto Y, Nakashima K, Nittono H, Ura M, Yamawaki S (2009) Decreased ventral anterior cingulate cortex activity is associated with reduced social pain during emotional support. Soc Neurosci 4:443–454

Rogers CR (1957) The necessary and sufficient conditions of therapeutic personality change. J Consult Psychol 21:95–103

Singer T, Seymour B, O'Doherty J, Kaube H, Dolan RJ, Frith CD (2004) Empathy for pain involves the affective but not sensory components of pain. Science 303:1157–1162

26 Brain Activation Related to the Imitative Learning of Bodily Actions Observed During the Construction of a Mousterian Stone Tool: A Functional Magnetic Resonance Imaging Study

Naoki Miura, Kenji Nagai, Mika Yamazaki, Yumiko Yoshida, Hiroki C. Tanabe, Takeru Akazawa, and Norihiro Sadato

Abstract

To comprehend the acquisition of technology during human evolution, it is import to elucidate the cognitive abilities underpinning social learning, such as imitating another's behavior. We focused on a neural mechanism to understand stone tool-making by observing another's behavior, and the existence of a shared neural mechanism with learning of linguistic information using functional magnetic resonance imaging. A learning-related activation change was found in the right cerebellum while observing stone tool-making, which reflected an internal model of motor control. A similar change in word pronunciation was found in the left superior temporal gyrus, which reflected the effect of learning on the perception of auditory stimuli. These results indicate that the progress of imitative learning is represented in a specific cortical region, and that the represented region depends on the information that the subject is focusing on learning.

N. Miura (✉)
Department of Information and Communication Engineering, Faculty of Engineering, Tohoku Institute of Technology, 35-1 Yagiyama Kasumi-cho, Taihaku-ku, Sendai, Miyagi 982-8577, Japan
e-mail: miura.naoki@tohtech.ac.jp

K. Nagai
Department of Historic Heritage, Tohoku University of Art & Design, 3-4-5 Kami-sakurada, Yamagata, Yamagata 990-9530, Japan
e-mail: nagai.kenji@aga.tuad.ac.jp

M. Yamazaki
Child Development Research Center, Graduate School of Medical Sciences, National University Corporation University of Fukui, 23-3 Matsuokashimoaizuki, Eiheiji-cho, Yoshida-gun, Fukui 910-1193, Japan
e-mail: mika@u-fukui.ac.jp

Y. Yoshida
Division of Cerebral Integration, Department of Cerebral Research, National Institute for Physiological Sciences, 38 Nishigo-naka, Myodaiji, Okazaki, Aichi 444-8585, Japan
e-mail: yyumiko@nips.ac.jp

H.C. Tanabe
Department of Social and Human Environment, Graduate School of Environmental Studies, Nagoya University, Furo-cho, Chikusa-ku, Nagoya, Aichi 464-8601, Japan

Division of Cerebral Integration, Department of Cerebral Research, National Institute for Physiological Sciences, 38 Nishigo-naka, Myodaiji, Okazaki, Aichi 444-8585, Japan
e-mail: htanabe@lit.nagoya-u.ac.jp

T. Akazawa
Research Institute, Kochi University of Technology, 185 Miyanokuchi, Tosayamada, Kami, Kochi 782-8502, Japan
e-mail: akazawa.takeru@kochi-tech.ac.jp; akazawa0823@qd6.so-net.ne.jp

N. Sadato
Division of Cerebral Integration, Department of Cerebral Research, National Institute for Physiological Sciences, 38 Nishigo-naka, Myodaiji, Okazaki, Aichi 444-8585, Japan
e-mail: sadato@nips.ac.jp

T. Akazawa et al. (eds.), *Dynamics of Learning in Neanderthals and Modern Humans Volume 2: Cognitive and Physical Perspectives*, Replacement of Neanderthals by Modern Humans Series, DOI 10.1007/978-4-431-54553-8_26, © Springer Japan 2014

Keywords
Cognitive neuroscience • Functional magnetic resonance imaging • Imitative learning • Stone tool

26.1 Introduction

Since antiquity, humans have developed useful tools to improve their lives, and human culture was created by transmitting these technologies between individuals and generations. Technology is transferred by both social learning, which is learning from the behavior of another individual through social interaction, including imitating another's behavior, and individual learning through trial and error. In particular, social learning such as imitation plays an important role in the acquisition of knowledge about the social group to which the individual belongs. This kind of social learning is realized by developing cognitive abilities to comprehend the intentions of the other individual and learning a novel technology. Thus, elucidating the cognitive abilities underpinning social learning behavior is important to comprehend human evolutionary history, particularly the acquisition of technology. Neuroimaging techniques are highly effective for investigating the neural basis of cognitive abilities (Rilling 2008; for a review). Previous interdisciplinary studies between neuroscience and archaeology have investigated the neural correlates of execution during the construction of early Stone-age tools by experts (Stout et al. 2008) and examined the effect of motor-skill learning on the construction of stone tools by inexperienced subjects (Stout and Chaminade 2007). However, there is no direct evidence about which component of the neural mechanism is required to learn a novel technology from another individual.

In the present study, we examined the neural basis of social learning, particularly the contribution of linguistic ability. For this purpose, a social learning situation in which Mousterian stone tools were constructed was used as an experimental task because an expected neural activity in a historical environment can be depicted by reproducing the behaviors at that time. A previous study suggested that the development of cognitive abilities for tool use and language are closely represented in the cortex (Greenfield 1991), and the neural substrate for language and tool use shares a common region in Broca's area (Higuchi et al. 2009). Overlapping cortical regions contribute to the neural mechanisms of understanding actions (i.e., the mirror neuron system) (Buccino et al. 2004; Vogt et al. 2007) and tool use in non-human primates (Maravita and Iriki 2004). The importance of this region in language processing and its evolution has been widely discussed (Fogassi and Ferrari 2007; Corballis 2010 for reviews). However, it is unknown whether the cognitive ability to learn inexperienced tool use via social interaction during the prehistoric age was intervened in the cognitive ability for language processing. Humans in the prehistoric age transmitted their technology over a number of generations from the age when there was no explicit evidence about language use. Thus, even if the cognitive mechanism of tool use and language share a common neural basis, the key components of the social learning mechanism to acquire tool use and language might be different.

We assumed that imitative learning was the fundamental avenue for transmitting technology such as stone tool making in the prehistoric social environment. Observing the behavior of others is particularly important as a trigger for acquiring knowledge, and imitative learning is effective for acquiring generalized knowledge within a social group because learners can easily find good examples (e.g., elders) in their living space. It is speculated that imitative learning was essential to propagate technology or culture in the prehistoric social environment. We also expected that essential parts of the neural basis of imitative learning are different for stone tool making and language information processing. In imitative learning an individual needs to understand another's intention. In the case of stone tool making, the individual must extract intention from bodily actions, whereas in the case of spoken language s/he must extract it from articulated sounds. We speculate that the building process of an internal model for observed bodily action by imitative learning is different than that of internal model for observed speech by imitative learning. Humans in the prehistoric age may have used some kind of verbal communication even if there is no evidence of language at that time. If the essential neural bases of imitative learning to acquire the stone tool making skill and spoken language are different even though there are some common cortical regions that process both skills, this would help inform the cognitive mechanisms of tool-use and language.

To address this question, we used functional magnetic resonance imaging (fMRI) to investigate brain activity while subjects observed the bodily actions used to make a stone tool and observed an unknown spoken language. Common and different activations were analyzed to clarify the differences in the neural processes associated with observing bodily actions versus those associated with word pronunciation. We used a repetition suppression approach to identify the cortical areas in which imitative learning occurs that are different from those

in which other behaviors occur. Repetition suppression is a robust neural mechanism in which a neural activity is reduced when stimuli are repeated, and this suppression has been used to identify shared populations of neurons responsive to different stimuli (for a review, see Grill-Spector et al. 2006). Repetition-related reduction in neural activity was also used to probe the neural basis of learning. Repetitive-perceptual learning of auditory words shows a significant repetition-related decrease in the left superior temporal region (Rauschecker et al. 2008; Graves et al. 2008) and the frontal region related to articulation (Rauschecker et al. 2008). Similar repetition suppression effects have been reported in previous observational learning studies for bodily action in premotor and parietal regions (Hamilton and Grafton 2009). The neural mechanism of understanding another's intention from behavior is represented as a repetitive decrease in neural activity in the right superior temporal sulcus and intraparietal region (Ortigue et al. 2009). Thus, we hypothesized that when learning bodily actions and word pronunciation progress by observing the behavior of others, the neural activity that takes part in the observed behavior decreases due to repetitive observation. The repetition suppression of task-related activation was analyzed to detect the process by which a bodily action or word pronunciation is learned from the repetitively observed behavior of others.

26.2 Materials and Methods

26.2.1 Participants

Twenty-four healthy Japanese volunteers participated in this study (12 males and 12 females; mean age, 25 ± 5; range, 20–36 years). The experimental data from six subjects were excluded because of excessive head movement or an insufficient number of responses. Thus, we analyzed data from 18 participants (9 males and 9 females). All participants were right-handed according to the Edinburgh Handedness Inventory (Oldfield 1971), and none had a history of neurological or psychiatric disorders. We confirmed that all participants were inexperienced with stone tool-making and the Uzbek language. All participants provided written informed consent to the experimental protocol, which was approved by the Ethical Committee of the National Institute for Physiological Sciences. The experiments were conducted in compliance with national legislation and the Code of Ethical Principles for Medical Research Involving Human Subjects of the World Medical Association (Declaration of Helsinki).

26.2.2 Experimental Procedure

The fMRI experiment consisted of four runs of actual measurement and one practice run. A rapid event-related design was used for the fMRI experiment. During the fMRI session, all participants observed 15 moving pictures and one still picture of stone tool-making (mSTM and sSTM) and 15 moving pictures and one still picture of the pronunciation of an Uzbek word (mUWP and sUWP). Video clips of an expert making stone tools and of an Uzbek word pronounced by a native speaker were recorded using a digital video camera. The moving pictures were 1 s segments extracted from video clips. Each picture showed a kind of bodily action used to make a Mousterian stone tool from which it was easy to understand what kind of process was being depicted such as flaking, which includes a platform-preparation, or abrading (although it is unclear whether this abrading procedure accompanied the actual production of Mousterian stone tools) or to pronounce one Uzbek word. Each moving picture was presented twice in each run. In total, participants observed the same moving picture eight times throughout the fMRI session. The still pictures were used as a low-level control condition of visual stimuli to subtract the difference in the stone tool maker and Uzbek speaker on displayed moving pictures. Both still pictures were presented 15 times during each run. The practice run presented moving pictures that differed from those used in the actual run. The pictures were separated by resting intervals of approximately 4 s, during which time a white fixation cross was presented. The efficiency of the experimental design was highly dependent on the temporal pattern of the stimulus presentations (Dale 1999; Friston et al. 1999). We designed the order of moving and still pictures to become a highly efficient experimental design throughout the fMRI session. The detailed method has been described previously (Morita et al. 2008).

Participants were instructed to observe the pictures and to memorize the content of the bodily action or word pronunciation. To ensure that the participants were conscious of the task, an actual imitation task was conducted immediately after the fMRI measurements. The participants noticed the execution of the imitation task beforehand, and they were asked to imitate the observed bodily actions and the word pronunciation during an actual imitation task. The participant's imitations were video-recorded to evaluate the accuracy of the memorized content. To confirm the arousal state of the participants, the color of the fixation cross occasionally changed to yellow, and the participants were instructed to press a button when they noticed the change. Figure 26.1 illustrates the timeline of an fMRI run.

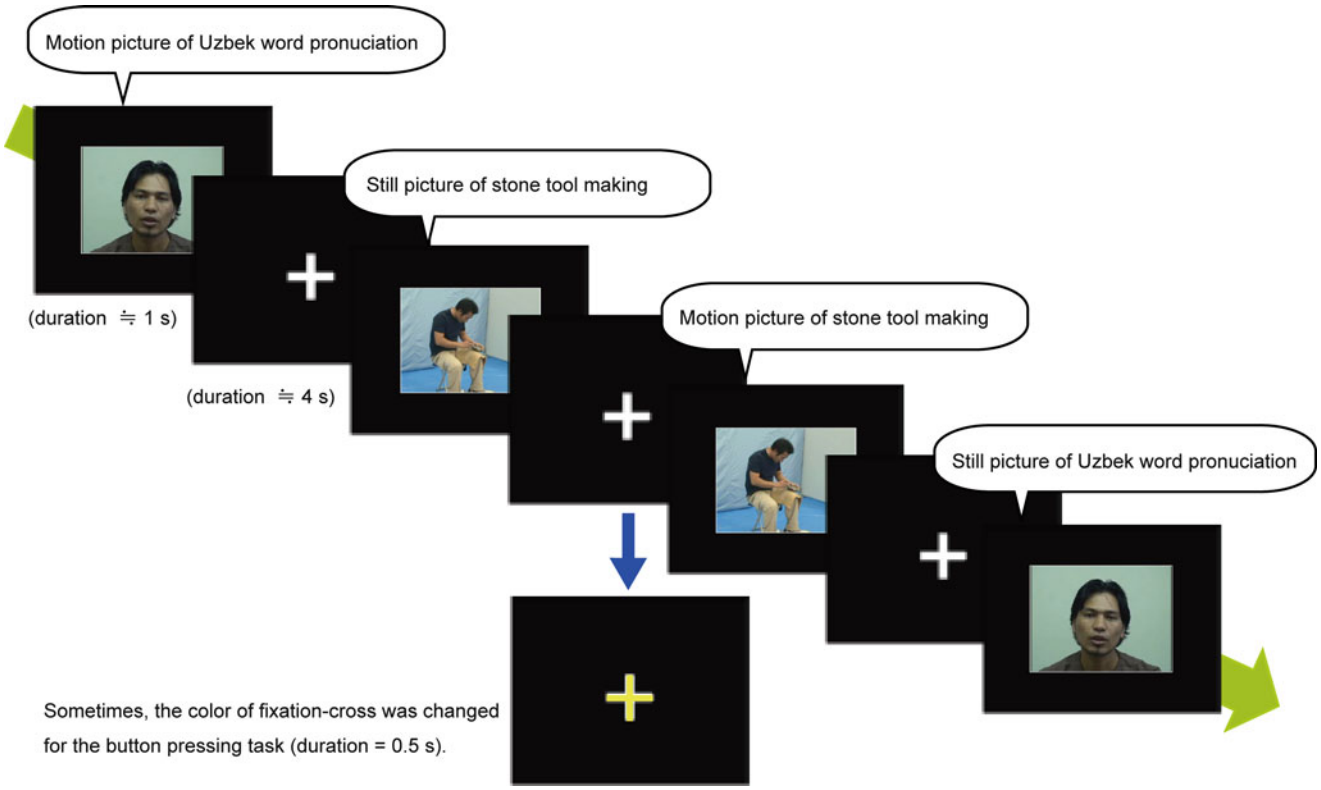

Fig. 26.1 Example of fMRI experimental stimulus

26.2.3 fMRI Scanning

All images were acquired using a 3-T Siemens Allegra scanner with a bird cage head coil (Siemens, Erlangen, Germany). To acquire a fine structural whole-brain image, magnetization-prepared rapid-acquisition gradient-echo (MP-RAGE) images were obtained (repetition time [TR], 2500 ms; echo time [TE], 4.38 ms; flip angle = 8°; field of view [FoV], 230 mm; one slab; number of slices per slab = 192; voxel dimensions = 0.9 × 0.9 × 1.0 mm). The fMRI time-series data covering the entire brain were acquired using a T2*-weighted gradient echo-echo planar imaging. Oblique scanning was used to exclude the artifacts of eyeballs and to cover the entire cerebrum. The parameters of the experiment were as follows: (TR, 3000 ms; acquisition time [TA], 2000 ms; TE, 30 ms; flip angle, 85°; 34 slices; FoV, 192 × 192 mm; 64 × 64 matrix; slice thickness, 3 mm; slice gap, 0.45 mm). The initial two scans of each run were dummy scans to equilibrate the state of magnetization and were discarded from the time-series data; thus, we collected 93 scans for each run. In total, 372 scans per subject were included in the analysis.

Stimulus presentation and response collection were performed using Presentation 1.21 (Neurobehavioral Systems, Albany, CA, USA) software implemented on a personal computer (Dimension 8200; Dell Computer Co., Round Rock, TX, USA). A liquid crystal display projector (DLA-M200L; Victor, Yokohama, Japan) located outside and behind the scanner projected the stimuli through another waveguide onto a translucent screen, which the subjects viewed via a mirror attached to the head coil of the MRI scanner. The auditory stimuli were presented via MRI-compatible headphones (Hitachi Advanced Systems, Yokohama, Japan). Behavioral responses were recorded using a fiber-optic response box (Current Designs Inc., Philadelphia, PA, USA).

26.2.4 Data Analysis

Data preprocessing and statistical analyses of fMRI data were performed using statistical parametric mapping (SPM8, Wellcome Trust Center for Neuroimaging, London, UK). The effect of head motion across the scans was corrected by realigning all scans to the first one. The whole-head MP-RAGE image volume was then co-registered with the first EPI image. All EPI images were spatially normalized to the Montréal Neurological Institute T1 template using the anatomical T1-weighted MRI image for each subject. Finally, each scan was smoothed with a Gaussian filter in a spatial domain (8-mm full-width at half-maximum).

The fMRI data were analyzed using a two-level approach in SPM8. During the first level, the hemodynamic responses produced under the different experimental conditions were assessed at each voxel on a subject base using a general linear model. We hypothesized that the hemodynamic responses under the mSTM, sSTM, mUWP, and sUWP conditions would be the canonical hemodynamic response functions with a 1-s duration. These hemodynamic responses were modeled for every repetition of the mSTM, sSTM, mUWP, and sUWP conditions. Hemodynamic responses to the observation of still pictures and to button responses were also modeled. Global changes were adjusted by proportional scaling, and low-frequency confounding effects were removed using a high-pass filter with a 128-s cutoff. Multiple regression analyses were performed on each voxel to detect the regions in which MR signal changes were correlated with the hypothesized model to obtain the partial regression coefficient of each voxel.

The second level of the analysis was performed on a population-based random-effects analysis using a two-way repeated-measures factorial design. One factor was the type of picture observed (STM or UWP; two conditions), and the other factor was the number of times the same moving picture was presented repeatedly (1–8, eight conditions). The contrast images obtained by subtraction of the (mSTM–sSTM) and (mUWP–sUWP) conditions were used for this analysis to subtract the difference between the visual stimulus and a simple repetitive effect caused by repetitively observing thhe same image. The statistical threshold was set at $p<0.05$ (corrected for family-wise error [FWE] by voxel level). The cytoarchitectonic location of each activation focus was confirmed by the SPM Anatomy toolbox (Eickhoff et al. 2005).

To identify the regions showing learning effects for each task, contrast images representing a repetition suppression effect of task-related activation were created and estimated. The contrast images were made using decreased linear contrasts (7, 5, 3, 1, −1, −3, −5, −7) for the factor of the number of repetitions (i.e., eight times) under each STM and UWP condition. Contrast images of the first repetition of the (mSTM–sSTM) and (mUWP–sUWP) contrast ($p<0.05$, corrected for FWE) were also made to specify brain activation when the subjects observed each stimulus for the first time, and were used as mask images to detect the repetition suppression effect of task-related activation. The statistical threshold was set at $p<0.05$ (corrected for FWE). In addition, to compare the task-specific learning effect on each task, the parameter estimate of the activation foci showing the repetition suppression effect with sphere radii of 4 mm were extracted using MarsBaR 0.42 toolbox (Brett et al. 2002). A gradient of the decrease in the activation profile associated with the repetition between (mSTM–sSTM) and (mUWP–sUWP) contrast was tested.

26.3 Results

The cortical activations during observation of STM and UWP pictures are summarized in Table 26.1. A cytoarchitectonic location was obtained by Anatomy toolbox 1.7 (Eickhoff et al. 2005, 2007). Significant activations in the bilateral premotor and pre-supplementary motor areas and the right superior and bilateral posterior parts of the middle temporal gyri were commonly manifested during observations of both STM and UWP moving pictures. The large activation cluster over the parietal cortex was found bilaterally during observation of the STM moving pictures, as determined by the procedure (mSTM–sSTM); activation peaks were identified in the bilateral superior and inferior parietal lobules, intraparietal sulcus, and supramarginal gyrus. The frontal activation clusters were extended dorsally to the superior frontal gyrus and ventrally to the middle or inferior frontal gyrus. Moreover, the left insula and right cerebellar posterior lobule were significantly activated (Fig. 26.2a). In contrast, significant activation clusters during observation of moving pictures of UWP were demonstrated by (mUWP–sUWP) in the bilateral temporal areas, including the superior temporal gyrus, and extended to the parietal operculum (Fig. 26.2b).

The common and differential activations in response to observation of the STM and UWP pictures are summarized in Tables 26.2 and 26.3, respectively. Significant activations depicted by conjunction analysis of the aforementioned conditions were observed in the left premotor and pre-supplementary motor areas and in the bilateral superior and posterior parts of the middle temporal gyri (Fig. 26.2c). Differential activations associated with (mSTM–sSTM)—(mUWP–sUWP) were obtained in the bilateral middle frontal gyrus, left premotor area, large regions of the bilateral intraparietal sulcus extending to the left supramarginal gyrus, right postcentral gyrus, posterior part of the bilateral middle temporal gyrus, left insula, and right cerebellar posterior lobule (Fig. 26.2d). In contrast, differential activations associated with (mUWP–sUWP)—(mSTM–sSTM) were obtained in the bilateral premotor area, pre-supplementary motor area, and superior temporal gyrus (Fig. 26.2e).

The repetition-suppression effect was found in a region of the right cerebellar posterior lobule under the STM condition and a border region of the left superior temporal gyrus and inferior parietal lobule under the UWP condition. Figure 26.3 depicts regions showing the effect of repetition-suppression on task-related activation and Table 26.4 summarizes anatomical location of those regions. The decrease in the activation profile associated with the repetition of the (mSTM–sSTM) condition was significantly larger than that associated with repetition of the (mUZP–sUZP) condition ($F_{(1,\ 284)}=14.88$, $p=0.0001$) on the ROI of the right cerebellar posterior lobule (Fig. 26.3a). Additionally, the decrease in the activation

Table 26.1 Cortical activation during observation of pictures under the STM and UWP conditions

		MNI coordinate (mm)			
Area	(Brodmann's area)	x	y	z	T-score
(mSTM–sSTM) contrast					
L. superior frontal gyrus	(BA6)	−24	−4	52	7.77
	(BA6)	−24	0	64	7.46
R. middle frontal gyrus	(BA6)	34	−2	54	7.20
R. inferior frontal gyrus	(BA44)	56	10	28	6.49
L. precentral gyrus	(BA6)	−34	0	56	7.80
	(BA6/44)	−56	6	34	11.22
L. supplementary motor area	(BA6)	−4	14	50	6.26
L. postcentral gyrus	(BA40)	−62	−20	34	13.16
R. postcentral gyrus	(BA2)	38	−40	46	7.16
R. supramarginal gyrus	(BA40)	62	−16	24	6.72
L. superior parietal lobule	(BA7a)	−18	−46	66	7.78
R. superior parietal lobule	(BA7p)	16	−66	52	6.98
L. inferior parietal lobule	(BA40)	−38	−42	48	10.10
	(BA40)	−52	−38	24	8.28
R. inferior parietal lobule	(BA40)	34	−46	52	6.99
R. superior temporal gyrus	(BA40)	68	−34	14	7.00
L. superior temporal sulcus	(BA21)	−54	−44	12	5.63
R. superior temporal sulcus	(BA21)	52	−38	8	4.77
L. middle temporal gyrus	(BA19/37)	−50	−66	6	15.28
R. middle temporal gyrus	(BA19/37)	52	−62	2	15.50
L. inferior temporal gyrus	(BA37)	−46	−50	−18	5.74
R. inferior temporal gyrus	(BA37)	48	−48	−18	5.24
L. insula		−42	−4	6	5.12
R. cerebellum		16	−76	−48	7.28
		26	−66	−26	6.53
(mUWP–sUWP) contrast					
R. precentral gyrus	(BA6)	56	0	40	10.47
L. precontral gyrus	(BA6/4a)	−52	−6	44	9.09
L. supplementary motor area	(BA6)	−2	4	62	7.63
L. postcentral gyrus	(BA3b/3a)	−56	−4	18	5.39
L. superior temporal gyrus	(BA22)	−54	−18	2	26.79
R. superior temporal gyrus	(BA22)	62	−14	2	25.78
L. middle temporal gyrus	(BA21)	−50	−64	8	7.57
R. middle temporal gyrus	(BA21)	50	−62	2	6.58

Anatomical location was obtained by the Anatomy toolbox (Eickhoff et al. 2005)

profile associated with the repetition of the (mUZP–sUZP) condition was significantly greater than that associated with the (mSTM–sSTM) condition ($F_{(1, 284)} = 20.44$, $p = 0.000001$) in the ROI of the left superior temporal gyrus (Fig. 26.3b).

26.4 Discussion

In the present study, we observed activity in the parietofrontal network when an inexperienced novice observed the STM actions of an expert. We also found that the cortical network was primarily involved in the experimental task, which is consistent with previous findings of the neural correlates of Acheulean stone tool-making by experts (Stout et al. 2008). A recent meta-analysis of action-observation and imitation tasks also reported similar patterns in cortical networks (Caspers et al. 2010). In contrast, the activation pattern in the dorsal premotor area and the supramarginal gyrus was different from the previous findings of a novice during execution of stone tool making (Stout and Chaminade 2007). This discrepancy may have depended on whether or not the actual execution process was involved. Moreover, we observed a repetition-related decrease in specific activation in the right posterior part of the cerebellum (lobule VI) under the STM picture-observation condition. In contrast, a border region of the superior temporal gyrus and left inferior parietal lobule

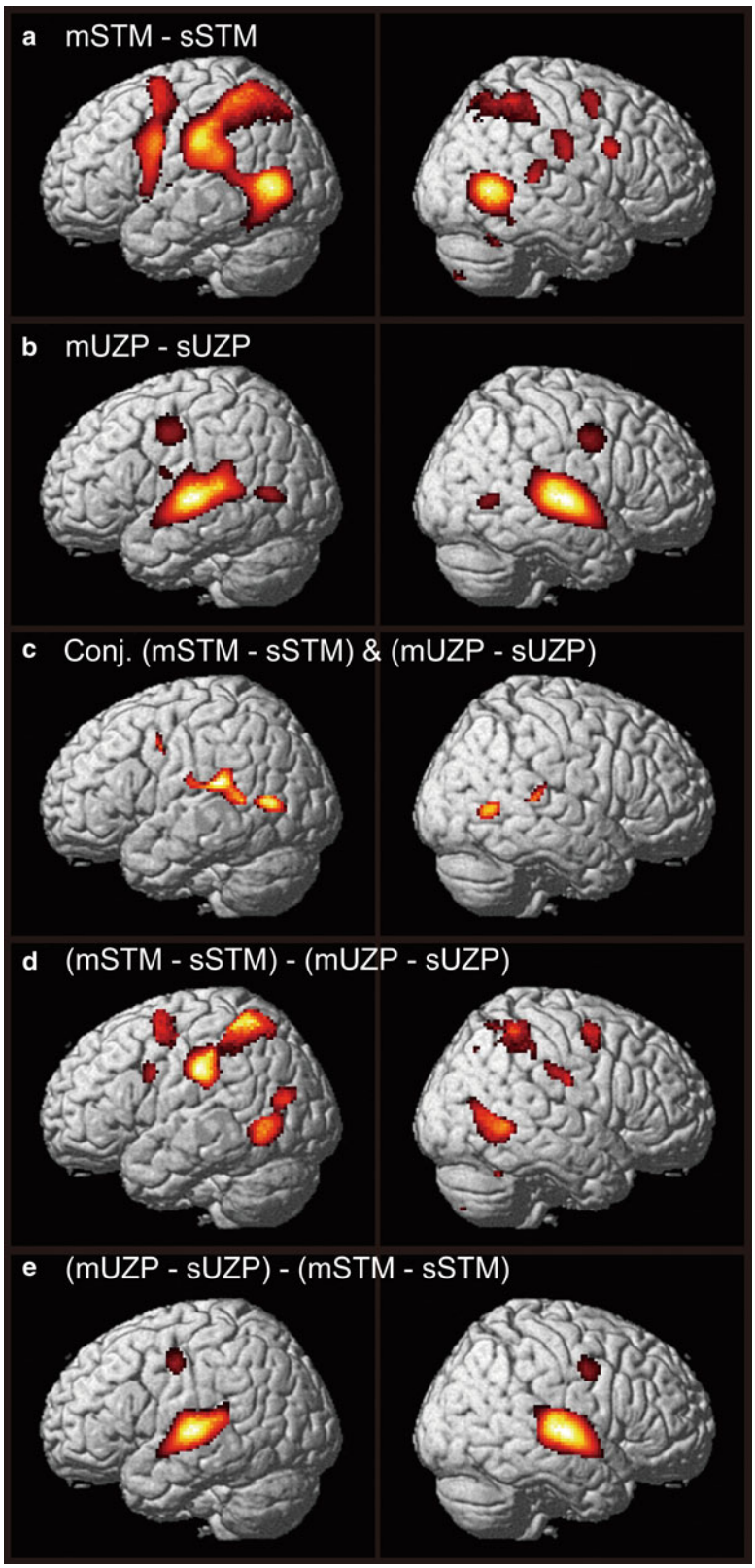

Fig. 26.2 Cortical activation associated with observation of stone tool-making and pronunciation of an Uzbek word. Comparison between moving and still pictures under (**a**) STM and (**b**) UWP conditions, and (**c**) result of conjunction analysis of (a) and (b). (**d**) and (**e**) show differential activations under STM and UWP conditions

Table 26.2 Common activations during observation of STM and UWP pictures

		MNI coordinate (mm)			
Area	(Brodmann's area)	x	y	z	T-score
Conjunction analysis of (mSTM–sSTM) & (mUWP–sUWP)					
L. precentral gyrus	(BA6/4a)	−50	0	40	5.64
L. supplementary motor area	(BA6)	−6	12	52	6.09
L. postcentral gyrus	(BA40/43)	−60	−18	18	6.31
	(BA40)	−50	−36	22	7.88
R. postcentral gyrus/superior temporal gyrus	(BA40)	66	−32	12	6.46
L. middle temporal gyrus	(BA19/37)	−50	−64	8	7.57
R. middle temporal gyrus	(BA19/37)	50	−62	2	6.58

Anatomical location was obtained by the Anatomy toolbox (Eickhoff et al. 2005)

Table 26.3 Differential activations during observation of STM and UWP pictures

		MNI coordinate (mm)			
Area	(Brodmann's area)	x	y	z	T-score
(mSTM–sSTM)-(mUWP–sUWP)					
L. superior frontal gyrus	(BA6)	−22	0	54	6.14
L. middle frontal gyrus/precentral gyrus	(BA6)	−26	−6	50	6.81
R. middle frontal gyrus	(BA6)	32	−2	52	7.14
L. precentral gyrus	(BA6/44)	−56	6	32	6.40
R. postcentral gyrus	(BA3b/40)	62	−14	26	5.82
L. supramarginal gyrus	(BA40)	−54	−24	34	9.33
R. supramarginal gyrus	(BA40)	56	−28	36	5.05
L. superior parietal lobule	(BA7a)	−22	−54	62	8.08
R. superior parietal lobule	(BA7a)	16	−60	54	7.45
L. inferior parietal lobule	(BA40)	−36	−44	48	7.10
R. inferior parietal lobule	(BA2/40)	38	−40	46	6.49
L. middle occipital gyrus	(BA39)	−38	−74	18	5.52
	(BA39)	−48	−72	12	5.28
R. middle occipital gyrus	(BA39)	48	−68	10	5.38
L. middle temporal gyrus	(BA19/37)	−50	−64	−4	7.56
R. middle temporal gyrus	(BA19/37)	56	−58	−2	6.47
L. insula		−42	−2	8	4.81
R. cerebellum		18	−76	−48	5.50
		44	−56	−28	4.96
(mUWP–sUWP)-(mSTM–sSTM)					
L. precentral/postcentral gyrus	(BA6/4a)	−52	−8	44	8.04
R. precentral gyrus	(BA6)	56	−2	42	9.02
L/R. supplementary motor area	(BA6)	0	2	64	5.11
L. superior temporal gyrus	(BA22)	−52	−18	2	21.75
	(BA22)	−44	−26	8	19.26
R. superior temporal gyrus	(BA22)	58	−14	2	20.32
	(BA22)	42	−24	10	14.47

Anatomical location was obtained by the Anatomy toolbox (Eickhoff et al. 2005)

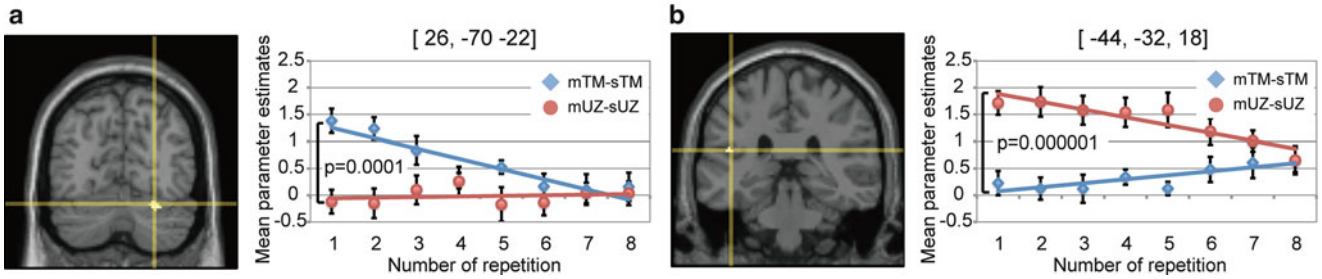

Fig. 26.3 Repetition-suppression effect in the (**a**) right cerebellar posterior lobule with STM task-related activation, and (**b**) in the left superior temporal gyrus with UWP task-related activation. The plot shows repetition-related changes of parameter estimates in each activation focus, and *error bar* shows the standard error of the mean

Table 26.4 Regions showing the repetition-suppression effect on task-related activation during observation of STM and UWP pictures

		MNI coordinate (mm)			
Area	(Brodmann's area)	x	y	z	T-score
Linear contrast of (mSTM–sSTM)					
R. cerebellum		26	−70	−22	4.59
Linear contrast of (mUWP–sUWP)					
L. superior temporal gyrus/inferior parietal lobule	(BA22) (BA40)	−44	−32	18	3.94

Anatomical location was obtained by the Anatomy toolbox (Eickhoff et al. 2005)

showed a significant decrease in specific activation under the UWP picture-observation condition. This result supports our hypothesis; the cognitive mechanism of imitative learning for stone tool-making and that of word-pronunciation involves different cortical regions.

26.4.1 Effect of Learning on Task-Related Activation

The activation of the right cerebellar posterior lobule (lobule VI) showed a significant repetition-related decrease under the STM condition. A previous study suggested that changes in cerebellar activity reflect the progress of internal model formulation to learn a motor control to manipulate a novel tool (Imamizu et al. 2000). A learning-related decrease in cerebellar lobule VI activation was also observed in a neuroimaging study focused on acquisition of a bimanual coordination task (Debaere et al. 2004). Because the subjects were asked to imitate the observed STM action immediately after the fMRI scan, they had to be alert to acquire the STM action presented. Subjects must have observed the posture of the whole body and how to handle the hummerstone and stone core that the expert held in both hands to imitate the STM action. As each observed STM action itself was simple, the subjects could formulate the internal model of STM action using their own repertoires of motor control through a repetitive observation of another's action. Hence, it was expected that the subjects interpreted the observed STM action and could roughly translate it into their own motor representation via repetitive observation, and the repetition-related decline of cerebellar activation reflected the progress of learning to construct an internal model of STM actions.

In contrast, the border area of the left superior temporal gyrus and inferior parietal lobule showed repetition-dependent suppression of activation. A repetition-related decrease in neural activity associated with the learning of pseudo-words was observed in the left superior temporal gyrus as well as the left frontal cortex, suggesting that the repetition-related decreases in the left superior temporal gyrus reflected the effect of learning on the neural processing of the perception of auditory stimuli (Rauschecker et al. 2008). Graves et al. (2008) also reported that the posterior superior temporal gyrus showed reduced neural activity related to repetitive lexical phonological processing. In the present study, subjects were asked to vocalize an Uzbek word after the fMRI scan as well as to imitate an STM action. Because subjects were inexperienced with the Uzbek language and no information about the meaning of the words presented was provided during the experiment, they had to concentrate on catching the phonological information about the presented word during the mUWP task. Thus, the repetition-dependent suppression in the activity of the left superior temporal gyrus reflected the progress in learning

the phonological information. A learning-related decrease in cortical activation was not observed in the common cortical regions of both imitation tasks, suggesting that activity in these regions was not being reflected in the progress of imitative learning by observation without execution such as with the present experimental task. If individual learning accompanied by actual execution such as trial-and-error learning is performed, the learning-related activation change may also be observed in common regions.

Stout et al. (2011) suggested that brain activation specific to naïve subjects reflects kinematic information and visuospatial attention that represents a strategy of observational learning to simulate low-level aspects of task performance such as understanding action elements. The present results support their assertion; that is, a learning effect based on repetitive observation of stone tool-making was found in the neural basis to construct an internal model of action in the cerebellum, whereas the neural basis to understand an action intention such as the mirror neuron system did not show that kind of learning effect. A similar interpretation is possible for the case of Uzbek word articulation. The learning effect due to repetitive observation of Uzbek word articulation was observed in the neural basis of phonological processing, whereas cortical regions representing articulatory processes, such as the dorsal premotor area (Brown et al. 2009; Koelsch et al. 2009), did not show such a learning effect. Therefore, participants who had no exact knowledge about stone tool-making or the Uzbek language focused on a low-level aspect of task information during repetitive observational learning, that is, to acquire the motor sequence of each bodily action for stone tool-making or to follow the sequence of the phoneme for the Uzbek word. It can be predicted that when trained subjects or experts perform the same experiment, subjective attention is turned to a higher-level aspect of task information, that is, to understand the intention of each process of stone tool-making or to simulate articulation of Uzbek words. Cortical regions that show repetition-related decreases in trained subjects may also differ via the aforementioned differences between naïve and trained subjects. Further investigations using trained subjects are necessary to clarify this point.

These results suggest a decrease in brain activation by repetitive observation of another's behavior, but we did not investigate the quantitative relationship between changes in brain activation and skill progress to carry out the actual behavior. It is expected that there is a relationship between not only social learning such as imitation but also individual learning such as trial-and-error and skill progress. In addition, the internal model of observed behavior may be preliminarily constructed by imitative learning and the model may be refined to suit the personal characteristics of each individual through individual learning. To clarify this point, it is necessary to measure brain activity at each stage of skill acquisition, which can be evaluated from an outside learner as in Stout and Chaminade (2007) and Stout et al. (2011).

26.4.2 Common Activation for Both Imitation Tasks

The posterior part of the bilateral superior temporal gyrus showed significant activation in the conjunction analysis of the STM and UWP conditions. The location of the activation site was close to that identified by previous studies on biological motion (Grossman and Blake 2002; Thompson et al. 2005; Peelen et al. 2006). The activity of this area is involved in the perception of dynamic facial motion (Sato et al. 2004; Schultz and Pilz 2009). Because the participants observed motion pictures to memorize the projected bodily action or speech for the *post-hoc* mimicking test in our fMRI experiment, the activity of this region reflected bodily or facial motion for learning the observed behavior of others.

Activation in the superior part of the dorsal premotor area was observed under the STM condition. From the conjunction analysis, a part of the activated region was also observed under the UWP condition. A previous study suggested that the dorsolateral prefrontal cortex was active during tool-use action-planning tasks (Johnson-Frey et al. 2005), and the influence of spatial information on observed behavior has also been suggested (Vogt et al. 2007). Thus, dorsal premotor activation reflected the cognitive process used to integrate an observer's motor representation with the observed bodily or facial action. However, it has also been reported that stone tool making by a novice does not involve activation of the dorsal premotor area (Stout and Chaminade 2007). The discrepancy in the results of these two studies may be attributable to differences in the actual interpretation of the practice of stone tool making by participants. In the present study, participants did not have an execution session until they were tested with video recordings after the fMRI measurement. Thus, it would be expected that they interpreted and planned to imitate the observed action by substituting their own motor representation, which was similar to the STM action presented during the fMRI measurement, because they were inexperienced and did not have an actual motor representation of the STM action.

Cognitive functions in the pre-supplementary motor area have been suggested to be important for response inhibition (Duann et al. 2009; Chen et al. 2009). In the fMRI experiment, participants were asked to mentally imitate the presented action or speech to memorize them. However, they were asked not to move or vocalize during the experiment. Therefore, the activity of the pre-supplementary motor area was observed in relation to suppression of imitative body movement. Activation of the bilateral posterior part of the middle temporal gyrus that has been reported as a visual motion processing area (Tootell et al. 1995; Malikovic et al. 2007) was commonly observed under the STM and UWP conditions. Because the contrast between the motion-picture minus the still-picture condition was used for the second-level analysis, that activation reflected the perception of visual motion.

26.4.3 Differential Activation for Each Imitation Task

Ventral premotor activation, which was also specifically induced by observing STM action, was included in the region that has been interpreted as part of the mirror neuron system in previous studies (Buccino et al. 2004; Vogt et al. 2007). Furthermore, execution of stone tool-making involves activity in the ventral premotor region (Stout and Chaminade 2007; Stout et al. 2008, 2011). To imitate an STM action, subjects must observe the posture of the whole body and learn how to handle the hummerstone and stone core that the expert held in both hands. Thus, ventral premotor activation reflected the cognitive process used to analyze the observed action. Caspers et al. (2010) reported that the dorsal part of BA44 is commonly involved in action-observation and imitation tasks, whereas the caudoventral part of BA44 is consistently involved during action imitation. Based on the activation induced by observing the STM action, the peak location of the ventral premotor area was located on the border region between the probabilistic map of BA6 and BA44, and the activation cluster was more expansive on the ventral side of the inferior frontal region. These results suggest that the cognitive mechanism to manipulate the self-motor representations contribute to the action observation during imitative learning. In contrast, the activation peak in the dorsal premotor area under the UWP compared with the STM condition was observed in the inferior portion. Previous neuroimaging studies of phonological processing have reported that the inferior part of the dorsal premotor area plays an important role in the articulatory process (Brown et al. 2009; Koelsch et al. 2009). The participants were not familiar with the pronunciation of Uzbek words because the sequence of the phonemes differed from that of Japanese words. We concluded that the increase in activity reflected the cognitive load of the mental rehearsal needed to pronounce the Uzbek words.

Activations were observed in the parietal cortex adjacent to the bilateral intraparietal sulcus and extended to the left supramarginal gyrus specifically under the STM condition. These findings are consistent with those of a previous study on the neural correlates in the posterior parietal region associated with the observation of action (Caspers et al. 2010). Previous studies have suggested that intraparietal sulcus regions are involved in stone tool making by both novices and experts (Stout and Chaminade 2007; Stout et al. 2008, 2011). In the present study, subjects were asked to memorize observed unfamiliar STM actions that consisted of an interpretable bimanual manipulation using a hummerstone and stone core. Therefore, the activations reflected the acquisition of the procedure of bimanual motor representation for stone tool making by observing the actions of others. Additionally, a differential activation pattern in the supramarginal gyrus of the dorsal premotor area was observed and compared with the results of a previous study of stone tool-making by a novice (Stout and Chaminade 2007). Activity in the left posterior parietal regions including the supramarginal gyrus occurred while planning the bodily actions associated with the use of a familiar tool, even though the execution of actual motor actions was not involved (Johnson-Frey et al. 2005). Moreover, stone tool making by experts was associated with activation in the bilateral supramarginal gyrus (Stout et al. 2008). This may also indicate that participants were using their own motor representations, which would be similar to the STM action, to plan the imitative action instead of using an actual motor representation of an STM action that they had not yet learned.

A direct comparison of (mSTM–sSTM)—(mUWP–sUWP) showed activation of the junction areas of the bilateral middle temporal and occipital region, which had a slightly inferior peak location compared with that during common activation. The pictures under the mSTM condition presented all the bodily motions involved in stone tool-making. By contrast, the pictures under the mUWP condition presented only the facial motion. A previous study reported that the occipitotemporal region was particularly sensitive to the perception of the human body (Astafiev et al. 2004). Thus, differential activation was induced by the perception of motion enacted by the whole human body. In contrast, observation of the pronunciation of a Uzbek word involved large activation clusters in the bilateral superior temporal gyrus. Because only the mUWP condition contained auditory information in the form of pronunciation of a Uzbek word, these activations were considered to reflect audiovisual speech perception (Murase et al. 2008).

26.5 Conclusion

The progress of imitation learning by repetitive observation was represented in a specific cortical region, and the represented region was dependent on the information that the subject focused on to learn, although a common mechanism representing the premotor and supplementary motor area and posterior part of the temporal region existed between both imitative learning tasks. That is, the subject had to focus on the internal model formulation of the observed action to imitate the stone tool-making procedure, and the imitative learning of observed action caused activity to decrease in the right cerebellum. In contrast, the subject had to focus on the phonological components of the auditory information to imitate an unknown Uzbek word, and the imitative learning of the Uzbek word caused an activity decrease in the left superior temporal gyrus. These results support our hypothesis that the cortical region where imitative learning by repetitive observation of stone tool-making appears as a change in neural activity differs from that of word pronunciation. Our results demonstrate the cortical mechanisms of social learning behavior that were assumed to have been used in the prehistoric age.

Acknowledgements This study was supported by Grant-in-Aid for Scientific Research on Innovative Areas (Grand No. 22101007), MEXT, Japan. The fMRI experiment was carried out using a 3-Tesla MR scanner located at National Institute for Physiological Sciences.

References

Astafiev SV, Stanley CM, Shulman GL, Corbetta M (2004) Extrastriate body area in human occipital cortex responds to the performance of motor actions. Nat Neurosci 7:542–548

Brett M, Anton JJ, Valabregue R, Poline JB (2002) Region of interest analysis using an SPM toolbox. NeuroImage 16 (available in CD-ROM)

Brown S, Laird AR, Pfordresher PQ, Thelen SM, Turkeltaub P, Liotti M (2009) The somatotopy of speech: phonation and articulation in the human motor cortex. Brain Cogn 70:31–41

Buccino G, Vogt S, Ritzl A, Fink GR, Zilles K, Freund HJ, Rizzolatti G (2004) Neural circuits underlying imitation learning of hand actions: an event-related fMRI study. Neuron 42:323–334

Caspers S, Zilles K, Laird AR, Eickhoff SB (2010) ALE meta-analysis of action observation and imitation in the human brain. Neuroimage 50:1148–67

Chen CY, Muggleton NG, Tzeng OJL, Humg DL, Juan CH (2009) Control of prepotent responses by the superior medial frontal cortex. Neuroimage 44:537–545

Corballis MC (2010) Mirror neuron and the evolution of language. Brain Lang 112:25–35

Dale AM (1999) Optimal experimental design for event-related fMRI. Hum Brain Mapp 8:109–114

Debaere F, Wenderoth N, Sunaert S, Van Hecke P, Swinnen SP (2004) Changes in brain activation during the acquisition of a new bimanual coordination task. Neuropsychologia 42:855–867

Duann JP, Ide JS, Luo X, Li CR (2009) Functional connectivity delineates distinct roles of the inferior frontal cortex and presupplementary motor area in stop signal inhibition. J Neurosci 29:10171–10179

Eickhoff SB, Stephan KE, Mohlberg H, Grefkes C, Fink GR, Amunts K, Zilles K (2005) A new SPM toolbox for combining probabilistic cytoarchitectonic maps and functional imaging data. Neuroimage 25:1325–1335

Eickhoff SB, Paus T, Caspers S, Grosbras MH, Evans A, Zilles K, Amunts K (2007) Assignment of functional activations to probabilistic cytoarchitectonic areas revisited. Neuroimage 36:511–521

Fogassi L, Ferrari PF (2007) Mirror neurons and the evolution of embodied language. Curr Dir Psychol Sci 16:136–141

Friston KJ, Zarahn E, Josephs O, Henson RN, Dale AM (1999) Stochastic designs in event-related fMRI. Neuroimage 10:607–619

Greenfield PM (1991) Language, tools and brain: the ontogeny and phylogeny of hierarchically organized sequential behavior. Behav Brain Sci 14:531–595

Grill-Spector K, Henson R, Martin A (2006) Repetition and the brain: neural models of stimulus-specific effects. Trends Cogn Sci 10:14–23

Graves WW, Grabowski TJ, Mehta S, Gupta P (2008) Left posterior superior temporal gyrus participates specifically in accessing lexical phonology. J Cogn Neurosci 20:1698–1710

Grossman ED, Blake R (2002) Brain areas active during visual perception of biological motion. Neuron 35:1167–1175

Hamilton AF, Grafton ST (2009) Repetition suppression for performed hand gestures revealed by fMRI. Hum Brain Mapp 30:2898–2906

Higuchi S, Chaminade T, Imamizu H, Kawato M (2009) Shared neural correlates for language and tool use. Neuroreport 20:1376–1381

Imamizu H, Miyauchi S, Tamada T, Sasaki Y, Takino R, Puetz B, Yoshioka T, Kawato M (2000) Human cerebellar activity reflecting an acquired internal model of a novel tool. Nature 403:192–195

Johnson-Frey SH, Newman-Norlund R, Grafton ST (2005) A Distributed left hemisphere network active during planning of everyday tool use skills. Cereb Cortex 15:681–695

Koelsch S, Schulze K, Sammler D, Fritz T, Müller K, Gruber O (2009) Functional architecture of verbal and tonal working memory: an FMRI study. Hum Brain Mapp 30:859–873

Malikovic A, Amunts K, Schleicher A, Mohlberg H, Eickhoff SB, Wilms M, Palomero-Gallagher N, Armstrong E, Zilles K (2007) Cytoarchitectonic analysis of the human extrastriate cortex in the region of V5/ MT1: a probabilistic, stereotaxic map of area hOc5. Cereb Cortex 17:562–574

Maravita A, Iriki A (2004) Tools for the body (schema). Trends Cogn Sci 8:79–86

Morita T, Itakura S, Saito DN, Nakashita S, Harada T, Kochiyama T, Sadato N (2008) The role of the right prefrontal cortex in self-evaluation of the face: a functional magnetic resonance imaging study. J Cogn Neurosci 20:342–355

Murase M, Saito DN, Kochiyama T, Tanabe HC, Tanaka S, Harada T, Aramaki Y, Honda M, Sadato N (2008) Cross-modal integration during vowel identification in audiovisual speech: a functional magnetic resonance imaging study. Neurosci lett 434:71–76

Oldfield R (1971) The assessment and analysis of handedness: the Edinburgh inventory. Neuropsychologia 9:812–815

Ortigue S, Thompson JC, Parasuraman R, Grafton ST (2009) Spatio-temporal dynamics of human intention understanding in temporo-parietal cortex: a combined EEG/fMRI repetition suppression paradigm. PLoS ONE 4(9):e6962

Peelen MV, Wiggett AJ, Downing PE (2006) Patterns of fMRI activity dissociate overlapping functional brain areas that respond to biological motion. Neuron 49:815–822

Rauschecker AM, Pringle A, Watkins KE (2008) Changes in neural activity associated with learning to articulate novel auditory pseudowords by covert repetition. Hum Brain Mapp 29:1231–1242

Rilling K (2008) Neuroscientific approaches and applications within anthropology. Am J Phys Anthropol Suppl 47:2–32

Sato W, Kochiyaman T, Yoshikawa S, Naito E, Matsumura M (2004) Enhanced neural activity in response to dynamic facial expressions of emotion: an fMRI study. Cogn Brain Res 20:81–91

Schultz J, Pilz KS (2009) Natural facial motion enhances cortical responses to faces. Exp Brain Res 194:465–475

Stout D, Chaminade T (2007) The evolutionary neuroscience of tool making. Neuropsychologia 45:1091–1100

Stout D, Toth N, Schick K, Chaminade T (2008) Neural correlates of early stone age toolmaking: technology, language and cognition in human evolution. Philos Trans R Soc Lond B Biol Sci 363:1939–1949

Stout D, Passingham R, Frith C, Apel J, Chaminade T (2011) Technology, expertise and social cognition in human evolution. Eur J Neurosci 33:1328–38

Thompson JC, Clarke M, Stewart T, Puce A (2005) Configural processing of biological motion in human superior temporal sulcus. J Neurosci 25:9059–9066

Tootell RBH, Reppas JB, Kwong KK, Malach R, Born RT, Brady TJ, Rosen BR, Belliveau JW (1995) Functional analysis of human MT and related visual cortical areas using magnetic resonance imaging. J Neurosci 15:3125–3230

Vogt S, Buccino G, Wohlschläger AM, Canessa N, Shah NJ, Zilles K, Eickhoff SB, Freund HJ, Rizzolatti G, Fink GR (2007) Prefrontal activation in imitation learning of hand actions: effect of practice and expertise. Neuroimage 37:1371–1383

Neural Substrates Associated with Motivation to Learn in Modern Humans

27

Kei Mizuno

Abstract

Differences in learning abilities are thought to be demonstrated by elucidating the brain regions involved in individual and social learning of modern humans using neuropsychological methods, and by comparing the differences in brain regions between modern and ancient humans based on fossil reconstruction of ancient human brains. Although motivation to learn is an enforced factor in individual and social learning, the neural substrates associated with motivation to learn have not previously been determined. Therefore, I investigated the neural substrates of motivation to learn in modern humans using functional magnetic resonance imaging (fMRI). I confirmed that sense of accomplishment, which is an intrinsic reward, is associated with motivation to learn. In addition, the striatum was strongly activated by sense of accomplishment, and striatal activation levels were positively associated with a motivation-to-learn score derived from a questionnaire. I explored the association between motivation to learn and other cognitive functions, and found that motivation to learn was positively correlated with performance on a divided attention task. The fMRI study revealed that processing of divided attention activates the dorsal inferior frontal gyrus and superior parietal lobule, found in the frontal and parietal cortices, and fosters higher synchronization between these regions. In modern humans, the frontal and parietal cortices develop from childhood to adulthood. Morphological and functional comparisons of these regions between modern and ancient humans are expected to help elucidate differences in learning abilities between modern and ancient humans.

Keywords

Divided attention • Functional magnetic resonance imaging • Intrinsic reward • Motivation to learn • Striatum

27.1 Introduction

Comparative anatomy has been used to elucidate differences in learning abilities between modern and ancient humans based on differences in brain morphology related to learned behaviors. In modern humans, the brain regions involved in individual and social learning are determined using neuropsychological methods. By comparing those brain regions with morphological reconstruction of fossils of the ancient human brain, the differences in learning abilities may be established. The study project for Replacement of

K. Mizuno (✉)
Molecular Probe Dynamics Laboratory, RIKEN Center for Molecular Imaging Science, 6-7-3 Minatojima-minamimachi, Chuo-ku, Kobe, Hyogo 650-0047, Japan

Pathophysiological and Health Science Team, RIKEN Center for Life Science Technologies, 6-7-3 Minatojima-minamimachi, Chuo-ku, Kobe, Hyogo 650-0047, Japan
e-mail: keimizuno@riken.jp

T. Akazawa et al. (eds.), *Dynamics of Learning in Neanderthals and Modern Humans Volume 2: Cognitive and Physical Perspectives*, Replacement of Neanderthals by Modern Humans Series, DOI 10.1007/978-4-431-54553-8_27, © Springer Japan 2014

Neanderthals by Modern Humans (RNMH) has focused on the neural bases of learning control (enforced learning) in individual learning and of imitative learning in social learning. Although motivation to learn is an enforced factor for individual and social learning, the neural substrates associated with it have been unclear. Therefore, I investigated the neural substrates of motivation to learn in modern humans using functional magnetic resonance imaging (fMRI). In addition, I tried to determine what cognitive function is associated with level of motivation to learn. The neural substrates of that cognitive function may provide evidence for discussion of the differences in learning abilities between modern and ancient humans based on the differences in the brain morphologies and functions between them.

27.2 Neural Basis of Motivation to Learn

Academic rewards for motivational arousal include sense of accomplishment and competence, self-efficacy, and acceptance by others (Deci et al. 1991, 1996). Although acceptance by others corresponds to the social reward in the RNMH projects, and is induced by the relationship between self and others, sense of accomplishment and competence and self-efficacy are induced comparatively without dependence on others. In other words, sense of accomplishment and competence and self-efficacy are intrinsic rewards. Therefore, not only social rewards but also intrinsic rewards are important factors for enforced learning (Fig. 27.1).

Neural bases of acceptance by others and sense of accomplishment have been reported using fMRI. Perception of a good reputation by others induces activation of the medial prefrontal cortex and striatum (Izuma et al. 2008). Additionally, when all pieces fit comfortably into a square puzzle with the correct answer to a working memory task (2-back task), a sense of accomplishment occurred (Yoshida et al. 2008) and striatal activation was observed (Mizuno et al. 2008). However, although striatal activation levels were positively correlated with scores on Waugh's academic achievement motivation scale (Waugh 2002), which is a scale of motivation to learn (Fig. 27.2), and with accuracy of the task during this academic reward (sense of accomplishment) condition, these correlations were not observed during a monetary reward condition. In this case, the task was not a learning task. However, an association between good performance on the task or high motivation to learn and striatal activation was observed, suggesting that intrinsic rewards may be effective in enforced learning.

27.3 Attentional Function Involved in Motivation to Learn

When students graduate to junior high school from elementary school, rapid changes in the environment occur, which may cause various behavioral and emotional problems (Spear 2000). One example is the number of Japanese students with school refusal, which was observed in 7,154 out of 1,201,134 sixth-graders of elementary school and 21,084 out of 1,177,557 seventh-graders of junior high school in 2010 (MEXT 2010). Chronic fatigue and low motivation to learn in students are closely correlated to school refusal (Miike et al. 2004). I reported that from elementary school to junior high school, fatigue and intrinsic

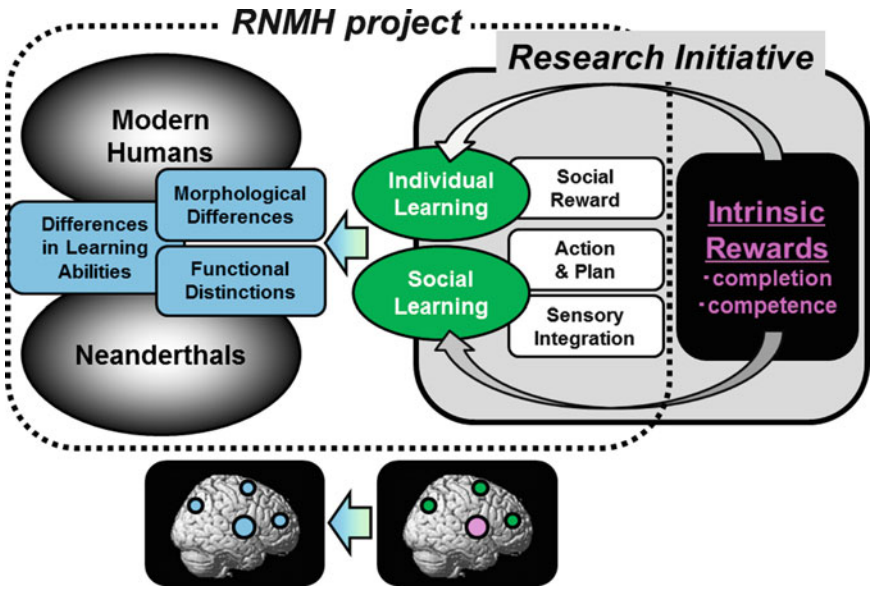

Fig. 27.1 Research initiative

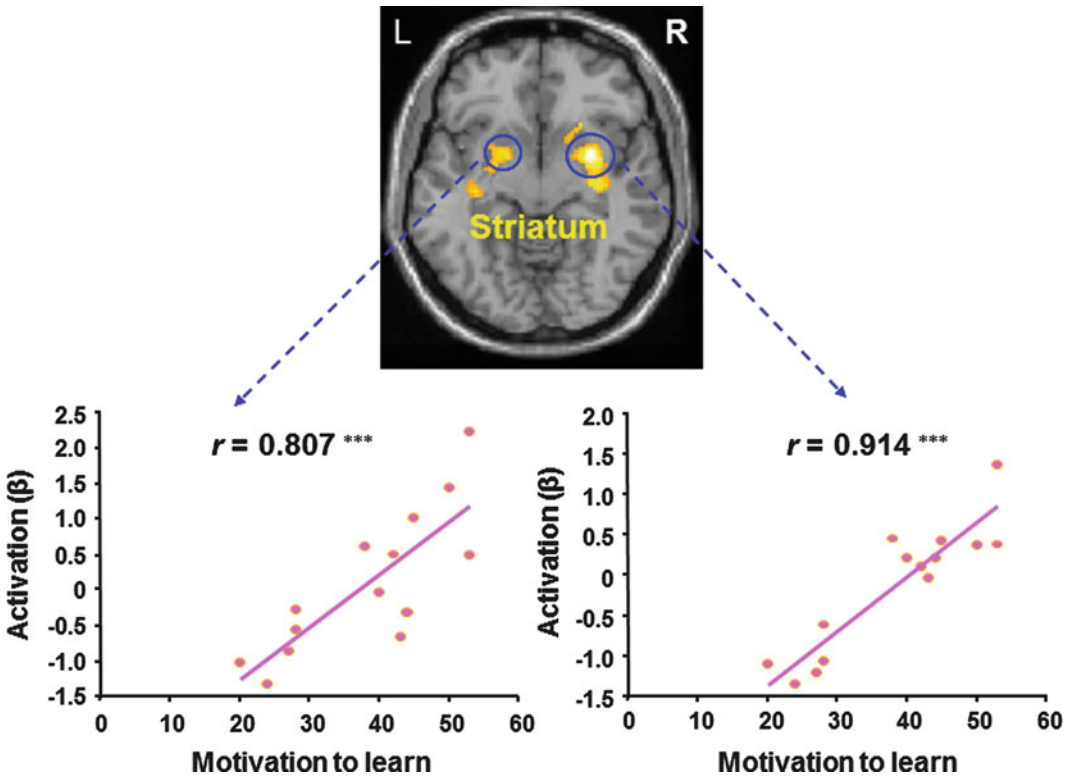

Fig. 27.2 Relationship between striatal activation and motivation-to-learn score

motivation to learn in students also markedly increases and decreases, respectively (Mizuno et al. 2011b, c). On the other hand, performance of executive functions, such as working memory and attention control, develops dramatically from elementary school to junior high school (Mizuno et al. 2011a).

Based on these findings, in elementary and junior high school students, I investigated correlations between motivation-to-learn scores calculated by the intrinsic motivation to learn scale (Sakurai and Takano 1985) and performance of various cognitive functions including motor processing, spatial construction ability, semantic fluency, immediate memory, delayed memory, spatial and non-spatial working memory, and selective, switching, and divided attention (Mizuno et al. 2011a). In multivariate logistic regression analyses adjusted for grade and gender, none of the cognitive test scores were correlated with intrinsic motivation to learn in elementary school students. However, the scores for the divided attention task (kana pick-out test) were positively correlated with intrinsic motivation to learn in junior high school students (Mizuno et al. 2011b). The kana pick-out test demands performance of parallel processing during a reading task. Participants must pick out a subset of letters contained within a story while reading the story for comprehension. The task requires appropriate allocation of attentional resources to the two activities (Kaneko 1996).

27.4 Neural Basis of Divided Attention

Based on finding a relationship between motivation to learn and divided attention, I used fMRI to investigate the neural substrates associated with the kana pick-out test. I found that in the dual-task condition, the left dorsal inferior frontal gyrus and superior parietal lobule were more highly activated than they were in the two single-task conditions (Mizuno et al. 2012) (Fig. 27.3). In addition, higher functional connectivity (synchronization) between the left dorsal inferior frontal gyrus and superior parietal lobule in the dual-task condition than in the two single-task conditions was observed. These results suggest that increased activation of the left dorsal inferior frontal gyrus and superior parietal lobule during dual-task performance may be associated with capacity for attentional resources, and the increase in synchronization between the left dorsal inferior frontal gyrus and superior parietal lobule in the dual-task condition may induce effective communication between these brain regions, leading to more attentional processing due to greater and more complex demands on voluntary attentional resources.

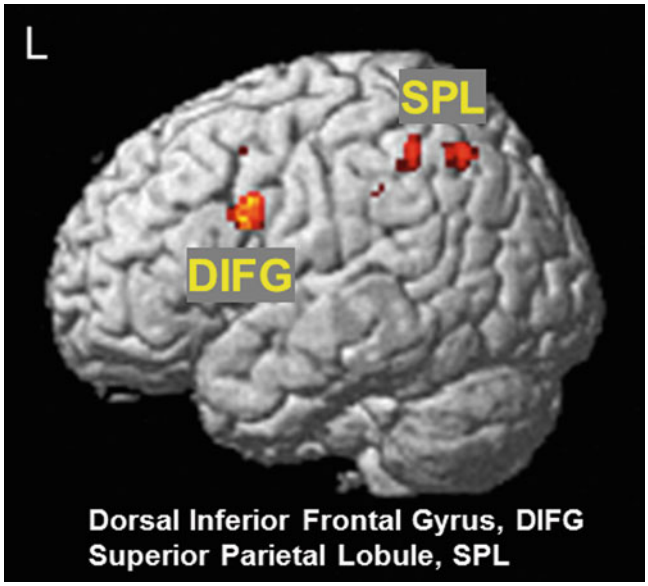

Fig. 27.3 Activation of frontal and parietal cortices during divided attention

27.5 Conclusion

In modern humans, intrinsic reward for motivational arousal, such as sense of accomplishment, induces activation of the striatum. Motivation to learn is related to the ability to divide attention. The dorsal inferior frontal gyrus and superior parietal lobule, found in the frontal and parietal cortices, are activated during divided attention processing on the kana pick-out test. It is known that the frontal and parietal cortices are some of the last regions to mature from childhood to adolescence. Morphological and functional comparisons of these regions between modern and ancient humans are expected to help elucidate differences in learning abilities between modern and ancient humans.

27.6 Ethics

The protocols of these studies were approved by each Ethics Committee, and all participants gave written informed consent for participation in the studies. The experiments were undertaken in compliance with national legislation and the Code of Ethical Principles for Medical Research Involving Human Subjects of the World Medical Association (Declaration of Helsinki).

Acknowledgments These studies were supported by Grants-in-Aid for Scientific Research on Innovative Areas (No. 23101508) from the Ministry of Education, Culture, Sports, Science and Technology (MEXT) of Japan and the Japan Science and Technology Corporation (JST)/Research Institute of Science and Technology for Society (RISTEX) (No. 07052628).

References

Deci EL, Vallerand RJ, Pelletier LG, Ryan RM (1991) Motivation and education: the self-determination perspective. Educ Psychol 26:325–346

Deci EL, Ryan RM, Williams GC (1996) Need satisfaction and the self-regulation of learning. Learn Individ Differ 8:165–183

Izuma K, Saito DN, Sadato N (2008) Processing of social and monetary rewards in the human striatum. Neuron 58:284–294. doi:10.1016/j.neuron.2008.03.020

Kaneko M (1996) A neuropsychological index of aging data from 9000 elderly people. Nihon Ronen Igakkai Zasshi 33:811–815 (in Japanese)

MEXT (Ministry of Education, Culture, Sports, Science and Technology-Japan) (2010) Statistics on student guidance

Miike T, Tomoda A, Jhodoi T, Iwatani N, Mabe H (2004) Learning and memorization impairment in childhood chronic fatigue syndrome manifesting as school phobia in Japan. Brain Dev 26:442–447

Mizuno K, Tanaka M, Ishii A, Tanabe HC, Onoe H, Sadato N, Watanabe Y (2008) The neural basis of academic achievement motivation. Neuroimage 42:369–378. doi:10.1016/j.neuroimage.2008.04.253

Mizuno K, Tanaka M, Fukuda S, Sasabe T, Imai-Matsumura K, Watanabe Y (2011a) Changes in cognitive functions of students in the transitional period from elementary school to junior high school. Brain Dev 33:412–420. doi:10.1016/j.braindev.2010.07.005

Mizuno K, Tanaka M, Fukuda S, Imai-Matsumura K, Watanabe Y (2011b) Relationship between cognitive function and prevalence of decrease in intrinsic academic motivation in adolescents. Behav Brain Funct 7:4. doi:10.1186/1744-9081-7-4

Mizuno K, Tanaka M, Fukuda S, Imai-Matsumura K, Watanabe Y (2011c) Relationship between cognitive functions and prevalence of fatigue in elementary and junior high school students. Brain Dev 33:470–479. doi:10.1016/j.braindev.2010.08.012

Mizuno K, Tanaka M, Tanabe HC, Sadato N, Watanabe Y (2012) The neural substrates associated with attentional resources and difficulty of concurrent processing of the two verbal tasks. Neuropsychologia 50:1998–2009. doi:10.1016/j.neuropsychologia.2012.04.025

Sakurai S, Takano S (1985) A new self-report scale of intrinsic versus extrinsic motivation toward learning in children. Tsukuba Psychol Res 7:43–54 (in Japanese)

Spear LP (2000) The adolescent brain and age-related behavioral manifestations. Neurosci Biobehav Rev 24:417–463

Waugh RF (2002) Creating a scale to measure motivation to achieve academically linking attitudes and behaviours using Rasch measurement. Br J Educ Psychol 72:65–86

Yoshida M, Tanaka M, Mizuno K, Ishii A, Nozaki K, Urakawa A, Cho Y, Kataoka Y, Watanabe Y (2008) Factors influencing the academic motivation of individual college students. Int J Neurosci 118:1400–1411. doi:10.1080/00207450701242982

Index

T. Akazawa et al. (eds.), *Dynamics of Learning in Neanderthals and Modern Humans Volume 2: Cognitive and Physical Perspectives*, Replacement of Neanderthals by Modern Humans Series, DOI 10.1007/978-4-431-54553-8, © Springer Japan 2014